BETA AMYLOID: FROM PHYSIOLOGY TO PATHOGENESIS

EDITED BY: Robert A. Nichols, Daniela Puzzo and Walter Gulisano

PUBLISHED IN: Frontiers in Molecular Neuroscience

frontiers Research Topics

frontiers

ISSN 1664-8714
ISBN 978-2-88974-458-9
DOI 10.3389/978-2-88974-458-9

About Frontiers

Frontiers is more than just an open-access publisher of scholarly articles: it is a pioneering approach to the world of academia, radically improving the way scholarly research is managed. The grand vision of Frontiers is a world where all people have an equal opportunity to seek, share and generate knowledge. Frontiers provides immediate and permanent online open access to all its publications, but this alone is not enough to realize our grand goals.

Frontiers Journal Series

The Frontiers Journal Series is a multi-tier and interdisciplinary set of open-access, online journals, promising a paradigm shift from the current review, selection and dissemination processes in academic publishing. All Frontiers journals are driven by researchers for researchers; therefore, they constitute a service to the scholarly community. At the same time, the Frontiers Journal Series operates on a revolutionary invention, the tiered publishing system, initially addressing specific communities of scholars, and gradually climbing up to broader public understanding, thus serving the interests of the lay society, too.

Dedication to Quality

Each Frontiers article is a landmark of the highest quality, thanks to genuinely collaborative interactions between authors and review editors, who include some of the world's best academicians. Research must be certified by peers before entering a stream of knowledge that may eventually reach the public - and shape society; therefore, Frontiers only applies the most rigorous and unbiased reviews.
Frontiers revolutionizes research publishing by freely delivering the most outstanding research, evaluated with no bias from both the academic and social point of view. By applying the most advanced information technologies, Frontiers is catapulting scholarly publishing into a new generation.

What are Frontiers Research Topics?

Frontiers Research Topics are very popular trademarks of the Frontiers Journals Series: they are collections of at least ten articles, all centered on a particular subject. With their unique mix of varied contributions from Original Research to Review Articles, Frontiers Research Topics unify the most influential researchers, the latest key findings and historical advances in a hot research area! Find out more on how to host your own Frontiers Research Topic or contribute to one as an author by contacting the Frontiers Editorial Office: frontiersin.org/about/contact

BETA AMYLOID: FROM PHYSIOLOGY TO PATHOGENESIS

Topic Editors:
Robert A. Nichols, University of Hawaii at Manoa, United States
Daniela Puzzo, University of Catania, Italy
Walter Gulisano, University of Catania, Italy

Citation: Nichols, R. A., Puzzo, D., Gulisano, W., eds. (2022). Beta Amyloid: From Physiology to Pathogenesis. Lausanne: Frontiers Media SA.
doi: 10.3389/978-2-88974-458-9

Table of Contents

frontiers in Molecular Neuroscience

EDITORIAL
published: 14 March 2022
doi: 10.3389/fnmol.2022.876224

Editorial: Beta Amyloid: From Physiology to Pathogenesis

Robert A. Nichols[1]*, *Walter Gulisano*[2] *and Daniela Puzzo*[2]*

[1] Department of Cell and Molecular Biology, University of Hawaii, Honolulu, HI, United States, [2] Department of Biomedical and Biotechnological Sciences, University of Catania, Catania, Italy

Keywords: beta amyloid, Alzheimer's disease, pathogenesis, synaptic plasticity, cognitive deficits, neuroinflammation, neurogenesis

Editorial on the Research Topic

Beta Amyloid: From Physiology to Pathogenesis

The neuropeptide beta amyloid (Aβ) is present in the brain throughout life, but accumulates with age, with levels rising dramatically years prior to the diagnosis of Alzheimer's disease (AD) (Bateman et al., 2012). In AD, elevated levels of Aβ assemble into extracellular plaques, notable histological hallmarks of the disease along with accumulation of intracellular neurofibrillary tangles and neuronal loss in select regions of the brain. Curiously, the level of Aβ at synapses is regulated by nerve activity and the pool of Aβ in brain turns over at a remarkable rate (Cirrito et al., 2005; Bateman et al., 2006). These observations, and others, led to the postulate that in the absence of dementia the low levels of soluble oligomeric Aβ present in brain impact synaptic and neural circuit function, now borne out in a range of functional studies (Puzzo et al., 2008, 2012; Morley et al., 2010; Lawrence et al., 2014; Gulisano et al., 2019).

The objective of this Frontiers Research Topic collection was to bring together a cross-section of reports on Aβ as a physiological regulator in relation to studies on the contribution of Aβ pathology to AD pathogenesis. A fundamental issue in the study of AD pathogenesis revolves around the role of supranormal levels of Aβ arising during the prodromic period before AD, linked to synaptic dysfunction and, ultimately, synapse loss as well as neural circuit hyperactivity and select cognitive dysfunction, which are to varying extents inter-related to neuroinflammation. Approaches to lower pathological levels of Aβ in AD would thus be expected to normalize function, but, for humans, has largely failed in the vast majority of clinical trials. This conundrum underscores the need to better understand all aspects of Aβ function and regulation, informing new approaches, possibly identifying new targets and, especially, avoiding misleading methodological and conceptual pitfalls.

For this Research Topic we received a large number of submissions from which 14 articles by a total of 70 authors from 10 countries were published. The articles included seven original research papers along with a diverse array of reviews, mini-reviews and perspectives. These articles range from confrontation of the conceptual and methodological pitfalls in AD research (Puzzo and Conti) to Aβ regulation of synaptic function (Fagiani et al.; Forest et al.; Karisetty et al.; Guan et al.), neural circuitry (Hector and Brouillette), organelle trafficking (Fabbrietti et al.), transcriptional regulation (Jesko et al.); neuroepigenic gene regulation (Karisetty et al.), neurogenesis (Li Puma et al.); glia and neuroinflammation (Guzman et al.; Spampinato et al.; Oberstein et al.; Seol et al.); and cognitive processes (Zhang et al.; Guan et al.). This wide range of topics underscores the breadth of impact of Aβ as a synaptic, neuronal, neuroimmune and cognitive regulator.

OPEN ACCESS

Edited and reviewed by:
Detlev Boison,
The State University of New Jersey, United States

***Correspondence:**
Robert A. Nichols
robert.nichols@hawaii.edu
Daniela Puzzo
danypuzzo@yahoo.it

Specialty section:
This article was submitted to Brain Disease Mechanisms, a section of the journal Frontiers in Molecular Neuroscience

Received: *15 February 2022*
Accepted: *15 February 2022*
Published: *14 March 2022*

Citation:
Nichols RA, Gulisano W and Puzzo D (2022) Editorial: Beta Amyloid: From Physiology to Pathogenesis. Front. Mol. Neurosci. 15:876224. doi: 10.3389/fnmol.2022.876224

The Perspective by Puzzo and Conti confront many of the limitations, experimenter bias, conceptual bias and paucity of rigor and reproducibility in methodology. Of particular note is over-reach in regard to the experimental model under study, particularly in preclinical studies using rodent models that have repeatedly failed to translate to the clinic, wherein intrinsic variables are not properly considered. For Aβ in AD, *confirmation* bias, extrapolation from preclinical rodent models and dismissing a role for Aβ out of hand have compromised the need for open, neutral, question-driven research on the fundamental role for Aβ in the brain as a foundation for understanding Aβ in AD pathogenesis.

As the progressive elevation of Aβ levels appear to correlate with synaptic dysfunction, new insights into synaptic regulation by Aβ are reviewed by Karisetty et al. in which both direct action on the synapse and neuroepigenetic regulation of synaptic genes contribute to synaptic impairment, focusing on DNA methylation and histone acetylation. The current status of selective demethylase and HDAC inhibitors in clinical trials is also reviewed. Similarly, Fagiani et al. review the impact of Aβ on synaptic function but from the point of view of Aβ as endogenous regulator, with elevation levels leading to a disruption of synaptic homeostasis as one of the earliest stages in AD pathogenesis, separate but related to Aβ disruption of synaptic plasticity.

Delving into molecular mechanisms for synaptic dysregulation by Aβ, Guan et al. reviewed the current understanding of the role for calcium, ranging from neuroinflammatory processes with a focus on proinflammatory cytokines, neuronal apoptosis in relation to ER and mitochondrial calcium dysregulation, dysregulation of neurogenesis, excitotoxicity, lysosomal degradation pathways and autophagy. Zhang et al. demonstrated that glucocorticoids can accelerate disease development and progression in a mouse model of AD by interfering with plasticity-related proteins and apoptotic pathways, indicating a potential detrimental effect of long-term cortisone treatments. Jésko et al. found that a sphingosine-1-phosphate receptor modulator reversed, in part, synaptic dysfunction in an aged familial AD mouse model. These findings provide new insights into the disruption of sphingolipids in AD, which appears to be an early event in disease progression. Continuing with approaches with therapeutic potential, Forest et al. demonstrated that the neuroprotective N-terminal Aβ core hexapeptide, YEVHHQ, potently reversed impaired synaptic plasticity in AD pathology models in manner dependent upon PI3 kinase via mTOR, in addition to its previously noted protection against neuronal toxicity.

In a parallel with synaptic dysfunction, Aβ induces neurite atrophy and compromised neurite trafficking. Fabbrietti et al. addressed fundamental mechanisms in Aβ-triggered dendrite atrophy by studying trafficking of Golgi-like organelles, essential for dendritic arborization, tagged for live imaging. Aβ treatment led to rapid reduction in Golgi-like organelle trafficking, most pronounced in higher order dendritic arbors, and a tetracyclic antidepressant with neurotrophin-like activity was able to rescue the Aβ-induced reduction in trafficking concomitant with reversal of neuritic atrophy, offering a novel means to prevent or reverse this very early Aβ-linked neuropathology.

Moving to the level of neural circuits, Hector and Brouillette review neuronal network hyperactivity in rodent AD pathology models as well as humans with mild cognitive impairment, as an early pathological event in AD pathogenesis, replicated in *in vitro* studies applying Aβ. While a number of mechanisms may contribute to an excess of excitation in neural circuits leading to hyperactivity, several factors converge on altered glutamatergic signaling, suggesting a range of potential sites for intervention.

Examining the impact of neuroimmune responses catalyzed by direct application of Aβ by injection into the CA1 region of the hippocampus, as a highly simplified *in vivo* model, Guzman et al. found rapid mobilization of reactive astrocytes and microglia as well as endothelial dysfunction, correlated with spatial memory deficits, well before onset of tau-based pathology or neurodegeneration. Spampinato et al. addressed more broadly the cross-talk between neuroinflammation and the peripheral immune system as AD develops, particularly in the context of a compromised blood-brain barrier (BBB) in AD allowing lymphocyte infiltration. Using *in vitro* models, it was found that Aβ-primed reactive astrocytes altered CD4+ T cell cytokine and neurotrophin expression, and in turn, the CD4+ cell moderated the inflammatory response of the Aβ-primed astrocytes. The latter finding is intriguing as a possible transient mitigating impact of the peripheral T cells on the Aβ-triggered inflammatory response in the astrocytes at the BBB. Regarding the interaction of astrocytes with Aβ, specifically intracellular Aβ degradation leading to the formation of N-terminally truncated forms of the amyloid peptide, which are prominent in extracellular amyloid deposits, Oberstein et al. examined the effect of deletion or inhibition of the degradative enzyme cathepsin B and observed a sharp reduction in the amount of secreted N-terminal truncated Aβ, while secretion of full-length Aβ increased. These findings add complexity to understanding of the degradative pathways for internalized Aβ, indicating that the N-terminal truncated forms of Aβ are generated outside of the lysosomal compartment. Turning to microglial responses to Aβ, Seol et al. reviewed cell-based Aβ clearance as a limited compensatory response in contrast to a developing feed-forward response of microglia to advancing Aβ pathology, wherein induction of the inflammasome contributes to seeding and spreading of Aβ pathology via released ASC-Aβ complexes, providing another unique target for intervention in AD pathogenesis.

Lastly, Li Puma et al. reviewed the controversial association of Aβ accumulation with the development of impaired neurogenesis. As to whether organized neurogenesis continues into adulthood in humans remains in question; however, well defined AD pathology models indicate that altered hippocampal neurogenesis occurs prior to dysfunction in memory formation, and more importantly, suggests that increased hippocampal neurogenesis would improve memory acquisition.

Altogether, we hope that this collection of reviews and original research for this Research Topic provides new perspectives and insights into the wide range of connections between Aβ as

regulator of multiple physiological processes in the brain and supranormal Aβ in AD pathogenesis.

AUTHOR CONTRIBUTIONS

All authors listed have made a substantial, direct, and intellectual contribution to the work and approved it for publication.

ACKNOWLEDGMENTS

We thank all of the authors for their contributions to this Research Topic. We acknowledge funding support from the University of Hawaii Foundation, #125-8320-4, to RN and University of Catania Project Piaceri, Linea 2 to DP.

REFERENCES

Bateman, R. J., Munsell, L. Y., Morris, J. C., Swarm, R., Yarasheski, K. E., and Holtzman, D. M. (2006). Human amyloid-? synthesis and clearance rates as measured in cerebrospinal fluid *in vivo*. *Nature Med.* 12, 856–861. doi: 10.1038/nm1438

Bateman, R. J., Xiong, C., Benzinger, T. L., Fagan, A. M., Goate, A., Fox, N. C., et al. (2012). Clinical and biomarker changes in dominantly inherited Alzheimer's disease. *N. Engl. J. Med.* 367, 795–804. doi: 10.1056/NEJMoa1202753

Cirrito, J. R., Yamada, K. A., Finn, M. B., Sloviter, R. S., Bales, K. R., May, P. C., et al. (2005). Synaptic activity regulates interstitial fluid amyloid-? levels in vivo. *Neuron.* 48, 913–922. doi: 10.1016/j.neuron.2005.10.028

Gulisano, W., Melone, M., Ripoli, C., Tropea, M. R., Li Puma, D. D., Giunta, S., et al. (2019). Neuromodulatory action of picomolar extracellular A?42 oligomers on presynaptic and postsynaptic mechanisms underlying synaptic function and memory. *J. Neurosci.* 39, 5986–6000. doi: 10.1523/JNEUROSCI.0163-19.2019

Lawrence, J. L., Tong, M., Alfulaij, N., Sherrin, T., Contarino, M., White, M. M., et al. (2014). Regulation of presynaptic Ca^{2+}, synaptic plasticity and contextual fear conditioning by a N-terminal?-amyloid fragment. *J. Neurosci.* 34, 14210–14218. doi: 10.1523/JNEUROSCI.0326-14.2014

Morley, J. E., Farr, S. A., Banks, W. A., Johnson, S. N., Yamada, K. A., and Xu, L. (2010). A physiological role for amyloid-beta protein: enhancement of learning and memory. *J. Alzheimers Dis.* 19:441–449. doi: 10.3233/JAD-2010-1230

Puzzo, D., Privitera, L., Leznik, E., Fa,' M., Staniszewski, A., Palmeri, A., et al. (2008). Picomolar amyloid-beta positively modulates synaptic plasticity and memory in hippocampus. *J. Neurosci.* 28:14537–14545. doi: 10.1523/JNEUROSCI.2692-08.2008

Puzzo, D., Privitera, L., and Palmeri, A. (2012). Hormetic effect of amyloid-? peptide in synaptic plasticity and memory. *Neurobiol. Aging.* 33, 1484.e15–24. doi: 10.1016/j.neurobiolaging.2011.12.020

Conflict of Interest: The authors declare that the research was conducted in the absence of any commercial or financial relationships that could be construed as a potential conflict of interest.

Publisher's Note: All claims expressed in this article are solely those of the authors and do not necessarily represent those of their affiliated organizations, or those of the publisher, the editors and the reviewers. Any product that may be evaluated in this article, or claim that may be made by its manufacturer, is not guaranteed or endorsed by the publisher.

frontiers in Molecular Neuroscience

ORIGINAL RESEARCH
published: 03 July 2020
doi: 10.3389/fnmol.2020.00120

Reciprocal Interplay Between Astrocytes and CD4+ Cells Affects Blood-Brain Barrier and Neuronal Function in Response to β Amyloid

*Simona Federica Spampinato[1], Sara Merlo[1], Evelina Fagone[2], Mary Fruciano[2], Yasuteru Sano[3], Takashi Kanda[3] and Maria Angela Sortino[1]**

[1]Section of Pharmacology, Department of Biomedical and Biotechnological Sciences, University of Catania, Catania, Italy, [2]Department of Clinical and Experimental Medicine, University of Catania, Catania, Italy, [3]Department of Neurology and Clinical Neuroscience, Yamaguchi University Graduate School of Medicine, Ube, Japan

Background: In Alzheimer's disease (AD) neuronal degeneration is associated with gliosis and infiltration of peripheral blood mononuclear cells (PBMCs), which participate in neuroinflammation. Defects at the blood-brain barrier (BBB) facilitate PBMCs migration towards the central nervous system (CNS) and in particular CD4+ T cells have been found in areas severely affected in AD. However, the role of T cells, once they migrate into the CNS, is not well defined. CD4+ cells interact with astrocytes able to release several factors and cytokines that can modulate T cell polarization; similarly, astrocytic properties are modulated after interaction with T cells.

Methods: In *in vitro* models, astrocytes were primed with β-amyloid (Aβ; 2.5 μM, 5 h) and then co-cultured with magnetically isolated CD4+ cells. Cytokines expression was evaluated both in co-cultured CD4+ cells and astrocytes. The effects of this crosstalk were further evaluated by co-culturing CD4+ cells with the neuronal-like SH-SY5Y cell line and astrocytes with endothelial cells.

Results: The pattern of cytokines and trophic factors expressed by CD4+ cells were strongly modulated in the presence of Aβ-primed astrocytes. Specifically, the percentage of IL-4+ and IFNγ+ CD4+ cells was significantly increased and reduced, respectively. Further, increased BDNF mRNA levels were observed in CD4+ cells. When SH-SY5Y cells were co-cultured with astrocyte-conditioned CD4+ cells and exposed to Aβ, the reduction of the presynaptic protein synaptophysin was prevented with a BDNF-dependent mechanism. In astrocytes co-cultured with CD4+ cells, reduced mRNA levels of inflammatory cytokines and VEGF were observed. This was paralleled by the prevention of the reduction of claudin-5 when astrocytes were co-cultured with endothelial cells.

OPEN ACCESS

Edited by:
Robert A. Nichols, University of Hawaii at Manoa, United States

Reviewed by:
Carsten Theiss, Ruhr University Bochum, Germany
Francesco Ria, Catholic University of the Sacred Heart, Italy

***Correspondence:**
Maria Angela Sortino
msortino@unict.it

Received: *02 April 2020*
Accepted: *10 June 2020*
Published: *03 July 2020*

Citation:
Spampinato SF, Merlo S, Fagone E, Fruciano M, Sano Y, Kanda T and Sortino MA (2020) Reciprocal Interplay Between Astrocytes and CD4+ Cells Affects Blood-Brain Barrier and Neuronal Function in Response to β Amyloid. Front. Mol. Neurosci. 13:120. doi: 10.3389/fnmol.2020.00120

Abbreviations: AC, astrocytes; AD, Alzheimer's disease; Aβ, β-amyloid; BBB, blood-brain barrier; BDNF, brain-derived neurotrophic factor; CD, cluster of differentiation; CNS, central nervous system; ICAM-1, intercellular adhesion molecule 1; IFNγ, interferon γ; IL-4, interleukin 4; MHC, major histocompatibility complex; MW, molecular weight; PBMCs, peripheral blood mononuclear cells; TEM, trans-endothelial migration; Th, T-helper; TJ, tight junctions; TrkB, Tropomyosin receptor kinase B; VCAM-1, vascular cell adhesion molecule 1; VEGF, vascular endothelial growth factor.

Conclusion: Following Aβ exposure, there exists reciprocal crosstalk between infiltrating peripheral cells and astrocytes that in turn affects not only endothelial function and thus BBB properties, but also neuronal behavior. Since astrocytes are the first cells that lymphocytes interact with and are among the principal players in neuroinflammation occurring in AD, understanding this crosstalk may disclose new potential targets of intervention in the treatment of neurodegeneration.

Keywords: BBB, Th2, IL-4, BDNF, synaptophysin, neurodegeneration, neuroinflammation, Alzheimer's disease

INTRODUCTION

Alzheimer's disease (AD) is a neurodegenerative disorder whose typical pathological hallmarks are β-amyloid (Aβ) plaques and neurofibrillary tangles. The neuronal degeneration that characterizes the disease is associated with microgliosis and astrocytosis, causing an inflammatory state that has been described in the brain of AD patients. Peripheral inflammation can affect the central nervous system (CNS) and increased infiltration of immune cells in the brain of AD patients and corresponding animal models has been reported (Togo et al., 2002; Michaud et al., 2013; Zenaro et al., 2015). Also, in particular in AD patients, changes in the distribution of monocytes and lymphocytes as well as cytokines production have been described (Pellicano et al., 2012; Zhang et al., 2013). Enhanced blood-brain barrier (BBB) leakage and endothelial overexpression of adhesion molecules (such as vascular cell adhesion molecule 1, VCAM-1, and intercellular adhesion molecule-1, ICAM-1) induce leukocytes migration into the CNS close to Aβ plaques (Zenaro et al., 2015). Above the others, migration of both CD4+ and CD8+ T cells into the CNS of AD patients is significantly increased and observed mainly in areas that are typically affected in AD (Togo et al., 2002). However, the role of T cells, once they migrate through the BBB, is still not completely clarified. CD4+ subsets may differently influence CNS responses. T-helper (Th)1 and Th17 infiltration causes increased microglial activation and Aβ load (Browne et al., 2013) and enhanced neuronal degeneration through the release of specific interleukins (IL-1β, -6, -17, -21 and -22; Zhang et al., 2013). In contrast, Th2, that above the others, release factors like IL-4, IL-10 and brain-derived neurotrophic factor (BDNF; Eremenko et al., 2019), associate with decreased pathological exacerbation (Cao et al., 2009) and reduce glial response to inflammatory cytokines (McQuillan et al., 2010).

Astrocytes support neurons, but their involvement in CNS immunity has been underestimated. For their physical association with endothelial cells at the BBB, they are indeed the first cell type facing infiltrating cells (Iadecola and Nedergaard, 2007). They are directly involved in innate CNS immunity (Farina et al., 2007), but their ability to prime T cells seems relatively weak if compared to dendritic cells or microglia (McQuillan et al., 2010). Astrocytes further support endothelial cells function at the BBB, physically and through the release of several factors, including growth factors, such as vascular endothelial growth factor (VEGF), and inflammatory interleukins (IL-1β and IL-6) that may modulate the response of the barrier both in physiological and pathological conditions (Spampinato et al., 2019a).

Starting from the interaction between T cells and astrocytes, the aim of our study was then to analyze, in an *in vitro* system based on independent cellular cultures, the reciprocal interplay among infiltrating peripheral T cells, CNS resident cells, including astrocytes and neurons, and endothelial cells and to establish whether this crosstalk can be modified when the different cell types are exposed to Aβ.

MATERIALS AND METHODS

Reagent

All cell culture plastics were from BD Falcon. Polycarbonate membrane transwell inserts (0.4, μm pores, no. 353090 and 8 μm pores no. 3422), collagen I rat tail (no. 354236) and lymphocyte separation medium (no. 25-072-cv) were provided by Corning. β-amyloid 1–42 peptide (Aβ; Innovagen, no. SP-BA42-1) was solubilized in dimethylsulfoxide as a 5 mM stock solution. Subsequent dilutions were made in the medium. A concentrated solution of Aβ 100 μM was aggregated by overnight incubation at room temperature, followed by freeze-thaw cycles for enrichment in oligomers, as previously described (Merlo and Sortino, 2012). For experiments, Aβ (1–42) was diluted in culture medium to a final concentration of 2.5 μM. The state of oligomerization of the peptide was evaluated by western blot analysis showing a mixture of monomers, dimers, tetramers, and different size oligomers, as previously shown (Merlo and Sortino, 2012). Human recombinant brain-derived neurotrophic factor (BDNF, no. 450-02) and human recombinant interleukin 4 (IL-4, no. 200-04) were from Peprotech Inc. The selective TrkB antagonist ANA-12 was provided by Sigma-Aldrich (no. 5063040001).

Cell Cultures

TY-10 cells, brain microvascular endothelial cells, and hAST, astrocytic cells, are adult human immortalized cell lines, transfected with a plasmid expressing temperature-sensitive Simian virus-40 large T-antigen (ts-SV40-LT) and the catalytic subunit of human telomerase, as previously described (Haruki et al., 2013). Both cell lines were developed at Yamaguchi University (Japan), in the labs of Dr. Sano and Kanda. TY-10 cells were grown in MCDB-131 media (Sigma–Aldrich, no.

10372019) supplemented with EGM-2 SingleQuots (Lonza, no. LOCC4176) and 20% heat-inactivated fetal bovine serum (FBS, Thermo Fisher Scientific). hAST were grown in astrocyte medium containing 2% heat-inactivated FBS, astrocyte growth supplement, and penicillin/streptomycin (P/S) solution, as provided with the Astrocyte media kit (ScienCell Research Laboratories, no. 1801-SC). For experiments, both TY-10 and hAST cells were grown at 33°C for 2 days and then transferred to 37°C, where they exhibited growth arrest and differentiation. After differentiation for 2 days at 37°C, cells were exposed to Aβ. The continuous human neuroblastoma cell line, SH-SY5Y cells, were grown in DMEM/F12 medium (ThermoFisher Scientific, no. 21331-020) supplemented with 10% FBS and P/S. The amount of serum in the medium was progressively reduced to 1% to allow differentiation. The protocol here described was set in our lab and lasted 5 DIV. Gradual serum reduction induced cell cycle arrest and neuronal differentiation. The reduction of neuronal-like cell proliferation in these conditions was confirmed by cytofluorometric analysis of cell cycle distribution following propidium iodide incorporation, as previously demonstrated (Merlo et al., 2018). Experiments were performed in DMEM/F12 supplemented with 1% FBS. Peripheral blood mononuclear cells (PBMCs) were isolated from fresh heparinized blood of healthy subjects by density centrifugation with Lymphocyte Separation Medium (Corning, Thermo Fisher Scientific), as previously described (Man et al., 2008). Blood was from de-identified subjects donating to the Hospital blood bank for transfusion purposes. This exempted the study from Ethics Committee authorization. We used buffy coats derived from six healthy donors for the transmigration assay, from eight healthy donors to evaluate CD4 polarization and from seven healthy donors for CD4/SH-SY5Y co-cultures. For the transmigration assay, PBMCs were resuspended in transendothelial migration (TEM) buffer (RPMI 1640 without phenol red, 1% bovine serum albumin, Hepes, L-glutamine, Na-pyruvate, MEM non-essential amino acids, all from Thermo Fisher Scientific). CD4+ cells were negatively selected using the $CD4^+$ T Cell Isolation Kit (MiltenyiBiotec, no. 130-096-533) and grown in phenol red-free RPMI medium supplemented with FBS 10%, glutamine and non-essential amino acids, either alone or in co-culture with astrocytes.

Co-cultures of Astrocytes and CD4+ Cells and SH-SY5Y Cells and CD4+ Cells

Co-cultures were set on culture transwell inserts, allowing the passage of cytokines and growth factors, but no direct physical contact between different cell lines. Astrocytes (3×10^5 cells per wells) were plated on six multiwell dish plates, grown in astrocyte medium for 2 days at 33°C, and then kept for 2 days at 37°C. Aβ (2.5 μM) treatment was performed in astrocyte medium for 5 h at 37°C, the time point we chose to induce an early astrocytic response to Aβ, as already observed (Spampinato et al., 2019b). CD4+ cells (1×10^6 cells per wells) were transferred on culture transwell inserts with 0.4 μm pore (Falcon). At the time of co-culture, the ratio astrocytes/CD4 was 1:2. Co-cultures were maintained for 18/48 h, according to different experimental settings, grown in phenol red-free RPMI medium supplemented with 10% FBS, glutamine and non-essential amino acids (all from Thermo Fisher Scientific). To evaluate variations in mRNA levels, CD4+ cells and astrocytes co-cultured for 18 h were collected and pellets were processed for RT-PCR analysis. After 48 h in co-culture, a longer time point chosen to evaluate cytokine expression, CD4+ cells were collected and counted and an aliquot was fixed and processed for flow cytometry. Remaining cells were co-cultured with SH-SY5Y neuronal-like cells as follows. SH-SY5Y (4.5×10^5 cells per wells) were plated on 12 multiwell dish plates and progressively deprived of serum to allow differentiation. After 5 DIV, CD4+ cells (1.5×10^6 cells per wells) were transferred on culture transwell inserts with 0.4 μm pore, and the ratio between SH-SY5Y/CD4 at the time of co-culture was 1:2,5. Co-cultures were exposed to Aβ (2.5 μM) for 24 h, and then SH-SY5Y cells were processed for western blot analysis.

Migration Assay

The protocol for static transmigration assay has been previously described (Spampinato et al., 2019b). For the static transmigration assay, 6.5 mm polycarbonate membrane cell culture inserts with 8.0 μm *pore* (Corning® Transwell®) were used. hAST (3×10^5 cells per wells) were seeded on the abluminal side of the membrane, and after attachment, inserts were flipped and TY-10 (5×10^5 per membrane, with a ratio astrocytes/endothelial cells of 1:1,6), seeded on the luminal side. This setting allowed the passage of soluble factors between endothelial cells and astrocytes layer, but not their direct physical contact. Co-cultures were grown in astrocyte medium for 2 days at 33°C and then kept for 2 days at 37°C. Aβ (2.5 μM) treatment was performed in astrocyte medium for 18 h at 37°C, a time point at which Aβ exposure induces PBMCs migration through the endothelial barrier (Spampinato et al., 2019b). At this time point, the ratio astrocytes/endothelial cells was 1:1,7. Before the assay, the apical endothelial layer was exposed to CXCL12 (50 ng/ml in TEM buffer, Peprotech, no. 300-28A) and incubated for 15 min at 37°C. FBS 1% was used as chemoattractant in the abluminal side. PBMCs (2.8×10^6 cells per assay, with a ratio of endothelial cells/ PBMCs of 1:3, six at the time of co-culture) were added on the top of the endothelial layer. The assay was ended after a total of 18 h. Migrated PBMCs were recovered from the bottom chamber and counted.

Western Blot

After treatments, pellets were collected and lysed in RIPA lysis buffer (Sigma-Aldrich, no. R0278) supplemented with protease and phosphatase inhibitors. Thirty micrograms of each sample were separated by sodium dodecyl sulfate page and transferred to nitrocellulose membranes. Membranes were blocked with Blocker™ FL Fluorescent Blocking Buffer (Thermo Fisher Scientific, no. 37565) and probed with the following primary antibodies overnight: anti-rabbit Claudin-5 (1:300; Thermo Fisher Scientific, no. 34-1600), anti-mouse ICAM-1 (1:800; Santa Cruz Biotechnology, no. SC-8439), anti-mouse GAPDH (1:800;

Millipore, no. MAB 374); anti-mouse synaptophysin (1:5,000, Santa Cruz Biotechnology no. SC-17750). Membranes were then processed for immunodetection using specific fluorescent AlexaFluor® 647 and AlexaFluor® 488 Plus-conjugated secondary antibodies. Fluorescent signals were detected using IBright 1500 (Thermo Fisher Scientific). Band intensity was analyzed using the image processing software "ImageJ" developed by NIH and in the public domain.

Flow Cytometry

CD4+ cells were either cultured alone and exposed to Aβ 2.5 μm for 48 h or co-cultured for 48 h with astrocytes previously exposed to Aβ for 5 h. Both CD4+ cells and astrocytes were then collected and fixed using the Inside stain kit (Miltenyi Biotec, no. 130-090-477), following the manufacturer protocols and stained using either anti-human IL4-phycoerythrin (PE) antibody (1 h at RT, 1:50 Miltenyi Biotec, no. 130-091-647) or mouse anti-human interferon (IFN)-γ (overnight at 4°C, 1:120, Thermo Fisher Scientific no. 710287), followed by staining with the secondary anti-mouse-PE antibody (1:500, 1 h at RT). The samples were examined using Amnis® ImageStream® (Millipore), and data were analyzed using the Amnis Ideas® software.

Quantitative Real-Time Polymerase Chain Reaction (PCR)

CD4+ cells were either cultured alone and exposed to Aβ 2.5 μm or co-cultured for 18 h with astrocytes previously exposed to Aβ for 5 h. Both CD4+ cells and astrocytes were then collected and total RNA was extracted from cell cultures using the RNeasy Plus Mini Kit or Micro Kit (Qiagen, no. 74134). One microgram of RNA was used for cDNA synthesis, using the Superscript-VILO kit (Thermo Fisher Scientific). Quantitative RT-PCR was performed with Rotor-Gene Q using QuantiNova SYBR Green PCR Kit (Qiagen, no. 208054). The melting curves obtained after each PCR amplification reaction confirmed the specificity of the 2-[N-(3-dimethylaminopropyl)-N-propylamino]-4-[2,3-dihydro-3-methyl-(benzo-1,3-thiazol-2-yl)-methyli-dene]-1-phenyl-quinolinium (SYBR Green assays). The following Quantitec primers (Qiagen) were used: IL-6 (QT00083720), IL-1β (QT00021385), IL-4 (QT00012565), vascular endothelial growth factor (VEGF)-A (QT01010184) and human RPLP0 (QT00075012) as an endogenous control. Expression fold changes were calculated by applying the $2^{-\Delta Ct}$ method.

Statistical Analysis

All data are expressed as means ± SEM of 3–10 different experiments each run in duplicates or triplicates as specified in the figure legends. Intra assay variability was always less than 5%. Data were analyzed by one-way ANOVA, followed by Newman–Keuls test for significance. $p < 0.05$ was taken as the criterion for statistical significance when three or more conditions were compared. Student's *t*-test was applied between two groups. $p < 0.05$ was taken as the criterion for statistical significance.

RESULTS

CD4+ Cells Cross the BBB in Response to Aβ

Endothelial/astrocyte co-cultures were exposed to Aβ 2.5 μM for 18 h. Freshly isolated PBMCs from healthy donors were used to evaluate the capability of PBMCs to migrate through the *in vitro* BBB model. PBMCs migration rate through the barrier was significantly induced after 18 h of Aβ exposure (**Figure 1A**); this effect was accompanied by endothelial overexpression of the lower MW ICAM-1 glycoform (75 kDa), tightly involved in TEM (Spampinato et al., 2019b), as shown by western blot analysis on endothelial extracts (**Figure 1B**). At the end of the assay, PBMCs migrated through the *in vitro* barrier were recovered, enumerated, and analyzed by flow cytometry to evaluate their cellular subsets. Compared to PBMCs not subjected to the assay and maintained under the same conditions (input), the population of migrated cells was enriched in the percentage of CD3+ cells (**Figure 1C**). About 50% (53.5 ± 2.8%) of the migrated CD3+ population was represented by CD4+ cells, suggesting, as a consequence, a slight enrichment in the population of CD4+ cells crossing the *in vitro* barrier. However, direct analysis of the CD4+ cells within the CD3+ population showed only a trend toward an increase, without yielding statistical significance (**Figure 1D**).

Aβ Through Astrocytes Modifies CD4+ Cell Polarization

CD4+ cells were isolated from freshly prepared PBMCs and co-cultured with either control astrocytes (ACctr) or astrocytes primed with Aβ for 5 h (2.5 μM, ACAβ). The 5 h pretreatment time and the Aβ concentration were chosen since, in our experience, responses to Aβ are already measurable at these conditions, without affecting endothelial and astrocytic viability (Spampinato et al., 2019b). Astrocytes/CD4+ co-cultures were maintained for 48 h. Simultaneously, CD4+ cells were directly exposed to Aβ (2.5 μM). At the end of the incubation, CD4+ cells were collected and counted before being fixed and processed for flow cytometry. The 48 h time point was chosen because, according to preliminary data (not shown), a 24 h astrocytes/CD4 co-culture was not sufficient to induce any modifications in the expression and storage of cytokines in CD4+ cells. Aβ exposure did not modify *per se* the total number of CD4+ cells (**Figure 2A**). However, when co-cultured with ACAβ, CD4+ cell number increased (**Figure 2B**). Once collected, CD4+ cells, directly exposed to Aβ (2.5 μM) or co-cultured with ACctr or ACAβ for 48 h, were processed for flow cytometry. The expression of specific markers for both Th1 and Th2 cells (IFNγ and IL-4, respectively) was evaluated. The expression of Foxp3+ cells in our system was very limited, thus Treg polarization was not evaluated. When directly exposed to Aβ, the percentage of CD4+ cells expressing IFNγ or IL-4 was not affected (**Figures 2C,D**, upper panels). In contrast, when CD4+ cells were co-cultured with Aβ-pretreated astrocytes (ACAβ), the percentage of IFNγ+ cells was reduced (**Figure 2C**, lower panel) and accordingly, the percentage of IL-4+ cells significantly increased (**Figure 2D**

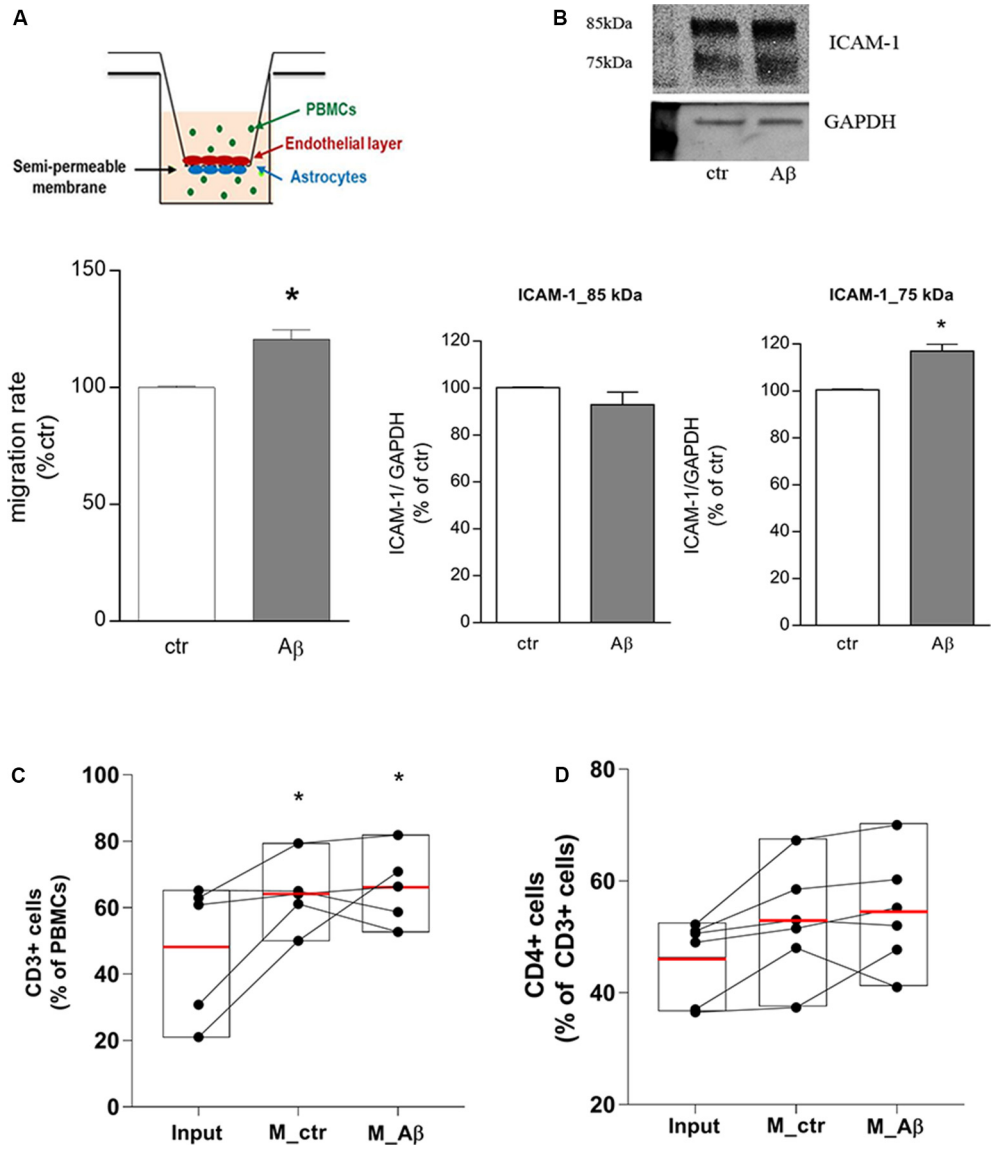

FIGURE 1 | Aβ induces CD3+/CD4+ cells transmigration through an *in vitro* blood-brain barrier (BBB) model. Endothelial/astrocytes co-cultures were exposed to Aβ (2.5 μM) for 18 h and the number of PBMCs migrating through the barrier was evaluated after an additional 18 h. PBMCs migration represents the ratio of migrated cells through the barrier, given a constant input, expressed as a percentage of migration in control conditions **(A)**. Protein expression of ICAM-1 in endothelial cells co-cultured with astrocytes and exposed to Aβ (2.5 μM) for 18 h was evaluated by western blot analysis. Densitometric analyses of the two isoform bands (85 and 75 kDa) and a representative blot are reported **(B)**. PBMCs migrated through the *in vitro* BBB were immunostained for the T cell co-receptor CD3 **(C)** and CD4 **(D)** and processed through flow cytometry analysis. Boxplots for total cells (input), cells migrated under control conditions (M_ctr), and cells migrated after treatment of astrocytes/endothelial cells with Aβ (2.5 μM) for 18 h (M_Aβ) are shown. Data are mean ± SEM of four **(A)** to six **(B–D)** independent experiments. *$p < 0.05$ vs. control, ctr **(A)** and input **(C)**. Significance was assessed by Student's *t*-test **(A,B)** and by one-way ANOVA followed by Newman–Keuls test **(C,D)**.

lower panel). Representative plots of flow cytometric analysis are reported in **Figures 2E,F**.

CD4+ Cells Cultured With Aβ-Pretreated Astrocytes Modify the Expression of Synaptic Proteins

CD4+ cells, cultured for 48 h with either control astrocytes (CD4/ACctr) or Aβ-treated astrocytes (CD4/ACAβ), were then transferred on top of an insert and co-cultured with differentiated human neuronal-like SH-SY5Y cells. Co-cultures were exposed to Aβ (2.5 μM) for 24 h and neuronal damage was assessed by evaluating the expression of the presynaptic protein synaptophysin. As expected, the expression of synaptophysin was significantly reduced by 24 h treatment with Aβ (2.5 μM). This effect was not modified in the presence of CD4/ACctr (**Figure 3A**). In contrast, Aβ exposure affected only slightly the expression of synaptophysin when SH-SY5Y cells were

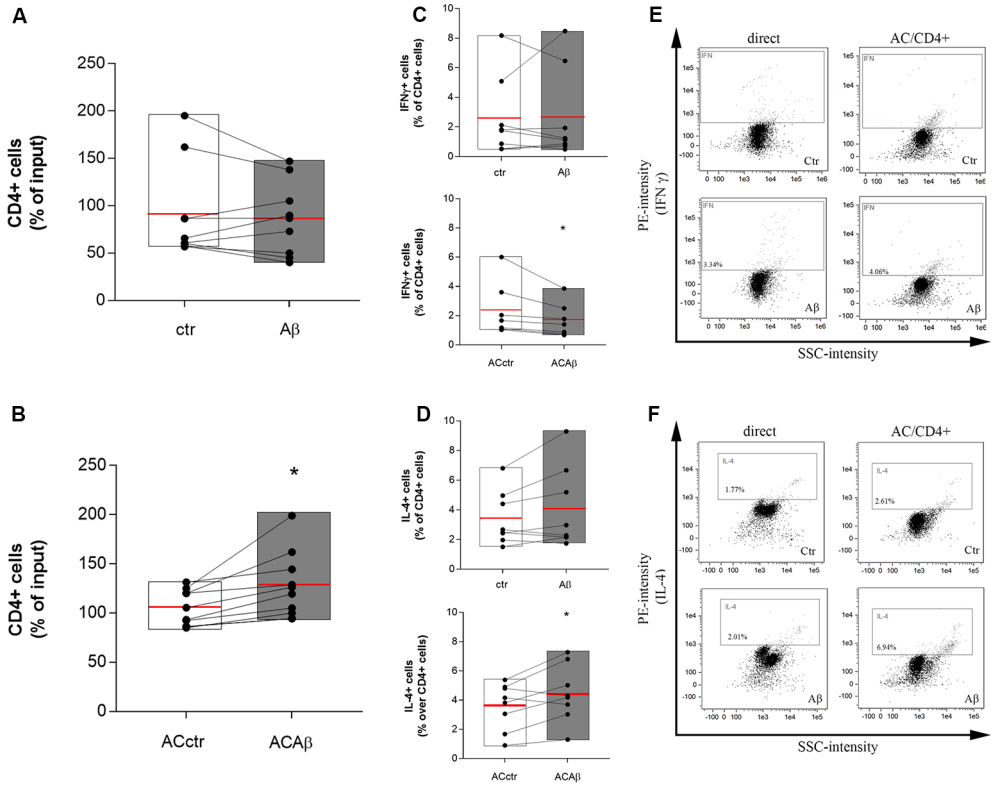

FIGURE 2 | Aβ treated astrocytes support CD4+ cell survival and skew their phenotype. CD4+ cells were exposed either directly to Aβ (2.5 μM) **(A)** or co-cultured with control (ACctr) or Aβ pre-exposed astrocytes (ACAβ) **(B)** for 48 h. After treatments, CD4+ cells were collected and enumerated. Given a constant input, values express the percentage of viable cells counted vs. the input. Through cytofluorometric analysis the expression of IFNγ **(C,E)** and IL-4 **(D,F)** was evaluated in CD4+ cells exposed either directly to Aβ (2.5 μM, **C,D**, upper panels) or to control (ACctr) or Aβ-pretreated astrocytes (ACAβ; **C,D**, lower panels) for 48 h. Representative plots of flow cytometric analysis for IFNγ **(E)** and IL-4 **(F)** are reported. Data are mean ± SEM of six **(A,B)** or eight **(C,D)** independent experiments. *$p < 0.05$ vs control (ctr) Significance was assessed by Student's *t*-test.

co-cultured with CD4+ cells polarized in the presence of Aβ-pretreated astrocytes (CD4/ACAβ, **Figure 3A**). To establish whether the observed effects on expression of the synaptic protein were due to changes of CD4+ cells, we investigated their expression of IL-4 and BDNF. When co-cultured for 18 h with Aβ-pretreated astrocytes (ACAβ), IL-4 and BDNF mRNA levels were significantly increased in CD4+ cells compared to those cultured in the presence of control astrocytes (ACctr). No changes of IL-4 and BDNF mRNA levels were observed when CD4+ cells were directly exposed to Aβ, whereas they were significantly increased in the presence of Aβ-pretreated astrocytes (ACAβ, **Figure 3B**). To ascertain whether BDNF and IL-4 could indeed affect neuronal response to Aβ, we treated SH-SY5Y cells in the presence of exogenously added IL-4 (10 ng/ml) and BDNF (10 ng/ml) for 24 h and analyzed the expression of synaptophysin. Both treatments prevented the reduced expression of synaptophysin induced by Aβ (**Figure 3C**).

Interestingly, prevention of Aβ-induced synaptophysin reduction in the presence of CD4/ACAβ was not observed any more on SH-SY5Y cells treated with the BDNF receptor TrkB selective antagonist ANA-12, known to counteract, *in vitro*, BDNF functions at the concentration of 20 μM (Merlo et al., 2018, **Figure 3D**). In contrast, when added directly to SH-SY5Y cells, ANA-12 did not modify Aβ effects on synaptophysin expression (**Figure 3D**).

CD4+ Cells Interfere With Cytokine Expression in Astrocytes and Modify BBB Function

We then evaluated whether and how CD4+ cells affected astrocytic response to Aβ. Gene expression of inflammatory cytokines (IL-1β and IL-6) was investigated in astrocytes pre-exposed to Aβ for 5 h and then cultured either alone (AC) or in the presence of CD4+ cells (AC/CD4) for further 18 h. Aβ induced enhanced expression of both IL-6 and IL-1β, as measured by RT-PCR, an effect prevented by pre-exposure to Aβ followed by co-culture with CD4+ cells (AC/CD4, **Figures 4A,B**). Also, under the same conditions, Aβ failed to induce enhanced VEGF expression in astrocytes co-cultured with CD4+ (**Figure 4C**). Astrocytes previously exposed to Aβ for 5 h and then cultured either alone or in the presence of CD4+ (AC/CD4) for 48 h, were co-cultured with endothelial cells and exposed to 2.5 μM Aβ for 24 h.

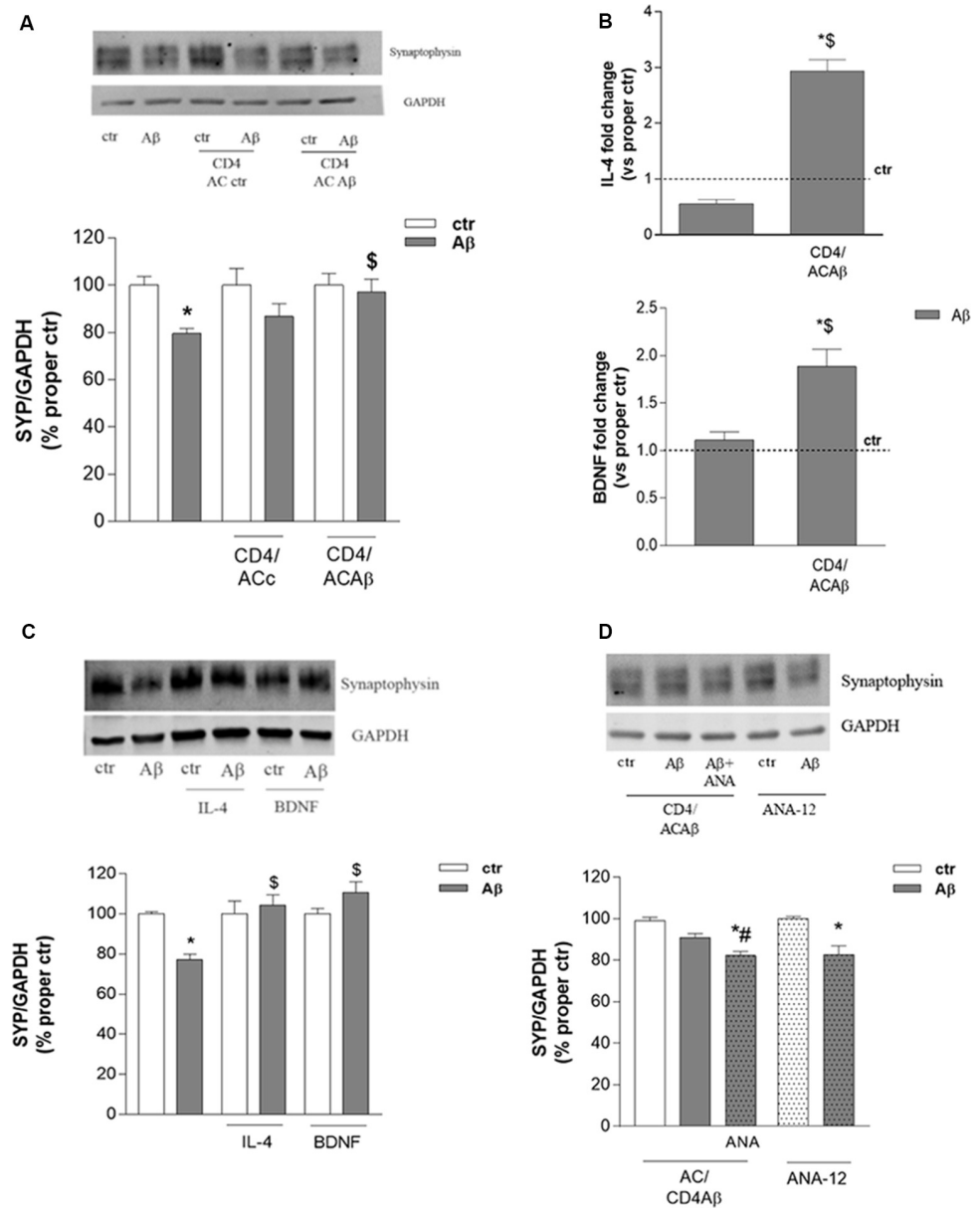

FIGURE 3 | CD4+ cells co-cultured with Aβ-treated astrocytes express BDNF and prevent Aβ-induced changes in synaptic protein expression. The expression of the synaptic protein synaptophysin was evaluated by western blot in SH-SY5Y cells treated with Aβ (2.5 μM) for 24 h either alone or in the presence of CD4+ cells previously co-cultured with astrocytes under control (ACctr) or Aβ-treated conditions **(A)**. IL-4 and BDNF mRNA levels were evaluated in CD4+ cells exposed to Aβ (2.5 μM) either directly or in co-culture with astrocytes (CD4/ACAβ) for 18 h **(B)**. Data are reported as fold change vs. proper control. Expression of synaptophysin in SH-SY5Y cells treated with Aβ (2.5 μM) alone or in co-treatment with IL-4 (10 ng/ml) and BDNF (10 ng/ml) are reported in **(C)**. Expression of synaptophysin under conditions described in A in the presence of the TrkB antagonist ANA-12 (20 μM) added 30 min before Aβ (2.5 μM, 24 h; CD4/ACAβ) **(D)**. Representative blots are reported in **(A,C,D)**. Data are mean ± SEM of six **(A)**, four **(C)**, and three **(B,D)** independent experiments. $^{*}p < 0.05$ vs. control, ctr. $^{\$}p < 0.05$ vs. direct Aβ. $^{\#}p < 0.05$ vs. Aβ alone. Significance was assessed by one-way ANOVA followed by Newman–Keuls test.

Endothelial expression of claudin-5 and ICAM-1 was evaluated by western blot analysis. Aβ reduced claudin-5 expression, but this effect was prevented in endothelial cells co-cultured with AC/CD4 (**Figure 4D**). Modifications in ICAM-1 expression were observed only for the lower MW glycoform of the protein. In particular, ICAM-1 (75 kDa) was induced in endothelial/astrocytes co-cultures exposed to Aβ for 24 h, but not when astrocytes were previously exposed to CD4+ cells (**Figure 4E**).

DISCUSSION

During AD, in particular in the late stages of the disease, the BBB can be severely damaged, and thus the access to

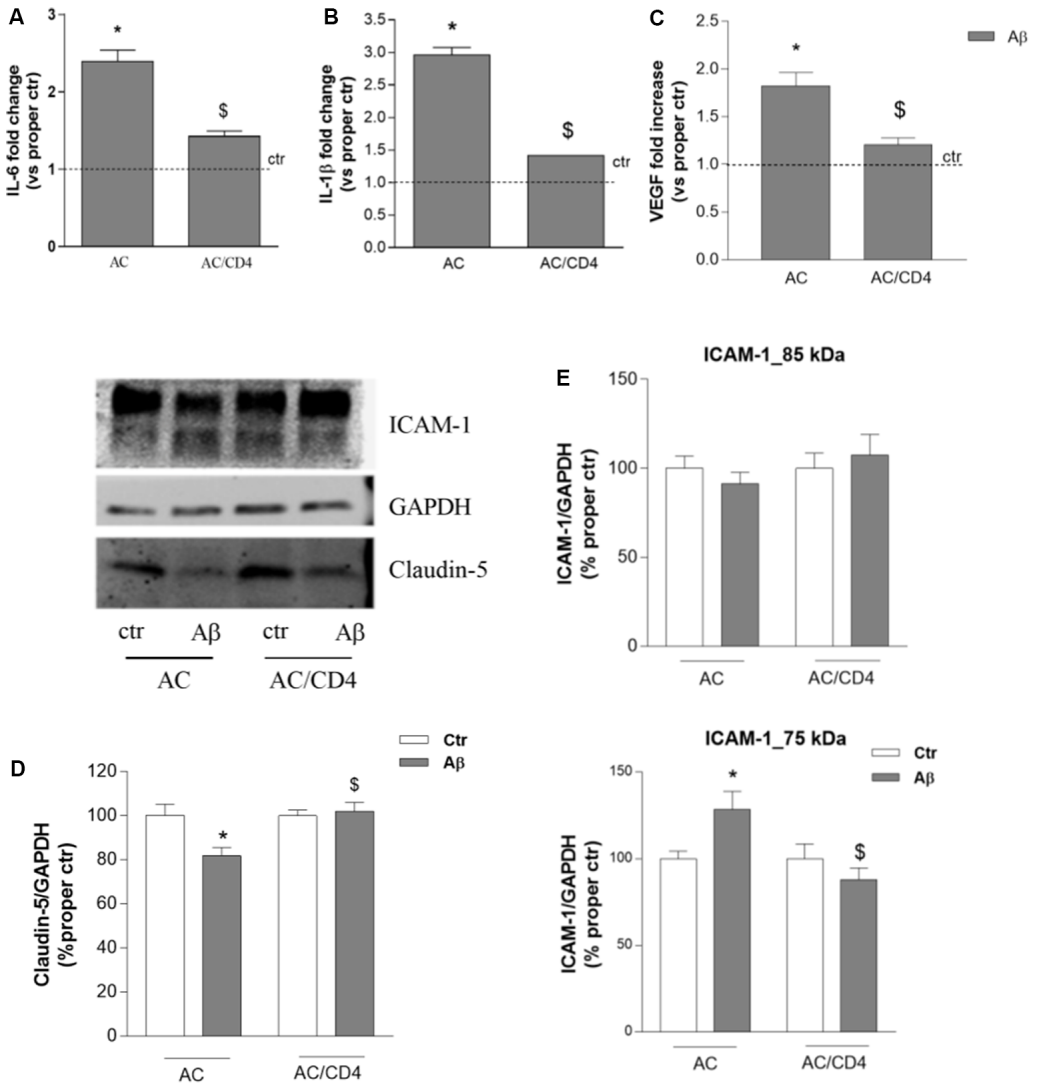

FIGURE 4 | CD4+ cells modulate astrocyte ability to affect endothelial properties. Astrocytes (AC) were pre-exposed to Aβ (2.5 μM) for 5 h and then co-cultured with CD4+ cells (AC/CD4). Astrocytic mRNA levels of IL-6 **(A)**, IL-1β **(B)**, and VEGF **(C)** were evaluated by RT-PCR. Endothelial cells were co-cultured with naïve astrocytes (AC) or astrocytes co-cultured with CD4+ cells (AC/CD4) and treated with Aβ (2.5 μM) for 18 h. Protein expression of claudin-5 and ICAM-1 was evaluated by western blot analysis. A representative blot and densitometric analysis of claudin-5 **(D)** and the two ICAM-1 isoforms (85 and 75 kDa) are reported **(E)**. Data are mean ± SEM of three **(A–C)**, four **(D)**, and six **(E)** independent experiments. $^{*}p < 0.05$ vs. control, ctr. $^{\$}p < 0.05$ vs. the condition without CD4 (AC). Significance was assessed by one-way ANOVA followed by Newman–Keuls test.

the CNS of solutes and immune cells is altered. T cells in particular may easily cross the damaged BBB in these conditions. In the cerebrospinal fluid and the brain of AD patients, the proportion of CD4+ and CD8+ T cells is elevated (Laurent et al., 2017). Accordingly, increased levels of peripheral T cells have been described in postmortem brains from AD patients, as a consequence of damaged BBB and increased release of chemokines and cytokines by degenerating and activated cells in the CNS (Mietelska-Porowska and Wojda, 2017). Once they cross the BBB, T cells immediately reach the glia *limitans*, and herein they interact with astrocytes. It has been widely reported that microglia are the main resident cells in the CNS and they can thus act as potential antigen-presenting cells. Astrocytes also express major histocompatibility complex (MHCI and II) and under inflammatory challenge, they overexpress the co-stimulatory factors CD80 and CD86 (reviewed in Xie and Yang, 2015), although their ability to prime T cells seems relatively weak if compared to dendritic cells or microglia (McQuillan et al., 2010). However, the interaction between astrocytes and CD4+ cells is not exclusively dependent on the contact between astrocytic MHC/T cell receptors. Astrocytes release several cytokines and chemokines that can potentially modify T cell functions. We first noticed that when co-cultured with astrocytes and in particular with Aβ-pretreated astrocytes, CD4+ cell number increased. We have not investigated what

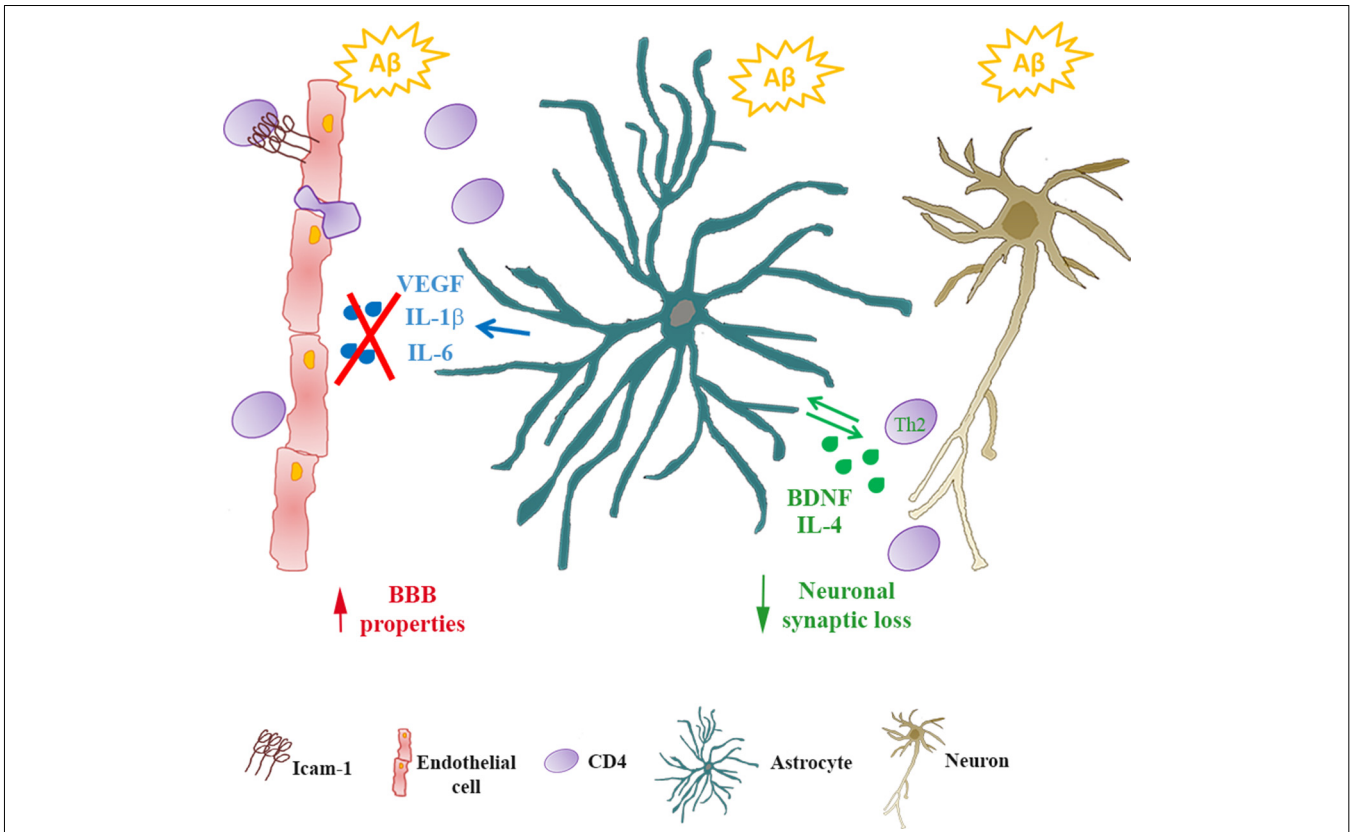

FIGURE 5 | Astrocytes/CD4+ reciprocal crosstalk. In Alzheimer's disease (AD), infiltrating CD4+ cells cross the BBB reaching the *glia limitans*. Through reciprocal crosstalk, Aβ-exposed astrocytes skew CD4+ towards a Th2 phenotype, inducing the production of IL-4 and BDNF. In the presence of BDNF, Aβ-induced synaptic loss in neurons is prevented. Conversely, in the presence of CD4+ cells, Aβ-exposed astrocytes reduce the release of inflammatory cytokines (IL-6 and IL-1β) and VEGF. As a consequence, endothelial properties at the BBB are preserved.

is at the basis of this effect, but it appears in accordance with what was previously observed in astrocytes/CD4 co-cultures, where glutamate released by astrocytes promoted CD4 cell division (Beurel et al., 2014).

CD4+ cells changed their response to Aβ when co-cultured with Aβ-pretreated astrocytes, as shown by reduced and increased levels of IFNγ and IL-4, respectively. Of note, only these CD4+ cells prevented the loss of neuronal synaptic function. When co-cultured with unstimulated astrocytes (ACctr), this effect was not observed, clearly indicating that Aβ modifies astrocytes which in turn affect CD4+ cells polarization toward a less inflammatory phenotype. Accordingly, it has been described that, when damage occurs in the CNS, astrocytes may stimulate the innate immune response skewing it towards the production of Th2 cytokines (Schmitz et al., 2005; Neill et al., 2010). In these conditions, the production of IL-4 is increased (Walsh et al., 2015), and infiltrating T cells appear to be the main source of this cytokine in the CNS, as both microglia and astrocytes release very low levels of IL-4 (Walsh et al., 2015). A protective role for IL-4 has been described in AD transgenic mice, where administration of this cytokine, in association with IL-13, improved cognitive function (Kiyota et al., 2010; Kawahara et al., 2012). Administration of amyloid-specific Th2 cells improved spatial memory, decreased microglial reactivity and reduced Aβ pathology in AD animal models (Cao et al., 2009), pointing out the role played by IL4-producing cells in reducing AD damage. Higher peripheral IL-4 concentration was found in MCI patients whereas increased disease severity seemed to be associated with reduced IL-4 levels (King et al., 2018). Finally, interacting with the neuronal IL-4 receptor, IL-4 could mediate a protective function (Steinman, 2015; Walsh et al., 2015), inducing actin modifications and axonal sprouting, as observed in experimental autoimmune encephalomyelitis (EAE) models (Vogelaar et al., 2018).

Together with the increased production of IL-4, CD4+ cells co-cultured with Aβ-pretreated astrocytes showed also an enhanced expression of BDNF. We did not measure IL-4 and BDNF released by astrocytes, but the increase of BDNF mRNA expression was remarkable and suggestive of an enhanced release, as previously described (Kerschensteiner et al., 1999). As for IL-4, the increase of its mRNA expression was paralleled by enhanced intracellular content as by flow cytometric analysis. We focused our attention on BDNF, a known regulator of the expression, function and localization of presynaptic protein synaptophysin, as our

marker of choice to evaluate neuronal damage (Tartaglia et al., 2001; Bamji et al., 2006; Zhang et al., 2017). Of note, partial preservation of pre-synaptic function observed with CD4+ cells pre-exposed to Aβ-treated astrocytes was blunted, at least in part, under conditions of a blockade of the BDNF receptor TrkB, confirming the main role for the growth factor in the observed effect. This is not surprising since the role of BDNF in preserving neuronal function is largely proved. Increased BDNF serum levels are associated with reduced cognitive decline (Laske et al., 2011), while BDNF therapy results in increased synaptic efficiency and plasticity (Murer et al., 2001; Nagahara et al., 2009; Budni et al., 2015) and increased neuronal survival (Arancibia et al., 2008). What probably appears unexpected is that CD4+ cells are the main source of BDNF. However, supportive data emerge from studies in which CD4+ cells overexpressing BDNF were injected ICV in 5XFAD mice, resulting in increased neuronal viability and synaptic rescue (Eremenko et al., 2019). Further, BDNF serum levels are increased in preclinical stages of AD (Angelucci et al., 2010; Laske et al., 2011), when compensatory mechanisms are initiated in the attempt to prevent neuronal degeneration (Merlo et al., 2019), and in PBMCs derived from MCI patients, when exposed *ex vivo* to Aβ include CD4+ cells with higher levels of BDNF in comparison to PBMCs derived from AD patients (Baglio et al., 2013).

The crosstalk appears reciprocal since not only astrocytes are capable to modify CD4+ cell functions, but also CD4+ cells modulate astrocytes by reducing their inflammatory response to Aβ, as shown by decreased expression of inflammatory cytokines IL-6 and IL-1β. The role played by astrocytes in the CNS is pleiotropic, as they can support neuronal activity as well as modulate BBB functions in healthy and pathological conditions (Spampinato et al., 2019a). Here, we wondered whether, after their interaction with CD4+ cells, astrocytes may differently affect endothelial properties. This happened to be the case since Aβ failed to induce the reported VEGF up-regulation in astrocytes (Spampinato et al., 2017) in the presence of CD4+ cells. We have previously shown that acting on endothelial cells, astrocytic derived VEGF induces endothelial expression and activity of matrix metalloproteinase (MMP)-9 and subsequent reduction of one of its substrates, the junctional protein claudin-5 (Spampinato et al., 2017). Accordingly, in our study, following exposure of astrocytes to CD4+ cells, we did not detect any change in endothelial claudin-5 expression, thus reinforcing the hypothesis that astrocytic response to Aβ is modified in the presence of CD4+ cells.

Finally, it was established that astrocytes modify the expression of endothelial ICAM-1. In particular, we have previously demonstrated that ICAM-1 is expressed in two different glycoforms, depending on the glycosylation status, and astrocytes in response to Aβ induce the high mannose, low molecular weight, ICAM-1 glycoform (Spampinato et al., 2019b) that is involved in increased migration through the endothelial layer at the BBB (Chacko et al., 2011; Scott et al., 2012). This effect appeared dampened when astrocytes were co-cultured with CD4+ cells, suggesting a series of events by which migrated lymphocytes, after their interaction with astrocytes, can induce changes in BBB function, promoting a negative control mechanism that limits their transmigration through the BBB. Although very speculative, this interpretation let us conclude that initial migration of CD4+ cells through the damaged BBB in AD may trigger, through astrocytes, an auto-limiting outcome that plays as a preventing mechanism to limit further peripheral cell infiltration.

Data here reported have been observed in *in vitro* models, that only partially represent the complexity of the *in vivo* system. For example, in our experimental setting, we did not take into account the differences between naïve and memory T cells that are known to differ in phenotype, the pattern of migration, responsiveness to antigen and cytokines (Pennock et al., 2013). Although these limitations and the consequent attention that should be used when transferring observations *in vitro* to human pathology, the use of the *in vitro* setting allowed us to analyze the reciprocal crosstalk among peripheral cells, cellular components of the BBB and neurons under conditions of exposure to Aβ. We confirmed that astrocytes, at least in the early phases of AD disease, play a central role in this interaction as they can modify endothelial properties as well as CD4+ cell phenotype and features (**Figure 5**). As a result, neurons appeared less vulnerable to the effects of Aβ. CD4+ cells, on their side, modified the ability of astrocytes to affect endothelial properties in response to Aβ implying a potential protective effect on the function of the BBB itself.

DATA AVAILABILITY STATEMENT

All datasets presented in this study are included in the article.

AUTHOR CONTRIBUTIONS

All authors gave a significant contribution to the study. SS participated in the study conception and design, carried out the experimental part, and wrote the manuscript. MF and EF participated in selected experimental procedures. YS and TK established and provided the human astrocytic and endothelial cell lines. SM contributed to the interpretation of data and critically revised the manuscript. MS participated in study conception, acquired funding, and reviewed the manuscript.

FUNDING

This study was supported by intramural research funding (Università di Catania; 20130143075) and in part by PRIN17 (Ministero dell'Istruzione, dell'Università e della Ricerca; 2017XZ7A37_004) both to MS. The initial part of this study was done also thanks to a SIF/MSD fellowship 2017 to SS.

REFERENCES

Angelucci, F., Spalletta, G., di Iulio, F., Ciaramella, A., Salani, F., Colantoni, L., et al. (2010). Alzheimer's disease (AD) and Mild Cognitive Impairment (MCI) patients are characterized by increased BDNF serum levels. *Curr. Alzheimer Res.* 7, 15–20. doi: 10.2174/156720510790274473

Arancibia, S., Silhol, M., Moulière, F., Meffre, J., Höllinger, I., Maurice, T., et al. (2008). Protective effect of BDNF against β-amyloid induced neurotoxicity *in vitro* and *in vivo* in rats. *Neurobiol. Dis.* 31, 316–326. doi: 10.1016/j.nbd.2008.05.012

Baglio, F., Saresella, M., Preti, M. G., Cabinio, M., Griffanti, L., Marventano, I., et al. (2013). Neuroinflammation and brain functional disconnection in Alzheimer's disease. *Front. Aging Neurosci.* 5:81. doi: 10.3389/fnagi.2013.00081

Bamji, S. X., Rico, B., Kimes, N., and Reichardt, L. F. (2006). BDNF mobilizes synaptic vesicles and enhances synapse formation by disrupting cadherin-β-catenin interactions. *J. Cell Biol.* 174, 289–299. doi: 10.1083/jcb.200601087

Beurel, E., Harrington, L. E., Buchser, W., Lemmon, V., and Jope, R. S. (2014). Astrocytes modulate the polarization of $CD4^+$ T cells to Th1 cells. *PLoS One* 9:e86257. doi: 10.1371/journal.pone.0086257

Browne, T. C., McQuillan, K., McManus, R. M., O'Reilly, J. A., Mills, K. H., and Lynch, M. A. (2013). IFN-γ Production by amyloid β-specific Th1 cells promotes microglial activation and increases plaque burden in a mouse model of Alzheimer's disease. *J. Immunol.* 190, 2241–2251. doi: 10.4049/jimmunol.1200947

Budni, J., Bellettini-Santos, T., Mina, F., Garcez, M. L., and Zugno, A. I. (2015). The involvement of BDNF, NGF and GDNF in aging and Alzheimer's disease. *Aging Dis.* 6, 331–341. doi: 10.14336/ad.2015.0825

Cao, C., Arendash, G. W., Dickson, A., Mamcarz, M. B., Lin, X., and Ethell, D. W. (2009). Aβ-specific Th2 cells provide cognitive and pathological benefits to Alzheimer's mice without infiltrating the CNS. *Neurobiol. Dis.* 34, 63–70. doi: 10.1016/j.nbd.2008.12.015

Chacko, B. K., Scott, D. W., Chandler, R. T., and Patel, R. P. (2011). Endothelial surface N-glycans mediate monocyte adhesion and are targets for anti-inflammatory effects of peroxisome proliferator-activated receptor γ ligands. *J. Biol. Chem.* 286, 38738–38747. doi: 10.1074/jbc.m111.247981

Eremenko, E., Mittal, K., Berner, O., Kamenetsky, N., Nemirovsky, A., Elyahu, Y., et al. (2019). BDNF-producing, amyloid β-specific CD4 T cells as targeted drug-delivery vehicles in Alzheimer's disease. *EBioMedicine* 43, 424–434. doi: 10.1016/j.ebiom.2019.04.019

Farina, C., Aloisi, F., and Meinl, E. (2007). Astrocytes are active players in cerebral innate immunity. *Trends Immunol.* 28, 138–145. doi: 10.1016/j.it.2007.01.005

Haruki, H., Sano, Y., Shimizu, F., Omoto, M., Tasaki, A., Oishi, M., et al. (2013). NMO sera down-regulate AQP4 in human astrocyte and induce cytotoxicity independent of complement. *J. Neurol. Sci.* 331, 136–144. doi: 10.1016/j.jns.2013.05.035

Iadecola, C., and Nedergaard, M. (2007). Glial regulation of the cerebral microvasculature. *Nat. Neurosci.* 10, 1369–1376. doi: 10.1038/nn2003

Kawahara, K., Suenobu, M., Yoshida, A., Koga, K., Hyodo, A., Ohtsuka, H., et al. (2012). Intracerebral microinjection of interleukin-4/interleukin-13 reduces β-amyloid accumulation in the ipsilateral side and improves cognitive deficits in young amyloid precursor protein 23 mice. *Neuroscience* 207, 243–260. doi: 10.1016/j.neuroscience.2012.01.049

Kerschensteiner, M., Gallmeier, E., Behrens, L., Leal, V. V., Misgeld, T., Klinkert, W. E., et al. (1999). Activated human T cells, B cells, and monocytes produce brain-derived neurotrophic factor *in vitro* and in inflammatory brain lesions: a neuroprotective role of inflammation? *J. Exp. Med.* 189, 865–870. doi: 10.1084/jem.189.5.865

King, E., O'Brien, J. T., Donaghy, P., Morris, C., Barnett, N., Olsen, K., et al. (2018). Peripheral inflammation in prodromal Alzheimer's and Lewy body dementias. *J. Neurol. Neurosurg. Psychiatry* 89, 339–345. doi: 10.1136/jnnp-2017-317134

Kiyota, T., Okuyama, S., Swan, R. J., Jacobsen, M. T., Gendelman, H. E., and Ikezu, T. (2010). CNS expression of anti-inflammatory cytokine interleukin-4 attenuates Alzheimer's disease-like pathogenesis in APP+PS1 bigenic mice. *FASEB J.* 24, 3093–3102. doi: 10.1096/fj.10-155317

Laske, C., Stellos, K., Hoffmann, N., Stransky, E., Straten, G., Eschweiler, G. W., et al. (2011). Higher BDNF serum levels predict slower cognitive decline in Alzheimer's disease patients. *Int. J. Neuropsychopharmacol.* 14, 399–404. doi: 10.1017/S1461145710001008

Laurent, C., Dorothée, G., Hunot, S., Martin, E., Monnet, Y., Duchamp, M., et al. (2017). Hippocampal T cell infiltration promotes neuroinflammation and cognitive decline in a mouse model of tauopathy. *Brain* 140, 184–200. doi: 10.1093/brain/aww270

Man, S., Ubogu, E. E., Williams, K. A., Tucky, B., Callahan, M. K., and Ransohoff, R. M. (2008). Human brain microvascular endothelial cells and umbilical vein endothelial cells differentially facilitate leukocyte recruitment and utilize chemokines for T cell migration. *Clin. Dev. Immunol.* 2008:384982. doi: 10.1155/2008/384982

McQuillan, K., Lynch, M. A., and Mills, K. H. (2010). Activation of mixed glia by Aβ-specific Th1 and Th17 cells and its regulation by Th2 cells. *Brain Behav. Immun.* 24, 598–607. doi: 10.1016/j.bbi.2010.01.003

Merlo, S., and Sortino, M. A. (2012). Estrogen activates matrix metalloproteinases-2 and -9 to increase β-amyloid degradation. *Mol. Cell. Neurosci.* 49, 423–429. doi: 10.1016/j.mcn.2012.02.005

Merlo, S., Spampinato, S. F., Beneventano, M., and Sortino, M. A. (2018). The contribution of microglia to early synaptic compensatory responses that precede β-amyloid-induced neuronal death. *Sci. Rep.* 8:7297. doi: 10.1038/s41598-018-25453-1

Merlo, S., Spampinato, S. F., and Sortino, M. A. (2019). Early compensatory responses against neuronal injury: a new therapeutic window of opportunity for Alzheimer's disease? *CNS Neurosci. Ther.* 25, 5–13. doi: 10.1111/cns.13050

Michaud, J. P., Bellavance, M. A., Préfontaine, P., and Rivest, S. (2013). Real-time *in vivo* imaging reveals the ability of monocytes to clear vascular amyloid β. *Cell Rep.* 5, 646–653. doi: 10.1016/j.celrep.2013.10.010

Mietelska-Porowska, A., and Wojda, U. (2017). T lymphocytes and inflammatory mediators in the interplay between brain and blood in Alzheimer's disease: potential pools of new biomarkers. *J. Immunol. Res.* 2017:4626540. doi: 10.1155/2017/4626540

Murer, M. G., Yan, Q., and Raisman-Vozari, R. (2001). Brain-derived neurotrophic factor in the control human brain and in Alzheimer's disease and Parkinson's disease. *Prog. Neurobiol.* 63, 71–124. doi: 10.1016/s0301-0082(00)00014-9

Nagahara, A. H., Merrill, D. A., Coppola, G., Tsukada, S., Schroeder, B. E., Shaked, G. M., et al. (2009). Neuroprotective effects of brain-derived neurotrophic factor in rodent and primate models of Alzheimer's disease. *Nat. Med.* 15, 331–337. doi: 10.1038/nm.1912

Neill, D. R., Wong, S. H., Bellosi, A., Flynn, R. J., Daly, M., Langford, T. K., et al. (2010). Nuocytes represent a new innate effector leukocyte that mediates type-2 immunity. *Nature* 464, 1367–1370. doi: 10.1038/nature08900

Pellicano, M., Larbi, A., Goldeck, D., Colonna-Romano, G., Buffa, S., Bulati, M., et al. (2012). Immune profiling of Alzheimer patients. *J. Neuroimmunol.* 242, 52–59. doi: 10.1016/j.jneuroim.2011.11.005

Pennock, N. D., White, J. T., Cross, E. W., Cheney, E. E., Tamburini, B. A., and Kedl, R. M. (2013). T cell responses: naive to memory and everything in between. *Adv. Physiol. Educ.* 37, 273–283. doi: 10.1152/advan.00066.2013

Schmitz, J., Owyang, A., Oldham, E., Song, Y., Murphy, E., McClanahan, T. K., et al. (2005). IL-33, an interleukin-1-like cytokine that signals *via* the IL-1 receptor-related protein ST2 and induces T helper type 2-associated cytokines. *Immunity* 23, 479–490. doi: 10.1016/j.immuni.2005.09.015

Scott, D. W., Chen, J., Chacko, B. K., Traylor, J. G. Jr., Orr, A. W., and Patel, R. P. (2012). Role of endothelial N-glycan mannose residues in monocyte recruitment during atherogenesis. *Arterioscler. Thromb. Vasc. Biol.* 32, e51–e59. doi: 10.1161/ATVBAHA.112.253203

Spampinato, S. F., Bortolotto, V., Canonico, P. L., Sortino, M. A., and Grilli, M. (2019a). Astrocyte-derived paracrine signals: relevance for neurogenic niche regulation and blood-brain barrier integrity. *Front. Pharmacol.* 10:1346. doi: 10.3389/fphar.2019.01346

Spampinato, S. F., Merlo, S., Fagone, E., Fruciano, M., Barbagallo, C., Kanda, T., et al. (2019b). Astrocytes modify migration of PBMCs induced by β-amyloid in a blood-brain barrier *in vitro* model. *Front. Cell. Neurosci.* 13:337. doi: 10.3389/fncel.2019.00337

Spampinato, S. F., Merlo, S., Sano, Y., Kanda, T., and Sortino, M. A. (2017). Astrocytes contribute to Aβ-induced blood-brain barrier damage through activation of endothelial MMP9. *J. Neurochem.* 142, 464–477. doi: 10.1111/jnc.14068

Steinman, L. (2015). Role reversal: infiltrating T cells protect the brain. *J. Clin. Invest.* 125, 493–494. doi: 10.1172/jci80279

Tartaglia, N., Du, J., Tyler, W. J., Neale, E., Pozzo-Miller, L., and Lu, B. (2001). Protein synthesis-dependent and -independent regulation of hippocampal synapses by brain-derived neurotrophic factor. *J. Biol. Chem.* 276, 37585–37593. doi: 10.1074/jbc.m101683200

Togo, T., Akiyama, H., Iseki, E., Kondo, H., Ikeda, K., Kato, M., et al. (2002). Occurrence of T cells in the brain of Alzheimer's disease and other neurological diseases. *J. Neuroimmunol.* 124, 83–92. doi: 10.1016/s0165-5728(01)00496-9

Vogelaar, C. F., Mandal, S., Lerch, S., Birkner, K., Birkenstock, J., Buhler, U., et al. (2018). Fast direct neuronal signaling *via* the IL-4 receptor as therapeutic target in neuroinflammation. *Sci. Transl. Med.* 10:eaao2304. doi: 10.1126/scitranslmed.aao2304

Walsh, J. T., Hendrix, S., Boato, F., Smirnov, I., Zheng, J., Lukens, J. R., et al. (2015). MHCII-independent $CD4^+$ T cells protect injured CNS neurons *via* IL-4. *J. Clin. Invest.* 125, 699–714. doi: 10.1172/JCI76210

Xie, L., and Yang, S. H. (2015). Interaction of astrocytes and T cells in physiological and pathological conditions. *Brain Res.* 1623, 63–73. doi: 10.1016/j.brainres.2015.03.026

Zenaro, E., Pietronigro, E., Della Bianca, V., Piacentino, G., Marongiu, L., Budui, S., et al. (2015). Neutrophils promote Alzheimer's disease-like pathology and cognitive decline *via* LFA-1 integrin. *Nat. Med.* 21, 880–886. doi: 10.1038/nm.3913

Zhang, J., Ke, K. F., Liu, Z., Qiu, Y. H., and Peng, Y. P. (2013). Th17 cell-mediated neuroinflammation is involved in neurodegeneration of aβ1–42-induced Alzheimer's disease model rats. *PLoS One* 8:e75786. doi: 10.1371/journal.pone.0075786

Zhang, R., Miller, R. G., Madison, C., Jin, X., Honrada, R., Harris, W., et al. (2013). Systemic immune system alterations in early stages of Alzheimer's disease. *J. Neuroimmunol.* 256, 38–42. doi: 10.1016/j.jneuroim.2013.01.002

Zhang, Y., Qiu, B., Wang, J., Yao, Y., Wang, C., and Liu, J. (2017). Effects of BDNF-transfected BMSCs on neural functional recovery and synaptophysin expression in rats with cerebral infarction. *Mol. Neurobiol.* 54, 3813–3824. doi: 10.1007/s12035-016-9946-7

Conflict of Interest: The authors declare that the research was conducted in the absence of any commercial or financial relationships that could be construed as a potential conflict of interest.

frontiers in Molecular Neuroscience

ORIGINAL RESEARCH
published: 02 November 2020
doi: 10.3389/fnmol.2020.552073

The Interplay Between Beta-Amyloid 1–42 ($A\beta_{1–42}$)-Induced Hippocampal Inflammatory Response, p-tau, Vascular Pathology, and Their Synergistic Contributions to Neuronal Death and Behavioral Deficits

*Beatriz Calvo-Flores Guzmán[1], Tessa Elizabeth Chaffey[1], Thulani Hansika Palpagama[1], Sarah Waters[1], Jordi Boix[2], Warren Perry Tate[3], Katie Peppercorn[3], Michael Dragunow[4], Henry John Waldvogel[1], Richard Lewis Maxwell Faull[1] and Andrea Kwakowsky[1]**

[1]Centre for Brain Research, Department of Anatomy and Medical Imaging, Faculty of Medical and Health Sciences, University of Auckland, Auckland, New Zealand, [2]Centre for Brain Research, NeuroDiscovery Behavioural Unit, Faculty of Medical and Health Sciences, University of Auckland, Auckland, New Zealand, [3]Department of Biochemistry, University of Otago, Dunedin, New Zealand, [4]Centre for Brain Research, Department of Pharmacology, Faculty of Medical and Health Sciences, University of Auckland, Auckland, New Zealand

OPEN ACCESS

Edited by:
Robert A. Nichols,
University of Hawaii at Manoa,
United States

Reviewed by:
Fernando Peña-Ortega,
National Autonomous University of Mexico, Mexico
Annakaisa Haapasalo,
University of Eastern Finland, Finland

***Correspondence:**
Andrea Kwakowsky
a.kwakowsky@auckland.ac.nz

Received: 15 April 2020
Accepted: 22 September 2020
Published: 02 November 2020

Citation:
Calvo-Flores Guzmán B, Chaffey TE, Palpagama TH, Waters S, Boix J, Tate WP, Peppercorn K, Dragunow M, Waldvogel HJ, Faull RLM and Kwakowsky A (2020) The Interplay Between Beta-Amyloid 1–42 ($A\beta_{1–42}$)-Induced Hippocampal Inflammatory Response, p-tau, Vascular Pathology, and Their Synergistic Contributions to Neuronal Death and Behavioral Deficits. Front. Mol. Neurosci. 13:552073. doi: 10.3389/fnmol.2020.552073

Alzheimer's disease (AD), the most common chronic neurodegenerative disorder, has complex neuropathology. The principal neuropathological hallmarks of the disease are the deposition of extracellular β-amyloid (Aβ) plaques and neurofibrillary tangles (NFTs) comprised of hyperphosphorylated tau (p-tau) protein. These changes occur with neuroinflammation, a compromised blood-brain barrier (BBB) integrity, and neuronal synaptic dysfunction, all of which ultimately lead to neuronal cell loss and cognitive deficits in AD. $A\beta_{1–42}$ was stereotaxically administered bilaterally into the CA1 region of the hippocampi of 18-month-old male C57BL/6 mice. This study aimed to characterize, utilizing immunohistochemistry and behavioral testing, the spatial and temporal effects of $A\beta_{1–42}$ on a broad set of parameters characteristic of AD: p-tau, neuroinflammation, vascular pathology, pyramidal cell survival, and behavior. Three days after $A\beta_{1–42}$ injection and

Abbreviations: Aβ, β-amyloid; ACSF, artificial cerebrospinal fluid; AD, Alzheimer's disease; BBB, blood-brain barrier; CA 1, cornu ammonis region 1; CX3CR1, CX3C chemokine receptor 1; DR, discrimination ratio; E/I, excitatory/inhibitory; FPLC, fast protein liquid chromatography; IBA-1, ionized calcium-binding adaptor molecule 1; ICV, intracerebroventricular; LTP, long-term potentiation; $GABA_A$Rs, GABA type (A) receptors; GFAP, glial fibrillary acidic protein; IP-10, interferon-inducible protein 10; MAPT, microtubule-associated protein Tau; MBP, maltose-binding protein; MCP-1, monocyte chemotactic protein-1; MWM, Morris water maze; NC, naïve control; NeuN, neuronal nuclei; NFTs, neurofibrillary tangles; NOA, novel object alteration; NOR, novel object recognition; NVU, neurovascular unit; OM, O-maze; PBST, phosphate-buffered saline with Tween-20; PFA, paraformaldehyde; PC, pyramidal cell; PMSF, phenylmethanesulfonyl fluoride; RT, room temperature; Str, stratum; TBS, Tris-buffered saline; TBST, tris-buffered saline Tween-20; TFA, trifluoroacetic acid; Tg, transgenic; TGF-β1, transforming growth factor-β 1; TTB, 0.05 M TBS/0.3% Triton/0.25% BSA; YM, Y-maze; α-SMA, alpha-smooth muscle actin.

before significant neuronal cell loss was detected, acute neuroinflammatory and vascular responses were observed. These responses included the up-regulation of glial fibrillary acidic protein (GFAP), cell adhesion molecule-1 (PECAM-1, also known as CD31), fibrinogen labeling, and an increased number of activated astrocytes and microglia in the CA1 region of the hippocampus. From day 7, there was significant pyramidal cell loss in the CA1 region of the hippocampus, and by 30 days, significant localized up-regulation of p-tau, GFAP, Iba-1, CD31, and alpha-smooth muscle actin (α-SMA) in the $A\beta_{1-42}$-injected mice compared with controls. These molecular changes in $A\beta_{1-42}$-injected mice were accompanied by cognitive deterioration, as demonstrated by long-term spatial memory impairment. This study is reporting a comprehensive examination of a complex set of parameters associated with intrahippocampal administration of $A\beta_{1-42}$ in mice, their spatiotemporal interactions and combined contribution to the disease progression. We show that a single Aβ injection can reproduce aspects of the inflammatory, vascular, and p-tau induced pathology occurring in the AD human brain that lead to cognitive deficits.

Keywords: Alzheiemer's disease, β-amyloid, tau phosphorylation, cognition, neuroinflamamation

INTRODUCTION

Alzheimer's disease (AD) is a progressive neurodegenerative disorder characterized by a widespread loss of neuronal synapses and spines, the presence of intracellular neurofibrillary tangles (NFTs), and extracellular β-amyloid (Aβ) plaques (Huang and Mucke, 2012; Brun and Englun, 1981). During the last two decades, these features have been incorporated into the amyloid cascade hypothesis (Eric et al., 2011). Today, the successive downstream events occurring as a result of Aβ aggregation and spread represent a key thread of the hypotheses to explain the pathology observed in AD (Hardy and Selkoe, 2002). Despite a large number of clinical trials, there is still currently no effective treatment to prevent, significantly delay, or ameliorate the debilitating symptoms of AD. This is largely due to our limited understanding of the connecting factors underlying the disease, as well as the poor translation of promising treatment options derived from animal models to human clinical trials (Franco and Cedazo-Minguez, 2014; Souchet et al., 2018). With the prevalence of AD increasing alarmingly, it is crucial to develop animal models that more closely mimic the pathological and clinical symptoms of human AD. Importantly, such a model has to be well characterized to document its limitations (Drummond and Wisniewski, 2017) and to determine whether it might effectively support drug screening for the development of novel and effective treatments for AD.

A rising concentration of Aβ in the brain is a critical factor in the development of late-onset sporadic AD, playing a key role in triggering the "amyloid cascade." Although transgenic models, such as amyloid protein precursor (APP)- and presenilin-1 (PS-1)-overexpressing models are known to be useful in the study of genetic aspects of early-onset AD (Ohno et al., 2004, 2007), the late-onset sporadic form of the disease, that accounts for approximately 90% of all cases (Bekris et al., 2010), requires unique approaches to model this form of AD. Growing evidence indicates that Aβ-injected rodent models of AD might closely mimic the main neuropathological symptoms present in AD patients when concentrations of Aβ are increasing (Puzzo et al., 2014; Kwakowsky et al., 2016; Facchinetti et al., 2018; Baluchnejadmojara et al., 2019; Mudò et al., 2019; Yeung et al., 2020a,b). With this model, many aspects of AD-related pathology post-Aβ-injection and their link to the cognitive deficits are not fully characterized. Some of the key events occurring in the AD brain as a consequence of increased Aβ load include neuroinflammation and the disruption of the blood-brain barrier (BBB), both of which contribute to the progression of the disease (Soto-Rojas et al., 2015). For example, the abnormal accumulation and spread of Aβ can lead to localized inflammation involving reactive astrocytes with increased glial fibrillary acidic protein (GFAP) expression (Kamphuis et al., 2012), as well as the activation of the microglia that surround Aβ plaques early in the disease (Navarro et al., 2018). In response to high Aβ load and as part of the initiation of the inflammatory process, both astrocytes and microglia likely up-regulate their expression of a surface receptor for the monocyte chemotactic protein-1 (MCP-1), a β-chemokine involved in inflammation that regulates infiltration/migration of macrophages and microglia (Conductier et al., 2010). It has been recently shown that both the severity of AD (Lee et al., 2018b) and the associated memory deficits (Bettcher et al., 2019) correlate with increased plasma levels of MCP-1 in affected humans. Despite evidence supporting microgliosis as a direct response to Aβ load in the AD brain, and/or an indirect process underlying neuronal death (Marín-Teva et al., 2011), the precise role of microglia in the progression of the disease and response to Aβ load has not been fully elucidated. Interferon gamma-induced protein 10 (IP-10) is a pro-inflammatory chemokine that plays a key role in the inflammatory process and is highly expressed in astrocytes in the AD brain (Xia et al., 2000). Furthermore, increasing severity of AD is associated with increased levels of IP-10

(Leung et al., 2013). Aβ load also correlates with the level of astrocytic GFAP expression in 3xTg-AD mice and AD patients (Wyssenbach et al., 2016).

There is increasing evidence to suggest that the BBB is affected by Aβ deposition, which might contribute to its leakage and dysfunction (Erickson and Banks, 2013). The basic functional unit of the BBB is the neurovascular unit (NVU). In capillaries, this consists of endothelial cells connected by tight junctions, pericytes, astrocyte end-feets and extracellular matrix components of the basement membrane (Muoio et al., 2014). Most components of the BBB have been found to contribute to vascular dysfunction in AD (Govindpani et al., 2019, 2020).

A triggering event of AD pathology might be the accumulation of Aβ in the vasculature, leading to a vicious cycle of Aβ aggregation and BBB dysfunction (Govindpani et al., 2020). In this regard, the leakage of fibrinogen, a protein excluded from the brain by the BBB, has been implicated in AD vascular pathology. The fibrinogen-Aβ interaction causes aggregation of fibrinogen and significantly increased BBB permeability through the down-regulation of endothelial tight junction proteins (Cortes-Canteli et al., 2012). Aβ deposition in the vasculature also affects endothelial cell function in the NVU. For instance, endothelial cell adhesion molecules PECAM-1 and ICAM-1 (also known as CD31 and CD54, respectively) play a role in regulating interactions between leukocytes and the endothelium and are involved in the AD pathology through their contribution to the inflammatory process within blood vessels (Wennström and Nielsen, 2012). In the same way, the up-regulation of α-SMA, which plays a role in the contraction of the vessels, might be a compensatory mechanism in late-stage of the AD pathology in response to early vascular disruption in the BBB (Hutter-Schmid and Humpel, 2016).

NFT load has also been found to correlate with the severity of AD (Arriagada et al., 1992). The pathological effect of p-tau in AD may be due to the loss of function of normal tau together with the toxic gain of function of p-tau, which ultimately leads to impaired axonal transport and compromises cell function and homeostasis (Pritchard et al., 2011; Kruger and Mandelkow, 2015; Huber et al., 2017). Neuroinflammation (Lee et al., 2008), compromised BBB function (Nelson et al., 2016) and p-tau accumulation (Huber et al., 2017) are inferred to be the main pathological mechanisms underlying cognitive impairment in AD (Zempel and Mandelkow, 2014; van de Haar et al., 2016; Bettcher et al., 2019). These mechanisms likely promote extensive degeneration of excitatory pathways in brain areas such as the cerebral cortex and hippocampus.

Excitatory N-methyl-D-aspartate receptors are known to mediate $A\beta_{1-42}$-induced excitotoxicity during AD (Liu et al., 2008). Nevertheless, inhibitory pathway disruptions are also well identified in the AD brain (Rissman and Mobley, 2011; Limon et al., 2012; Fuhrer et al., 2017; Govindpani et al., 2017; Kwakowsky et al., 2018). It has been shown that $A\beta_{1-42}$ can increase ambient γ-aminobutyric acid (GABA) concentrations (Kwakowsky et al., 2020; Vinnakota et al., 2020). Recent evidence postulates that this increased ambient GABA level might activate extrasynaptic $GABA_A$ receptors ($GABA_A$Rs) in the hippocampus leading to a chronic depolarizing block through increased tonic inhibition in this area. This results in neural dystrophy and contributes to cognitive decline (Marczynski, 1998; Calvo-Flores Guzmán et al., 2020; Yeung et al., 2020b).

Despite the extensive research in this area, both utilizing *in vitro* and *in vivo* transgenic animal models as well as AD patients, both the definition and the understanding of the disease pathophysiology are far from precise (Govindpani et al., 2017, 2019; Boche and Nicoll, 2020; Harris et al., 2020). Consequently there is a need for a better understanding of the mechanisms underlying Aβ-induced molecular, cellular, and behavioral changes. Some AD rodent models injected with different types of Aβ fragments intraventricularly, or to specific brain regions, have been used to model the disease (Cetin et al., 2013; Faucher et al., 2016; Kwakowsky et al., 2016; Nicole et al., 2016; Schmid et al., 2017). However, it has been shown that the $A\beta_{1-42}$ peptide introduced to neurons *in vitro* and *in vivo* is considerably more neurotoxic than that generated in the AD brain (Klein et al., 1999). This may be because it contains misfolded $A\beta_{1-42}$ and thereby already has enhanced aggregation (Hillen, 2019).

The goal of this study is to elucidate the spatiotemporal progression of $A\beta_{1-42}$-induced pathology and its connection to the resulting synergies of the molecular and cellular changes in p-tau, GFAP, IBA-1, IP-10, MCP-1, ICAM-1, αSMA, CD31, and fibrinogen in the hippocampus, and the resulting behavioral deficits. We have examined the local layer-specific changes of p-tau, and these neuroinflammatory and vascular markers in the CA1 region of the mouse hippocampus using immunohistochemistry and have shown they lead to severe impairment of long-term spatial memory.

MATERIALS AND METHODS

Animals and Brain Tissue Preparation

All experiments were approved and performed following the regulations of the University of Otago and the University of Auckland. All mice were bred and housed at the Hercus Taieri Resource Unit, the University of Otago and Vernon Jansen Unit, University of Auckland, under 12-h reverse light-cycle conditions (lights on at 8 PM), with *ad libitum* access to food and water. All experiments were conducted following the National Animal Ethics Advisory Committee guidelines and with the approval of the institutional animal ethics committee of the University of Otago and the University of Auckland. All experiments were performed on old (18 months; immunohistochemistry, n = 6/group; behavioral testing, n = 12/group) C57BL/6 wild-type male mice.

$A\beta_{1-42}$ Preparation

$A\beta_{1-42}$ is routinely produced as a recombinant protein fused with maltose-binding protein (MBP), with a proteolytic cleavage site for Factor X protease between the two segments based on as used in (Kwakowsky et al., 2020, 2016; Calvo-Flores Guzmán et al., 2020; Yeung et al., 2020a,b). This strategy utilizes the solubilizing character of the MBP, a product of the MalE gene, to ensure the expression of the soluble fusion protein at a high concentration in *Escherichia coli*. After the bacterial expression of

this recombinant fusion protein, the product was purified on an amylose column to which the MBP segment of the protein binds. The affinity selected fusion protein was eluted from the resin with maltose and concentrated by ammonium sulfate precipitation. The carrier MBP was then cleaved off the fusion protein by Factor X protease, and the released $A\beta_{1-42}$ was isolated and further purified by hydrophobic chromatography with 0–50% v/v acetonitrile/0.1% v/v Trifluoroacetic acid (TFA), using fast protein liquid chromatography (FPLC). The fractions containing pure $A\beta_{1-42}$ were detected immunologically with an antibody against residues 17–24 of $A\beta_{1-42}$ and lyophilized to remove the solvent. Mass spectrometry was used to confirm the expected molecular ion for the desired product. The concentration of the protein fragment has been determined by bicinchoninic acid assay at 60°C for 30 min. Before intra-hippocampal injection of this product, we diluted the prepared monomer in artificial cerebrospinal fluid [ACSF: 147 mM Na^+, 3.5 mM K^+, 2 mM Ca^{2+}, 1 mM Mg^{2+} (pH 7.3)] and "aged" the solution at 37°C for 48 h to facilitate the formation of soluble aggregates, which was confirmed by SDS/PAGE and by non-dissociating PAGE (Yeung et al., 2020a). The optimal incubation time required to produce the highly toxic oligomers is 48–120 h depending on the preparation (Kwakowsky et al., 2016; Calvo-Flores Guzmán et al., 2020; Yeung et al., 2020a).

$A\beta_{1-42}$ Stereotaxic Injection

Mice were anesthetized by subcutaneous injection of 75 mg/kg ketamine and 1 mg/kg domitor. Bilateral coordinates for stereotaxic $A\beta_{1-42}$ injection at three depths (antero-posterior, −2.0 mm; medio-lateral, ±1.3 mm; dorso-ventral, −1.8, 2.0, and 2.2 mm from the dura) within the CA1 region of the hippocampus were determined relative to the bregma according to the Paxinos and Franklin's mouse brain atlas (Yeung et al., 2020a,b). Stereotaxic bilateral administration of 1 μl of 20 μM neurotoxic $A\beta_{1-42}$ or scrambled $A\beta_{1-42}$ ($scrA\beta_{1-42}$, AS-25382, AnaSpec) or artificial cerebrospinal fluid (ACSF, used as a vehicle) into the CA1 region was performed at a rate of 0.1 μl/min. The mice in this study were categorized into four groups: naïve control (NC), ACSF, $scrA\beta_{1-42}$, and $A\beta_{1-42}$ injected groups. Naïve control animals did not undergo any surgical procedures.

Behavioral Testing

Behavioral testing was performed to elucidate the effects of $A\beta_{1-42}$ on the cognitive performance of the mice. Specific behavioral tests were used to target different types of hippocampal-dependent memories: (i) long-term spatial memory with the novel object alteration (NOA), novel object recognition (NOR) test, and the Morris water maze (MWM) tests; and (ii) short-term spatial memory with the Y-maze test (YM), as well as short-term non-spatial memory with the passive avoidance test. The O-maze (OM) test was used as a measurement of the anxiety levels of the mice. All behavioral tests were started at 9 am, and analysis was performed using the tracking image analyzer system EthoVision XT 9 (Noldus).

Novel Object Alteration Test

The NOA test was performed to evaluate long-term working memory 7–8 days after injection. The test was performed in a square arena that was surrounded by non-transparent plexiglass walls (25 cm × 29 cm × 25 cm). Each mouse was placed in the arena individually and given 10 min to habituate to the environment. Next, two identical objects were introduced in the arena at designated locations, and the mice were given 5 min to interact with and explore the objects. Following this, each mouse was returned to its cage. The following day (24 h later), one of the identical objects was placed in a new location, and the behavior of the mice was recorded over a 5 min testing period. The testing apparatus was cleaned between animals with 5% acetic acid to minimize olfactory cues. The discrimination ratio (DR) for a novel over a familiar object was calculated as follows: time spent near the object at the new position minus the time spent near the object at the old position, divided by time spent near the object at the new position plus the time spent near the object at the old position.

Novel Object Recognition Test

The NOR test to evaluate long-term recognition memory was performed 11 days after injection. in the same arena as the NOA. During the first 10 min session on day 1, the animal was free to explore the arena, and during the second 5 min session, the animal was able to explore two identical objects. On day 2, one of the objects was replaced by a novel, unfamiliar object, and animal behavior was recorded for 5 min.

The amount of time spent to explore the new object is considered as an index of recognition memory. The DR for a novel over a familiar object was calculated as follows: time spent near the new object minus the time spent near the old object, divided by time spent near the new object plus the time spent near the old object.

Y-Maze Test

Spontaneous exploration and responsiveness to novel environments and short-term spatial memory functions were evaluated with the YM test 15 days post-injection. The apparatus used for the YM study was constructed out of plexiglass with the three arms of the maze positioned at a 120° angle relative to each other. Each arm is identical (52 cm × 12.5 cm); however, different spatial cues were placed in each arm. The start arm for each experiment was chosen randomly: each mouse was placed in the YM environment on two occasions that were separated by a 2 min interval. During the first 5 min trial, one of the three arms was randomly blocked. In the second trial, all the arms were opened for exploration; the total amount of time the mouse took to explore each arm was recorded for 3 min. During the inter-trial interval (2 min), the animal was returned to its home cage and the maze was cleaned. The alternation percentage was calculated as the percentage of the ratio of actual to possible alternations. An index of the time spent in the new, previously unexplored arm as opposed to the familiar explored arm was used to assess any behavioral differences between each group and was calculated as follows: time spent in the new arm minus

time spent in the old arm, divided by time spent in the new arm plus time spent in the old arm.

Morris Water Maze Test

The MWM, a reliable test of spatial memory and hippocampal-dependent learning, was performed at 20 days post-injection (D'Hooge and De Deyn, 2001). The MWM apparatus comprised a circular black tank (diameter, 130 cm; height, 130 cm) filled with tap water and powdered non-fat milk that was added to the tank before the experiment. A constant temperature of 20°C was maintained during the test. A circular escape platform of ∼10 cm diameter and several navigation cues were used to provide spatial orientation for the mice. The starting position of every mouse was assigned randomly. The location of the hidden platform was kept constant (except on the last day of the experiment). If the mouse did not find the hidden platform within 60 s, the animal was guided to the platform for 10 s before being returned to the cage. Spatial learning was tested across four repeat trials over the following 4 days. Between trials, mice were dried with a towel and placed in their cages, located over heating blankets. On the fifth day in each trial, the escape platform was removed, and the time taken to reach the platform quadrant, time spent in the platform quadrant, and distance traveled to reach the platform for each animal were assessed.

Passive Avoidance Test

The passive avoidance test was performed 27 days post-injection. This associative learning task was conducted in a two-compartment box made of one bright compartment and one dark compartment (16 cm × 18 cm). During habituation, the mouse was placed in the bright compartment, and the mouse gained access to the dark compartment. When the mouse entered the dark compartment the door was closed, and the mouse was briefly administered a 0.3-mA electric shock on the foot for 2 s as an aversive stimulus. After 30 s the animal was returned to its home cage. Three hours later, the animal was returned to the bright compartment with the sliding door open. The animal now had the option to avoid or enter the dark compartment. The latency period before the mouse entered the dark compartment was measured.

O-Maze Test

The OM test was performed at 17 days post-injection to assess anxiety-like behaviors. The OM apparatus consisted of a circular maze (40 cm diameter) with two protected (closed) arms, where the mice usually feel safer, and two unprotected (open) arms. Each mouse was randomly placed in one of the closed arms and the behavior was recorded for 5 min. The total time spent by each mouse in the closed and protected arms was measured. Anxiety-like behavior was estimated based on the total time spent in the closed arms of the apparatus, indicating the amount of time spent avoiding the new environment.

Western Blotting

The specificity of the antibodies used in this study had either been tested and reported previously (Yang et al., 2014; Llorian et al., 2016; Wang et al., 2016) or was examined using Western blotting (**Figure 1I**; using a method published previously; Palpagama et al., 2019a,b; Pandya et al., 2019). Mice were euthanized by cervical dislocation and the brains rapidly removed. The brain was cut in half separating the hemispheres on ice; the hippocampus was dissected from each hemisphere of the brain, freshly snap-frozen on dry ice, and stored at −80°C. Tissue was homogenized using a lysis buffer: 4% SDS, 50 mM Tris-HCL, 2 mM EDTA, pH 6.8 supplemented with 0.1% protease inhibitor cocktail (Sigma-Aldrich Co., Saint Louis, MO, USA: P8340) and with 1 mM phenylmethylsulfonyl fluoride (PMSF; Sigma–Aldrich Co., Saint Louis, MO, USA: P7626). A mixture of tissue and lysis buffer was then transferred to centrifuge tubes containing 0.5 mm glass beads. Tissue was homogenized using a Bullet Blender Tissue Homogeniser (Next Advance, Inc., Troy, NY, USA) at speed 8 for 4 min. Samples were then left on the ice to incubate for 1 h and centrifuged at 10,621 *g* for 10 min at 4°C. The supernatant was collected and stored at −20°C. Protein concentrations were determined using a detergent-compatible protein assay (DC Protein assay, 500-0116, Bio-Rad, Hercules, CA, USA), following the manufacturer's instructions. Twenty μg of each protein extract was run on a gradient-polyacrylamide electrophoresis gel (NU PAGE 4–12% BT 1.5, Life Technologies, CA, USA) at 200 V for 45 min using a Thermo Fisher Mini Gel Tank and transferred onto nitrocellulose membranes using the XCell Blot Module (Invitrogen, Waverley, VIC, Australia) at 30 V for 90 min. Membranes were washed in Tris-HCl buffered saline (TBS; pH 7.6) with 0.1% Tween (TBST) and blocked for 30 min at room temperature (RT) with Odyssey blocking buffer (LI-COR Biosciences, USA). The membranes were incubated with primary antibodies (**Table 1**) overnight at 4°C in TBST with 4% BSA (BSA-TBST). The following day, after 3 × 10 min washes in TBST, membranes were incubated at RT for 1 h with an appropriate IRDye (1:10,000, goat anti-rabbit IRDye 680RD, 926-68071, RRID:AB_10956166; goat anti-mouse IRDye 800CW, 926-32210, RRID:AB_621842; donkey anti-goat IRDye 800CW, 926-32214, RRID:AB_621846; LI-COR Biosciences, Lincoln, NE, USA) secondary antibody diluted in 4% BSA-TBST. Detection of immunoreactive bands was performed using the Odyssey Infrared Imaging System (LI-COR Biosciences, USA).

Free-Floating Fluorescence Immunohistochemistry

Mice were deeply anesthetized with 75 mg/kg ketamine and 1 mg/kg domitor and perfused transcardially with 20 ml of ice-cold 4% paraformaldehyde in phosphate buffer (pH 7.6). Brains were removed and postfixed in 4% paraformaldehyde solution for 2 h at RT and then incubated in 30% sucrose in TBS (pH 7.6; 0.05 M Tris-HCl, 0.15 M NaCl) overnight at 4°C. Hippocampal coronal sections (30 μm) were cut on a freezing microtome (Microm International GmbH, Walldorf, Germany) and collected in TBS.

Free-floating fluorescent immunohistochemistry was performed using the method described by Kwakowsky et al. (2016). Briefly, hippocampal sections were washed 3 × 10 min with TBS and incubated in 0.05 M TBS/0.3% Triton/0.25% BSA (TTB)/1% goat serum for 1 h at RT. Sections were then incubated with primary antibodies (**Table 1**) diluted in TTB for 72 h at

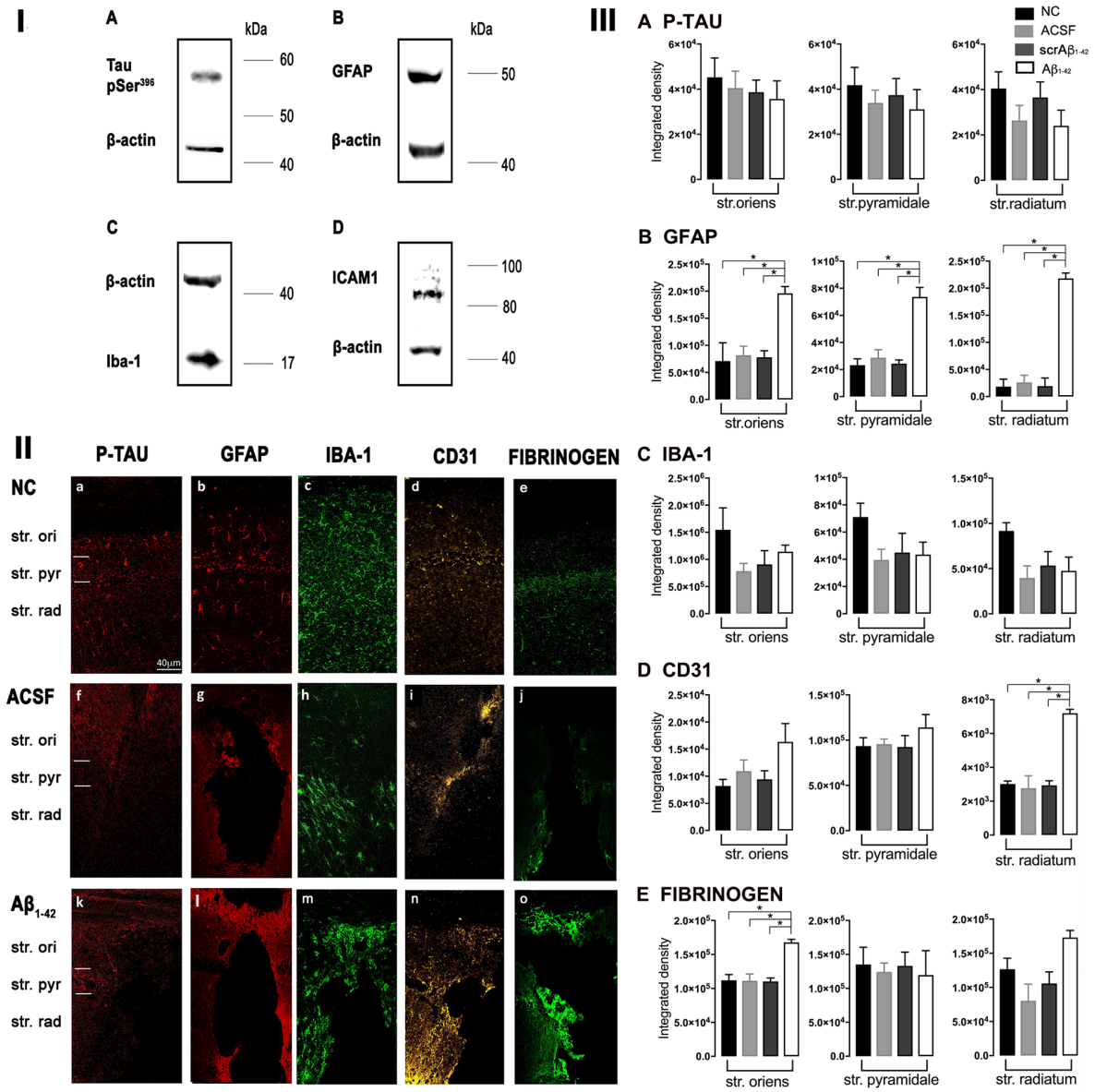

FIGURE 1 | Panel I: Western blot against mouse brain protein homogenates probed with p-tau **(A)**, glial fibrillary acidic protein (GFAP; **B**), Iba-1 **(C)**, and ICAM-1 **(D)**. Observed band sizes: p-tau ∼58 kDA, GFAP ∼50 kDA, Iba-1 ∼17 kDA and ICAM-1 ∼85 kDA. **Panel II:** Representative images showing immunolabeling of p-tau, GFAP, Iba-1, CD31, and fibrinogen at the injection site, 3 days post-injection in NC **(a–e)**, ACSF- **(f–j)**, and $A\beta_{1-42}$-injected **(k–o)** mice. Scale bar (40 μm). **Panel III:** Graphs showing quantification at the injection site in the CA1 hippocampal region of p-tau, GFAP, Iba-1, CD31, and fibrinogen immunolabeling density, 3 days post-injection in NC, ACSF-, $scrA\beta_{1-42}$- and $A\beta_{1-42}$-injected mice. Data expressed as mean ± SEM (Kruskal–Wallis test; $^*p < 0.05$, $n = 3–5$).

4°C on two hippocampal sections from each group. Following 3 × 10 min washes in TBS, sections were incubated in secondary antibodies, goat anti-rabbit Alexa Fluor 647 (1:500, A21245, RRID:AB_141775; Invitrogen, Carlsbad, CA, USA), goat anti-mouse Alexa Fluor 488 (1:500, A11029, RRID: AB_138404; Invitrogen), goat anti-mouse Alexa Fluor 647 (1:500, A21236, RRID:AB_141725; Invitrogen), goat anti-rabbit Alexa Fluor 488 (1:500, A11034, RRID:AB_2576217; Invitrogen), donkey anti-goat Alexa Fluor 647 (1:500, A21447, RRID:AB_141844; Invitrogen) and donkey anti-rabbit Alexa Fluor 488 (1:500, A21206, RRID:AB_141708; Invitrogen) diluted in TTB for 2 h at RT. Finally, the sections were incubated in Hoechst nuclear counterstain (1/10,000 in TTB) for 15 min at RT. Stained sections were examined under a Zeiss LSM 710 confocal laser-scanning microscope (Carl Zeiss, Jena, Germany). The layer-specific labeling of each marker within the CA1 region of the hippocampus was locally analyzed at two specific sites (injection site or needle track, 0–50 μm from the needle track, and adjacent to injection site, 50–500 μm from the needle track) using ImageJ software (U. S. National Institutes of

TABLE 1 | Primary antibodies used in this study.

Antigen	Immunogen	Source, host species, catalog number	Dilution for WB	Dilution for IHC
Anti- Tau pSer396	MAPT(human) mapping to 17q21.31; Mapt(mouse) mapping to 11 E1	Santa Cruz, polyclonal rabbit, sc-101815	1/200	1/100
GFAP cocktail	Equal concentrations of all three monoclonal antibodies (4A11, 1B4, 2E1) that specifically recognize GFAP	BD Biosciences, monoclonal mouse, 556330	1/10,000	1/5,000
Iba-1	A synthetic peptide corresponding to human Iba-1 amino acid 135–147 (C-terminal)	Abcam, polyclonal goat, ab5076	1/500	1/1,000
IP-10	Highly pure (>98%) recombinant hIP 10	Abcam, polyclonal rabbit, ab9807	-	1/100
MCP-1	A recombinant fragment corresponding to human MCP-1	Abcam, polyclonal rabbit, ab9669	-	1/100
α-SMA	N-terminal synthetic decapeptide of α-SMA coupled to keyhole limpet hemocyanin (KLH)	Dako, monoclonal, mouse, M0851	-	1/10
ICAM-1 (CD54)	ICAM-1 (human) mapping too 19p13.2; ICAM-1 (mouse) mapping to 9A3	Santa Cruz, monoclonal mouse, sc-107	1/50	1/50
Fibrinogen	Fibrinogen isolated from human plasma	Dako, polyclonal rabbit, A0080	-	1/500
PECAM-1 (CD31)	Human extracellular domain 1	Dako, monoclonal mouse, M0823	-	1/50
NeuN	Purified cell nuclei from mouse brain	Millipore, monoclonal mouse, MAB377	-	1/1,000

IHC, immunohistochemistry; WB, Western blotting.

Health, Bethesda, MD, USA). After background subtraction and greyscale threshold determination, density measurements were performed for each marker from a defined area of interest measuring 22,748 μm^2 at the injection site and 152,132 μm^2 in each analyzed layer [stratum (str.) oriens, str. pyramidale, str. radiatum] at a location adjacent to the injection site. Particle count and area coverage measurements were conducted using this protocol on the entire field of view of acquired images. Manual counting was performed to determine the number of primary astrocytic and microglial branches. The percentage area coverage by large particles is an indicator of area coverage by activated cells, set at threshold >150 pixels. The percentage area coverage by small particles is the measure of the area covered by the astrocyte and microglia processes. Cells with activated morphology tend to be larger, with more primary branches and an increased number of smaller processes (Glenn et al., 1992; Wilhelmsson et al., 2006; Boche et al., 2013; Palpagama et al., 2019b). The experimenter was blinded to the experimental groupings to eliminate any bias during the experiment, including during image acquisition and analysis. To assess the extent of pyramidal cell loss in the str. pyramidale of the CA1 region of the hippocampus post-$A\beta_{1-42}$ injection, the number of NeuN-positive pyramidal neurons was counted in a 10,296 μm^2 area of the str. pyramidale of the CA1 region. Sections in which the needle track was detected were used for analysis. Two sections were counted per animal (n = 6 in each group) and the results are presented as the number of NeuN-positive pyramidal neurons in the region of interest. Sections with NeuN labeling were examined under a Zeiss LSM 710 inverted confocal laser-scanning microscope (Carl Zeiss, Jena, Germany).

Statistical Analysis

To examine the differences between groups, a Kruskal–Wallis test was conducted for the data obtained, using Graph-Pad Prism software version 8 (GraphPad software, RRID:SCR_002798) with a p-value of $p \leq 0.05$ considered significant, as the data did not meet the assumptions of parametric tests assessed by the D'Agostino–Pearson omnibus and Brown–Forsythe tests. Correlation analysis was performed using Spearman's test. Adobe Photoshop CC 2017 (Adobe Systems Software) was used to prepare the figures.

RESULTS

To assess cell layer-specific changes in tau pathology, density, and morphological changes in neuroinflammatory (GFAP, IBA-1, IP-10, MCP-1) and vascular markers (ICAM-1, αSMA, CD31, fibrinogen) within the CA1 hippocampal region, free-floating fluorescent immunohistochemistry was performed on tissues from NC, ACSF, $scrA\beta_{1-42}$- and $A\beta_{1-42}$-injected mice. Quantification was performed 3 and 30 days post-$A\beta_{1-42}$ injection at sites adjacent to the injection site, as well as at the injection site itself within the CA1 hippocampal region.

Localized $A\beta_{1-42}$-Induced Up-Regulation of GFAP and CD31 by 3 Days Post-$A\beta_{1-42}$ Injection

At the injection site, $A\beta_{1-42}$-injected mice did not display any significant cell loss in the str. pyramidale of the CA1 region at 3 days post-$A\beta_{1-42}$ injection compared with control mice (Yeung et al., 2020a). Localized inflammatory- and vascular pathology-related changes were found in $A\beta_{1-42}$-injected mice compared with ACSF-, $scrA\beta_{1-42}$-injected and NC mice (**Figure 1**, **panel II**). By contrast, p-tau did not show altered expression at the injection site 3 days post-$A\beta_{1-42}$ injection (**Figures 1IIa,f,k,IIIA**). $A\beta_{1-42}$-injected mice exhibited stronger immunostaining of GFAP, Iba-1, CD31, and fibrinogen (**Figure 1III**), markers in the CA1 region at the injection site in comparison with controls. There was an increased GFAP labeling density in comparison with NC, ACSF- and $scrA\beta_{1-42}$-injected mice within the str. oriens (p = 0.0415 vs. NC; p = 0.0499 vs.

ACSF; $p = 0.0315$ vs. $scrA\beta_{1-42}$), str. pyramidale ($p = 0.041$ vs. NC; $p = 0.0491$ vs. ACSF; $p = 0.032$ vs. $scrA\beta_{1-42}$) and str. radiatum ($p = 0.0416$ vs. NC; $p = 0.0421$ vs. ACSF; $p = 0.417$ vs. $scrA\beta_{1-42}$) of the CA1 region (**Figure 1IIIB**). $A\beta_{1-42}$-injected mice showed an increased area coverage by activated cells ($p = 0.049$ vs. NC; $p = 0.049$ vs. ACSF; $p = 0.0235$ vs. $scrA\beta_{1-42}$), a greater number of astrocytes with reactive morphology ($p = 0.0003$ vs. NC; $p = 0.1838$ vs. ACSF; $p = 0.1554$ vs. $scrA\beta_{1-42}$) with increased number of primary branches ($p < 0.0001$ vs. NC; $p = 0.0499$ vs. ACSF; $p = 0.0398$ vs. $scrA\beta_{1-42}$) and increased area coverage by astrocytic processes ($p = 0.0315$ vs. NC; $p = 0.049$ vs. ACSF; $p = 0.0415$ vs. $scrA\beta_{1-42}$; **Figures 2A–D**).

$A\beta_{1-42}$-injected mice also showed an increase in numbers of reactive and dystrophic microglia, but the Iba-1 staining density did not increase (**Figures 1IIm,IIIC**, **2K**). There was also an increased area coverage by activated cells ($p = 0.021$ vs. NC; $p = 0.9321$ vs. ACSF; $p = 0.99$ vs. $scrA\beta_{1-42}$), a greater number of microglia with reactive morphology ($p = 0.0053$ vs. NC; $p = 0.2170$ vs. ACSF; $p = 0.2170$ vs. $scrA\beta_{1-42}$) with increased number of primary branches ($p = 0.0044$ vs. NC; $p = 0.0399$ vs. ACSF; $p = 0.0399$ vs. $scrA\beta_{1-42}$) but the area covered by microglial processes did not change (**Figures 2I–L**).

$A\beta_{1-42}$-injected mice also showed an increased CD31 labeling density in comparison with NC, ACSF- and $scrA\beta_{1-42}$-injected mice within the str. radiatum ($p = 0.0415$ vs. NC; $p = 0.049$ vs. ACSF; $p = 0.0315$ vs. $scrA\beta_{1-42}$) of the CA1 region (**Figure 1IIID**). Fibrinogen displayed increased labeling in the brain parenchyma at the injection site compared with NC, ACSF- and $scrA\beta_{1-42}$-injected mice with a significant increase detected within the str. oriens ($p = 0.042$ vs. NC; $p = 0.042$ vs. ACSF; $p = 0.042$ vs. $scrA\beta_{1-42}$). A similar trend occurred in the str. radiatum but did not reach significance (**Figures 1Ie,j,o,IIE**).

Adjacent to the injection site, despite changes in the pattern of p-tau distribution between groups (**Figure 3Ia,j,s**), quantification of Tau $pSer^{396}$ did not reveal any significant differences between NC, ACSF-, and $scrA\beta_{1-42}$-injected or $A\beta_{1-42}$-injected mice in any layer of the CA1 region 3 days post-$A\beta_{1-42}$ injection (**Figure 3IIA**). However, astrogliosis was revealed by a significant increase in the GFAP labeling intensity between NC, $scrA\beta_{1-42}$-injected and $A\beta_{1-42}$–injected mice in the str. oriens ($p = 0.0021$ vs. NC; $p = 0.0173$ vs. $scrA\beta_{1-42}$), str. pyramidale ($p = 0.036$ vs. NC; $p = 0.0076$ vs. $scrA\beta_{1-42}$) and str. radiatum ($p = 0.0003$ vs. NC; $p = 0.0071$ vs. $scrA\beta_{1-42}$) of the CA1 region of the hippocampus (**Figures 3Ib,k,t,IIB**). $A\beta_{1-42}$-injected mice also displayed an increased GFAP labeling in comparison with ACSF-injected mice within the str. radiatum ($p = 0.0114$) of the CA1 region (**Figure 3IIB**). $A\beta_{1-42}$-injected mice showed a greater number of astrocytes with a highly reactive morphology indicated by numerous branching, elongated processes and hypertrophic cell bodies (**Figure 3It**). $A\beta_{1-42}$-injected mice showed an increased area coverage by activated cells ($p < 0.0001$ vs. NC; $p = 0.02$ vs. ACSF; $p = 0.0305$ vs. $scrA\beta_{1-42}$), a greater number of astrocytes with reactive morphology ($p < 0.0001$ vs. NC; $p = 0.0410$ vs. ACSF; $p = 0.0142$ vs. $scrA\beta_{1-42}$) with increased number of primary branches ($p < 0.0001$ vs. NC; $p = 0.0499$ vs. ACSF; $p = 0.0398$ vs. $scrA\beta_{1-42}$) and increased area coverage by astrocytic processes ($p < 0.0001$ vs. NC; $p = 0.0312$ vs. ACSF; $p = 0.0077$ vs. $scrA\beta_{1-42}$; **Figures 2E–H**).

Despite $A\beta_{1-42}$-injected mice displaying a greater increase in reactive and dystrophic microglia (**Figure 3Iu**), there were no significant differences in Iba-1 density among the groups at 3 days post-$A\beta_{1-42}$ injection at locations adjacent to the injection site (**Figure 3IIc**). $A\beta_{1-42}$-injected mice displayed an increased area coverage by activated microglia ($p < 0.0001$ vs. NC; $p = 0.0275$ vs. ACSF; $p = 0.016$ vs. $scrA\beta_{1-42}$), a greater number of microglia with reactive morphology ($p < 0.0001$ vs. NC; $p = 0.049$ vs. ACSF; $p = 0.0475$ vs. $scrA\beta_{1-42}$) with increased number of primary branches ($p = 0.0012$ vs. NC; $p = 0.0286$ vs. ACSF; $p = 0.0286$ vs. $scrA\beta_{1-42}$) but the area covered by microglial processes did not change (**Figures 2M–P**). Neither IP-10 nor MCP-1 levels, chemokines involved in inflammation, showed significant differences between the groups at 3 days post-$A\beta_{1-42}$ injection (**Figures 3Id,m,v,e,n,w,IID,E**).

Concerning early vasculature disruption, labeling intensity was not significantly different among the groups in the markers ICAM-1 (**Figures 3If,o,x,IIF**), α-SMA (**Figures 3Ig,p,y,IIG**), or fibrinogen (**Figures 3Ii,r,aa,III**). However, $A\beta_{1-42}$-injected mice showed early signs of vascular disruption with significantly up-regulated levels of the endothelial cell marker CD31 adjacent to the injection site in the str. oriens of the CA1 region of the hippocampus compared with NC ($p = 0.0031$), as well as in the str. radiatum of the CA1 region of the hippocampus compared with NC ($p = 0.0131$), ACSF-injected ($p = 0.0387$) and $scrA\beta_{1-42}$-injected mice ($p = 0.0226$; **Figures 3Ih,q,z,IIH**).

These inflammatory (number of GFAP and IBA-1 positive activated cells) and vascular (CD31 and fibrinogen density) pathology markers showed multiple positive cross-correlations (**Figure 4**). For the data obtained at the injections site, these correlations were not statistically significant due to the limited number of sections available from the same animal to test all these markers (**Figures 4A–F**). However, significant positive correlations were observed for most of these markers adjacent to the injection site. The number of activated GFAP positive cells positively correlated with the number of activated microglia ($r = 0.8704$, $p = 0.0028$) and CD31 integrated density ($r = 0.8857$, $p = 0.0333$; **Figures 3G,H**). The number of IBA-1 positive activated cells also correlated with CD31 integrated density ($r = 0.9429$, $p = 0.0167$; **Figure 4I**).

Localized $A\beta_{1-42}$-Induced Pyramidal Cell Loss and Increase in p-tau, GFAP, Iba-1, CD31, and α-SMA by 30 Days Post-injection

By day 30 post-$A\beta_{1-42}$ injection the mice displayed significant neuronal cell loss in the str. pyramidale of the CA1 region of the hippocampus in comparison with the NC (23 ± 0.6 vs. 34.44 ± 1.02, $p < 0.0001$), ACSF-injected (23 ± 0.6 vs. 31.44 ± 0.75, $p = 0.0412$) and $scrA\beta_{1-42}$-injected mice (23 ± 0.6 vs. 32.38 ± 0.86, $p = 0.0069$; **Figure 5IB**). This 33%, 37% and 39% neuronal cell loss in the str. pyramidale of the CA1 region of the hippocampus in the $A\beta_{1-42}$-injected

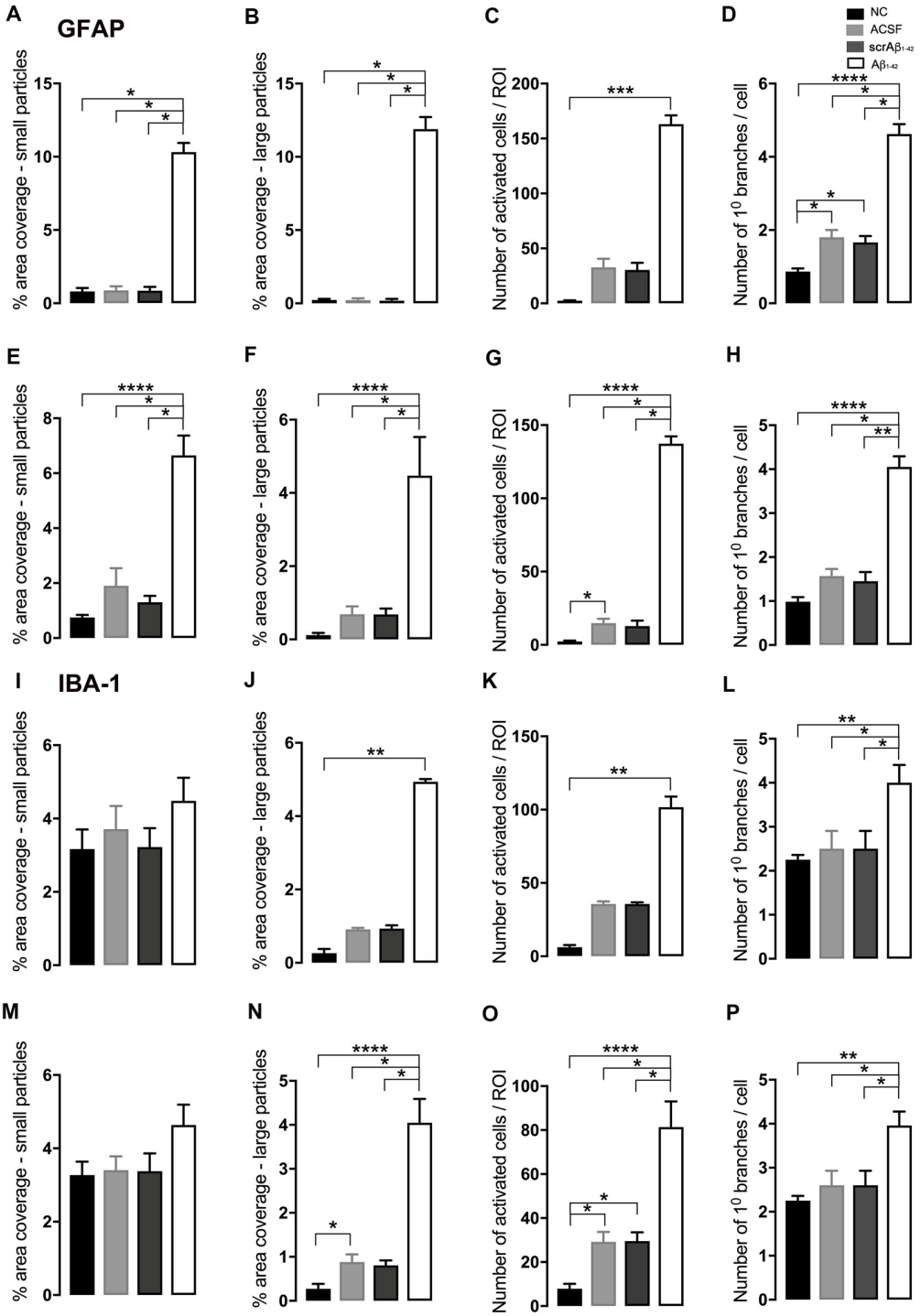

FIGURE 2 | Graphs showing quantification of astrocytic and microglial morphology at the injection site **(A–D,I–L)** and a location adjacent to the injection site **(E–H,M–P)** in the CA1 hippocampal region 3 days post-injection in NC, ACSF-, scrAβ_{1-42}- and Aβ_{1-42}-injected mice. Data expressed as mean ± SEM (Kruskal–Wallis test; *$p < 0.05$; **$p < 0.01$, ***$p < 0.001$, ****$p < 0.0001$, $n = 3$–6).

mice in comparison with the NC mice, ACSF-, and scrAβ_{1-42}-injected controls respectively (**Figure 5IB**) is indicative of Aβ_{1-42}-induced neurotoxicity, as well as the long-lasting impact of a single bilateral intra-hippocampal injection of Aβ_{1-42}. Visualization of NeuN-positive pyramidal cells in the str. pyramidale of the CA1 hippocampal region of Aβ_{1-42}-injected mice demonstrated that apart from the considerable amount of cell loss, the remaining pyramidal cells had an irregular shape

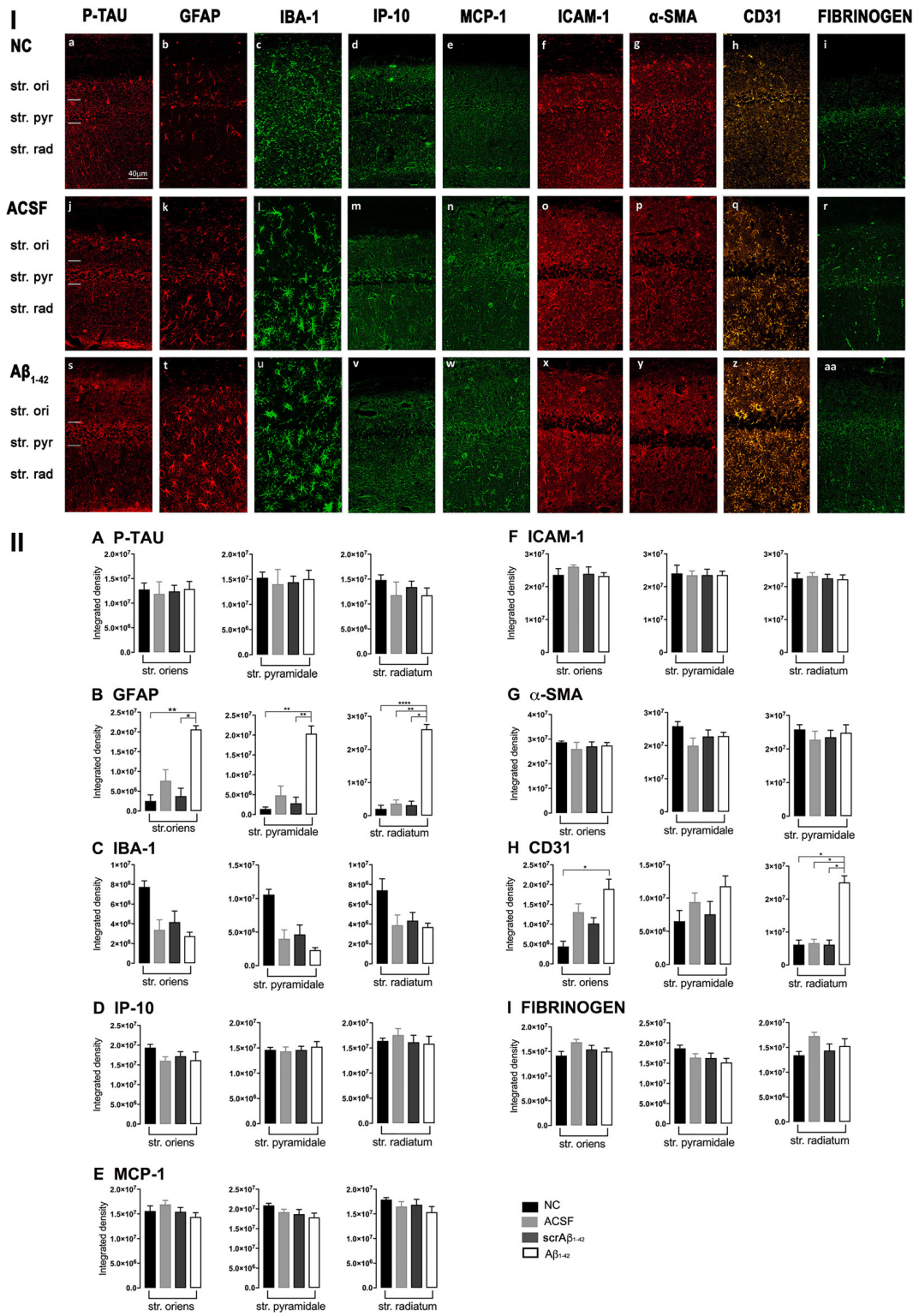

FIGURE 3 | Panel I: Representative images showing immunolabeling of p-tau, GFAP, Iba-1, IP-10, MCP-1, ICAM-1, α-SMA, CD31, and fibrinogen at a location adjacent to the injection site, 3 days after injection in NC **(a–i)**, ACSF- **(j–r)** and $A\beta_{1-42}$-injected **(s–aa)** mice. Scale bar (40 μm). **Panel II:** Graphs showing quantification at a location adjacent to the injection site in the CA1 hippocampal region of p-tau, GFAP, Iba-1, IP-10, MCP-1, ICAM-1, α-SMA, CD31, and fibrinogen **(A–I)** immunolabeling density, 3 days post-injection in NC, ACSF-, $scrA\beta_{1-42}$- and $A\beta_{1-42}$-injected mice. Data expressed as mean ± SEM (Kruskal–Wallis test; $^{*}p < 0.05$; $^{**}p < 0.01$, $^{****}p < 0.0001$, $n = 6$).

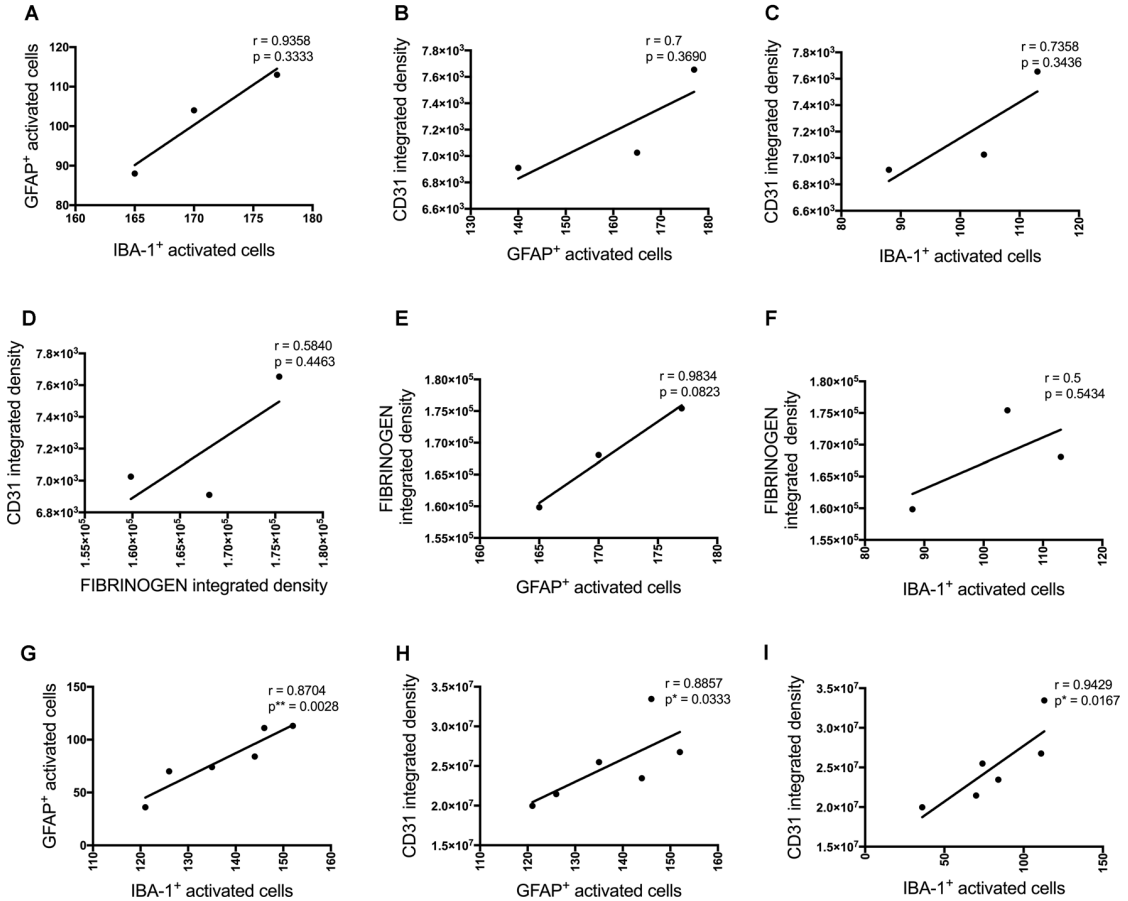

FIGURE 4 | Correlation between the number of activated astrocytes and microglia and vascular markers at the injection site (**A–F**, $n = 3$) and a location adjacent to the injection site (**G–I**, $n = 6$) in the CA1 hippocampal region 3 days post-injection in NC, ACSF-, scrAβ$_{1-42}$- and Aβ$_{1-42}$-injected mice. This relationship is represented by a Spearman's r-value (*$p < 0.05$, **$p < 0.01$).

in Aβ$_{1-42}$-injected mice (**Figure 5IC**). We have also found a significant 12%, 15% and 13% pyramidal cell loss at 7 days after Aβ$_{1-42}$ injection in the CA1 hippocampal region of the mice compared to NC (56 ± 1.2 vs. 64 ± 1.34, $p = 0.0458$), ACSF- (56 ± 1.2 vs. 66 ± 1.59, $p = 0.0164$) and scrAβ$_{1-42}$-injected mice, respectively (**Figure 5IA**).

At the injection site, significant localized tau hyperphosphorylation, inflammation, and vascular changes were found in Aβ$_{1-42}$-injected mice 30 days post-injection compared with ACSF-injected and NC mice (**Figures 5II,III**). This conclusion was derived from localized Aβ$_{1-42}$ injection-induced increase in p-tau, GFAP, and Iba-1 levels and the up-regulation of CD31 at the injection site (**Figure 5IIk–m**). By 30 days after the injection, p-tau immunoreactivity in the str. oriens, str. pyramidale and str. radiatum of the CA1 region of the hippocampus was significantly higher in the Aβ$_{1-42}$-injected mice compared to NC ($p < 0.0001$), ACSF- ($p = 0.0439$; $p = 0.044$; $p = 0.0123$) and scrAβ$_{1-42}$-injected mice ($p = 0.0057$; $p = 0.0058$; $p = 0.0229$; **Figures 5IIa,f,k,IIIA**). Aβ$_{1-42}$-injected mice showed stronger p-tau immunoreactivity within the somatodendritic compartments of neurons in the str. pyramidale and along axonal processes extending from the str. pyramidale compared with control mice (**Figure 5IIa,f,k**).

In addition, astrogliosis was observed at the injection site by 30 days after the Aβ$_{1-42}$ injection, as indicated by the significant increase in GFAP labeling in the str. oriens, str. pyramidale and str. radiatum in the Aβ$_{1-42}$-injected mice in comparison with the NC ($p < 0.0001$), ACSF- ($p = 0.0168$; $p = 0.0439$; $p = 0.0058$) and scrAβ$_{1-42}$-injected mice ($p = 0.0168$; $p = 0.0057$; $p = 0.044$; **Figure 5IIIB**). The ACSF- and scrAβ$_{1-42}$-injected mice also displayed significantly higher GFAP immunoreactivity than the NC mice in the str. oriens ($p = 0.0168$; $p = 0.0168$), str. pyramidale ($p = 0.0057$; $p = 0.0439$) and str. radiatum ($p = 0.044$; $p = 0.0058$; **Figure 5IIIB**). Aβ$_{1-42}$-injected mice showed an increased area coverage by activated cells ($p = 0.0001$ vs. NC; $p = 0.0151$ vs. ACSF; $p = 0.0095$ vs. scrAβ$_{1-42}$), a greater number of astrocytes with reactive morphology ($p = 0.0005$ vs. NC; $p = 0.049$ vs. ACSF; $p = 0.037$ vs. scrAβ$_{1-42}$), increased area coverage by astrocytic processes ($p = 0.0128$ vs. NC; $p = 0.1651$ vs. ACSF; $p = 0.0455$ vs. scrAβ$_{1-42}$) but the number of primary branches did not change (**Figures 6A–D**).

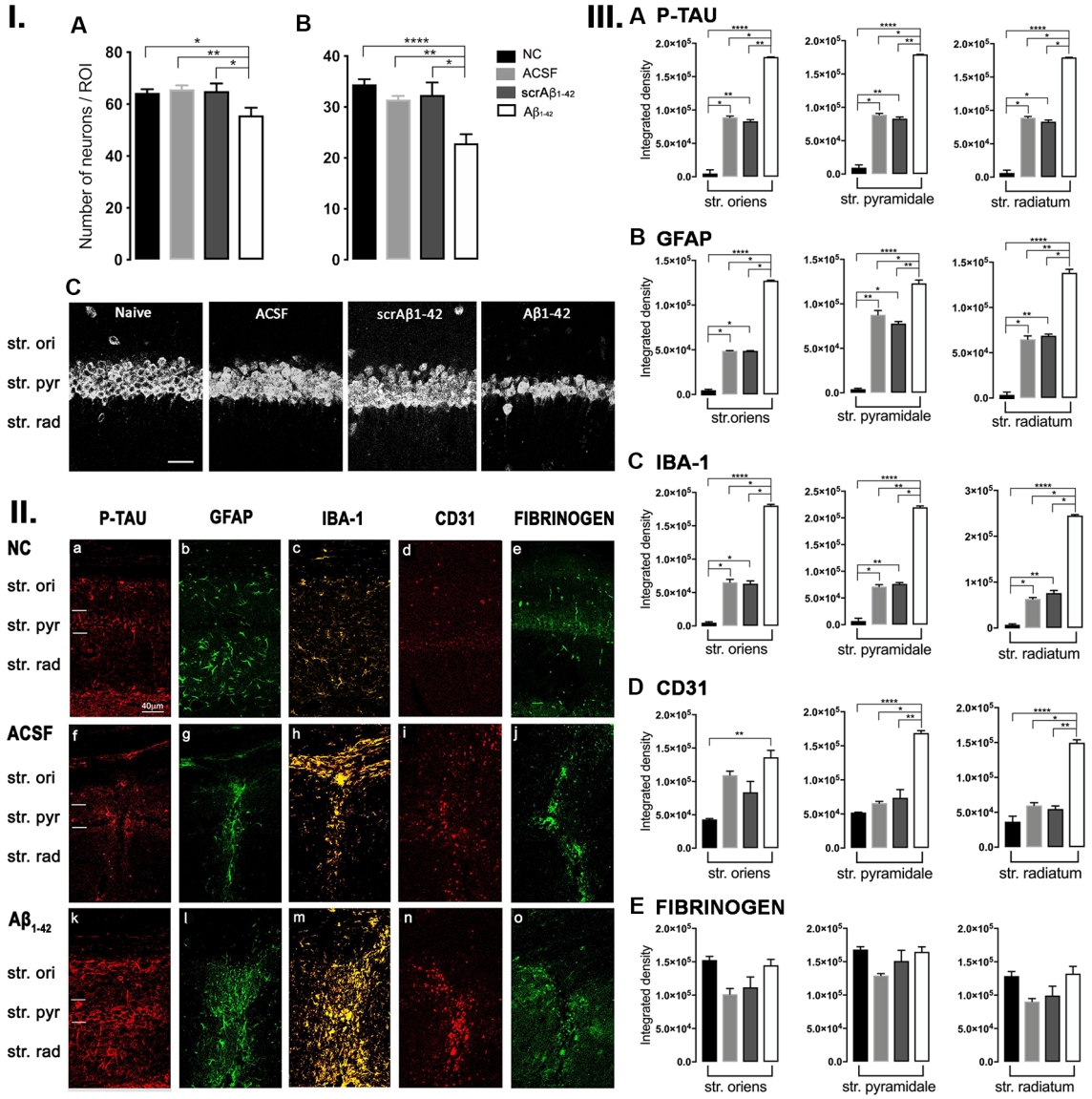

FIGURE 5 | Panel I: Graphs showing the number of NeuN-positive pyramidal cells in the str. pyramidale of the CA1 hippocampal layer in NC, ACSF-, scrAβ_{1-42}- and Aβ_{1-42}-injected mice 7 days post-injection **(A)** and 30 days post-injection **(B)**. Representative images of the CA1 hippocampal subregion at a location adjacent to the injection site showing NeuN-positive pyramidal cells from the str. pyramidale in NC, ACSF-, scrAβ_{1-42}- and Aβ_{1-42}-injected mice 30 days post-injection **(C)**. **Panel II:** Representative images showing immunolabeling of p-tau, GFAP, Iba-1, CD31, and fibrinogen at the injection site 30 days post-injection in NC **(a–e)**, ACSF-injected **(f–j)**, and Aβ_{1-42}-injected **(k–o)** mice. Scale bar (40 μm). **Panel III:** Graphs showing quantification at the injection site in the CA1 hippocampal region of p-tau, GFAP, Iba-1, CD31, and fibrinogen, 30 days post-injection in NC, ACSF-, scrAβ_{1-42}- and Aβ_{1-42}-injected mice. Data expressed as mean ± SEM (Kruskal–Wallis test; *$p < 0.05$; **$p < 0.01$, ****$p < 0.0001$, $n = 6$).

Likewise, localized microgliosis, as indicated by the increase in Iba-1 density, in the str. oriens, str. pyramidale and str. radiatum was significantly increased in the Aβ_{1-42}-injected mice compared with the NC ($p < 0.0001$), ACSF- ($p = 0.0229$; $p = 0.0058$; $p = 0.0052$) and scrAβ_{1-42}-injected mice ($p = 0.0124$; $p = 0.044$; $p = 0.0475$; **Figure 5IIIC**). The ACSF- and scrAβ_{1-42}-injected mice also displayed higher Iba-1 levels than the NC mice in the str. oriens ($p = 0.0124$; $p = 0.0229$), str. pyramidale ($p = 0.044$; $p = 0.0058$) and str. radiatum ($p = 0.0475$; 0.0052) of the CA1 region (**Figure 5IIIC**). Aβ_{1-42}-injected mice displayed an increased area coverage by activated microglia ($p < 0.0001$ vs. NC; $p = 0.0269$ vs. ACSF; $p = 0.049$ vs. scrAβ_{1-42}) and a greater number of microglia with reactive morphology ($p < 0.0001$ vs. NC; $p = 0.0151$ vs. ACSF; $p = 0.0261$ vs. scrAβ_{1-42}) but the number of primary branches and the area covered by microglial processes did not change (**Figures 6I–L**).

Localized changes in vascular markers at the injection site were also observed in Aβ_{1-42}-injected mice by 30 days

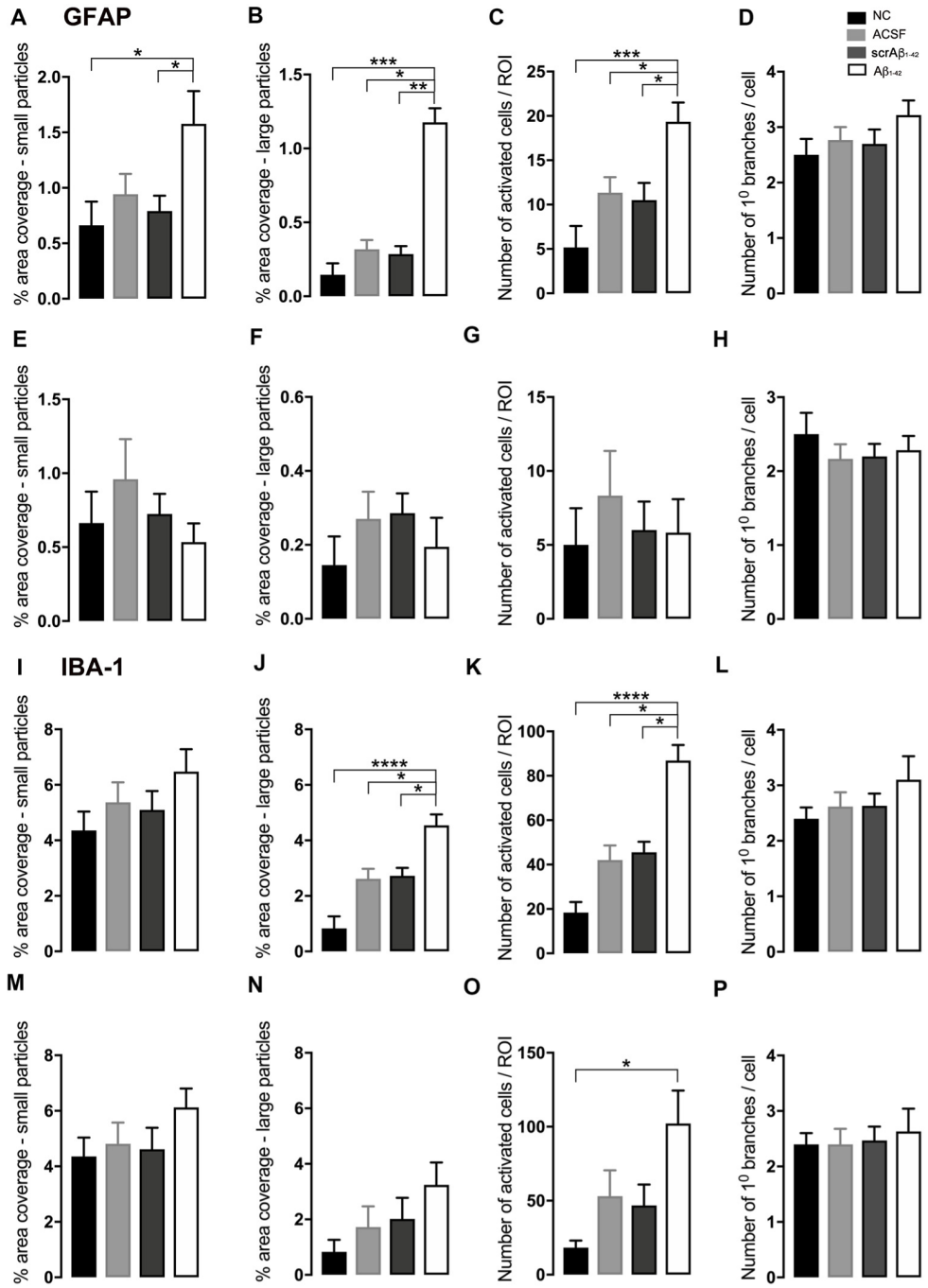

FIGURE 6 | Graphs showing quantification of astrocytic and microglial morphology at the injection site **(A–D,I–L)** and a location adjacent to the injection site **(E–H,M–P)** in the CA1 hippocampal region 30 days post-injection in NC, ACSF-, scrAβ_{1-42}- and Aβ_{1-42}-injected mice. Data expressed as mean ± SEM (Kruskal–Wallis test; *$p < 0.05$, **$p < 0.01$, ***$p < 0.001$, ****$p < 0.0001$, $n = 6$).

after the injection as compared to the controls. CD31 levels were significantly higher in the Aβ_{1-42}-injected mice than in the NC mice in the str. oriens, str. pyramidale, and str. radiatum of the CA1 region of the hippocampus ($p = 0.0002$; $p < 0.0001$; $p < 0.0001$; **Figures 5IIn,IIID**). The Aβ_{1-42}-injected mice also displayed higher CD31 levels than the ACSF- and scrAβ_{1-42}-injected mice in the str. pyramidale ($p = 0.0135$; $p = 0.0025$) and str. radiatum ($p = 0.0162$; $p = 0.0042$) of the CA1 region of the hippocampus (**Figure 5IIID**).

In addition to the vascular changes found at the injection site, 30 days post-injection, there was a significant increase

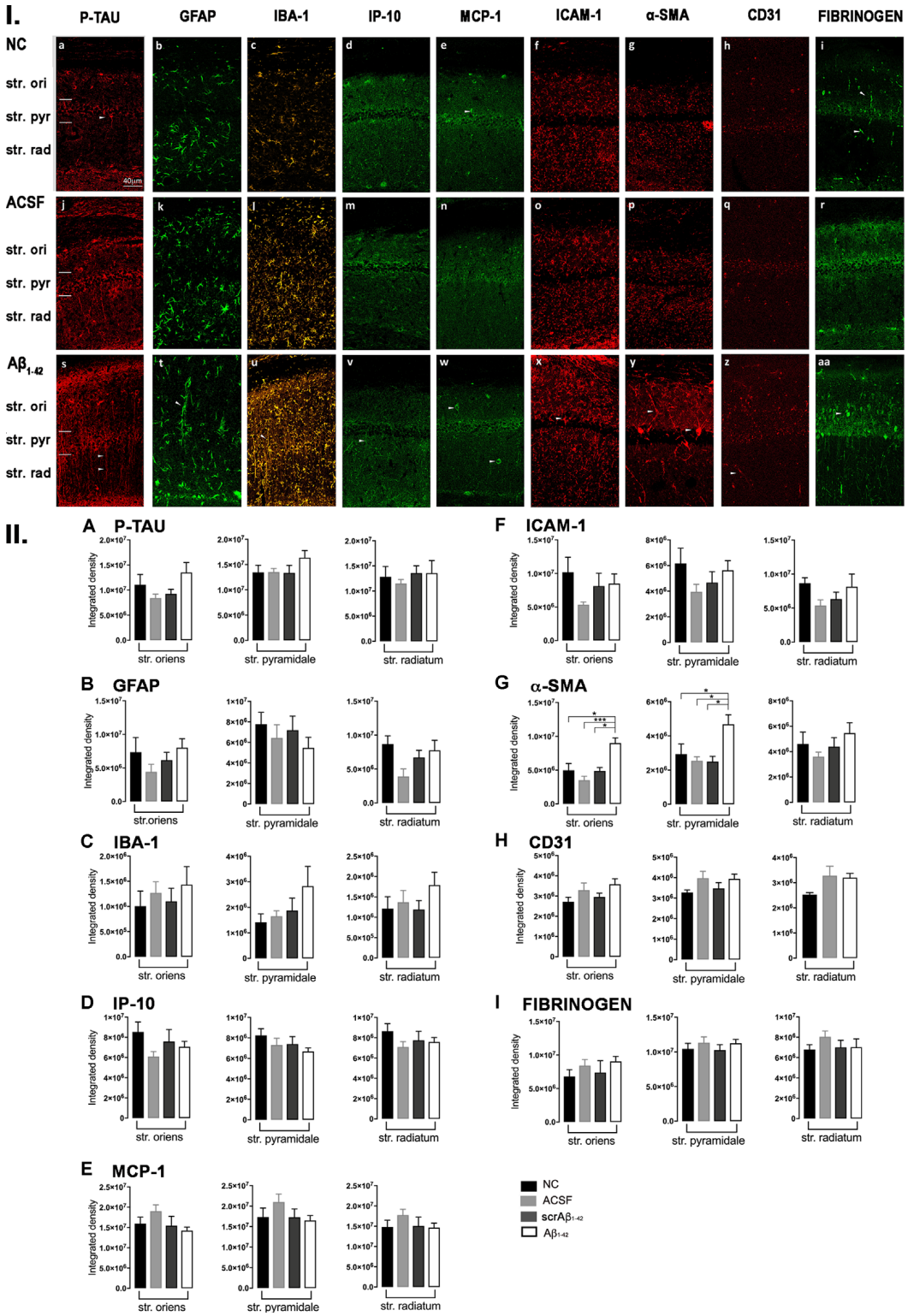

FIGURE 7 | Panel I: Representative images showing immunolabeling of p-tau, GFAP, Iba-1, IP-10, MCP-1, ICAM-1, a-SMA, CD31 and fibrinogen at a location adjacent to the injection site, 30 days post- injection in NC **(a–i)**, ACSF-injected **(j–r)** and $A\beta_{1-42}$-injected **(s–aa)** mice. **Panel II:** Graphs showing quantification at a location adjacent to the injection site in the CA1 hippocampal region of p-tau, GFAP, Iba-1, IP-10, MCP-1, ICAM-1, α-SMA, CD31 and fibrinogen immunolabeling density, 30 days post injection in NC, ACSF-, scrAb1–42- and Ab1–42-injected mice. Data expressed as mean SEM (Kruskall–Wallis test; $^{*}p < 0.05$; $^{***}p < 0.001$, $n = 6$).

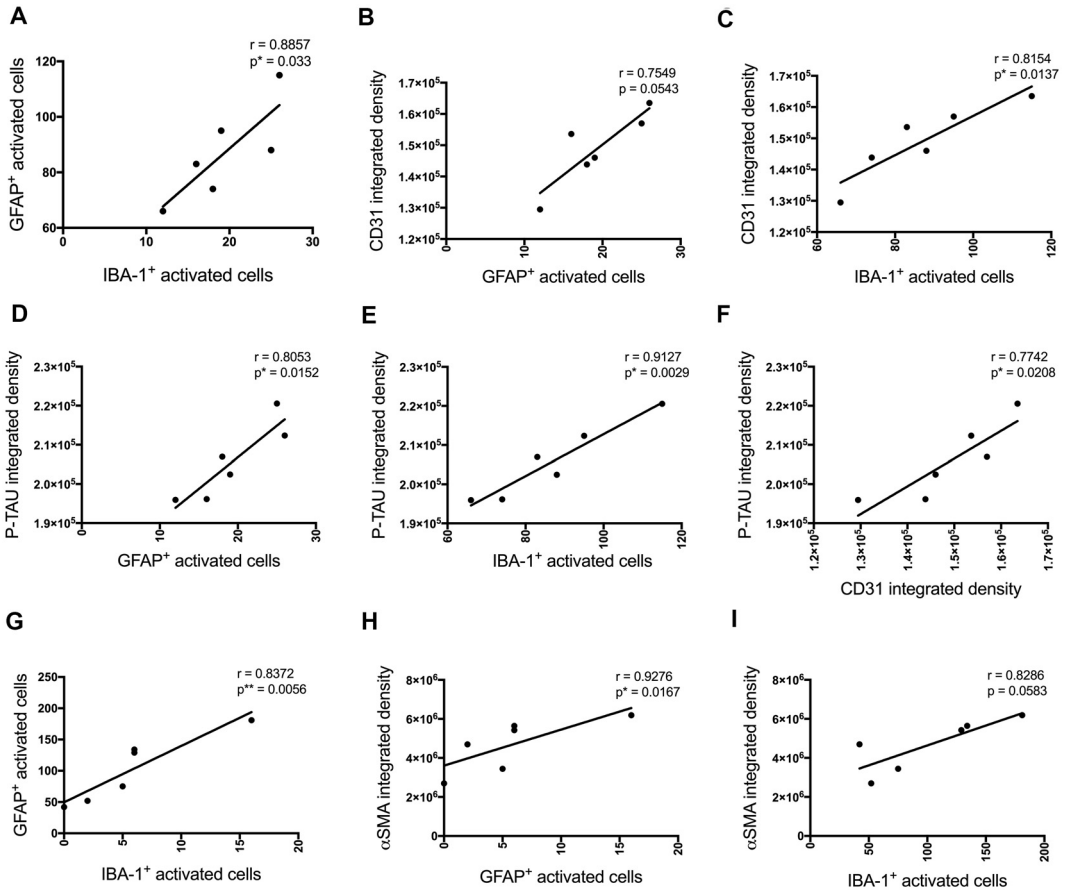

FIGURE 8 | Correlation between the number of activated astrocytes and microglia, p-tau, and vascular markers at the injection site **(A–F)** and at a location adjacent to the injection site **(G–I)** in the CA1 hippocampal region 30 days post-injection in NC, ACSF-, scrAβ$_{1-42}$- and Aβ$_{1-42}$-injected mice. This relationship is represented by a Spearman's *r*-value (*$p < 0.05$, **$p < 0.01$, $n = 6$).

in α-SMA density at a location adjacent to the injection site in Aβ$_{1-42}$-injected mice compared with NC, ACSF and scrAβ$_{1-42}$-injected mice in the str. oriens ($p = 0.0180$ vs. NC; $p = 0.0008$ vs. ACSF; $p = 0.0143$ vs. scrAβ$_{1-42}$) and str. pyramidale ($p = 0.0241$; vs. NC; $p = 0.0246$ vs. ACSF; $p = 0.0136$ vs. scrAβ$_{1-42}$; **Figures 7Iy,IIG**). Although we did not find any other significant Aβ$_{1-42}$-induced effects at the location adjacent to the injection site for p-tau, Iba-1, IP-10, MCP-1, ICAM-1, CD31, and fibrinogen (**Figures 7I;IIA,D,E,F,H,I**), Aβ$_{1-42}$-injected mice showed a non-significant trend towards increased p-tau in the str. oriens of the CA1 hippocampal region (**Figure 7Is**). Astrocyte morphology did not differ from controls in Aβ$_{1-42}$-injected mice (**Figures 6E–H**) but activated microglia numbers were slightly increased compared with NC ($p = 0.0019$), ACSF- ($p = 0.1208$) and scrAβ$_{1-42}$-injected mice ($p = 0.0864$; **Figures 6M–P**).

P-tau, some inflammatory- (number of GFAP and IBA-1 positive activated cells) and vascular (CD31 and α-SMA density) pathology markers showed multiple positive correlations (**Figure 8**). Significant positive correlations were observed for most of these markers at the injection site and adjacent to the injection site as well. The number of activated GFAP positive cells positively correlates with the number of activated microglia ($r = 0.8857$, $p = 0.033$ injection site; $r = 0.8372$, $p = 0.0056$ adjacent injection site), CD31 ($r = 0.7549$, $p = 0.0543$), p-tau ($r = 0.8053$, $p = 0.0152$) and α-SMA ($r = 0.9276$, $p = 0.0167$ adjacent injection site) integrated density (**Figures 8A,B,D,G,H**). The number of IBA-1 positive activated cells also correlates with CD31 ($r = 0.8154$, $p = 0.0137$) and p-tau ($r = 0.9127$, $p = 0.0029$) integrated density (**Figures 8C,E**).

Aβ$_{1-42}$-Induced Behavioral and Cognitive Changes

To elucidate the long-lasting effect of Aβ$_{1-42}$ treatment on cognitive function at the 7–30-day time points the NOA, NOR and MWM tests for long-term spatial-memory were performed, as well as the YM test for short-term spatial memory, the passive avoidance test for short-term non-spatial memory, and the OM test as a measurement of the anxiety levels in the mice (**Figures 9A–F**).

According to the results of NOA (**Figure 9A**), the Aβ$_{1-42}$-injected mice showed significant cognitive deterioration in long-term spatial memory as compared with the NC ($p = 0.0308$),

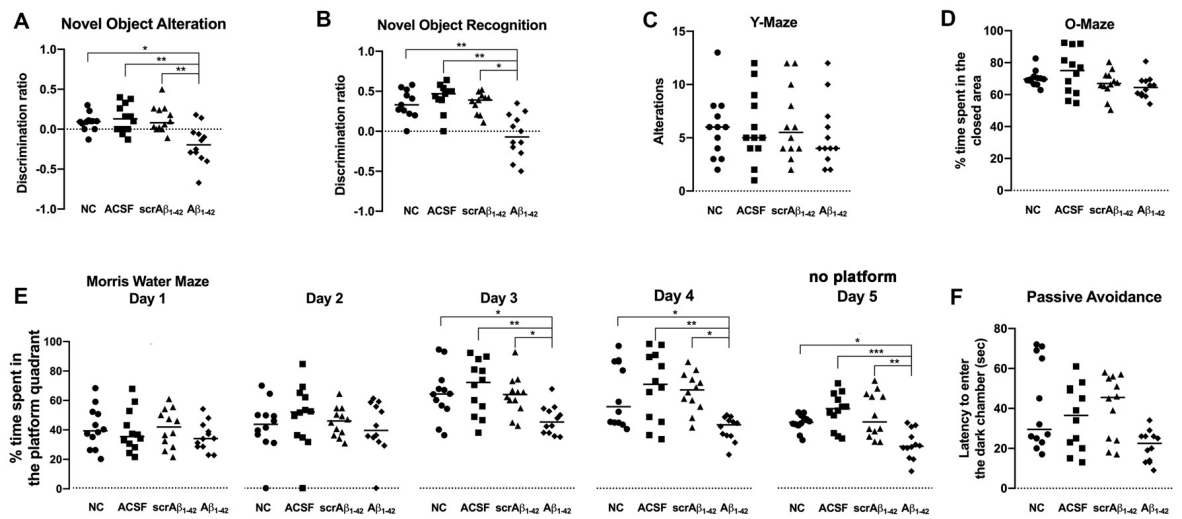

FIGURE 9 | $A\beta_{1-42}$-injected mice showed long-term spatial memory impairment revealed by the novel object alteration (**A**, performed on days 7, 8), novel object recognition (**B**, performed on days 11, 12), and Morris Water Maze (**E**, performed on days 20–24) tests. Short-term spatial memory assessed by the Y maze showed no significant difference in $A\beta_{1-42}$-injected mice compared with controls (**C**, performed on day 15). Non-spatial memory remained unchanged in $A\beta_{1-42}$-injected mice compared with controls (**F**, performed on day 27), and $A\beta_{1-42}$ and/or the injection itself did not produce any anxiogenic effect (**D**, performed on day 17). Scatter plot showing all of the data values used with the median (Kruskal-Wallis test; $^{*}p < 0.05$; $^{**}p < 0.01$, $^{***}p < 0.001$, $n = 12$).

ACSF- ($p = 0.0082$), and $scrA\beta_{1-42}$-injected mice ($p = 0.0089$), with significantly lower DR at 8 days post-injection (**Figure 9A**).

The $A\beta_{1-42}$-injected mice also showed significant cognitive deterioration in long-term spatial memory as compared with the NC ($p = 0.0099$), ACSF- ($p = 0.0003$), and $scrA\beta_{1-42}$-injected mice ($p = 0.0127$) according to the results of the NOR test at 12 days post-injection (**Figure 9B**).

According to the MWM test, the $A\beta_{1-42}$-injected mice also showed significant long-term spatial memory impairment when compared with the NC, ACSF- and $scrA\beta_{1-42}$-injected mice (**Figure 9E**). During day 1 and 2 of the MWM test (20 and 21 days post-injection), the mice from the three groups spent a similar amount of time in the platform quadrant of the maze, but significant differences were found between the NC, ACSF- and $scrA\beta_{1-42}$-injected mice and the $A\beta_{1-42}$-injected mice during day 3 and 4 of the experiment: the $A\beta_{1-42}$-injected mice spent significantly less time in the platform quadrant than the NC ($p = 0.0401$; $p = 0.0498$), ACSF-injected mice ($p = 0.008$; $p = 0.0064$) and the $scrA\beta_{1-42}$ mice ($p = 0.0437$; $p = 0.0129$ for day 3 and 4 respectively). During the fifth and last day of the test, when the platform was removed, the time spent by each group at the "platform quadrant" was also assessed. The $A\beta_{1-42}$-injected mice spent significantly less time in the platform quadrant on day 5, as compared with the NC ($p = 0.0287$), ACSF- ($p = 0.0003$) and $scrA\beta_{1-42}$-injected mice ($p = 0.0072$; **Figure 9E**). Therefore, data from the MWM test show that whereas the control mice showed successful learning from day 3, the $A\beta_{1-42}$-injected mice presented with long-term spatial memory impairment which affected their performance on days 3 and 4, as well as the last day of the test (**Figure 9E**).

According to the findings of the YM test, there was no significant difference in short-term spatial memory between any of the treatment groups 15 days post-injection. This indicates that short-term spatial memory was not affected by $A\beta_{1-42}$ injection. Alternatively, it is also possible that any effect on short-term spatial memory could not be detected by this test. However, although the performance of the mice was similar across all the groups, the $A\beta_{1-42}$-injected mice showed a slightly decreased number of alternations as compared with the NC, ACSF- and $scrA\beta_{1-42}$-injected mice (**Figure 9C**).

The $A\beta_{1-42}$-injected mice showed no significant difference in non-spatial memory performance as compared with the NC ($p = 0.0739$), ACSF- ($p = 0.3766$) and $scrA\beta_{1-42}$-injected mice ($p = 0.0539$) by 28 days post-injection (**Figure 9F**). In phase 3 of the passive avoidance test (post-shock 3 h), similar latency to enter the dark chamber was found in the control and $A\beta_{1-42}$-injected mice (**Figure 9F**).

Since anxiety is likely to influence cognitive performance, the OM test was performed to determine whether the mice from the different treatment groups exhibited anxiety. The $A\beta_{1-42}$-injected mice showed no significant difference in anxiety levels as compared with the NC, ACSF- and $scrA\beta_{1-42}$-injected mice (**Figure 9D**), as mice from all the groups were found to spend a similar amount of time in the closed (protected) arm of the O-maze apparatus. Thus, $A\beta_{1-42}$ and/or the injection itself did not produce any anxiogenic effect (**Figure 9D**).

Cognitive performance of $A\beta_{1-42}$-injected mice after showed a negative correlation with p-tau density (NOA $r = -0.8469$, $p = 0.0238$; NOR $r = -0.8117$, $p = 0.0722$; MWM $r = -0.8286$, $p = 0.0573$; **Figures 10G–I**), the number of activated astrocytes (NOA $r = -0.6571$, $p = 0.175$; NOR $r = -0.8986$, $p = 0.0278$; MWM $r = -0.8857$, $p = 0.0333$; **Figures 10A–C**) and microglia (NOA $r = -0.9429$, $p = 0.0167$; NOR $r = -0.8986$,

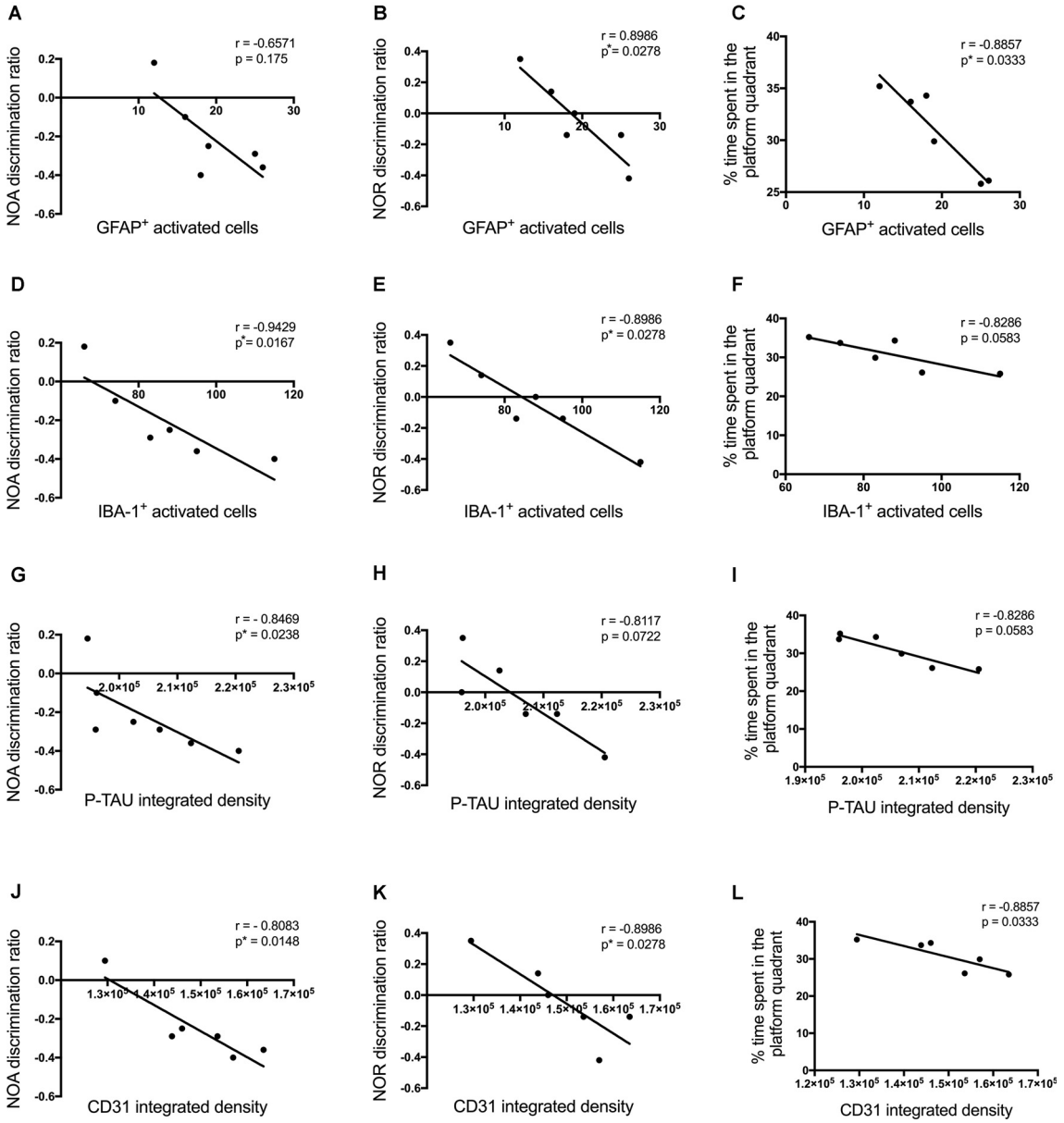

FIGURE 10 | Correlation between the number of activated astrocytes and microglia **(A–F)**, p-tau **(G–I)**, CD31 **(J–L)**at the injection site in the CA1 hippocampal region, and behavioral scores 30 days post-injection in NC, ACSF-, scrAβ$_{1–42}$- and Aβ$_{1–42}$-injected mice. This relationship is represented by a Spearman's *r*-value (*$p < 0.05$, $n = 6$).

$p = 0.0278$; MWM $r = -0.8286$, $p = 0.0583$; **Figures 10D–F**) and CD31 density (NOA $r = -0.8083$, $p = 0.0148$; NOR $r = -0.8986$, $p = 0.0278$; MWM $r = -0.8857$, $p = 0.0333$; **Figures 10J–L**), but no significant correlations were observed with other inflammatory, vascular markers or neuronal loss.

DISCUSSION

The present study is an in-depth holistic molecular, cellular, and behavioral characterization of the acute and chronic effects of increased hippocampal Aβ$_{1–42}$ concentration, achieved through bilateral intra-hippocampal Aβ$_{1–42}$ injection in mice. We report that a single hippocampal Aβ$_{1–42}$ injection resulted in localized layer-specific alterations in the abundance of inflammatory- and vascular markers and phosphorylated tau, at the injection site. At all the time points examined post-injection (7–30 days) significant long-term spatial memory impairments were found in Aβ$_{1–42}$-injected mice compared to controls along with a significant neuronal cell loss in the str. pyramidale of the CA1 region. Our data suggest that inflammation and vascular disruption along with the local tau pathology observed in the CA1 region of the hippocampus might represent a

relevant, complex, and interactive combination of leading factors that synergistically contribute to the hippocampus-dependent spatial memory impairment observed in the $A\beta_{1-42}$-injected mice.

Pyramidal Cell Loss in the CA1 Hippocampal Region of $A\beta_{1-42}$-Injected Mice

We found a significant $A\beta_{1-42}$ mediated pyramidal cell loss by 7 days in the str. pyramidale of the CA1 region of the hippocampus despite finding of an earlier study that hippocampal cell loss was not observed until 14 and 28 days, and not at 7 days (Takuma et al., 2004). This delayed response might be explained if there was a lower concentration of misfolded Aβ, and thereby fewer aggregates, perhaps because the less aggregation-prone $A\beta_{1-40}$ was used. Although extrapolation of findings from rodent models to human AD must be made with caution, the excitatory pyramidal cell loss observed here does occur in late-stage AD in humans (Rossler et al., 2002) and, was at a relatively late outcome in our study as well.

The neurotoxic effect induced by high concentrations of $A\beta_{1-42}$ observed in this study likely arose from a combination of factors, including damage from oxidative stress (Behl et al., 1995), activation of glial cells (Farfara et al., 2008), changes in intracellular Ca^{2+} concentrations and mitochondrial dysfunction (Arbel-Ornath et al., 2017). Aβ-induced apoptosis is likely mediated by the caspase-3-apoptotic cascade (Takuma et al., 2004; Brouillette et al., 2012; Vinnakota et al., 2020). $A\beta_{1-42}$-induced cell death might also result from oxidative stress and the generation of oxidative modifications to lipid and protein in the cell—the presence of intracerebral $A\beta_{1-42}$ in rats is associated with increased levels of oxidized proteins in the rat hippocampus (Boyd-Kimball et al., 2005). $A\beta_{1-42}$-induced activation of glial cells and the generation of pro-inflammatory cytokines may also contribute to neurodegeneration *in vivo* (Farfara et al., 2008). Cell loss induced by hippocampal injection of $A\beta_{1-42}$ in mice has been prevented by the administration of transforming growth factor (TGF)-β1, an immunosuppressive cytokine, which prevents glial activation and accumulation of $A\beta_{1-42}$ (Chen et al., 2015). In the present study, the significant local upregulation of activated microglia and reactive astrocytes that were observed in the $A\beta_{1-42}$-injected mice might also partially be responsible for the neural cell loss.

Tau Pathology-Related Changes in $A\beta_{1-42}$-Injected Mice

We report locally increased tau hyperphosphorylation by 30 days after $A\beta_{1-42}$ injection in the str. oriens, str. pyramidale, and str. radiatum of the CA1 region of the hippocampus. Microglial activation seems to precede both tau hyperphosphorylation (Yoshiyama et al., 2007) and NFT formation (Maphis et al., 2016) and this might explain why, despite other changes, there is no p-tau pathology at day 3 after injection of $A\beta_{1-42}$. The mechanism by which Aβ induces the activation of p-tau-dependent degeneration pathways in the cell has been widely investigated (Hurtado et al., 2010; Hu et al., 2014; Bennett et al., 2017). Hu et al. (2014) provide support for our conclusions as they demonstrated intra-hippocampal injection of aggregation susceptible $A\beta_{1-42}$, but not $A\beta_{1-40}$, in mice is responsible for the subsequent p-tau pathology of cell loss (Hu et al., 2014). Microglia may regulate tau phosphorylation through the microglial-specific fractalkine receptor (CX3CR1; Bhaskar et al., 2010). The ligand CX3CL1 is by contrast exclusively expressed by neurons and so neuron-microglia crosstalk likely precedes the p-tau pathology in AD. Indeed, disruption of the CX3CL1-CX3CR1 association has been shown to have a neuroprotective effect in a triple Tg AD mouse model (Fuhrmann et al., 2010).

Apart from contributions to both neuronal cell and synapse loss in the AD brain, p-tau pathology affects the generation of hippocampal theta oscillations, underlying the dysfunctional network circuitry in a triple Tg AD mouse model. A recent study reported that early tau pathology in the triple Tg AD mouse model resulted in a reduction in theta oscillations and overall excitability in the CA1 region of the hippocampus; perhaps as a compensatory mechanism for the prevention of Aβ-induced NMDA-mediated overexcitation (Mondragón-Rodríguez et al., 2018). Additionally, the accumulation of p-tau in parvalbumin-positive interneurons may also influence the changes in hippocampal activity and functionality (Soler et al., 2017). The tau pathology observed in the hippocampus and the activation of microglia might be one of the factors contributing to neurotoxicity and pyramidal cell loss in the CA1 region. While activation of microglia was observed further away from the injection site 3-day post $A\beta_{1-42}$ injection, long-distance spreading from the injection site of the p-tau protein along the CA1 region was not found, indicating a longer-term activation of microglia might be required to trigger p-tau pathology. At day 30, p-tau correlates with the number of activated astrocytes and microglia at the injection site, but not at day 3 or adjacent to the injection site at day 30 where we did not observe activation of these cells.

Inflammatory Changes in $A\beta_{1-42}$-Injected Mice

$A\beta_{1-42}$-induced inflammatory responses were confirmed by the local up-regulation of GFAP levels at day 3, as well as up-regulation of GFAP and Iba-1 levels by day 30, in $A\beta_{1-42}$-injected mice compared with controls. Whereas control mice displayed sparse resting astrocytes, $A\beta_{1-42}$-injected mice had an increased number of astrocytes with highly reactive morphologies depicted by numerous branching, elongated processes, and hypertrophic cell bodies. Astrogliosis, observable at day 3 and still present by day 30, occurred in the absence of significant increases in the immunoreactivity of the chemotactic factors IP-10 and MCP-1. Some studies have shown MCP-1 labeling near senile Aβ plaques, as well as reactive astrocytes expressing IP-10 in AD (McLarnon, 2012). Therefore, we hypothesize that the local acute inflammation following a single $A\beta_{1-42}$ injection might not be sufficient to trigger the detectable production of chemotactic factors in the mouse hippocampus,

as chemotactic factors in AD have been observed only during chronic neuroinflammation (McLarnon, 2012).

The activation of astrocytes seen on day 3 at the injection site was not maintained at an adjacent location until day 30. A previous study of Aβ-injection in a rat model showed that significantly elevated GFAP levels were observed 1 day after soluble Aβ injection, but not at day 30 (Weldon et al., 1998). We hypothesize that the system might be self-regulating with compensatory mechanisms for the inflammatory process in the proximity of the injection site and that acute astrocyte activation after $A\beta_{1-42}$ injection could be transient. Activated astrocytes surrounding and isolating Aβ aggregates might represent the beginning of the Aβ clearance. On the other hand, the observed microglia activation responses on day 3 and day 30 post-injection had also occurred, which implies a phagocytic role for the microglia after the $A\beta_{1-42}$ injection. Relationships between Aβ, neurons, astrocytes, and microglia in the AD brain are complex and should be further investigated.

Vascular Changes in $A\beta_{1-42}$-Injected Mice

$A\beta_{1-42}$-injected mice also displayed signs of early vascular dysfunction by day 3 as revealed by the up-regulation of the endothelial cell marker CD31 in the str. radiatum of the CA1 region of the hippocampus. Consistent with this, early endothelial cell dysfunction has already been seen in other mouse models of AD (Lee et al., 2018a,b) and also in AD patients (Kelleher and Soiza, 2013), suggesting early alterations in blood flow regulation and in BBB permeability. Aβ-mediated increase in reactive oxygen species generation could lead to endothelial cell dysfunction through the alteration of endothelial tight junctions (Carrano et al., 2011). The acute up-regulation of the CD31 levels seen in this study might play a role in counteracting early Aβ-mediated effects on the endothelial cell and/or be involved with an early inflammatory process around the BBB. At this stage, the beginning of a disruptive process might affect BBB integrity.

Importantly, the early vascular dysfunction seen in $A\beta_{1-42}$-injected mice is maintained up to day 30, and at this time point, CD31 labeling intensity was increased in the str. pyramidale and str. radiatum of the CA1 region of the hippocampus. In contrast to our results, reduced CD31 density was observed in 9-month-old Tg APP mice (Lee et al., 2018b), and Religa and colleagues demonstrated an inverse correlation between the number of plaques and CD31-labeled vessel density, which indicates that $A\beta_{1-42}$ destroys the integrity of the BBB. They further suggested that $A\beta_{1-42}$ led to apoptosis of endothelial and smooth muscle cells in AD patients and Tg TCRND8 APP mice (Religa et al., 2013). This apparent conflict with our findings might be resolved if the localized up-regulation of CD31 we observed is a compensatory molecular mechanism to re-establish homeostasis of the BBB, and to compensate for the loss of endothelial cells in cerebral capillaries during AD. Interestingly, tau overexpression affected endothelial cell functionality, as well as inducing vascular remodeling in a Tg AD mouse model (Bennett et al., 2018). Thus, local up-regulation of p-tau levels at the injection site in the present study may contribute to the dysfunction of endothelial cells in the BBB of $A\beta_{1-42}$-injected mice. Indeed, p-tau levels show a positive correlation with CD31 levels on day 30 after $A\beta_{1-42}$ injection.

Essential for the maintenance of vascular integrity in the brain, α-SMA has been extensively investigated in the context of AD pathogenesis. Here we report up-regulated α-SMA levels at the injection site in the CA1 region of the hippocampus in $A\beta_{1-42}$-injected mice at day 30 post-injection. Furthermore, this up-regulation of α-SMA spread along the entire CA1 region. A lower degree of α-SMA immunostaining was found in the blood vessels of AD patients compared to controls (Ervin et al., 2004) but also increased expression of α-SMA in preclinical AD cases (Ervin et al., 2004). Consistent with our results, another AD mouse model was found to express high α-SMA immunostaining near Aβ plaques in the blood vessels in the cortex (Hutter-Schmid and Humpel, 2016). In preliminary studies, we have also detected an increase in α-SMA immunostaining in the middle temporal cortex of AD cases using tissue microarray methods (Austria et al., unpublished). It has been shown that smooth muscle cells undergo degeneration and atrophy during AD (Farkas and Luiten, 2001); therefore, the up-regulated α-SMA levels observed here might be an indicator of a systemic compensatory mechanism. Alternatively, since α-SMA regulates blood vessel contraction, its expression may be up-regulated to counteract any early dysfunction in blood flow occurring following $A\beta_{1-42}$'injection.

In the present study, up-regulated fibrinogen labeling at day 3 post-injection was also observed in the str. oriens of the CA1 region of the hippocampus. Three Tg AD mouse models, TgCRND8, PDAPP, and Tg2576, also have high levels of fibrinogen (Paul et al., 2007); confirming the contribution of fibrinogen to the pathology of AD, mostly *via* inflammatory processes. In agreement with this, in mouse models overexpressing APP in which fibrinogen was eliminated, microgliosis was found to be reduced (Paul et al., 2007). Fibrinogen infiltration and microglial reactivity have also been observed in $A\beta_{1-42}$ intrahippocampal injected rodent brains and the human AD brain (Ryu and McLarnon, 2009). Indeed, increased fibrinogen density at day 3 shows a positive correlation with increased astrogliosis and microglia activation at day 3 after $A\beta_{1-42}$ injection. Furthermore, increased fibrinogen deposition in $A\beta_{1-42}$-injected mice might promote microvascular permeability through a negative effect on endothelial tight junction proteins (Tyagi et al., 2008), resulting in the accumulation of fibrinogen outside of circulation. Another possible mechanism by which fibrinogen could mediate BBB disruption is by affecting the accumulation and/or clearance process of Aβ in the vessels. Indeed, when fibrinogen levels were reduced in TgCRND8 AD mice, cerebral amyloid angiopathy was significantly diminished and reduced fibrinogen levels were linked to significant improvement in spatial memory (Cortes-Canteli et al., 2010). This finding indicates that one of the multiple factors associated with cognitive decline in the present AD mouse model could be the infiltration of fibrinogen into the hippocampal areas of the brain of $A\beta_{1-42}$-injected mice, with the subsequent associated pathological events.

Cognitive and Behavioral Changes in $A\beta_{1-42}$-Injected Mice

A large number of Aβ-injected AD rodent models have demonstrated cognitive decline after infusion of the neurotoxic Aβ into rodent brains (Yamada et al., 1999; Nakamura et al., 2001; Tohda et al., 2003; Tsukuda et al., 2009; Takeda et al., 2014; Sadigh-Eteghad et al., 2015; Faucher et al., 2016). Spatial memory impairment is likely a result of the effects of increased Aβ concentrations at localized sites, confirmed by Aβ administration through both the i.c.v (Tsukuda et al., 2009; Kasza et al., 2017; Schmid et al., 2017) and hippocampal routes (Xuan et al., 2012).

Much evidence has shown that spatial memory impairment is caused by Aβ deposition and the subsequent synaptic dysfunction, among other Aβ-mediated effects, in the hippocampal area (Balducci et al., 2010). Exploration of novel objects is a critical approach to assess hippocampal-dependent spatial memory in AD rodent models. Our results demonstrate that $A\beta_{1-42}$-injected mice showed hippocampal-dependent spatial memory impairment, as indicated by the results of the NOA, NOR and MWM tests on days 3 (Yeung et al., 2020b) and 30 post-injection, respectively. Previous studies have reported cognitive decline after Aβ infusion into rodent brains, assessed by NOR. $A\beta_{1-42}$-mediated impairment of long-term spatial recognition memory was reported following a single injection of neurotoxic $A\beta_{1-42}$ (i.c.v) into male C57BL/6 mice (Balducci et al., 2010). Takeda and colleagues found only very transient cognitive impairment after infusion of $A\beta_{1-42}$ into the DG region of rats using the NOR test, and it was found to be associated with decreased long-term potentiation (LTP; Takeda et al., 2014). The short duration of the cognitive impairment indicates that the Aβ-mediated effect might vary among different areas of the hippocampus. Unlike this finding, our results demonstrated long-lasting $A\beta_{1-42}$ effects on cognition, with the MWM test performed 20 days after the injection showing long-term spatial memory impairment in $A\beta_{1-42}$-injected mice.

The MWM test is one of the most robust and most popular cognitive tests to assess hippocampal-dependent spatial memory (Tsukuda et al., 2009; Xuan et al., 2012; Esfandiary et al., 2015). We demonstrated that $A\beta_{1-42}$-injected mice spent significantly less time in the platform quadrant than control mice during the last 2 days of the MWM test. In agreement with our findings, Xuan and colleagues also reported spatial memory impairment (using the MWM test) following the injection of $A\beta_{1-40}$ into the dentate gyrus of the hippocampus of rats (Xuan et al., 2012). They observed astrogliosis and microgliosis in the hippocampus of the $A\beta_{1-40}$-injected rats, consistent with our results in $A\beta_{1-42}$-injected mice. Cognitive deficits were also demonstrated in $A\beta_{25-35}$-injected mice (i.c.v administration) by the MWM test. Esfandiary and colleagues also demonstrated spatial-memory impairment (assessed by the MWM test) in an AD mouse model in which $A\beta_{1-42}$ was intra-hippocampally injected into the CA1 region of the mice. In agreement with our findings, this study failed to demonstrate impairment in non-spatial memory, according to assessment with the passive avoidance test (Esfandiary et al., 2015). $A\beta_{1-42}$ injection (i.c.v) in rats also resulted in cognitive deficits according to the MWM test (Zhang et al., 2015).

We did not find significant short-term spatial memory deficits with the YM test in $A\beta_{1-42}$-injected mice, although there was a trend towards decreased alternations. Huh et al. (2014) found the percentage of alternations in mice where the DG was intra-hippocampally injected with $A\beta_{1-42}$ was significantly lower than in the control group. Other studies have confirmed this with $A\beta_{1-42}$-i.c.v injected mice (Yan et al., 2001) and rats (Zhang et al., 2015). Thus, the YM test might be a valid method to assess cognitive impairment in short-term memory induced by $A\beta_{1-42}$ in rodent models.

In our study, no significant deficits were observed in non-spatial memory in the $A\beta_{1-42}$-injected mice, utilizing the passive avoidance test (Esfandiary et al., 2015). These findings imply that the hippocampus might not be overly involved with non-spatial memory processes (Cave and Squire, 1991) and that Aβ affects only hippocampal-dependent memory processes. The passive avoidance test is used to assess a type of contextual memory which partly involves processing in the CA3 region of the hippocampus (Daumas et al., 2004) but our model is based on a single $A\beta_{1-42}$ injection into the CA1 region, and that the CA1 area might be more critical in recognizing the novelty or familiarity of an object rather than contextual related-memories (Nakazawa et al., 2004; Daumas et al., 2005). This type of non-spatial memory likely remains unaffected in our experiments. An earlier study found that soon after $A\beta_{1-42}$ i.c.v injection (day 1 and 7), mice exhibited deteriorated long-term non-spatial memory (Yan et al., 2001). Differences in the injected brain area, along with slight variations in the behavioral task design, might be factors that can potentially contribute to the divergence of results to those found in the literature.

The observed short-term spatial memory deficits correlate with p-tau, inflammatory and vascular pathology. Cognitive performance of $A\beta_{1-42}$-injected mice showed a negative correlation with p-tau density, the number of activated astrocytes and microglia, and CD31 density. Most likely all these pathological changes are contributing factors to the cognitive deficits observed in these mice along with other molecular and cellular deficits. Short-term spatial memory deficits at day 3 occur before any significant neuronal loss (Yeung et al., 2020a), suggesting that all these pathological changes are sufficient to impair neural activity and information processing. The hippocampal $A\beta_{1-42}$ injection in our study likely results in dysfunctional neural networks within the CA1, CA3 and the dentate gyrus, as there are widespread and complex interconnections within these hippocampal regions (Amaral et al., 2007). Likewise, it is well known that tau and amyloid can propagate throughout synaptically connected networks in the hippocampus (Cirrito et al., 2005; de Calignon et al., 2012). The physiological changes induced directly by $A\beta_{1-42}$ throughout the hippocampus and other brain areas have been extensively studied but the link of network dysfunction with the complex pathological and behavioral changes needs to be further explored in future experiments.

In summary, our study shows that a single Aβ injection can reproduce aspects of the molecular, cellular, and vascular changes occurring in the AD human brain and can lead to cognitive deficits. We have demonstrated that not only classic Aβ and tau pathology features of AD contribute to the cognitive decline, but that neuroinflammation and vascular pathology may also play a key role in hippocampal-memory and learning deficits in AD.

DATA AVAILABILITY STATEMENT

All datasets presented in this study are included in the article.

ETHICS STATEMENT

The animal study was reviewed and approved by the University of Otago Animal Ethics Committee and the University of Auckland Animal Ethics Committee.

AUTHOR CONTRIBUTIONS

BC-F, TC, TP, SW, KP, and AK: performed research. BC-F, TC, TP, SW, KP, JB, and AK: analyzed data. BC-F, TC, WT, HW, RF, and AK: wrote the article. WT, MD, and AK: designed research. MD, RF, and AK: funding acquisition. AK: project administration. WT, HW, RF, and AK: supervision. All authors contributed to the article and approved the submitted version.

FUNDING

This work was supported by Alzheimer's New Zealand Charitable Trust (AK; 3720863); Alzheimer's New Zealand (AK; 3718869); Freemasons New Zealand (AK; 3719321); Aotearoa Foundation, Centre for Brain Research, University of Auckland (AK; 3705579); Brain Research New Zealand (BC-F, HW, RF, AK; 3710638); Health Research Council of New Zealand (MD, RF, HW; 3627373), Neurological Foundation of New Zealand (AK and TP; 848010).

ACKNOWLEDGMENTS

We thank Kristina Hubbard, Jacqueline Ross and Marika Eszes for their excellent work and assistance, and members of the Hercus Taieri Resource Unit, University of Otago, and Vernon Jansen Unit, University of Auckland also for their excellent work.

REFERENCES

Amaral, D. G., Scharfman, H. E., and Lavenex, P. (2007). The dentate gyrus: fundamental neuroanatomical organization (dentate gyrus for dummies). *Prog. Brain Res.* 163, 3–22. doi: 10.1016/S0079-6123(07)63001-5

Arbel-Ornath, M., Hudry, E., Boivin, J. R., Hashimoto, T., Takeda, S., Kuchibhotla, K. V., et al. (2017). Soluble oligomeric amyloid-β induces calcium dyshomeostasis that precedes synapse loss in the living mouse brain. *Mol. Neurodegener.* 12:27. doi: 10.1186/s13024-017-0169-9

Arriagada, P. V., Growdon, J. H., Hedley-Whyte, E. T., and Hyman, B. T. (1992). Neurofibrillary tangles but not senile plaques parallel duration and severity of Alzheimer's disease. *Neurology* 42, 631–639. doi: 10.1212/wnl.42.3.631

Balducci, C., Beeg, M., Stravalaci, M., Bastone, A., Sclip, A., Biasini, E., et al. (2010). Synthetic amyloid-β oligomers impair long-term memory independently of cellular prion protein. *Proc. Natl. Acad. Sci. U S A* 107, 2295–2300. doi: 10.1073/pnas.0911829107

Baluchnejadmojara, D. T., Mohamadi-Zarch, S., and Roghani, M. (2019). Safranal, an active ingredient of saffron, attenuates cognitive deficits in amyloid β-induced rat model of Alzheimer's disease: underlying mechanisms metabolic brain disease. *Metab. Brain Dis.* 34, 1747–1759. doi: 10.1073/pnas.0911829107

Behl, C., Widmann, M., Trapp, T., and Holsboer, F. (1995). 17-β estradiol protects neurons from oxidative stress-induced cell death *in vitro*. *Biochem. Biophys. Res. Commun.* 216, 473–482. doi: 10.1006/bbrc.1995.2647

Bekris, L. M., Yu, C.-E., Bird, T. D., and Tsuang, D. W. (2010). Genetics of Alzheimer disease. *J. Geriatr. Psychiatry Neurol.* 23, 213–227. doi: 10.1177/0891988710383571

Bennett, R. E., DeVos, S. L., Dujardin, S., Corjuc, B., Gor, R., Gonzalez, J., et al (2017). Enhanced tau aggregation in the presence of amyloid-β. *Am. J. Pathol.* 187, 1601–1612. doi: 10.1016/j.ajpath.2017.03.011

Bennett, R. E., Robbins, A. B., Hu, M., Cao, X., Betensky, R. A., Clark, T., et al. (2018). Tau induces blood vessel abnormalities and angiogenesis-related gene expression in P301L transgenic mice and human Alzheimer's disease. *Proc. Natl. Acad. Sci. U S A* 115:E1289. doi: 10.1073/pnas.1710329115

Bettcher, B. M., Neuhaus, J., Wynn, M. J., Elahi, F. M., Casaletto, K. B., Saloner, R., et al. (2019). Increases in a pro-inflammatory chemokine, MCP-1, are related to decreases in memory over time. *Front. Aging Neurosci.* 11, 25–25. doi: 10.3389/fnagi.2019.00025

Bhaskar, K., Konerth, M., Kokiko-Cochran, O. N., Cardona, A., Ransohoff, R. M., and Lamb, B. T. (2010). Regulation of tau pathology by the microglial fractalkine receptor. *Neuron* 68, 19–31. doi: 10.1016/j.neuron.2010.08.023

Boche, D., and Nicoll, J. A. R. (2020). Understanding cause and effect in Alzheimer's pathophysiology: implications for clinical trials. *Neuropathol. Appl. Neurobiol.* doi: 10.1111/nan.12642.

Boche, D., Perry, V. H., and Nicoll, J. A. R. (2013). Review: activation patterns of microglia and their identification in the human brain. *Neuropathol. Appl. Neurobiol.* 39, 3–18. doi: 10.1111/nan.12011

Boyd-Kimball, D., Sultana, R., Poon, H. F., Lynn, B., Casamenti, F., Pepeu, G., et al. (2005). Proteomic identification of proteins specifically oxidized by intracerebral injection of amyloid-β-peptide (1–42) into rat brain: implications for Alzheimer's disease. *Neuroscience* 132, 313–324. doi: 10.1016/j.neuroscience.2004.12.022

Brouillette, J., Caillierez, R., Zommer, N., Alves-Pires, C., Benilova, I., Blum, D., et al. (2012). Neurotoxicity and memory deficits induced by soluble low-molecular-weight amyloid-β_{1-42} oligomers are revealed *in vivo* by using a novel animal model. *J. Neurosci.* 32, 7852–7861. doi: 10.1523/jneurosci.5901-11.2012

Brun, A., and Englun, E. (1981). Regional pattern of degeneration in Alzheimer's disease: neuronal loss and histopathological grading. *Histopathology* 5, 549–564. doi: 10.1111/j.1365-2559.1981.tb01818.x

Calvo-Flores Guzmán, B., Kim, S., Chawdhary, B., Peppercorn, K., Tate, W. P., Waldvogel, H. J., et al. (2020). Amyloid-β_{1-42}-induced increase in GABAergic tonic conductance in mouse hippocampal CA1 pyramidal cells. *Molecules* 25:693.

Carrano, A., Hoozemans, J. J., van der Vies, S. M., Rozemuller, A. J., van Horssen, J., and de Vries, H. E. (2011). Amyloid Beta induces oxidative stress-mediated blood-brain barrier changes in capillary amyloid angiopathy. *Antioxid. Redox Signal.* 15, 1167–1178. doi: 10.1089/ars.2011.3895

Cave, C. B., and Squire, L. R. (1991). Equivalent impairment of spatial and nonspatial memory following damage to the human hippocampus. *Hippocampus* 1, 329–340. doi: 10.1002/hipo.450010323

Cetin, F., Yazihan, N., Dincer, S., and Akbulut, G. (2013). The effect of intracerebroventricular injection of beta amyloid peptide (1–42) on caspase-3 activity, lipid peroxidation, nitric oxide and NOS expression in young adult and aged rat brain. *Turk. Neurosurg.* 23, 144–150. doi: 10.5137/1019-5149.Jtn.5855-12.1

Chen, J.-H., Ke, K.-F., Lu, J.-H., Qiu, Y.-H., and Peng, Y.-P. (2015). Protection of TGF-β against neuroinflammation and neurodegeneration in Aβ1–42-induced

Alzheimer's disease model rats. *PLoS One* 10:e0116549. doi: 10.1371/journal.pone.0116549

Cirrito, J. R., Yamada, K. A., Finn, M. B., Sloviter, R. S., Bales, K. R., May, P. C., et al. (2005). Synaptic activity regulates interstitial fluid amyloid-beta levels *in vivo*. *Neuron* 48, 913–922. doi: 10.1016/j.neuron.2005.10.028

Conductier, G., Blondeau, N., Guyon, A., Nahon, J. L., and Rovere, C. (2010). The role of monocyte chemoattractant protein MCP1/CCL2 in neuroinflammatory diseases. *J. Neuroimmunol.* 224, 93–100. doi: 10.1016/j.jneuroim.2010.05.010

Cortes-Canteli, M., Paul, J., Norris, E. H., Bronstein, R., Ahn, H. J., Zamolodchikov, D., et al. (2010). Fibrinogen and β-amyloid association alters thrombosis and fibrinolysis: a possible contributing factor to Alzheimer's disease. *Neuron* 66, 695–709. doi: 10.1016/j.neuron.2010.05.014

Cortes-Canteli, M., Zamolodchikov, D., Ahn, H., Strickland, S., and Norris, E. (2012). Fibrinogen and altered hemostasis in Alzheimer's disease. *J. Alzheimers Dis.* 32, 599–608. doi: 10.3233/JAD-2012-120820

Daumas, S., Halley, H., and Lassalle, J.-M. (2004). Disruption of hippocampal CA3 network: effects on episodic-like memory processing in C57BL/6J mice. *Eur. J. Neurosci.* 20, 597–600. doi: 10.1111/j.1460-9568.2004.03484.x

Daumas, S., Halley, H., Francés, B., and Lassalle, J.-M. (2005). Encoding, consolidation and retrieval of contextual memory: differential involvement of dorsal CA3 and CA1 hippocampal subregions. *Learn. Mem.* 12, 375–382. doi: 10.1101/lm.81905

de Calignon, A., Polydoro, M., Suarez-Calvet, M., William, C., Adamowicz, D. H., Kopeikina, K. J., et al. (2012). Propagation of tau pathology in a model of early Alzheimer's disease. *Neuron* 73, 685–697. doi: 10.1016/j.neuron.2011.11.033

D'Hooge, R., and De Deyn, P. P. (2001). Applications of the Morris water maze in the study of learning and memory. *Brain Res. Brain Res. Rev.* 36, 60–90. doi: 10.1016/s0165-0173(01)00067-4

Drummond, E., and Wisniewski, T. (2017). Alzheimer's disease: experimental models and reality. *Acta Neuropathol.* 133, 155–175. doi: 10.1007/s00401-016-1662-x

Erickson, M. A., and Banks, W. A. (2013). Blood-brain barrier dysfunction as a cause and consequence of Alzheimer's disease. *J. Cereb. Blood Flow Metab.* 33, 1500–1513. doi: 10.1038/jcbfm.2013.135

Ervin, J. F., Pannell, C., Szymanski, M., Welsh-Bohmer, K., Schmechel, D. E., and Hulette, C. M. (2004). Vascular smooth muscle actin is reduced in Alzheimer disease brain: a quantitative analysis. *J. Neuropathol Exp. Neurol.* 63, 735–741. doi: 10.1093/jnen/63.7.735

Esfandiary, E., Karimipour, M., Mardani, M., Ghanadian, M., Alaei, H. A., Mohammadnejad, D., et al. (2015). Neuroprotective effects of *Rosa damascena* extract on learning and memory in a rat model of amyloid-β-induced Alzheimer's disease. *Adv. Biomed. Res.* 4:131. doi: 10.4103/2277-9175.161512

Facchinetti, R., Bronzuoli, M. R., and Scuderi, C. (2018). An animal model of Alzheimer disease based on the intrahippocampal injection of amyloid β-peptide (1–42). *Methods Mol. Biol.* 1727, 343–352. doi: 10.1007/978-1-4939-7571-6_25

Farfara, D., Lifshitz, V., and Frenkel, D. (2008). Neuroprotective and neurotoxic properties of glial cells in the pathogenesis of Alzheimer's disease. *J. Cell. Mol. Med.* 12, 762–780. doi: 10.1111/j.1582-4934.2008.00314.x

Farkas, E., and Luiten, P. G. (2001). Cerebral microvascular pathology in aging and Alzheimer's disease. *Prog. Neurobiol.* 64, 575–611. doi: 10.1016/s0301-0082(00)00068-x

Faucher, P., Mons, N., Micheau, J., Louis, C., and Beracochea, D. J. (2016). Hippocampal injections of oligomeric amyloid β-peptide (1–42) induce selective working memory deficits and long-lasting alterations of ERK signaling pathway. *Front. Aging Neurosci.* 7, 245–245. doi: 10.3389/fnagi.2015.00245

Franco, R., and Cedazo-Minguez, A. (2014). Successful therapies for Alzheimer's disease: why so many in animal models and none in humans? *Front. Pharmacol.* 5:146. doi: 10.3389/fphar.2014.00146

Fuhrer, T. E., Palpagama, T. H., Waldvogel, H. J., Synek, B. J. L., Turner, C., Faull, R. L., et al. (2017). Impaired expression of GABA transporters in the human Alzheimer's disease hippocampus, subiculum, entorhinal cortex and superior temporal gyrus. *Neuroscience* 351, 108–118. doi: 10.1016/j.neuroscience.2017.03.041

Fuhrmann, M., Bittner, T., Jung, C. K. E., Burgold, S., Page, R. M., Mitteregger, G., et al. (2010). Microglial Cx3cr1 knockout prevents neuron loss in a mouse model of Alzheimer's disease. *Nat. Neurosci.* 13, 411–413. doi: 10.1038/nn.2511

Glenn, J. A., Ward, S. A., Stone, C. R., Booth, P. L., and Thomas, W. E. (1992). Characterisation of ramified microglial cells: detailed morphology, morphological plasticity and proliferative capability. *J. Anat.* 180, 109–118.

Govindpani, K., Calvo-Flores Guzmán, B., Vinnakota, C., Waldvogel, H. J., Faull, R. L., and Kwakowsky, A. (2017). Towards a better understanding of GABAergic remodeling in Alzheimer's disease. *Int. J. Mol. Sci.* 18:1813. doi: 10.3390/ijms18081813

Govindpani, K., McNamara, L. G., Smith, N. R., Vinnakota, C., Waldvogel, H. J., Faull, R. L., et al. (2019). Vascular dysfunction in Alzheimer's disease: a prelude to the pathological process or a consequence of it? *J. Clin. Med.* 8:651. doi: 10.3390/jcm8050651

Govindpani, K., Vinnakota, C., Waldvogel, H. J., Faull, R. L., and Kwakowsky, A. (2020). Vascular dysfunction in Alzheimer's disease: a biomarker of disease progression and a potential therapeutic target. *Neural Regen. Res.* 15, 1030–1032. doi: 10.4103/1673-5374.270306

Hardy, J., and Selkoe, D. J. (2002). The amyloid hypothesis of Alzheimer's disease: progress and problems on the road to therapeutics. *Science* 297, 353–356. doi: 10.1126/science.1072994

Harris, S. S., Wolf, F., De Stooper, B., and Busche, M. A. (2020). Tipping the scales: peptide-dependent dysregulation of neural circuit dynamics in Alzheimer's disease. *Neuron* 107, 417–435. doi: 10.1016/j.neuron.2020.06.005.

Hillen, H. (2019). The beta amyloid dysfunction (BAD) hypothesis for Alzheimer's disease. *Front. Neurosci.* 13:1154. doi: 10.3389/fnins.2019.01154

Hu, X., Li, X., Zhao, M., Gottesdiener, A., Luo, W., and Paul, S. (2014). Tau pathogenesis is promoted by $A\beta_{1-42}$ but not $A\beta_{1-40}$. *Mol. Neurodegener.* 9:52. doi: 10.1186/1750-1326-9-52

Huang, Y., and Mucke, L. (2012). Alzheimer mechanisms and therapeutic strategies. *Cell* 148, 1204–1222.

Huber, C. M., Yee, C., May, T., Dhanala, A., and Mitchell, C. S. (2017). Cognitive decline in preclinical Alzheimer's disease: amyloid-β versus tauopathy. *J. Alzheimers Dis.* 61, 265–281. doi: 10.3233/JAD-170490

Huh, E., Kim, H. G., Park, H., Kang, M. S., Lee, B., and Oh, M. S. (2014). Houttuynia cordata improves cognitive deficits in cholinergic dysfunction Alzheimer's disease-like models. *Biomol. Ther.* 22, 176–183. doi: 10.4062/biomolther.2014.040

Hurtado, D. E., Molina-Porcel, L., Iba, M., Aboagye, A. K., Paul, S. M., Trojanowski, J. Q., et al (2010). Aβ accelerates the spatiotemporal progression of tau pathology and augments tau amyloidosis in an alzheimer mouse model. *Am. J. Pathol.* 177, 1977–1988. doi: 10.2353/ajpath.2010.100346.

Hutter-Schmid, B., and Humpel, C. (2016). Alpha-smooth muscle actin mRNA and protein are increased in isolated brain vessel extracts of Alzheimer mice. *Pharmacology* 98, 251–260. doi: 10.1159/000448007

Kamphuis, W., Mamber, C., Moeton, M., Kooijman, L., Sluijs, J. A., Jansen, A. H., et al. (2012). GFAP isoforms in adult mouse brain with a focus on neurogenic astrocytes and reactive astrogliosis in mouse models of Alzheimer disease. *PLoS One* 7:e42823. doi: 10.1371/journal.pone.0042823

Karran, E., Mercken, M., and De Strooper, B. (2011). The amyloid cascade hypothesis for Alzheimer's disease: an appraisal for the development of therapeutics. *Nat. Rev. Drug Discov.* 10, 698–712. doi: 10.1038/nrd3505

Kasza, Á., Penke, B., Frank, Z., Bozsó, Z., Szegedi, V., Hunya, Á., et al. (2017). Studies for improving a rat model of Alzheimer's disease: Icv administration of well-characterized β-amyloid 1–42 oligomers induce dysfunction in spatial memory. *Molecules* 22:2007. doi: 10.3390/molecules22112007

Kelleher, R. J., and Soiza, R. L. (2013). Evidence of endothelial dysfunction in the development of Alzheimer's disease: Is Alzheimer's a vascular disorder? *Am. J. Cardiovasc Dis.* 3, 197–226.

Klein, A. M., Kowall, N. W., and Ferrante, R. J. (1999). Neurotoxicity and oxidative damage of beta amyloid 1–42 versus beta amyloid 1–40 in the mouse cerebral cortex. *Ann. N Y Acad. Sci.* 893, 314–320. doi: 10.1111/j.1749-6632.1999.tb07845.x

Kruger, L., and Mandelkow, E. M. (2015). Tau neurotoxicity and rescue in animal models of human Tauopathies. *Curr Opin Neurobiol* 36, 52–58. doi: 10.1016/j.conb.2015.09.004

Kwakowsky, A., Calvo-Flores Guzman, B., Pandya, M., Turner, C., Waldvogel, H. J., and Faull, R. L. (2018). GABAA receptor subunit expression changes in the human Alzheimer's disease hippocampus, subiculum, entorhinal cortex and superior temporal gyrus. *J. Neurochem.* 145, 374–392. doi: 10.1111/jnc.14325

Kwakowsky, A., Potapov, K., Kim, S., Peppercorn, K., Tate, W. P., and Abraham, I. M. (2016). Treatment of beta amyloid 1–42 ($A\beta_{1-42}$)-induced basal forebrain cholinergic damage by a non-classical estrogen signaling activator *in vivo*. *Sci. Rep.* 6:21101. doi: 10.1038/srep21101

Kwakowsky, A., Waldvogel, H. J., and Faull, R. L. M. (2020). Therapeutic potential of a5 subunit containing GABAA receptors in Alzheimer's disease. *Neural Regener. Res.* 16:2021.

Lee, D., Cho, S. -J., Lim, H. J., Seok, J., Jo, C., Jo, S. A., et al. (2018a). Alteration of vascular endothelial cadherin in Alzheimer's disease patient and mouse model. *BioRxiv* 430140. doi: 10.1101/430140

Lee, W. J., Liao, Y. C., Wang, Y. F., Lin, I. F., Wang, S. J., and Fuh, J. L. (2018b). Plasma MCP-1 and cognitive decline in patients with Alzheimer's disease and mild cognitive impairment: a two-year follow-up study. *Sc.i Rep.* 8:1280. doi: 10.1038/s41598-018-19807-y

Lee, J. W., Lee, Y. K., Yuk, D. Y., Choi, D. Y., Ban, S. B., Oh, K. W., et al. (2008). Neuro-inflammation induced by lipopolysaccharide causes cognitive impairment through enhancement of beta-amyloid generation. *J. Neuroinflammation* 5, 37–37. doi: 10.1186/1742-2094-5-37

Leung, R., Proitsi, P., Simmons, A., Lunnon, K., Güntert, A., Kronenberg, D., et al. (2013). Inflammatory proteins in plasma are associated with severity of Alzheimer's disease. *PLoS One* 8:e64971. doi: 10.1371/journal.pone.0064971

Limon, A., Reyes-Ruiz, J. M., and Miledi, R. (2012). Loss of functional GABA(A) receptors in the Alzheimer diseased brain. *Proc. Natl. Acad. Sci. U S A* 109, 10071–10076. doi: 10.1073/pnas.1204606109

Liu, J., Gao, X., and Wu, Y. (2008). N-Methyl-*D*-aspartate receptors mediate excitotoxicity in amyloid beta-induced synaptic pathology of Alzheimer's disease. *Neuroembryol. Aging* 5, 134–143. doi: 10.1159/000193851

Llorian, M., Gooding, C., Bellora, N., Hallegger, M., Buckroyd, A., Wang, X., et al. (2016). The alternative splicing program of differentiated smooth muscle cells involves concerted non-productive splicing of post-transcriptional regulators. *Nucleic Acids Res.* 44, 8933–8950. doi: 10.1093/nar/gkw560

Maphis, N., Jiang, S., Xu, G., Kokiko-Cochran, O. N., Roy, S. M., Van Eldik, L. J., et al. (2016). Selective suppression of the α isoform of p38 MAPK rescues late-stage tau pathology. *Alzheimers Res. Ther.* 8:54. doi: 10.1186/s13195-016-0221-y

Marczynski, T. J. (1998). GABAergic deafferentation hypothesis of brain aging and Alzheimer's disease revisited. *Brain Res. Bull.* 45, 341–379. doi: 10.1016/s0361-9230(97)00347-x

Marín-Teva, J. L., Cuadros, M. A., Martín-Oliva, D., and Navascués, J. (2011). Microglia and neuronal cell death. *Neuron Glia Biol.* 7, 25–40. doi: 10.1017/s1740925x12000014

McLarnon, J. G. (2012). Microglial chemotactic signaling factors in Alzheimer's disease. *Am. J. Neurodegener Dis.* 1, 199–204.

Mondragón-Rodríguez, S., Salas-Gallardo, A., González-Pereyra, P., Macías, M., Ordaz, B., Peña-Ortega, F., et al. (2018). Phosphorylation of Tau protein correlates with changes in hippocampal theta oscillations and reduces hippocampal excitability in Alzheimer's model. *J. Biol. Chem.* 293, 8462–8472. doi: 10.1074/jbc.RA117.001187

Mudò, G., Frinchi, M., Nuzzo, D., Scaduto, P., Plescia, F., Massenti, M. F., et al. (2019). Anti-inflammatory and cognitive effects of interferon-β1a (IFNβ1a) in a rat model of Alzheimer's disease. *J. Neuroinflammation* 16:44. doi: 10.1186/s12974-019-1417-4.

Muoio, V., Persson, P. B., and Sendeski, M. M. (2014). The neurovascular unit – concept review. *Acta Physiol.* 210, 790–798. doi: 10.1111/apha.12250

Nakamura, S., Murayama, N., Noshita, T., Annoura, H., and Ohno, T. (2001). Progressive brain dysfunction following intracerebroventricular infusion of beta1–42-amyloid peptide. *Brain Res.* 912, 128–136. doi: 10.1016/s0006-8993(01)02704-4

Nakazawa, K., McHugh, T. J., Wilson, M. A., and Tonegawa, S. (2004). NMDA receptors, place cells and hippocampal spatial memory. *Nat. Rev. Neurosci.* 5, 361–372. doi: 10.1038/nrn1385

Navarro, V., Sanchez-Mejias, E., Jimenez, S., Muñoz-Castro, C., Sanchez-Varo, R., Davila, J. C., et al. (2018). Microglia in Alzheimer's disease: activated, dysfunctional or degenerative. *Front. Aging Neurosci.* 10:140. doi: 10.3389/fnagi.2018.00140

Nelson, A. R., Sweeney, M. D., Sagare, A. P., and Zlokovic, B. V. (2016). Neurovascular dysfunction and neurodegeneration in dementia and Alzheimer's disease. *Biochim. Biophys. Acta* 1862, 887–900. doi: 10.1016/j.bbadis.2015.12.016

Nicole, O., Hadzibegovic, S., Gajda, J., Bontempi, B., Bem, T., and Meyrand, P. (2016). Soluble amyloid beta oligomers block the learning-induced increase in hippocampal sharp wave-ripple rate and impair spatial memory formation. *Sci. Rep.* 6:22728. doi: 10.1038/srep22728

Ohno, M., Cole, S. L., Yasvoina, M., Zhao, J., Citron, M., Berry, R., et al. (2007). BACE1 gene deletion prevents neuron loss and memory deficits in 5XFAD APP/PS1 transgenic mice. *Neurobiol. Dis.* 26, 134–145. doi: 10.1016/j.nbd.2006.12.008

Ohno, M., Sametsky, E. A., Younkin, L. H., Oakley, H., Younkin, S. G., Citron, M., et al. (2004). BACE1 deficiency rescues memory deficits and cholinergic dysfunction in a mouse model of Alzheimer's disease. *Neuron* 41, 27–33. doi: 10.1016/s0896-6273(03)00810-9

Palpagama, T. H., Sagniez, M., Kim, S., Waldvogel, H. J., Faull, R. L., and Kwakowsky, A. (2019a). $GABA_A$ receptor subunit expression is well preserved in the aged mouse hippocampus. *eNeuro*. 0496-18. –. doi: 10.1523/ENEURO.0496-18.2019

Palpagama, H. T., Waldvogel, H. J., Faull, R. L., and Kwakowsky, A. (2019b). The role of microglia and astrocytes in Huntington's disease. *Front. Mol. Neurosci.* 12:258. doi: 10.3389/fnmol.2019.00258

Pandya, M., Palpagama, T. H., Turner, C., Waldvogel, H. J., Faull, R. L., and Kwakowsky, A. (2019). Sex- and age-related changes in GABA signaling components in the human cortex. *Biol. Sex Differ.* 10:5. doi: 10.1186/s13293-018-0214-6

Paul, J., Strickland, S., and Melchor, J. P. (2007). Fibrin deposition accelerates neurovascular damage and neuroinflammation in mouse models of Alzheimer's disease. *J. Exp. Med.* 204, 1999–2008. doi: 10.1084/jem.20070304

Pritchard, S. M., Dolan, P. J., Vitkus, A., and Johnson, G. V. (2011). The toxicity of tau in Alzheimer disease: turnover, targets and potential therapeutics. *J. Cell. Mol. Med.* 15, 1621–1635. doi: 10.1111/j.1582-4934.2011.01273.x

Puzzo, D., Lee, L., Palmeri, A., Calabrese, G., and Arancio, O. (2014). Behavioral assays with mouse models of Alzheimer's disease: practical considerations and guidelines. *Biochem. Pharmacol.* 88, 450–467. doi: 10.1016/j.bcp.2014.01.011

Religa, P., Cao, R., Religa, D., Xue, Y., Bogdanovic, N., Westaway, D., et al. (2013). VEGF significantly restores impaired memory behavior in Alzheimer's mice by improvement of vascular survival. *Sci. Rep.* 3:2053. doi: 10.1038/srep02053

Rissman, R. A., and Mobley, W. C. (2011). Implications for treatment: GABAA receptors in aging, down syndrome and Alzheimer's disease. *J. Neurochem.* 117, 613–622. doi: 10.1111/j.1471-4159.2011.07237.x

Rossler, M., Zarski, R., Bohl, J., and Ohm, T. G. (2002). Stage-dependent and sector-specific neuronal loss in hippocampus during Alzheimer's disease. *Acta Neuropathol.* 103, 363–369. doi: 10.1007/s00401-001-0475-7

Ryu, J. K., and McLarnon, J. G. (2009). A leaky blood-brain barrier, fibrinogen infiltration and microglial reactivity in inflamed Alzheimer's disease brain. *J. Cell. Mol. Med.* 13, 2911–2925. doi: 10.1111/j.1582-4934.2008.00434.x

Sadigh-Eteghad, S., Mahmoudi, J., Babri, S., and Talebi, M. (2015). Effect of alpha-7 nicotinic acetylcholine receptor activation on beta-amyloid induced recognition memory impairment. Possible role of neurovascular function. *Acta Cir. Bras.* 30, 736–742. doi: 10.1590/S0102-86502015011000003

Schmid, S., Jungwirth, B., Gehlert, V., Blobner, M., Schneider, G., Kratzer, S., et al. (2017). Intracerebroventricular injection of beta-amyloid in mice is associated with long-term cognitive impairment in the modified hole-board test. *Behav. Brain Res.* 324, 15–20. doi: 10.1016/j.bbr.2017.02.007

Soler, H., Dorca-Arévalo, J., González, M., Rubio, S. E., Ávila, J., Soriano, E., et al. (2017). The GABAergic septohippocampal connection is impaired in a mouse model of tauopathy. *Neurobiol. Aging* 49, 40–51. doi: 10.1016/j.neurobiolaging.2016.09.006

Soto-Rojas, L. O., de la Cruz-López, F., Torres, M. A. O., Viramontes-Pintos, A., del Carmen Cárdenas-Aguayo, M., Meraz-Ríos, M. A., et al. (2015). Neuroinflammation and alteration of the blood-brain barrier in Alzheimer's disease. In Alzheimer's Disease-Challenges for the Future: IntechOpen. doi: 10.5772/60024

Souchet, B., Audrain, M., Billoir, B., Lecanu, L., Tada, S., Braudeau, J., et al. (2018). Is it time to rethink the Alzheimer's disease drug development strategy by targeting its silent phase? *Neural Regen. Res.* 13, 224–225. doi: 10.4103/1673-5374.226389

Takeda, A., Nakamura, M., Fujii, H., Uematsu, C., Minamino, T., Adlard, P. A., et al. (2014). Amyloid β-mediated Zn^{2+} influx into dentate granule cells transiently induces a short-term cognitive deficit. *PLoS One* 9:e115923. doi: 10.1371/journal.pone.0115923

Takuma, H., Tomiyama, T., Kuida, K., and Mori, H. (2004). Amyloid beta peptide-induced cerebral neuronal loss is mediated by caspase-3 *in vivo*. *J. Neuropathol. Exp. Neurol.* 63, 255–261. doi: 10.1093/jnen/63.3.255

Tohda, C., Tamura, T., and Komatsu, K. (2003). Repair of amyloid β(25–35)-induced memory impairment and synaptic loss by a Kampo formula, Zokumei-to. *Brain Res.* 990, 141–147. doi: 10.1016/S0006-8993(03)03449-8

Tsukuda, K., Mogi, M., Iwanami, J., Min, L. J., Sakata, A., Jing, F., et al. (2009). Cognitive deficit in amyloid-beta-injected mice was improved by pretreatment with a low dose of telmisartan partly because of peroxisome proliferator-activated receptor-gamma activation. *Hypertension* 54, 782–787. doi: 10.1161/hypertensionaha.109.136879

Tyagi, N., Roberts, A. M., Dean, W. L., Tyagi, S. C., and Lominadze, D. (2008). Fibrinogen induces endothelial cell permeability. *Mol. Cell. Biochem.* 307, 13–22. doi: 10.1007/s11010-007-9579-2

van de Haar, H. J., Jansen, J. F. A., van Osch, M. J. P., van Buchem, M. A., Muller, M., Wong, S. M., et al. (2016). Neurovascular unit impairment in early Alzheimer's disease measured with magnetic resonance imaging. *Neurobiol. Aging* 45, 190–196. doi: 10.1016/j.neurobiolaging.2016.06.006

Vinnakota, C., Govondpani, K., Tate, W. P., Peppercorn, K., Aneka, P. V., Waldvogel, H. J., et al. (2020). An α5 $GABA_A$ receptor inverse agonist, α5IA, attenuates amyloid beta-induced neuronal death in mouse hippocampal cultures. *Int. J. Mol. Sci.* 21:3284. doi: 10.3390/ijms21093284

Wang, W., Nguyen, L. T. T., Burlak, C., Chegini, F., Guo, F., Chataway, T., et al. (2016). Caspase-1 causes truncation and aggregation of the Parkinson's disease-associated protein α-synuclein. *Proc. Natl. Acad. Sci.* 113, 9587–9592. doi: 10.1073/pnas.1610099113

Weldon, D. T., Rogers, S. D., Ghilardi, J. R., Finke, M. P., Cleary, J. P., O'Hare, E., et al. (1998). Fibrillar beta-amyloid induces microglial phagocytosis, expression of inducible nitric oxide synthase and loss of a select population of neurons in the rat CNS *in vivo*. *J. Neurosci.* 18, 2161–2173. doi: 10.1523/JNEUROSCI.18-06-02161.1998

Wennström, M., and Nielsen, H. M. (2012). Cell adhesion molecules in Alzheimer's disease. *Degener. Neurol. Neuromuscul. Dis.* 2, 65–77. doi: 10.2147/dnnd.S19829

Wilhelmsson, U., Bushong, E. A., Price, D. L., Smarr, B. L., Phung, V., Terada, M., et al. (2006). Redefining the concept of reactive astrocytes as cells that remain within their unique domains upon reaction to injury. *Proc. Natl. Acad. Sci. U S A* 103, 17513–17518. doi: 10.1073/pnas.0602841103

Wyssenbach, A., Quintela, T., Llavero, F., Zugaza, J. L., Matute, C., and Alberdi, E. (2016). Amyloid β-induced astrogliosis is mediated by β1-integrin *via* NADPH oxidase 2 in Alzheimer's disease. *Aging Cell* 15, 1140–1152. doi: 10.1111/acel.12521

Xia, M. Q., Bacskai, B. J., Knowles, R. B., Qin, S. X., and Hyman, B. T. (2000). Expression of the chemokine receptor CXCR3 on neurons and the elevated expression of its ligand IP-10 in reactive astrocytes: *in vitro* ERK1/2 activation and role in Alzheimer's disease. *J. Neuroimmunol.* 108, 227–235. doi: 10.1016/S0165-5728(00)00285-X

Xuan, A., Long, D., Li, J., Ji, W., Zhang, M., Hong, L., et al. (2012). Hydrogen sulfide attenuates spatial memory impairment and hippocampal neuroinflammation in β-amyloid rat model of Alzheimer's disease. *J. Neuroinflammation* 9:202. doi: 10.1186/1742-2094-9-202

Yamada, K., Tanaka, T., Han, D., Senzaki, K., Kameyama, T., and Nabeshima, T. (1999). Protective effects of idebenone and alpha-tocopherol on beta-amyloid-(1–42)-induced learning and memory deficits in rats: implication of oxidative stress in beta-amyloid-induced neurotoxicity *in vivo*. *Eur. J. Neurosci.* 11, 83–90. doi: 10.1046/j.1460-9568.1999.00408.x

Yan, J. J., Cho, J. Y., Kim, H. S., Kim, K. L., Jung, J. S., Huh, S. O., et al. (2001). Protection against beta-amyloid peptide toxicity *in vivo* with long-term administration of ferulic acid. *Br. J. Pharmacol.* 133, 89–96. doi: 10.1038/sj.bjp.0704047

Yang, S., Xia, C., Li, S., Du, L., Zhang, L., and Zhou, R. (2014). Defective mitophagy driven by dysregulation of rheb and KIF5B contributes to mitochondrial reactive oxygen species (ROS)-induced nod-like receptor 3 (NLRP3) dependent proinflammatory response and aggravates lipotoxicity. *Redox Biol.* 3, 63–71. doi: 10.1016/j.redox.2014.04.001

Yeung, J. H. Y., Calvo-Flores Guzmán, B., Palpagama, T. H., Ethira, J., Zhai, Y., Tate, W. P., et al. (2020a). Beta amyloid 1–42 ($A\beta_{1-42}$)-induced alterations in glutamate receptor and transporter expression in the mouse hippocampus. *J. Neurochemistry* 155, 62–80. doi: 10.1111/jnc.15099.

Yeung, J. H. Y., Palpagama, T. H., Tate, W. P., Peppercorn, K., Waldvogel, H. J., Faull, R. L. M., et al. (2020b). The acute effects of amyloid-$beta_{(1-42)}$ on glutamatergic receptor and transporter expression in the mouse hippocampus. *Front. Neurosci.* 13:1427. doi: 10.3389/fnins.2019.01427

Yoshiyama, Y., Higuchi, M., Zhang, B., Huang, S. M., Iwata, N., Saido, T. C., et al. (2007). Synapse loss and microglial activation precede tangles in a P301S tauopathy mouse model. *Neuron* 53, 337–351. doi: 10.1016/j.neuron.2007.01.010

Zempel, H., and Mandelkow, E. (2014). Lost after translation: missorting of Tau protein and consequences for Alzheimer disease. *Trends Neurosci.* 37, 721–732. doi: 10.1016/j.tins.2014.08.004

Zhang, L., Fang, Y., Lian, Y., Chen, Y., Wu, T., Zheng, Y., et al. (2015). Brain-derived neurotrophic factor ameliorates learning deficits in a rat model of Alzheimer's disease induced by $A\beta_{1-42}$. *PLoS One* 10:e0122415. doi: 10.1371/journal.pone.0122415

Conflict of Interest: The authors declare that the research was conducted in the absence of any commercial or financial relationships that could be construed as a potential conflict of interest.

frontiers in Molecular Neuroscience

REVIEW
published: 13 November 2020
doi: 10.3389/fnmol.2020.577622

Amyloid-β Peptide Impact on Synaptic Function and Neuroepigenetic Gene Control Reveal New Therapeutic Strategies for Alzheimer's Disease

*Bhanu Chandra Karisetty, Akanksha Bhatnagar†, Ellen M. Armour†, Mariah Beaver, Haolin Zhang and Felice Elefant**

Department of Biology, Drexel University, Philadelphia, PA, United States

Amyloid-β (Aβ) peptides can form protease-resistant aggregates within and outside of neurons. Accumulation of these aggregates is a hallmark of Alzheimer's disease (AD) neuropathology and contributes to devastating cognitive deficits associated with this disorder. The primary etiological factor for Aβ aggregation is either an increase in Aβ production or a decrease in its clearance. Aβ is produced by the sequential activity of β- and γ-secretase on the amyloid precursor protein (APP) and the clearance is mediated by chaperone-mediated mechanisms. The Aβ aggregates vary from soluble monomers and oligomers to insoluble senile plaques. While excess intraneuronal oligomers can transduce neurotoxic signals into neurons causing cellular defects like oxidative stress and neuroepigenetic mediated transcriptional dysregulation, extracellular senile plaques cause neurodegeneration by impairing neural membrane permeabilization and cell signaling pathways. Paradoxically, senile plaque formation is hypothesized to be an adaptive mechanism to sequester excess toxic soluble oligomers while leaving native functional Aβ levels intact. This hypothesis is strengthened by the absence of positive outcomes and side effects from immunotherapy clinical trials aimed at complete Aβ clearance, and support beneficial physiological roles for native Aβ in cellular function. Aβ has been shown to modulate synaptic transmission, consolidate memory, and protect against excitotoxicity. We discuss the current understanding of beneficial and detrimental roles for Aβ in synaptic function and epigenetic gene control and the future promising prospects of early therapeutic interventions aimed at mediating Aβ induced neuroepigenetic and synaptic dysfunctions to delay AD onset.

Keywords: neuroepigenetics, TIP60, synaptic function, therapeutics, amyloid beta, KAT5

OPEN ACCESS

Edited by:
Daniela Puzzo,
University of Catania, Italy

Reviewed by:
Takashi Saito,
Nagoya City University, Japan
Chunyu Wang,
Rensselaer Polytechnic Institute, United States

****Correspondence:***
Felice Elefant
fe22@drexel.edu

† These authors have contributed equally to this work and share second authorship

Received: *29 June 2020*
Accepted: *22 October 2020*
Published: *13 November 2020*

Citation:
Karisetty BC, Bhatnagar A, Armour EM, Beaver M, Zhang H and Elefant F (2020) Amyloid-β Peptide Impact on Synaptic Function and Neuroepigenetic Gene Control Reveal New Therapeutic Strategies for Alzheimer's Disease. Front. Mol. Neurosci. 13:577622. doi: 10.3389/fnmol.2020.577622

INTRODUCTION

Alzheimer's disease (AD) affects 5.8 million Americans aged 65 and older and is estimated to grow to 13.8 million by mid-century. AD is the most common cause of dementia, presenting with hallmarks such as amyloid-β (Aβ) plaques, tau neurofibrillary tangles, neuronal cell death, cognitive dysfunction, and altered brain morphology. Aβ-plaques comprise of aggregated Aβ, a

cleaved product of the glycoprotein amyloid precursor protein (APP). According to the amyloid cascade hypothesis, it is these plaques that are responsible for AD pathology.

Newly generated Aβ released into the extracellular space remain in soluble form or aggregate into insoluble Aβ-plaques. Soluble Aβ species can bind to various neuronal cell receptors and transduce neurotoxic signals causing cellular defects that include oxidative stress and epigenetic-mediated transcriptional dysregulation (Chen et al., 2017). However, recent evidence demonstrates that soluble Aβ shows beneficial physiological roles such as regulating cellular signaling pathways and synaptic function as well as possessing antimicrobial and antioxidant properties (Brothers et al., 2018). In this review, we summarize recent progress in understanding the beneficial and detrimental aspects of Aβ in mediating processes underlying synaptic and cognitive function and epigenetic neuronal gene control. We further discuss therapeutic interventions aimed at synaptic plasticity and epigenetic regulation to delay AD progression.

Aβ REGULATION OF SYNAPTIC PLASTICITY

Synaptic plasticity mediated changes in neuronal connections have long been established as the primary mechanism of learning and memory (Martin et al., 2000; Ramirez and Arbuckle, 2016). Accordingly, loss of synaptic connections is an early event in AD pathogenesis and cognitive impairment (Selkoe, 2002; Scheff et al., 2006; Kashyap et al., 2019). Although the precise mechanisms underlying synaptic dysfunction in AD are obscure, emerging studies have uncovered a feedback regulation between Aβ and synaptic plasticity.

Multiple studies demonstrate that soluble Aβ oligomers in pre- and post-synaptic compartments can disrupt synaptic morphology and inhibit long-term potentiation (LTP) that trigger cognitive dysfunction. Intriguingly, insoluble Aβ-plaques are less active in promoting such alterations (Lambert et al., 1998; Takahashi et al., 2002; Walsh et al., 2002; Shankar et al., 2008; **Figure 1**). For example, studies in amyloid mice reveal that reduction of synaptophysin puncta correlates with soluble Aβ and not plaque load (Mucke et al., 2000). Further, AD-associated apolipoprotein E4 has been implicated in facilitating the transport of soluble Aβ species to synapses elucidating toxic effects (Koffie et al., 2012). Aberrant activation of neuronal signal transduction pathways can arise via Aβ directly binding to Aβ receptors or competing with essential ligands to bind their receptors (Xia et al., 2016). For example, soluble Aβ dimers cause glutamate excitotoxicity via blockage of glutamate reuptake in the synaptic cleft, activating glutamate receptors and ion channels like N-Methyl-D-aspartate (NMDA) receptors that trigger downstream cell signaling transduction cascades to pathologically alter gene expression profiles (Li et al., 2009). Additionally, accumulation of extracellular $A\beta_{42}$ triggers the loss of synaptic mushroom spines via hyperactivation of metabotropic glutamate receptor type 5 (mGluR5) receptors, resulting in elevated endoplasmic reticulum Ca^{2+} levels and downregulation of the Ca^{2+}/calmodulin kinase II signaling pathway (Zhang et al., 2015). Interestingly, soluble APP has also been shown to directly modulate synaptic plasticity by binding to the gamma-aminobutyric acid (GABA) receptor and inducing a conformational change that facilitates reduced neurotransmitter release and neuronal activity (Rice et al., 2019; **Figure 1**). Together, these findings support the concept that soluble APP and Aβ oligomers promote synaptic impairment and cognitive deficits during the early stages of AD, followed by neurodegeneration in the later stages (Ferreira and Klein, 2011).

Conversely, synaptic activity positively modulates Aβ production to promote synaptic function (Kamenetz et al., 2003; Cirrito et al., 2005). Increased synaptic activity promotes APP endocytosis, and β-secretase 1 (BACE1) mediated Aβ production (Cirrito et al., 2008). Since Aβ depresses synaptic activity, the activity-dependent modulation of endogenous Aβ production has been suggested to be a finely tuned negative feedback loop that regulates the neuronal activity and appropriate function by preventing hyperactivation (Kamenetz et al., 2003). Perturbation in this homeostatic mechanism may interfere with synaptic activity and contribute to cognitive decline, as seen in AD. These studies support the premise that physiological levels of Aβ are critical for optimal synaptic activity (Kamenetz et al., 2003; Parihar and Brewer, 2010; Jang and Chung, 2016).

Aβ AND EPIGENETIC MECHANISMS UNDERLYING AD

Epigenetic modifications of DNA and histone proteins regulate gene expression profiles via controlling chromatin accessibility. The neuroepigenome has been proven to be critical in memory formation and consolidation through dynamic control of neural genes essential for these functions (Feng et al., 2007; Sultan and Day, 2011). Neuroepigenetic imbalance in the brain causes transcriptional dysregulation, a pivotal step in AD etiology (Esposito and Sherr, 2019). Here, we summarize primary epigenetic alterations that affect or are affected by Aβ production.

DNA methylation: DNA methylation occurs at cytosine bases in CpG repeats and primarily controls gene repression (Saxonov et al., 2006; Miranda and Jones, 2007). Reports on DNA methylation and AD are conflicting with several studies reporting global DNA hypermethylation in the AD brain (Rao et al., 2012; Di Francesco et al., 2015; Liu et al., 2019), while other studies show reduction (Chen et al., 2009; Chouliaras et al., 2013; Li et al., 2019) or no alterations in global DNA methylation (Lashley et al., 2015). Common AD-associated methylation alterations often increase Aβ production. For example, AD-associated genes APP, Apolipoprotein E, and BACE1 are hypomethylated in AD brains with concomitant BACE1 activation increasing Aβ levels via the amyloidogenic processing pathway (West et al., 1995; Tulloch et al., 2018; Li et al., 2019). Conversely, the neprilysin gene that encodes for an Aβ degrading enzyme is hypermethylated and repressed in AD, also leading to increased Aβ levels (Chen et al., 2009).

Histone acetylation: Histone modifications, including acetylation, methylation, and phosphorylation on histone

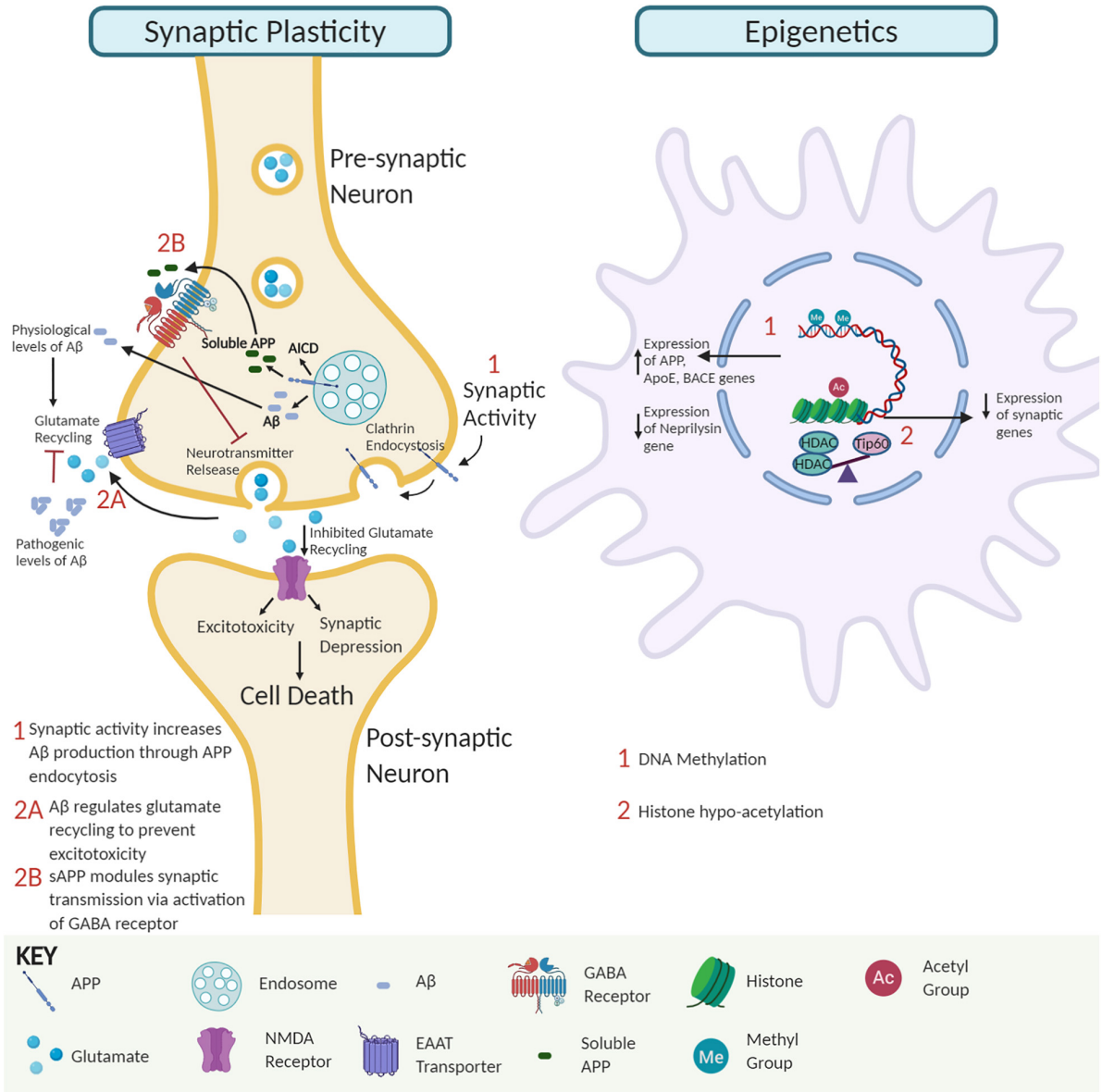

FIGURE 1 | The interplay of amyloid precursor protein (APP) and amyloid-β (Aβ) impact on synaptic activity and neuroepigenetic gene control. Synaptic activity module. APP endocytosis and cleavage yield Aβ peptides and APP intracellular domain (AICD). Soluble APP regulates GABA receptor function to modulate synaptic transmission and plasticity. At physiological levels, Aβ peptides promote glutamate recycling keeping glutamate levels in check. In contrast, at pathological Aβ levels, impaired glutamate recycling increases post-synaptic uptake, leading to excitotoxicity, synaptic depression, and eventually neural cell death. Epigenetic module. Soluble Aβ monomer and dimer competition for binding of essential ligands to receptors can alter signal transduction pathways causing global changes in neuroepigenetic gene control. Such alterations include DNA methylation changes that alter the expression of genes involved in APP processing and Aβ degradation pathways to favor increased Aβ levels and disruption of Tip60/HDAC balance causing hypoacetylation of chromatin with concomitant repression of associated critical synaptic plasticity genes.

protein tails, modulate chromatin accessibility to control gene expression. Of these modifications, histone acetylation is best characterized for its role in learning and memory and contribution to AD when altered (Saha and Pahan, 2006; Sharma, 2010; Peixoto and Abel, 2013). Histone acetylation homeostasis is regulated by the antagonistic activity of histone acetyltransferases (HATs) and histone deacetylases (HDACs). Evidence from our group and others shows that neural histone acetylation dysregulation, caused by an imbalance between specific HATs and HDACs, is a crucial early step in AD pathology. Downregulation of the HAT Tip60 (KAT5) and upregulation of HDAC2 causes epigenetic repression of critical neuroplasticity genes in multiple types of AD animal models and patients (Graff et al., 2012; Panikker et al., 2018). Further, alteration of Tip60 epigenetic mediated control in the brain by either APP or Aβ driven Alzheimer's disease pathology leads

to repression of a set of neuronal genes critical for synaptic function (Panikker et al., 2018). Restoring such alterations in Tip60/HDAC2 balance protects against AD-associated pathologies in the AD *Drosophila* model expressing APP.

How might Aβ influence early HAT/HDAC disruption? Our findings reveal that APP expression results in a reduction of Tip60 protein levels but not Tip60 mRNA levels (Panikker et al., 2018), suggesting a mechanism of post-transcriptional regulation. Thus far, there is no evidence to demonstrate a direct Aβ and Tip60 interaction underlying reduced Tip60 levels, but a potential mechanism is via ubiquitin-mediated Aβ-induced Tip60 degradation. Another consideration is soluble Aβ monomer and dimer competition for the binding of essential ligands to receptors (Xia et al., 2016). Such interactions possibly alter signal transduction pathways that disrupt Tip60/HDAC balance and acetylation levels, inducing altered gene expression profiles contributing to AD.

THERAPEUTIC INTERVENTION FOR Aβ INDUCED NEUROEPIGENETIC AND SYNAPTIC DYSFUNCTION

Currently, the Food and Drug Administration (FDA) approved drugs for AD are limited to palliative medications: cholinesterase inhibitors and a non-competitive NMDA antagonist (National Institute on Aging, 2018, April 01). As Aβ-plaques are considered as primary effector molecules in AD pathogenesis, therapeutic strategies are focused on developing agents that can block Aβ production or clear Aβ-plaques. The clinical trials are ongoing, but the initial results thus far are not encouraging. The β- and γ-secretase inhibitors, aimed to block Aβ production, were discontinued due to unfavorable risk/benefit profile and cognitive worsening. Also, Aβ immunotherapies, intended to clear the Aβ-plaques, were terminated due to toxicity and cognitive worsening. Efforts are in progress to refine the approaches to these trials (reviewed in Panza et al., 2019). Further, it is hypothesized that the complete reduction of Aβ as a principal reason for these failures, underscoring the necessity to understand the physiological roles of Aβ.

The U-shaped natural course of cerebrospinal fluid Aβ levels in aging suggests it as physiologically active (Shoji and Kanai, 2001). One of the main reasons for clinical trial failures is the toxicity resulting from reducing Aβ, supporting a critical role for Aβ in neuronal survival and function. In support of this concept, synthetic $Aβ_{42}$ monomers (30–100 nM) have been shown to promote survival in developing neurons deprived with trophic factors (Giuffrida et al., 2009). Further, in different neuronal cell types, exogenous $Aβ_{40}$ had a neuroprotective effect on cells dying from Aβ immunodepletion, while the same levels of exogenous $Aβ_{42}$ oligomers proved to be toxic (Plant et al., 2003). These studies demonstrate a hormetic effect of Aβ in neuroprotection and the neurotoxicity of soluble oligomeric forms over insoluble aggregates. Considering the physiological importance of monomeric Aβ, monoclonal antibody Aducanumab was developed with a much greater affinity to Aβ-aggregates versus monomeric forms. Currently, Phase 3 trials have been discontinued based on futility analysis but not on safety concerns (U.S. National Library of Medicine, 2020a,b). In the future, the predicted aggregate-specific N-terminal binding motif of Aducanumab could potentially serve as a basis to re-engineer Aducanumab for further enhanced preference to bind Aβ -aggregates versus monomers (Frost and Zacharias, 2020).

Another disappointing outcome from clinical trials focused on Aβ depletion is the failure to alleviate cognitive decline. Studies show that Aβ affects memory by regulating synaptic vesicle dynamics and synaptic plasticity with physiological levels increasing recycling and supraphysiological levels decreasing recycling (Lazarevic et al., 2017). Similarly, exogenously applied $Aβ_{42}$ shows a biphasic dose-response curve on hippocampal LTP and reference memory (Puzzo et al., 2012). Additional studies carried out to understand the synaptic plasticity and memory formation by different isoforms ($Aβ_{40}$ and $Aβ_{42}$) and aggregation status (monomer and oligomer) revealed that lower levels of oligomeric $Aβ_{42}$ enhanced LTP and spatial memory while higher concentrations of oligomeric $Aβ_{40}$, oligomeric $Aβ_{42}$ & monomeric $Aβ_{42}$ impaired LTP and spatial memory (Gulisano et al., 2018). In addition to memory formation, Aβ is required for memory consolidation and stability. Intrahippocampal administration of picomolar concentrations of exogenous $Aβ_{42}$, following training, enhances memory retention (Garcia-Osta and Alberini, 2009). Elevated soluble $Aβ_{42}$ in the amygdala of adult rats, during the formation of auditory fear memories, is required for memory consolidation and stability (Finnie and Nader, 2020). These studies signify the importance of physiological concentrations of Aβ on memory formation and retention and substantiate the hypothesis that cognitive deficits increase due to Aβ depletion.

The two major histopathological hallmarks of AD are extracellular Aβ-plaques and intracellular neurofibrillary tangles. These changes predominantly occur in the later stages of AD. In contrast, synaptic dysfunction typically appears early in prodromal or mild cognitive impairment (MCI) stages of the disease, thus serving as a potent target for early stage therapeutic intervention to slow AD progression. Soluble $Aβ_{42}$ oligomers can interact with proteins participating in the regulation of the synaptic vesicle life cycle that includes Syntaxin1a, Synaptophysin, and Synapsin1 (Snp1), causing aberrant glutamate release and reduction in synaptic vesicle recycling (reviewed in Marsh and Alifragis, 2018). Currently, there are three publicly disclosed drug trials with endpoints that specifically inform on synapse density and/or function (reviewed in Jackson et al., 2019). First, Elayta (CT1812) is a small-molecule that prevents and displaces beta-amyloid binding to the sigma-2 receptor on the nerve cells and interferes with its toxicity. Elayta lowered the neurogranin and synaptotagmin-1, markers of synaptic damage, in AD patients (U.S. National Library of Medicine, 2020d). A second trial is using imaging techniques and cognitive performance testing to assess the efficiency of LMTX (methylthioninium chloride), a tau aggregation inhibitor, to elicit changes in brain function (U.S. National Library of Medicine, 2020c). Finally, Saracatinib inhibition of Fyn is another potential synaptic specific therapeutic intervention in AD. Fyn is a non-receptor tyrosine kinase

that is activated by Aβ oligomers and alters synaptic plasticity (U.S. National Library of Medicine, 2019). These studies have moved the field forward toward clinical trials testing therapuetic drugs designed specifically for synaptic plasticity enhancement (**Figure 2**). Indeed, recent years have shown an increase in the number of drugs/biologics targeting pathways other than amyloid or tau (Cummings et al., 2020).

Compelling evidence demonstrates that repression of histone acetylation mediated epigenetic gene control involving an increase in HDAC2 and a reduction of Tip60 are early contributors to AD (Panikker et al., 2018). Thus, epigenetic therapeutic approaches that involve increasing acetylation levels using HDAC inhibitors (HDACi) and HAT activators is a promising therapeutic approach. At present, there are two HDACi at clinical trials targeting AD pathology (**Figure 2**; Cummings et al., 2020). Nicotinamide is at Phase 2 testing to assess the reduction of phosphorylated tau in patients that display MCI or mild AD dementia. Another HDACi vorinostat is in Phase 1b to determine the maximal tolerable dose in AD patients between (including) 55 and 90 years with mild symptoms. The epigenetic drug valproic acid restores the physiological regulation of Snp1, a pre-synaptic protein that regulates the availability of synaptic vesicles, in $A\beta_{42}$ treated primary rat hippocampal neurons (Marsh et al., 2017). Mithramycin A (FDA approved antineoplastic antibiotic) significantly upregulates the synaptic plasticity gene expression and downregulates HDAC2 in SH-SY5Y cells overexpressing APP (Atluri et al., 2019).

HDACi can be either multitargeting like M344, an inhibitor of class I and IIB HDACs, or specific like CM-695 and RGFP966 selectively inhibiting HDAC6 and HDAC3, respectively. M344 regulated multiple AD-related genes and exhibited significant cognitive benefits *in vivo* (Volmar et al., 2017). CM-695 inhibits HDAC6 and phosphodiesterase 9 (PDE9) and ameliorates memory impairment, and reduces $A\beta_{42}$ levels *in vivo* (Cuadrado-Tejedor et al., 2019). RGFP966 inhibits HDAC3 and reverse the attenuation of LTP by Aβ oligomers in rat CA1 pyramidal neurons (Krishna et al., 2016). Selective inhibition by specific HDACi can reduce the side effects and serves as a viable therapeutic strategy. An alternative approach to improve target specificity is to target the binding partners in the HDAC complex rather than the HDAC. Utilizing weighted gene co-expression network analysis (WGCNA), transcription factor Sp3 identified as a putative HDAC2 co-regulator, and its expression was also elevated in AD patients. The knockdown of Sp3 reduced the HDAC2 occupancy and reversed the HDAC2 associated synaptic gene repression (Yamakawa et al., 2017). Therefore, targeting the HDAC2-Sp3 complex may be a feasible approach for AD therapy.

Many HATs as opposed to HDACs have non-redundant physiological functions as different HATs exhibit a specialized preference for site-specific chromatin marks that regulate synaptic gene expression and cognitive function. Thus, HAT activators are a potentially powerful epigenetic therapeutic tool for the treatment of neurodegenerative diseases. As such, chemical modifications are being made to existing drugs to increase their cell permeability in the brain. For example, TTK21, an activator of the HAT CBP/p300, is conjugated to a glucose-based carbon nanosphere enabling it to cross the blood-brain barrier (Chatterjee et al., 2013). It promotes neurogenesis and extends memory duration *in vivo*. A patent publication (US20180050982A1) covers the use of HAT activators to enhance learning and memory and to treat AD (Francis et al., 2018). Alternatively, downstream molecules/pathways regulated by HATs can also be targeted for therapeutic effects.

A recent growing interest among many researchers is moving toward exploration of non-coding RNA (ncRNA) related

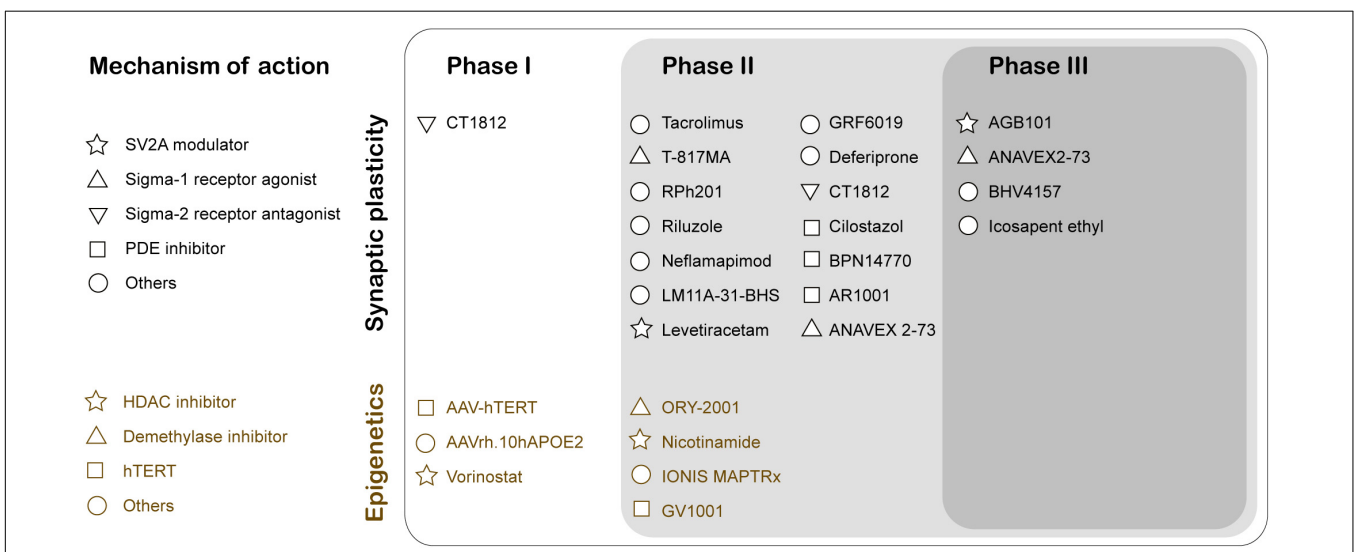

FIGURE 2 | Clinical Trials for therapeutic drugs targeting synaptic activity and neuroepigenetic mechanisms for Alzheimer's disease treatment. The mechanism of action of the drug is classified using Common Alzheimer's and Related Dementias Research Ontology (CADRO) (Cummings et al., 2020). SV2A, Synaptic vesicle glycoprotein 2A; PDE, Phosphodiesterase; HDAC, Histone deacetylases; hTERT, human telomerase reverse transcriptase.

neuroepigenetic alterations in AD and its relationship with synaptic dysfunction. Notably, some microRNAs (miRNAs) are particularly enriched in presynaptic and postsynaptic compartments. For example, miR-34a can target the synaptic proteins synaptotagmin-1 and syntaxin-1A to regulate neurite outgrowth and dendritic spine morphology and function (Agostini et al., 2011). Further, in AD-associated HDAC2-induced tauopathy, 5′ AMP-activated protein kinase (AMPK) activation is correlated with the loss of spine density. AMPK expression is under the control of the miR-101b promoter and as such, miR-101b mimics have been shown to block dendritic impairments *in vitro* (Liu et al., 2017). Thus, understanding the various ncRNAs in AD pathology should lead to new pharmacological interventions. Interestingly, non-pharmacological approaches like an enriched environment (EE) and non-invasive brain stimulation techniques can be utilized to attenuate early stage synaptic dysfunction and appear to act via neuroepigenetic mechanisms. For example, EE triggers hippocampal induction of histone acetylation at specific sites linked to synaptic plasticity and learning and memory enhancement and also ameliorates soluble Aβ oligomer induced synaptic dysfunction by upregulating miRNA-132 and reducing HDAC3 signaling (Wei et al., 2020). Currently, transcranial magnetic stimulation (TMS) and transcranial direct current stimulation (tDCS) usage have been shown to be beneficial for stroke and Parkinson's patients to positively modulate brain plasticity (reviewed in Schulz et al., 2013). Thus, exciting new avenues involving these types of non-invasive treatment methods likely hold promise for AD patients as well.

OUTLOOK

In AD patients, Aβ accumulation and associated neuroepigenetic transcriptional alterations contribute to synaptic dysfunction and cognitive impairment (Panikker et al., 2018). However, failure to attenuate or reverse the cognitive decline by anti-amyloid therapeutics in clinical trials raises concerns toward these strategies. Intriguingly, recent studies demonstrate roles for Aβ in neuroprotection, synaptic function, and memory consolidation (Giuffrida et al., 2009; Lazarevic et al., 2017; Finnie and Nader, 2020). These beneficial roles are Aβ concentration- and species-specific. Picomolar concentrations and monomers proved to be beneficial, while higher concentrations and soluble oligomers proved to be detrimental. These findings underscore the necessity to understand the physiological and pathological roles of Aβ for refining the current amyloid-based therapeutic strategies. As AD is a multifactorial disease, targeting AD-associated processes like tau-associated pathology, inflammatory responses, synaptic activity, and neuroepigenetic regulation of AD-related genes may provide alternative therapeutic strategies during early AD progression. Additionally, exploring the synergistic effects of HDACi and HAT activators to restore histone acetylation homeostasis, opens new less invasive and early avenues for treatment. Recent studies utilizing methodological improvements to specifically target toxic Aβ species demonstrate encouraging results. Thus, the development of early therapeutic interventions aimed at mediating Aβ induced neuroepigenetic and synaptic dysfunctions while simultaneously maintaining beneficial physiological levels and forms of Aβ provide exciting new avenues for preventing or treating AD.

AUTHOR CONTRIBUTIONS

BK, AB, EMA, FE, and HZ contributed to writing and reviewing the manuscript. MB and BK contributed to figures and reviewing the manuscript. All authors contributed to the article and approved the submitted version.

FUNDING

Funding for this work was provided by National Institutes of Health Grant NINDS/NIA 1R01NS095799 to FE.

REFERENCES

Agostini, M., Tucci, P., Steinert, J. R., Shalom-Feuerstein, R., Rouleau, M., Aberdam, D., et al. (2011). microRNA-34a regulates neurite outgrowth, spinal morphology, and function. *Proc. Natl. Acad. Sci. U.S.A.* 108, 21099–21104. doi: 10.1073/pnas.1112063108

Atluri, V. S. R., Tiwari, S., Rodriguez, M., Kaushik, A., Yndart, A., Kolishetti, N., et al. (2019). Inhibition of amyloid-beta production, associated neuroinflammation, and histone deacetylase 2-mediated epigenetic modifications prevent neuropathology in alzheimer's disease in vitro model. *Front. Aging Neurosci.* 11:342. doi: 10.3389/fnagi.2019.00342

Brothers, H. M., Gosztyla, M. L., and Robinson, S. R. (2018). The physiological roles of amyloid-beta peptide hint at new ways to treat Alzheimer's disease. *Front. Aging Neurosci.* 10:118. doi: 10.3389/fnagi.2018.00118

Chatterjee, S., Mizar, P., Cassel, R., Neidl, R., Selvi, B. R., Mohankrishna, D. V., et al. (2013). A novel activator of CBP/p300 acetyltransferases promotes neurogenesis and extends memory duration in adult mice. *J. Neurosci.* 33, 10698–10712. doi: 10.1523/JNEUROSCI.5772-12.2013

Chen, G. F., Xu, T. H., Yan, Y., Zhou, Y. R., Jiang, Y., Melcher, K., et al. (2017). Amyloid beta: structure, biology and structure-based therapeutic development. *Acta Pharmacol. Sin.* 38, 1205–1235. doi: 10.1038/aps.2017.28

Chen, K. L., Wang, S. S., Yang, Y. Y., Yuan, R. Y., Chen, R. M., and Hu, C. J. (2009). The epigenetic effects of amyloid-beta(1-40) on global DNA and neprilysin genes in murine cerebral endothelial cells. *Biochem. Biophys. Res. Commun.* 378, 57–61. doi: 10.1016/j.bbrc.2008.10.173

Chouliaras, L., Mastroeni, D., Delvaux, E., Grover, A., Kenis, G., Hof, P. R., et al. (2013). Consistent decrease in global DNA methylation and hydroxymethylation in the hippocampus of Alzheimer's disease patients. *Neurobiol. Aging* 34, 2091–2099. doi: 10.1016/j.neurobiolaging.2013.02.021

Cirrito, J. R., Kang, J.-E., Lee, J., Stewart, F. R., Verges, D. K., Silverio, L. M., et al. (2008). Endocytosis is required for synaptic activity-dependent release of amyloid-β in vivo. *Neuron* 58, 42–51. doi: 10.1016/j.neuron.2008.02.003

Cirrito, J. R., Yamada, K. A., Finn, M. B., Sloviter, R. S., Bales, K. R., May, P. C., et al. (2005). Synaptic activity regulates interstitial fluid amyloid-β levels in vivo. *Neuron* 48, 913–922. doi: 10.1016/j.neuron.2005.10.028

Cuadrado-Tejedor, M., Perez-Gonzalez, M., Garcia-Munoz, C., Muruzabal, D., Garcia-Barroso, C., Rabal, O., et al. (2019). Taking advantage of the selectivity of histone deacetylases and phosphodiesterase inhibitors to design better therapeutic strategies to treat Alzheimer's disease. *Front. Aging Neurosci.* 11:149. doi: 10.3389/fnagi.2019.00149

Cummings, J., Lee, G., Ritter, A., Sabbagh, M., and Zhong, K. J. A. S. (2020). Alzheimer's disease drug development pipeline: 2020. *Alzheimers Dement (N. Y.)* 6:e12050.

Di Francesco, A., Arosio, B., Falconi, A., Micioni Di Bonaventura, M. V., Karimi, M., Mari, D., et al. (2015). Global changes in DNA methylation in Alzheimer's disease peripheral blood mononuclear cells. *Brain Behav. Immun.* 45, 139–144. doi: 10.1016/j.bbi.2014.11.002

Esposito, M., and Sherr, G. L. (2019). Epigenetic modifications in Alzheimer's neuropathology and therapeutics. *Front. Neurosci.* 13:476. doi: 10.3389/fnins.2019.00476

Feng, J., Fouse, S., and Fan, G. (2007). Epigenetic regulation of neural gene expression and neuronal function. *Pediatric Res.* 61, 58–63. doi: 10.1203/pdr.0b013e3180457635

Ferreira, S. T., and Klein, W. L. (2011). The Aβ oligomer hypothesis for synapse failure and memory loss in Alzheimer's disease. *Neurobiol. Learn. Memory* 96, 529–543. doi: 10.1016/j.nlm.2011.08.003

Finnie, P. S. B., and Nader, K. (2020). Amyloid beta secreted during consolidation prevents memory malleability. *Curr. Biol.* 30, 1934–1940.e1934. doi: 10.1016/j.cub.2020.02.083

Francis, Y., Arancio, O., and Fa, M. (2018). *Uses of Histone Acetyltransferase Activators*. New York: Google Patents.

Frost, C. V., and Zacharias, M. J. (2020). From monomer to fibril: abeta−amyloid binding to Aducanumab antibody studied by molecular dynamics simulation. *Protiens Struct. Func. Bioinform.* 88, 1592–1606. doi: 10.1002/prot.25978

Garcia-Osta, A., and Alberini, C. M. (2009). Amyloid beta mediates memory formation. *Learn. Mem.* 16, 267–272. doi: 10.1101/lm.1310209

Giuffrida, M. L., Caraci, F., Pignataro, B., Cataldo, S., De Bona, P., Bruno, V., et al. (2009). Beta-amyloid monomers are neuroprotective. *J. Neurosci.* 29, 10582–10587. doi: 10.1523/JNEUROSCI.1736-09.2009

Graff, J., Rei, D., Guan, J. S., Wang, W. Y., Seo, J., Hennig, K. M., et al. (2012). An epigenetic blockade of cognitive functions in the neurodegenerating brain. *Nature* 483, 222–226. doi: 10.1038/nature10849

Gulisano, W., Melone, M., Li Puma, D. D., Tropea, M. R., Palmeri, A., Arancio, O., et al. (2018). The effect of amyloid-beta peptide on synaptic plasticity and memory is influenced by different isoforms, concentrations, and aggregation status. *Neurobiol. Aging* 71, 51–60. doi: 10.1016/j.neurobiolaging.2018.06.025

Jackson, J., Jambrina, E., Li, J., Marston, H., Menzies, F., Phillips, K., et al. (2019). Targeting the synapse in Alzheimer's disease. *Front. Neurosci.* 13:735. doi: 10.3389/fnins.2019.00735

Jang, S.-S., and Chung, H. J. (2016). Emerging link between Alzheimer's disease and homeostatic synaptic plasticity. *Neural. Plasticity* 2016:7969272. doi: 10.1155/2016/7969272

Kamenetz, F., Tomita, T., Hsieh, H., Seabrook, G., Borchelt, D., Iwatsubo, T., et al. (2003). APP processing and synaptic function. *Neuron* 37, 925–937. doi: 10.1016/S0896-6273(03)00124-7

Kashyap, G., Bapat, D., Das, D., Gowaikar, R., Amritkar, R. E., Rangarajan, G., et al. (2019). Synapse loss and progress of Alzheimer's disease -A network model. *Sci. Rep.* 9:6555. doi: 10.1038/s41598-019-43076-y

Koffie, R. M., Hashimoto, T., Tai, H.-C., Kay, K. R., Serrano-Pozo, A., Joyner, D., et al. (2012). Apolipoprotein E4 effects in Alzheimer's disease are mediated by synaptotoxic oligomeric amyloid-β. *Brain* 135, 2155–2168. doi: 10.1093/brain/aws127

Krishna, K., Behnisch, T., and Sajikumar, S. J. (2016). Inhibition of histone deacetylase 3 restores amyloid-β oligomer-induced plasticity deficit in hippocampal CA1 pyramidal neurons. *J. Alzheimers Dis.* 51, 783–791. doi: 10.3233/jad-150838

Lambert, M. P., Barlow, A. K., Chromy, B. A., Edwards, C., Freed, R., Liosatos, M., et al. (1998). Diffusible, nonfibrillar ligands derived from Abeta1-42 are potent central nervous system neurotoxins. *Proc. Natl. Acad. Sci. U.S.A.* 95, 6448–6453. doi: 10.1073/pnas.95.11.6448

Lashley, T., Gami, P., Valizadeh, N., Li, A., Revesz, T., and Balazs, R. (2015). Alterations in global DNA methylation and hydroxymethylation are not detected in Alzheimer's disease. *Neuropathol. Appl. Neurobiol.* 41, 497–506. doi: 10.1111/nan.12183

Lazarevic, V., Fienko, S., Andres-Alonso, M., Anni, D., Ivanova, D., Montenegro-Venegas, C., et al. (2017). Physiological concentrations of amyloid beta regulate recycling of synaptic vesicles via alpha7 acetylcholine receptor and CDK5/calcineurin signaling. *Front. Mol. Neurosci.* 10:221. doi: 10.3389/fnmol.2017.00221

Li, P., Marshall, L., Oh, G., Jakubowski, J. L., Groot, D., He, Y., et al. (2019). Epigenetic dysregulation of enhancers in neurons is associated with Alzheimer's disease pathology and cognitive symptoms. *Nat. Commun.* 10:2246. doi: 10.1038/s41467-019-10101-7

Li, S., Hong, S., Shepardson, N. E., Walsh, D. M., Shankar, G. M., and Selkoe, D. (2009). Soluble oligomers of amyloid Beta protein facilitate hippocampal long-term depression by disrupting neuronal glutamate uptake. *Neuron* 62, 788–801. doi: 10.1016/j.neuron.2009.05.012

Liu, D., Tang, H., Li, X.-Y., Deng, M.-F., Wei, N., Wang, X., et al. (2017). Targeting the HDAC2/HNF-4A/miR-101b/AMPK pathway rescues tauopathy and dendritic abnormalities in Alzheimer's disease. *Mol. Ther.* 25, 752–764. doi: 10.1016/j.ymthe.2017.01.018

Liu, Y., Wang, M., Marcora, E. M., Zhang, B., and Goate, A. M. (2019). Promoter DNA hypermethylation – Implications for Alzheimer's disease. *Neurosci. Lett.* 711:134403. doi: 10.1016/j.neulet.2019.134403

Marsh, J., and Alifragis, P. J. N. (2018). Synaptic dysfunction in Alzheimer's disease: the effects of amyloid beta on synaptic vesicle dynamics as a novel target for therapeutic intervention. *Neural. Regen Res.* 13:616. doi: 10.4103/1673-5374.230276

Marsh, J., Bagol, S. H., Williams, R. S. B., Dickson, G., and Alifragis, P. (2017). Synapsin I phosphorylation is dysregulated by beta-amyloid oligomers and restored by valproic acid. *Neurobiol. Dis.* 106, 63–75. doi: 10.1016/j.nbd.2017.06.011

Martin, S. J., Grimwood, P. D., and Morris, R. G. (2000). Synaptic plasticity and memory: an evaluation of the hypothesis. *Ann. Rev. Neurosci.* 23, 649–711. doi: 10.1146/annurev.neuro.23.1.649

Miranda, T. B., and Jones, P. A. (2007). DNA methylation: the nuts and bolts of repression. *J. Cell. Physiol.* 213, 384–390. doi: 10.1002/jcp.21224

Mucke, L., Masliah, E., Yu, G.-Q., Mallory, M., Rockenstein, E. M., Tatsuno, G., et al. (2000). High-level neuronal expression of Aβ1–42 in wild-type human amyloid protein precursor transgenic mice: synaptotoxicity without plaque formation. *J. Neurosci.* 20, 4050–4058. doi: 10.1523/jneurosci.20-11-04050.2000

National Institute on Aging (2018). *How Is Alzheimer's Disease Treated? [Online]*. Available online at: https://www.nia.nih.gov/health/how-alzheimers-disease-treated (accessed April 1, 2018).

Panikker, P., Xu, S.-J., Zhang, H., Sarthi, J., Beaver, M., Sheth, A., et al. (2018). Restoring Tip60 HAT/HDAC2 balance in the neurodegenerative brain relieves epigenetic transcriptional repression and reinstates cognition. *J. Neurosci.* 38, 4569–4583. doi: 10.1523/jneurosci.2840-17.2018

Panza, F., Lozupone, M., Logroscino, G., and Imbimbo, B. P. (2019). A critical appraisal of amyloid-beta-targeting therapies for Alzheimer disease. *Nat. Rev. Neurol.* 15, 73–88. doi: 10.1038/s41582-018-0116-6

Parihar, M. S., and Brewer, G. J. (2010). Amyloid-β as a modulator of synaptic plasticity. *J. Alzheimers Dis.* 22, 741–763. doi: 10.3233/JAD-2010-101020

Peixoto, L., and Abel, T. (2013). The role of histone acetylation in memory formation and cognitive impairments. *Neuropsychopharmacology* 38, 62–76. doi: 10.1038/npp.2012.86

Plant, L. D., Boyle, J. P., Smith, I. F., Peers, C., and Pearson, H. A. J. J. (2003). The production of amyloid β peptide is a critical requirement for the viability of central neurons. *J. Neurosci.* 23, 5531–5535. doi: 10.1523/jneurosci.23-13-05531.2003

Puzzo, D., Privitera, L., and Palmeri, A. (2012). Hormetic effect of amyloid-beta peptide in synaptic plasticity and memory. *Neurobiol. Aging* 33, e1415–e1424. doi: 10.1016/j.neurobiolaging.2011.12.020

Ramirez, A., and Arbuckle, M. R. (2016). Synaptic plasticity: the role of learning and unlearning in addiction and beyond. *Biol. Psychiatry* 80, e73–e75. doi: 10.1016/j.biopsych.2016.09.002

Rao, J. S., Keleshian, V. L., Klein, S., and Rapoport, S. I. (2012). Epigenetic modifications in frontal cortex from Alzheimer's disease and bipolar disorder patients. *Transl. Psychiatry* 2:e132. doi: 10.1038/tp.2012.55

Rice, H. C., De Malmazet, D., Schreurs, A., Frere, S., Van Molle, I., Volkov, A. N., et al. (2019). Secreted amyloid-β precursor protein functions as a GABABR1a ligand to modulate synaptic transmission. *Science* 363:6423.

Saha, R., and Pahan, K. (2006). HATs and HDACs in neurodegeneration: a tale of disconcerted acetylation homeostasis. *Cell Death Different.* 13:539. doi: 10.1038/sj.cdd.4401769

Saxonov, S., Berg, P., and Brutlag, D. L. (2006). A genome-wide analysis of CpG dinucleotides in the human genome distinguishes two distinct classes of promoters. *Proc. Natl. Acad. Sci. U.S.A.* 103, 1412–1417. doi: 10.1073/pnas.0510310103

Scheff, S. W., Price, D. A., Schmitt, F. A., and Mufson, E. J. (2006). Hippocampal synaptic loss in early Alzheimer's disease and mild cognitive impairment. *Neurobiol. Aging* 27, 1372–1384. doi: 10.1016/j.neurobiolaging.2005.09.012

Schulz, R., Gerloff, C., and Hummel, F. C. J. N. (2013). Non-invasive brain stimulation in neurological diseases. *Neuropharmacology* 64, 579–587. doi: 10.1016/j.neuropharm.2012.05.016

Selkoe, D. J. (2002). Alzheimer's disease is a synaptic failure. *Science* 298, 789–791.

Shankar, G. M., Li, S., Mehta, T. H., Garcia-Munoz, A., Shepardson, N. E., Smith, I., et al. (2008). Amyloid-β protein dimers isolated directly from Alzheimer's brains impair synaptic plasticity and memory. *Nat. Med.* 14:837. doi: 10.1038/nm1782

Sharma, S. K. (2010). Protein acetylation in synaptic plasticity and memory. *Neurosci. Biobehav. Rev.* 34, 1234–1240. doi: 10.1016/j.neubiorev.2010.02.009

Shoji, M., and Kanai, M. J. J. (2001). Cerebrospinal fluid Aβ40 and Aβ42: natural course and clinical usefulness. *J. Alzheimers Dis.* 3, 313–321. doi: 10.3233/jad-2001-3306

Sultan, F. A., and Day, J. J. (2011). Epigenetic mechanisms in memory and synaptic function. *Epigenomics* 3, 157–181. doi: 10.2217/epi.11.6

Takahashi, R. H., Milner, T. A., Li, F., Nam, E. E., Edgar, M. A., Yamaguchi, H., et al. (2002). Intraneuronal Alzheimer abeta42 accumulates in multivesicular bodies and is associated with synaptic pathology. *Am. J. Pathol.* 161, 1869–1879. doi: 10.1016/s0002-9440(10)64463-x

Tulloch, J., Leong, L., Thomson, Z., Chen, S., Lee, E.-G., Keene, C. D., et al. (2018). Glia-specific APOE epigenetic changes in the Alzheimer's disease brain. *Brain Res.* 1698, 179–186. doi: 10.1016/j.brainres.2018.08.006

U.S. National Library of Medicine (2019). *NCT02167256 A Phase IIa Multi-Center Study of 18F-FDG PET, Safety, and Tolerability of AZD0530 in Mild Alzheimer's Disease*. Available online at: https://ClinicalTrials.gov/show/NCT02167256 (accessed August 14, 2019).

U.S. National Library of Medicine (2020a). *NCT02477800 221AD301 Phase 3 Study of Aducanumab (BIIB037) in Early Alzheimer's Disease*. Availble online at: https://ClinicalTrials.gov/show/NCT02477800 (accessed August 14, 2020).

U.S. National Library of Medicine (2020b). *NCT02484547 221AD302 Phase 3 Study of Aducanumab (BIIB037) in Early Alzheimer's Disease*. Available online at: https://ClinicalTrials.gov/show/NCT02484547 (August 7, 2020).

U.S. National Library of Medicine (2020c). *NCT03446001 Safety and Efficacy of TRx0237 in Subjects With Alzheimer's Disease Followed by Open-Label Treatment*. Available online at: https://ClinicalTrials.gov/show/NCT03446001 (accessed September 1, 2020).

U.S. National Library of Medicine (2020d). *NCT03493282 Effect of CT1812 Treatment on Brain Synaptic Density*. Available online at: https://ClinicalTrials.gov/show/NCT03493282 (accessed February 5, 2020).

Volmar, C.-H., Salah-Uddin, H., Janczura, K. J., Halley, P., Lambert, G., Wodrich, A., et al. (2017). M344 promotes nonamyloidogenic amyloid precursor protein processing while normalizing Alzheimer's disease genes and improving memory. *Proc. Natl. Acad. Sci. U.S.A.* 114, E9135–E9144. doi: 10.1097/00002093-199709000-00012

Walsh, D. M., Klyubin, I., Fadeeva, J. V., Cullen, W. K., Anwyl, R., Wolfe, M. S., et al. (2002). Naturally secreted oligomers of amyloid β protein potently inhibit hippocampal long-term potentiation in vivo. *Nature* 416, 535–539. doi: 10.1038/416535a

Wei, Z., Meng, X., El Fatimy, R., Sun, B., Mai, D., Zhang, J., et al. (2020). Environmental enrichment prevents Aβ oligomer-induced synaptic dysfunction through mirna-132 and hdac3 signaling pathways. *Neurobiol. Dis.* 134:104617. doi: 10.1016/j.nbd.2019.104617

West, R. L., Lee, J. M., and Maroun, L. E. (1995). Hypomethylation of the amyloid precursor protein gene in the brain of an alzheimer's disease patient. *J. Mol Neurosci.* 6, 141–146. doi: 10.1007/BF02736773

Xia, M., Cheng, X., Yi, R., Gao, D., and Xiong, J. (2016). The binding receptors of aβ: an alternative therapeutic target for Alzheimer's disease. *Mol. Neurobiol.* 53, 455–471. doi: 10.1007/s12035-014-8994-0

Yamakawa, H., Cheng, J., Penney, J., Gao, F., Rueda, R., Wang, J., et al. (2017). The transcription factor Sp3 cooperates with HDAC2 to regulate synaptic function and plasticity in neurons. *Cell Rep.* 20, 1319–1334. doi: 10.1016/j.celrep.2017.07.044

Zhang, H., Wu, L., Pchitskaya, E., Zakharova, O., Saito, T., Saido, T., et al. (2015). Neuronal store-operated calcium entry and mushroom spine loss in amyloid precursor protein knock-in mouse model of Alzheimer's disease. *J. Neurosci.* 35, 13275–13286. doi: 10.1523/jneurosci.1034-15.2015

Conflict of Interest: The authors declare that the research was conducted in the absence of any commercial or financial relationships that could be construed as a potential conflict of interest.

frontiers in Molecular Neuroscience

REVIEW
published: 17 November 2020
doi: 10.3389/fnmol.2020.593724

How Microglia Manages Non-cell Autonomous Vicious Cycling of Aβ Toxicity in the Pathogenesis of AD

*YunHee Seol[1], Soomin Ki[2], Hannah L. Ryu[3], Sooyoung Chung[1], Junghee Lee[3,4] and Hoon Ryu[1,3]**

[1]Center for Neuroscience, Brain Science Institute, Korea Institute of Science and Technology, Seoul, South Korea, [2]Department of Brain and Cognitive Science, Ewha Womens University, Seoul, South Korea, [3]Department of Neurology, Boston University Alzheimer's Disease Center, Boston University School of Medicine, Boston, MA, United States, [4]VA Boston Healthcare System, Boston, MA, United States

Alzheimer's disease (AD) is a progressive neurodegenerative disease and a common form of dementia that affects cognition and memory mostly in aged people. AD pathology is characterized by the accumulation of β-amyloid (Aβ) senile plaques and the neurofibrillary tangles of phosphorylated tau, resulting in cell damage and neurodegeneration. The extracellular deposition of Aβ is regarded as an important pathological marker and a principal-agent of neurodegeneration. However, the exact mechanism of Aβ-mediated pathogenesis is not fully understood yet. Recently, a growing body of evidence provides novel insights on the major role of microglia and its non-cell-autonomous cycling of Aβ toxicity. Hence, this article provides a comprehensive overview of microglia as a signifi cant player in uncovering the underlying disease mechanisms of AD.

Keywords: Alzheimer's disease, microglia, amyloid-β, non-cell-autonomous toxicity, vicious cycle

OPEN ACCESS

Edited by:
Daniela Puzzo, University of Catania, Italy

Reviewed by:
Roberto Piacentini, Catholic University of the Sacred Heart, Italy
Simona Federica Spampinato, University of Catania, Italy

****Correspondence:***
Hoon Ryu
hoonryu@kist.re.kr

Received: *11 August 2020*
Accepted: *20 October 2020*
Published: *17 November 2020*

Citation:
Seol Y, Ki S, Ryu HL, Chung S, Lee J and Ryu H (2020) How Microglia Manages Non-cell Autonomous Vicious Cycling of Aβ Toxicity in the Pathogenesis of AD. Front. Mol. Neurosci. 13:593724. doi: 10.3389/fnmol.2020.593724

INTRODUCTION

Alzheimer's disease (AD) is the most common form of dementia, with increasing prevalence as global life expectancy increases. The aggregation of β-amyloid (Aβ), the main component of senile plaques, is a pathological hallmark in AD. In the context of abnormal Aβ processing, ineffective Aβ phagocytosis and clearance by non-neuronal cells including microglia and astrocytes are linked to AD pathogenesis, but the exact mechanism is not understood yet. Microglia, the resident macrophages of the brain, constantly survey the microenvironment for pathogen-associated (PAMPs) or damage-associated molecular patterns (DAMPs), and clear unwanted toxins for steady-brain maintenance (Janeway, 1992; Kigerl et al., 2014; Clayton et al., 2017). As such, microglia have been widely viewed as a homogenous population of ancillary cells, which nevertheless become neurotoxic under neurodegenerative conditions (Lee et al., 2016).

Recent studies have yielded new interpretations of the involvement of microglia in Aβ pathogenesis. Comprehensive single-cell RNA analysis of brain immune cells revealed a disease-associated reactive microglia phenotype called DAM (disease-associated reactive microglia). Owing to the microglial receptors TREM2 (triggering receptor expressed on myeloid cells 2) and Tyrobp (Tyro protein tyrosine kinase binding protein), DAM cells exhibit remarkable morphological changes polarized from homeostatic microglia in response to Aβ (Clayton et al., 2017). Additionally, in studies of the brain immune

system regarding pyrin domain-containing protein 3 (NLRP3) positive (+) inflammasomes, ASC Specks (Apoptosis-associated speck-like protein) containing a C-terminal caspase recruitment domain (CARD), and Aβ-ASC composites, the view upon microgliosis or the secondary cellular responses to Aβ pathology have been increased.

Previous studies report that microglia undergo prominent morphological and functional changes with a marked decline in homeostatic signatures in AD (Krasemann et al., 2017; Mathys et al., 2017; Zhou et al., 2020). Hypothetically, cross Aβ aggregation (so-called cross-seeding activity) of different amyloid proteins *via* a synergetic relationship between non-neuronal cells may contribute to neuronal injury. Contrary to previous dogma, microglia are not merely subsidiary to the disease mechanisms of AD. Accordingly, in this review, we revisit the pathway of Aβ aggregation and focus on microglia function in non-cell-autonomous pathways of sustained Aβ-dependent pathogenesis in AD.

BIRTH OF AMYLOID-BETA PEPTIDE

Amyloid Precursor Protein (APP) Synthesis and Trafficking

The overproduction and extracellular deposition of Aβ1–42 peptides by neurons is a major component of Aβ senile plaque formation and maturation (Lee and Ryu, 2010; Schmit et al., 2011; Campion et al., 2016; Daria et al., 2017; Picone et al., 2020). How Aβ accumulates in the brains of the elderly individual is unclear, but could be initiated by changes in amyloid precursor protein (APP) metabolism (**Figure 1**). Under normal conditions, APP synthesis continues at a high rate in which a portion of APP proteins are inserted into subcellular organelles *via* the early secretory pathway (Anelli and Sitia, 2008; Campion et al., 2016). APP is transported and inserted into the plasma membrane, where more than 90%; is cleaved non-amyloidogenically by α-secretase and γ-secretase activity (Hernández-Zimbrón and Rivas-Arancibia, 2014; Sole-Domenech et al., 2016). APP is also re-internalized and directed to late endosomes in a clathrin-dependent manner where it is cleaved by β-secretase (BACE1) at the N-terminal and γ-secretase at the C terminal (Hernández-Zimbrón and Rivas-Arancibia, 2014; Sun et al., 2015; Webers et al., 2020). Sequence divergence at the internal Aβ site generates Aβ1–40, Aβ1–42, and a long-form of APP (sAPPβ) fated to dispatch into the extracellular space. As well as the amino-terminal APP intracellular domain (AICD) which is released into the cytosol (**Figure 2**; Campion et al., 2016).

Studies show that soluble Aβ oligomers or small Aβ aggregates are toxic to neurons in AD (Jarrett et al., 1993; Sun et al., 2015; Picone et al., 2020), whereas Aβ fibril formation has been proposed as a neural-protective process, possibly segregating neurons from soluble Aβ (Sun et al., 2015; Campion et al., 2016; Picone et al., 2020). Indeed, now, it is well accepted that Aβ toxicity, which disrupts neuronal cell structures and cellular function, resulting in cell death, is mainly represented by oligomers or small aggregates (Daria et al., 2017; Reiss et al., 2018; Picone et al., 2020).

Notably, previous studies show evidence of Aβ associated toxicity in larger Aβ species or plaques that are surrounded by microglia (Sheng et al., 2019; Dickson et al., 1999; Serrano-Pozo et al., 2016). Interestingly, microglia surround Aβ plaques and exhibit decreased Aβ clearance in late-stage AD (Condello et al., 2015; Yuan et al., 2016; Webers et al., 2020). Furtheri nvestigation into the various forms of Aβ depositions and its relationship to non-cell-autonomous mechanisms are necessary for understanding exactly how microglia engage in Aβ clearance and how they are responsible for Aβ accumulation (Sole-Domenech et al., 2016).

Endoplasmic Reticulum (ER) Stress

Considering only 10%; of APP is inserted into the plasma membrane, APP processing may not be isolated to late-endosomes (**Figures 1**, **2**). For instance, Aβ and β-secretases have been identified in cellular compartments involved in APP processing, recycling, and degradation (Picone et al., 2020). One such area of interest is the endoplasmic reticulum (ER; Hashimoto and Saido, 2018). Increased levels of unfolded protein response (UPR) in AD post mortem brain tissues, perhaps with the retention of Aβ or APP in the ER lumen, have been described (Hoozemans et al., 2005, 2009; Nijholt et al., 2012; Picone et al., 2020). Aβ oligomers activate mitochondrion-ER stress-mediated apoptosis, in which, a special sub-compartment called the mitochondria-associated membrane (MAM) is responsible for Ca^{2+} homeostasis. Subsequently, Ca^{2+} uptake due to exogenous Aβ results in eventual apoptosis, promoting the release of Aβ and Ca^{2+} into the extracellular space and triggering inflammatory responses (Resende et al., 2008; Song et al., 2008; Costa et al., 2010; Plácido et al., 2014; Picone et al., 2020). The role of ER stress in AD is still poorly understood. Therefore, more investigation is necessary to determine the Aβ-associated neuronal damage along this cell-autonomous pathway (Plácido et al., 2014; Hashimoto and Saido, 2018).

WHICH CELL TYPE WORKS ON AMYLOID-BETA CLEARANCE?

Homeostatic Microglia

Microglia are extremely sensitive resident myeloid cells of the central nervous system (CNS; Anwar and Rivest, 2020). Microglia play a variety of roles to clear dying neurons, proteins, and debris *via* active phagocytosis and micropinocytosis activity (Rogers et al., 2002; Webers et al., 2020). Phagocytosis by microglia is the process of "eating" large unwanted or toxic macromolecules that are delivered to the lysosome to break down materials, similar to the autophagy process in neurons (Malik et al., 2019; van Weering and Scheper, 2019; Anwar and Rivest, 2020). This includes the clearance of both soluble and insoluble Aβ peptides in the healthy brain, preventing Aβ over-accumulation, and thus, preempting AD initiation (Anwar and Rivest, 2020; Webers et al., 2020). However, in the majority of AD cases, it is unclear whether the faster production or slower clearance of Aβ species is responsible for plaque accumulation (Sole-Domenech et al., 2016). It has been reported that microglia sufficiently clear Aβ in the early stages of AD while late-stage AD is characterized by

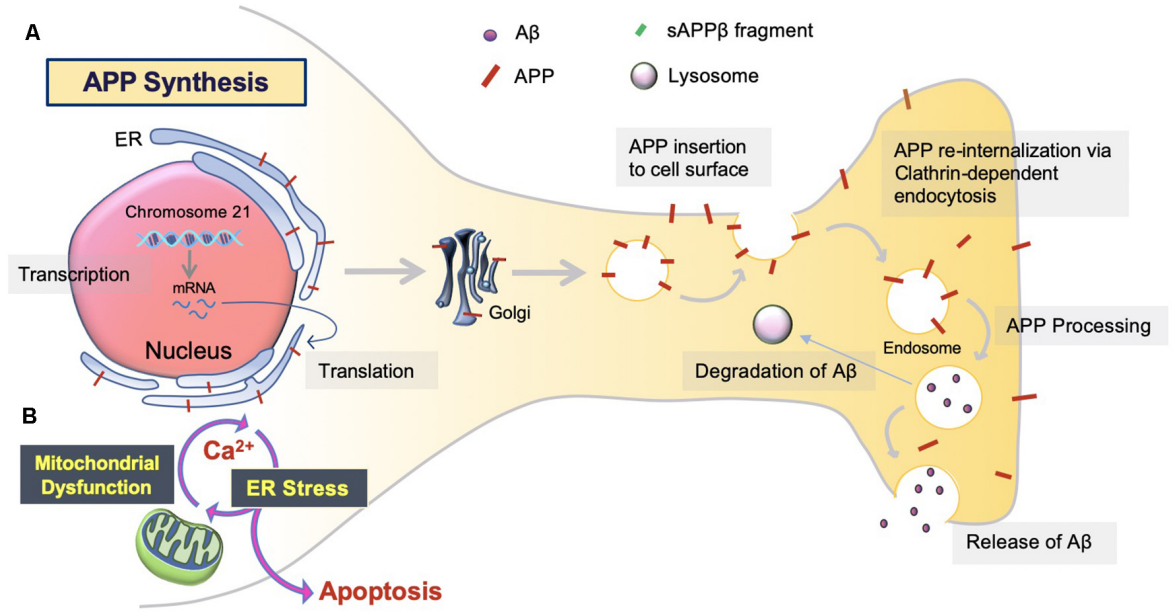

FIGURE 1 | Amyloid precursor protein (APP) synthesis and trafficking. **(A)** APP synthesis. APP synthesis commences with transcription on chromosome 21. Then, it is translated by endoplasmic reticulum (ER) bound ribosomes, translocated into the ER, and trafficked to the Golgi to assume native structure and folding (Sun et al., 2015; Sole-Domenech et al., 2016). Eventually, the APP is inserted into the plasma membrane and reinternalized to produce Aβ. Otherwise, APP can be redirected to non-amyloidogenic pathways by the retromer complex and transported back to the Golgi or plasma membrane *via* the recycling pathway. Nascent Aβ peptides are either extracellularly released or degraded by the lysosome (Hernández-Zimbrón and Rivas-Arancibia, 2014). **(B)** ER stress. Aβ toxicity responds with consequential disruption of Ca^{2+} permeability *via* mitochondria-associated membrane (MAM), mitochondrial Ca^{2+} uptake, and eventual apoptosis.

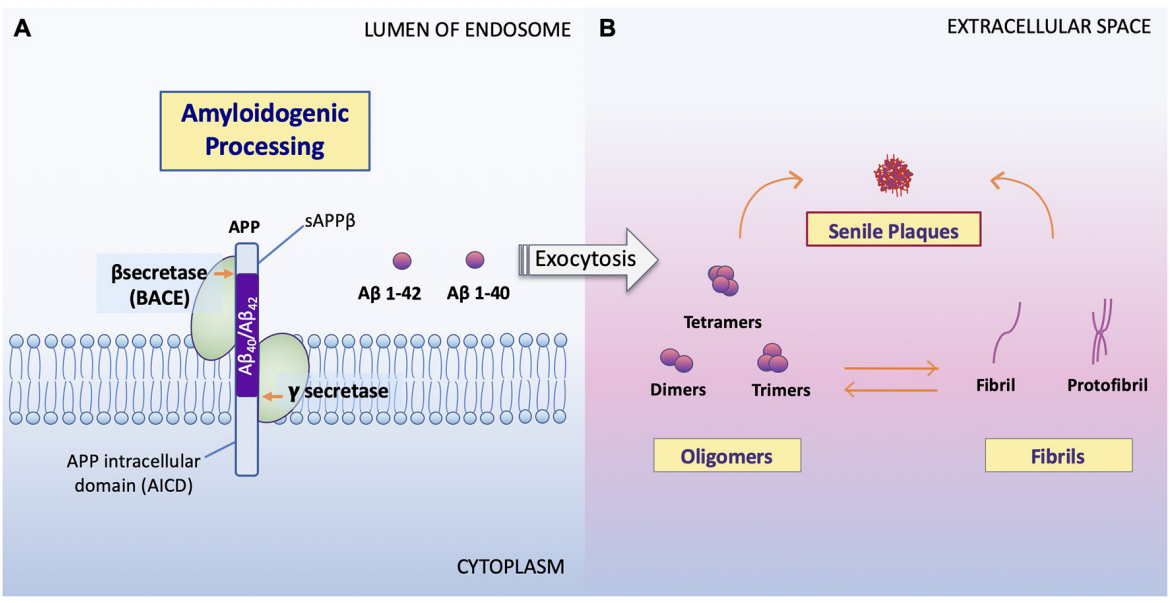

FIGURE 2 | Processing of APP and formation of Aβ oligomers vs. fibrils. **(A)** Amyloidogenic processing. Sequence divergence at the internal Aβ site by γ-secretase produces the monomers Aβ1–40 and Aβ1–42 (Campion et al., 2016) to be deposited to the extracellular space. **(B)** Aβ oligomers vs. fibrils formation. Amyloid oligomers are small with few-chain, soluble, disordered clusters. Fibrils are long, many-chained, highly structured, β-sheet-like aggregates. The hydrophobic amino acids of Aβ1–40 and Aβ1–42 peptides confer to the hydrophobicity of the C terminal. Fibrils then arrange in a beta-pleated sheet and form the amyloid plaques seen on conventional hematoxylin and eosin (HE) staining or amyloid specific staining (Sun et al., 2015). It has been noted that the high peptide concentration tips the balance towards fibrils regardless of monomer concentrations and that the onset of fibrilization limits the concentration of oligomers in solution (Schmit et al., 2011).

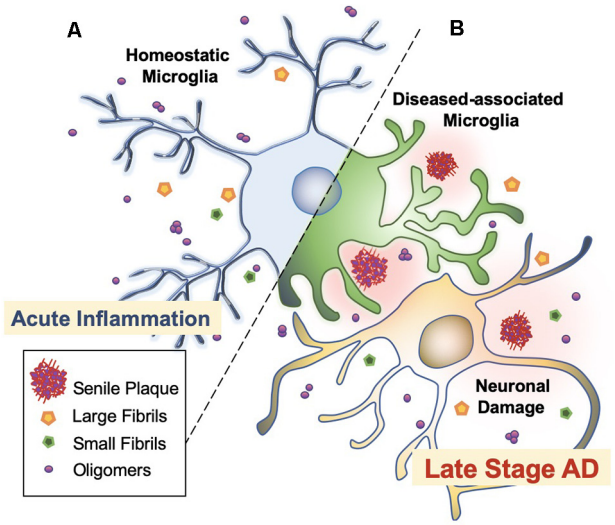

FIGURE 3 | Microglial activation checkpoints. **(A)** Homeostatic microglia. Resting microglia, under non-inflammatory healthy conditions, have a small soma with processes extending into the microenvironment (Webers et al., 2020). Triggering of PAMP or DAMP signals may occur intermittently, in which ramified microglia exhibit "controlled phagocytosis," a process by which cells engage in the clearance of damaged cells and debris as part of their scavenging role within the brain (Sole-Domenech et al., 2016; Webers et al., 2020). **(B)** Disease-associated microglia. Intermediate activation of microglia exhibits larger and elongated soma, where microglia become highly motile with enhanced phagocytic activity and release pro-inflammatory cytokines (O'Brien and Wong, 2011). Fully activated microglia are located nearby Aβ plaques. In AD transgenic mice, gene set enrichment analysis revealed significant involvement in phagocytotic pathways, endocytosis, and regulation of anti-inflammatory and immune response in DAM (Keren-Shaul et al., 2017).

the phagocytosis of fibrils and plaques with an overflow of Aβ in the brain (**Figure 3**; Hickman et al., 2008; O'Brien and Wong, 2011; Keren-Shaul et al., 2017; Anwar and Rivest, 2020; Webers et al., 2020). A shortage of protein clearance by microglia may ultimately swing the balance between neuronal health and death (Zhao et al., 2017; Malik et al., 2019). Thus, the progression of AD may strongly depend on microglial phagocytosis and autophagy-lysosomal activity. In this paradigm, the connection between phagocytosis and microglia-mediated neurotoxicity is closely linked to the pathogenesis of AD (O'Brien and Wong, 2011).

Disease-Associated Reactive Microglia (DAM)

In general, the healthy hippocampal parenchyma is characterized by an even distribution of microglia. However, in human cases and animal models of AD, microglia in the vicinity of Aβ deposits lose their Aβ clearing ability (**Figure 4**). IBA1 positive (+) cells express an accumulation of autophagy receptor p62 in the late stages of AD (O'Brien and Wong, 2011; Daria et al., 2017; Tejera et al., 2019; Anwar and Rivest, 2020). This phenomenon has been attributed to a specific subpopulation of microglial cells. Microglia in *5xFAD* mice and human post mortem AD brains transit from a homeostatic phenotype to DAM population, accompanied by alterations to their morphology and gene transcription (O'Brien and Wong, 2011; Sole-Domenech et al., 2016; Keren-Shaul et al., 2017; Lučiūnaitė et al., 2019). Immunohistochemical staining also revealed the DAM as autophagosomes with positively stained intracellular Aβ (Keren-Shaul et al., 2017).

Two activation states of microglia have been defined: Stage I and Stage II DAM (Da Mesquita and Kipnis, 2017). Importantly, Aβ1–42 has been identified as one of the damage-associated molecular patterns (DAMPs) that triggers the microglial transformation (Cho et al., 2014; Terrill-Usery et al., 2014; Deczkowska et al., 2018). In its diseased state, microglia express a single-pass transmembrane receptor (*Trem2*) which associates with the signaling adaptor tyrosine kinase-binding protein (Tyrobp). Studies have indicated the role of Trem2 in phagocytosis along the activation spectrum that generates DAM in microglia (Kleinberger et al., 2014). In a study by Ulland et al., increased $LC3^{+}$ puncta, an autophagosome marker, was observed in human post-mortem brain sections from AD patients with a rare R47H variant of the Trem2 gene compared to controls (Ulland et al., 2017; Filipello et al., 2018; Ulland and Colonna, 2018). In *Trem2*$^{-}$*/5xFAD* mice, similar results were observed in addition to the failure of microglia to migrate around Aβ plaques compared to controls (Kleinberger et al., 2014; Ulland et al., 2017; Ulland and Colonna, 2018). Furthermore, Keren-Shaul et al. demonstrated an absence of full DAM in *Trem2*$^{-}$*/5xFAD* mice, instead, a large population of partially activated or Stage I DAM was accumulated in the brain, indicating that DAM activation occurs in a TREM2-independent manner (Haure-Mirande et al., 2019). Whereas, entering Stage II DAM required the activation of Tyrobp in a TREM2-dependent manner (Keren-Shaul et al., 2017). It is well known that in both mouse and AD patient brains, Tyrobp is significantly upregulated (Ma et al., 2015). Mice expressing a decrease in Tyrobp protein resulted in impaired microglial activation decreased microglial recruitment and clustering around Aβ plaques (Haure-Mirande et al., 2017). This may indicate an enhanced phagocytotic role of Tyrobp in close association with Trem2, however, its role remains elusive. Overall, homeostatic microglia phenotype from Stage I and then Stage II DAM is accompanied by pronounced DAM-specific gene expression with full microglial activation (Keren-Shaul et al., 2017). The loss of function or partial defect in the trajectory of microglial activation is likely to accumulate and facilitate in the development of AD.

Such findings coincide with Johnson et al.'s (2020) recent large-scale proteomic study uncovering the cellular changes complementary to AD. A consensus view of the proteomic changes within each progressive AD state was developed using a co-expression analysis and a weighted correlation network analysis algorithm (WGCNA). Interestingly, the co-expression module with the most strongly altered AD proteins linked to AD genetic risk was the Astrocyte/Microglia metabolism module, which was enriched in proteins linked to microglia, astrocytes, and sugar metabolism. Specifically, its principal component (PC) was more strongly associated with the neuropathological hallmarks of AD (CERAD, Braak-staging-system, MMSE, CDR) compared to other biological processes (mitochondria, RNA binding/splicing). Importantly, in this module, the microglia

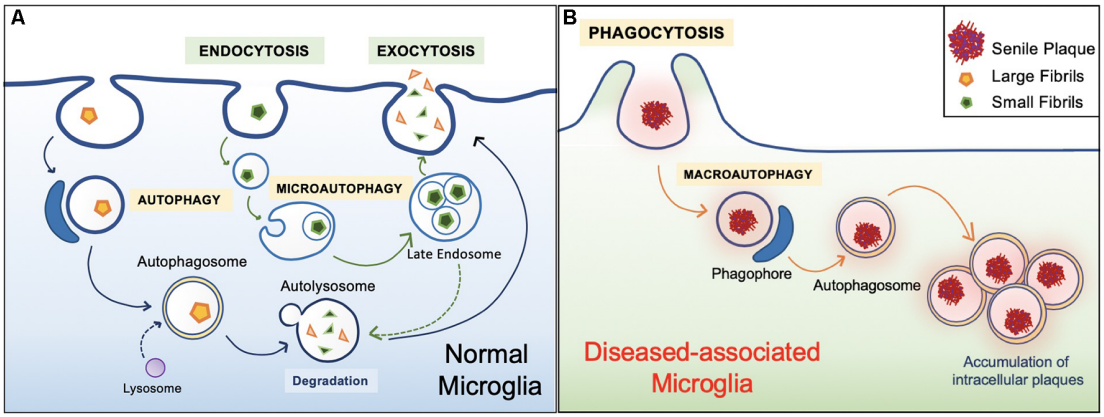

FIGURE 4 | Healthy vs. diseased Aβ clearance. **(A)** Homeostatic autophagy. In the healthy brain, endocytosis of Aβ oligomers and fibrils are normal (Lee and Landreth, 2010; Webers et al., 2020). Internalized Aβ substrates are sorted within the endocytic pathway. Aβ substrates are delivered to acidic lysosomes and late endosomes. Compartment acidification leads to degradation of Aβ oligomers and fibrils, then released *via* exocytosis (Sole-Domenech et al., 2016). **(B)** Diseased Aβ clearance. In the unhealthy brain, microglia engulf large Aβ plaques *via* phagocytosis. However, Aβ plaques are not properly degraded and instead harbored within the cell, ultimately leading to inflammatory conditions (Malik et al., 2019; Zhao and Zhang, 2019).

protein markers were identified to be in an anti-inflammatory disease-associated state. Synonymous with current studies on microglia activation, it also exhibited one of the strongest increasing patterns along with AD progression in the dorsolateral prefrontal cortex (DLPC; Johnson et al., 2020). It is noticeable that most phenotypic markers amongst a thousand AD risk factor genes were categorized into an anti-inflammatory phagocytotic DAM state. Thus, the strong AD correlations with DAM highlights the importance of heterogeneous microglia populations in the brain. Microglia may be characterized by a heterogeneous pool with local and cross-seeding effects on Aβ clearance (Mandrekar-Colucci and Landreth, 2010). On this note, depletion of either old or young microglial cells prevented Aβ plaque clearance in AD brains, indicating the modulation effect of old microglial populations by young microglia (Malik et al., 2019). Furthermore, Daria et al. (2017) found that co-cultured organotypic brain slices of amyloid bearing APP/PS1 transgenic AD mice with the brain slices of young neonatal wild-type mice revealed almost a 60%; reduction in Aβ plaque levels. After microglia were depleted of clodronate in young brain slices and then added to old APP/PS1 mouse brain slices, the clearance of plaques was less effective. Moreover, young microglia-derived conditioned media increased the proliferation of old microglia and decreased the size of Aβ plaques. This study suggests that microglia activity can be reversibly regulated and that microglial aging is an instrumental factor in Aβ plaque phagocytosis and clearance (Daria et al., 2017).

Phagocytosis and Autophagy of Aβ

Recent studies suggest a "critical threshold" of microglial capacity or limitation in Aβ degradation (Anwar and Rivest, 2020; Pomilio et al., 2020). Pomilio et al. (2020) monitored the autophagic flux and inflammation of microglia in AD. Prolonged inflammatory responses or persistent exposure to Aβ1–42 peptides and fibrillar Aβ resulted in microglial exhaustion and decreased autophagy markers. In this case, short vs. long exposure of Aβ on microglia (*in vitro* cultured BV-2 cells) showed significant and differential changes in autophagy activity. Short (2 h) exposure of Aβ1–42 peptide exhibited functional autophagy and enhanced autophagic flux in an inflammasome-mediated manner. However, prolonged Aβ1–42 exposure (longer than 24 h) resulted in a decreased autophagic flux. Together, aggregated Aβ peptides affect the autophagy flux in microglia in a time-dependent manner (Pomilio et al., 2020). Consequently, such microglial autophagy dysfunction enhances toxic Aβ protein aggregates, possibly leading to neuronal damage in AD patients (**Figure 3**; Anwar and Rivest, 2020).

Lysosomal Damage

In microglia, internalized Aβ substances are delivered to the lysosome for degradation (Nakanishi, 2003; Halle et al., 2008; Ries and Sastre, 2016). This interplay between autophagy machinery and lysosomal activity has been considered in the context of chronic Aβ exposure (Zhang et al., 2017). Lysosomal damage was associated with autophagic impairment and membrane permeabilization of acid hydrolase cathepsin-D, which altered LysoTracker staining in the cytoplasm of microglia. Furthermore, microglia in the vicinity of amyloid deposits in post-mortem AD brains showed phagocytic CD69 positive (+) microglia with displaced LC3 positive (+) autophagosome accumulation and autophagic vesicles (Anwar and Rivest, 2020). It is proposed that the lysosomal damage may be a key factor in inducing microglial dysfunction and poor clearance of Aβ in the late stages of AD. Further study is needed to address the relationship between lysosomal damage and autophagy due to chronic Aβ exposure.

Phagocytosis at the Synapse

Amongst the many important roles of microglia and its involvement in Aβ clearance, microglial involvement at the

synaptic level in response to Aβ warrants attention. In AD patients, a significant reduction in the number of synapses has been observed, even forgoing senile plaque deposition (Cardozo et al., 2019). Studies suggest that the role of microglia in synaptic removal, normally operated during the refinement period of brain development, can be reactivated in aging or in disease. The trajectory has been best described by the complement cascade. Increased levels of the complement component 1q (C1q) and its downstream complement compound 3 (C3) at the synapse are activated, then targeted by microglia for elimination (Rajendran and Paolicelli, 2018). Recent studies show that this action occurs through tight interactions between astrocytes, microglia, and the pre and post-synapses in response to Aβ (**Figure 5**).

At the synapse, APP has been proposed to be an Aβ receptor which becomes internalized, increasing Aβ toxicity intracellularly and suppressing long term potentiation (LTP) in the neuron (Ripoli et al., 2014; Fá et al., 2016; Puzzo et al., 2017). Aβ also activates the complement cascade by directly binding to C1q, contributing to the upregulation of C3 which is recognized by microglial complement receptor (CR3) and triggering microglial engulfment of the synapse (Hong et al., 2016; Cardozo et al., 2019; Hemonnot et al., 2019). The complement cascade is also activated indirectly *via* astrocytes. Talantova et al. (2013) discovered that the activation of α-7 nicotinic receptor (α7nachr) by Aβ, increases intracellular Ca^{2+}, and prompts glutamate release in astrocytes. Glutamate binds to metabotropic glutamate receptor 1 (mGluR1) and eNMDAR at the synapse, both of which lead to LTD and the later activating the complement cascade (Talantova et al., 2013; Cardozo et al., 2019; **Figure 5**). In synchrony, synaptic engulfment may be actionable when microglia and astrocytes tightly interact with pre and post-synapses, a key site previously termed the "tetrapartite synapse" (Dodds et al., 2016; Rial et al., 2016; Jay et al., 2019).

"A DROP HOLLOWS THE STONE, NOT BY FORCE, BUT BY ITS FREQUENCY": CHRONIC Aβ STRESS LEADS TO BRAIN INJURY

Traditionally, the pathways of Aβ production and microglia-dependent neuroinflammation have been considered separately. However, as more studies have been performed, these processes are converging to promote understanding of neuropathology associated with AD. Recent research indicates that microglia induce continuous inflammation when Aβ levels are elevated (Webers et al., 2020). Activated microglia secrete proinflammatory cytokines that trigger a vicious and positive feedback cycle to the microglia itself and neighboring neurons, inducing persistent low-grade inflammation in the parenchyma and subsequently implementing chronic pathogenesis (Keren-Shaul et al., 2017; Webers et al., 2020). Now, it is well accepted that the neuroinflammation response is a pivotal and central player in AD pathogenesis as the third hallmark of the disease beyond Aβ plaques and fibrillary tau tangles (Webers et al., 2020).

Importantly, the chemical nature of Aβ oligomers harboring a major number of open active ends can spread easily in tissues and interact with target cells. This has shown the capacity of Aβ monomers and oligomers to penetrate, insert, or coat the plasma membrane, potentially increasing Aβ aggregations by inducing structural transitions from random coil to β sheets in Aβ1–42 peptides in neurons (Rushworth and Hooper, 2010; Drolle et al., 2014). Importantly, the dysfunction of these cellular components may lead to the activation of cellular death mechanisms and subsequent neurodegeneration observed in AD pathologies (Lansbury and Lashuel, 2006; Picone et al., 2020). In the following section, we will discuss the vicious and positive feedback mechanisms of inflammation and subsequent neurotoxicity.

NLRP3 and ASC Specks: The Vicious Positive-Feedback Mechanism

NLRP3 Inflammasome

Microglia are capable of binding to soluble Aβ oligomers and fibrils *via* cell-surface receptors (CD36, CD14, and CD47) and Toll-like receptors (TLR2, 4, 6, and 9) including NACHT-, LRR-, and pyrin domain-containing protein 3 (NLRP3). Engagement of these receptors induces the release of proinflammatory cytokines and chemokines such as tumor necrosis factor (TNF) α and IL-1β, which cause sustained low-grade inflammation and neurotoxicity (Lu et al., 2008; Tejera et al., 2019; Webers et al., 2020).

PAMP or DAMP signals, which trigger DAM activation and phagocytosis in microglia, also induce NOD-like receptor (NLR) family and NLRP3 inflammasome activity in microglia (**Figure 6**; Lučiūnaitė et al., 2019; Tejera et al., 2019). The NLRP3 inflammasome is a multiprotein complex bridged to procaspase-1 zymogen *via* the adaptor protein ASC (apoptosis-associated speck-like protein) containing a C-terminal caspase recruitment domain (CARD; Lučiūnaitė et al., 2019; Friker et al., 2020). Its assembly and activation depend on two signals: transcriptional upregulation of inflammasome components *via* the transcription factor nuclear factor κB (NF-κB), and a second signal generated by DAMP-induced ion fluxes, mitochondrial reactive oxygen species (ROS) production, or lysosomal destabilization. Indeed, both small and large Aβ molecular aggregates such as oligomers, protofibrils, and large fibrils, act as a DAMP and rapidly trigger NLRP3 (Lučiūnaitė et al., 2019).

ASC Specks

Following NLRP3 activation, ASC, also known as PYCARD, engages in ASC helical fibrillar assembly (Venegas et al., 2017). ASC is composed of an N-terminal pyrin domain (PYD) and a CARD. The homotypic intramolecular PYD-PYD interactions of the ASC adaptor protein initiate the formation of a helical filament, which allows intermolecular CARD-CARD interactions with the CARD domain of procaspase-1. Then, it causes the activation of mature caspase-1, which can cleave the pro-forms of inflammatory cytokines into their active forms such as IL-1B and IL-18 (Lučiūnaitė et al., 2019; Tejera et al., 2019; Friker et al., 2020; Webers et al., 2020). Interactions

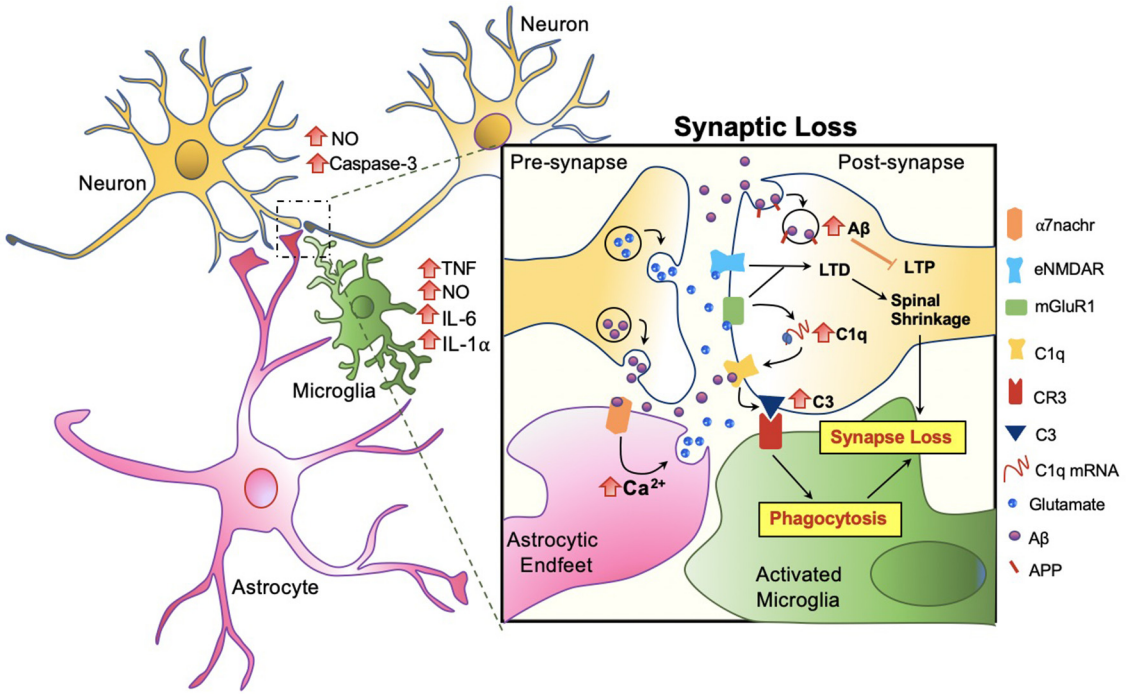

FIGURE 5 | Microglia mediated synaptic loss in AD. Synaptic engulfment by activated microglia can occur through the direct effects of Aβ on synapses or indirect action *via* astrocytes. Soluble factors, tumor necrosis factor (TNF), nitric oxide (NO), interleukin-6 (IL-6), interleukin 1 alpha (IL-1α) are released by microglia, and NO and Caspase-3 by neurons, contributing towards the overall toxicity at the synapse (Rajendran and Paolicelli, 2018). In synchrony, these mechanisms result in spinal shrinkage, activated microglia, and ultimately the loss of the synapse.

between ASC and caspase-1 generate large para nuclear ASC specks and release them into the intracellular space (Venegas et al., 2017; Lučiūnaitė et al., 2019; Tejera et al., 2019). ASC specks are also NLRP3 dependent and only observed in *NLRP3*$^{-/-}$ mice (Tejera et al., 2019). Released ASC or ASC specks can be functionally built into NLRP3 inflammasomes of neighboring microglia and trigger the ongoing immune response *via* microglial activity (Baroja-Mazo et al., 2014; Franklin et al., 2014; Venegas et al., 2017; Tejera et al., 2019; Friker et al., 2020).

ASC-Aβ Composites

Recent findings support the concept that NLRP3 inflammasome activation is connected to the seeding and spreading of Aβ pathology (**Figure 6**; Cho et al., 2014; Venegas et al., 2017). In AD patient brains and APP/PS1 transgenic mice, Aβ1–42 aggregates composited with ASC specks are observed rapidly after its release. Using purified ASC specks generated by immunoprecipitation and enzymatic cleavage, Aβ cross-seeding activity resulted in the acceleration of Aβ oligomerization and aggregation in injected APP/PS1 mice (Venegas et al., 2017; Friker et al., 2020) compared to ASC-deficient APP/PS1 mice. Analysis of thioflavin-T (ThT) fluorescence assays and Western blot analysis further revealed that ASC-Aβ composites are produced in a time and concentration-dependent manner (Venegas et al., 2017). Increasing evidence shows that sustained microglial activation and its peripheral inflammation increases Aβ production as a direct result of neuroinflammation. Tejera et al. (2019) found a significant increase in Aβ deposit number and size in old (15 months) APP/PS1 mice by LPS administrations but not in APP/PS1/NLRP3$^{-/-}$ mice (Tejera et al., 2019). In this condition, ASC specks were correlatively increased. These results suggest that the NLRP-3 activation and pro-inflammation pathway affects amyloid deposition in aged APP/PS1 mice (Tejera et al., 2019).

To examine whether endogenous ASC specks contribute to this phenomenon, Venegas et al. (2017) performed direct intrahippocampal injections of ASC specks to wild-type mice and APP/PS1 mice. Administration of ASC specks increased the total number and area of Aβ immunopositive deposits compared to the contralateral injection site without changes in expression of APP or APP-cleavage products or phagocytosis. The phenomenon was absent in APP/PS1/ASC$^{-/-}$ mice (Venegas et al., 2017). These studies suggest that an increase in ASC-Aβ composites due to the inflammatory response in microglia results in a vicious cycle between neurons and microglia, resulting in ongoing low-grade inflammation and ultimately AD progression (**Figure 6**; Webers et al., 2020).

Microglial Pyroptosis

Pyroptosis ("pyro" means fever/fire in Greek) is a unique kind of cell death by inflammatory caspases (Caspase 1, Caspase 4/5, and Caspase 11) and shows nuclear condensation, cellular

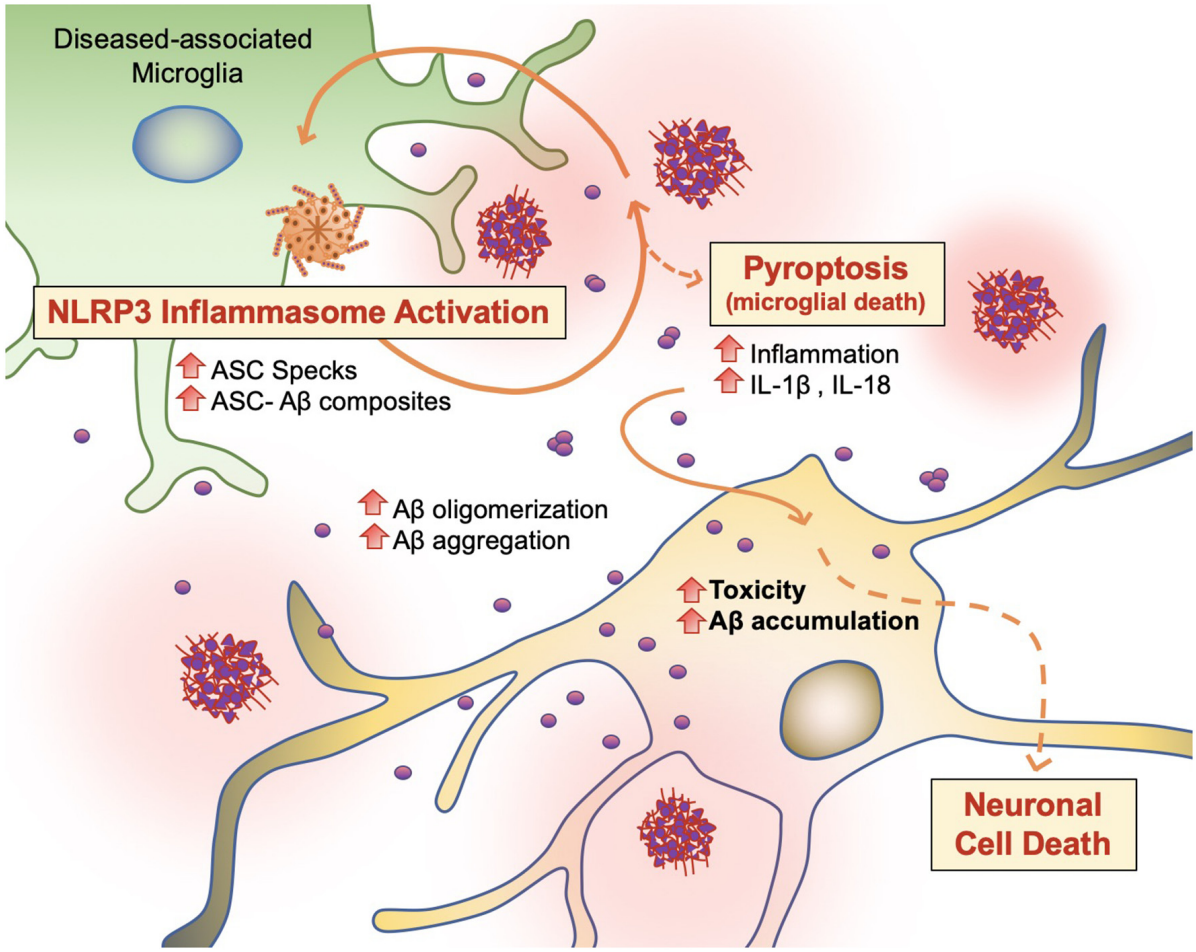

FIGURE 6 | Vicious cycling of Aβ. The NLRP3 inflammasome, which behaves as an intracellular sensor for DAMP signals, is activated in diseased microglia. Specifically, in the later stages of AD, microglia activation releases ASC specks, which bind to Aβ. ASC-Aβ composites reactivate the NLRP3 inflammasome *via* a vicious cycle, prolonging inflammation and the release of inflammatory cytokines such as interleukin IL-1β and IL-18, consequently damaging neurons (Voet et al., 2019).

swelling, and lysis. Microglial pyroptosis can be a factor in AD progression as it may release withheld Aβ plaques and ASC specks (**Figure 6**). In a study by Friker et al. (2020), lipopolysaccharide (LPS) primed cells were treated with ASC, Aβ, or ASC-Aβ composites. Irrespective of LPS priming, microglia exposed to ASC-Aβ composites showed a significant increase in cell death compared to ASC or Aβ alone. Interestingly, the metabolic activity in microglia treated with ASC-Aβ composites did not change within 12 h but was significantly reduced after 24 h compared to cells only treated with ASC or Aβ. ASC-Aβ composites amplified NLRP3 inflammasome activation, resulting in pyroptotic cell death. Exposure to ASC-Aβ composites amplifies the proinflammatory response, resulting in pyroptotic cell death and setting free functional ASC, and consequently inducing a vicious cycle of pathogenesis (**Figure 6**; Friker et al., 2020).

Caspase-1 has also been noted to be involved in microglial pyroptosis, which cleaves pyroptosis executioner protein gasdermin D (GSDMD), resulting in the formation of pores in the plasma membrane and leading to cell lysis because of ion flux and subsequent cytosolic swelling (Friker et al., 2020). When it comes to microglial pyroptosis, inflammation that results from active microglia seem to jeopardize their viability as lower molecular aggregates such as Aβ oligomers and protofibrils do not have such effects (Lučiūnaitė et al., 2019).

CONCLUSION

Since the discovery of microglia types, the mechanisms for microglial activation and its possible contributions towards neuronal degeneration has become an intense topic of debate and research. A common theme amongst the players responsible for microglial activation has been its changing role on Aβ clearance depending on the stage of AD severity. It seems likely that microglial-activation is pre-programmed in homeostatic conditions or pre-clinical stages of AD, suggesting that microglia play a useful role in normal conditions and then progress into dysfunctional cells in pathological conditions as if "friends

become foes" (Lee et al., 2016; Venegas et al., 2017; Tejera et al., 2019; Johnson et al., 2020). Indeed, AD pathology is through to begin 10–20 years before the first clinical manifestation, with Aβ accumulation in the cerebral spinal fluid preceding changes in the cortex (Braak and Braak, 1991; Hölttä et al., 2013; Palmqvist et al., 2016). Consistent with these observations, in both humans and AD mouse models, the absence of normally functioning microglia exacerbates Aβ pathology. On the other hand, activated microglia not only trigger inflammation but also cross-seed with neighboring neurons and astrocytes, sustaining, and accelerating diseased conditions. In combination, reconciling these contradictory functions may further uncover the role of non-cell-autonomous pathways on Aβ aggregate formation. We may find that microglia are deeply involved in the pathogenesis of AD (Anwar and Rivest, 2020; Johnson et al., 2020). In this context, future studies of the vicious cycling of Aβ aggregation *via* microglia with consideration of characterizing heterogeneous microglial types can improve our understanding of the complex pathological events in AD.

AUTHOR CONTRIBUTIONS

YS and HR wrote the manuscript and drew the schemes. SK, YS, and HR organized the references. JL and HR read, reviewed, and edited the manuscript. All authors contributed to the article and approved the submitted version.

FUNDING

This study was also supported by the National Research Foundation of Korea Grant (NRF-2016M3C7A1904233, NRF-2018M3C7A1056894, and NRF-2020M3E5D9079742) from the Ministry of Science, ICT and Future Planning, the National Research Council of Science and Technology (NST) Grant (No. CRC-15-04-KIST) from the Korea government (MSIP), and Grants from Korea Institute of Science and Technology (2E30320 and 2E30762). In part, this study was supported by NIH Grants (NS109537 to JL and AG054156 to HR).

REFERENCES

Anelli, T., and Sitia, R. (2008). Protein quality control in the early secretory pathway. *EMBO J.* 27, 315–327. doi: 10.1038/sj.emboj.7601974

Anwar, S., and Rivest, S. (2020). Alzheimer's disease: microglia targets and their modulation to promote amyloid phagocytosis and mitigate neuroinflammation. *Expert Opin. Ther. Targets* 24, 331–344. doi: 10.1080/14728222.2020.1738391

Baroja-Mazo, A., Martín-Sánchez, F., Gomez, A. I., Martínez, C. M., Amores-Iniesta, J., Compan, V., et al. (2014). The NLRP3 inflammasome is released as a particulate danger signal that amplifies the inflammatory response. *Nat. Immunol.* 15, 738–748. doi: 10.1038/ni.2919

Braak, H., and Braak, E. (1991). Neuropathological stageing of Alzheimer-related changes. *Acta Neuropathol.* 82, 239–259. doi: 10.1007/BF00308809

Campion, D., Pottier, C., Nicolas, G., Le Guennec, K., and Rovelet-Lecrux, A. (2016). Alzheimer disease: modeling an Aβ-centered biological network. *Mol. Psychiatry* 21, 861–871. doi: 10.1038/mp.2016.38

Cardozo, P. L., de Lima, I. B. Q., Maciel, E. M. A., Silva, N. C., Dobransky, T., and Ribeiro, F. M. (2019). Synaptic elimination in neurological disorders. *Curr. Neuropharmacol.* 17, 1071–1095. doi: 10.2174/1570159X17666190603170511

Cho, M. H., Cho, K., Kang, H. J., Jeon, E. Y., Kim, H. S., Kwon, H. J., et al. (2014). Autophagy in microglia degrades extracellular β-amyloid fibrils and regulates the NLRP3 inflammasome. *Autophagy* 10, 1761–1775. doi: 10.4161/auto.29647

Clayton, K. A., Van Enoo, A. A., and Ikezu, T. (2017). Alzheimer's disease: the role of microglia in brain homeostasis and proteopathy. *Front. Neurosci.* 11:680. doi: 10.3389/fnins.2017.00680

Condello, C., Yuan, P., Schain, A., and Grutzendler, J. (2015). Microglia constitute a barrier that prevents neurotoxic protofibrillar Aβ42 hotspots around plaques. *Nat. Commun.* 6:6176. doi: 10.1038/ncomms7176

Costa, R. O., Ferreiro, E., Cardoso, S. M., Oliveira, C. R., and Pereira, C. M. (2010). ER stress-mediated apoptotic pathway induced by Aβ peptide requires the presence of functional mitochondria. *J. Alzheimers Dis.* 20, 625–636. doi: 10.3233/JAD-2010-091369

Da Mesquita, S., and Kipnis, J. (2017). DAMed in (trem) 2 steps. *Cell* 169, 1172–1174. doi: 10.1016/j.cell.2017.05.039

Daria, A., Colombo, A., Llovera, G., Hampel, H., Willem, M., Liesz, A., et al. (2017). Young microglia restore amyloid plaque clearance of aged microglia. *EMBO J.* 36, 583–603. doi: 10.15252/embj.201694591

Deczkowska, A., Keren-Shaul, H., Weiner, A., Colonna, M., Schwartz, M., and Amit, I. (2018). Disease-associated microglia: a universal immune sensor of neurodegeneration. *Cell* 173, 1073–1081. doi: 10.1016/j.cell.2018.05.003

Dickson, T. C., King, C. E., McCormack, G. H., and Vickers, J. C. (1999). Neurochemical diversity of dystrophic neurites in the early and late stages of Alzheimer's disease. *Exp. Neurol.* 156, 100–110. doi: 10.1006/exnr.1998.7010

Dodds, K. N., Beckett, E. A. H., Evans, S. F., Grace, P. M., Watkins, L. R., and Hutchinson, M. R. (2016). Glial contributions to visceral pain: implications for disease etiology and the female predominance of persistent pain. *Transl. Psychiatry* 6:e888. doi: 10.1038/tp.2016.168

Drolle, E., Hane, F., Lee, B., and Leonenko, Z. (2014). Atomic force microscopy to study molecular mechanisms of amyloid fibril formation and toxicity in Alzheimer's disease. *Drug Metab. Rev.* 46, 207–223. doi: 10.3109/03602532.2014.882354

Fá, M., Puzzo, D., Piacentini, R., Staniszewski, A., Zhang, H., Baltrons, M. A., et al. (2016). Extracellular tau oligomers produce an immediate impairment of LTP and memory. *Sci. Rep.* 6:19393. doi: 10.1038/srep19393

Filipello, F., Morini, R., Corradini, I., Zerbi, V., Canzi, A., Michalski, B., et al. (2018). The Microglial innate immune receptor TREM2 is required for synapse elimination and normal brain connectivity. *Immunity* 48, 979–991.e8. doi: 10.1016/j.immuni.2018.04.016

Franklin, B. S., Bossaller, L., De Nardo, D., Ratter, J. M., Stutz, A., Engels, G., et al. (2014). The adaptor ASC has extracellular and "prionoid" activities that propagate inflammation. *Nat. Immunol.* 15, 727–737. doi: 10.1038/ni.2913

Friker, L. L., Scheiblich, H., Hochheiser, I. V., Brinkschulte, R., Riedel, D., Latz, E., et al. (2020). β-amyloid clustering around ASC fibrils boosts its toxicity in microglia. *Cell Rep.* 30, 3743.e6–3754.e6. doi: 10.1016/j.celrep.2020.02.025

Halle, A., Hornung, V., Petzold, G. C., Stewart, C. R., Monks, B. G., Reinheckel, T., et al. (2008). The NALP3 inflammasome is involved in the innate immune response to amyloid-β. *Nat. Immunol.* 9, 857–865. doi: 10.1038/ni.1636

Hashimoto, S., and Saido, T. C. (2018). Critical review: involvement of endoplasmic reticulum stress in the aetiology of Alzheimer's disease. *Open Biol.* 8:180024. doi: 10.1098/rsob.180024

Haure-Mirande, J. V., Audrain, M., Fanutza, T., Kim, S. H., Klein, W. L., Glabe, C., et al. (2017). Deficiency of TYROBP, an adapter protein for TREM2 and CR3 receptors, is neuroprotective in a mouse model of early Alzheimer's pathology. *Acta Neuropathol.* 134, 769–788. doi: 10.1007/s00401-017-1737-3

Haure-Mirande, J. V., Wang, M., Audrain, M., Fanutza, T., Kim, S. H., Heja, S., et al. (2019). Integrative approach to sporadic Alzheimer's disease: deficiency of TYROBP in cerebral Aβ amyloidosis mouse normalizes clinical phenotype and complement subnetwork molecular pathology without reducing Aβ burden. *Mol. Psychiatry* 24, 431–446. doi: 10.1038/s41380-018-0255-6

Hemonnot, A. L., Hua, J., Ulmann, L., and Hirbec, H. (2019). Microglia in Alzheimer disease: well-known targets and new opportunities. *Front. Aging Neurosci.* 11:233. doi: 10.3389/fnagi.2019.00233

Hernández-Zimbrón, L. F., and Rivas-Arancibia, S. (2014). Deciphering an interplay of proteins associated with amyloid β 1–42 peptide and molecular mechanisms of Alzheimer's disease. *Rev. Neurosci.* 25, 773–783. doi: 10.1515/revneuro-2014-0025

Hickman, S. E., Allison, E. K., and El Khoury, J. (2008). Microglial dysfunction and defective β-amyloid clearance pathways in aging Alzheimer's disease mice. *J. Neurosci.* 28, 8354–8360. doi: 10.1523/jneurosci.0616-08.2008

Hölttä, M., Hansson, O., Andreasson, U., Hertze, J., Minthon, L., Nägga, K., et al. (2013). Evaluating amyloid-β oligomers in cerebrospinal fluid as a biomarker for Alzheimer's disease. *PLoS One* 8:e66381. doi: 10.1371/journal.pone.0066381

Hong, S., Beja-Glasser, V. F., Nfonoyim, B. M., Frouin, A., Li, S., Ramakrishnan, S., et al. (2016). Complement and microglia mediate early synapse loss in Alzheimer mouse models. *Science* 352, 712–716. doi: 10.1126/science.aad8373

Hoozemans, J. J., van Haastert, E. S., Nijholt, D. A., Rozemuller, A. J., Eikelenboom, P., and Scheper, W. (2009). The unfolded protein response is activated in pretangle neurons in Alzheimer's disease hippocampus. *Am. J. Pathol.* 174, 1241–1251. doi: 10.2353/ajpath.2009.080814

Hoozemans, J. J., Veerhuis, R., Van Haastert, E. S., Rozemuller, J. M., Baas, F., Eikelenboom, P., et al. (2005). The unfolded protein response is activated in Alzheimer's disease. *Acta Neuropathol.* 110, 165–172. doi: 10.1007/s00401-005-1038-0

Janeway, C. A. Jr. (1992). The immune system evolved to discriminate infectious nonself from noninfectious self. *Immunol. Today* 13, 11–16. doi: 10.1016/0167-5699(92)90198-G

Jarrett, J. T., Berger, E. P., and Lansbury, P. T. Jr. (1993). The carboxy terminus of the β amyloid protein is critical for the seeding of amyloid formation: implications for the pathogenesis of Alzheimer's disease. *Biochemistry* 32, 4693–4697. doi: 10.1021/bi00069a001

Jay, T. R., von Saucken, V. E., Muñoz, B., Codocedo, J. F., Atwood, B. K., Lamb, B. T. et al. (2019). TREM2 is required for microglial instruction of astrocytic synaptic engulfment in neurodevelopment. *Glia* 67, 1873–1892. doi: 10.1002/glia.23664

Johnson, E. C. B., Dammer, E. B., Duong, D. M., Ping, L., Zhou, M., Yin, L., et al. (2020). Large-scale proteomic analysis of Alzheimer's disease brain and cerebrospinal fluid reveals early changes in energy metabolism associated with microglia and astrocyte activation. *Nat. Med.* 26, 769–780. doi: 10.1038/s41591-020-0815-6

Keren-Shaul, H., Spinrad, A., Weiner, A., Matcovitch-Natan, O., Dvir-Szternfeld, R., Ulland, T. K., et al. (2017). A unique microglia type associated with restricting development of Alzheimer's disease. *Cell* 169, 1276.e17–1290.e17. doi: 10.1016/j.cell.2017.05.018

Kigerl, K. A., de Rivero Vaccari, J. P., Dietrich, W. D., Popovich, P. G., and Keane, R. W. (2014). Pattern recognition receptors and central nervous system repair. *Exp. Neurol.* 258, 5–16. doi: 10.1016/j.expneurol.2014.01.001

Kleinberger, G., Yamanishi, Y., Suárez-Calvet, M., Czirr, E., Lohmann, E., Cuyvers, E., et al. (2014). TREM2 mutations implicated in neurodegeneration impair cell surface transport and phagocytosis. *Sci. Transl. Med.* 6:243ra286. doi: 10.1126/scitranslmed.3009093

Krasemann, S., Madore, C., Cialic, R., Baufeld, C., Calcagno, N., El Fatimy, R., et al. (2017). The TREM2-APOE pathway drives the transcriptional phenotype of dysfunctional microglia in neurodegenerative diseases. *Immunity* 47, 566.e9–581.e9. doi: 10.1016/j.immuni.2017.08.008

Lansbury, P. T., and Lashuel, H. A. (2006). A century-old debate on protein aggregation and neurodegeneration enters the clinic. *Nature* 443, 774–779. doi: 10.1038/nature05290

Lee, C. Y., and Landreth, G. E. (2010). The role of microglia in amyloid clearance from the AD brain. *J. Neural Transm.* 117, 949–960. doi: 10.1007/s00702-010-0433-4

Lee, J., and Ryu, H. (2010). Epigenetic modification is linked to Alzheimer's disease: is it a maker or a marker? *BMB Rep.* 43, 649–655. doi: 10.5483/BMBRep.2010.43.10.649

Lee, J., Hyeon, S. J., Im, H., Ryu, H., Kim, Y., and Ryu, H. (2016). Astrocytes and microglia as non-cell autonomous players in the pathogenesis of ALS. *Exp. Neurobiol.* 25, 233–240. doi: 10.5607/en.2016.25.5.233

Lu, Y. C., Yeh, W. C., and Ohashi, P. S. (2008). LPS/TLR4 signal transduction pathway. *Cytokine* 42, 145–151. doi: 10.1016/j.cyto.2008.01.006

Lučiūnaitė, A., McManus, R. M., Jankunec, M., Rácz, I., Dansokho, C., Dalgediene, I., et al. (2019). Soluble Aβ oligomers and protofibrils induce NLRP3 inflammasome activation in microglia. *J. Neurochem.*, e14945. doi: 10.1111/jnc.14945

Ma, J., Jiang, T., Tan, L., and Yu, J.-T. (2015). TYROBP in Alzheimer's disease. *Mol. Neurobiol.* 51, 820–826. doi: 10.1007/s12035-014-8811-9

Malik, B. R., Maddison, D. C., Smith, G. A., and Peters, O. M. (2019). Autophagic and endo-lysosomal dysfunction in neurodegenerative disease. *Mol. Brain* 12:100. doi: 10.1186/s13041-019-0504-x

Mandrekar-Colucci, S., and Landreth, G. E. (2010). Microglia and inflammation in Alzheimer's disease. *CNS Neurol. Disord. Drug Targets* 9, 156–167. doi: 10.2174/187152710791012071

Mathys, H., Adaikkan, C., Gao, F., Young, J. Z., Manet, E., Hemberg, M., et al. (2017). Temporal tracking of microglia activation in neurodegeneration at single-cell resolution. *Cell Rep.* 21, 366–380. doi: 10.1016/j.celrep.2017.09.039

Nakanishi, H. (2003). Microglial functions and proteases. *Mol. Neurobiol.* 27, 163–176. doi: 10.1385/mn:27:2:163

Nijholt, D. A., van Haastert, E. S., Rozemuller, A. J., Scheper, W., and Hoozemans, J. J. M. (2012). The unfolded protein response is associated with early tau pathology in the hippocampus of tauopathies. *J. Pathol.* 226, 693–702. doi: 10.1002/path.3969

O'Brien, R. J., and Wong, P. C. (2011). Amyloid precursor protein processing and Alzheimer's disease. *Annu. Rev. Neurosci.* 34, 185–204. doi: 10.1146/annurev-neuro-061010-113613

Palmqvist, S., Mattsson, N., and Hansson, O. (2016). Cerebrospinal fluid analysis detects cerebral amyloid-β accumulation earlier than positron emission tomography. *Brain* 139, 1226–1236. doi: 10.1093/brain/aww015

Picone, P., Nuzzo, D., Giacomazza, D., and Di Carlo, M. (2020). β-amyloid peptide: the cell compartment multi-faceted interaction in Alzheimer's disease. *Neurotox. Res.* 37, 250–263. doi: 10.1007/s12640-019-00116-9

Plácido, A. I., Pereira, C. M., Duarte, A. I., Candeias, E., Correia, S. C., Santos, R. X., et al. (2014). The role of endoplasmic reticulum in amyloid precursor protein processing and trafficking: implications for Alzheimer's disease. *Biochim. Biophys. Acta* 1842, 1444–1453. doi: 10.1016/j.bbadis.2014.05.003

Pomilio, C., Gorojod, R. M., Riudavets, M., Vinuesa, A., Presa, J., Gregosa, A., et al. (2020). Microglial autophagy is impaired by prolonged exposure to beta-amyloid peptides: evidence from experimental models and Alzheimer's disease patients. *Geroscience* 42, 613–632. doi: 10.1007/s11357-020-00161-9

Puzzo, D., Piacentini, R., Fá, M., Gulisano, W., Li Puma, D. D., Staniszewski, A., et al. (2017). LTP and memory impairment caused by extracellular Aβ and tau oligomers is APP-dependent. *eLife* 6:e26991. doi: 10.7554/eLife.26991

Rajendran, L., and Paolicelli, R. C. (2018). Microglia-mediated synapse loss in Alzheimer's disease. *J. Neurosci.* 38, 2911–2919. doi: 10.1523/JNEUROSCI.1136-17.2017

Reiss, A. B., Arain, H. A., Stecker, M. M., Siegart, N. M., and Kasselman, L. J. (2018). Amyloid toxicity in Alzheimer's disease. *Rev. Neurosci.* 29, 613–627. doi: 10.1515/revneuro-2017-0063

Resende, R., Ferreiro, E., Pereira, C., and Oliveira, C. R. (2008). ER stress is involved in Aβ-induced GSK-3β activation and tau phosphorylation. *J. Neurosci. Res.* 86, 2091–2099. doi: 10.1002/jnr.21648

Rial, D., Lemos, C., Pinheiro, H., Duarte, J. M., Gonçalves, F. Q., Real, J. I., et al. (2016). Depression as a glial-based synaptic dysfunction. *Front. Cell. Neurosci.* 9:521. doi: 10.3389/fncel.2015.00521

Ries, M., and Sastre, M. (2016). Mechanisms of Aβ clearance and degradation by glial cells. *Front. Aging Neurosci.* 8:160. doi: 10.3389/fnagi.2016.00160

Ripoli, C., Cocco, S., Li Puma, D. D., Piacentini, R., Mastrodonato, A., Scala, F., et al. (2014). Intracellular accumulation of amyloid-β (Aβ) protein plays a major role in Aβ-induced alterations of glutamatergic synaptic transmission and plasticity. *J. Neurosci.* 34, 12893–12903. doi: 10.1523/JNEUROSCI.1201-14.2014

Rogers, J., Strohmeyer, R., Kovelowski, C. J., and Li, R. (2002). Microglia and inflammatory mechanisms in the clearance of amyloid β peptide. *Glia* 40, 260–269. doi: 10.1002/glia.10153

Rushworth, J. V., and Hooper, N. M. (2010). Lipid rafts: linking Alzheimer's amyloid-β production, aggregation and toxicity at neuronal membranes. *Int. J. Alzheimers Dis.* 2011:603052. doi: 10.4061/2011/603052

Schmit, J. D., Ghosh, K., and Dill, K. (2011). What drives amyloid molecules to assemble into oligomers and fibrils? *Biophys. J.* 100, 450–458. doi: 10.1016/j.bpj.2010.11.041

Serrano-Pozo, A., Betensky, R. A., Frosch, M. P., and Hyman, B. T. (2016). Plaque-associated local toxicity increases over the clinical course of Alzheimer disease. *Am. J. Pathol.* 186, 375–384. doi: 10.1016/j.ajpath.2015.10.010

Sheng, L., Chen, M., Cai, K., Song, Y., Yu, D., Zhang, H., et al. (2019). Microglial trem2 induces synaptic impairment at early stage and prevents amyloidosis at late stage in APP/PS1 mice. *FASEB J.* 33, 10425–10442. doi: 10.1096/fj.201900527R

Sole-Domenech, S., Cruz, D. L., Capetillo-Zarate, E., and Maxfield, F. R. (2016). The endocytic pathway in microglia during health, aging and Alzheimer's disease. *Ageing Res. Rev.* 32, 89–103. doi: 10.1016/j.arr.2016.07.002

Song, S., Lee, H., Kam, T. I., Tai, M. L., Lee, J. Y., Noh, J. Y., et al. (2008). E2-25K/Hip-2 regulates caspase-12 in ER stress-mediated Abeta neurotoxicity. *J. Cell Biol.* 182, 675–684. doi: 10.1083/jcb.200711066

Sun, X., Chen, W. D., and Wang, Y. D. (2015). β-amyloid: the key peptide in the pathogenesis of Alzheimer's disease. *Front. Pharmacol.* 6:221. doi: 10.3389/fphar.2015.00221

Talantova, M., Sanz-Blasco, S., Zhang, X., Xia, P., Akhtar, M. W., Okamoto, S., et al. (2013). Aβ induces astrocytic glutamate release, extrasynaptic NMDA receptor activation and synaptic loss. *Proc. Natl. Acad. Sci. U S A* 110, E2518–E2527. doi: 10.1073/pnas.1306832110

Tejera, D., Mercan, D., Sanchez-Caro, J. M., Hanan, M., Greenberg, D., Soreq, H., et al. (2019). Systemic inflammation impairs microglial Aβ clearance through NLRP3 inflammasome. *EMBO J.* 38:e101064. doi: 10.15252/embj.201801064

Terrill-Usery, S. E., Mohan, M. J., and Nichols, M. R. (2014). Amyloid-β(1–42) protofibrils stimulate a quantum of secreted IL-1β despite significant intracellular IL-1β accumulation in microglia. *Biochim. Biophys. Acta* 1842, 2276–2285. doi: 10.1016/j.bbadis.2014.08.001

Ulland, T. K., and Colonna, M. (2018). TREM2—a key player in microglial biology and Alzheimer disease. *Nat. Rev. Neurol.* 14, 667–675. doi: 10.1038/s41582-018-0072-1

Ulland, T. K., Song, W. M., Huang, S. C., Ulrich, J. D., Sergushichev, A., Beatty, W. L., et al. (2017). TREM2 maintains microglial metabolic fitness in Alzheimer's disease. *Cell* 170, 649.e13–663.e13. doi: 10.1016/j.cell.2017.07.023

van Weering, J. R. T., and Scheper, W. (2019). Endolysosome and autolysosome dysfunction in Alzheimer's disease: where intracellular and extracellular meet. *CNS Drugs* 33, 639–648. doi: 10.1007/s40263-019-00643-1

Venegas, C., Kumar, S., Franklin, B. S., Dierkes, T., Brinkschulte, R., Tejera, D., et al. (2017). Microglia-derived ASC specks cross-seed amyloid-β in Alzheimer's disease. *Nature* 552, 355–361. doi: 10.1038/nature25158

Voet, S., Srinivasan, S., Lamkanfi, M., and van Loo, G. (2019). Inflammasomes in neuroinflammatory and neurodegenerative diseases. *EMBO Mol. Med.* 11:e10248. doi: 10.15252/emmm.201810248

Webers, A., Heneka, M. T., and Gleeson, P. A. (2020). The role of innate immune responses and neuroinflammation in amyloid accumulation and progression of Alzheimer's disease. *Immunol. Cell Biol.* 98, 28–41. doi: 10.1111/imcb.12301

Yuan, P., Condello, C., Keene, C. D., Wang, Y., Bird, T. D., Paul, S. M., et al. (2016). TREM2 haplodeficiency in mice and humans impairs the microglia barrier function leading to decreased amyloid compaction and severe axonal dystrophy. *Neuron* 90, 724–739. doi: 10.1016/j.neuron.2016.05.003

Zhang, Y., Chen, X., Zhao, Y., Ponnusamy, M., and Liu, Y. (2017). The role of ubiquitin proteasomal system and autophagy-lysosome pathway in Alzheimer's disease. *Rev. Neurosci.* 28, 861–868. doi: 10.1515/revneuro-2017-0013

Zhao, R., Hu, W., Tsai, J., Li, W., and Gan, W. B. (2017). Microglia limit the expansion of β-amyloid plaques in a mouse model of Alzheimer's disease. *Mol. Neurodegener.* 12:47. doi: 10.1186/s13024-017-0188-6

Zhao, Y. G., and Zhang, H. (2019). Autophagosome maturation: an epic journey from the ER to lysosomes. *J. Cell Biol.* 218, 757–770. doi: 10.1083/jcb.201810099

Zhou, Y., Song, W. M., Andhey, P. S., Swain, A., Levy, T., Miller, K. R., et al. (2020). Human and mouse single-nucleus transcriptomics reveal TREM2-dependent and TREM2-independent cellular responses in Alzheimer's disease. *Nat. Med.* 26, 131–142. doi: 10.1038/s41591-019-0695-9

Conflict of Interest: The authors declare that the research was conducted in the absence of any commercial or financial relationships that could be construed as a potential conflict of interest.

frontiers in Molecular Neuroscience

REVIEW
published: 07 January 2021
doi: 10.3389/fnmol.2020.600084

Hyperactivity Induced by Soluble Amyloid-β Oligomers in the Early Stages of Alzheimer's Disease

*Audrey Hector and Jonathan Brouillette**

Department of Pharmacology and Physiology, Hôpital du Sacré-Cœur de Montréal Research Center, Centre intégré universitaire de santé et de services sociaux du Nord-de-l'Île-de-Montréal (CIUSSS-NIM), Université de Montréal, Montreal, QC, Canada

Soluble amyloid-beta oligomers (Aβo) start to accumulate in the human brain one to two decades before any clinical symptoms of Alzheimer's disease (AD) and are implicated in synapse loss, one of the best predictors of memory decline that characterize the illness. Cognitive impairment in AD was traditionally thought to result from a reduction in synaptic activity which ultimately induces neurodegeneration. More recent evidence indicates that in the early stages of AD synaptic failure is, at least partly, induced by neuronal hyperactivity rather than hypoactivity. Here, we review the growing body of evidence supporting the implication of soluble Aβo on the induction of neuronal hyperactivity in AD animal models, *in vitro*, and in humans. We then discuss the impact of Aβo-induced hyperactivity on memory performance, cell death, epileptiform activity, gamma oscillations, and slow wave activity. We provide an overview of the cellular and molecular mechanisms that are emerging to explain how Aβo induce neuronal hyperactivity. We conclude by providing an outlook on the impact of hyperactivity for the development of disease-modifying interventions at the onset of AD.

Keywords: amyloid-beta oligomers, hyperactivity, neurodegeneration, memory, epileptiform activity, gamma oscillations, slow wave

OPEN ACCESS

Edited by:
Robert A. Nichols, University of Hawaii at Manoa, United States

Reviewed by:
Shaomin Li, Brigham and Women's Hospital and Harvard Medical School, United States
Patrizia Hrelia, Alma Mater Studiorum University of Bologna, Italy

***Correspondence:**
Jonathan Brouillette
jonathan.brouillette@umontreal.ca

Received: *28 August 2020*
Accepted: *01 December 2020*
Published: *07 January 2021*

Citation:
Hector A and Brouillette J (2021) Hyperactivity Induced by Soluble Amyloid-β Oligomers in the Early Stages of Alzheimer's Disease. Front. Mol. Neurosci. 13:600084. doi: 10.3389/fnmol.2020.600084

INTRODUCTION

Synapse loss that precedes neuronal death is the strongest predictor of cognitive decline in Alzheimer's disease (AD) (Alzheimer's, 2020). Although we still need to uncover all the cellular and molecular events leading to neurodegeneration in AD, it is well-established that toxic soluble low-molecular-weight amyloid-beta oligomers (Aβo) play an essential role in synapse loss and strongly correlate with the clinical state of AD patients (Selkoe, 2002; Brouillette, 2014). Since soluble Aβo start to accumulate in the brain up to two decades before the appearance of clinical symptoms (Cline et al., 2018), understanding how Aβ pathology disturbs cell functioning and neuronal networks would be exceedingly beneficial to develop novel therapeutic approaches to prevent memory deficits at the onset of AD before neurodegeneration induces irreversible brain damages that drastically compromises the quality of life of the patient.

Aβ peptides are composed of 36–43 amino acids and are produced by the proteolytic cleavage of the transmembrane amyloid precursor protein (APP) by β- and γ-secretases (Haass et al., 2012). Given their hydrolytic properties, Aβ peptides (especially $A\beta_{1-42}$) tend to oligomerize rapidly and dynamically until they form insoluble fibrils that aggregate into plaques. Many Aβ species have been shown to be neurotoxic such as dimers, trimers, tetramers, nonamers, dodecamers, protofibrils, and fibrils (Brouillette, 2014). Whereas some reports have highlighted the neurotoxic effects of

particular Aβ intermediates with a defined size and structure, other studies have used mixtures of various Aβ species to measure the global impact of the different species that are found simultaneous in the brain. Although a large amount of studies have consistently reported the deleterious impact of soluble Aβo on synapse function and cognitive performance using different types of Aβ preparations in AD mouse models, *in vitro*, and in humans, the primary events disturbed by Aβo which drive the neurodegenerative process still need to be elucidated.

Cognitive impairment in AD was traditionally assumed to originate from lower synaptic activity that eventually lead to neurodegeneration. Multiple lines of evidence now indicate that, particularly in the early stages of AD, synapse dysfunction and loss are first induced by neuronal hyperactivity rather than hypoactivity (Busche et al., 2012, 2015a). Over the past few years, a growing body of evidence has highlighted the major role of soluble Aβo in the induction of neuronal hyperactivity at the onset of AD. Based on AD animal models, *in vitro* experiments and human studies, Aβo-induced neuronal hyperactivity has emerged as an early functional hallmark of AD which triggers synaptic failure, memory dysfunction, epileptiform activity, and neurodegeneration.

NEURONAL NETWORK HYPERACTIVITY IN HUMANS

In human, brain activity can be investigated by functional magnetic resonance imaging (fMRI), positron emission tomography (PET), single-photon emission computed tomography (SPECT), and electroencephalogram (EEG) recordings at resting state or while executing a cognitive task. Hippocampal hyperactivation has been detected by fMRI during memory-encoding tasks in people with mild cognitive impairment (MCI), a prodromal stage of AD, as well as in pre-symptomatic individuals carrying the E280A presenilin-1 (PS1) mutation, the most common cause of early-onset familial AD (Dickerson et al., 2005; Celone et al., 2006; Quiroz et al., 2010; Bakker et al., 2012; Sepulveda-Falla et al., 2012) (**Table 1**). Higher hippocampal activation was also observed before any clinical symptoms in carriers of the APOE4 allele, the most important genetic risk factor for late-onset sporadic AD (Bookheimer et al., 2000; Trivedi et al., 2008; Filippini et al., 2009; Kunz et al., 2015).

As the disease progresses, neuronal networks gradually switch to hypoactivity in AD during memory encoding (Celone et al., 2006; Persson et al., 2008; Reiman et al., 2012). Although there is currently many different compounds such as the Pittsburgh Compound B that can efficiently detect Aβ plaques in the brain using imaging techniques (Chetelat et al., 2020), the level of soluble Aβo cannot yet be directly measured in the brain of live patients. Although we know that the level of soluble Aβo begin to increase in the brain ∼10–15 years before any clinical symptoms of AD (Cline et al., 2018), it still need to be established if the hyperactivity observed in early AD patients is induced, at least partly, by this progressive accumulation of soluble Aβo in the brain as shown *in vitro* and in animal models. A way to bypass this limitation would be to investigate the level of $A\beta_{1-42}$ and $A\beta_{1-40}$ in the CSF or plasma of AD patients while measuring hippocampal hyperactivity by imaging techniques, although this method would only allow to investigate the global impact of Aβo on specific brain area dysfunctions.

HYPERACTIVITY IN AD ANIMAL MODELS

Neuronal hyperactivity has been detected in many transgenic AD mice such as the hAPP-J20, 3×Tg-AD, APP23×PS45, APP23, and APPswe/PS1D9 mice (Busche et al., 2008, 2012, 2015a; Rudinskiy et al., 2012; Sanchez et al., 2012; Maier et al., 2014; Nygaard et al., 2015) (**Table 1**). Using two-photon Ca^{2+} imaging, it was observed that 21% of cortical neurons displayed an increase of Ca^{2+} influx predominantly near the amyloid plaques in the APP23×PS45 mouse model (Busche et al., 2008). A similar level of hyperactivity was also observed in the CA1 region of the hippocampus in young (1–2 months of age) APP23×PS45 mice when Aβo begin to accumulate but no plaques are detected (Busche et al., 2012).

These results suggest that hyperactivity is an early pathological event that depends on the accumulation of Aβo rather than plaques *per se*, and that plaques might serve as a reservoir of toxic Aβo that amplify this excessive neuronal activity responsible, at least in part, for the marked synaptic and neuronal losses observed around plaques (Hefendehl et al., 2016). In parallel to this hyperactivity, another fraction (29%) of cortical neurons were also found to be hypoactive in 6–10 months old APP23×PS45 mice when plaques are present (Busche et al., 2008). Since hypoactive neurones were only found after plaque formation, it is hypothesized that initial neuronal hyperactivity progressively switch to hypoactivity in AD (Busche and Konnerth, 2016), although the cellular and molecular mechanisms underpinning this shift still need to be determined.

To determine the direct implication of soluble Aβo on neuronal hyperactivation *in vivo*, exogenous Aβ species were also injected into the brain of wild-type mice. A single injection of Aβ-containing AD brain extracts and Aβ dimers were both found to induce a marked neuronal hyperactivity in CA1 neurons of wild-type mice (Busche et al., 2012; Zott et al., 2019). However, it should be noted that overexpression of additional APP fragments other than Aβo were also shown to induce hyperactivity and seizures in another mouse model (APP/TTA) (Born et al., 2014). Since it is difficult to tease apart the specific effects of each APP metabolites that are overexpressed in transgenic mouse models, the use of an animal model where fresh solutions of soluble Aβo are injected chronically into the hippocampus, such as the one we developed (Brouillette et al., 2012), could be advantageous to investigate the specific impact of Aβo on neuronal hyperactivity over time.

AβO-INDUCED NEURONAL HYPERACTIVITY *IN VITRO*

In line with these observations in AD mouse models, a myriad of studies performed *in vitro* also support the implication of Aβ on

TABLE 1 | Neuronal hyperactivity in humans, AD animal models, and cell cultures.

Humans, animal models, and cell cultures		Periods of neuronal hyperactivity	Brain regions	References
Humans	MCI	Prodromal AD	Hippocampus	Dickerson et al., 2005; Celone et al., 2006; Bakker et al., 2012
	PS1 E280A	Pre-symptomatic AD	Hippocampus	Quiroz et al., 2010; Sepulveda-Falla et al., 2012
	APOE4	Before clinical symptoms of AD	Hippocampus	Bookheimer et al., 2000; Trivedi et al., 2008; Filippini et al., 2009; Kunz et al., 2015
Animal models	APP23×PS45	1–2 mo old	Hippocampus and cortex	Busche et al., 2008, 2012
	APP23, APPPS1	18 mo old	Frontal cortex	Maier et al., 2014
	hAPP-J20	4–6 mo old	Parietal cortex	Sanchez et al., 2012
	3×Tg-AD	8–10 mo old	Cortex	Nygaard et al., 2015
	APPswe/PS1D9	6–7 mo old	Visual cortex	Rudinskiy et al., 2012
	Aβ-containing AD brain extracts, Aβ dimers	Immediately after Aβ injection in WT mice	CA1 area	Busche et al., 2012; Zott et al., 2019
Cell cultures	$A\beta_{25-35}$	Immediately after Aβ application	Rat hippocampal cultures and slices	Brorson et al., 1995
	$A\beta_{1-42}$ oligomers	24 h after Aβ application	Mouse hippocampal cultures	Ciccone et al., 2019
	Tg2576 mice	Embryos (cultures) and 3 mo old (slices)	Hippocampal cultures and slices	Ciccone et al., 2019
	Endogenously released human Aβ	1 h after inhibition of neprilysin	Rat hippocampal cultures and slices	Abramov et al., 2009
	$A\beta_{1-40}$ monomers and dimers	15 min after Aβ application	Hippocampal cultures and slices	Fogel et al., 2014
	Aβ-containing AD brain extracts, Aβ dimers	Immediately after Aβ application	Mouse hippocampal slices	Zott et al., 2019
	PS1ΔE9, PS1M146V, APPswedish mutants	5–6 weeks of differentiation	hiPSC-derived neurons	Park et al., 2018; Ghatak et al., 2019

neuronal hyperexcitability using different types of Aβ solutions (**Table 1**). Indeed, application of the toxic Aβ peptide fragment consisting of amino acid residues 25 through 35 ($A\beta_{25-35}$) to rat hippocampal cultures increased the intracellular levels of Ca^{2+} and the action potential activity in neurons (Brorson et al., 1995). Another study found that synthetic $A\beta_{1-42}$ oligomers applied in primary neuronal cultures induced a dose-dependent decrease in neuronal viability that was cause, at least partly, by neuronal overexcitation (Sanchez-Mejia et al., 2008). Moreover, $A\beta_{1-42}$ oligomers were found to induce aberrant neuronal activity in primary hippocampal neurons and in hippocampal slices from 3-month-old Tg2576 mice (Ciccone et al., 2019). Extracellular elevation of endogenously released human Aβ induced by inhibiting its degradation also rise up the synaptic vesicle release probability, and results in neuronal overexcitation in rat hippocampal cultures and in acute hippocampal slices (Abramov et al., 2009).

Similarly, higher levels of extracellular human $A\beta_{1-40}$ monomers and dimers augmented synaptic vesicle release which in turn leads to hyperactivity of excitatory synapses in cultured hippocampal neurons and acute hippocampal slices (Fogel et al., 2014). More recently, it was shown that Aβ-containing AD brain extracts and purified cross-linked Aβ dimers were able to induce hyperactivity in active CA1 neurons treated with bicuculline in wild-type mouse hippocampal slices (Zott et al., 2019). Furthermore, increased Ca^{2+} transients and excessive neuronal excitability have been observed in neurons derived from human induced pluripotent stem cell (hiPSC) lines carrying familial AD mutations (Park et al., 2018; Ghatak et al., 2019).

CELLULAR AND MOLECULAR MECHANISMS UNDERPINNING AβO-INDUCED NEURONAL HYPERACTIVITY

Different studies have revealed various cellular and molecular mechanisms to explain how Aβo might induce neuronal hyperactivity (**Figure 1**). Several lines of evidence obtained in AD mouse models suggest that soluble Aβo alter the excitation/inhibition balance by decreasing the inhibitory GABAergic function, which in turn induced an excessive activation of the excitatory glutamatergic system in AD mice (Busche et al., 2008; Palop and Mucke, 2010; Busche and Konnerth, 2016; Styr and Slutsky, 2018). Indeed, hyperactivity of the cortical neurons in APP23×PS45 mice was linked to lower GABAergic inhibition instead of higher glutamatergic transmission, and the activity of the hyperactive neurons was

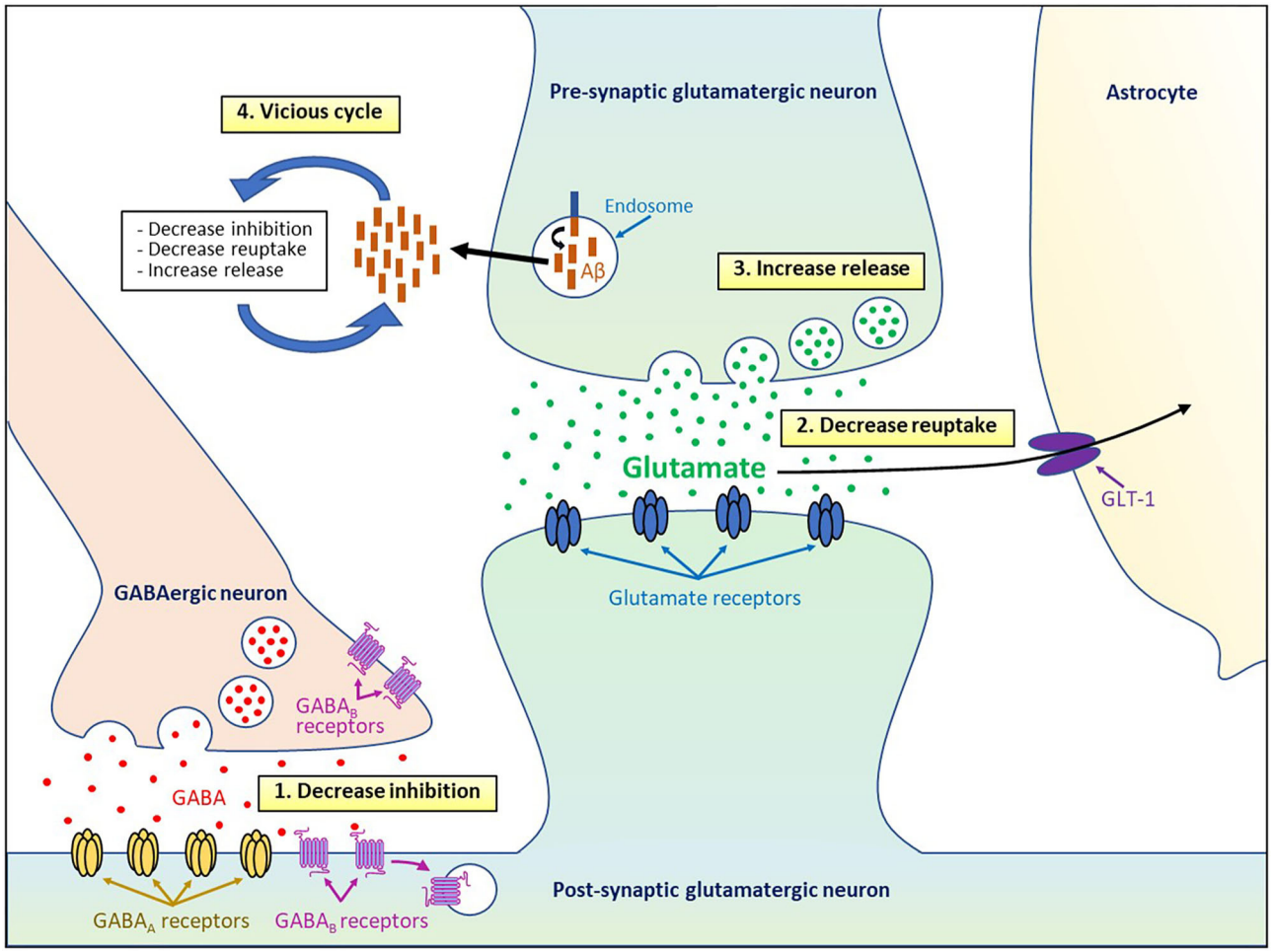

FIGURE 1 | Cellular and molecular mechanisms underpinning Aβo-induced neuronal hyperactivity.

found to be decreased by diazepam, a benzodiazepine that increase the probability of opening the γ-aminobutyric acid type A ($GABA_A$) receptor channels (Busche et al., 2008).

These results are consistent with another study showing that $GABA_A$ receptors localized in the temporal cortex of AD patients have a reduction of current, a higher rate of desensitization, and are less sensitive to GABA (Limon et al., 2012). Higher excitatory and lower inhibitory synaptic activities have also been reported in AD hiPSC-derived neurons (Ghatak et al., 2019). On the other hand, aberrant excitatory neuronal activity triggers by Aβ in the cortex and hippocampus of hAPP-J20 mice was found to induce subsequent maladaptive inhibitory mechanisms that reduce overexcitation (Palop et al., 2007), which could potentially be involved in the gradual switch to hypoactivity seen in animal models and AD patients (Celone et al., 2006; Persson et al., 2008; Sperling et al., 2009; Reiman et al., 2012; Busche and Konnerth, 2016).

Another mechanism that could explain hyperactivity generates by Aβo relies on the accumulation of glutamate at the synapse. Indeed, *in vivo* infusion of $A\beta_{1-42}$ and $A\beta_{25-35}$ into the rat cholinergic magnocellular nucleus basalis was shown to induce extracellular glutamate accumulation (Harkany et al., 2000). Fibrillar Aβ was also reported to decrease glutamate reuptake by both neuronal and glial cells (Harris et al., 1996; Parpura-Gill et al., 1997). More recently, it was found that Aβo-dependent hyperactivity in active CA1 neurons was triggered by impaired reuptake of synaptically released glutamate, which in turn potentiate excitatory glutamatergic transmission (Zott et al., 2019).

This reuptake suppression was shown to be induced by lower levels and membrane diffusion obstruction of the astroglial excitatory amino-acid transporter 2 (EAAT2; termed GLT-1 in mice) (Jacob et al., 2007; Hefendehl et al., 2016; Zott et al., 2019), a glutamate transporter that is predominant in the CA1 area and whose activity is reduced in the early stages of AD (Masliah et al., 1996; Hefendehl et al., 2016). In line with these observations, neuronal hyperexcitability observed in 5×FAD mice was attenuated by increasing the expression of GLT-1 and by reducing changes in dendrite morphology, synaptic strength, and NMDA/AMPA receptors activity ratios after inhibiting the nuclear factor of activated T cells 4 (Sompol et al., 2017), a protein overactivated in the early stages of AD (Abdul et al., 2009).

An alternative mechanism by which Aβo may deregulate glutamate homeostasis implicates aberrant release of glutamate stored in pre-synaptic vesicles. Soluble Aβo have been shown to increase the release of pre-synaptic vesicles in hippocampal neuronal cultures, whereas the activation of inhibitory $GABA_A$ receptors by the agonist taurine was able to block the accumulation of glutamate at the synaptic cleft (Brito-Moreira et al., 2011). Moreover, application of $A\beta_{1-42}$ oligomers on hippocampal cultures was reported to increase the amount of synaptic vesicles and their exocytosis by disrupting the synaptophysin/VAMP2 complex at the pre-synaptic terminals (Russell et al., 2012). Even a small elevation of endogenous $A\beta_{40}$ and $A\beta_{42}$ peptides of different lengths and molecular conformations was able to accelerate the vesicle exocytosis rate and increased release probability of active neurons in hippocampal cultures (Abramov et al., 2009). Given that both higher and lower levels of endogenous extracellular Aβ oligomers reduced short-term facilitation of vesicle release (Abramov et al., 2009), these results indicate that the level of Aβ peptides needs to be tightly control to keep the vesicle release probability in the optimal range. Application of $A\beta_{40}$ monomers or dimers was also shown to induce hyperactivity by augmenting vesicle release probability at excitatory synapses after promoting pre-synaptic CA^{2+} influx via APP homodimerization in hippocampal cultures and slices (Fogel et al., 2014). Interestingly, various Aβ peptides such as $A\beta_{1-42}$, $A\beta_{1-40}$, $A\beta_{1-28}$, and $A\beta_{25-35}$ were all found to increase potassium-evoked glutamate release from hippocampal slices in a dose-dependent manner (Kabogo et al., 2010).

Lower reuptake and higher release of glutamate can also act synergistically to increase the load of glutamate in the synaptic cleft and lead to its "spillover" to activate extrasynaptic GluN2B-containing NMDA receptors that were found to promote neuronal death (Parsons and Raymond, 2014). Interestingly, prolonged activation of NMDA receptors has been shown to induce endocytosis and lysosomal degradation of the post-synaptic $GABA_B$ receptors (Terunuma et al., 2010), which could in turn amplify neuronal excitability by decreasing the inhibitory action of GABA in AD. Moreover, lower axonal trafficking and reduced expression of the pre-synaptic $GABA_B$ receptors in AD were reported to increase Aβ formation (Dinamarca et al., 2019). Since neuronal and synaptic activity were shown to increase the production and secretion of Aβ (Cirrito et al., 2005; Dolev et al., 2013; Yamamoto et al., 2015), the hyperactivity induced by Aβo can also favor an excessive release of Aβ and consequently causes a vicious cycle that amplifies and perpetuates the deleterious effects of Aβo on cell function. Using a chemogenetic approach, it was reported that chronic attenuation of aberrant neuronal activity was able to reduce amyloid plaque formation and synapse loss (Yuan and Grutzendler, 2016).

IMPACT OF AβO-INDUCED HYPERACTIVITY ON CELL DEATH

By blocking glutamate reuptake and facilitating its pre-synaptic release, soluble Aβo increased glutamate concentration at the synaptic cleft and subsequently affect post-synaptic neurons by overactivating glutamatergic NMDA and AMPA receptors. It was shown that higher pre-synaptic release of glutamate induced by soluble Aβ generated a massive entry of Ca^{2+} and Na^{+} through NMDA receptors, which in turn impaired intracellular signaling pathways involved in synaptic plasticity and produced deleterious effects on neurons leading ultimately to cell death (Calvo-Rodriguez and Bacskai, 2020) (**Figure 2**). In physiological condition, Ca^{2+} concentration is finely balanced to maintain a lower level in the cytosol than in the extracellular space or some cell organelles such as the endoplasmic reticulum (ER) and lysosome. When this balance is disturbed in AD, overactivation of Ca^{2+}-dependent intracellular pathways impaired energy metabolism, produced reactive oxygen species (ROS), and oxidative stress that eventually lead to cell death (Belkacemi and Ramassamy, 2012; Calvo-Rodriguez and Bacskai, 2020).

Using neuronal culture and entorhinal–hippocampal organotypic slices, it was found that $A\beta_{1-42}$ oligomers dysregulated Ca^{2+} homeostasis and triggered neuronal death through both NMDA and AMPA receptors by generating ROS that derived in part from mitochondrial sources (De Felice et al., 2007; Wang and Zheng, 2019). *In vivo* infusion of $A\beta_{1-42}$ and $A\beta_{25-35}$ in the rat cholinergic magnocellular nucleus basalis induced a rapid accumulation of intracellular Ca^{2+} in the vicinity of the injection site followed by cell death 3 days post-injection (Harkany et al., 2000). In human cortical cell cultures, $A\beta_{1-38}$ and $A\beta_{25-35}$ increased the intracellular basal level of Ca^{2+} and amplified Ca^{2+} influx induced by excitatory amino acid (EAA), thereby potentiating EAA-induced neuronal degeneration (Mattson et al., 1992). Injection of Aβ-containing AD extracts in the CA1 area was also reported to reduce neurite length and the number of branch points in wild-type mice (Zott et al., 2019).

At the level of the plasma membrane, Aβo can also increase the intracellular levels of Ca^{2+} by (1) inhibiting the Ca^{2+}-efflux ATPase or exchangers (Wu et al., 1997; Kim et al., 1999; Mata, 2018), and by (2) intensifying Ca^{2+} influx through L-type, T-type, and N-type voltage-gated Ca^{2+} channels (Ueda et al., 1997; Ekinci et al., 1999; MacManus et al., 2000; Thibault et al., 2012; Min et al., 2013). Moreover, Aβo were found to increase Ca^{2+} release from the ER to the cytosol by enhancing the function of ryanodine receptors and by increasing inositol 1,4,5-trisphosphate receptor (IP3) production and binding to its receptors (Cowburn et al., 1995; Shtifman et al., 2010; Demuro and Parker, 2013; SanMartin et al., 2017). These results are in line with the beneficial effects observed in some AD patients with the memantine compound, an antagonist of the NMDA receptors that reduced Ca^{2+} influx into cells (Robinson and Keating, 2006).

IMPACT OF AβO-INDUCED HYPERACTIVITY ON MEMORY PERFORMANCE

It is well-established that in healthy individuals hippocampal activity increased when performing different types of memory tasks such as spatial navigation, episodic and associative memory tasks (Sperling et al., 2003; Zeineh et al., 2003; Moser et al., 2017). This higher neuronal activity is essential to induce

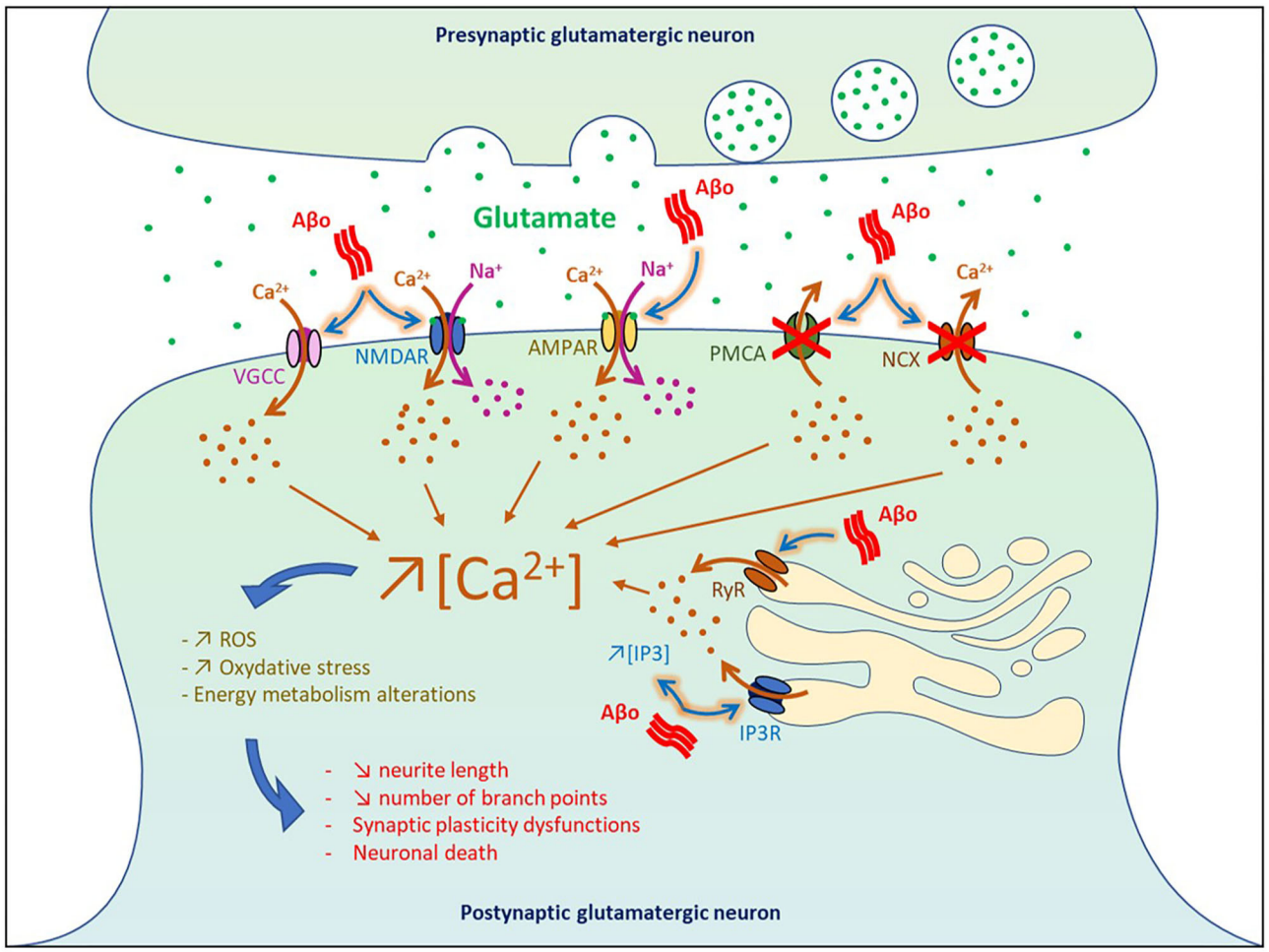

FIGURE 2 | Impact of Aβo-induced hyperactivity on cell death. VGCC, voltage-gated Ca^{2+} channel; NMDAR, NMDA receptor; AMPAR, AMPA receptor; PMCA, plasma membrane calcium ATPase NCX, Na+/Ca2+ exchanger; IP3, inositol 1,4,5-trisphosphate; IP3R, IP3 receptor; RyR, ryanodine receptor.

synaptic plasticity to encode and consolidate new information learned while executing the task. But what happen when the hippocampus gets overactivated? Excessive neuronal activity in the hippocampus was first observed in animal models of aging and has been shown to induce age-related memory deficits (Koh et al., 2010; Thome et al., 2016; Haberman et al., 2017). In AD, hippocampal hyperactivity can be detected in the preclinical et prodromal stages of the disease when memory deficits are still very subtle and can hardly be perceived by neurocognitive exams (Mondadori et al., 2006; Filippini et al., 2009; Bateman et al., 2012; Reiman et al., 2012). Indeed, before clinical symptoms become apparent in APOE4 carriers, higher hippocampal activation was associated with lower grid-cell like representation in the entorhinal cortex when performing a virtual spatial-memory task (Bookheimer et al., 2000; Kunz et al., 2015).

In APP knock-in mice with human APP containing three mutations, grid cells were shown to degenerate when Aβ depositions are emerging, and started to lose connection with place cells in the hippocampus when mice were getting old, which prevented the hippocampus to recreate spatial maps to distinguish between different environments (Jun et al., 2020). Memory deficits were also observed in APOE4 knock-in mice, in which the APOE gene is replaced by knocking in the human ε4 allele (Andrews-Zwilling et al., 2010). Transplantation of interneuron precursor cells and treatment with pentobarbital to promote the inhibitory action of GABA were both able to attenuate these cognitive dysfunctions in APOE4 knock-in mice (Andrews-Zwilling et al., 2010).

In presymptomatic individuals carrying the AD-associated PS1 E280A mutation, increased activation of the right anterior hippocampus was observed when performing a face-name associative encoding task (Quiroz et al., 2010). Hippocampal hyperactivity was even detected in elderly with Aβ plaque deposition who doesn't showed episodic memory impairment (Mormino et al., 2012), suggesting that Aβ-dependent hyperactivation is an early event that might be present before memory deficits become apparent in some hippocampal-dependent memory tasks. In cognitively normal

elderly, higher hippocampal activation at baseline has been shown to be correlated with increased longitudinal Aβ plaque deposition and progressive memory decline across time (Leal et al., 2017).

In another study, the presence of Aβ plaques in the neocortex was associated with impaired episodic memory deficits in both asymptomatic elderly and MCI individuals (Pike et al., 2007). Amnestic MCI and non-demented older adults also showed aberrant activity in the dentate gyrus and CA3 regions of the hippocampus during a pattern-separation task, which markedly depends on the hippocampus (Yassa et al., 2011; Bakker et al., 2012, 2015). Moreover, MCI patients with Aβ plaque depositions were found to have more pronounce hippocampal activation at baseline and faster clinical progression compared to Aβ negative MCI elderly (Huijbers et al., 2015).

Transcranial magnetic stimulation (TMS) is a non-invasive form of brain stimulation technique that not only allow to monitor variations in intracortical inhibition and excitation but might also serve as a diagnostic tool and a way to modulate cortex activity to ameliorate memory function in AD patients. Indeed, repetitive TMS (rTMS) applied to the dorsolateral prefrontal cortex (DLPFC) has been shown to improve performance on an action naming memory task in mild AD as well as object naming in moderate to severe AD patients (Cotelli et al., 2006, 2008). A longer treatment (five times a week for 4 weeks) with rTMS over the left DLPFC was even able to enhance language performance of AD patients that lasted for 8 weeks after ending the stimulations (Cotelli et al., 2011). Moreover, high-frequency rTMS over the DLPFC improved memory performance in the mini-mental state examination (MMSE) in patients with mild to moderate AD, whereas high-frequency rTMS over the right inferior frontal gyrus increased attention and psychomotor speed of MCI and mild AD patients in the trail making test (Eliasova et al., 2014). Another study has found that application of rTMS for 6 weeks over the parietal P3/P4 and posterior temporal T5/T6 areas improved cognitive function in mild to moderate AD patients in three different neuropsychological tests (Zhao et al., 2017). Although we still don't know if rTMS can impact Aβ accumulation, this technique holds great promise to tackle neuronal hyperactivity and acts on it to improve cognitive performance of AD patients.

Neuronal hyperactivity also affects memory performance in various animal models. All the transgenic AD mouse models showing network hyperexcitability such as the hAPP-J20, 3×Tg-AD, APP23×PS45, APP23, Tg2576, and APPswe/PS1D9 mice, were found to have memory deficits in various memory tasks (Busche et al., 2008, 2012, 2015a; Rudinskiy et al., 2012; Sanchez et al., 2012; Maier et al., 2014; Nygaard et al., 2015). Direct injections of soluble $A\beta_{1-42}$ oligomers into the hippocampus also induced memory deficits that were reversed by sequestering Aβo with transthyretin (Brouillette et al., 2012). Cognitive functions were also improved in hAPP-J20 and 3×Tg-AD mice by suppressing neuronal overactivation with levetiracetam, an anti-epileptic drug that facilitate inhibitory GABAergic neurotransmission (Sanchez et al., 2012; Nygaard et al., 2015).

Memory plasticity can be modeled by inducing long-term potentiation (LTP) or long-term depression (LTD) in cell cultures or animal models (Nabavi et al., 2014). Nanomolar and micromolar levels of Aβ dimers and trimers were shown to inhibit LTP, increase LTD and reduce dendritic spine density in organotypic hippocampal slices (Townsend et al., 2006; Shankar et al., 2007, 2008; Li et al., 2009). It was found that Aβo altered LTP and LTD by decreasing neuronal glutamate reuptake, thereby contributing to the diffusion of glutamate outside the post-synaptic density where it can activate extrasynaptic GluN2B-containing NMDA receptors and induced cell death (Li et al., 2009, 2011; Hardingham and Bading, 2010). On the contrary, smaller (picomolar) concentration of $A\beta_{42}$ was shown to enhance LTP and memory formation (Puzzo et al., 2008), suggesting that the level of Aβ needs to be finely tuned to prevent synaptic failure and ensuing cognitive impairment.

As the disease progresses and cognitive decline worsens, hippocampal activation decreased gradually at the basal level and when AD patients performed a task-related hippocampal activity (Dickerson et al., 2005; Pariente et al., 2005; Celone et al., 2006). In a prospective study it was found that MCI individuals shifted from hippocampal hyperexcitability to hypoactivation at the baseline level over time, and that deterioration of memory performance was associated with the rate of decrease in hippocampal activity (O'Brien et al., 2010). Collectively, these studies suggest that high neuronal activity induced, at least in part, by Aβ accumulation is a very early phenomenon in AD pathogenesis that has a deleterious impact on memory abilities.

IMPACT OF AβO-INDUCED HYPERACTIVITY ON EPILEPTIFORM ACTIVITY

Since neuronal hyperactivation is characterized by an increase in frequency and amplitude of neuronal firing, it is not surprising to observe abnormal level of synchronization between excitatory glutamatergic neurons that fired together at the same time, which in turn increased the incidence of epileptiform activity and seizure observed in AD patients and AD animal models. Although the prevalence rates vary considerably between studies (1.5–64%) because of limitation and methodological issues to detect non-convulsive epileptiform activity, a rate of 64% has been observed in cohorts monitored carefully at all stages of AD (Friedman et al., 2012).

Interestingly, seizures have been shown to occur more frequently in younger AD patients (Vossel et al., 2013; Sherzai et al., 2014), when neuronal hyperactivity is more prominent. In patients with early-onset AD that developed the disease before 65 years old, seizures were detected in 45% of cases (Samson et al., 1996). A seizure rate of 28% was also observed in people with familial AD carrying mutations in *APP*, *PS1*, or *PS2* genes (Shea et al., 2016). In a prospective study of 8 years, seizures were observed in 84% of patients with Down's syndrome who developed AD because of the duplication of chromosome 21 that contains the *APP* gene (Lai and Williams, 1989). The higher and earlier accumulation of Aβ in familial cases of AD and Down's syndrome supports the notion that neuronal hyperactivation

induced by soluble Aβo is involved in epileptogenic activity seen at the onset of AD.

In the more common form of sporadic AD, epileptiform activity might be more prominent than previously recognized. Indeed, it was first found that only 2% of AD patients had subclinical non-convulsive epileptiform activity when recording EEGs for 30 min in awake patients (Liedorp et al., 2010). However, a more recent study detected subclinical epileptiform activity in 42% of the cases (four times more often than in healthy controls), using 24h EEGs in combination with 1 h magnetoencephalography (MEG) (Vossel et al., 2016). Interestingly, 90% of epileptiform activity occurred during sleep, and AD patients with subclinical epileptiform activity showed a faster rate of cognitive decline (Vossel et al., 2016). Using intracranial recording, clinically silent hippocampal seizures and epileptiform spikes were also observed during sleep in two AD patients without a history or EEG evidence of seizures (Lam et al., 2017).

These results are in line with the manifestation of non-convulsive seizure activity and epileptiform spike discharges observed using EEGs in various AD transgenic models. Like in humans, most of the epilepsies seen in AD mice are non-convulsive, with the exception of mice overexpressing human APPswe and PS1ΔE9 which have recurrent motor seizures (Minkeviciene et al., 2009; Palop and Mucke, 2010; Um et al., 2012). In hAPP-J20 and APPswe/PS1ΔE9 mice, pathological elevation of Aβo has been shown to elicit hyperexcitability and spontaneous non-convulsive epileptic activity, including spikes and sharp waves, in cortical and hippocampal networks (Palop et al., 2007; Minkeviciene et al., 2009).

As in humans, spontaneous epileptiform discharges were found to arise mainly during resting periods in hAPPJ20 mice (Verret et al., 2012). Enhancing inhibitory GABA current by restoring the level of voltage-gated sodium channels subunit Nav1.1 was shown to reduce network hypersynchrony, memory deficits, and premature mortality in hAPP-J20 mice (Verret et al., 2012). $A\beta_{1-42}$ oligomers were also found to up-regulate the level of Nav1.6 subtype, which contribute to neuronal hyperexcitability observed in primary hippocampal neurons and in hippocampal slices from 3-month-old Tg2576 mice (Ciccone et al., 2019). In APPswe/PS1ΔE9 mice, electrographic and motor seizures were prevented by deleting the cellular prion protein, which was shown to interact with Aβ and triggered dendritic spine loss (Um et al., 2012).

EFFECT OF AβO-INDUCED HYPERACTIVITY ON GAMMA OSCILLATIONS AND SLOW WAVE ACTIVITY

Normal neuronal synchrony is critical to generate oscillatory rhythmic activities within a certain range that allow different brain regions to communicate efficiently together in function of the brain state. Brain rhythms are formed when neuronal ensembles depolarized (most often with firing) and hyperpolarized their membrane potentials together in synchronized repeating sequences (Buzsaki and Watson, 2012). Five widely recognized brain waves have been characterized in function of their frequencies; delta (1–4 Hz), theta (4–8 Hz), alpha (8–12 Hz), beta (12–30 Hz), and gamma (30–150 Hz) oscillations. Each brain waves have been associated with a particular brain state, where delta oscillations are more prominent during non-rapid eye movement (NREM) sleep whereas gamma oscillations are mostly detected when concentration is required, and tend to be localized to neuronal networks directly implicated in the task (Timofeev and Chauvette, 2017; Adaikkan and Tsai, 2020). For example, the amplitude (power) of gamma oscillatory activity was shown to be increased in the hippocampus during memory encoding and to predict effective memory formation in humans and mice (Jensen et al., 2007; Sederberg et al., 2007; Matsumoto et al., 2013; Yamamoto et al., 2014).

Given that Aβo-induced hyperactivity favors hypersynchrony, which in turn affects brain waves, one could expect that brain rhythms are altered at the onset of AD. In fact, gamma power has been shown to be reduced in MCI and AD patients (Herrmann and Demiralp, 2005; van Deursen et al., 2008), as well as in various AD mouse models (Verret et al., 2012; Goutagny et al., 2013; Iaccarino et al., 2016; Mably et al., 2017; Mondragon-Rodriguez et al., 2018). Interestingly, it was found recently that restoring slow gamma oscillation (40 Hz) in a non-invasive manner by simply exposing AD mice to 1 h of 40 Hz tons per day for a week was sufficient to reduce amyloid and tau pathologies not only in the auditory cortex but also in the hippocampus, to activate microglia, and to improve cognitive performance (Martorell et al., 2019). A stronger microglia response and a larger reduction of amyloid plaques were also found by combining auditory with visual stimulation to induce 40 Hz gamma waves (Martorell et al., 2019). Moreover, optogenetic stimulation of medial septal parvalbumin neurons at 40 Hz was reported to restore hippocampal slow gamma oscillations power and to ameliorate spatial memory in hAPP J20 mice (Etter et al., 2019).

Slow wave activity (SWA)—comprising slow oscillations (0.6–1 Hz) and delta waves—that is present during NREM sleep was also found to be disrupted in the early stages of AD (Lee et al., 2020). It is well-established that NREM sleep is particularly important to consolidate memories newly acquired during the awake state, and that SWA is critical to transfer novel information from the hippocampus to long-term memory storage across cortical areas (Steriade et al., 1993; Clemens et al., 2005; Diekelmann and Born, 2010). In individuals with MCI, lower delta and theta power during sleep was associated with declarative memory impairments, and more fragmentation of slow-wave sleep was observed relative to healthy elders (Hita-Yanez et al., 2012; Westerberg et al., 2012). It was shown that disruption of NREM SWA and deficits in hippocampus-dependent memory consolidation correlated with the level of Aβ plaque deposition in the medial prefrontal cortex of older adults (Mander et al., 2015). Cortical Aβ burden was also able to predict the lower amplitude of slow oscillations in elderly (Winer et al., 2019). Moreover, reduce slow-wave sleep was associated with higher level of Aβ in the plasma of MCI individuals

(Sanchez-Espinosa et al., 2014). Interestingly, restoring slow oscillations by transcranial direct current stimulation was shown to improve memory performance in patients with early AD (Ladenbauer et al., 2017).

In line with these human studies showing the involvement of Aβ on SWA impairment at the onset of AD, disruption of SWA was also detected in mouse models of β-amyloidosis. SWA has been shown to be markedly disrupted in the hippocampus, neocortex and thalamus of APP23×PS45 mice and in wild-type mice injected with synthetic Aβ (Busche et al., 2015b). Slow wave power was also decreased in young and older APPswe/PS1ΔE9 mice (Kastanenka et al., 2017, 2019). Moreover, both the APP/PS1 and Tg2576 mouse models exhibited an age-dependent decreased in delta and theta power (Kent et al., 2018), whereas 3×Tg-AD mice showed slow waves at lower frequency (Castano-Prat et al., 2019). Remarkably, restoring slow oscillations using a GABA receptors agonist (benzodiazepine), a suppressor of Aβ production (β-secretase), or by optogenetic manipulation have all been shown to rescue memory deficits in various AD mouse models (Busche et al., 2015b; Kastanenka et al., 2017; Keskin et al., 2017).

TREATMENTS TO COUNTERACT NEURONAL HYPERACTIVATION IN AD

Since Aβo-induced hyperactivity is an early pathological event that precedes plaque formation when soluble low-molecular-weight Aβo begin to accumulate in the human brain up to two decades before the symptomatic phase of the disease (Cline et al., 2018), acting on this detrimental phenomenon might prove beneficial to develop therapeutic approaches to prevent or at least slow down the disease progression. Since the excitation/inhibition balance has been shown to be compromised at the onset of AD primarily because of insufficient GABAergic inhibition (Busche et al., 2008; Palop and Mucke, 2010; Busche and Konnerth, 2016; Styr and Slutsky, 2018), using drugs that are capable of restoring the GABAergic system might potentially lower the hyperactivity triggers by Aβo and consequently AD pathogenesis.

The $GABA_A$ receptors agonist taurine was found to attenuate neuronal hyperactivity by decreasing glutamate level released at the synapse (Brito-Moreira et al., 2011) (**Table 2**). Hyperactivity was also reduced in cortical neurons of APP23×PS45 mice by increasing the inhibitory effect of GABA with diazepam

TABLE 2 | Treatments to counteract neuronal hyperactivation in AD.

Compounds	Types	Models	Effects	References
Taurine	$GABA_A$ receptors agonist	$Aβ_{1-42}$ oligomers in hippocampal cultures	↘ hyperactivity by ↘ glutamate release	Brito-Moreira et al., 2011
Diazepam	Benzodiazepine	APP23×PS45 mice	↘ hyperactivity ↗ opening of $GABA_A$ receptor channels	Busche et al., 2008
GABA	Neurotransmitter	APP mice	Restore slow oscillations	Kastanenka et al., 2017, 2019
Midazolam	Benzodiazepine	APP23×PS45 mice, Aβo injected mice	Rescue the frequency and long-range coherence of slow waves	Busche et al., 2015b
Clonazepam	Benzodiazepine	APP23×PS45 mice	Rescue slow waves and sleep-dependent memory consolidation	Busche et al., 2015b
GNE-0723	Modulator of NMDAR-GluN2A	hAPP-J20 mice	↘ low-frequency oscillations, network hypersynchrony, and memory deficits	Hanson et al., 2020
NB-360	Inhibitor of β-secretase BACE	APP23×PS45 mice	↘ prefibrillary Aβ, hyperactivity, and memory deficits	Keskin et al., 2017
LY-411575	Inhibitor of γ-secretase	APP23×PS45 mice	↘ soluble Aβ levels, hyperactivity, and cognitive deficits	Busche et al., 2012
Levetiracetam	Anti-epileptic	hAPP mice	↘ epileptiform activity, hyperactivity, hypersynchrony, DNA double-strand breaks; ↗ memory performance	Sanchez et al., 2012; Suberbielle et al., 2013, 2015; Nygaard et al., 2015
		Humans with MCI	↘ hyperactivity; ↗ memory performance	Putcha et al., 2011; Bakker et al., 2012
Pyruvate and 3-β-hydroxybutyrate supplement	Dietary energy substrates	APPswe/PS1ΔE9 mice	Prevent energy metabolism deficits, hyperactivity, epileptiform activity	Zilberter et al., 2013
		Protofibrillar $Aβ_{1-42}$ in hippocampal slices	Rescue network activity, synaptic function, LTP and energy metabolism	Zilberter et al., 2013

(Busche et al., 2008). Topical application of GABA directly on the somatosensory cortex was reported to restore slow oscillations in APP mice (Kastanenka et al., 2017, 2019), whereas the topical application of the $GABA_A$ agonist midazolam rescued the frequency and long-range coherence of slow waves in the frontal and occipital cortex of APP23×PS45 mice and in wild-type mice infused with Aβo (Busche et al., 2015b). Moreover, intraperitoneal injection of the benzodiazepine clonazepam, which increase GABAergic function by acting on $GABA_A$ receptors, has been shown to rescue slow waves and sleep-dependent memory consolidation in APP23×PS45 mice (Busche et al., 2015b).

Recently, a positive allosteric modulator called GNE-0723 that can boost the activity of NMDAR containing GluN2A subunit contained in both excitatory pyramidal neurons and inhibitory interneurons has been tested in hAPP-J20 mice (Hanson et al., 2020). This compound was found to decrease aberrant low-frequency oscillations (12–20 Hz), network hypersynchrony, and memory deficits in hAPP-J20 mice, suggesting that this drug is able to reinstate the excitation/inhibition balance. Inhibitors of β-secretase BACE and γ-secretase, two enzymes involved in the production of Aβ, have also been shown to decrease Aβo-induced hyperactivity and cognitive impairments in APP23×PS45 mice (Busche et al., 2012; Keskin et al., 2017). However, given the clinical trial failures obtained so far with these types of compounds, additional experiments are requested to develop more Aβ specific BACE and γ-secretase inhibitors and to find the appropriate doses and time of administration for an efficient therapeutic intervention.

Levetiracetam (Keppra) is an atypical anti-epileptic drug that is assumed to decrease impulse conduction across excitatory synapses by inhibiting pre-synaptic Ca^{2+} channels, and by acting on the synaptic vesicle protein SV2A (Lynch et al., 2004; Vogl et al., 2012). Interestingly, levetiracetam not only decreased epileptiform activity in hAPP mice, but also lower neuronal hyperactivation and hypersynchrony, improved memory performance, and reduced neuronal DNA double-strand breaks in AD mouse models (Sanchez et al., 2012; Suberbielle et al., 2013, 2015; Nygaard et al., 2015). In MCI individuals, treatment with a low dose of levetiracetam for two weeks was found to attenuate hippocampal hyperactivation and to ameliorate performance in a pattern-separation memory task (Putcha et al., 2011; Bakker et al., 2012).

Since higher level of glucose is required to provide the increase of energy associated with neuronal hyperexcitability, several cellular energy deficiencies have also been detected at the onset of AD (Velliquette et al., 2005; Guglielmotto et al., 2009; Avila et al., 2010). To compensate for this neuronal energy supply deficiency, an energy substrate-enriched diet (standard diet supplemented with pyruvate and 3-β-hydroxybutyrate) was administered for 5 weeks to APPswe/PS1ΔE9 mice (Zilberter et al., 2013). By restoring the level of glycogen in the brain of these AD mice, this treatment was able to prevent energy metabolism deficits, neuronal hyperexcitability, and epileptiform activity. Moreover, alterations in network activity, synaptic function, LTP, and energy metabolism induced by protofibrillar $A\beta_{1-42}$ in hippocampal slices were rescued by using artificial cerebrospinal fluid supplemented with pyruvate and 3-β-hydroxybutyrate (Zilberter et al., 2013).

CONCLUSION

A myriad of studies performed in humans, cell cultures, hiPSC lines carrying familial AD mutations, AD mouse models, and wild-type mice injected with soluble Aβo indicate that neuronal hyperactivity is an early detrimental event in AD pathogenesis. Multiple lines of evidence strongly suggest that the accumulation of soluble low-molecular-weight Aβo plays a major role in neuronal hyperexcitability observed at the onset of AD, although other factors might also contribute, such as tau, other APP metabolites, APOE4, glial responses, neuroinflammation, and oxidative stress. Encouragingly, a growing body of evidence indicates that neuronal hyperactivity may be potentially reversed, which could prevent cell death, improve cognitive impairments, decrease epileptiform activity, restore gamma oscillations, and slow wave activity. Decreasing the abnormal accumulation of soluble Aβo to avoid an excess of glutamate at the synaptic cleft and re-establishing the balance between synaptic excitation and inhibition might prove useful to ameliorate memory performance in the early stages of AD and prevent, or at least slow down, the neurodegenerative process that progressively takes place in the course of AD.

AUTHOR CONTRIBUTIONS

AH and JB wrote and approved the final manuscript. All authors contributed to the article and approved the submitted version.

REFERENCES

Abdul, H. M., Sama, M. A., Furman, J. L., Mathis, D. M., Beckett, T. L., Weidner, A. M., et al. (2009). Cognitive decline in Alzheimer's disease is associated with selective changes in calcineurin/NFAT signaling. *J. Neurosci.* 29, 12957–12969. doi: 10.1523/JNEUROSCI.1064-09.2009

Abramov, E., Dolev, I., Fogel, H., Ciccotosto, G. D., Ruff, E., and Slutsky, I. (2009). Amyloid-β as a positive endogenous regulator of release probability at hippocampal synapses. *Nat. Neurosci.* 12, 1567–1576. doi: 10.1038/nn.2433

Adaikkan, C., and Tsai, L. H. (2020). Gamma entrainment: impact on neurocircuits, glia, and therapeutic opportunities. *Trends Neurosci.* 43, 24–41. doi: 10.1016/j.tins.2019.11.001

Alzheimer's, A. (2020). 2020 Alzheimer's disease facts and figures. *Alzheimers Dement*. 16, 391–460. doi: 10.1002/alz.12068

Andrews-Zwilling, Y., Bien-Ly, N., Xu, Q., Li, G., Bernardo, A., Yoon, S. Y., et al. (2010). Apolipoprotein E4 causes age- and Tau-dependent impairment of GABAergic interneurons, leading to learning and memory deficits in mice. *J. Neurosci.* 30, 13707–13717. doi: 10.1523/JNEUROSCI.4040-10.2010

Avila, J., Wandosell, F., and Hernandez, F. (2010). Role of glycogen synthase kinase-3 in Alzheimer's disease pathogenesis and glycogen synthase

kinase-3 inhibitors. *Expert Rev. Neurother.* 10, 703–710. doi: 10.1586/ern.10.40

Bakker, A., Albert, M. S., Krauss, G., Speck, C. L., and Gallagher, M. (2015). Response of the medial temporal lobe network in amnestic mild cognitive impairment to therapeutic intervention assessed by fMRI and memory task performance. *Neuroimage Clin.* 7, 688–698. doi: 10.1016/j.nicl.2015.02.009

Bakker, A., Krauss, G. L., Albert, M. S., Speck, C. L., Jones, L. R., Stark, C. E., et al. (2012). Reduction of hippocampal hyperactivity improves cognition in amnestic mild cognitive impairment. *Neuron* 74, 467–474. doi: 10.1016/j.neuron.2012.03.023

Bateman, R. J., Xiong, C., Benzinger, T. L., Fagan, A. M., Goate, A., Fox, N. C., et al. (2012). Clinical and biomarker changes in dominantly inherited Alzheimer's disease. *N. Engl. J. Med.* 367, 795–804. doi: 10.1056/NEJMoa1202753

Belkacemi, A., and Ramassamy, C. (2012). Time sequence of oxidative stress in the brain from transgenic mouse models of Alzheimer's disease related to the amyloid-beta cascade. *Free Radic. Biol. Med.* 52, 593–600. doi: 10.1016/j.freeradbiomed.2011.11.020

Bookheimer, S. Y., Strojwas, M. H., Cohen, M. S., Saunders, A. M., Pericak-Vance, M. A., Mazziotta, J. C., et al. (2000). Patterns of brain activation in people at risk for Alzheimer's disease. *N. Engl. J. Med.* 343, 450–456. doi: 10.1056/NEJM200008173430701

Born, H. A., Kim, J. Y., Savjani, R. R., Das, P., Dabaghian, Y. A., Guo, Q., et al. (2014). Genetic suppression of transgenic APP rescues Hypersynchronous network activity in a mouse model of Alzeimer's disease. *J. Neurosci.* 34, 3826–3840. doi: 10.1523/JNEUROSCI.5171-13.2014

Brito-Moreira, J., Paula-Lima, A. C., Bomfim, T. R., Oliveira, F. B., Sepulveda, F. J., De Mello, F. G., et al. (2011). Abeta oligomers induce glutamate release from hippocampal neurons. *Curr. Alzheimer Res.* 8, 552–562. doi: 10.2174/156720511796391917

Brorson, J. R., Bindokas, V. P., Iwama, T., Marcuccilli, C. J., Chisholm, J. C., and Miller, R. J. (1995). The Ca^{2+} influx induced by beta-amyloid peptide 25-35 in cultured hippocampal neurons results from network excitation. *J. Neurobiol.* 26, 325–338. doi: 10.1002/neu.480260305

Brouillette, J. (2014). The effects of soluble Abeta oligomers on neurodegeneration in Alzheimer's disease. *Curr. Pharm. Des.* 20, 2506–2519. doi: 10.2174/13816128113199990498

Brouillette, J., Caillierez, R., Zommer, N., Alves-Pires, C., Benilova, I., Blum, D., et al. (2012). Neurotoxicity and memory deficits induced by soluble low-molecular-weight amyloid-β_{1-42} oligomers are revealed *in vivo* by using a novel animal model. *J. Neurosci.* 32, 7852–7861. doi: 10.1523/JNEUROSCI.5901-11.2012

Busche, M. A., Chen, X., Henning, H. A., Reichwald, J., Staufenbiel, M., Sakmann, B., et al. (2012). Critical role of soluble amyloid-beta for early hippocampal hyperactivity in a mouse model of Alzheimer's disease. *Proc. Natl. Acad. Sci. U. S. A.* 109, 8740–8745. doi: 10.1073/pnas.1206171109

Busche, M. A., Eichhoff, G., Adelsberger, H., Abramowski, D., Wiederhold, K. H., Haass, C., et al. (2008). Clusters of hyperactive neurons near amyloid plaques in a mouse model of Alzheimer's disease. *Science* 321, 1686–1689. doi: 10.1126/science.1162844

Busche, M. A., Grienberger, C., Keskin, A. D., Song, B., Neumann, U., Staufenbiel, M., et al. (2015a). Decreased amyloid-beta and increased neuronal hyperactivity by immunotherapy in Alzheimer's models. *Nat. Neurosci.* 18, 1725–1727. doi: 10.1038/nn.4163

Busche, M. A., Kekus, M., Adelsberger, H., Noda, T., Forstl, H., Nelken, I., et al. (2015b). Rescue of long-range circuit dysfunction in Alzheimer's disease models. *Nat. Neurosci.* 18, 1623–1630. doi: 10.1038/nn.4137

Busche, M. A., and Konnerth, A. (2016). Impairments of neural circuit function in Alzheimer's disease. *Philos. Trans. R. Soc. Lond. B Biol. Sci.* 371:20150429. doi: 10.1098/rstb.2015.0429

Buzsaki, G., and Watson, B. O. (2012). Brain rhythms and neural syntax: implications for efficient coding of cognitive content and neuropsychiatric disease. *Dialogues Clin. Neurosci.* 14, 345–367. doi: 10.31887/DCNS.2012.14.4/gbuzsaki

Calvo-Rodriguez, M., and Bacskai, B. J. (2020). Mitochondria and calcium in Alzheimer's disease: from cell signaling to neuronal cell death. *Trends Neurosci.* 4. doi: 10.1016/j.tins.2020.10.004

Castano-Prat, P., Perez-Mendez, L., Perez-Zabalza, M., Sanfeliu, C., Gimenez-Llort, L., and Sanchez-Vives, M. V. (2019). Altered slow (<1 Hz) and fast (beta and gamma) neocortical oscillations in the 3×Tg-AD mouse model of Alzheimer's disease under anesthesia. *Neurobiol. Aging* 79, 142–151. doi: 10.1016/j.neurobiolaging.2019.02.009

Celone, K. A., Calhoun, V. D., Dickerson, B. C., Atri, A., Chua, E. F., Miller, S. L., et al. (2006). Alterations in memory networks in mild cognitive impairment and Alzheimer's disease: an independent component analysis. *J. Neurosci.* 26, 10222–10231. doi: 10.1523/JNEUROSCI.2250-06.2006

Chetelat, G., Arbizu, J., Barthel, H., Garibotto, V., Law, I., Morbelli, S., et al. (2020). Amyloid-PET and (18)F-FDG-PET in the diagnostic investigation of Alzheimer's disease and other dementias. *Lancet Neurol.* 19, 951–962. doi: 10.1016/S1474-4422(20)30314-8

Ciccone, R., Franco, C., Piccialli, I., Boscia, F., Casamassa, A., de Rosa, V., et al. (2019). Amyloid beta-induced upregulation of Nav1.6 underlies neuronal hyperactivity in Tg2576 Alzheimer's disease mouse model. *Sci. Rep.* 9, 13592. doi: 10.1038/s41598-019-50018-1

Cirrito, J. R., Yamada, K. A., Finn, M. B., Sloviter, R. S., Bales, K. R., May, P. C., et al. (2005). Synaptic activity regulates interstitial fluid amyloid-beta levels *in vivo*. *Neuron* 48, 913–922. doi: 10.1016/j.neuron.2005.10.028

Clemens, Z., Fabo, D., and Halasz, P. (2005). Overnight verbal memory retention correlates with the number of sleep spindles. *Neuroscience* 132, 529–535. doi: 10.1016/j.neuroscience.2005.01.011

Cline, E. N., Bicca, M. A., Viola, K. L., and Klein, W. L. (2018). The amyloid-beta oligomer hypothesis: beginning of the third decade. *J. Alzheimers Dis.* 64, S567–S610. doi: 10.3233/JAD-179941

Cotelli, M., Calabria, M., Manenti, R., Rosini, S., Zanetti, O., Cappa, S. F., et al. (2011). Improved language performance in Alzheimer disease following brain stimulation. *J. Neurol. Neurosurg. Psychiatry* 82, 794–797. doi: 10.1136/jnnp.2009.197848

Cotelli, M., Manenti, R., Cappa, S. F., Geroldi, C., Zanetti, O., Rossini, P. M., et al. (2006). Effect of transcranial magnetic stimulation on action naming in patients with Alzheimer disease. *Arch. Neurol.* 63, 1602–1604. doi: 10.1001/archneur.63.11.1602

Cotelli, M., Manenti, R., Cappa, S. F., Zanetti, O., and Miniussi, C. (2008). Transcranial magnetic stimulation improves naming in Alzheimer disease patients at different stages of cognitive decline. *Eur. J. Neurol.* 15, 1286–1292. doi: 10.1111/j.1468-1331.2008.02202.x

Cowburn, R. F., Wiehager, B., and Sundstrom, E. (1995). β-Amyloid peptides enhance binding of the calcium mobilising second messengers, inositol(1,4,5)trisphosphate and inositol-(1,3,4,5)tetrakisphosphate to their receptor sites in rat cortical membranes. *Neurosci. Lett.* 191, 31–34. doi: 10.1016/0304-3940(94)11549-3

De Felice, F. G., Velasco, P. T., Lambert, M. P., Viola, K., Fernandez, S. J., Ferreira, S. T., et al. (2007). Abeta oligomers induce neuronal oxidative stress through an N-methyl-D-aspartate receptor-dependent mechanism that is blocked by the Alzheimer drug memantine. *J. Biol. Chem.* 282, 11590–11601. doi: 10.1074/jbc.M607483200

Demuro, A., and Parker, I. (2013). Cytotoxicity of intracellular aβ42 amyloid oligomers involves Ca^{2+} release from the endoplasmic reticulum by stimulated production of inositol trisphosphate. *J Neurosci.* 33, 3824–3833. doi: 10.1523/JNEUROSCI.4367-12.2013

Dickerson, B. C., Salat, D. H., Greve, D. N., Chua, E. F., Rand-Giovannetti, E., Rentz, D. M., et al. (2005). Increased hippocampal activation in mild cognitive impairment compared to normal aging and AD. *Neurology* 65, 404–411. doi: 10.1212/01.wnl.0000171450.97464.49

Diekelmann, S., and Born, J. (2010). The memory function of sleep. *Nat. Rev. Neurosci.* 11, 114–126. doi: 10.1038/nrn2762

Dinamarca, M. C., Raveh, A., Schneider, A., Fritzius, T., Fruh, S., Rem, P. D., et al. (2019). Complex formation of APP with GABAB receptors links axonal trafficking to amyloidogenic processing. *Nat Commun.* 10, 1331. doi: 10.1038/s41467-019-09164-3

Dolev, I., Fogel, H., Milshtein, H., Berdichevsky, Y., Lipstein, N., Brose, N., et al. (2013). Spike bursts increase amyloid-beta 40/42 ratio by inducing a presenilin-1 conformational change. *Nat. Neurosci.* 16, 587–595. doi: 10.1038/nn.3376

Ekinci, F. J., Malik, K. U., and Shea, T. B. (1999). Activation of the L voltage-sensitive calcium channel by mitogen-activated protein (MAP) kinase following exposure of neuronal cells to β-amyloid. MAP kinase mediates

beta-amyloid-induced neurodegeneration. *J. Biol. Chem.* 274, 30322–30327. doi: 10.1074/jbc.274.42.30322

Eliasova, I., Anderkova, L., Marecek, R., and Rektorova, I. (2014). Non-invasive brain stimulation of the right inferior frontal gyrus may improve attention in early Alzheimer's disease: a pilot study. *J. Neurol. Sci.* 346, 318–322. doi: 10.1016/j.jns.2014.08.036

Etter, G., van der Veldt, S., Manseau, F., Zarrinkoub, I., Trillaud-Doppia, E., and Williams, S. (2019). Optogenetic gamma stimulation rescues memory impairments in an Alzheimer's disease mouse model. *Nat. Commun.* 10, 5322. doi: 10.1038/s41467-019-13260-9

Filippini, N., MacIntosh, B. J., Hough, M. G., Goodwin, G. M., Frisoni, G. B., Smith, S. M., et al. (2009). Distinct patterns of brain activity in young carriers of the APOE-ε4 allele. *Proc. Natl. Acad. Sci. U. S. A.* 106, 7209–7214. doi: 10.1073/pnas.0811879106

Fogel, H., Frere, S., Segev, O., Bharill, S., Shapira, I., Gazit, N., et al. (2014). APP homodimers transduce an amyloid-beta-mediated increase in release probability at excitatory synapses. *Cell Rep.* 7, 1560–1576. doi: 10.1016/j.celrep.2014.04.024

Friedman, D., Honig, L. S., and Scarmeas, N. (2012). Seizures and epilepsy in Alzheimer's disease. *CNS Neurosci. Ther.* 18, 285–294. doi: 10.1111/j.1755-5949.2011.00251.x

Ghatak, S., Dolatabadi, N., Trudler, D., Zhang, X., Wu, Y., Mohata, M., et al. (2019). Mechanisms of hyperexcitability in Alzheimer's disease hiPSC-derived neurons and cerebral organoids vs isogenic controls. *Elife.* 8:e50333. doi: 10.7554/eLife.50333.sa2

Goutagny, R., Gu, N., Cavanagh, C., Jackson, J., Chabot, J. G., Quirion, R., et al. (2013). Alterations in hippocampal network oscillations and theta-gamma coupling arise before Abeta overproduction in a mouse model of Alzheimer's disease. *Eur. J. Neurosci.* 37, 1896–1902. doi: 10.1111/ejn.12233

Guglielmotto, M., Tamagno, E., and Danni, O. (2009). Oxidative stress and hypoxia contribute to Alzheimer's disease pathogenesis: two sides of the same coin. *ScientificWorldJournal* 9, 781–791. doi: 10.1100/tsw.2009.93

Haass, C., Kaether, C., Thinakaran, G., and Sisodia, S. (2012). Trafficking and proteolytic processing of APP. *Cold Spring Harb. Perspect. Med.* 2, a006270. doi: 10.1101/cshperspect.a006270

Haberman, R. P., Koh, M. T., and Gallagher, M. (2017). Heightened cortical excitability in aged rodents with memory impairment. *Neurobiol. Aging* 54, 144–151. doi: 10.1016/j.neurobiolaging.2016.12.021

Hanson, J. E., Ma, K., Elstrott, J., Weber, M., Saillet, S., Khan, A. S., et al. (2020). GluN2A NMDA receptor enhancement improves brain oscillations, synchrony, and cognitive functions in dravet syndrome and Alzheimer's disease models. *Cell Rep.* 30, 381–396.e384. doi: 10.1016/j.celrep.2019.12.030

Hardingham, G. E., and Bading, H. (2010). Synaptic versus extrasynaptic NMDA receptor signalling: implications for neurodegenerative disorders. *Nat. Rev. Neurosci.* 11, 682–696. doi: 10.1038/nrn2911

Harkany, T., Abraham, I., Timmerman, W., Laskay, G., Toth, B., Sasvari, M., et al. (2000). β-amyloid neurotoxicity is mediated by a glutamate-triggered excitotoxic cascade in rat nucleus basalis. *Eur. J. Neurosci.* 12, 2735–2745. doi: 10.1046/j.1460-9568.2000.00164.x

Harris, M. E., Wang, Y., Pedigo, N. W. Jr., Hensley, K., Butterfield, D. A., and Carney, J. M. (1996). Amyloid beta peptide (25-35) inhibits Na+-dependent glutamate uptake in rat hippocampal astrocyte cultures. *J. Neurochem.* 67, 277–286. doi: 10.1046/j.1471-4159.1996.67010277.x

Hefendehl, J. K., LeDue, J., Ko, R. W., Mahler, J., Murphy, T. H., and MacVicar, B. A. (2016). Mapping synaptic glutamate transporter dysfunction *in vivo* to regions surrounding Abeta plaques by iGluSnFR two-photon imaging. *Nat. Commun.* 7, 13441. doi: 10.1038/ncomms13441

Herrmann, C. S., and Demiralp, T. (2005). Human EEG gamma oscillations in neuropsychiatric disorders. *Clin. Neurophysiol.* 116, 2719–2733. doi: 10.1016/j.clinph.2005.07.007

Hita-Yanez, E., Atienza, M., Gil-Neciga, E., and Cantero, J. L. (2012). Disturbed sleep patterns in elders with mild cognitive impairment: the role of memory decline and ApoE ε4 genotype. *Curr. Alzheimer Res.* 9, 290–297. doi: 10.2174/156720512800107609

Huijbers, W., Mormino, E. C., Schultz, A. P., Wigman, S., Ward, A. M., Larvie, M., et al. (2015). Amyloid-beta deposition in mild cognitive impairment is associated with increased hippocampal activity, atrophy and clinical progression. *Brain* 138, 1023–1035. doi: 10.1093/brain/awv007

Iaccarino, H. F., Singer, A. C., Martorell, A. J., Rudenko, A., Gao, F., Gillingham, T. Z., et al. (2016). Gamma frequency entrainment attenuates amyloid load and modifies microglia. *Nature* 540, 230–235. doi: 10.1038/nature20587

Jacob, C. P., Koutsilieri, E., Bartl, J., Neuen-Jacob, E., Arzberger, T., Zander, N., et al. (2007). Alterations in expression of glutamatergic transporters and receptors in sporadic Alzheimer's disease. *J. Alzheimers Dis.* 11, 97–116. doi: 10.3233/JAD-2007-11113

Jensen, O., Kaiser, J., and Lachaux, J. P. (2007). Human gamma-frequency oscillations associated with attention and memory. *Trends Neurosci.* 30, 317–324. doi: 10.1016/j.tins.2007.05.001

Jun, H., Bramian, A., Soma, S., Saito, T., Saido, T. C., and Igarashi, K. M. (2020). Disrupted place cell remapping and impaired grid cells in a knockin model of Alzheimer's disease. *Neuron.* 107, 1095–1112.e6. doi: 10.1016/j.neuron.2020.06.023

Kabogo, D., Rauw, G., Amritraj, A., Baker, G., and Kar, S. (2010). ss-amyloid-related peptides potentiate K+-evoked glutamate release from adult rat hippocampal slices. *Neurobiol. Aging* 31, 1164–1172. doi: 10.1016/j.neurobiolaging.2008.08.009

Kastanenka, K. V., Calvo-Rodriguez, M., Hou, S. S., Zhou, H., Takeda, S., Arbel-Ornath, M., et al. (2019). Frequency-dependent exacerbation of Alzheimer's disease neuropathophysiology. *Sci. Rep.* 9, 8964. doi: 10.1038/s41598-019-44964-z

Kastanenka, K. V., Hou, S. S., Shakerdge, N., Logan, R., Feng, D., Wegmann, S., et al. (2017). Optogenetic restoration of disrupted slow oscillations halts amyloid deposition and restores calcium homeostasis in an animal model of Alzheimer's disease. *PLoS One* 12, e0170275. doi: 10.1371/journal.pone.0170275

Kent, B. A., Strittmatter, S. M., and Nygaard, H. B. (2018). Sleep and EEG power spectral analysis in three transgenic mouse models of Alzheimer's disease: APP/PS1, 3×TgAD, and Tg2576. *J. Alzheimers Dis.* 64, 1325–1336. doi: 10.3233/JAD-180260

Keskin, A. D., Kekus, M., Adelsberger, H., Neumann, U., Shimshek, D. R., Song, B., et al. (2017). BACE inhibition-dependent repair of Alzheimer's pathophysiology. *Proc. Natl. Acad. Sci. U. S. A.* 114, 8631–8636. doi: 10.1073/pnas.1708106114

Kim, H. S., Lee, J. H., and Suh, Y. H. (1999). C-terminal fragment of Alzheimer's amyloid precursor protein inhibits sodium/calcium exchanger activity in SK-N-SH cell. *Neuroreport* 10, 113–116. doi: 10.1097/00001756-199901180-00022

Koh, M. T., Haberman, R. P., Foti, S., McCown, T. J., and Gallagher, M. (2010). Treatment strategies targeting excess hippocampal activity benefit aged rats with cognitive impairment. *Neuropsychopharmacology* 35, 1016–1025. doi: 10.1038/npp.2009.207

Kunz, L., Schroder, T. N., Lee, H., Montag, C., Lachmann, B., Sariyska, R., et al. (2015). Reduced grid-cell-like representations in adults at genetic risk for Alzheimer's disease. *Science* 350, 430–433. doi: 10.1126/science.aac8128

Ladenbauer, J., Ladenbauer, J., Kulzow, N., de Boor, R., Avramova, E., Grittner, U., et al. (2017). Promoting sleep oscillations and their functional coupling by transcranial stimulation enhances memory consolidation in mild cognitive impairment. *J. Neurosci.* 37, 7111–7124. doi: 10.1523/JNEUROSCI.0260-17.2017

Lai, F., and Williams, R. S. (1989). A prospective study of Alzheimer disease in Down syndrome. *Arch. Neurol.* 46, 849–853. doi: 10.1001/archneur.1989.00520440031017

Lam, A. D., Deck, G., Goldman, A., Eskandar, E. N., Noebels, J., and Cole, A. J. (2017). Silent hippocampal seizures and spikes identified by foramen ovale electrodes in Alzheimer's disease. *Nat. Med.* 23, 678–680. doi: 10.1038/nm.4330

Leal, S. L., Landau, S. M., Bell, R. K., and Jagust, W. J. (2017). Hippocampal activation is associated with longitudinal amyloid accumulation and cognitive decline. *Elife.* 6:e22978. doi: 10.7554/eLife.22978.012

Lee, Y. F., Gerashchenko, D., Timofeev, I., Bacskai, B. J., and Kastanenka, K. V. (2020). Slow wave sleep is a promising intervention target for Alzheimer's disease. *Front. Neurosci.* 14, 705. doi: 10.3389/fnins.2020.00705

Li, S., Hong, S., Shepardson, N. E., Walsh, D. M., Shankar, G. M., and Selkoe, D. (2009). Soluble oligomers of amyloid Beta protein facilitate hippocampal long-term depression by disrupting neuronal glutamate uptake. *Neuron* 62, 788–801. doi: 10.1016/j.neuron.2009.05.012

Li, S., Jin, M., Koeglsperger, T., Shepardson, N. E., Shankar, G. M., and Selkoe, D. J. (2011). Soluble Abeta oligomers inhibit long-term potentiation through

a mechanism involving excessive activation of extrasynaptic NR2B-containing NMDA receptors. *J. Neurosci.* 31, 6627–6638. doi: 10.1523/JNEUROSCI.0203-11.2011

Liedorp, M., Stam, C. J., van der Flier, W. M., Pijnenburg, Y. A., and Scheltens, P. (2010). Prevalence and clinical significance of epileptiform EEG discharges in a large memory clinic cohort. *Dement. Geriatr. Cogn. Disord.* 29, 432–437. doi: 10.1159/000278620

Limon, A., Reyes-Ruiz, J. M., and Miledi, R. (2012). Loss of functional GABA (A) receptors in the Alzheimer diseased brain. *Proc. Natl. Acad. Sci. U. S. A.* 109, 10071–10076. doi: 10.1073/pnas.1204606109

Lynch, B. A., Lambeng, N., Nocka, K., Kensel-Hammes, P., Bajjalieh, S. M., Matagne, A., et al. (2004). The synaptic vesicle protein SV2A is the binding site for the antiepileptic drug levetiracetam. *Proc. Natl. Acad. Sci. U. S. A.* 101, 9861–9866. doi: 10.1073/pnas.0308208101

Mably, A. J., Gereke, B. J., Jones, D. T., and Colgin, L. L. (2017). Impairments in spatial representations and rhythmic coordination of place cells in the 3×Tg mouse model of Alzheimer's disease. *Hippocampus* 27, 378–392. doi: 10.1002/hipo.22697

MacManus, A., Ramsden, M., Murray, M., Henderson, Z., Pearson, H. A., and Campbell, V. A. (2000). Enhancement of (45)Ca(2+) influx and voltage-dependent Ca(2+) channel activity by beta-amyloid-(1-40) in rat cortical synaptosomes and cultured cortical neurons. Modulation by the proinflammatory cytokine interleukin-1β. *J. Biol. Chem.* 275, 4713–4718. doi: 10.1074/jbc.275.7.4713

Maier, F. C., Wehrl, H. F., Schmid, A. M., Mannheim, J. G., Wiehr, S., Lerdkrai, C., et al. (2014). Longitudinal PET-MRI reveals beta-amyloid deposition and rCBF dynamics and connects vascular amyloidosis to quantitative loss of perfusion. *Nat. Med.* 20, 1485–1492. doi: 10.1038/nm.3734

Mander, B. A., Marks, S. M., Vogel, J. W., Rao, V., Lu, B., Saletin, J. M., et al. (2015). β-amyloid disrupts human NREM slow waves and related hippocampus-dependent memory consolidation. *Nat. Neurosci.* 18, 1051–1057. doi: 10.1038/nn.4035

Martorell, A. J., Paulson, A. L., Suk, H. J., Abdurrob, F., Drummond, G. T., Guan, W., et al. (2019). Multi-sensory gamma stimulation ameliorates Alzheimer's-associated pathology and improves cognition. *Cell* 177, 256–271.e222. doi: 10.1016/j.cell.2019.02.014

Masliah, E., Alford, M., DeTeresa, R., Mallory, M., and Hansen, L. (1996). Deficient glutamate transport is associated with neurodegeneration in Alzheimer's disease. *Ann. Neurol.* 40, 759–766. doi: 10.1002/ana.410400512

Mata, A. M. (2018). Functional interplay between plasma membrane Ca(2+)-ATPase, amyloid beta-peptide and tau. *Neurosci. Lett.* 663, 55–59. doi: 10.1016/j.neulet.2017.08.004

Matsumoto, J. Y., Stead, M., Kucewicz, M. T., Matsumoto, A. J., Peters, P. A., Brinkmann, B. H., et al. (2013). Network oscillations modulate interictal epileptiform spike rate during human memory. *Brain* 136, 2444–2456. doi: 10.1093/brain/awt159

Mattson, M. P., Cheng, B., Davis, D., Bryant, K., Lieberburg, I., and Rydel, R. E. (1992). β-Amyloid peptides destabilize calcium homeostasis and render human cortical neurons vulnerable to excitotoxicity. *J. Neurosci.* 12, 376–389. doi: 10.1523/JNEUROSCI.12-02-00376.1992

Min, D., Guo, F., Zhu, S., Xu, X., Mao, X., Cao, Y., et al. (2013). The alterations of Ca^{2+}/calmodulin/CaMKII/CaV1.2 signaling in experimental models of Alzheimer's disease and vascular dementia. *Neurosci. Lett.* 538, 60–65. doi: 10.1016/j.neulet.2013.02.001

Minkeviciene, R., Rheims, S., Dobszay, M. B., Zilberter, M., Hartikainen, J., Fulop, L., et al. (2009). Amyloid beta-induced neuronal hyperexcitability triggers progressive epilepsy. *J. Neurosci.* 29, 3453–3462. doi: 10.1523/JNEUROSCI.5215-08.2009

Mondadori, C. R., Buchmann, A., Mustovic, H., Schmidt, C. F., Boesiger, P., Nitsch, R. M., et al. (2006). Enhanced brain activity may precede the diagnosis of Alzheimer's disease by 30 years. *Brain* 129, 2908–2922. doi: 10.1093/brain/awl266

Mondragon-Rodriguez, S., Gu, N., Manseau, F., and Williams, S. (2018). Alzheimer's transgenic model is characterized by very early brain network alterations and beta-CTF fragment accumulation: reversal by beta-secretase inhibition. *Front. Cell Neurosci.* 12, 121. doi: 10.3389/fncel.2018.00121

Mormino, E. C., Brandel, M. G., Madison, C. M., Marks, S., Baker, S. L., and Jagust, W. J. (2012). Abeta Deposition in aging is associated with increases in brain activation during successful memory encoding. *Cereb. Cortex* 22, 1813–1823. doi: 10.1093/cercor/bhr255

Moser, E. I., Moser, M. B., and McNaughton, B. L. (2017). Spatial representation in the hippocampal formation: a history. *Nat. Neurosci.* 20, 1448–1464. doi: 10.1038/nn.4653

Nabavi, S., Fox, R., Proulx, C. D., Lin, J. Y., Tsien, R. Y., and Malinow, R. (2014). Engineering a memory with LTD and LTP. *Nature* 511, 348–352. doi: 10.1038/nature13294

Nygaard, H. B., Kaufman, A. C., Sekine-Konno, T., Huh, L. L., Going, H., Feldman, S. J., et al. (2015). Brivaracetam, but not ethosuximide, reverses memory impairments in an Alzheimer's disease mouse model. *Alzheimers Res. Ther.* 7, 25. doi: 10.1186/s13195-015-0110-9

O'Brien, J. L., O'Keefe, K. M., LaViolette, P. S., DeLuca, A. N., Blacker, D., Dickerson, B. C., et al. (2010). Longitudinal fMRI in elderly reveals loss of hippocampal activation with clinical decline. *Neurology* 74, 1969–1976. doi: 10.1212/WNL.0b013e3181e3966e

Palop, J. J., Chin, J., Roberson, E. D., Wang, J., Thwin, M. T., Bien-Ly, N., et al. (2007). Aberrant excitatory neuronal activity and compensatory remodeling of inhibitory hippocampal circuits in mouse models of Alzheimer's disease. *Neuron* 55, 697–711. doi: 10.1016/j.neuron.2007.07.025

Palop, J. J., and Mucke, L. (2010). Amyloid-beta-induced neuronal dysfunction in Alzheimer's disease: from synapses toward neural networks. *Nat. Neurosci.* 13, 812–818. doi: 10.1038/nn.2583

Pariente, J., Cole, S., Henson, R., Clare, L., Kennedy, A., Rossor, M., et al. (2005). Alzheimer's patients engage an alternative network during a memory task. *Ann. Neurol.* 58, 870–879. doi: 10.1002/ana.20653

Park, J., Wetzel, I., Marriott, I., Dreau, D., D'Avanzo, C., Kim, D. Y., et al. (2018). A 3D human triculture system modeling neurodegeneration and neuroinflammation in Alzheimer's disease. *Nat. Neurosci.* 21, 941–951. doi: 10.1038/s41593-018-0175-4

Parpura-Gill, A., Beitz, D., and Uemura, E. (1997). The inhibitory effects of beta-amyloid on glutamate and glucose uptakes by cultured astrocytes. *Brain Res.* 754, 65–71. doi: 10.1016/S0006-8993(97)00043-7

Parsons, M. P., and Raymond, L. A. (2014). Extrasynaptic NMDA receptor involvement in central nervous system disorders. *Neuron* 82, 279–293. doi: 10.1016/j.neuron.2014.03.030

Persson, J., Lind, J., Larsson, A., Ingvar, M., Sleegers, K., Van Broeckhoven, C., et al. (2008). Altered deactivation in individuals with genetic risk for Alzheimer's disease. *Neuropsychologia* 46, 1679–1687. doi: 10.1016/j.neuropsychologia.2008.01.026

Pike, K. E., Savage, G., Villemagne, V. L., Ng, S., Moss, S. A., Maruff, P., et al. (2007). Beta-amyloid imaging and memory in non-demented individuals: evidence for preclinical Alzheimer's disease. *Brain* 130, 2837–2844. doi: 10.1093/brain/awm238

Putcha, D., Brickhouse, M., O'Keefe, K., Sullivan, C., Rentz, D., Marshall, G., et al. (2011). Hippocampal hyperactivation associated with cortical thinning in Alzheimer's disease signature regions in non-demented elderly adults. *J. Neurosci.* 31, 17680–17688. doi: 10.1523/JNEUROSCI.4740-11.2011

Puzzo, D., Privitera, L., Leznik, E., Fa, M., Staniszewski, A., Palmeri, A., et al. (2008). Picomolar amyloid-beta positively modulates synaptic plasticity and memory in hippocampus. *J. Neurosci.* 28, 14537–14545. doi: 10.1523/JNEUROSCI.2692-08.2008

Quiroz, Y. T., Budson, A. E., Celone, K., Ruiz, A., Newmark, R., Castrillon, G., et al. (2010). Hippocampal hyperactivation in presymptomatic familial Alzheimer's disease. *Ann. Neurol.* 68, 865–875. doi: 10.1002/ana.22105

Reiman, E. M., Quiroz, Y. T., Fleisher, A. S., Chen, K., Velez-Pardo, C., Jimenez-Del-Rio, M., et al. (2012). Brain imaging and fluid biomarker analysis in young adults at genetic risk for autosomal dominant Alzheimer's disease in the presenilin 1 E280A kindred: a case-control study. *Lancet Neurol.* 11, 1048–1056. doi: 10.1016/S1474-4422(12)70228-4

Robinson, D. M., and Keating, G. M. (2006). Memantine: a review of its use in Alzheimer's disease. *Drugs* 66, 1515–1534. doi: 10.2165/00003495-200666110-00015

Rudinskiy, N., Hawkes, J. M., Betensky, R. A., Eguchi, M., Yamaguchi, S., Spires-Jones, T. L., et al. (2012). Orchestrated experience-driven Arc responses

are disrupted in a mouse model of Alzheimer's disease. *Nat. Neurosci.* 15, 1422–1429. doi: 10.1038/nn.3199

Russell, C. L., Semerdjieva, S., Empson, R. M., Austen, B. M., Beesley, P. W., and Alifragis, P. (2012). Amyloid-beta acts as a regulator of neurotransmitter release disrupting the interaction between synaptophysin and VAMP2. *PLoS One* 7, e43201. doi: 10.1371/journal.pone.0043201

Samson, W. N., van Duijn, C. M., Hop, W. C., and Hofman, A. (1996). Clinical features and mortality in patients with early-onset Alzheimer's disease. *Eur. Neurol.* 36, 103–106. doi: 10.1159/000117218

Sanchez, P. E., Zhu, L., Verret, L., Vossel, K. A., Orr, A. G., Cirrito, J. R., et al. (2012). Levetiracetam suppresses neuronal network dysfunction and reverses synaptic and cognitive deficits in an Alzheimer's disease model. *Proc. Natl. Acad. Sci. U. S. A.* 109, E2895–2903. doi: 10.1073/pnas.1121081109

Sanchez-Espinosa, M. P., Atienza, M., and Cantero, J. L. (2014). Sleep deficits in mild cognitive impairment are related to increased levels of plasma amyloid-beta and cortical thinning. *Neuroimage* 98, 395–404. doi: 10.1016/j.neuroimage.2014.05.027

Sanchez-Mejia, R. O., Newman, J. W., Toh, S., Yu, G. Q., Zhou, Y., Halabisky, B., et al. (2008). Phospholipase A2 reduction ameliorates cognitive deficits in a mouse model of Alzheimer's disease. *Nat. Neurosci.* 11, 1311–1318. doi: 10.1038/nn.2213

SanMartin, C. D., Veloso, P., Adasme, T., Lobos, P., Bruna, B., Galaz, J., et al. (2017). RyR2-Mediated Ca(2+) release and mitochondrial ROS generation partake in the synaptic dysfunction caused by amyloid beta peptide oligomers. *Front. Mol. Neurosci.* 10, 115. doi: 10.3389/fnmol.2017.00115

Sederberg, P. B., Schulze-Bonhage, A., Madsen, J. R., Bromfield, E. B., McCarthy, D. C., Brandt, A., et al. (2007). Hippocampal and neocortical gamma oscillations predict memory formation in humans. *Cereb. Cortex* 17, 1190–1196. doi: 10.1093/cercor/bhl030

Selkoe, D. J. (2002). Alzheimer's disease is a synaptic failure. *Science* 298, 789–791. doi: 10.1126/science.1074069

Sepulveda-Falla, D., Glatzel, M., and Lopera, F. (2012). Phenotypic profile of early-onset familial Alzheimer's disease caused by presenilin-1 E280A mutation. *J. Alzheimers Dis.* 32, 1–12. doi: 10.3233/JAD-2012-120907

Shankar, G. M., Bloodgood, B. L., Townsend, M., Walsh, D. M., Selkoe, D. J., and Sabatini, B. L. (2007). Natural oligomers of the Alzheimer amyloid-beta protein induce reversible synapse loss by modulating an NMDA-type glutamate receptor-dependent signaling pathway. *J. Neurosci.* 27, 2866–2875. doi: 10.1523/JNEUROSCI.4970-06.2007

Shankar, G. M., Li, S., Mehta, T. H., Garcia-Munoz, A., Shepardson, N. E., Smith, I., et al. (2008). Amyloid-beta protein dimers isolated directly from Alzheimer's brains impair synaptic plasticity and memory. *Nat. Med.* 14, 837–842. doi: 10.1038/nm1782

Shea, Y. F., Chu, L. W., Chan, A. O., Ha, J., Li, Y., and Song, Y. Q. (2016). A systematic review of familial Alzheimer's disease: Differences in presentation of clinical features among three mutated genes and potential ethnic differences. *J. Formos. Med. Assoc.* 115, 67–75. doi: 10.1016/j.jfma.2015.08.004

Sherzai, D., Losey, T., Vega, S., and Sherzai, A. (2014). Seizures and dementia in the elderly: Nationwide Inpatient Sample 1999-2008. *Epilepsy Behav.* 36, 53–56. doi: 10.1016/j.yebeh.2014.04.015

Shtifman, A., Ward, C. W., Laver, D. R., Bannister, M. L., Lopez, J. R., Kitazawa, M., et al. (2010). Amyloid-beta protein impairs Ca2+ release and contractility in skeletal muscle. *Neurobiol. Aging* 31, 2080–2090. doi: 10.1016/j.neurobiolaging.2008.11.003

Sompol, P., Furman, J. L., Pleiss, M. M., Kraner, S. D., Artiushin, I. A., Batten, S. R., et al. (2017). Calcineurin/NFAT signaling in activated astrocytes drives network hyperexcitability in abeta-bearing mice. *J. Neurosci.* 37, 6132–6148. doi: 10.1523/JNEUROSCI.0877-17.2017

Sperling, R., Chua, E., Cocchiarella, A., Rand-Giovannetti, E., Poldrack, R., Schacter, D. L., et al. (2003). Putting names to faces: successful encoding of associative memories activates the anterior hippocampal formation. *Neuroimage* 20, 1400–1410. doi: 10.1016/S1053-8119(03)00391-4

Sperling, R. A., Laviolette, P. S., O'Keefe, K., O'Brien, J., Rentz, D. M., Pihlajamaki, M., et al. (2009). Amyloid deposition is associated with impaired default network function in older persons without dementia. *Neuron* 63, 178–188. doi: 10.1016/j.neuron.2009.07.003

Steriade, M., Nunez, A., and Amzica, F. (1993). A novel slow (< 1 Hz) oscillation of neocortical neurons *in vivo*: depolarizing and hyperpolarizing components. *J. Neurosci.* 13, 3252–3265. doi: 10.1523/JNEUROSCI.13-08-03252.1993

Styr, B., and Slutsky, I. (2018). Imbalance between firing homeostasis and synaptic plasticity drives early-phase Alzheimer's disease. *Nat. Neurosci.* 21, 463–473. doi: 10.1038/s41593-018-0080-x

Suberbielle, E., Djukic, B., Evans, M., Kim, D. H., Taneja, P., Wang, X., et al. (2015). DNA repair factor BRCA1 depletion occurs in Alzheimer brains and impairs cognitive function in mice. *Nat. Commun.* 6, 8897. doi: 10.1038/ncomms9897

Suberbielle, E., Sanchez, P. E., Kravitz, A. V., Wang, X., Ho, K., Eilertson, K., et al. (2013). Physiologic brain activity causes DNA double-strand breaks in neurons, with exacerbation by amyloid-beta. *Nat. Neurosci.* 16, 613–621. doi: 10.1038/nn.3356

Terunuma, M., Vargas, K. J., Wilkins, M. E., Ramirez, O. A., Jaureguiberry-Bravo, M., Pangalos, M. N., et al. (2010). Prolonged activation of NMDA receptors promotes dephosphorylation and alters postendocytic sorting of GABAB receptors. *Proc. Natl. Acad. Sci. U. S. A.* 107, 13918–13923. doi: 10.1073/pnas.1000853107

Thibault, O., Pancani, T., Landfield, P. W., and Norris, C. M. (2012). Reduction in neuronal L-type calcium channel activity in a double knock-in mouse model of Alzheimer's disease. *Biochim. Biophys. Acta* 1822, 546–549. doi: 10.1016/j.bbadis.2012.01.004

Thome, A., Gray, D. T., Erickson, C. A., Lipa, P., and Barnes, C. A. (2016). Memory impairment in aged primates is associated with region-specific network dysfunction. *Mol. Psychiatry* 21, 1257–1262. doi: 10.1038/mp.2015.160

Timofeev, I., and Chauvette, S. (2017). Sleep slow oscillation and plasticity. *Curr. Opin. Neurobiol.* 44, 116–126. doi: 10.1016/j.conb.2017.03.019

Townsend, M., Shankar, G. M., Mehta, T., Walsh, D. M., and Selkoe, D. J. (2006). Effects of secreted oligomers of amyloid beta-protein on hippocampal synaptic plasticity: a potent role for trimers. *J. Physiol.* 572, 477–492. doi: 10.1113/jphysiol.2005.103754

Trivedi, M. A., Schmitz, T. W., Ries, M. L., Hess, T. M., Fitzgerald, M. E., Atwood, C. S., et al. (2008). fMRI activation during episodic encoding and metacognitive appraisal across the lifespan: risk factors for Alzheimer's disease. *Neuropsychologia* 46, 1667–1678. doi: 10.1016/j.neuropsychologia.2007.11.035

Ueda, K., Shinohara, S., Yagami, T., Asakura, K., and Kawasaki, K. (1997). Amyloid beta protein potentiates Ca2+ influx through L-type voltage-sensitive Ca^{2+} channels: a possible involvement of free radicals. *J. Neurochem.* 68, 265–271. doi: 10.1046/j.1471-4159.1997.68010265.x

Um, J. W., Nygaard, H. B., Heiss, J. K., Kostylev, M. A., Stagi, M., Vortmeyer, A., et al. (2012). Alzheimer amyloid-beta oligomer bound to postsynaptic prion protein activates Fyn to impair neurons. *Nat. Neurosci.* 15, 1227–1235. doi: 10.1038/nn.3178

van Deursen, J. A., Vuurman, E. F., Verhey, F. R., van Kranen-Mastenbroek, V. H., and Riedel, W. J. (2008). Increased EEG gamma band activity in Alzheimer's disease and mild cognitive impairment. *J. Neural Transm. (Vienna)* 115, 1301–1311. doi: 10.1007/s00702-008-0083-y

Velliquette, R. A., O'Connor, T., and Vassar, R. (2005). Energy inhibition elevates beta-secretase levels and activity and is potentially amyloidogenic in APP transgenic mice: possible early events in Alzheimer's disease pathogenesis. *J. Neurosci.* 25, 10874–10883. doi: 10.1523/JNEUROSCI.2350-05.2005

Verret, L., Mann, E. O., Hang, G. B., Barth, A. M., Cobos, I., Ho, K., et al. (2012). Inhibitory interneuron deficit links altered network activity and cognitive dysfunction in Alzheimer model. *Cell* 149, 708–721. doi: 10.1016/j.cell.2012.02.046

Vogl, C., Mochida, S., Wolff, C., Whalley, B. J., and Stephens, G. J. (2012). The synaptic vesicle glycoprotein 2A ligand levetiracetam inhibits presynaptic Ca^{2+} channels through an intracellular pathway. *Mol. Pharmacol.* 82, 199–208. doi: 10.1124/mol.111.076687

Vossel, K. A., Beagle, A. J., Rabinovici, G. D., Shu, H., Lee, S. E., Naasan, G., et al. (2013). Seizures and epileptiform activity in the early stages of Alzheimer disease. *JAMA Neurol.* 70, 1158–1166. doi: 10.1001/jamaneurol.2013.136

Vossel, K. A., Ranasinghe, K. G., Beagle, A. J., Mizuiri, D., Honma, S. M., Dowling, A. F., et al. (2016). Incidence and impact of subclinical epileptiform activity in Alzheimer's disease. *Ann. Neurol.* 80, 858–870. doi: 10.1002/ana.24794

Wang, X., and Zheng, W. (2019). Ca(2+) homeostasis dysregulation in Alzheimer's disease: a focus on plasma membrane and cell organelles. *FASEB J.* 33, 6697–6712. doi: 10.1096/fj.201801751R

Westerberg, C. E., Mander, B. A., Florczak, S. M., Weintraub, S., Mesulam, M. M., Zee, P. C., et al. (2012). Concurrent impairments in sleep and memory in amnestic mild cognitive impairment. *J. Int. Neuropsychol. Soc.* 18, 490–500. doi: 10.1017/S135561771200001X

Winer, J. R., Mander, B. A., Helfrich, R. F., Maass, A., Harrison, T. M., Baker, S. L., et al. (2019). Sleep as a potential biomarker of tau and β-amyloid burden in the human brain. *J. Neurosci.* 39, 6315–6324. doi: 10.1523/JNEUROSCI.0503-19.2019

Wu, A., Derrico, C. A., Hatem, L., and Colvin, R. A. (1997). Alzheimer's amyloid-beta peptide inhibits sodium/calcium exchange measured in rat and human brain plasma membrane vesicles. *Neuroscience* 80, 675–684. doi: 10.1016/S0306-4522(97)00053-5

Yamamoto, J., Suh, J., Takeuchi, D., and Tonegawa, S. (2014). Successful execution of working memory linked to synchronized high-frequency gamma oscillations. *Cell* 157, 845–857. doi: 10.1016/j.cell.2014.04.009

Yamamoto, K., Tanei, Z. I., Hashimoto, T., Wakabayashi, T., Okuno, H., Naka, Y., et al. (2015). Chronic optogenetic activation augments abeta pathology in a mouse model of Alzheimer disease. *Cell Rep.* 11, 859–865. doi: 10.1016/j.celrep.2015.04.017

Yassa, M. A., Lacy, J. W., Stark, S. M., Albert, M. S., Gallagher, M., and Stark, C. E. (2011). Pattern separation deficits associated with increased hippocampal CA3 and dentate gyrus activity in nondemented older adults. *Hippocampus* 21, 968–979. doi: 10.1002/hipo.20808

Yuan, P., and Grutzendler, J. (2016). Attenuation of β-amyloid deposition and neurotoxicity by chemogenetic modulation of neural activity. *J. Neurosci.* 36, 632–641. doi: 10.1523/JNEUROSCI.2531-15.2016

Zeineh, M. M., Engel, S. A., Thompson, P. M., and Bookheimer, S. Y. (2003). Dynamics of the hippocampus during encoding and retrieval of face-name pairs. *Science* 299, 577–580. doi: 10.1126/science.1077775

Zhao, J., Li, Z., Cong, Y., Zhang, J., Tan, M., Zhang, H., et al. (2017). Repetitive transcranial magnetic stimulation improves cognitive function of Alzheimer's disease patients. *Oncotarget* 8, 33864–33871. doi: 10.18632/oncotarget.13060

Zilberter, M., Ivanov, A., Ziyatdinova, S., Mukhtarov, M., Malkov, A., Alpar, A., et al. (2013). Dietary energy substrates reverse early neuronal hyperactivity in a mouse model of Alzheimer's disease. *J. Neurochem.* 125, 157–171. doi: 10.1111/jnc.12127

Zott, B., Simon, M. M., Hong, W., Unger, F., Chen-Engerer, H. J., Frosch, M. P., et al. (2019). A vicious cycle of beta amyloid-dependent neuronal hyperactivation. *Science* 365, 559–565. doi: 10.1126/science.aay0198

Conflict of Interest: The authors declare that the research was conducted in the absence of any commercial or financial relationships that could be construed as a potential conflict of interest.

frontiers in Molecular Neuroscience

ORIGINAL RESEARCH
published: 12 January 2021
doi: 10.3389/fnmol.2020.615740

The Role of Cathepsin B in the Degradation of Aβ and in the Production of Aβ Peptides Starting With Ala2 in Cultured Astrocytes

Timo Jan Oberstein[1]*, *Janine Utz*[1], *Philipp Spitzer*[1], *Hans Wolfgang Klafki*[2], *Jens Wiltfang*[2,3,4], *Piotr Lewczuk*[1,5], *Johannes Kornhuber*[1] and *Juan Manuel Maler*[1]

[1] Department of Psychiatry and Psychotherapy, Friedrich-Alexander-University of Erlangen-Nuremberg, Erlangen, Germany, [2] Department of Psychiatry and Psychotherapy, University Medical Center, Georg-August-University, Göttingen, Germany, [3] German Center for Neurodegenerative Diseases, Göttingen, Germany, [4] Neurosciences and Signaling Group, Department of Medical Sciences, Institute of Biomedicine, University of Aveiro, Aveiro, Portugal, [5] Department of Neurodegeneration Diagnostics and Department of Biochemical Diagnostics, University Hospital of Bialystok, Bialystok, Poland

OPEN ACCESS

Edited by:
Robert A. Nichols, University of Hawaii at Manoa, United States

Reviewed by:
Janko Kos, University of Ljubljana, Slovenia
Takashi Saito, Nagoya City University, Japan

***Correspondence:**
Timo Jan Oberstein
timo.oberstein@uk-erlangen.de

Received: *09 October 2020*
Accepted: *03 December 2020*
Published: *12 January 2021*

Citation:
Oberstein TJ, Utz J, Spitzer P, Klafki HW, Wiltfang J, Lewczuk P, Kornhuber J and Maler JM (2021) The Role of Cathepsin B in the Degradation of Aβ and in the Production of Aβ Peptides Starting With Ala2 in Cultured Astrocytes. Front. Mol. Neurosci. 13:615740. doi: 10.3389/fnmol.2020.615740

Astrocytes may not only be involved in the clearance of Amyloid beta peptides (Aβ) in Alzheimer's disease (AD), but appear to produce N-terminally truncated Aβ ($Aβ_{n-x}$) independently of BACE1, which generates the N-Terminus of Aβ starting with Asp1 ($Aβ_{1-x}$). A candidate protease for the generation of $Aβ_{n-x}$ is cathepsin B (CatB), especially since CatB has also been reported to degrade Aβ, which could explain the opposite roles of astrocytes in AD. In this study, we investigated the influence of CatB inhibitors and the deletion of the gene encoding CatB (CTSB) using CRISPR/Cas9 technology on $Aβ_{2-x}$ and $Aβ_{1-x}$ levels in cell culture supernatants by one- and two-dimensional Urea-SDS-PAGE followed by immunoblot. While the cell-permeant inhibitors E64d and CA-074 Me did not significantly affect the $Aβ_{1-x}$ levels in supernatants of cultured chicken and human astrocytes, they did reduce the $Aβ_{2-x}$ levels. In the glioma-derived cell line H4, the $Aβ_{2-x}$ levels were likewise decreased in supernatants by treatment with the more specific, but cell-impermeant CatB-inhibitor CA-074, by CA-074 Me treatment, and by CTSB gene deletion. Additionally, a more than 2-fold increase in secreted $Aβ_{1-x}$ was observed under the latter two conditions. The CA-074 Me-mediated increase of $Aβ_{1-x}$, but not the decrease of $Aβ_{2-x}$, was influenced by concomitant treatment with the vacuolar H^+-ATPase inhibitor Bafilomycin A1. This indicated that non-lysosomal CatB mediated the production of $Aβ_{2-x}$ in astrocytes, while the degradation of $Aβ_{1-x}$ seemed to be dependent on lysosomal CatB in H4 cells, but not in primary astrocytes. These findings highlight the importance of considering organelle targeting in drug development to promote Aβ degradation.

Keywords: Alzheimer's disease, amyloid beta, cathepsin B, N-terminus, astrocytes, lysosomal

INTRODUCTION

Alzheimer's disease (AD) is the most common neurodegenerative disease in the elderly with neuritic plaques and the neurofibrillary tangles as its neuropathological hallmarks (Glenner and Wong, 1984; Masters et al., 1985; Delacourte and Defossez, 1986; Grundke-Iqbal et al., 1986). The major protein compound of neurofibrillary tangles is hyperphosphorylated tau protein, whereas in neuritic plaques, Amyloid beta (Aβ) peptides represent the predominant protein compound. Aβ peptides are generated from the amyloid precursor protein (APP) by consecutive proteolytic cleavages by β- and γ-secretase and appear to be part of the physiological cell metabolism (Haass and Selkoe, 1993). The most extensively studied β-secretase is the beta-site APP cleaving enzyme 1 (BACE1), which generates the N-terminus of Aβ 1-x by cleaving APP between methionine (671) and aspartic acid (672) (APP770 numbering) (Hussain et al., 1999; Vassar et al., 1999). The highest BACE 1 activity is commonly found in neurons, which seem to be the major source of Aβ 1-x in the central nervous system (Vassar et al., 1999; Lee et al., 2003; Oberstein et al., 2015). However, a major fraction of the Aβ peptides in neuritic plaques in AD brains does not start with the canonical L-aspartic acid residue (Asp1), but is N-terminally truncated or modified (Aβ n-x). These Aβ variants include e.g., Aβ starting with isoaspartate (Aβ 1isoD-x), Aβ starting at Glu3, which is eventually cyclized to pyroglutamate (Aβ 3pE-x), and truncated Aβ peptide variants starting with Ala2, Phe4, and Arg5 (Glenner and Wong, 1984; Masters et al., 1985; Miller et al., 1993; Saido et al., 1995, 1996; Guntert et al., 2006; Bayer and Wirths, 2014). At present, it is not clear how exactly the different N-terminally modified or truncated Aβ variants, that have been detected in neuritic plaques, are generated and which cell types or proteolytic enzymes are involved. An imbalance between the production and degradation of Aβ as well as a shift toward increased proportions of more amyloidogenic Aβ variants via different proteases may promote cerebral Aβ accumulation and amyloid plaque formation (Selkoe, 1998). Aβ variants with truncated N-termini, in particular Aβ variants starting with pyroglutamic acid (Aβ N3pE), and those Aβ variants ending at Ala (42) (Aβ x-42) tend to be more hydrophobic and more amyloidogenic than e.g., Aβ 1-40 and 1-38, which are the most abundant Aβ variants in cerebrospinal fluid, blood plasma and cell culture supernatants (Haass and Selkoe, 1993; Pike et al., 1995; Wang et al., 1996; Thal et al., 2006; Bayer and Wirths, 2014; Oberstein et al., 2015; Schonherr et al., 2016). The vascular deposits do not possess a dense core primarily made of Ab x-42 like the parenchymal neuritic or senile plaques (Thal et al., 2006). They contain mainly Aβ x-40 (Glenner and Wong, 1984; Akiyama et al., 1997). The N-terminally truncated Aβ 2-x peptides were found in particular in parenchymal and vascular amyloid deposits in AD brains (Wiltfang et al., 2001; Schieb et al., 2011; Savastano et al., 2016; Wildburger et al., 2017; Zampar et al., 2020). Aβ 2-40 seemed to be elevated in AD cases with severe cerebral amyloid angiopathy (CAA) compared to AD cases without CAA (Gkanatsiou et al., 2019). A potential source for these N-terminally modified Aβ may be reactive astrocytes and microglia, as they are located in the immediate vicinity of neuritic plaques. They seem to be involved in changes in the amyloid plaque composition by means of ineffective phagocytosis, secretion of proteases, and interactions with the peripheral immune system (Selkoe, 2001; Nagele et al., 2003; Thal et al., 2006). In previous studies we have shown that the role of astrocytes and microglia in AD may not be limited to Aβ plaque removal or modification: In cell culture, these cells secrete higher proportions of N-terminally modified or truncated Aβ variants like Aβ 2/3-40 and Aβ 4/5-40 in relation to Aβ 1-x than neuronal cells (Oberstein et al., 2015). The cellular production of the presumed Aβ 2-40 variant was found to be independent of BACE1. A number of different candidate proteases, such as cathepsin B (CatB), meprin β, neprilysin, myelin basic protein, the metalloproteinase ADAM TS4 or aminopeptidases, have been proposed to act in cooperation with or independently of BACE1 to produce these N-terminally modified Aβ variants (Howell et al., 1995; Saido, 1998; Hook et al., 2005; Liao et al., 2009; Sevalle et al., 2009; Bien et al., 2012; Bayer and Wirths, 2014; Walter et al., 2019). In this study, we chose to investigate the cysteine protease CatB for its ability to generate Aβ in astrocytes, because assays from cell extracts and purified secretory vesicles indicated that CatB exerts β-secretase activity and thereby promotes the production of Aβ (Hook et al., 2005; Bohme et al., 2008; Schechter and Ziv, 2011). On the other hand, CatB seemed to degrade Aβ via C-Terminal truncation, leaving its role for the Aβ metabolism unclear (Mackay et al., 1997; Mueller-Steiner et al., 2006). Accordingly, both protective and deleterious effects of CatB on memory loss and Aβ plaque load have been described (Mueller-Steiner et al., 2006; Sun et al., 2008; Hook et al., 2010, 2011; Kindy et al., 2012; Moon et al., 2016; Embury et al., 2017). In general, CatB seems to be involved in cell cycle regulation, the pathophysiology of multiple cancers, autophagy and neuroinflammation (Yan and Sloane, 2003; Chai et al., 2019). CatB has also been linked to a plethora of other diseases of the central nervous system, including AD, intracerebral hemorrhages, and traumatic brain injury (Cataldo and Nixon, 1990; Hook et al., 2005, 2014; Mueller-Steiner et al., 2006; Kindy et al., 2012). In AD, elevated levels of CatB have been detected in brains of AD patients extracellularly near neuritic plaques in membrane bound organelles, in degenerating neuronal perikarya, and in reactive astrocytes (Cataldo and Nixon, 1990; Cataldo et al., 1991; Nakamura et al., 1991). Elevated CatB activity in plasma samples of AD patients has been published (Sundelof et al., 2010; Morena et al., 2017). CatB has both endopeptidase and exopeptidase activities (Taralp et al., 1995). Under physiological conditions, CatB is mainly active in early endosomes and lysosomes (Taralp et al., 1995). At low

Abbreviations: AD, Alzheimer's disease; Aβ, Amyloid beta; ADAM, A Disintegrin and Metalloproteinase; APP, Amyloid Precursor Protein; BACE1, beta-site APP cleaving enzyme 1; Baf-A1, Bafilomycin A1; CatB, cathepsin B; CRISPR, Clustered Regularly Interspaced Short Palindromic Repeats; CTSB, gene enconding CatB; con., vehicle treated controls, DMEM, Dulbecco's Modified Eagle's Medium; DMSO, Dimethylsulfoxid; d.f., degrees of freedom, HEPES, 4-(2-hydroxyethyl)-1-piperazineethanesulfonic acid; LLOD, lower limit of detection; n, sample size; mAb 82E1, monoclonal antibody, which specifically recognizes Aβ 1-x; pAb p77, polyclonal antibody, which specifically recognizes Aβ 2-x; PAGE, Polyacrylamide gel electrophoresis; SDS, sodium dodecyl sulfate.

pH, it exerts a high carboxypeptidase activity on APP and Aβ in cell free assays (Mackay et al., 1997). Tumor cells secrete CatB into extracellular space, where it is stabilized by heparin sulfate on the plasma membrane, and its endopeptidase activity is favored due to neutral pH values (Almeida et al., 2001; Cotrin et al., 2004). To investigate whether CatB was involved in the generation of Aβ 1-x and the N-terminally truncated Aβ 2-x variants by astrocytes, we tested the cysteine protease inhibitor E64d and the CatB inhibitor CA-074 Me on chicken and human primary astrocytes. We selected the chicken as a model organism, because the Aβ amino acid sequence is the same as in humans. To further confirm the observed effects of the CA-074 Me treatment the gene encoding CatB (CTSB) was deleted via CRISPR/Cas 9 technology in the glioma derived cell line H4. The patterns of Aβ variants in the conditioned cell culture media were assessed by one- (1D) and two-dimensional (2D) Urea-SDS-PAGE followed by Western blotting.

MATERIALS AND METHODS

Isolation and Cultivation of Primary Cells

Chicken neurons and astrocytes from specific pathogen free eggs (Valo Biomedia, Osterholz-Scharmbeck, Germany) were prepared and cultivated as previously described. Human fetal astrocytes (provitro/Sciencell, Berlin, Germany) were cultivated as previously described (Oberstein et al., 2015).

Cultivation of Cell Lines

Untransfected human brain neuroglioma H4 cells (H4, LGC Standards GmbH/ATCC, Wesel, Germany), H4 cells stably transfected with human APP 751 (H4 APP 751) or H4 APP 751 (see below) with and without bi-allelic deletion of CTSB via CRISPR/Cas9 (H4 APP754 CTSB –/–) were maintained in DMEM medium supplemented with 10% superior fetal bovine serum (FBS, Biochrom, Berlin, Germany), 100 IU/ml penicillin and 100 µg/ml streptomycin (Biochrom) with or without 500 µg/ml G418 (Thermo Fisher Scientific/Roche, Grenzach-Wyhlen, Germany) and/or 2 µg/ml Puromycin (Santa Cruz Biotechnology, Heidelberg, Germany) respectively. A complete change of the medium was performed every two to three days. For the assessment of Aβ in conditioned supernatants, the medium was changed to serum-free DMEM/Ham's F12 (Biochrom) with G5 supplement (Thermo Fisher Scientific/Gibco, Darmstadt, Germany) and 10 mM Hepes (Biochrom).

Drug Treatment and Sample Preparation

The cysteine protease inhibitor E64d (100 mM, Peptanova, Sandhausen, Germany), the H^+-ATPase inhibitor Bafilomycin A1 (20 µM, Sigma Aldrich, Munich, Germany) the cathepsin B inhibitors CA-074 Me (25 mM, Peptanova), and CA-074 (25 mM, Sigma Aldrich, Munich, Germany) were dissolved in dimethyl sulphoxide (DMSO, Carl Roth, Karlsruhe, Germany) and stored at −20 °C. For the analysis of the released Aβ, the expression of APP, of BACE1, and of CatB, a complete medium change with serum-free medium was performed prior to treatment with drugs or with DMSO alone, yielding maximum final concentrations of 0.2% v/v DMSO. The cells were treated over 48 h. The conditioned media were subsequently centrifuged at 500 g for 5 min and stored at −20°C. Cells were washed with phosphate buffered saline (PBS, Biochrom) for 5 min at room temperature (RT) and lysed in detergent buffer [50 mM HEPES, 0.037 w/v Complete Mini Protease Inhibitor Cocktail (Thermo Fisher Scientific/Roche), 150 mM NaCl, 1% v/v Non-idet P-40, 0.5% w/v sodium deoxycholate, and 0.1% w/v sodium dodecylsulfate (SDS)] or in CytoBuster™ Protein Extraction Reagent (Merck Millipore) for 10 min at 4°C. The lysed cells were centrifuged (13,000 g, 5 min, 4°C), and supernatants were stored at −70°C.

Transfection of APP 751 Into H4 Cells

Full-length cDNA of human amyloid beta A4 protein isoform b precursor (also known as PreA4 751, APP 751) cloned into a pCI-neo mammalian expression vector (Promega, Mannheim, Germany) was kindly provided by Prof. Dr. Oliver Wirths (University Medical Center Goettingen, Goettingen). Twenty four hours post-seeding, the construct (7.5 µg / 9.5 cm² growth area) was transfected in 70% confluent H4 neuroglioma cells by calcium phosphate co-precipitation in serum-free medium. After 48 h, G418 (Thermo Fisher Scientific/Roche) resistant clones were selected by limiting dilution at <0.2 cells/well in DMEM with 10%FBS 100 IU/ml penicillin, 100 µg/ml streptomycin, 500 µg/ml G418 and maintained in the presence of G418. Six clones were isolated and assessed for the level of APP expression in 1D Aβ-PAGE.

Knockout of CTSB in H4 APP 751 wt Cells *via* CRISPR/Cas9

CTSB –/– cell lines were generated from H4 cells and H4 APP 751 cells using CRISPR/Cas9 KO and HDR Plasmid (Santa Cruz Biotechnology) according to the protocol of the supplier. Empty CRISPR/Cas9 plasmids (Santa Cruz Biotechnology) were used as control. For generation of single-cell colonies, Puromycin (Santa Cruz Biotechnology) resistant clones were selected by limiting dilution at <0.2 cells/well and maintained in the presence of 2 µg/ml puromycin. Five clones of H4 and two clones of H4 APP 751 cells were identified having a bi-allelic knockout for CTSB by western blot analysis.

Cell Viability Assays

Cell viability was assessed after drug treatment and knockout using the CytoTox 96® lactate dehydrogenase (LDH) assay (Promega) according to the manufacturer's instructions and for cells treated with CA-074 Me or E64d using the MTT [3-(4,5-dimethylthiazol-2-yl)-2,5-diphenyltetrazolium bromide] assay, as previously described (Mosmann, 1983).

Immunoprecipitation of Aβ

For the immunoprecipitation of Aβ, 40 µg mouse anti- Aβ n-x 6E10 (mAb 6E10, BioLegend formerly Covance, Koblenz, Germany) were covalently coupled to 10 mg magnetic sheep anti-mouse Dynabeads® M-280 (Dynal, Hamburg, Germany) according to the manufacturer's instructions.

For the detection of N-terminally truncated Aβ, 5, 10, or 20 ml of conditioned cell culture supernatant of chicken astrocytes, human astrocytes or H4 cells were supplemented

with Complete Mini Protease Inhibitor Cocktail (Thermo Fisher Scientific/ Roche) and concentrated 5 to 10-fold with 3,000 MWCO Vivaspin Protein Concentrators (GE Healthcare, Munich, Germany) at 4,000 g and 4°C. Conditioned media (with or without prior concentration) were mixed with 5-fold triple detergent buffer concentrate and 25 µl of magnetic beads coupled with mouse anti-Aβ antibody (mAb 6E10); yielding final concentrations of 1 µg/ml of immobilized mAb 6E10 in 50 mM HEPES, 150 mM NaCl, 0.5% v/v Non-idet P-40, 0.25% w/v sodium deoxycholate, and 0.05% w/v SDS. Immunoprecipitation was performed under rotation for 15 h at 4°C. For the analysis with Urea-SDS–PAGE, the samples were rinsed three times with PBS/0.1% BSA for 5 min at 4°C and once with 10 mM Tris-HCl, pH 7.5. For 1D-Aβ-PAGE and for 2D-Aβ-PAGE, the Aβ were eluted as previously described (Maler et al., 2007; Oberstein et al., 2015).

BCA Assay and Tris/glycine SDS-PAGE (SDS-PAGE) Followed by Western Blot and Immunodetection (IB)

The concentration of total protein in cell lysates was assessed with the bicinchoninic acid assay (BCA assay, Thermo Fisher Scientific/Pierce) as previously described (Smith et al., 1985). The absorption at 562 nm was measured with a Benchmark Microplate Reader (Bio-Rad, München, Germany) and was analyzed with Microplate Manager 5.1 software (Bio-Rad, München, Germany). 0.5 µg of protein sample per lane in sample buffer (63 mM Tris/HCl pH 6,8; 0.5% w/v SDS; 2.5% v/v glycerol; 100 mM w/v dithiothreitol; 0,0125% w/v bromophenol blue) were separated by 25 mM Tris pH 8,3/0,192 M glycine 0.1 w/v% SDS-PAGE with a 4% T/2.67% C stacking gel and a 7.5% T/2.67% C running gel for the detection of APP and a 10% T/2.67% C running gel for the detection of cathepsin B or BACE1 at RT and 200 V constant voltage (Laemmli, 1970). Separated proteins were transferred to Immobilon-FL PVDF membranes (Merck Millipore, Darmstadt, Germany), blocked with 2% w/v Amersham ECL advance blocking agent (GE Healthcare, Munich, Germany), probed with mouse anti-Cathepsin B CA10 (1:400 in PBS/0.1% v/v Tween (PBS-T); abcam, Cambridge, UK), rabbit anti-BACE1 PA1-757 (1:200 in PBS-T, Thermo Fisher Scientific) or mouse anti-APP 22C11 (1:1000 in PBS-T, Merck Millipore). After three times washing for 10 min with PBS-T the blots were incubated for 60 min with horseradish peroxidase (POD) conjugated goat anti-mouse or horse anti-rabbit antibodies (Merck Millipore). Mouse anti-GAPDH 374 (1:5000; Merck/Millipore) served to detect GAPDH as a loading control. Chemiluminescence was recorded after 5 min incubation at room temperature with ECL Prime Western Blotting Detection Reagent (GE Healthcare) with an Amersham Imager 600 (GE Healthcare).

CatB Activity Assay

CatB activity in cells lysed with the CytoBuster™ Protein Extraction Reagent was assessed with the InnoZyme™ Cathepsin B Activity Assay Kit (Merck Millipore/Calbiochem) according to the supplier's information. The different samples were adjusted to equal protein concentrations according to the results from BCA protein assay. Free AMC was measured using a Victor 3 multilabel plate reader (Perkin Elmer, Rodgau, Germany) with 355 nm excitation and 460 nm emission wavelengths and was quantified with Wallac 1420 software (Perkin Elmer).

Urea-Bicine/Bis-Tris/Tris/Sulfate SDS-PAGE Followed by Western Blot and Immunodetection

Stock solutions of synthetic peptides $A\beta_{1-40}$, $A\beta_{2-40}$, $A\beta_{3-40}$, $A\beta_{pE3-40}$ and $A\beta_{4-40}$ and $A\beta_{5-40}$ (1 mg/ml, MoBiTec/Anaspec, Goettingen, Germany) were prepared in sample buffer (0.36 M Bis–Tris, 0.16 M Bicine, 15% w/v sucrose, 1% w/v SDS, and 0.0075% w/v bromophenol blue) and stored at −80°C. Aβ levels in cell culture supernatants, were analyzed by urea-bicine/bis-tris/tris/sulfate SDS-PAGE followed by immunoblot as previously described (Klafki et al., 1996; Oberstein et al., 2015). The development of the immunoblots with mouse monoclonal anti-Aβ 1-x 82E1 (mAb 82E1, 1:1000 in PBS-T; IBL) or rabbit polyclonal anti-Aβ 2-x p77 (Savastano et al., 2016) was performed as previously described (Oberstein et al., 2015; Savastano et al., 2016).

2D Urea-SDS-PAGE and Immunoblot

Two-dimensional electrophoretic separation of Aβ peptides and immunoblot analysis were performed as previously described (Maler et al., 2007; Oberstein et al., 2015). The procedure for immunodetection with different anti-Aβ antibodies was as described above.

Organelle Stains

LysoTracker® as an organelle dye was used to examine the effects of chemical protease inhibitors and deletion of CatB on the morphology of lysosomes. Human astrocytes and H4 CTSB ± and CTSB –/– cells, were incubated with 75 nM working concentration of LysoTracker® Red DND-99 (Thermo Fisher) at 37°C for 30 min according to the manufacturer's instructions. Visualization was performed under a Leica DM IL HC Bio fluorescence microscope (excitation filter: BP 561/14, beamsplitter: BS R561, suppression filter: 609/54). Particle analysis was performed using ImageJ v1.46R.

Statistical Analysis

The data were analyzed with GraphPad Prism version 6.02 (GraphPad Software, San Diego, CA, USA) and SPSS Statistics version 22.0 (IBM, San Jose, CA, USA). Differences between groups were assessed with unpaired and ratio paired *T*-test, Kruskal-Wallis Test, one-way analysis of variance (ANOVA), and two-way ANOVA followed by Dunnett's or Tukey's multiple comparisons test, as a *post-hoc* test when a significant effect was observed. The degrees of freedom (d.f.) for the associated tests are given in brackets. All data are expressed as the mean ± standard deviation (SD). Significance levels are indicated as follows: $^{***}p < 0.001$; $^{**}p < 0.01$; $^{*}p < 0.05$; and ns, not significant.

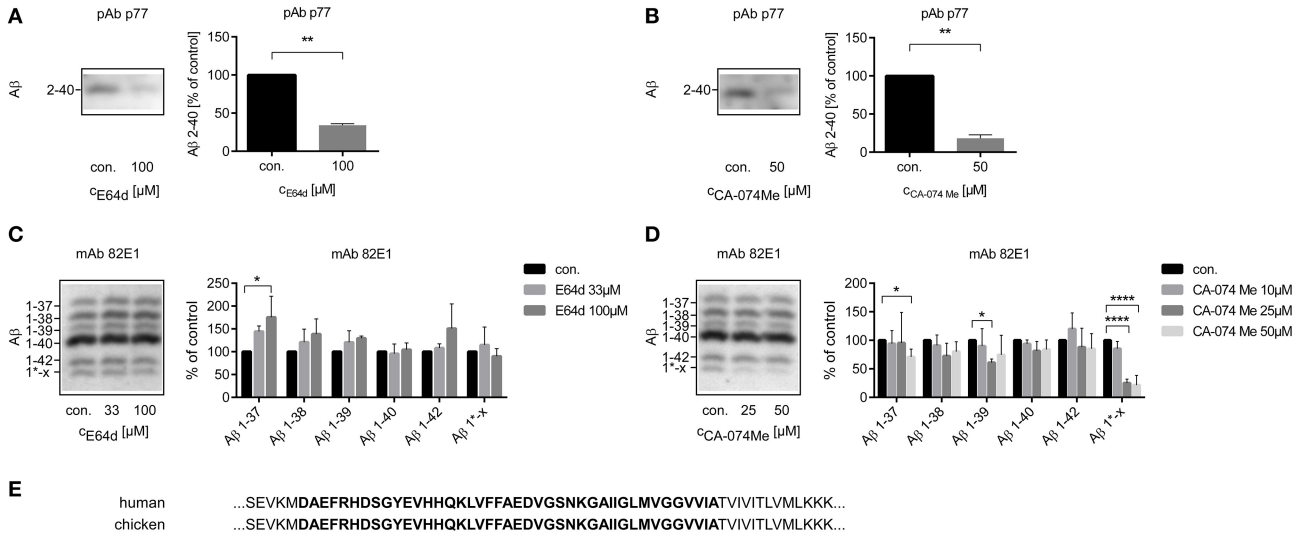

FIGURE 1 | Quantification of the relative amounts of Aβ 2-x **(A,B)** and of Aβ 1-x **(C,D)** in conditioned medium of cultured chicken astrocytes after the treatment with E64d **(A,C)** or CA-074 Me **(B,D)** over 48 h compared to controls using 1D Urea-SDS-PAGE followed by immunoblot analysis with anti-Aβ 2-x polyclonal antibody (pAb) p77 **(A,B)** or anti-Aβ 1-x monoclonal antibody (mAb) 82E1 **(C,D)**. Twenty milliliter **(A,B)** or 4 ml **(C,D)** sample volume were used. Aβ 2-40 was significantly reduced after the treatment with E64d **(A)** or CA-074 Me **(B)**. No significant reduction of the amounts of Aβ 1-40 or Aβ 1-42 was detected after E64d **(C)** or CA-074 Me **(D)** treatment. The labeling of the different Aβ 1-x peptide variants is based on a series of synthetic Aβ (Aβ 1-37, Aβ 1-38, Aβ 1-39, Aβ 1-40, and Aβ 1-42) and their isoelectric point in 2D Urea-SDS-PAGE (**Supplementary Figure 1**). A specific Aβ variant, designated as Aβ 1*-x, was effectively reduced by CA-074 Me treatment **(D)**. Panel **(E)** shows a section of the amino acid sequences of human and chicken APP, which contains the amino acid sequence of Aβ 1-42 (bold) and adjacent amino acids. In contrast to rodents, no differences in the amino acid sequence exist between humans (NP _958816.1) and chicken (NP _989639.1) in this part of APP (NCBI Reference Sequences are given, http://www.uniprot.org). Statistics: **(A)** $n = 3$, ratio paired T-Test $t_{(2)} = 31.43$ $p < 0.01$, **(B)** $n = 3$, ratio paired T-Test $t_{(2)} = 12.05$ $p < 0.01$, **(C)** $n = 3$, Kruskal-Wallis test Aβ 1-37, H (2) = 5. 793, $p < 0.05$, eta$^2 = 0.63$, Kruskal-Wallis test Aβ 1-38, H (2) = 3.310, $p > 0.05$, Kruskal-Wallis test Aβ 1-39, H (2) = 3.310, $p > 0.05$, Kruskal-Wallis test Aβ 1-40, H (2) = 0.8276, $p > 0.05$, Kruskal-Wallis test Aβ 1-42, H (2) = 0.1036, $p > 0.05$, Kruskal-Wallis test Aβ1*-x, H (2) = 1.471, $p > 0.05$, **(D)** $n = 5$, Kruskal-Wallis test Aβ 1-37, H (3) = 10.45, $p < 0.05$, eta$^2 = 0.41$, Kruskal-Wallis test Aβ 1-38, H (3) = 6.529, $p > 0.05$, Kruskal-Wallis test Aβ 1-39, H (3) = 8.236, $p < 0.05$, Kruskal-Wallis test Aβ 1-40, H (3) = 6.101, $p > 0.05$, Kruskal-Wallis test Aβ 1-42, H (3) = 4.178, $p > 0.05$, Kruskal-Wallis test Aβ 1*-x, H (3) = 17.23, $p < 0.001$, eta$^2 = 0.79$. Dunn's *post-hoc* test was performed for comparisons to vehicle treated control (con.). Selected comparisons are indicated as follows*$p < 0.05$; **$p < 0.01$, and ****$p < 0.0001$).

RESULTS

The Cell Permeant-Cysteine Proteinase Inhibitor E64d and the Cell-Permeant CatB Inhibitor CA-074 Me Reduced the Amount of Aβ 2–40

The amounts of Aβ 2-x or Aβ 1-x in cell culture supernatants were assessed by 1D Urea-SDS-PAGE followed by immunoblot. Treatment with the irreversible cysteine proteinase inhibitor E64d or with the CatB inhibitor CA-074 Me significantly reduced the amount of Aβ 2-x in conditioned media of cultured chicken astrocytes to 34.2 ± 1.2% and 18.2 ± 2.6 of the respective controls (**Figures 1A,B**). In contrast, separate immunoblots probed with the monoclonal antibody (mAb) 82E1, which specifically recognizes Aβ 1-x, indicated that the levels of Aβ 1-37, Aβ 1-38, Aβ 1-39, Aβ 1-40, and Aβ 1-42 were not decreased by E64d (**Figure 1C**). Treatment of cultured chicken astrocytes with high concentrations of CA-074 Me appeared to slightly reduce the levels of Aβ 1-37, Aβ 1-38, and Aβ 1-39 without significantly affecting the amount of Aβ 1-40 or Aβ 1-42 compared to controls (**Figure 1D**). The separation of Aβ peptide variants by 2D Urea-SDS-PAGE was used to further characterize the detected Aβ 1-x and 2-x variants. 2D-immunoblots probed with mAb p77 showed that the most abundant Aβ 2-x variant in supernatants of cultivated chicken astrocytes had the same pI and electrophoretic mobility in the second dimension as Aβ 2-40. Additionally, Aβ variants co-migrating with Aβ 2-38 and Aβ 2-42 were observed (**Supplementary Figure 1**). On 1D-immunoblots, Aβ 2-38 and Aβ 2-42 were usually not detected, presumably due to lower analytical sensitivity. Interestingly, a single, specific Aβ variant (designated Aβ* 1-x) was substantially and statistically significantly reduced by CA-074 Me treatment (**Figure 1D**). The exact length and chemical structure of Aβ* 1-x remains elusive, however, it is recognized by mAb 82E1, which is highly selective for Aβ starting with Asp (1) (Oberstein et al., 2015). On 2D-immunoblots, Aβ* 1-x showed a shifted isoelectric point (pI) of ∼6.4, which is substantially different from that of Aβ 1-38, Aβ 1-40, and Aβ 1-42, which all have a pI of ∼5.4 (**Supplementary Figure 2**). In order to find out whether not only the amino acid sequence of Aβ between chickens and humans is identical (**Figure 1E**), but the CatB inhibition has a similar effect on the processing of APP, cultured human astrocytes were also treated with CA-074 Me (**Supplementary Figure 3**).

In human astrocytes, data from two individual experiments indicated that the amount of Aβ 2-40 was reduced after 48h incubation with 25 µM CA-074 Me (**Supplementary Figure 3A**).

TABLE 1 | Comparison of the effects of 50 μM CA-074 Me, 50 μM CA-074 and 100 μM E64d on the relative abundances of different Aβ peptide variants in supernatants of H4 cells, H4 APP 751 cells, H4 APP 751 CTSB –/– cells, chicken astrocytes, and human astrocytes compared to controls.

H4APP 751/(H4)	**$A\beta_{1-40}$**	**$A\beta_{1-42}$**	**$A\beta_{2-40}$**
CA-074 Me (50 μM)	↑↑/(↑)	↑↑	↓
CA-074 (50 μM)	⟷	⟷	↓
H4APP 751 CTSB–/–	**$A\beta_{1-40}$**	**$A\beta_{1-42}$**	**$A\beta_{2-40}$**
CA-074 Me (50 μM)	⟷	⟷	⟷
Chicken astrocytes/(Human astrocytes)	**$A\beta_{1-40}$**	**$A\beta_{1-42}$**	**$A\beta_{2-40}$**
E64d	⟷	↑	↓↓
CA-074 Me	⟷/(⟷)	⟷/(⟷)	↓↓/(↓↓*)

*The decrease of Aβ 2-40 in supernatants from human astrocytes after CA-074 Me treatment has to be considered as preliminary (n = 2, *).*
x-fold increase: ↑↑ ≙ x > 200%; ↑ ≙ 125% < x < 200%, ⟷ ≙ 75% < x < 125%; ↓ ≙ 50% < x < 75%; ↓↓ ≙ 10% < x < 50%.

The level of the highly abundant Aβ 1-40 remained unchanged by CA-74 Me treatment in supernatants of cultured human astrocytes (**Supplementary Figure 3B**). Aβ 1-37 was significantly increased by 25μM CA-74 Me (169 ± 43% of controls). Aβ 1-37 is generally low abundant in cell culture supernatants, and even after its increase by CA-074Me treatment, its level was only 4.8 ± 2.1% of Aβ 1-40.

Collectively, the treatment with the cell permeant proteinase inhibitors E64d and CA-074 Me reduced the relative amount of Aβ 2-x in cell culture supernatants of primary astrocytes mostly without displaying significant effects on the secretion of Aβ 1 -x (see **Table 1**).

The tested concentrations of E64d or CA-074 Me did not lead to a significant decrease in cell viability or cytotoxicity (data not shown). In cell extracts of cultured chicken astrocytes treated with 25 and 50 μM CA-074 Me, the activity of CatB was below the detection range of the cathepsin B activity assay (**Supplementary Figure 4A**). The cellular CatB, BACE1 and APP levels in western blot analysis as well as total protein according to BCA assay were not significantly changed after the treatment with 50 μM CA-074 Me for 48 h (**Supplementary Figures 4B,C**).

Mature CatB Protein Levels and CatB Activity Were Higher in Cultured Chicken Astrocytes Than in Neurons

CA-074 Me appeared to affect mainly Aβ 2-x peptides, which are typically secreted by astrocytes. Thus, the relative abundance of CatB protein and its enzymatic activity were compared between cultured chicken astrocytes and chicken neurons. Expression of mature CatB, as assessed by western blot, and CatB activity in cell lysates were more than 4-fold higher in astrocytes than in neurons (**Supplementary Figures 5A,B**). Immature and mature BACE1 proteins (67 and 59 kDa, respectively) were detected in cultured chicken neurons but not in chicken astrocytes by SDS-PAGE followed by immunoblot (**Supplementary Figure 5C**). Chicken astrocytes predominantly expressed longer isoforms of APP compared to chicken neurons (**Supplementary Figure 5D**), which was in line with previous reports (Rohan de Silva et al., 1997). Accordingly, the APP 751 isoform and not the shorter APP 695 isoform was chosen for the transfection of cell lines (**Figure 2A**).

CRISPR/Cas9 Induced Knockout of CTSB and CatB-Inhibition With CA-074 Me in H4 APP 751 Neuroglioma Cells Increased the Amount of Secreted Total Aβ

Aβ 2-x concentrations are small and cannot be reliably measured by Western blot in primary cell culture experiments with sample volumes that are typically used e.g., in gene silencing experiments. Thus, a H4 neuroglioma cell line stably overexpressing the amyloid precursor protein transcript variant b (APP 751; H4 APP 751) was established, and the effect of a CRISPR/Cas9 induced CTSB knockout (H4 APP 751 CTSB–/–) on Aβ peptide variants in the conditioned media was investigated (**Figures 2E–H**).

In contrast to the findings in primary cell culture experiments (see above), the concentrations of Aβ 1-38, Aβ 1-40, and Aβ 1-42 in the supernatant of H4 APP 751 cells were increased after treatment with 50 μM CA-074 Me according to Aβ immunoblot analysis (**Figure 2B**) In sharp contrast, Aβ 2-x was reduced after CA-074 Me treatment (**Figure 2C**). The increase in Aβ 1-x in conditioned medium after treatment with 25 and 50 μM CA-074 Me was also observed after normalization to total cellular protein levels of H4 APP 751 cells. According to BCA protein assay, the cellular protein levels were slightly increased after CA-074 Me treatment (25 μM: 1.26 ± 0.34 of control and 50 μM: 1.21 ± 0.21 of control). The CatB level in cell lysates of H4 APP 751 cells remained unchanged by CA-074 Me treatment (**Supplementary Figure 6**).

The CRISPR/Cas9 induced knockout of CTSB in H4 APP 751 cells (H4 APP 751 CTSB –/–; **Figure 2D**) led to a strong increase in Aβ 1-40, Aβ 1-42, and Aβ 1-38 in supernatants compared to mock treated H4 APP 751 cells (**Figure 2E**). In contrast, the abundance of Aβ 2-x in supernatants of H4 APP 751 CTSB –/– cells was moderately reduced to 0.55 ± 0.22 in comparison to H4 APP 751 cells (**Figure 2F**). Treating H4 APP 751 CTSB –/– cells with 50 μM CA-074 Me did not have an additional effect, and thus did not significantly change the amounts of Aβ 1-38, Aβ 1-40, and Aβ 1-42 in conditioned medium compared to controls (**Figures 2G,H**).

Collectively, the observations after pharmacological inhibition of CatB with CA-074 Me and CatB knockout suggested that CatB was probably involved in the degradation of Aβ in H4 APP 751 cell cultures but not in primary astrocytes (see **Table 1**). To exclude that this was a consequence of the APP 751 overexpression, non–transfected H4 cells were treated with CA-074 Me. This resulted in a similar increase in the abundance of Aβ 1-40 as observed in H4 APP 751 cells (**Supplementary Figure 7**).

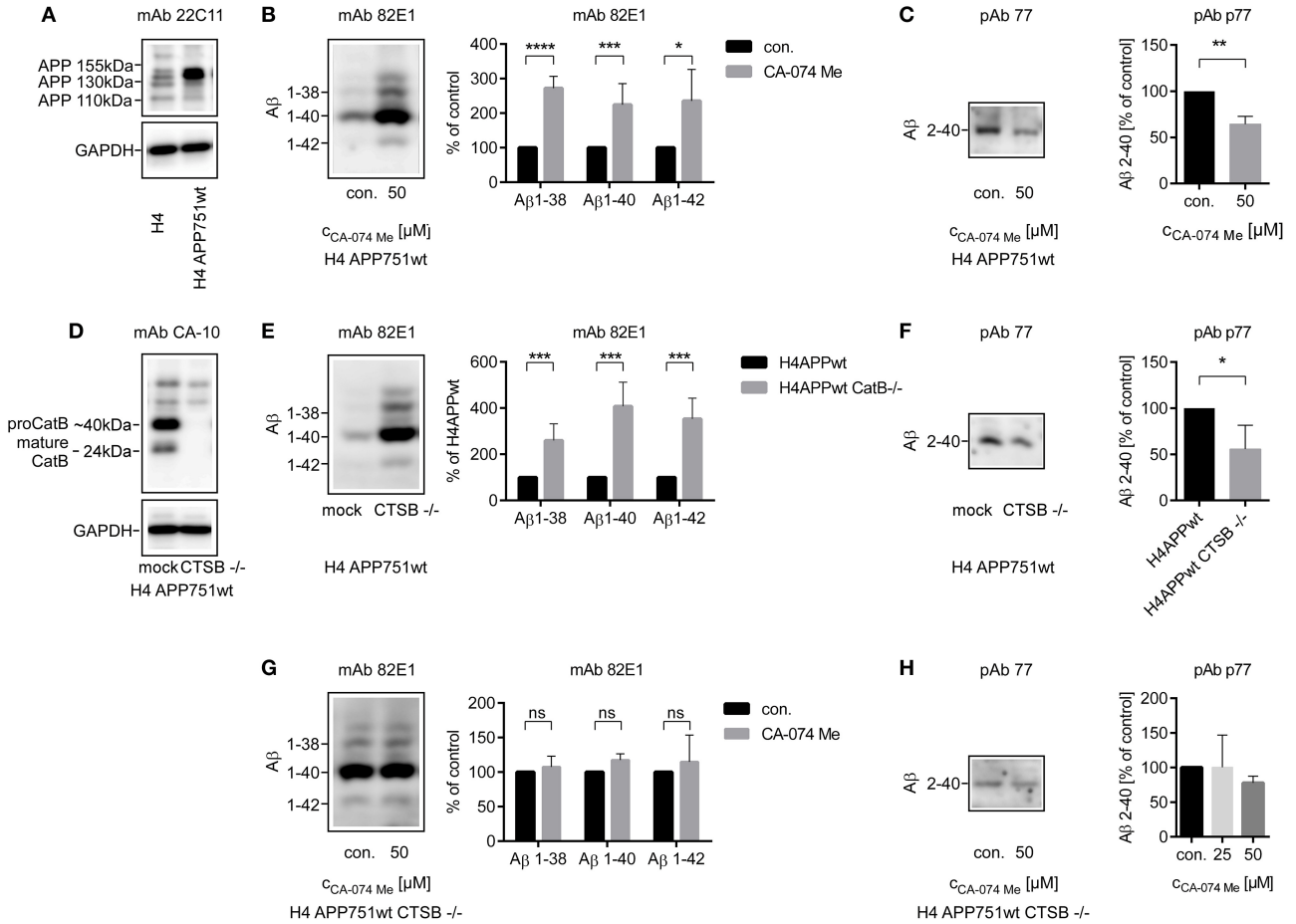

FIGURE 2 | Stable transfection of APP751 in H4 cells was controlled by SOS-PAGE followed by immunoblot probed with anti-APP mAb 22C11 **(A)**. Four milliliters **(B,E,G)** or 10 ml **(C,F,H)** of conditioned media from H4 APP751wt cells were used for the analysis of secreted Aβ peptides. The relative abundance of Aβ 1-x **(B)** was increased after the stimulation with CA-074 Me over 48 h in supernatants of H4 APP751wt cells as assessed by 1D Urea-SDS-PAGE followed by immunoblot, whereas the amount of Aβ co-migrating with Aβ 2-40 was decreased compared to controls **(C)**. Deletion of CTSB *via* CRISPR/Cas9 technology was controlled by SOS-PAGE followed by immunoblot probed with anti-CatB mAb CA-10 **(D)**. The abundance of Aβ 1-x was increased in H4 APP751wt CTSB –/– cells compared to H4 APP751wt cells **(E)**, whereas Aβ co-migrating with Aβ 2-40 was slightly decreased **(F)**. In H4 APP751wt CTSB –/– cells, treatment with CA-074 Me did not significantly alter the abundance of Aβ co-migrating with synthetic Aβ 1-38, Aβ 1-40 or Aβ 1-42 **(G)**, but it slightly reduced the amount of Aβ 2-x **(H)**. Statistics: **(B)** ratio paired *T*-Test Aβ 1-38, $t_{(4)} = 18.04$, $p < 0.001$, **(F)** $n = 4$, ratio paired *T*-Test $t_{(3)} = 3.435$, $p < 0.05$ **(G)** $n = 3$, ratio paired *T*-Test Aβ 1-38, $t_{(2)} = 0.3416$, $p > 0.05$, ratio paired *T*-Test Aβ 1-40, $t_{(2)} = 3.857$, $p > 0.05$, ratio paired *T*-Test Aβ 1-42, $t_{(2)} = 2.776$, $p > 0.05$ **(H)** $n = 3$, Kruskal-Wallis test $H\,(2) = 3.310$, $p > 005$. Selected comparisons are indicated as follows $^{*}p < 0.05$; $^{**}p < 0.01$; $^{***}p < 0.001$; and $^{***}p < 0.0001$.

Secreted Aβ 1-x Was Reduced by the Cell-Impermeant CatB Inhibitor CA-074 and H^{+}-ATPase Inhibitor Baf-A1 in H4 APP 751 Cells

As the different effects of CatB inhibition on the Aβ profile of primary astrocytes or H4 cells might be due to different localizations of active CatB, H4 APP 751 cells and their supernatants alone were treated with the cell-impermeant CatB-inhibitor CA-074. In contrast to treatment with the cell-permeant Cat- inhibitor CA-074 Me, the treatment of H4 APP 751 cells with CA-074 over 48 h resulted not in an increase, but in a small decrease in secreted Aβ 1-40 to 82.2 ± 6.0% of control (**Figure 3A**; *T*-test $t_{(4)} = 2.980$, $p < 0.05$). The amount of Aβ 2-40 was decreased by CA-074 to a similar extent as CA-074 Me (**Figure 3B**). Incubation of cell-free, conditioned medium of H4 APP 751 cells with CA-074 over 48 h at 37°C did not change the amount of Aβ 1-x (**Figure 3C**). The CatB activity in cell culture supernatants varied substantially according to a CatB activity assay (data not shown). This indicated that the increase of total Aβ in H4 APP 751 cell culture supernatant was mediated by the inhibition of an intracellular enzyme, whilst the decrease of Aβ 2-40 after CA-074 Me and CA-074 treatment was probably mediated by the inhibition of a plasma membrane-associated enzyme. This is in accordance with our previous observation that Aβ peptide variants that were co-migrating with synthetic Aβ 1-40 in 2D SDS Urea-PAGE were detectable in lysates of cultured astrocytes, whereas Aβ peptide variants

co-migrating with synthetic Aβ 2-40 could be detected in cell culture supernatants but not in cell lysates (Oberstein et al., 2015). Next, we investigated the effect of the vacuolar H^+-ATPase inhibitor Bafilomycin A1 (Baf-A1), as Baf-A1 is known to inhibit the acidification of intracellular organelles such as lysosomes. Baf-A1 treatment resulted in a significant reduction of Aβ 1-x compared to controls in conditioned media of H4 APP 751 cells (**Figures 3A,D**), whereas the amount of Aβ 2-40 was increased (**Figures 3D,E**). Two-way ANOVA with Baf-A1 and CA-074 Me treatment as independent variables and Aβ 1-40 as dependent variable showed a significant interaction between the drug treatments (**Figure 3D**). The slopes of the corresponding interaction plot suggested that Baf-A1 treatment may reduce the degradation of Aβ 1-40 via CatB, as the slope steepness of the CA-074Me group was higher than the control group. Two-way ANOVA with Aβ 2-40 as the dependent variable showed no interaction between the Ca-074 Me and the Baf-A1 group (**Figure 3E**).

Treatment With CA-074 Me Changed the Morphology of Lysosomes in Human Astrocytes and H4 Cells

As not only the involved enzymes but also the different cell compartment seemed to be crucial for the generation of the different Aβ variants, the effect of CA-074 Me on the morphology of lysosomes was studied (**Figure 3F**). Staining with LysoTracker® indicated an increased mean fluorescence intensity (MFI) of the detected particles in CA-074 Me treated human astrocytes (**Figure 3H**) and H4 CTSB –/+ cells compared to controls after 24 h (**Figure 3G**). In H4 cells, an increase in particle size was also detected after CA-074 Me treatment (**Figure 3G**). However, the increase of the particle MFI and size after CA-074 Me treatment was also detected in H4 CTSB –/– cells, and no differences in the MFI and particle volume were observed between CA-074 Me treated H4 CTSB +/− and H4 CTSB –/– cells (**Figure 3H**), which indicates that this effect was independent of the inhibition of CatB.

DISCUSSION

The present study shows that the treatment of different astroglial cell cultures with the CatB-inhibitor CA-074 Me resulted in varying effects on the abundance of Aβ in supernatants depending on whether primary cells or a cell line was studied. Treatment with cell-impermeant CatB inhibitor CA-074 and the vacuolar H^+-ATPase inhibitor Baf-A1 further indicated that the capacity of degrading Aβ 1-x and the generation of Aβ 2-x by CatB might be dependent on the different cellular localizations of active CatB (**Figure 4**).

The amount of secreted Aβ 2-40, but not that of Aβ 1-40 in supernatants of cultured primary chicken or human astrocytes was reduced by treatment with CatB inhibitors. Thus, our data indicate that CatB is probably involved in the production of the N-terminally truncated Aβ 2-x. However, small amounts of these N-terminally modified Aβ peptide variants were detected, even after CatB inhibition with CA-074 Me. The observed decrease in Aβ 2-40 after CatB inhibition in cultured primary astrocytes is in accordance with a previous report, showing that purified CatB can cleave peptide substrates flanking the β-secretase site within APP between Lys and Met and between Asp and Ala (Schechter and Ziv, 2011). Bien et al. (2012) and we have previously reported that the production of Aβ 2-x was independent of BACE1 (Bien et al., 2012; Oberstein et al., 2015). Butler et al. (2011) reported that the activity of CatB was not influenced by commonly used BACE1 inhibitors. However, CatB does not seem to be the only endopeptidase, which is capable of cleaving APP N-terminal to Ala2 of the Aβ-Sequence. Previous reports state that Aβ 2-x can also be produced by the endoproteolytic activity of meprin β (Bien et al., 2012; Schonherr et al., 2016). Furthermore, Aminopeptidases, such as Aminopeptidase A, may be involved in the N-terminal truncation of Aβ following the primary cleavage of APP by BACE1 (Saido, 1998; Sevalle et al., 2009). Additionally, it has been reported that CatB cleaves APP-derived substrates at Asp and isoAsp as assessed by cell-free enzymatic assays (Bohme et al., 2008). However, in our cell culture model, the inhibition of CatB by CA-074 Me resulted in a slight, non-significant decrease of Aβ 1-40 in primary chick or human astrocytes. Given the differences in the sequence of APP between chickens and humans, these might alter the specificity and selectivity of CatB and other proteases to perform cleavage of APP at the beta-site. In our study, however, Aβ 1-37 was the only detected Aβ peptide variant that was changed in a statistically significantly different manner by CA-074Me-treatment in human astrocytes compared to chicken astrocytes. Since there was no difference in the levels of Aβ 1-40 and Aβ 1-42, we speculate that the difference observed for Aβ 1-37 was not due to cleavage of the beta-site of APP by CatB. Collectively, our data suggest that CatB is involved in the production of N-terminally truncated Aβ 2-x in primary astrocytes but not in the generation of Aβ 1-x. In H4 APP751 cells, the N-terminally truncated Aβ 2-40 was also reduced after inhibition with CA-074Me or with CA-074 as well as after the deletion of CTSB via CRISPR/Cas9 technology.

In contrast to the observations from primary cell culture experiments, CA-074 Me treatment and deletion of CTSB via CRISPR/Cas9 technology in H4 APP751 cells led to a significant increase of Aβ 1-x. Thus, it appears that CatB takes part in the degradation of Aβ 1-x in H4 cells overexpressing APP. In line with that, Mueller-Steiner et al. (2006) reported that CatB reduced Aβ levels in hippocampal CA1 pyramidal neurons of hAPP mice. In our study, the vacuolar H^+-ATPase inhibitor Baf-A1 reduced the amounts of Aβ 1-40, Aβ 1-42, and Aβ 1-38 in conditioned media, and simultaneous treatment with CA-074 Me suggested that the CA-074 Me-mediated increase of Aβ 1-40 was dependent on acidified compartments. This is in accordance with the reported dipeptidyl carboxypeptidase activity of CatB, which has its optimum at pH 5.0, i.e., the pH of late endosomes and lysosomes (Mach et al., 1994; Almeida et al., 2001; Mueller-Steiner et al., 2006; Butler et al., 2011; Wang et al., 2012). As we did not observe any increase of Aβ 1-x after treatment with the cell-impermeant inhibitor CA-074 in supernatants of H4 cells, we concluded that Aβ 1-x was not degraded extracellularly by CatB. It appears that CA-074 did not enter lysosomes via extensive pinocytosis/fluid phase endocytosis. This is in line with the report of Bogyo et al. (2000) who stated that the derivatives of CA-074, CA-074b and MB-074, were not capable of entering the lysosome

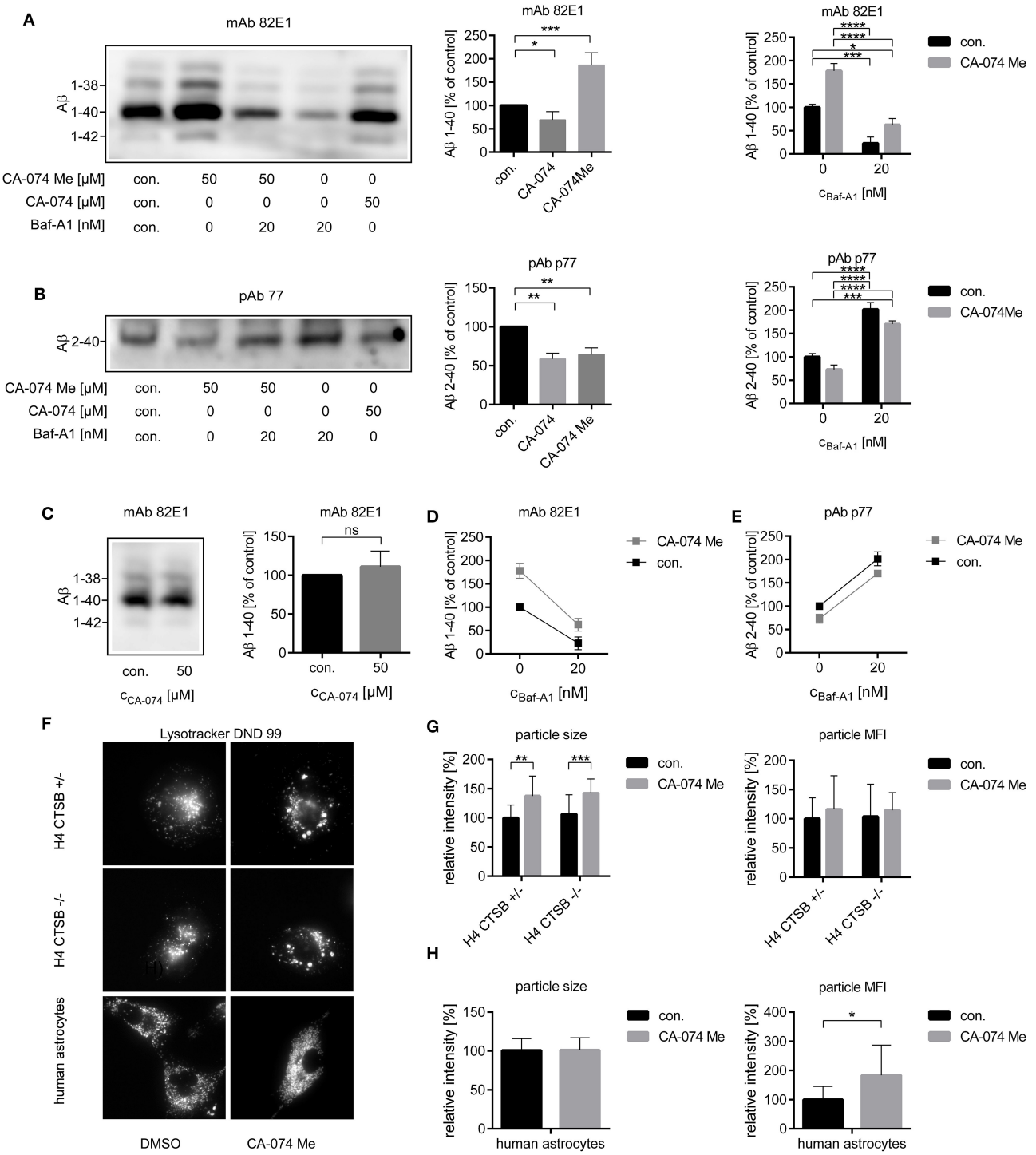

FIGURE 3 | Four milliliters **(A,C,D)** or 20 ml **(B,E)** of conditioned media from H4 APP751 wt cells were used for the analysis of secreted Aβ. The relative amounts of Aβ 1-x **(A)** and of Aβ 2-40 **(B)** were decreased after the treatment of H4 APP741 wt cells with the cell-impermeant CatB-inhibitor CA-074 over 48 h. In supernatants of CA-074 Me treated cells, only the amount of Aβ 2-40 was decreased and the amount of Aβ 1-40 was conversely increased compared to controls. In cell free-conditioned media incubated over 48 h at 37°C, no decrease of the secreted Aβ 1-40 was observed, when CA-074 was added **(C)**. Treatment with the H^+-ATPase inhibitor Bafilomycin A1 (Baf-A1) decreased the amount of Aβ 1-40 **(A)** and increased Aβ 2-40 **(B)** compared to controls. Interaction plots with CA-074 Me and Baf-A1 as independent variables suggested, that the increase of dependent variable Aβ 1-40 after CA-074 Me treatment was dependent on the level of Baf-A1 **(D)**, whereas no interaction was found for the dependent variable Aβ 2-40 **(E)**. Stains with Lysotracker **(F)** showed an increased particle size in H4 cells **(G)** and an increased particle mean fluorescence intensity (MFI) in human astrocytes **(H)** after the treatment with CA-074 Me compared to vehicle treated cells (con.). This

(Continued)

FIGURE 3 | effect was also observed in H4 CTSB –/– cells, which indicated a CatB-independent effect of CA-074 Me on the morphology of lysosomes. Statistics: **(A)** $n = 5$, ratio paired *T*-Test DMSO|CA-074 $t_{(4)} = 3.395$, $p < 0.05$, ratio paired *T*-Test DMSOICA-074Me $t_{(4)} = 10.59$, $p < 0.001$, **(B)** $n = 4$, ratio paired *T*-Test DMSO|CA-074 $t_{(3)} = 8.544$, $p < 0.01$, ratio paired *T*-Test DMSO|CA-074Me $t_{(4)} = 6.868$ $p < 0.01$, **(C)** $n = 4$, ratio paired *T*-Test $t_{(3)} = 1.056$, $p > 0.05$ **(D)** $n = 3$, Two-way ANOVA column *F* Baf-A1 (1, 8) = 68.54, $p < 0.0001$, row *F* CA-074 Me (1, 8) = 24.45, $p < 0.0001$, *F* interaction (1, 8) = 2.687, $p < 0.05$, **(E)** Two-way ANOVA F Baf-A1 (1, 8) = 89.70, $p < 0.0001$, *F* CA-074 Me (1, 8) = 7.734, $p < 0.01$, *F* interaction (1, 8) = 0.04241, $p > 0.05$, **(G)** Two-way ANOVA particle size *F* con. |CA-074 Me (1, 84) = 32.85, $p < 0.0001$, *F* CTSB +/−|CTSB –/– (1, 84) = 0.7853, $p > 0.05$, *F* interaction (1, 84) = 0.02116, $p > 0.05$, Two-way ANOVA particle MFI *F* con.|CA-074 Me (1, 80) = 5.279, $p < 0.05$, FCTSB +/−|CTSB –/– (1, 80) = 0.3039, $p > 0.05$, *F* interaction (1, 80) = 0.1415, $p > 0.05$, **(H)** unpaired *T*-Test particle size, $t_{(16)} = 0.05915$, $p > 0.05$, unpaired *T*-Test particle MFI, $t_{(15)} = 2.351$, $p < 0.05$. Tukey's *post-hoc* test was performed for multiple comparisons. Selected comparisons are indicated as follows ns $p > 0.05$, *$p < 0.05$; **$p < 0.01$; ***$p < 0.001$, and ****$p < 0.0001$). Each experiment was performed at least three times.

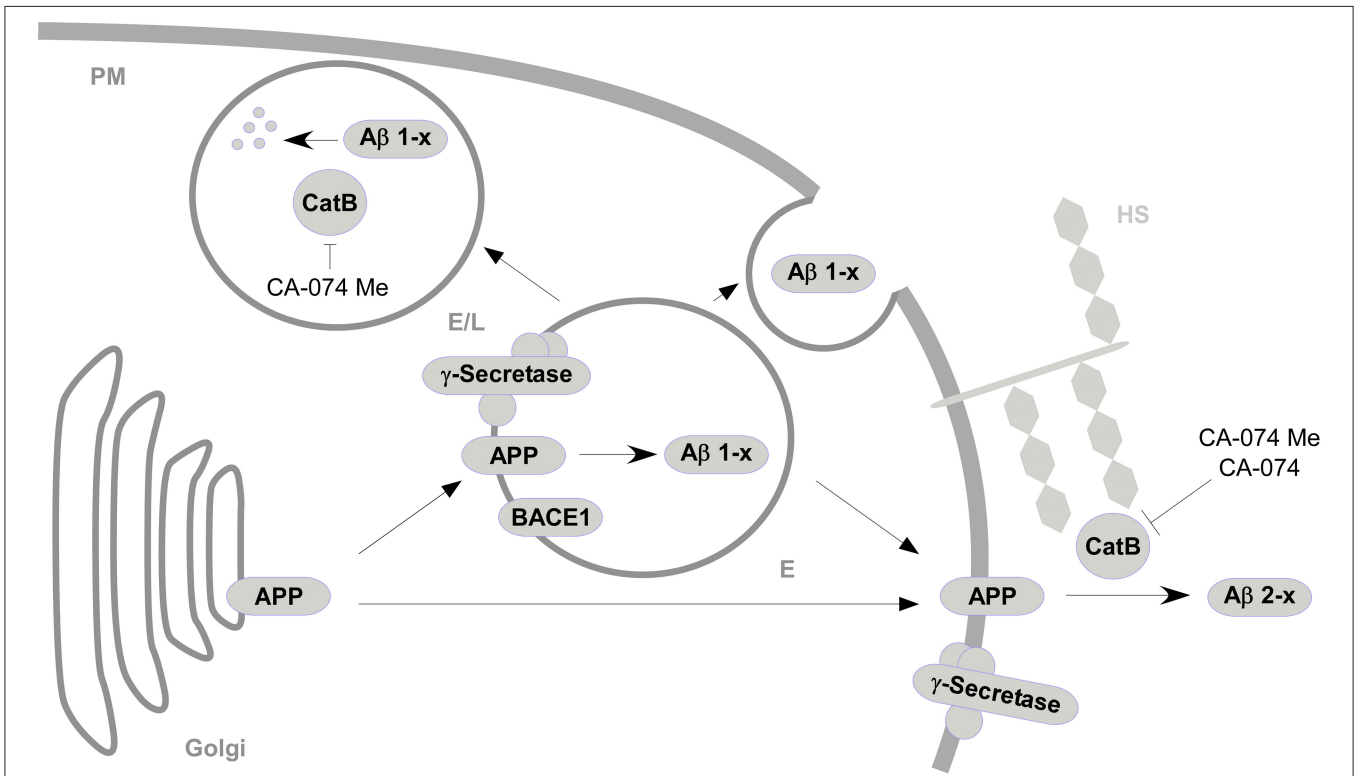

FIGURE 4 | A simplified model for the sites of interaction between CatB, APP, and Aβ and the subsequent generation or degradation of Aβ based on the effects of CatB inhibition (|) with cell-permeable CA-074 Me and cell-impermeable CA-074. APP from the golgi apparatus is transported to acidified vesicles (E) or to the plasma membrane (PM) via vesicular transport (⊣►). At the acificed vesicles, APP is processed (➤) by BACE1 and γ-secretase to Aβ 1-x, which are secreted to the extracellular space or degraded in endosomes/lysosomes (E/L) by CatB. APP at the plasma membrane is processed to Aβ 2-x mediated by CatB presumably associated to heparan sulfate (HS) (Almeida et al., 2001).

and inhibiting the target. In summary, the findings suggest that lysosomal CatB might be involved in Aβ 1-x degradation. In our cell culture model, all detected Aβ 1-x variants, including Aβ 1-42 and Aβ 1-38, were similarly increased after inhibition of CatB or deletion of CTSB. In cell-free assays, the carboxypeptidase activity of CatB did not produce C-terminally truncated Aβ peptide variants from Aβ 1-42 that were shorter than 38 or 37 amino acids (Mackay et al., 1997; Mueller-Steiner et al., 2006). Correspondingly, Butler et al. (2011) and Hwang et al. (2019) reported that the pharmacological modulation of lysosomes and thereby increased levels and activity of CatB resulted in a decrease of Aβ 42 and an increase of Aβ 38 in APPswe/PSEN1dE9 mice. We can only speculate, why we did not observe a shift toward Aβ 1-42 after CatB inhibition with CA-074 Me or deletion of CTSB in H4 APP751 cells in our study. One possible explanation might be that in our model other proteases rapidly degrade these CatB-produced, C-truncated Aβ fragments further into smaller fragments. A variety of proteases have been implicated in the degradation of Aβ, like neprilysin, plasmin, and insulin degrading enzyme (Howell et al., 1995; Qiu et al., 1998; Van Nostrand and Porter, 1999). Recently, Kidana et al. (2018) reported that kallikrein-related peptidase 7, a serine protease, contributes to the degradation of Aβ in astrocytes. Additionally, the overexpression of APP751 might also lead to an aberrant trafficking and/or C-Terminal truncation. The work of Butler et al. (2011) and Hwang et al. (2019) suffers from a similar dilemma, as they use transgenic animal models: The use of the so-called Swedish mutation of APP and the PSEN1dE9 mutation in both of the animal models should result in a pattern of secreted Aβ with abnormal high percentages of Aβ 1-42, because

the Swedish mutations increases the affinity of APP for BACE1 cleavage and the PSEN1dE9 mutations reduces the inherent carboxypeptidase activity of the γ-secretase. Conversely, the lower amount of APP and the unrestricted carboxypeptidase activity of the γ-secretase could be the reason why lysosomal CatB was apparently not involved in the degradation of Aβ in primary chicken and human astrocytes. However, the increased amount of Aβ 1-40 in supernatants of CA-074 Me-treated, untransfected H4 cells indicates that the overexpression of APP is not sufficient to explain the differences between H4 cells and primary astrocytes.

In contrast to Aβ 1-x, the decrease of Aβ 2-x in conditioned media after treatment of cultured cells with either CA-074Me or CA-074 and its increase upon Baf-A1 treatment suggests that Aβ 2-x is preferentially generated outside lysosomal compartments, i.e., extracellularly or near the plasma membrane in non-acidic cellular compartments. It has been reported before that CatB is frequently redistributed to the plasma membrane (Frosch et al., 1999; Cavallo-Medved and Sloane, 2003). CatB must then be stabilized by heparin sulfate at the cell surface, as otherwise it loses it proteolytic activity (Taralp et al., 1995; Almeida et al., 2001). Congruently, CatB activity in cell free medium was mostly below the LLOD and subject to great variances in the CatB activity assay. An abberant extracellular distribution of CatB has been described for AD near senile plaques (Cataldo et al., 1990). It has recently been hypothesized that leakage of lysosomal CatB into the cytosol contributes to neurodegeneration and behavioral deficits in AD and traumatic brain injury (Hook et al., 2020). The presumed generation of Aβ 2-x by non-lysosomal CatB in astrocytes in this study supports the hypothesis of deleterious effects of non-lysosomal CatB, as Aβ 2-40 is potentially associated with CAA in AD (Gkanatsiou et al., 2019).

Our study indicates that the decrease of Aβ 2-40 after CA-074 Me treatment might be mediated by both CatB-dependent and CatB-independent mechanisms: CA-074 has been reported to inhibit CatB more selectively than CA-074 Me (Bogyo et al., 2000; Montaser et al., 2002). This is in favor of a CatB-dependent decrease of Aβ 2-40 after inhibitor treatment, as CA-074 treatment lowered the amount of Aβ 2-40 to the same extent as CA-074 Me in our study. Additionally, Aβ 2-40 in conditioned media of H4 APP 751 CTSB –/– cells was moderately decreased in comparison to H4 APP 751 cells. However, CA-074 Me had an additional effect and further decreased the amount of Aβ 2-40 in conditioned medium of H4 APP 751 CTSB –/– cells. This additional reduction in Aβ 2-40, which was apparently not directly related to CatB inhibition, might be the consequence of altered lysosomal function and trafficking. In H4 cells LysoTracker© organelle dyes revealed enlarged vesicles after the CA-074 Me treatment. This effect was observed even after the deletion of CTSB in H4 cells. CA-074 Me is considered to be a specific CatB inhibitor (Murata et al., 1991; Buttle et al., 1992). Nevertheless, there have been previous reports of CA-074 Me effects that were independent of CatB inhibition. These might possibly be due to the methylation of the proline carboxyl group facilitating binding to cathepsins other than CatB, like cathepsin L, or increasing the lysosomal membrane integrity (Bogyo et al., 2000; Montaser et al., 2002; Mihalik et al., 2004; Xu et al., 2016). In accordance with previous studies from Hook et al. (2010) and Mueller-Steiner et al. (2006), the treatment with CA-074 Me and E64d, did not alter the cellular levels of the different APP isoforms and BACE1 in our study.

This study indicates that the observed adverse and positive effects of CatB and its inhibitors may depend on the sites of interaction with APP and its metabolites. The use of techniques like fluorescence (life cell) imaging, activity-based probes and small molecule inhibitors with different effects on the endo- and exopeptidase activity of CatB will be helpful in further elucidating the sites of interaction between CatB and APP both *in vitro* and ultimately *in vivo* and possibly contribute to the development of suitable drugs.

CONCLUSION

Lysosomal CatB seems to be involved the degradation of Aβ 1-x in neuroglioma cell culture but not in primary astrocytes. The generation of N-terminally truncated Aβ 2-x in astrocytes, however seemed to be mediated by plasma-membrane associated CatB.

DATA AVAILABILITY STATEMENT

The raw data supporting the conclusions of this article will be made available by the authors, without undue reservation.

AUTHOR CONTRIBUTIONS

TO designed the study, performed experiments, analyzed the data, and drafted the manuscript. JU performed experiments and contributed to revision of the manuscript. JK and JM provided reagents and contributed to the interpretation of findings and revision of the manuscript. PS, PL, JW, and HK contributed to the interpretation of findings and revision of the manuscript. All the authors read and approved the final manuscript.

FUNDING

PL received consultation and/or lecture honoraria from IBL International, Fujirebio Europe, AJ Roboscreen, and Roche. None of them were involved in the study design, collection, analysis, interpretation of data, the writing of this article or the decision to submit it for publication. JW was supported by an Ilídio Pinho professorship, iBiMED (UIDB/04501/2020) at the University of Aveiro, Portugal. TO's work was partly supported by grants from the Interdisciplinary Center for Clinical Research (IZKF), Erlangen. We acknowledge support from Deutsche Forschungsgemeinschaft (DFG) and Friedrich-Alexander-Universität ErlangenNürnberg (FAU) within the funding program Open Access Publishing.

SUPPLEMENTARY MATERIAL

The Supplementary Material for this article can be found online at: https://www.frontiersin.org/articles/10.3389/fnmol.2020.615740/full#supplementary-material

REFERENCES

Akiyama, H., Mori, H., Sahara, N., Kondo, H., Ikeda, K., Nishimura, T., et al. (1997). Variable deposition of amyloid beta-protein (A beta) with the carboxy-terminus that ends at residue valine40 (A beta 40) in the cerebral cortex of patients with Alzheimer's disease: a double-labeling immunohistochemical study with antibodies specific for A beta 40 and the A beta that ends at residues alanine42/threonine43 (A beta 42). *Neurochem. Res.* 22, 1499–1506. doi: 10.1023/A:1021910729963

Almeida, P. C., Nantes, I. L., Chagas, J. R., Rizzi, C. C., Faljoni-Alario, A., Carmona, E., et al. (2001). Cathepsin B activity regulation. Heparin-like glycosaminogylcans protect human cathepsin B from alkaline pH-induced inactivation. *J. Biol. Chem.* 276, 944–951. doi: 10.1074/jbc.M003820200

Bayer, T. A., and Wirths, O. (2014). Focusing the amyloid cascade hypothesis on N-truncated Abeta peptides as drug targets against Alzheimer's disease. *Acta Neuropathol.* 127, 787–801. doi: 10.1007/s00401-014-1287-x

Bien, J., Jefferson, T., Causevic, M., Jumpertz, T., Munter, L., Multhaup, G., et al. (2012). The metalloprotease meprin beta generates amino terminal-truncated amyloid beta peptide species. *J. Biol. Chem.* 287, 33304–33313. doi: 10.1074/jbc.M112.395608

Bogyo, M., Verhelst, S., Bellingard-Dubouchaud, V., Toba, S., and Greenbaum, D. (2000). Selective targeting of lysosomal cysteine proteases with radiolabeled electrophilic substrate analogs. *Chem. Biol.* 7, 27–38. doi: 10.1016/S1074-5521(00)00061-2

Bohme, L., Hoffmann, T., Manhart, S., Wolf, R., and Demuth, H. U. (2008). Isoaspartate-containing amyloid precursor protein-derived peptides alter efficacy and specificity of potential beta-secretases. *Biol. Chem.* 389, 1055–1066. doi: 10.1515/BC.2008.125

Butler, D., Hwang, J., Estick, C., Nishiyama, A., Kumar, S. S., Baveghems, C., et al. (2011). Protective effects of positive lysosomal modulation in Alzheimer's disease transgenic mouse models. *PLoS ONE* 6:e20501. doi: 10.1371/journal.pone.0020501

Buttle, D. J., Murata, M., Knight, C. G., and Barrett, A. J. (1992). CA074 methyl ester: a proinhibitor for intracellular cathepsin B. *Arch. Biochem. Biophys.* 299, 377–380. doi: 10.1016/0003-9861(92)90290-D

Cataldo, A. M., and Nixon, R. A. (1990). Enzymatically active lysosomal proteases are associated with amyloid deposits in Alzheimer brain. *Proc. Natl. Acad. Sci. U.S.A.* 87, 3861–3865. doi: 10.1073/pnas.87.10.3861

Cataldo, A. M., Paskevich, P. A., Kominami, E., and Nixon, R. A. (1991). Lysosomal hydrolases of different classes are abnormally distributed in brains of patients with Alzheimer disease. *Proc. Natl. Acad. Sci. U.S.A.* 88, 10998–11002. doi: 10.1073/pnas.88.24.10998

Cataldo, A. M., Thayer, C. Y., Bird, E. D., Wheelock, T. R., and Nixon, R. A. (1990). Lysosomal proteinase antigens are prominently localized within senile plaques of Alzheimer's disease: evidence for a neuronal origin. *Brain Res.* 513, 181–192. doi: 10.1016/0006-8993(90)90456-L

Cavallo-Medved, D., and Sloane, B. F. (2003). Cell-surface cathepsin B: understanding its functional significance. *Curr. Top. Dev. Biol.* 54, 313–341. doi: 10.1016/S0070-2153(03)54013-3

Chai, Y. L., Chong, J. R., Weng, J., Howlett, D., Halsey, A., Lee, J. H., et al. (2019). Lysosomal cathepsin D is upregulated in Alzheimer's disease neocortex and may be a marker for neurofibrillary degeneration. *Brain Pathol.* 29, 63–74. doi: 10.1111/bpa.12631

Cotrin, S. S., Puzer, L., de Souza Judice, W. A., Juliano, L., Carmona, A. K., and Juliano, M. A. (2004). Positional-scanning combinatorial libraries of fluorescence resonance energy transfer peptides to define substrate specificity of carboxydipeptidases: assays with human cathepsin B. *Anal. Biochem.* 335, 244–252. doi: 10.1016/j.ab.2004.09.012

Delacourte, A., and Defossez, A. (1986). Alzheimer's disease: tau proteins, the promoting factors of microtubule assembly, are major components of paired helical filaments. *J. Neurol. Sci.* 76, 173–186. doi: 10.1016/0022-510X(86)90167-X

Embury, C. M., Dyavarshetty, B., Lu, Y., Wiederin, J. L., Ciborowski, P., Gendelman, H. E., et al. (2017). Cathepsin B improves ss-amyloidosis and learning and memory in models of Alzheimer's disease. *J. Neuroimmune Pharmacol.* 12, 340–352. doi: 10.1007/s11481-016-9721-6

Frosch, B. A., Berquin, I., Emmert-Buck, M. R., Moin, K., and Sloane, B. F. (1999). Molecular regulation, membrane association and secretion of tumor cathepsin B. *APMIS* 107, 28–37. doi: 10.1111/j.1699-0463.1999.tb01523.x

Gkanatsiou, E., Portelius, E., Toomey, C. E., Blennow, K., Zetterberg, H., Lashley, T., et al. (2019). A distinct brain beta amyloid signature in cerebral amyloid angiopathy compared to Alzheimer's disease. *Neurosci. Lett.* 701, 125–131. doi: 10.1016/j.neulet.2019.02.033

Glenner, G. G., and Wong, C. W. (1984). Alzheimer's disease: initial report of the purification and characterization of a novel cerebrovascular amyloid protein. *Biochem. Biophys. Res. Commun.* 120, 885–890. doi: 10.1016/S0006-291X(84)80190-4

Grundke-Iqbal, I., Iqbal, K., Tung, Y. C., Quinlan, M., Wisniewski, H. M., and Binder, L. I. (1986). Abnormal phosphorylation of the microtubule-associated protein tau (tau) in Alzheimer cytoskeletal pathology. *Proc. Natl. Acad. Sci. U.S.A.* 83, 4913–4917. doi: 10.1073/pnas.83.13.4913

Guntert, A., Dobeli, H., and Bohrmann, B. (2006). High sensitivity analysis of amyloid-beta peptide composition in amyloid deposits from human and PS2APP mouse brain. *Neuroscience* 143, 461–475. doi: 10.1016/j.neuroscience.2006.08.027

Haass, C., and Selkoe, D. J. (1993). Cellular processing of beta-amyloid precursor protein and the genesis of amyloid beta-peptide. *Cell* 75, 1039–1042. doi: 10.1016/0092-8674(93)90312-E

Hook, G., Hook, V., and Kindy, M. (2011). The cysteine protease inhibitor, E64d, reduces brain amyloid-beta and improves memory deficits in Alzheimer's disease animal models by inhibiting cathepsin B, but not BACE1, beta-secretase activity. *J. Alzheimers. Dis.* 26, 387–408. doi: 10.3233/JAD-2011-110101

Hook, G. R., Yu, J., Sipes, N., Pierschbacher, M. D., Hook, V., and Kindy, M. S. (2014). The cysteine protease cathepsin B is a key drug target and cysteine protease inhibitors are potential therapeutics for traumatic brain injury. *J. Neurotrauma* 31, 515–529. doi: 10.1089/neu.2013.2944

Hook, V., Hook, G., and Kindy, M. (2010). Pharmacogenetic features of cathepsin B inhibitors that improve memory deficit and reduce beta-amyloid related to Alzheimer's disease. *Biol. Chem.* 391, 861–872. doi: 10.1515/bc.2010.110

Hook, V., Toneff, T., Bogyo, M., Greenbaum, D., Medzihradszky, K. F., Neveu, J., et al. (2005). Inhibition of cathepsin B reduces beta-amyloid production in regulated secretory vesicles of neuronal chromaffin cells: evidence for cathepsin B as a candidate beta-secretase of Alzheimer's disease. *Biol. Chem.* 386, 931–940. doi: 10.1515/BC.2005.108

Hook, V., Yoon, M., Mosier, C., Ito, G., Podvin, S., Head, B. P., et al. (2020). Cathepsin B in neurodegeneration of Alzheimer's disease, traumatic brain injury, and related brain disorders. *Biochim. Biophys. Acta Proteins Proteom.* 1868:140428. doi: 10.1016/j.bbapap.2020.140428

Howell, S., Nalbantoglu, J., and Crine, P. (1995). Neutral endopeptidase can hydrolyze beta-amyloid(1-40) but shows no effect on beta-amyloid precursor protein metabolism. *Peptides* 16, 647–652. doi: 10.1016/0196-9781(95)00021-B

Hussain, I., Powell, D., Howlett, D. R., Tew, D. G., Meek, T. D., Chapman, C., et al. (1999). Identification of a novel aspartic protease (Asp 2) as beta-secretase. *Mol. Cell. Neurosci.* 14, 419–427. doi: 10.1006/mcne.1999.0811

Hwang, J., Estick, C. M., Ikonne, U. S., Butler, D., Pait, M. C., Elliott, L. H., et al. (2019). The role of lysosomes in a broad disease-modifying approach evaluated across transgenic mouse models of Alzheimer's disease and Parkinson's disease and Models of mild cognitive impairment. *Int. J. Mol. Sci.* 20:4432. doi: 10.3390/ijms20184432

Kidana, K., Tatebe, T., Ito, K., Hara, N., Kakita, A., Saito, T., et al. (2018). Loss of kallikrein-related peptidase 7 exacerbates amyloid pathology in Alzheimer's disease model mice. *EMBO Mol. Med.* 10:e8184. doi: 10.15252/emmm.201708184

Kindy, M. S., Yu, J., Zhu, H., El-Amouri, S. S., Hook, V., and Hook, G. R. (2012). Deletion of the cathepsin B gene improves memory deficits in a transgenic ALZHeimer's disease mouse model expressing AbetaPP containing the wild-type beta-secretase site sequence. *J. Alzheimers. Dis.* 29, 827–840. doi: 10.3233/JAD-2012-111604

Klafki, H., Abramowski, D., Swoboda, R., Paganetti, P. A., and Staufenbiel, M. (1996). The carboxyl termini of beta-amyloid peptides 1-40 and 1-42 are generated by distinct gamma-secretase activities. *J. Biol. Chem.* 271, 28655–28659. doi: 10.1074/jbc.271.45.28655

Laemmli, U. K. (1970). Cleavage of structural proteins during the assembly of the head of bacteriophage T4. *Nature* 227, 680–685. doi: 10.1038/227680a0

Lee, E. B., Skovronsky, D. M., Abtahian, F., Doms, R. W., and Lee, V. M. (2003). Secretion and intracellular generation of truncated Abeta in beta-site amyloid-beta precursor protein-cleaving enzyme expressing human neurons. *J. Biol. Chem.* 278, 4458–4466. doi: 10.1074/jbc.M210105200

Liao, M. C., Ahmed, M., Smith, S. O., and Van Nostrand, W. E. (2009). Degradation of amyloid beta protein by purified myelin basic protein. *J. Biol. Chem.* 284, 28917–28925. doi: 10.1074/jbc.M109.050856

Mach, L., Mort, J. S., and Glossl, J. (1994). Maturation of human procathepsin B. Proenzyme activation and proteolytic processing of the precursor to the mature proteinase, *in vitro*, are primarily unimolecular processes. *J Biol Chem.* 269, 13030–13035.

Mackay, E. A., Ehrhard, A., Moniatte, M., Guenet, C., Tardif, C., Tarnus, C., et al. (1997). A possible role for cathepsins D, E, and B in the processing of beta-amyloid precursor protein in Alzheimer's disease. *Eur. J. Biochem.* 244, 414–425. doi: 10.1111/j.1432-1033.1997.00414.x

Maler, J. M., Klafki, H. W., Paul, S., Spitzer, P., Groemer, T. W., Henkel, A. W., et al. (2007). Urea-based two-dimensional electrophoresis of beta-amyloid peptides in human plasma: evidence for novel Abeta species. *Proteomics* 7, 3815–3820. doi: 10.1002/pmic.200700311

Masters, C. L., Simms, G., Weinman, N. A., Multhaup, G., McDonald, B. L., and Beyreuther, K. (1985). Amyloid plaque core protein in Alzheimer disease and down syndrome. *Proc. Natl. Acad. Sci. U.S.A.* 82, 4245–4249. doi: 10.1073/pnas.82.12.4245

Mihalik, R., Imre, G., Petak, I., Szende, B., and Kopper, L. (2004). Cathepsin B-independent abrogation of cell death by CA-074-OMe upstream of lysosomal breakdown. *Cell Death Differ.* 11, 1357–1360. doi: 10.1038/sj.cdd.4401493

Miller, D. L., Papayannopoulos, I. A., Styles, J., Bobin, S. A., Lin, Y. Y., Biemann, K., et al. (1993). Peptide compositions of the cerebrovascular and senile plaque core amyloid deposits of Alzheimer's disease. *Arch. Biochem. Biophys.* 301, 41–52. doi: 10.1006/abbi.1993.1112

Montaser, M., Lalmanach, G., and Mach, L. (2002). CA-074, but not its methyl ester CA-074Me, is a selective inhibitor of cathepsin B within living cells. *Biol. Chem.* 383, 1305–1308. doi: 10.1515/BC.2002.147

Moon, H. Y., Becke, A., Berron, D., Becker, B., Sah, N., Benoni, G., et al. (2016). Running-Induced systemic cathepsin b secretion is associated with memory function. *Cell Metab.* 24, 332–340. doi: 10.1016/j.cmet.2016.05.025

Morena, F., Argentati, C., Trotta, R., Crispoltoni, L., Stabile, A., Pistilli, A., et al. (2017). A Comparison of lysosomal enzymes expression levels in peripheral blood of mild- and severe-Alzheimer's disease and MCI patients: implications for regenerative medicine approaches. *Int. J. Mol. Sci.* 18:1806. doi: 10.3390/ijms18081806

Mosmann, T. (1983). Rapid colorimetric assay for cellular growth and survival: application to proliferation and cytotoxicity assays. *J. Immunol. Methods* 65, 55–63. doi: 10.1016/0022-1759(83)90303-4

Mueller-Steiner, S., Zhou, Y., Arai, H., Roberson, E. D., Sun, B., Chen, J., et al. (2006). Antiamyloidogenic and neuroprotective functions of cathepsin B: implications for Alzheimer's disease. *Neuron* 51, 703–714. doi: 10.1016/j.neuron.2006.07.027

Murata, M., Miyashita, S., Yokoo, C., Tamai, M., Hanada, K., Hatayama, K., et al. (1991). Novel epoxysuccinyl peptides. Selective inhibitors of cathepsin B, *in vitro*. *FEBS Lett.* 280, 307–310. doi: 10.1016/0014-5793(91)80318-W

Nagele, R. G., D'Andrea, M. R., Lee, H., Venkataraman, V., and Wang, H. Y. (2003). Astrocytes accumulate A beta 42 and give rise to astrocytic amyloid plaques in Alzheimer disease brains. *Brain Res.* 971, 197–209. doi: 10.1016/S0006-8993(03)02361-8

Nakamura, Y., Takeda, M., Suzuki, H., Hattori, H., Tada, K., Hariguchi, S., et al. (1991). Abnormal distribution of cathepsins in the brain of patients with Alzheimer's disease. *Neurosci. Lett.* 130, 195–198. doi: 10.1016/0304-3940(91)90395-A

Oberstein, T. J., Spitzer, P., Klafki, H. W., Linning, P., Neff, F., Knolker, H. J., et al. (2015). Astrocytes and microglia but not neurons preferentially generate N-terminally truncated abeta peptides. *Neurobiol. Dis.* 73, 24–35. doi: 10.1016/j.nbd.2014.08.031

Pike, C. J., Overman, M. J., and Cotman, C. W. (1995). Amino-terminal deletions enhance aggregation of beta-amyloid peptides *in vitro*. *J. Biol. Chem.* 270, 23895–23898. doi: 10.1074/jbc.270.41.23895

Qiu, W. Q., Walsh, D. M., Ye, Z., Vekrellis, K., Zhang, J., Podlisny, M. B., et al. (1998). Insulin-degrading enzyme regulates extracellular levels of amyloid beta-protein by degradation. *J. Biol. Chem.* 273, 32730–32738. doi: 10.1074/jbc.273.49.32730

Rohan de Silva, H. A., Jen, A., Wickenden, C., Jen, L. S., Wilkinson, S. L., and Patel, A. J. (1997). Cell-specific expression of beta-amyloid precursor protein isoform mRNAs and proteins in neurons and astrocytes. *Brain Res. Mol. Brain Res.* 47, 147–156. doi: 10.1016/S0169-328X(97)00045-4

Saido, T. C. (1998). Alzheimer's disease as proteolytic disorders: anabolism and catabolism of beta-amyloid. *Neurobiol. Aging* 19, S69–75. doi: 10.1016/S0197-4580(98)00033-5

Saido, T. C., Iwatsubo, T., Mann, D. M., Shimada, H., Ihara, Y., and Kawashima, S. (1995). Dominant and differential deposition of distinct beta-amyloid peptide species, A beta N3(pE), in senile plaques. *Neuron* 14, 457–466. doi: 10.1016/0896-6273(95)90301-1

Saido, T. C., Yamao-Harigaya, W., Iwatsubo, T., and Kawashima, S. (1996). Amino- and carboxyl-terminal heterogeneity of beta-amyloid peptides deposited in human brain. *Neurosci. Lett.* 215, 173–176. doi: 10.1016/0304-3940(96)12970-0

Savastano, A., Klafki, H., Haussmann, U., Oberstein, T. J., Muller, P., Wirths, O., et al. (2016). N-truncated Abeta2-X starting with position two in sporadic Alzheimer's disease cases and two Alzheimer mouse models. *J. Alzheimers. Dis.* 49, 101–110. doi: 10.3233/JAD-150394

Schechter, I., and Ziv, E. (2011). Cathepsins S, B and L with aminopeptidases display beta-secretase activity associated with the pathogenesis of Alzheimer's disease. *Biol. Chem.* 392, 555–569. doi: 10.1515/bc.2011.054

Schieb, H., Kratzin, H., Jahn, O., Mobius, W., Rabe, S., Staufenbiel, M., et al. (2011). Beta-amyloid peptide variants in brains and cerebrospinal fluid from amyloid precursor protein (APP) transgenic mice: comparison with human Alzheimer amyloid. *J. Biol. Chem.* 286, 33747–33758. doi: 10.1074/jbc.M111.246561

Schonherr, C., Bien, J., Isbert, S., Wichert, R., Prox, J., Altmeppen, H., et al. (2016). Generation of aggregation prone N-terminally truncated amyloid beta peptides by meprin beta depends on the sequence specificity at the cleavage site. *Mol. Neurodegener.* 11:19. doi: 10.1186/s13024-016-0084-5

Selkoe, D. J. (1998). The cell biology of beta-amyloid precursor protein and presenilin in Alzheimer's disease. *Trends Cell Biol.* 8, 447–453. doi: 10.1016/S0962-8924(98)01363-4

Selkoe, D. J. (2001). Alzheimer's disease results from the cerebral accumulation and cytotoxicity of amyloid beta-protein. *J. Alzheimers Dis.* 3, 75–80. doi: 10.3233/JAD-2001-3111

Sevalle, J., Amoyel, A., Robert, P., Fournie-Zaluski, M. C., Roques, B., and Checler, F. (2009). Aminopeptidase A contributes to the N-terminal truncation of amyloid beta-peptide. *J. Neurochem.* 109, 248–256. doi: 10.1111/j.1471-4159.2009.05950.x

Smith, P. K., Krohn, R. I., Hermanson, G. T., Mallia, A. K., Gartner, F. H., Provenzano, M. D., et al. (1985). Measurement of protein using bicinchoninic acid. *Anal. Biochem.* 150, 76–85. doi: 10.1016/0003-2697(85)90442-7. Erratum in: Anal. Biochem. (1987) 163:279.

Sun, B., Zhou, Y., Halabisky, B., Lo, I., Cho, S. H., Mueller-Steiner, S., et al. (2008). Cystatin C-cathepsin B axis regulates amyloid beta levels and associated neuronal deficits in an animal model of Alzheimer's disease. *Neuron* 60, 247–257. doi: 10.1016/j.neuron.2008.10.001

Sundelof, J., Sundstrom, J., Hansson, O., Eriksdotter-Jonhagen, M., Giedraitis, V., Larsson, A., et al. (2010). Higher cathepsin B levels in plasma in Alzheimer's disease compared to healthy controls. *J. Alzheimers. Dis.* 22, 1223–1230. doi: 10.3233/JAD-2010-101023

Taralp, A., Kaplan, H., Sytwu, I. I., Vlattas, I., Bohacek, R., Knap, A. K., et al. (1995). Characterization of the S3 subsite specificity of cathepsin B. *J. Biol. Chem.* 270, 18036–18043. doi: 10.1074/jbc.270.30.18036

Thal, D. R., Capetillo-Zarate, E., Del Tredici, K., and Braak, H. (2006). The development of amyloid beta protein deposits in the aged brain. *Sci Aging Knowledge Environ.* 2006:re1. doi: 10.1126/sageke.2006.6.re1

Van Nostrand, W. E., and Porter, M. (1999). Plasmin cleavage of the amyloid beta-protein: alteration of secondary structure and stimulation of tissue plasminogen activator activity. *Biochemistry* 38, 11570–11576. doi: 10.1021/bi990610f

Vassar, R., Bennett, B. D., Babu-Khan, S., Kahn, S., Mendiaz, E. A., Denis, P., et al. (1999). Beta-secretase cleavage of Alzheimer's amyloid precursor

protein by the transmembrane aspartic protease BACE. *Science* 286, 735–741. doi: 10.1126/science.286.5440.735

Walter, S., Jumpertz, T., Huttenrauch, M., Ogorek, I., Gerber, H., Storck, S. E., et al. (2019). The metalloprotease ADAMTS4 generates N-truncated Abeta4-x species and marks oligodendrocytes as a source of amyloidogenic peptides in Alzheimer's disease. *Acta Neuropathol.* 137, 239–257. doi: 10.1007/s00401-018-1929-5

Wang, C., Sun, B., Zhou, Y., Grubb, A., and Gan, L. (2012). Cathepsin B degrades amyloid-beta in mice expressing wild-type human amyloid precursor protein. *J. Biol. Chem.* 287, 39834–39841. doi: 10.1074/jbc.M112.371641

Wang, R., Sweeney, D., Gandy, S. E., and Sisodia, S. S. (1996). The profile of soluble amyloid beta protein in cultured cell media. Detection and quantification of amyloid beta protein and variants by immunoprecipitation-mass spectrometry. *J. Biol. Chem.* 271, 31894–31902. doi: 10.1074/jbc.271.50.31894

Wildburger, N. C., Esparza, T. J., LeDuc, R. D., Fellers, R. T., Thomas, P. M., Cairns, N. J., et al. (2017). Diversity of amyloid-beta proteoforms in the Alzheimer's disease brain. *Sci. Rep.* 7:9520. doi: 10.1038/s41598-017-10422-x

Wiltfang, J., Esselmann, H., Cupers, P., Neumann, M., Kretzschmar, H., Beyermann, M., et al. (2001). Elevation of beta-amyloid peptide 2-42 in sporadic and familial Alzheimer's disease and its generation in PS1 knockout cells. *J. Biol. Chem.* 276, 42645–42657. doi: 10.1074/jbc.M102790200

Xu, Y., Wang, J., Song, X., Wei, R., He, F., Peng, G., et al. (2016). Protective mechanisms of CA074-me (other than cathepsin-B inhibition) against programmed necrosis induced by global cerebral ischemia/reperfusion injury in rats. *Brain Res. Bull.* 120, 97–105. doi: 10.1016/j.brainresbull.2015.11.007

Yan, S., and Sloane, B. F. (2003). Molecular regulation of human cathepsin B: implication in pathologies. *Biol. Chem.* 384, 845–854. doi: 10.1515/BC.2003.095

Zampar, S., Klafki, H. W., Sritharen, K., Bayer, T. A., Wiltfang, J., Rostagno, A., et al. (2020). N-terminal heterogeneity of parenchymal and vascular amyloid-beta deposits in Alzheimer's disease. *Neuropathol. Appl. Neurobiol.* 46, 673–685. doi: 10.1111/nan.12637

Conflict of Interest: The authors declare that the research was conducted in the absence of any commercial or financial relationships that could be construed as a potential conflict of interest.

frontiers in Molecular Neuroscience

ORIGINAL RESEARCH
published: 15 January 2021
doi: 10.3389/fnmol.2020.613421

The Molecular Mechanism of Chronic High-Dose Corticosterone-Induced Aggravation of Cognitive Impairment in APP/PS1 Transgenic Mice

*Shen-Qing Zhang†, Long-Long Cao†, Yun-Yue Liang and Pu Wang**

College of Life and Health Sciences, Northeastern University, Shenyang, China

Clinical studies have found that some Alzheimer's disease (AD) patients suffer from Cushing's syndrome (CS). CS is caused by the long-term release of excess glucocorticoids (GCs) from the adrenal gland, which in turn, impair brain function and induce dementia. Thus, we investigated the mechanism of the effect of corticosterone (CORT) on the development and progression of AD in a preclinical model. Specifically, the plasma CORT levels of 9-month-old APP/PS1 Tg mice were abnormally increased, suggesting an association between GCs and AD. Long-term administration of CORT accelerated cognitive dysfunction by increasing the production and deposition of β-amyloid (Aβ). The mechanism of action of CORT treatment involved stimulation of the expression of BACE-1 and presenilin (PS) 1 in *in vitro* and *in vivo*. This observation was confirmed in mice with adrenalectomy (ADX), which had lower levels of GCs. Moreover, the glucocorticoid receptor (GR) mediated the effects of CORT on the stimulation of the expression of BACE-1 and PS1 *via* the PKA and CREB pathways in neuroblastoma N2a cells. In addition to these mechanisms, CORT can induce a cognitive decline in APP/PS1 Tg mice by inducing apoptosis and decreasing the differentiation of neurons.

Keywords: Alzheimer's disease, corticosterone, glucocorticoid receptor, BACE-1, CREB, apoptosis, neuronal differentiation

OPEN ACCESS

Edited by:
Daniela Puzzo,
University of Catania, Italy

Reviewed by:
Utpal Das,
University of California, San Diego, United States
Mario Buffelli,
University of Verona, Italy

***Correspondence:**
Pu Wang
wangpu@mail.neu.edu.cn

†These authors have contributed equally to this work

Received: *02 October 2020*
Accepted: *17 December 2020*
Published: *15 January 2021*

Citation:
Zhang S-Q, Cao L-L, Liang Y-Y and Wang P (2021) The Molecular Mechanism of Chronic High-Dose Corticosterone-Induced Aggravation of Cognitive Impairment in APP/PS1 Transgenic Mice. Front. Mol. Neurosci. 13:613421. doi: 10.3389/fnmol.2020.613421

INTRODUCTION

Clinical studies have found that Alzheimer's disease (AD) patients usually suffer from corticosteronism, which is characterized by the secretion of high levels of glucocorticoids (GCs) from the adrenal cortex (Guldiken and Guldiken, 2008; Haraguchi et al., 2016). In an A mouse model of an anxiety/depression-like state, long-term exposure to GCs results in structural changes in the brain, similar to those observed in aging (David et al., 2009; Herbert and Lucassen, 2016). In detail, the long-term administration of GCs can impair specific cognitive regions, such as the neocortex and hippocampus (Starkman et al., 2001). When the cortisol dropped to the basal level, the size of the hippocampus will be enlarged accompanied by improving the learning ability (Starkman et al., 2001, 2003). Reciprocally, chronic high levels of GC lead to a decrease in the volume of the hippocampus, which results in impairing cognitive ability (Starkman et al., 1992; Sheline et al., 1996; Bettio et al., 2017). More closely, patients with high levels of GC show long-term

impairment of memory and concentration (Ragnarsson et al., 2012). Based on these prior works, GCs potentially contribute to accelerating the progression of AD.

The production of GCs is tightly regulated under physiological conditions to avoid pathological effects. GCs is a self-regulating molecule in the endocrine system and is responsible for modulating stress reaction. GCs are synthesized and secreted by the fascicular zone of the adrenal cortex. GCs can be classified into two categories, hydrocortisone (HC) and cortisone, the synthesis and secretion of which are regulated by the hypothalamic-pituitary-adrenal (HPA) axis (Turnbull and Rivier, 1999). In detail, the nucleus of the paraventricular hypothalamus releases corticotropin-releasing factor (CRF), which promotes the secretion of adrenocorticotropic hormone (ACTH) by acting on the anterior pituitary, leading to the synthesis of GCs by the fascicular zone of the posterior adrenal cortex (Curran and Chalasani, 2012). GCs is primarily synthesized and secreted from the adrenal cortex and penetrates the blood-brain barrier (BBB) to function in the central nervous system (CNS).

The physiological and pharmacological functions of GCs are mediated by the intracellular glucocorticoid receptor (GR), which belongs to the family of nuclear receptors. Thus, the GR can promote or inhibit the transcription of target genes by directly binding to the glucocorticoid response element (GRE) or interacting with other transcription factors (Ratman et al., 2013; Meijer et al., 2018). Mineralocorticoid receptors (MR) have higher GCs binding activity than the GR (Richardson et al., 2016; Faught and Vijayan, 2019). Under resting conditions, the level of GCs is relatively low and GCs mainly bind to MR. When the level of GCs is elevated under pathological conditions, GCs bind to and activate the GR to induce biological effects (Brinks et al., 2007). In AD patients, GR-expressing neurons undergo progressive atrophy and loss, resulting in a decrease in the expression of the GR, leading to the excessive loading of GCs by disrupting the negative feedback of the GR on the HPA axis that regulates GCs synthesis (Sapolsky et al., 1986; Jacobson and Sapolsky, 1991). Also, overexpression of the GR in male C57BL/6L mice accelerates the aging phenotype, including neuroendocrine dysregulation and deficit in cognitive function (Wei et al., 2007). Specifically, blocking the GR for only 3 days in 12-month-old APP/PS1 Tg mice reduced the production of $A\beta_{1-40}$ and $A\beta_{1-42}$ in the hippocampus, resulting in the rescue of cognitive deficit (Lesuis et al., 2018). These observations were confirmed by reports that showed that treatment with a GR antagonist (mifepristone) completely reversed synaptic deficits and hippocampal apoptosis and partially reversed cognitive deficit, which are effects of the hippocampal amyloidogenic pathway and neuroinflammation (Pineau et al., 2016). Also, selective GR modulators can reverse hippocampal Aβ generation, neuroinflammation, and apoptosis; restore the hippocampal levels of synaptic markers; and improve cognitive function (Pineau et al., 2016).

GCs have certain GR-independent effects on the regulation of AD development. For instance, administration of stress-level GCs increases the formation of Aβ by increasing the steady-state levels of amyloid precursor protein (APP) and β-APP-cleaving enzyme (BACE-1) in APP/PS1/tau^{P301L} Tg mice (Green et al., 2006). This process is mediated by lipid raft-dependent CREB activation (Choi et al., 2017). Additionally, GCs considerably reduce the degradation and clearance of Aβ by astrocytes, inducing a decrease in the neuroprotective ability of astrocytes (Wang et al., 2011). GCs act *via* these mechanisms to impair learning and memory by inducing apoptosis of neurons (Li et al., 2010).

Based on these considerations, we aimed to examine the multiple roles of GCs in the production and deposition of Aβ, neuronal apoptosis, and neuronal differentiation. The results demonstrate that GCs significantly increase the production of Aβ by enhancing the expression of BACE-1 and PS1. Moreover, GCs induce neuronal apoptosis by reducing the ratio of Bcl-2 and Bax and inhibiting neuronal differentiation. These effects eventually induce a cognitive decline in APP/PS1 Tg mice.

MATERIALS AND METHODS

Reagents

Corticosterone (CORT) was obtained from Solarbio Life Sciences (Beijing, China). A PKA inhibitor, H89; an antibody specific for Aβ (A8354, mouse, dilution 1:100 for immunohistochemistry, IHC); and secondary antibodies were purchased from Sigma–Aldrich (St. Louis, MO, USA). Antibodies against APP (ab241592, rabbit, 1:2,000 for Western blot analysis), BACE1 (ab2077, rabbit, 1:2,000 for Western blot analysis; 1:100 for IHC and immunofluorescence, IF) and NeuN (ab104224, mouse, 1:100 for IF) were obtained from Abcam (Cambridge, MA, USA). Fluorescence-tagged secondary antibodies (A32727 mouse, A32732 rabbit, A11034 rabbit, A11029 mouse, 1:500 for IF) were purchased from Thermo Fisher Scientific (Waltham, MA, USA). Other antibodies, including ADAM10 (#14194, rabbit, 1:2,000 for Western blot analysis), PS1 (#5643, rabbit, 1:2,000 for Western blot analysis; 1:100 for IHC and IF), PS2 (#2192, rabbit, 1:2,000 for Western blot analysis), PEN2 (#5451, rabbit, 1:2,000 for Western blot analysis), nicastrin (#5665, rabbit, 1:2,000 for Western blot analysis), GR (#3660, rabbit, 1:2,000 for Western blot analysis; 1:100 for IF), CREB (#4820, rabbit, 1:2,000 for Western blot analysis), p-CREB (#9196, mouse, 1:2,000 for Western blot analysis), Bcl-2 (#3498, rabbit, 1:2,000 for Western blot analysis), Bax (#2774, rabbit, 1:2,000 for Western blot analysis), doublecortin (#14802, rabbit, 1:100 for IHC) and β-actin (#3700, mouse, 1:5,000 for Western blot analysis), were from Cell Signaling Technology (Danvers, MA, USA). All reagents for the sodium dodecyl sulfate-polyacrylamide gel electrophoresis (SDS–PAGE) experiments were purchased from Bio-Rad Laboratories (Hercules, CA, USA). All other reagents were from Thermo Fisher Scientific/Invitrogen (Waltham, MA, USA) unless specified otherwise.

Cell Culture and Treatment

Neuroblastoma N2a cells were cultured in DMEM with 10% FBS in a 37°C cell incubator containing 5% CO_2. Before treatment with corticosterone (CORT) or H89, the cells were cultured in a serum-free medium for 12 h. After changing the

serum-free medium, 1 μM CORT or 10 μM H89 was added to the fresh medium. After 24 h, the cells were lysed to extract protein or RNA.

Plasmid Construction

The primers for gRNA generation were synthesized by Genewiz, Inc. (Suzhou, Jiangsu, China). The sequences of the primers were as follows: NR3C1-1 forward, 5′-CACCGGCTTTGGAT AAATCTGGCTG-3′; reverse, 5′-AAACCAGCCAGATTTATC CAAAGCC-3′; NR3C1-2 forward, 5′-CACCGGGATCATCTTC TCCCGCCAA-3′; reverse, 5′-AAACTTGGCGGGAGAAGATG ATCCC-3′; and NR3C1-3 forward, 5′-CACCGCCAGCAGTT TGCTTGGCCGG-3′; reverse, 5′-AAACCCGGCCAAGCAAAC TGCTGGC-3′. The paired forward and reverse primers were annealed in NE buffer 2.1 (New England Biolabs, Beverly, MA, USA). LentiCRISPR V2 plasmid (Addgene, Cambridge, MA, USA) was linearized by incubation at 37°C with BsmBI restriction enzymes for 2 h. The annealed primers were used as insertion fragments, which were then inserted into the linearized LentiCRISPR v2 plasmid by incubating with T4 ligase at 16°C for 2 h. The constructed plasmids were transferred to Stbl3 competent cells for amplification and subsequent Sanger sequencing.

Transfection

LentiCRISPR v2 plasmids (6 μg) encoding gRNA of NR3C1 were cotransfected with 5 μg of psPAX2 and 3 μg of pMD2.G into HEK293T cells using Neofect (Neofect Biotech Company Limited, Beijing, China) transfecting reagent. The medium was replaced after 12 h. The virus was collected after 48 and 72 h of transfection by centrifugation at 8×10^4 rpm. The N2a cells were then infected with the virus in the presence of 10 μg/ml polybrene (Merck Millipore, Billerica, MA, USA). After 48 h, the cells were selected in the presence of 3 μg/ml puromycin to establish NR3C1 knockdown cells.

Animals and Treatment

APP/PS1 Tg mice were obtained from Jackson Laboratory (Bar Harbor, ME, USA). C57BL/6J mice were purchased from the Liaoning Changsheng Biotechnology Company Limited (Benxi, Liaoning, China). All mice were housed under the same conditions at standard room temperature and humidity in a light and dark cycle-controlled environment. To ensure that mice could freely move, eat, and drink, three to five mice were housed per cage. APP/PS1 Tg mice were used as a model for the AD study. The WT or APP/PS1 Tg mice at the age of 5 months were subcutaneously administered with CORT (10 mg/kg/day) for 3 months before assessment of their memory and physiological and biochemical parameters; the timeline and group sorting are shown in **Figures 1A,B**.

Adrenalectomy

The WT or APP/PS1 Tg mice were fasted overnight before surgery and anesthetized by tribromoethanol (Sigma–Aldrich, Beijing, China). Mice were fixed in a prone position, and the long hair from the middle of the back was removed. A 1.5 cm midline incision was made, and muscle was exfoliated layer by layer from the outside to the inside until the organs were visible. The spherical adrenal tissue around the kidney was identified and gently removed with scissors, which was then placed back in the body before closing the wound. The other side of the adrenal gland was removed using the same method. The sham operation group only received an incision, and the skin was sutured. From the 3rd day after adrenalectomy (ADX) surgery, intraperitoneal injection of CORT (10 mg/kg/day) was performed for 7 days. Then, tribromoethanol was used for anesthesia, and the animals were sacrificed to collect the cerebral cortex and hippocampus.

qRT-PCR

Total RNA was extracted by RNA isolator total RNA extraction reagent (Nanjing Vazyme Medical Technology Company Limited, Nanjing, Jiangsu, China). Purified RNA was reverse-transcribed into cDNA by a reverse transcription kit (Promega, Madison, WI, USA). qRT-PCR was performed according to the instructions of the qRT-PCR kit (Promega, Madison, WI, USA). The primer sequences for qRT-PCR were as follows: ADAM10 forward, 5′-CTCAAGCTTCGAAT TCATGGTG TTGCCGACAGTGTT-3′, reverse, 5′-GCGACCGGTGGATC CTTGCGTCGCATGTGTCCCAT-3′; BACE1 forward, 5′-CT CAAGCTTCGAATTCCAAGGCCCGGGCTCACTATG-3′, reverse, 5′-GGCGACCGGTGGATCCGCCTTGAGCAGGGA GATGTCATCA-3′ PS1 forward, 5′-CTCAAGCTTCGAATTC CTCCAATGACAGAGATACCTG-3′, reverse, 5′-GGCGACCG GTGGATCCGCGATATAAAACTGATGGAATG-3′; GAPDH forward, 5′-TGCAGTGGCAAAGTGGAGAT-3′, reverse, 5′-TT TGCCGTGAGTGGAGTCATA-3′. GAPDH was used as a housekeeping reference gene. The ratio was calculated as the following equation:

$$\text{Ratio} = \frac{2^{\Delta Ct(\text{Gene}_{\text{wt}} - \text{Gene}_{\text{Tg}})}}{2^{\Delta Ct(\text{GAPDH}_{\text{wt}} - \text{GAPDH}_{\text{Tg}})}}$$

The WT was always set to 1, and the value of the Tg mice was obtained from the previous equation.

Western Blots

Cells or tissues of the cerebral cortex and hippocampus were homogenized and lysed on ice in RIPA buffer [25 mM Tris-HCl (Ph 7.6), 150 mM NaCl, 1% NP-40, 1% sodium deoxycholate, and 0.1% SDS], containing protease inhibitor cocktail (Thermo Scientific-Pierce, Rockford, IL, USA). The supernatant was collected after centrifugation at 13,000 *g*. The concentration of protein in the supernatant was determined by a BCA kit (Beyotime Biotechnology, Shanghai, China). Protein (2 μg/μl) was loaded onto SDS–PAGE gels and, following SDS–PAGE, was transferred to a PVDF membrane. The membranes were incubated with a primary antibody at 4°C overnight. The membranes were washed with TBST five times for 5 min each time. Then, the corresponding secondary antibody was added to the membranes and incubated at room temperature for 2 h. The membranes were probed with an antibody, and the bands were visualized by an ECL kit (Thermo Fisher Scientific, Waltham, MA, USA). β-Actin was used as an internal reference control.

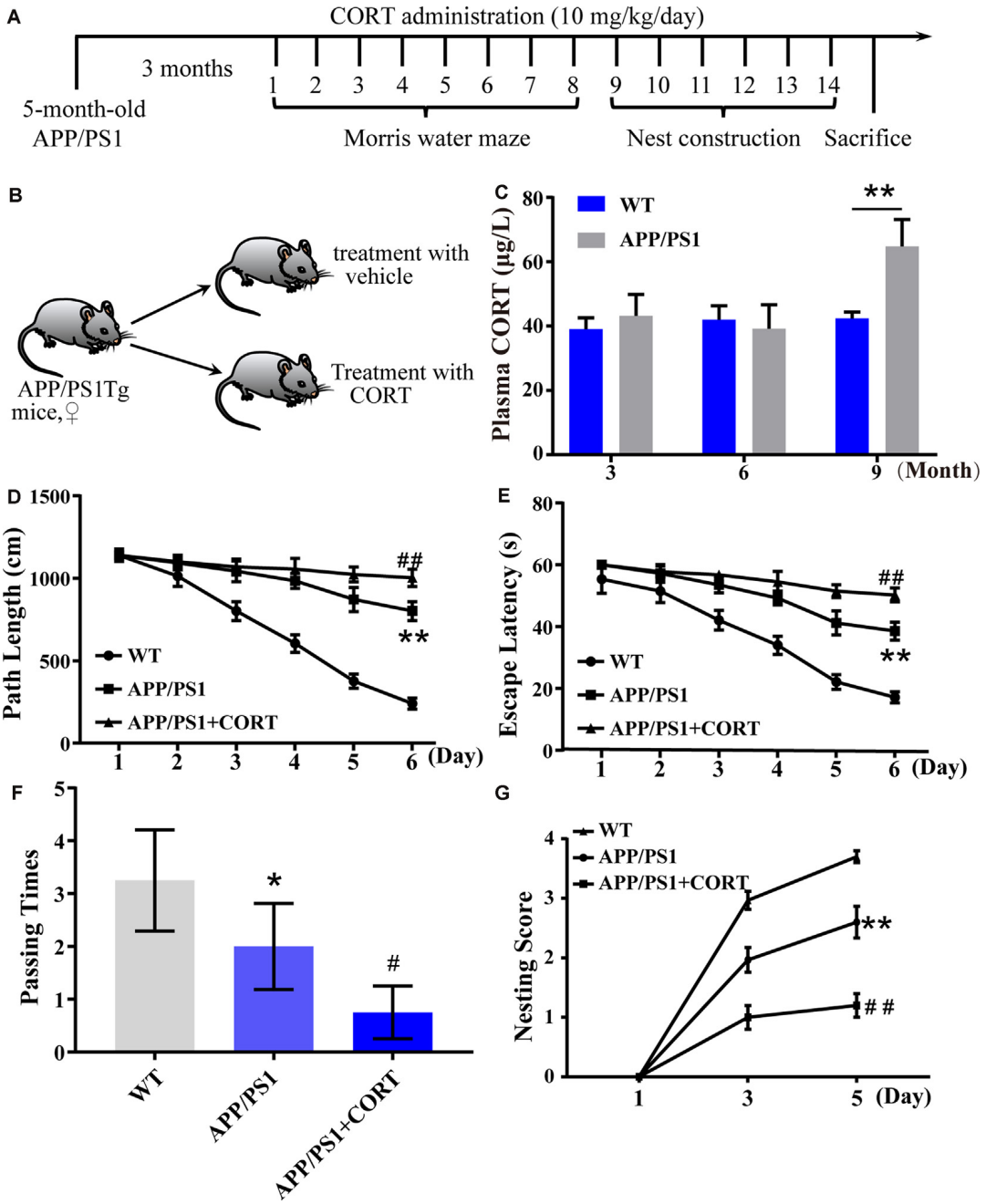

FIGURE 1 | Elevated plasma levels of corticosterone (CORT) result in impaired learning in APP/PS1 Tg mice. **(A)** Timeline of the treatment of APP/PS1 Tg mice with CORT. **(B)** Schematic diagram of the random grouping and treatment of mice. **(C)** Plasma was collected from 3-, 6- and 9-month-old APP/PS1 Tg and age-matched WT mice. The content of CORT was determined by enzyme-linked immunosorbent assay (ELISA). The data were analyzed by repeated-measures ANOVA ($n = 6$). **(D,E)** APP/PS1 Tg mice (5-month-old) were intraperitoneally injected with CORT (10 mg/kg/day) for 3 months. **(D,E)** The escape distance and latency of mice were observed in the hidden platform experiment. **(F)** In the space exploration experiment, the crossing times to the original platform were recorded by the software. The data were analyzed by repeated-measures ANOVA ($n = 6$). **(G)** The nesting score of various groups of mice was analyzed by the nest construction assay. The data were analyzed by a nonparametric statistical test. The data are presented as the mean ± SE of independent experiments ($n = 6$). $^{*}p < 0.05$; $^{**}p < 0.01$ compared with the WT mice. $^{\#}p < 0.05$; $^{\#\#}p < 0.01$ compared with vehicle-treated APP/PS1 Tg mice.

Immunohistochemistry (IHC)

The brains of WT or APP/PS1 Tg mice were fixed with 4% paraformaldehyde and dehydrated in a 30% sucrose solution. Sections (30 μm thickness) were prepared by a push slicer (Leica, Wetzlar, Germany). The slides were submerged in 3% hydrogen peroxide, to eliminate endogenous peroxidase activity. The sections were stained with antibodies specific for Aβ, BACE1, PS1, or doublecortin at 4°C overnight. A biotin-conjugated

secondary antibody was then incubated with the sections for 30 min at room temperature after rinsing three times with PBS. The sections were then stained using a DAB solution [7 mg DAB + 50 ml Tris-HCl (pH 7.6) + 12 μl H_2O_2]. Before mounting, the slides were dehydrated with graded ethanol and were washed with xylene for 20 min. Finally, the sections were observed and imaged under an optical microscope (Leica, Wetzlar, Germany) using a 10× or 20× objective lens.

Immunofluorescence

The cells or cerebral cortex and hippocampus tissue samples were fixed with 4% paraformaldehyde, permeabilized with 50 μg/ml digitonin for 10 min, and washed with PBS three times. The slides were blocked with 4% goat serum and incubated with a primary antibody specific to NeuN or GR at 4°C overnight. Then, the sections were incubated with Alexa 555-anti-rabbit IgG (1:500), Alexa 488-anti-rabbit IgG (1:500), and DAPI (1:1,000) for 1 h at room temperature. After rinsing, the sections were mounted using a fluorescent mounting reagent (Beyotime Biotechnology, Shanghai, China). The sections were visualized and imaged under a confocal microscope (Leica, Wetzlar, Germany) equipped with a 40× or 63× oil-immersion objective lens.

Enzyme-Linked Immunosorbent Assay (ELISA)

The production of $A\beta_{1-42}$ was determined by enzyme-linked immunosorbent assay (ELISA) kits (Thermo Fisher Scientific, Waltham, MA, USA). In brief, 50 μl of the standard curve storage solution and the sample solution were added to 96-well plates. Then, an $A\beta_{1-42}$ antibody was added to the plate. After rinsing with wash buffer, the HRP-conjugated secondary antibody was incubated with the samples. After another rinse, the stabilized chromogen TMB was added to the plate for 30 min before measurement at 450 nm in a microplate reader.

CORT was assayed by ELISA kits (Wuhan Enzyme Immuno-Biotechnology Company Limited, Wuhan, Hubei, China) according to the manufacturer's protocol. Briefly, 50 μl of the standard curve storage solution and the sample solution were added to 96-well plates. Enzyme-labeled reagent (50 μl) was added to the plates, which were incubated at 37°C for 30 min. After washing, 50 μl of developer A and developer B were added to the wells. After a 10 min incubation at 37°C, 50 μl stop solution was added to the wells before determination of the optical density of the CORT signal at 450 nm in a microplate reader.

Morris-Maze Test

APP/PS1 Tg mice at the age of 5 months were treated with CORT (10 mg/kg/day) for 3 months. The Morris maze test was used to determine spatial learning and memory. In brief, mice were placed into a 1.6 m diameter pool, which had labeled quadrants, I, II, III, and IV. Milk was added to the pool, and the water was then heated to 25 ± 2°C. In the first 2 days, the platform was set 1–2 cm above the water level in quadrant II. The time and distance required for mice to find the platform was recorded for 60 s. If a mouse was unable to find the platform in 60 s, the mouse was guided to the platform or placed on the platform and kept on the platform for an additional 10 s. Starting from day 3, the platform was submerged under the water. The time and distance required for mice to find the platform was recorded in the following 4 days. On day 7, the platform was removed, and the number of crosses to the original location of the platform was recorded for 60 s. The experimental timeline is shown in **Figure 1A**.

Nest Construction

After the Morris water maze test, each mouse was housed in a separate cage. Ten pieces of five 5 cm^2 filter paper were placed in the cage. Each mouse was imaged for 6 days at the same time every day. The specific evaluation rules were as follows: 0, no nesting behavior of mice and no tearing or moving of paper; 1, no obvious nesting behavior in mice, and only slight tearing and moving of paper; 2, no nesting behavior in mice, and obvious tearing and moving of paper; 3, nesting behavior in mice, and most of the paper was torn into wicker shapes; and 4, obvious nesting behavior in mice, and all the paper was torn and moved to a corner. Finally, the mice were anesthetized and sacrificed using tribromoethanol to collect the cerebral cortex and hippocampus.

Statistical Analysis

All data are presented as the mean ± SE, of at least three independent experiments. Data from the Morris water maze test and detection of CORT in plasma were analyzed using repeated-measures ANOVA. The paired *t*-test was used to analyze the nest construction data. Statistical significance of the differences between means was determined using Student's *t*-test or one-way analysis of variance when appropriate.

RESULTS

The Levels of CORT Are Elevated in the Plasma of APP/PS1 Tg Mice

In patients with sporadic AD, the plasma level of cortisol is increased in the early and late stages of the disease (Umegaki et al., 2000). The secretion of GCs is regulated by the HPA axis (Turnbull and Rivier, 1999). However, it is not known whether HPA axis dysfunction is the initial cause of AD. To detect whether the basic level of GCs is changed in AD animal models and whether the metabolic pathway of amyloid can change the production of GCs, the plasma CORT level of APP/PS1 Tg mice of various ages was detected. According to the data provided by Jackson Laboratory, APP/PS1 Tg mice express chimeric Mo/HuAPP695swe and mutant PS1-dE9 genes, Aβ is deposited in the brain of 6-month-old mice. Based on this information, plasma samples of wild-type (WT) and Tg mice were collected to determine the levels of CORT at the ages of 3, 6, and 9 months. The results demonstrated that the plasma levels in 3- and 6-month-old APP/PS1 animals were not significantly different from those of WT mice. In contrast, the plasma levels of 9-month-old APP/PS1 Tg mice were higher than those of the corresponding WT controls (**Figure 1C**). This observation suggests that enhanced production of GCs is associated with amyloidosis.

CORT Exposure Accelerates the Cognitive Decline of APP/PS1 Tg Mice

To determine whether CORT can promote the pathological process in AD model mice, 5-month-old APP/PS1 Tg mice were intraperitoneally injected with CORT at a dose of 10 mg/kg/day for 3 months. The Morris maze test was performed to determine the learning and memory ability of mice. The results showed that mice treated with GCs take more time and travel a longer distance to find the hidden platform compared to untreated APP/PS1 Tg mice (**Figures 1D,E**). In the space exploration experiment, the crossing times of GCs-treated mice were considerably lower than those of vehicle-treated controls (**Figure 1F**), suggesting that GCs impairs the leaning ability of APP/PS1 Tg mice.

The nest-building test is an experimental method to assess the social ability of mice. The results can reflect the instinctive learning and social ability of mice based on biting paper and constructing a nest. In the nesting experiment, the nesting ability of mice treated with CORT for 3 months was significantly decreased compared with that of vehicle-treated controls (**Figure 1G**). In conclusion, CORT can accelerate the decline in learning and memory ability in mice, suggesting that a high level of GCs can accelerate the occurrence and development of AD *in vivo*.

CORT Treatment Enhances the Deposition of Aβ in the Brain of APP/PS1 Tg Mice

According to Aβ theory, abnormal production and deposition of Aβ in the APs of the cerebral cortex and hippocampus is the key cause of the onset of AD (O'Brien and Wong, 2011). Thus, the effects of CORT on the production and deposition of Aβ in APP/PS1 Tg mice were assessed. APP/PS1 Tg mice (5-month-old) were intraperitoneally injected with CORT at a dose of 10 mg/kg/day for 3 months. The formation of APs was determined by IHC in CORT-treated APP/PS1 Tg mice. The results showed that the number of APs in the cerebral cortex and hippocampus of APP/PS1 Tg mice was increased by CORT treatment compared to that in vehicle-treated controls (**Figures 2A,B**). The plasma concentration of CORT was determined by ELISA, and the results showed that treatment with a high dose of CORT elevated the plasma levels of CORT in APP/PS1 Tg mice (**Figure 2C**). Moreover, the production of $A\beta_{1-42}$ was determined by ELISA. The results showed that the production of $A\beta_{1-42}$ in the cerebral cortex and hippocampus of APP/PS1 Tg mice was stimulated by long-term administration of CORT (**Figure 2D**). Therefore, these results demonstrate that GCs can enhance the production and deposition of Aβ in APP/PS1 Tg mice.

CORT Increases the Production of Aβ by Enhancing the Expression of BACE-1 and PS1

In the amyloid metabolic pathway, APP is sequentially cleaved by β- and γ-secretases to produce Aβ (O'Brien and Wong, 2011). To determine the mechanisms of Aβ production, the effects of CORT on the expression of α-, β- and γ-secretases was estimated. The results showed that CORT (1 μM) treatment increases the expression of the BACE1 and PS1 proteins in N2a cells (**Figures 3A,B**). In agreement with the results of the Western blot analysis, qRT-PCR data showed that CORT treatment upregulated the expression of BACE1 and PS1 mRNA in N2a cells (**Figure 3C**). The immunofluorescent imaging results confirmed the upregulation of BACE1 and PS1 in N2a cells (**Figures 3D,E**). Considering the *in vitro* observations, the ability of GCs to upregulate the expression of BACE1 and PS1 *in vivo* was tested. According to Western blot analysis, CORT treatment increased the expression of the BACE1, PS1, and protein level of β-CTF, while reduced the level of α-CTF without altering the protein level of APP in APP/PS1 Tg mice (**Figures 3F–H**). To assess the expression and distribution of BACE1 and PS1 in the brain of APP/PS1 Tg mice, sections were immunostained with antibodies against BACE1 and PS1. The results showed that the expression of BACE1 and PS1 was significantly increased in the CA3 region of the hippocampus (**Figures 3I,J**). Thus, CORT can promote the production of Aβ by activating BACE1 and PS1 in APP/PS1 Tg mice.

To investigate the role of CORT in the upregulation of the expression of BACE1 and PS1, WT, and APP/PS1 Tg mice were subjected to adrenalectomy (ADX) to establish a GCs-deficient animal model. After recovery for 3 days, ADX mice were randomly divided into vehicle and CORT (10 mg/kg/day) groups and treated for 7 days. The level of CORT in plasma was determined by ELISA. The results demonstrated that ADX lowered the plasma level of CORT in WT and APP/PS1 Tg mice, which was restored by treatment of WT mice with CORT (**Figures 4A,D**). Protein expression of BACE1 and PS1 was always consistent with the level of CORT (**Figures 4B,C,E,F**), suggesting the key role of CORT in the regulation of the expression of BACE1 and PS1 in mice.

GR Mediates the Effects of CORT on Stimulating the Expression of BACE1 and PS1

According to the classical hypothesis of the GCs cascade, the dysfunction of the HPA axis induced by a decrease in the GR level is the initial cause of AD. Thus, the expression of the GR was determined in CORT-treated mice. The results demonstrated that treatment with CORT (10 mg/kg/day) for 3 months did not significantly lower the expression of the GR (**Figures 5A,B**). However, the effects of the GR on the regulation of the expression of BACE1 and PS1 cannot be neglected. To assess these effects, the distribution of the GR was determined by immunofluorescence staining. The results demonstrated that the GR colocalized with neurons (**Figure 5C**). Therefore, the expression of NR3C1, which encodes the GR in N2a cells (Sevilla and Pérez, 2018) was knocked down and the efficacy of knocking down was determined by Western blots. The results demonstrated that gRNA targeted NR3C1 efficiently decreased the protein levels of NR3C1. The expression of BACE1 and PS1 was attenuated by knocking down the expression of NR3C1 in CORT-treated N2a cells (**Figures 5D,E**). Thus, the GR mediates the effects of GCs on stimulating the expression of BACE1 and PS1 in neurons.

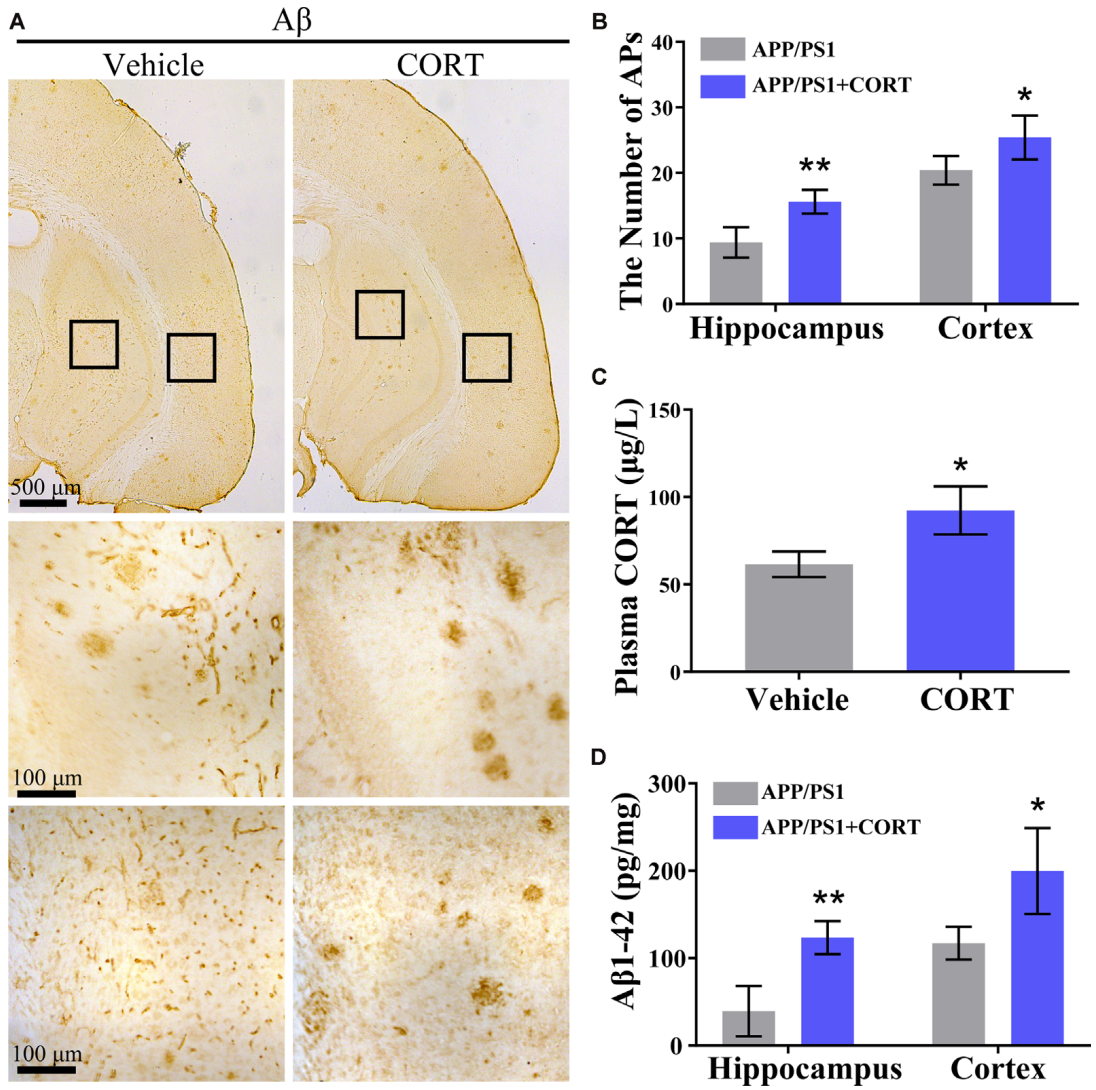

FIGURE 2 | CORT treatment increases the production of Aβ and the number of APs in the brain of APP/PS1 Tg mice. APP/PS1 Tg mice (5-month-old) were intraperitoneally injected with CORT (10 mg/kg/day) for 3 months. **(A,B)** The distribution of APs in the cerebral cortex and hippocampus of APP/PS1 Tg mice was determined by immunohistochemistry (IHC). **(C)** The content of CORT was determined by ELISA. **(D)** The contents of $A\beta_{1-42}$ in the cerebral cortex and hippocampus of APP/PS1 Tg mice were detected by ELISA. The data are present as the mean ± SE of independent experiments ($n = 6$). $^*p < 0.05$; $^{**}p < 0.01$ compared with the vehicle-treated mice by *t*-test.

CORT Upregulates the Expression of BACE1 and PS1 *via* the PKA and CREB Signaling Pathways

CREB is an important molecule involved in the regulation of memory in AD and was thus included in the current study to determine the mechanisms of its effects (Bartolotti and Lazarov, 2019). APP/PS1 mice were intraperitoneally injected with CORT at a dose of 10 mg/kg/day for 3 months. The Western blot analysis results indicated that phosphorylation of CREB was elevated in CORT-treated APP/PS1 Tg mice (**Figures 6A,B**). To validate these observations, N2a cells were treated with CORT (1 μM) in the absence or presence of a PKA/CREB inhibitor, H89 (10 μM). After 24 h, phosphorylation of CREB was blocked by H89 in CORT-stimulated N2a cells (**Figures 6C,D**). Deactivation of CREB resulted in attenuation of the effects of CORT on the stimulation of the expression of BACE1 and PS1 (**Figures 6C,D**). These results suggest the PKA and CREB signaling pathways are involved in mediating the effects of CORT on the upregulation of the expression of BACE1 and PS1.

CORT Promotes Apoptosis of Neurons and Inhibits Neuronal Differentiation in the Brain of APP/PS1 Tg Mice

Our results identified the mechanisms of action of CORT in the regulation of the production and deposition of Aβ; thus, the

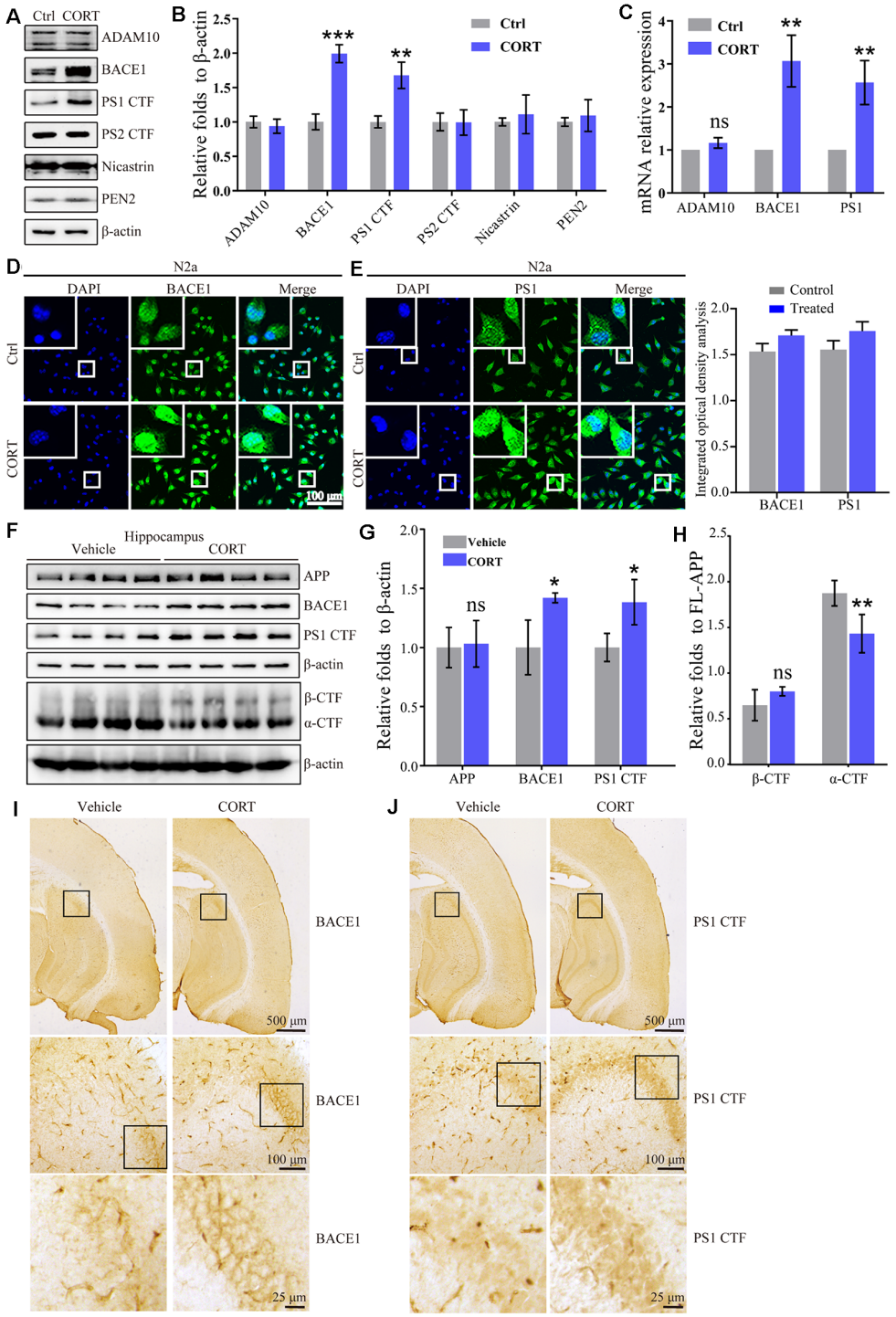

FIGURE 3 | CORT treatment upregulates the expression of BACE1 and PS1 *in vitro* and *in vivo*. **(A–E)** N2a cells were treated with CORT (1 μM) for 24 h. **(A)** Western blot analysis was used to detect the expression of ADAM10, BACE1, PS1, PS2, nicastrin, and PEN2. β-actin was used as an internal control. **(B)** The optical density of the bands was analyzed by ImageJ. The data of gene expression were analyzed by the *t*-test ($n = 6$). **(C)** mRNA expression of ADMA10, BACE1, and PS1 was determined by qRT-PCR. GAPDH was used as a housekeeping gene. The gene expression data were analyzed by the *t*-test ($n = 6$). $^{**}p < 0.01$; $^{***}p < 0.001$; ns: no significance compared with the vehicle-treated N2a cells. **(D,E)** The distribution of BACE1 and PS1 was detected by immunofluorescence and the immunofluorescence was semi-quantitatively analyzed by ImageJ software. **(F–I)** APP/PS1 Tg mice (5-month-old) were intraperitoneally injected with CORT (10 mg/kg/day) for 3 months. **(F–H)** The protein levels of APP, BACE1, PS1 α-CTF, and β-CTF were determined by Western blot analysis. β-Actin was used as an internal control. The optical density of the bands was analyzed by ImageJ. The gene expression data were analyzed by the *t*-test ($n = 6$). **(I,J)** The distribution of BACE1 and PS1 was determined by IHC. The data are presented as the mean ± SE of independent experiments. $^{*}p < 0.05$; $^{**}p < 0.01$; $^{***}p < 0.001$ compared with the vehicle-treated mice.

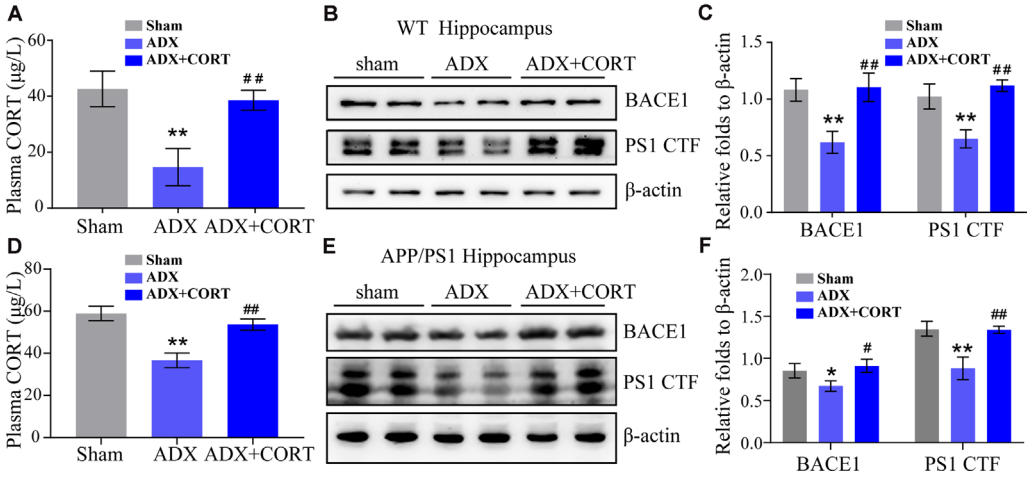

FIGURE 4 | CORT is essential for the expression of BACE1 and PS1. **(A–C)** WT mice were subjected to adrenalectomy (ADX). After 3 days, mice were intraperitoneally injected with CORT (10 mg/kg/day) for 7 days. **(A)** The content of CORT was determined by ELISA. The data were analyzed by repeated-measures ANOVA ($n = 4$). **(B,C)** Protein expression of BACE1 and PS1 was determined by Western blot analysis. β-Actin was used as an internal control. The optical density of the bands was analyzed by ImageJ. The gene expression data were analyzed by one-way ANOVA ($n = 4$). $^{**}p < 0.01$ compared with the sham-operated mice. $^{\#\#}p < 0.01$ compared with the ADX-operated C57BL/6 mice. **(D–F)** APP/PS1 mice were subjected to adrenalectomy (ADX). After 3 days, mice were intraperitoneally injected with CORT (10 mg/kg/day) for 7 days. **(D)** The content of CORT was determined by ELISA. The data were analyzed by repeated-measures ANOVA ($n = 4$). **(E,F)** Protein expression of BACE1 and PS1 was determined by Western blot analysis. β-Actin was used as an internal control. The optical density of the bands was analyzed by ImageJ. The gene expression data were analyzed by one-way ANOVA ($n = 4$). The data are presented as the mean ± SE of independent experiments. $^{*}p < 0.05$; $^{**}p < 0.01$ compared with the sham-operated mice. $^{\#}p < 0.05$, $^{\#\#}p < 0.01$ compared with the ADX-operated APP/PS1 Tg mice.

roles of CORT in neurons were further investigated. A series of studies have suggested the neurotoxic effects of Aβ on apoptosis of neurons (Reddy and Beal, 2008; Calvo-Rodriguez et al., 2019). To determine the effect of CORT on the brain of APP/PS1 Tg mice and to assess whether CORT can promote apoptosis of neurons in the brain, Western blot analysis was used to detect the expression of Bcl-2 and Bax in the hippocampus in all groups of mice. The results showed that the ratio of Bcl-2 to Bax was significantly downregulated in the brain of CORT-treated APP/PS1 Tg mice compared with that in the control groups (**Figures 7A,B**). This observation suggests that CORT promotes apoptosis of neurons in the brain of APP/PS1 transgenic mice. Since CORT induces apoptosis of neurons, the roles of CORT in neuronal differentiation were determined by staining doublecortin. The results demonstrated that axons and dendrites generated from neuronal stem cells are suppressed by treatment with CORT (**Figure 7C**). These results indicate that CORT can aggravate AD *via* multiple mechanisms, such as induction of the production and deposition of Aβ, triggering apoptosis of neurons, and inhibiting neuronal differentiation.

DISCUSSION

As the involvement of GCs in regulating the learning and cognitive functions (Starkman et al., 2001, 2003), we investigated the effects of GCs on AD. As a consequence, we found that the content of CORT in plasma was significantly increased in the 9-month-old APP/PS1 Tg mice. By subcutaneously injected CORT, the learning ability of APP/PS1 Tg mice was impaired with enhancing the production and deposition of A in a BACE1- and PS1-dependent mechanism. To the mechanism, CORT activates BACE1 and PS1 *via* the glucocorticoid receptor (GR)-PKA-CREB signaling pathway. These observations were further confirmed by ADX treatment, which downregulates the expression of BACE1 and PS1 by reducing the plasma levels of CORT.

Prior studies have shown that stress can accelerate brain aging, which results in the induction of dementia (Brinks et al., 2007). Additionally, stress has an impact on the major depressive disorder (MDD; Roy et al., 2017). Accumulating evidence shows that patients with MDD have cognitive disorders with symptoms similar to AD patients (Boedeker et al., 2020). These observations define a potential link between stress, MDD, and AD (Galts et al., 2019). Specifically, stress, MDD, and AD share the same characteristic of overproduction of GCs. Long-term exposure to a normal concentration of GCs accelerates brain aging, which results in a loss of the ability to regulate the levels of GCs, thus leading to further acceleration of brain aging and, eventually, causing brain impairment and onset of dementia. However, it is unclear whether GCs leads to the onset and development of AD or plays a role in AD-associated mechanisms. Certain controversies regarding the specific molecular mechanisms require additional clarification despite numerous studies on these issues. Therefore, the roles of CORT in the regulation of the development and progression of AD were investigated in the present study. The results indicate that CORT has multiple pathological functions in the progression of AD, including regulation of the production and aggregation of Aβ, apoptosis of neurons and suppression of neuronal differentiation.

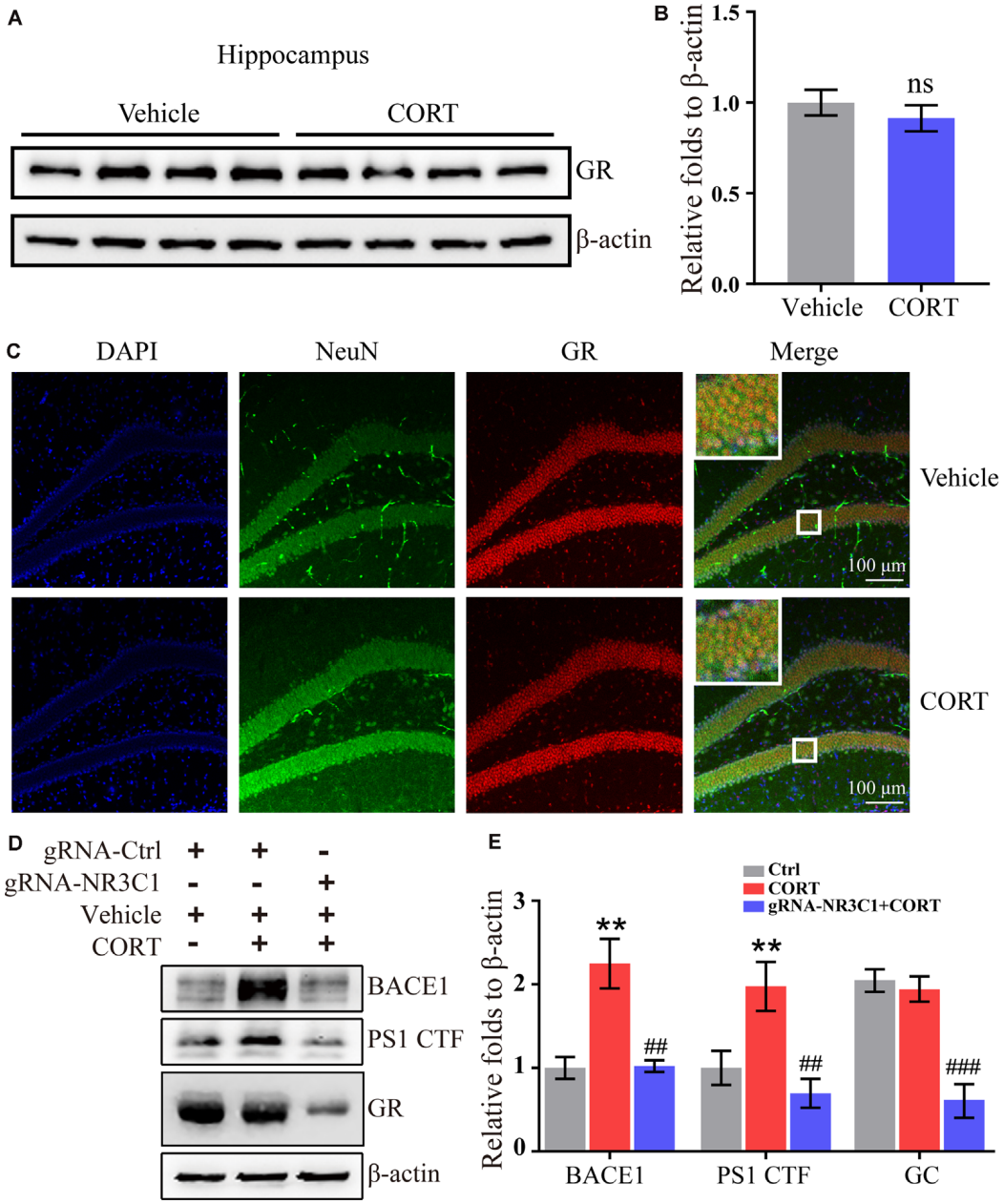

FIGURE 5 | Glucocorticoid receptor (GR) mediates the effects of CORT on the upregulation of the expression of BACE1 and PS1 in neurons. **(A–C)** APP/PS1 Tg mice (5-month-old) were intraperitoneally injected with CORT (10 mg/kg/day) for 3 months. **(A,B)** The expression of the GR was determined by Western blot analysis. β-Actin was used as an internal control. The optical density of the bands was analyzed by ImageJ. The data were analyzed by the *t*-test ($n = 6$). ns: no significance compared with the vehicle-treated controls. **(C)** Brain sections of mice were double-stained with NeuN and GR antibodies and observed by confocal microscopy. **(D,E)** N2a cells were treated with CORT with or without knockdown of NR3C1 expression. Western blot analysis was used to detect the expression of BACE1, PS1, and NR3C1. β-Actin was used as an internal control. The optical density of the bands was analyzed by ImageJ. The data were analyzed by one-way ANOVA ($n = 6$). The data are presented as the mean ± SE of independent experiments. $^{**}p < 0.01$ compared with the vehicle-treated controls. $^{\#\#}p < 0.01$; $^{\#\#\#}p < 0.001$ compared with the CORT-treated N2a cells.

Clinical data show that the average daily fluctuations of cortisol levels in elderly people are higher than those in younger people (Raskind et al., 1994). In the last century, elevated plasma levels of cortisol have been reported to induce a reduction in the volume of the hippocampus and impairment of memory in elderly people. Certain patients with high cortisol levels progressively develop AD (Lupien et al., 2005). Similarly, GCs are also responsible for a decrease in the volume of the hippocampus and memory impairment in patients with Cushing's syndrome (CS; Forget et al., 2000).

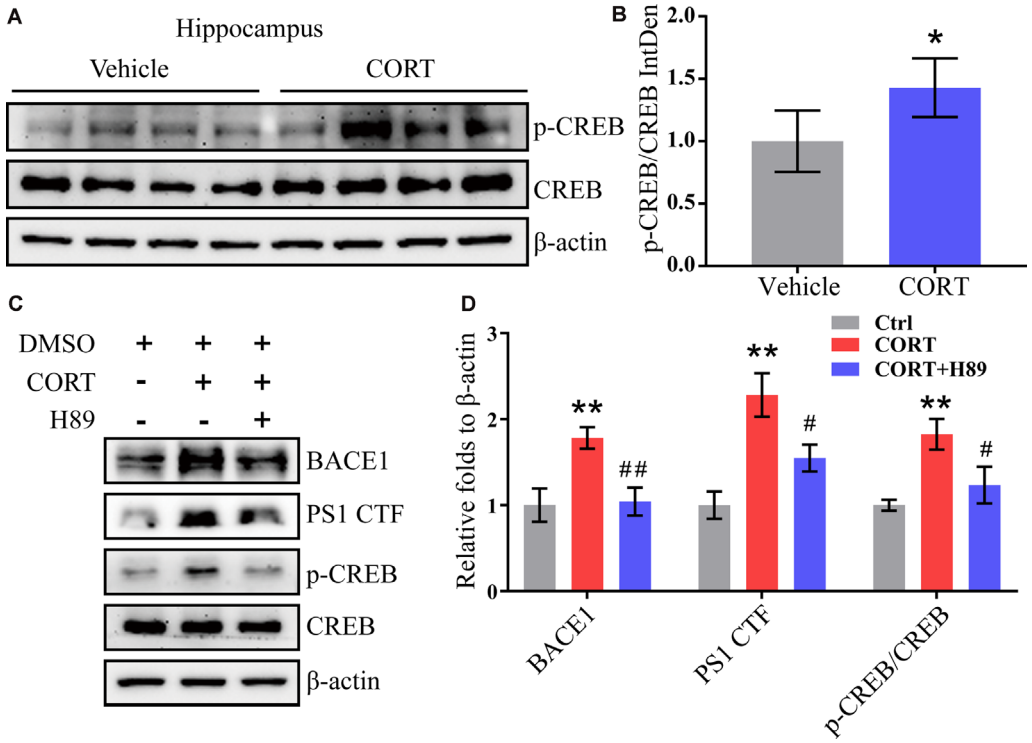

FIGURE 6 | CORT upregulates the expression of BACE1 and PS1 *via* the PKA and CREB signaling pathway. **(A,B)** APP/PS1 Tg mice (5-month-old) were intraperitoneally injected with CORT (10 mg/kg/day) for 3 months. The levels of phosphorylated and total CREB were determined by Western blot analysis. β-Actin was used as an internal control. The ratio of p-CREB to CREB was calculated using ImageJ software. The data were analyzed by the *t*-test ($n = 6$). **(C,D)** N2a cells were treated with CORT (1 μM) in the absence or presence of H89 (10 μM) for 24 h. The expression levels of BACE-1, PS1, p-CREB, and CREB were measured by Western blot analysis. β-Actin was used as an internal control. The optical density was measured using ImageJ software. The gene expression data were analyzed by one-way ANOVA ($n = 6$). The data are presented as the mean ± SE of independent experiments. $^{*}p < 0.05$; $^{**}p < 0.01$ compared with the vehicle-treated controls. $^{\#}p < 0.05$; $^{\#\#}p < 0.01$ compared with CORT-treated N2a cells.

In agreement with these observations, the level of cortisol is significantly higher in AD patients than in the control subjects (Raskind et al., 1982). Also, epidemiological studies have revealed that high levels of cortisol can upregulate the expression of AD-associated genes and can be used to diagnose AD *via* long-term monitoring of the level of cortisol (Ennis et al., 2017). The plasma concentration of CORT in 3×Tg AD mice was significantly higher than that in WT mice (Green et al., 2006). Thus, the prior studies have been expanded and it has been demonstrated that the plasma concentration of CORT is elevated in 9-month-old APP/PS1 Tg mice compared to that in WT mice.

However, overloading of GCs is not always bad for brain aging. For example, acute and transient secretion of GCs is beneficial to some types of learning and memory, such as emotional ability (McGaugh and Roozendaal, 2002) and spatial memory (Wingenfeld and Wolf, 2014). In contrast, a series of studies have demonstrated that GCs can increase the levels of Ca^{2+}-mediated electrophysiological biomarkers of hippocampal aging in the range from a few minutes to several hours (Kerr et al., 1989, 1992; Joëls and de Kloet, 1993). Therefore, the effects of short-term exposure to GCs on learning and memory remain a matter of debate. However, high levels of GCs or long-term exposure to a normal concentration of GCs will continuously activate the GR, which results in damage to memory (Zhang et al., 2020). In a preliminary study in the salmon and mammalian (including human) brain, an increase in GCs resulted in the degeneration of peripheral tissues, similar to the changes associated with aging (Sotiropoulos et al., 2008). In an ADX group of rats, several biomarkers of brain aging were significantly reduced, resulting in improved learning and memory performance in the Morris maze test compared with that in the sham group (Landfield et al., 1981). GCs have been shown to damage the hippocampus by increasing its vulnerability (Sapolsky et al., 1986). In detail, GCs impairs the energy metabolism of hippocampal neurons by inhibiting the uptake of glucose, which results in an increase in the susceptibility of cultured neurons to all types of destructive metabolic damage (Sapolsky et al., 1988). Additionally, CORT defines the relationship between hippocampal damage and cognitive impairment in elderly rats (Issa et al., 1990; Meaney et al., 1995), which is supported by other reports that demonstrated a negative correlation between GCs exposure and cognitive decline. On the other hand, excessive loading with GCs will cause atrophy of hippocampal dendrites and delay neurogenesis (McEwen, 1996; Mirescu and Gould, 2006). Based

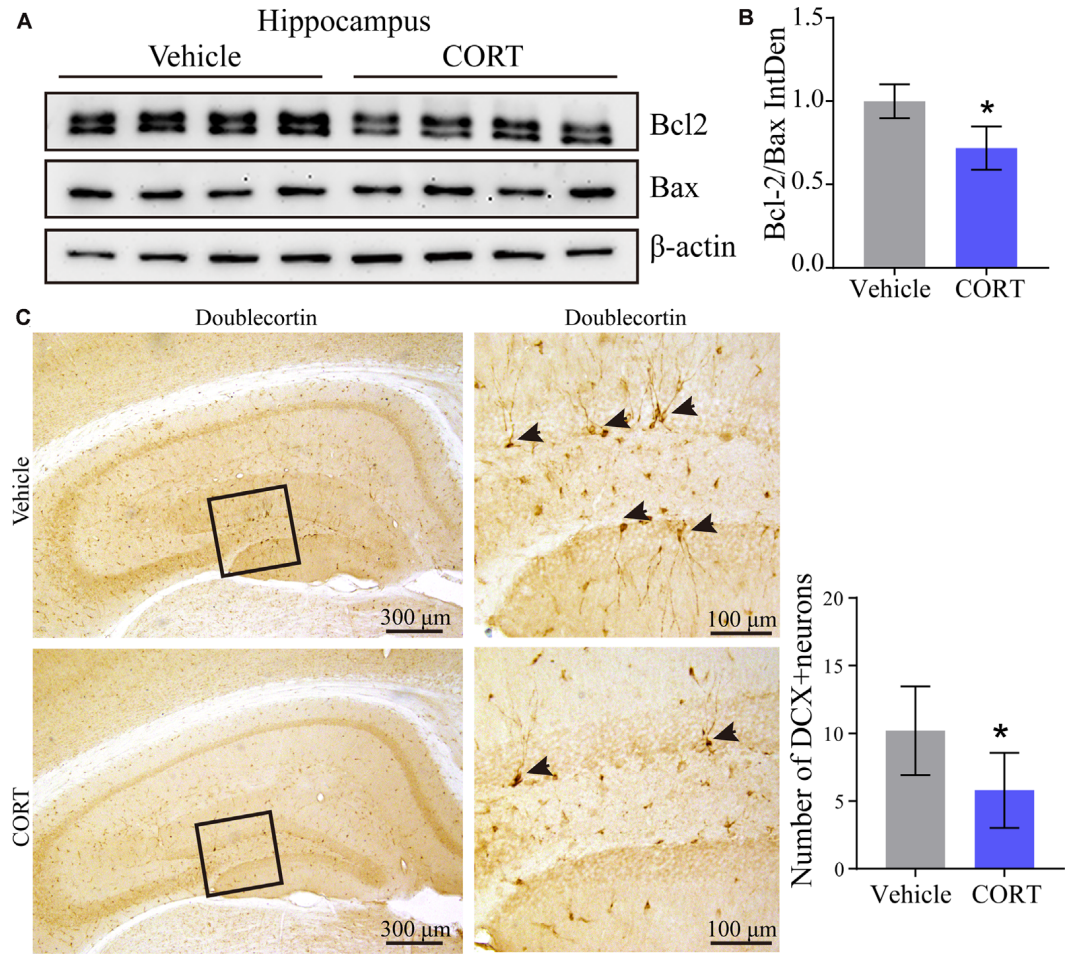

FIGURE 7 | CORT promotes apoptosis of neurons and inhibits neuronal differentiation in the brain of APP/PS1 Tg mice. APP/PS1 Tg mice (5-month-old) were intraperitoneally injected with CORT (10 mg/kg/day) for 3 months. **(A,B)** Western blot analysis was used to detect the expression of Bcl-2 and Bax in the hippocampus of mice in each group. β-Actin was used as an internal control. The bands were analyzed using ImageJ software. The data were analyzed by the *t*-test ($n = 6$). **(C)** Neuronal differentiation was determined by IHC staining of doublecortin. The positive neurons were semi-quantitatively analyzed by ImageJ software. The data are presented as the mean ± SE of independent experiments. $^*p < 0.05$ compared with the vehicle-treated controls.

on these studies, CORT treatment-induced cognitive decline in APP/PS1 Tg mice.

Secretion of GCs is regulated by the HPA axis. The GR is the key molecule of the HPA axis that regulates the level of GCs *in vivo*. Under pathological conditions, the concentrations of GCs increases *in vivo*. High levels of GCs act on the GR in the hippocampus, hypothalamus, and pituitary, which in turn, induce a decrease in GCs to the basal level *via* a negative feedback mechanism. Release of GCs leads to downregulation of the expression of the GR and its downstream signaling pathway and atrophy and loss of GR-containing neurons in the hippocampus, which suppresses the regulatory effects of the GR on the HPA axis (Sotiropoulos et al., 2008). The mRNA and protein levels of the GR are decreased with age in the hippocampus, damaging the negative feedback regulation of GCs and leading to continuous exposure of the brain to high concentrations of GCs, which results in loss of neuronal function (Landfield, 1978; Landfield et al., 1978; Jacobson and Sapolsky, 1991). Without chronic GCs stress, overexpression of the GR in the mouse forebrain has been reported to be responsible for the acceleration of the expression of brain aging-like phenotype (Wei et al., 2007). Also, subchronic inhibition of the GR in AD model mice can treat early defects of situational memory and synaptic plasticity (Lanté et al., 2015). The GR is a nuclear receptor that acts as a transcription factor to mediate the effects of CORT on the upregulated expression of BACE1 and PS1. GCs bind to the GR in the cytoplasm, which then enters the nucleus to regulate the transcription of APP and BACE1 *via* binding to the CRE sequence of the APP and BACE1 promoters (Green et al., 2006). The present study expands on these previous findings by demonstrating that knockdown of expression of NR3C1 blocks the effects of CORT on stimulating the expression of BACE1 and PS2, suggesting that CORT upregulates the expression of BACE1 and PS1 *via* the GR in neurons.

CREB is a transcription factor that plays an important role in regulating the transition from short-term memory to long-term memory (Tully et al., 2003; Saura and Valero, 2011). Additionally, the CREB signal is involved in the regulation of processes associated with many neurodegenerative diseases, such as AD. For example, CREB has been reported to regulate the expression of BACE1 and PS1 as a transcription factor (Lahiri et al., 2006; Choi et al., 2017). The results of the present study demonstrated that CORT can stimulate the phosphorylation of CREB at Ser 133, which results in upregulation of the expression of BACE1 and PS1 in neurons. The addition of H89 completely blocked the effects of CORT on stimulating the expression of BACE1 and PS1 *via* dephosphorylation of CREB, suggesting the key role of CREB in mediating the effects of CORT on regulating the expression of BACE1 and PS1 in neurons.

According to Aβ theory, APP is abnormally cleaved to produce Aβ, which can induce apoptosis of neurons *via* multiple pathways (Reddy and Beal, 2008; Calvo-Rodriguez et al., 2019). Aβ can concurrently upregulate the expression of Bax and downregulate the expression of Bcl-2, thus disrupting the balance between Bax and Bcl-2, leading to apoptosis of neurons during the course of AD development and progression (Hu et al., 2016). The results of the present study indicate that CORT can induce the production of Aβ and decrease the ratio of Bcl-2 to Bax, suggesting that CORT promotes apoptosis of neurons. Moreover, CORT inhibits neuronal differentiation in APP/PS1 Tg mice. In agreement with these results, chronic exposure to high concentrations of CORT has been shown to reduce neuronal differentiation in the dentate gyrus of rats (Brummelte and Galea, 2010). Inhibition of the secretion of CORT from midlife to the rest of the animal life increases neuronal differentiation in old animals, which prevents the onset of age-related memory disorders (Montaron et al., 2006). Thus, the effects of CORT trigger a loss of neurons during AD development and progression.

For neuroinflammation, more and more data proved the crosstalk between neuroinflammation and Aβ, which can accelerate the progression of AD (Cai et al., 2014). Since studies have shown that GCs induce the expression of nod-like receptor family in cultured macrophages and primary macrophages, leading to the secretion of pro-inflammatory cytokines IL-1, TNF-α, and IL-6 (Busillo et al., 2011), we continue to detect if CORT can regulate the neuroinflammation of APP/PS1 Tg mice. As the main cell types that mediate neuroinflammation in the brain are astrocytes and microglia (Sawikr et al., 2017), we immunostained the glial cells with GFAP and Iba1. The results demonstrated that CORT activates the glial cells of APP/PS1 Tg mice, leading to the secretion of TNF-α (data not shown). In agreement with our results, CORT has been reported to activate microglial cells (Zalewska et al., 2017) and astrocytes (Bridges et al., 2008). Moreover, intravenous infusion of CORT at non-stressed (35 ng/ml) and stressed levels (350 ng/ml) increased the release of TNF-α and/or IL-6 in the liver (Liao et al., 1995).

Apart from the above effects, high GCs can inhibit mTOR-dependent autophagy, leading to the aggregation and deposition of tau, which results in neuronal death of Tau^{P301L} mice (Silva et al., 2019). Also, GCs in the brain are the key regulators of dendritic spines. For example, Pedrazzoli et al. (2019) found that dexamethasone, an agonist of GRs, can significantly reduce the density of dendritic spines in the hippocampal CA1 area of 6- and 10-month-old 3×Tg-AD mice. Moreover, recent work suggests that GCs may regulate synaptic plasticity by interacting with glutamate-energy mechanisms and ultimately affect learning and memory processes (Sandi, 2011).

CONCLUSIONS

Elevated levels of CORT during the course of AD development and progression can induce the production and deposition of Aβ in APs by activating BACE1 and PS1 in APP/PS1 Tg mice. Additionally, the GR mediates the effects of high dose CORT exposure by stimulating the expression of BACE1 and PS1 *via* the PKA and CREB signaling cascades. These mechanisms of CORT promote apoptosis of neurons and inhibit neuronal differentiation, resulting in cognitive decline in APP/PS1 Tg mice.

DATA AVAILABILITY STATEMENT

The raw data supporting the conclusions of this article will be made available by the authors, without undue reservation.

ETHICS STATEMENT

The animal study was reviewed and approved by medical laboratory animals (Ministry of Health, Peoples Republic of China, 1998) and the laboratory animal ethical standards of Northeastern University of China were adhered to.

AUTHOR CONTRIBUTIONS

S-QZ and L-LC conceived and performed all of the experiments, participated in the design of the study, and wrote the manuscript. Y-YL carried out select experiments. PW interpreted the data and wrote the manuscript. All authors contributed to the article and approved the submitted version.

FUNDING

This work was supported, in part or in whole, by the National Natural Science Foundation of China (CN; 81870840) and the Fundamental Research Funds for the Central Universities, China (N172008008).

SUPPLEMENTARY MATERIAL

The Supplementary Material for this article can be found online at: https://www.frontiersin.org/articles/10.3389/fnmol.2020.613421/full#supplementary-material.

REFERENCES

Bartolotti, N., and Lazarov, O. (2019). CREB signals as PBMC-based biomarkers of cognitive dysfunction: a novel perspective of the brain-immune axis. *Brain Behav. Immun.* 78, 9–20. doi: 10.1016/j.bbi.2019.01.004

Bettio, L. E. B., Rajendran, L., and Gil-Mohapel, J. (2017). The effects of aging in the hippocampus and cognitive decline. *Neurosci. Biobehav. Rev.* 79, 66–86. doi: 10.1016/j.neubiorev.2017.04.030

Boedeker, S., Schulz, P., Beblo, T., Lenz, E., Sammer, G., Kreisel, S., et al. (2020). Symbol comprehension in patients with Alzheimer disease dementia, mild cognitive impairment and major depressive disorder. *Alzheimer Dis. Assoc. Disord.* 34, 85–93. doi: 10.1097/WAD.0000000000000347

Bridges, N., Slais, K., and Syková, E. (2008). The effects of chronic corticosterone on hippocampal astrocyte numbers: a comparison of male and female Wistar rats. *Acta Neurobiol. Exp.* 68, 131–138.

Brinks, V., van der Mark, M. H., de Kloet, E. R., and Oitzl, M. S. (2007). Differential MR/GR activation in mice results in emotional states beneficial or impairing for cognition. *Neural Plast.* 2007:90163. doi: 10.1155/2007/90163

Brummelte, S., and Galea, L. A. (2010). Chronic high corticosterone reduces neurogenesis in the dentate gyrus of adult male and female rats. *Neuroscience* 168, 680–690. doi: 10.1016/j.neuroscience.2010.04.023

Busillo, J. M., Azzam, K. M., and Cidlowski, J. A. (2011). Glucocorticoids sensitize the innate immune system through regulation of the NLRP3 inflammasome. *J. Biol. Chem.* 286, 38703–38713. doi: 10.1074/jbc.M111.275370

Cai, Z., Hussain, M. D., and Yan, L. J. (2014). Microglia, neuroinflammation and β-amyloid protein in Alzheimer's disease. *Int. J. Neurosci.* 124, 307–321. doi: 10.3109/00207454.2013.833510

Calvo-Rodriguez, M., Hernando-Perez, E., Nuñez, L., and Villalobos, C. (2019). Amyloid β oligomers increase ER-mitochondria Ca^{2+} cross talk in young hippocampal neurons and exacerbate aging-induced intracellular Ca^{2+} remodeling. *Front. Cell Neurosci.* 13:22. doi: 10.3389/fncel.2019.00022

Choi, G. E., Lee, S. J., Lee, H. J., Ko, S. H., Chae, C. W., and Han, H. J. (2017). Membrane-associated effects of glucocorticoid on BACE1 upregulation and Aβ generation: involvement of lipid raft-mediated CREB activation. *J. Neurosci.* 37, 8459–8476. doi: 10.1523/JNEUROSCI.0074-17.2017

Curran, K. P., and Chalasani, S. H. (2012). Serotonin circuits and anxiety: what can invertebrates teach us? *Invert. Neurosci.* 12, 81–92. doi: 10.1007/s10158-012-0140-y

David, D. J., Samuels, B. A., Rainer, Q., Wang, J. W., Marsteller, D., Mendez, I., et al. (2009). Neurogenesis-dependent and -independent effects of fluoxetine in an animal model of anxiety/depression. *Neuron* 62, 479–493. doi: 10.1016/j.neuron.2009.04.017

Ennis, G. E., An, Y., Resnick, S. M., Ferrucci, L., O'Brien, R. J., and Moffat, S. D. (2017). Long-term cortisol measures predict Alzheimer disease risk. *Neurology* 88, 371–378. doi: 10.1212/WNL.0000000000003537

Faught, E., and Vijayan, M. M. (2019). Postnatal triglyceride accumulation is regulated by mineralocorticoid receptor activation under basal and stress conditions. *J. Physiol.* 597, 4927–4941. doi: 10.1113/JP278088

Forget, H., Lacroix, A., Somma, M., and Cohen, H. (2000). Cognitive decline in patients with Cushing's syndrome. *J. Int. Neuropsychol. Soc.* 6, 20–29. doi: 10.1017/s1355617700611037

Galts, C. P. C., Bettio, L. E. B., Jewett, D. C., Yang, C. C., Brocardo, P. S., Rodrigues, A. L. S., et al. (2019). Depression in neurodegenerative diseases: common mechanisms and current treatment options. *Neurosci. Biobehav. Rev.* 102, 56–84. doi: 10.1016/j.neubiorev.2019.04.002

Green, K. N., Billings, L. M., Roozendaal, B., McGaugh, J. L., and LaFerla, F. M. (2006). Glucocorticoids increase amyloid-β and tau pathology in a mouse model of Alzheimer's disease. *J. Neurosci.* 26, 9047–9056. doi: 10.1523/JNEUROSCI.2797-06.2006

Guldiken, S., and Guldiken, B. (2008). Subclinical Cushing's syndrome is a potential cause of metabolic dementia and rapidly progressive Alzheimer-type dementia. *Med. Hypotheses* 71, 703–705. doi: 10.1016/j.mehy.2008.05.036

Haraguchi, Y., Mizoguchi, Y., Noguchi, T., Arai, T., Fukuyama, J., Kato, T. A., et al. (2016). A patient with Alzheimer's disease complicated by elderly-onset Cushing's syndrome who had undergone surgical treatment for adrenocorticotropic hormone-independent macronodular adrenal hyperplasia. *Psychogeriatrics* 16, 274–276. doi: 10.1111/psyg.12146

Herbert, J., and Lucassen, P. J. (2016). Depression as a risk factor for Alzheimer's disease: genes, steroids, cytokines and neurogenesis–what do we need to know? *Front. Neuroendocrinol.* 41, 153–171. doi: 10.1016/j.yfrne.2015.12.001

Hu, H., Wang, Y., Zhang, Y., Wang, W., Xu, D., Chen, Z., et al. (2016). Effect of Qingxinkaiqiao compound on cortical mRNA expression of the apoptosis-related genes Bcl-2, BAX, caspase-3 and Aβ in an Alzheimer's disease rat model. *J. Tradit. Chin. Med.* 36, 654–662. doi: 10.1016/s0254-6272(16)30086-3

Issa, A. M., Rowe, W., Gauthier, S., and Meaney, M. J. (1990). Hypothalamic-pituitary-adrenal activity in aged, cognitively impaired and cognitively unimpaired rats. *J. Neurosci.* 10, 3247–3254. doi: 10.1523/JNEUROSCI.10-10-03247.1990

Jacobson, L., and Sapolsky, R. (1991). The role of the hippocampus in feedback regulation of the hypothalamic-pituitary-adrenocortical axis. *Endocr. Rev.* 12, 118–134. doi: 10.1210/edrv-12-2-118

Joëls, M., and de Kloet, E. R. (1993). Corticosteroid actions on amino acid-mediated transmission in rat CA1 hippocampal cells. *J. Neurosci.* 13, 4082–4090. doi: 10.1021/acsami.0c18454

Kerr, D. S., Campbell, L. W., Hao, S. Y., and Landfield, P. W. (1989). Corticosteroid modulation of hippocampal potentials: increased effect with aging. *Science* 245, 1505–1509. doi: 10.1126/science.2781293

Kerr, D. S., Campbell, L. W., Thibault, O., and Landfield, P. W. (1992). Hippocampal glucocorticoid receptor activation enhances voltage-dependent Ca^{2+} conductances: relevance to brain aging. *Proc. Natl. Acad. Sci. U S A* 89, 8527–8531. doi: 10.1073/pnas.89.18.8527

Lahiri, D. K., Ge, Y. W., Rogers, J. T., Sambamurti, K., Greig, N. H., and Maloney, B. (2006). Taking down the unindicted co-conspirators of amyloid β-peptide-mediated neuronal death: shared gene regulation of BACE1 and APP genes interacting with CREB, Fe65 and YY1 transcription factors. *Curr. Alzheimer Res.* 3, 475–483. doi: 10.2174/156720506779025224

Landfield, P. W. (1978). An endocrine hypothesis of brain aging and studies on brain-endocrine correlations and monosynaptic neurophysiology during aging. *Adv. Exp. Med. Biol.* 113, 179–199. doi: 10.1007/978-1-4684-8893-7_11

Landfield, P. W., Baskin, R. K., and Pitler, T. A. (1981). Brain aging correlates: retardation by hormonal-pharmacological treatments. *Science* 214, 581–584. doi: 10.1126/science.6270791

Landfield, P. W., Waymire, J. C., and Lynch, G. (1978). Hippocampal aging and adrenocorticoids: quantitative correlations. *Science* 202, 1098–1102. doi: 10.1126/science.715460

Lanté, F., Chafai, M., Raymond, E. F., Pereira, A. R., Mouska, X., Kootar, S., et al. (2015). Subchronic glucocorticoid receptor inhibition rescues early episodic memory and synaptic plasticity deficits in a mouse model of Alzheimer's disease. *Neuropsychopharmacology* 40, 1772–1781. doi: 10.1371/journal.pone.0242588

Lesuis, S. L., Weggen, S., Baches, S., Lucassen, P. J., and Krugers, H. J. (2018). Targeting glucocorticoid receptors prevents the effects of early life stress on amyloid pathology and cognitive performance in APP/PS1 mice. *Transl. Psychiatry* 8:53. doi: 10.1038/s41398-018-0101-2

Li, W. Z., Li, W. P., Yao, Y. Y., Zhang, W., Yin, Y. Y., Wu, G. C., et al. (2010). Glucocorticoids increase impairments in learning and memory due to elevated amyloid precursor protein expression and neuronal apoptosis in 12-month old mice. *Eur. J. Pharmacol.* 628, 108–115. doi: 10.1016/j.ejphar.2009.11.045

Liao, J., Keiser, J. A., Scales, W. E., Kunkel, S. L., and Kluger, M. J. (1995). Role of corticosterone in TNF and IL-6 production in isolated perfused rat liver. *Am. J. Physiol.* 268, R699–R706. doi: 10.1152/ajpregu.1995.268.3.R699

Lupien, S. J., Schwartz, G., Ng, Y. K., Fiocco, A., Wan, N., Pruessner, J. C., et al. (2005). The douglas hospital longitudinal study of normal and pathological aging: summary of findings. *J. Psychiatry Neurosci.* 30, 328–334.

McEwen, B. S. (1996). Gonadal and adrenal steroids regulate neurochemical and structural plasticity of the hippocampus *via* cellular mechanisms involving NMDA receptors. *Cell. Mol. Neurobiol.* 16, 103–116. doi: 10.1007/BF02088170

McGaugh, J. L., and Roozendaal, B. (2002). Role of adrenal stress hormones in forming lasting memories in the brain. *Curr. Opin. Neurobiol.* 12, 205–210. doi: 10.1016/s0959-4388(02)00306-9

Meaney, M. J., O'Donnell, D., Rowe, W., Tannenbaum, B., Steverman, A., Walker, M., et al. (1995). Individual differences in hypothalamic-pituitary-adrenal activity in later life and hippocampal aging. *Exp. Gerontol.* 30, 229–251. doi: 10.1016/0531-5565(94)00065-b

Meijer, O. C., Koorneef, L. L., and Kroon, J. (2018). Glucocorticoid receptor modulators. *Ann. Endocrinol.* 79, 107–111. doi: 10.1016/j.ando.2018.03.004

Mirescu, C., and Gould, E. (2006). Stress and adult neurogenesis. *Hippocampus* 16, 233–238. doi: 10.1002/hipo.20155

Montaron, M. F., Drapeau, E., Dupret, D., Kitchener, P., Aurousseau, C., Le Moal, M., et al. (2006). Lifelong corticosterone level determines age-related decline in neurogenesis and memory. *Neurobiol. Aging* 27, 645–654. doi: 10.1016/j.neurobiolaging.2005.02.014

O'Brien, R. J., and Wong, P. C. (2011). Amyloid precursor protein processing and Alzheimer's disease. *Annu. Rev. Neurosci.* 34, 185–204. doi: 10.1146/annurev-neuro-061010-113613

Pedrazzoli, M., Losurdo, M., Paolone, G., Medelin, M., Jaupaj, L., Cisterna, B., et al. (2019). Glucocorticoid receptors modulate dendritic spine plasticity and microglia activity in an animal model of Alzheimer's disease. *Neurobiol. Dis.* 132:104568. doi: 10.1016/j.nbd.2019.104568

Pineau, F., Canet, G., Desrumaux, C., Hunt, H., Chevallier, N., Ollivier, M., et al. (2016). New selective glucocorticoid receptor modulators reverse amyloid-β peptide-induced hippocampus toxicity. *Neurobiol. Aging* 45, 109–122. doi: 10.1016/j.neurobiolaging.2016.05.018

Ragnarsson, O., Berglund, P., Eder, D. N., and Johannsson, G. (2012). Long-term cognitive impairments and attentional deficits in patients with Cushing's disease and cortisol-producing adrenal adenoma in remission. *J. Clin. Endocrinol. Metab.* 97, E1640–E1648. doi: 10.1210/jc.2012-1945

Raskind, M., Peskind, E., Rivard, M. F., Veith, R., and Barnes, R. (1982). Dexamethasone suppression test and cortisol circadian rhythm in primary degenerative dementia. *Am. J. Psychiatry* 139, 1468–1471. doi: 10.1176/ajp.139.11.1468

Raskind, M. A., Peskind, E. R., and Wilkinson, C. W. (1994). Hypothalamic-pituitary-adrenal axis regulation and human aging. *Ann. N. Y. Acad. Sci.* 746, 327–335. doi: 10.1111/j.1749-6632.1994.tb39251.x

Ratman, D., Vanden Berghe, W., Dejager, L., Libert, C., Tavernier, J., Beck, I. M., et al. (2013). How glucocorticoid receptors modulate the activity of other transcription factors: a scope beyond tethering. *Mol. Cell. Endocrinol.* 380, 41–54. doi: 10.1016/j.mce.2012.12.014

Reddy, P. H., and Beal, M. F. (2008). Amyloid β, mitochondrial dysfunction and synaptic damage: implications for cognitive decline in aging and Alzheimer's disease. *Trends Mol. Med.* 14, 45–53. doi: 10.1016/j.molmed.2007.12.002

Richardson, R. V., Batchen, E. J., Denvir, M. A., Gray, G. A., and Chapman, K. E. (2016). Cardiac GR and MR: from development to pathology. *Trends Endocrinol. Metab.* 27, 35–43. doi: 10.1016/j.tem.2015.10.001

Roy, B., Shelton, R. C., and Dwivedi, Y. (2017). DNA methylation and expression of stress related genes in PBMC of MDD patients with and without serious suicidal ideation. *J. Psychiatr. Res.* 89, 115–124. doi: 10.1016/j.jpsychires.2017.02.005

Sandi, C. (2011). Glucocorticoids act on glutamatergic pathways to affect memory processes. *Trends Neurosci.* 34, 165–176. doi: 10.1016/j.tins.2011.01.006

Sapolsky, R. M., Krey, L. C., and McEwen, B. S. (1986). The neuroendocrinology of stress and aging: the glucocorticoid cascade hypothesis. *Endocr. Rev.* 7, 284–301. doi: 10.1210/edrv-7-3-284

Sapolsky, R. M., Packan, D. R., and Vale, W. W. (1988). Glucocorticoid toxicity in the hippocampus: *in vitro* demonstration. *Brain Res.* 453, 367–371. doi: 10.1016/0006-8993(88)90180-1

Saura, C. A., and Valero, J. (2011). The role of CREB signaling in Alzheimer's disease and other cognitive disorders. *Rev. Neurosci.* 22, 153–169. doi: 10.1515/RNS.2011.018

Sawikr, Y., Yarla, N. S., Peluso, I., Kamal, M. A., Aliev, G., and Bishayee, A. (2017). Neuroinflammation in Alzheimer's disease: the preventive and therapeutic potential of polyphenolic nutraceuticals. *Adv. Protein Chem. Struct. Biol.* 108, 33–57. doi: 10.1016/bs.apcsb.2017.02.001

Sevilla, L. M., and Pérez, P. (2018). Roles of the glucocorticoid and mineralocorticoid receptors in skin pathophysiology. *Int. J. Mol. Sci.* 19:1906. doi: 10.3390/ijms19071906

Sheline, Y. I., Wang, P. W., Gado, M. H., Csernansky, J. G., and Vannier, M. W. (1996). Hippocampal atrophy in recurrent major depression. *Proc. Natl. Acad. Sci. U S A* 93, 3908–3913. doi: 10.1073/pnas.93.9.3908

Silva, J. M., Rodrigues, S., Sampaio-Marques, B., Gomes, P., Neves-Carvalho, A., Dioli, C., et al. (2019). Dysregulation of autophagy and stress granule-related proteins in stress-driven Tau pathology. *Cell Death Differ.* 26, 1411–1427. doi: 10.1038/s41418-018-0217-1

Sotiropoulos, I., Cerqueira, J. J., Catania, C., Takashima, A., Sousa, N., and Almeida, O. F. (2008). Stress and glucocorticoid footprints in the brain-the path from depression to Alzheimer's disease. *Neurosci. Biobehav. Rev.* 32, 1161–1173. doi: 10.1016/j.neubiorev.2008.05.007

Starkman, M. N., Gebarski, S. S., Berent, S., and Schteingart, D. E. (1992). Hippocampal formation volume, memory dysfunction and cortisol levels in patients with Cushing's syndrome. *Biol. Psychiatry* 32, 756–765. doi: 10.1016/0006-3223(92)90079-f

Starkman, M. N., Giordani, B., Berent, S., Schork, M. A., and Schteingart, D. E. (2001). Elevated cortisol levels in Cushing's disease are associated with cognitive decrements. *Psychosom. Med.* 63, 985–993. doi: 10.1097/00006842-200111000-00018

Starkman, M. N., Giordani, B., Gebarski, S. S., and Schteingart, D. E. (2003). Improvement in learning associated with increase in hippocampal formation volume. *Biol. Psychiatry* 53, 233–238. doi: 10.1016/s0006-3223(02)01750-x

Tully, T., Bourtchouladze, R., Scott, R., and Tallman, J. (2003). Targeting the CREB pathway for memory enhancers. *Nat. Rev. Drug Discov.* 2, 267–277. doi: 10.1038/nrd1061

Turnbull, A. V., and Rivier, C. L. (1999). Regulation of the hypothalamic-pituitary-adrenal axis by cytokines: actions and mechanisms of action. *Physiol. Rev.* 79, 1–71. doi: 10.1152/physrev.1999.79.1.1

Umegaki, H., Ikari, H., Nakahata, H., Endo, H., Suzuki, Y., Ogawa, O., et al. (2000). Plasma cortisol levels in elderly female subjects with Alzheimer's disease: a cross-sectional and longitudinal study. *Brain Res.* 881, 241–243. doi: 10.1016/s0006-8993(00)02847-x

Wang, Y., Li, M., Tang, J., Song, M., Xu, X., Xiong, J., et al. (2011). Glucocorticoids facilitate astrocytic amyloid-β peptide deposition by increasing the expression of APP and BACE1 and decreasing the expression of amyloid-β-degrading proteases. *Endocrinology* 152, 2704–2715. doi: 10.1210/en.2011-0145

Wei, Q., Hebda-Bauer, E. K., Pletsch, A., Luo, J., Hoversten, M. T., Osetek, A. J., et al. (2007). Overexpressing the glucocorticoid receptor in forebrain causes an aging-like neuroendocrine phenotype and mild cognitive dysfunction. *J. Neurosci.* 27, 8836–8844. doi: 10.1523/JNEUROSCI.0910-07.2007

Wingenfeld, K., and Wolf, O. T. (2014). Stress, memory and the hippocampus. *Front. Neurol. Neurosci.* 34, 109–120. doi: 10.1159/000356423

Zalewska, K., Ong, L. K., Johnson, S. J., Nilsson, M., and Walker, F. R. (2017). Oral administration of corticosterone at stress-like levels drives microglial but not vascular disturbances post-stroke. *Neuroscience* 352, 30–38. doi: 10.1016/j.neuroscience.2017.03.005

Zhang, B., Xu, X., Niu, F., Mao, X., Dong, J., Yang, M., et al. (2020). Corticosterone replacement alleviates hippocampal neuronal apoptosis and spatial memory impairment induced by dexamethasone *via* promoting brain corticosteroid receptor rebalance after traumatic brain injury. *J. Neurotrauma* 37, 262–272. doi: 10.1089/neu.2019.6556

Conflict of Interest: The authors declare that the research was conducted in the absence of any commercial or financial relationships that could be construed as a potential conflict of interest.

frontiers in Molecular Neuroscience

REVIEW
published: 22 January 2021
doi: 10.3389/fnmol.2020.578211

Does Impairment of Adult Neurogenesis Contribute to Pathophysiology of Alzheimer's Disease? A Still Open Question

Domenica Donatella Li Puma[1,2], *Roberto Piacentini*[1,2]* *and Claudio Grassi*[1,2]

[1] *Department of Neuroscience, Università Cattolica del Sacro Cuore, Rome, Italy,* [2] *Fondazione Policlinico Universitario A. Gemelli IRCCS, Rome, Italy*

Adult hippocampal neurogenesis is a physiological mechanism contributing to hippocampal memory formation. Several studies associated altered hippocampal neurogenesis with aging and Alzheimer's disease (AD). However, whether amyloid-β protein (Aβ)/tau accumulation impairs adult hippocampal neurogenesis and, consequently, the hippocampal circuitry, involved in memory formation, or altered neurogenesis is an epiphenomenon of AD neuropathology contributing negligibly to the AD phenotype, is, especially in humans, still debated. The detrimental effects of Aβ/tau on synaptic function and neuronal viability have been clearly addressed both in *in vitro* and *in vivo* experimental models. Until some years ago, studies carried out on *in vitro* models investigating the action of Aβ/tau on proliferation and differentiation of hippocampal neural stem cells led to contrasting results, mainly due to discrepancies arising from different experimental conditions (e.g., different cellular/animal models, different Aβ and/or tau isoforms, concentrations, and/or aggregation profiles). To date, studies investigating *in situ* adult hippocampal neurogenesis indicate severe impairment in most of transgenic AD mice; this impairment precedes by several months cognitive dysfunction. Using experimental tools, which only became available in the last few years, research in humans indicated that hippocampal neurogenesis is altered in cognitive declined individuals affected by either mild cognitive impairment or AD as well as in normal cognitive elderly with a significant inverse relationship between the number of newly formed neurons and cognitive impairment. However, despite that such information is available, the question whether impaired neurogenesis contributes to AD pathogenesis or is a mere consequence of Aβ/pTau accumulation is not definitively answered. Herein, we attempted to shed light on this complex and very intriguing topic by reviewing relevant literature on impairment of adult neurogenesis in mouse models of AD and in AD patients analyzing the temporal relationship between the occurrence of altered neurogenesis and the appearance of AD hallmarks and cognitive dysfunctions.

Keywords: neural stem cells, adult neurogenesis, amyloid-beta protein, tau, Alzheimer's disease, herpes simplex virus type 1

OPEN ACCESS

Edited by:
Robert A. Nichols, University of Hawaii at Manoa, United States

Reviewed by:
Orly Lazarov, University of Illinois at Chicago, United States
Juan Song, University of North Carolina at Chapel Hill, United States

***Correspondence:**
Roberto Piacentini
roberto.piacentini@unicatt.it

Received: *30 June 2020*
Accepted: *15 December 2020*
Published: *22 January 2021*

Citation:
Li Puma DD, Piacentini R and Grassi C (2021) Does Impairment of Adult Neurogenesis Contribute to Pathophysiology of Alzheimer's Disease? A Still Open Question. Front. Mol. Neurosci. 13:578211. doi: 10.3389/fnmol.2020.578211

HIPPOCAMPAL NEUROGENESIS AND MEMORY

The hippocampus is recognized as a brain area primarily involved in memory formation, e.g., pattern separation, emotional memory, and cognitive flexibility (Lazarov and Hollands, 2016; Anacker and Hen, 2017; Hainmueller and Bartos, 2020). The hippocampal circuitry consists of a unidirectional, trisynaptic excitatory pathway in which the dentate gyrus (DG) of the hippocampus receives inputs from the entorhinal cortex (EC), which are then delivered to the CA3 area of the hippocampus and from there to CA1. In turn, CA1 projects to the subiculum and hippocampal outputs are sent back to the deep layers of EC. The classical experimental paradigm used to investigate hippocampal plasticity, underlying memory formation, is the long-term potentiation (LTP) at the CA3-CA1 synapse not involving the DG (Malenka and Nicoll, 1999), and the EC-DG-CA3-CA1 axis could be strongly affected if this pathway is corrupted at the DG. In fact, DG supports various mnemonic functions including contextual discrimination, pattern separation, novelty detection, and integration of individual episodes into a framework of experiences (Hainmueller and Bartos, 2020). Interestingly, the subgranular zone (SGZ) of the DG in the hippocampus is known to be one of the two neurogenic niches in the adult brain, the other being the subventricular zone of the lateral ventricles (Gage, 2019). Adult neurogenesis occurring at the SGZ allows integration of newly formed neurons in the DG circuits (Kitabatake et al., 2007), thus providing this brain area with marked plasticity. As such, adult hippocampal neurogenesis at the DG has been proposed to strongly participate in formation of hippocampal-dependent memory (Gonçalves et al., 2016; Toda et al., 2019; Hainmueller and Bartos, 2020).

Additionally, the hippocampus is one of the brain areas primarily affected by aging and Alzheimer's disease (AD) (Selkoe, 2011). Alzheimer's disease is the most common cause of dementia in the elderly and is characterized by memory loss and cognitive dysfunction. The majority of AD cases are sporadic, and the remaining cases are associated with genetic factors [i.e., familial AD (FAD)]. Mutations in genes, encoding either the amyloid precursor protein (APP) or enzymes catalyzing its proteolytic cleavage (presenilin 1 and 2—PSEN1 and 2—subunits of γ-secretase responsible for amyloid-β peptide—Aβ–generation), along with microtubule-associated protein tau (MAPT) encoding the tau protein, are responsible for FAD. Nowadays, it is widely recognized that memory failure in AD is due to synaptic alterations caused by intra- and extracellular accumulation of Aβ and hyperphosphorylated tau oligomers (Crews et al., 2010; Puzzo et al., 2017). Experimental evidence also suggests that early alterations of DG neurogenesis may concur to the pathogenesis of this neurological disorder (Mu and Gage, 2011; Unger et al., 2016).

AD AND NEUROGENESIS: *IN VITRO* STUDIES

In the last 15 years, many studies investigated hippocampal neurogenesis [i.e., proliferation and neuronal differentiation of hippocampal neural stem cells (NSCs)] in *in vitro* and *in vivo* experimental AD models.

In vitro experimental paradigms usually consisted of NSC incubation with Aβ. However, researches carried out in various laboratories led to contrasting results about the effects of proliferation/differentiation of hippocampal NSCs, mainly because of different (i) Aβ preparations (monomeric, oligomeric, or fibrillar); (ii) peptide lengths (40 vs. 42 amino acids); and (iii) working concentrations, which are often irrelevant from a physiological point of view. For example, in 2004 López-Toledano and Shelanski reported that *in vitro* treatment of hippocampal NSCs with micromolar concentrations of Aβ42 oligomers dose-dependently increased their neuronal differentiation (López-Toledano and Shelanski, 2004). Conversely, more recent results obtained either with lower Aβ concentrations or in cultured NSCs isolated from mouse models harboring the most common genetic alterations observed in FAD indicated impaired proliferation and reduced neuronal differentiation of hippocampus-residing NSCs. In particular, Lee et al. (2013) found that exposure of human NSCs to Aβ-containing conditioned medium from SK-N-MC cells expressing APP Swedish mutation reduced NSC proliferation, impaired neurogenesis, and promoted gliogenesis via glycogen synthase kinase 3β (GSK-3β) activation. Moreover, the exposure of human neural stem cell line hNS1 to nanomolar concentrations of Aβ42 significantly promoted cell proliferation and glial cell specification by increasing the pool of proliferating glial precursors without affecting neuronal differentiation (Bernabeu-Zornoza et al., 2019). A recent study from our lab demonstrated that treatment of cultured murine hippocampal NSCs with Aβ42 oligomers (200 nM)—able to cross plasma membrane, to accumulate intracellularly, and to induce GSK-3 activation (Ripoli et al., 2013, 2014, Scala et al., 2015)—negatively affected their proliferation and neuronal differentiation (Li Puma et al., 2019). Similar results were obtained in NSCs infected with HSV-1, which triggered APP phosphorylation and cleavage with consequent accumulation of several APP fragments including Aβ in several cell types (De Chiara et al., 2010; Piacentini et al., 2011, 2015). The HSV-1-induced hyperproduction of Aβ was correlated with the antimicrobic activity of Aβ42 and interpreted as a defensive response of the infected cell (Soscia et al., 2010; Kumar et al., 2016). Strategies aimed at limiting the production and accumulation of Aβ inside cells (as the use of a γ-secretase inhibitor or the 4G8 antibody raised against Aβ oligomers able to be intracellularly uploaded; Tampellini et al., 2007) counteracted the effects of Aβ42 on *in vitro* neurogenesis (Li Puma et al., 2019). Altered proliferation and neuronal differentiation were also observed in NSCs isolated from 3 × Tg-AD mouse embryos (Leone et al., 2019). These cells exhibited high levels of Aβ oligomers compared with NSCs isolated from wild-type (WT) mouse. Emerging evidence also suggests that downregulated expression of the nucleoporin Nup153 negatively affects the neurogenic niche of 3 × Tg AD mice. Accordingly, restoration of Nup153 levels in hippocampal 3 × Tg-AD NSCs promoted their proliferation, migration, and neuronal maturation (Leone et al., 2019).

HIPPOCAMPAL NEUROGENESIS IN FAD MOUSE MODELS

More robust results have been obtained from studies performed in *in vivo* FAD mouse models often exhibiting impaired neurogenesis correlated with accumulation of molecular AD hallmarks (e.g., Taniuchi et al., 2007; Hollands et al., 2016, 2017; Baglietto-Vargas et al., 2017). However, depending on the FAD model used, this impairment may rely on reduced neurogenesis (lower NSC proliferation, decreased neuronal differentiation, and/or reduced survival of newly formed neurons) or increased gliogenesis (normal of even increased NSC proliferation, followed by differentiation toward the glial rather than neuronal phenotype). Nevertheless, despite the consensus about altered neurogenesis in these mouse models, a clear understanding of whether and how much this impairment contributes to memory/cognitive dysfunction in AD is still missing.

Various FAD mouse models have been developed resembling peculiar features of the disease, which are based on one or more gene-coding mutations in proteins critically involved in AD (Unger et al., 2016). The most applied models use *Tg2576 mice* (Hsiao, 1998), which overexpress APP harboring the Swedish double mutation—KM670/671NL; *PDAPP mice* (Games et al., 1995), which overexpress APP harboring the Indiana (V717F) mutation; and *J20 mice* (Mucke et al., 2000), which overexpress APP harboring both Swedish and Indiana mutations. Other models associate APP mutations to other mutations accounting for PSEN1 and 2 genes encoding for presenilin 1 and 2, as for example the double transgenic "*APP Swedish PS1ΔE9*" (APPswe/PS1ΔE9) mouse model (Jankowsky et al., 2001) or *APP/PS1 mice* harboring APP Swedish and London (V717I) along with the PS1 M146L mutation (Baglietto-Vargas et al., 2017). Finally, the 5 × FAD mouse model, which is a more complex model harboring all five AD-linked mutations accounting for Aβ formation, has also been developed (Oakley et al., 2006). All these models do not consider familial mutations involving the tau protein, which is the other key protein in AD. In this regard, a mouse model representative of the full AD pathology has been developed, associating mutation in the MAPT gene, encoding for tau protein, with those of the other key proteins in AD (APP and PS1). This 3 × Tg-AD model contains three mutations associated with FAD: APP Swedish, PSEN1 M146V, and MAPT P301L (Oddo et al., 2003).

What about neurogenesis in these FAD mouse models? Demars et al. (2010) reported a drastic reduction of NSC proliferation [identified through 5′-bromo-deoxyuridine (BrdU) incorporation] in the SGZ of the hippocampus of APPswe/PS1ΔE9 mice, at 2 months of age, with respect to the age-matched WT animals. These alterations, taking place before the formation of amyloid deposits, were followed by a significant reduction in the number of cells acquiring a neuronal (doublecortin$^+$ -DCX) phenotype (i.e., BrdU$^+$/DCX$^+$ cells) with respect to age-matched WT mice. In agreement with Demars's results, in the same experimental model Unger et al. (2016) found a reduced number of BrdU-positive cells evaluated at 3 months of age, 30 days after BrdU injection, but an increased numbers of PCNA$^+$ cells. PCNA is a protein expressed by proliferating cells in the late G1 and S phases of mitosis, and this difference, observed with these two methods of analysis, may suggest alteration in the cell cycle. However, most of these new cells (positive for either BrdU or PCNA) did not survive during maturation resulting in a reduced number of BrdU$^+$/DCX$^+$ and PCNA$^+$/DCX$^+$ cells, thus indicating impaired adult hippocampal neurogenesis. Similar findings were also obtained in Tg2576 mice, which showed increased NSC proliferation in the SGZ of the hippocampus DG but reduced integration of newly formed neurons in the DG at an age at which these mice exhibited neither amyloid extracellular deposits nor major cognitive impairment (Unger et al., 2016). Unger's data in Tg2576 mice were in agreement with those obtained by Krezymon et al. (2013) in the same mouse model. In APP/PS1 mice, Baglietto-Vargas et al. found a reduced number of SGZ precursor cells along with reduced numbers of BrdU$^+$/DCX$^+$ cells at 4–6 months, i.e., slightly before the onset of cognitive dysfunction (Baglietto-Vargas et al., 2017). Also, 5 × FAD mice exhibited an early impairment of neurogenesis with significantly reduced DCX$^+$ cells in the DG starting from 2 months of age (Moon et al., 2014). In 2008, Rodriguez et al. demonstrated impaired neurogenesis in terms of NSC proliferation and neuronal differentiation/integration of the DG even in 3 × Tg-AD mice. In this mouse, a significant reduction of neurogenesis was evident in females at 4 months of age with respect to age-matched controls, while male mice exhibited these alterations later. Findings about early alteration of hippocampal neurogenesis in 3 × Tg-AD mice were also confirmed by Hamilton et al. (2010). Interestingly, Zheng et al. (2017) demonstrated that intrahippocampal injection of Aβ42 in ovariectomized mice inhibited neurogenesis, which were recovered by 17β-estradiol (E2) treatment; this finding further supported the impact of estrogens in regulating neurogenesis and their potential role in AD pathogenesis. Of note, several conflicting results have been reported on the J20 mouse model, which was found to exhibit either increased neurogenesis with increasing age (López-Toledano and Shelanski, 2007) or impaired neurogenesis independently on Aβ (Pan et al., 2016) and additionally on the APP/PS1 mice, which exhibited increased neurogenesis at later age (Yu et al., 2009), thus indicating that effects on neurogenesis may also depend on a combination of mutations.

A detailed description of how neurogenesis is altered in different AD mouse models was reviewed by Chuang (2010) and Wirths (2017). In **Table 1**, we summarized how neurogenesis is altered in various AD models, highlighting the age at which neurogenesis was impaired and the age at which cognitive dysfunction started.

The finding that impairment of hippocampal neurogenesis in FAD mice occurs before (i) AD hallmarks accumulation and (ii) appearance of learning and memory dysfunction suggests that the former might have a causal role in cognitive decline characterizing prodromal AD.

In support of this hypothesis, experimental evidence indicates that ablation of hippocampal neurogenesis in APPswe/PS1ΔE9

TABLE 1 | Alteration of adult hippocampal neurogenesis in FAD and sporadic AD mouse models.

Mouse model	Alteration in hippocampal neurogenesis	Age at impaired neurogenesis	Age at the occurrence of cognitive decline	Reference(s)
APP Swe PS1 ΔE9 (FAD)	Reduced proliferation of NSCs ($BrdU^+$). Reduced survival of newly generated cells. Reduced neuronal commitment (DCX^+)	2 months	8 months	Demars et al., 2010
	Increased number of $PCNA^+$ and $PCNA^+/DCX^+$ NSCs. Reduced number of $BrdU^+$ NSCs 30 days after BrdU injection. Reduced number of newly generated cells neurons ($BrdU^+/NeuN^+$)	3 months		Unger et al., 2016
Tg2576 (FAD)	Increased proliferation of NSCs ($PCNA^+$) and of newly generated neuroblasts ($PCNA^+/DCX^+$ cells). Reduced survival of newly generated cells. Reduced number of newly generated cells neurons ($BrdU^+/NeuN^+$)	3 months	6–8 months	Unger et al., 2016
APP/PS1 (FAD)	Reduced proliferation of NSCs ($BLPL^+$). Reduced number of $BrdU^+/DCX^+$ cells	4–6 months	6 months	Baglietto-Vargas et al., 2017
	Increased proliferation of NSCs ($BrdU^+$); increased number of newly generated neuroblasts ($BrdU^+/DCX^+$) and mature neurons ($BrdU^+$/NeuN)	9 months	9 months	Yu et al., 2009
5xFAD (FAD)	Decrease of neuroblasts (DCX^+) in the DG	2 months	4–5 months	Moon et al., 2014
3xTg-AD (FAD)	Reduced proliferation and neuronal differentiation	3–4 months (for female mice)	6 months	Rodríguez et al., 2008
J20 (FAD)	Increased proliferation and neuronal differentiation	3 months	4 months	López-Toledano and Shelanski, 2007
HSV-1 infected (sporadic)	Reduced proliferation of NSCs ($BrdU^+$) along with reduced neuronal commitment (DCX^+)	5 months	10 months	De Chiara et al., 2019; Li Puma et al., 2019

mice alters hippocampal circuitry and excitability exacerbating performance deficits with respect to age-matched non-ablated animals (Hollands et al., 2017). Similar results were also observed in 5 × FAD mice, exhibiting worsened cognitive abilities after ablation of adult hippocampal neurogenesis (Choi et al., 2018). On the contrary, stimulation of neurogenesis with drugs (P7C3), Wnt3-expressing lentivirus, or physical exercise ameliorates cognitive deficits in transgenic 5 × FAD mice and reduces amyloid burden (Choi et al., 2018). These authors suggested that neither exercise nor stimulation of adult hippocampal neurogenesis alone had beneficial effects but only the association of the two stimuli was effective in this AD mouse model. In slight contrast with this study, physical exercise was sufficient to reduce Aβ plaque burden in 3 × Tg-AD mice, to increase neurogenesis at the DG, and to improve cognitive functions (Kim et al., 2019). Moreover, the experimental paradigm of "enriched environment" was effective in ameliorating cognitive functions in APPswe/PS1ΔE9 mice along with rescue of neural progenitor cell proliferation in the hippocampus, survival and incorporation of newly born cells in preexisting hippocampal circuits, and reduction of Aβ load and tau phosphorylation in the hippocampus of this FAD model (Lazarov et al., 2005; Hu et al., 2010). In any case, all these studies highlighted a positive correlation between hippocampal neurogenesis and cognitive functions in AD experimental models, even if it is known that physical exercise does not selectively improve neurogenesis but it acts on several targets (e.g., BDNF and other factors; Saraulli et al., 2017; Liu and Nusslock, 2018), which may support cognitive functions independently on neurogenesis. Finally, Yan et al. (2014) showed that adult bone marrow-derived mesenchymal stem cell transplantation improves memory and cognitive functions of APP/PS1 mice by enhancing endogenous neurogenesis in hippocampal SGZ. Another recent study (Micci et al., 2019) demonstrated that exosomes (containing miR-322, miR-17, and miR-485 miRNAs acting at the synaptic level), released from NSCs, significantly decrease Aβ oligomer binding at synapses and protect the hippocampus from Aβ oligomer-induced impairment of LTP and memory deficits. Therefore, NSCs might significantly contribute to fight the progression of the disease, independently on the replacement of lost neurons. Conversely, a partial rescue of the impairment of adult hippocampal neurogenesis was observed following reductions

of Aβ load in double transgenic APP/PS1 mice by passive Aβ immunotherapy (Biscaro et al., 2009).

Notably, all these studies demonstrated that stimuli ameliorating/increasing neurogenesis reduce the appearance of AD hallmarks; this suggests the possibility that not only Aβ/pTau affect neurogenesis, but also molecular mechanisms controlling neurogenesis influence Aβ clearance/degradation and/or tau phosphorylation.

Even if aging does not represent a pathological condition, it is a main risk factor for AD and aged people and experimental models often exhibit a decline of cognitive abilities. Dentate gyrus is one of the primary initial targets of normal aging (reviewed in Lazarov and Hollands, 2016), and hippocampal neurogenesis is negatively affected by this process, resulting in reduced NSC proliferation rates, neuroblast numbers, and immature neurons as well as differentiated granule cells in the DG (Lazarov and Hollands, 2016; Toda et al., 2019). These aging-dependent effects on neurogenesis could impact on structural and functional plasticity of the hippocampus, likely contributing to cognitive deficits in the elderly. Indeed, strategies aimed to increase adult neurogenesis in the hippocampus of aged mice [e.g., by transient overexpression of a negative regulator of dendritic spines, Kruppel-like factor 9 (McAvoy et al., 2016) or by attenuating bone morphogenetic protein signaling (Yousef et al., 2015)] improved their cognitive abilities and long-term memory (Toda et al., 2019). Notably, the above-cited FAD models also showed an age-dependent decrease in neurogenesis associated with an increase in the number of Aβ-containing neurons in the hippocampus and the presence of Aβ plaques.

HIPPOCAMPAL NEUROGENESIS IN HSV-1-INFECTED MOUSE MODEL

All the mouse models discussed above are genetically modified to develop AD hallmarks/pathology. This does not resemble what occurs in sporadic AD, in which a "normal" subject not carrying familial AD mutations starts exhibiting signs of impaired memory and learning because of undefined triggering factors. From this point of view, data obtained in a mouse model of HSV-1 infection and the recurrent reactivation that we recently set up are worth mentioning (De Chiara et al., 2019). This mouse model is reminiscent of sporadic AD phenotype. In fact, after infection and multiple cycles of virus reactivation promoting its spreading within the brain, the infected mice exhibited accumulation of amyloid-β and hyperphosphorylated tau proteins in several brain areas including the hippocampus. These molecular changes were accompanied by memory deficits that were very marked after 7 cycles of viral reactivation in mice and not found in age-matched mock-infected mice not exhibiting Aβ or pTau accumulation (De Chiara et al., 2019).

Infected mice also exhibited impaired adult hippocampal neurogenesis consisting in (i) reduced proliferation of NSCs residing in the SGZ and (ii) decreased differentiation toward the neuronal phenotype. These changes were statistically significant before the onset of memory deficits, i.e., after 2 cycles of thermal stress. Specifically, in the brain of infected mice the number of proliferating NSCs (identified through BrdU and Ki67 labeling) in the SGZ of the DG was significantly reduced with respect to mock-infected mice, and the percentage of cells acquiring glial phenotype [i.e., immunoreactive for the glial fibrillary acidic protein (GFAP)] vs. neuronal one [doublecortin (DCX)-positive] was significantly higher than in mock-infected cells (Li Puma et al., 2019). These findings suggested us that in this experimental model alteration of hippocampal neurogenesis precedes memory impairment, strongly supporting the contention that altered neurogenesis contributes to memory deficits also in sporadic AD.

HIPPOCAMPAL NEUROGENESIS, APP, AND APP CLEAVAGE PRODUCTS

Interestingly, mice lacking amyloid precursor protein (APP KO) did not exhibit alterations in neurogenesis following HSV-1 infection and recurrent virus reactivations (Li Puma et al., 2019) despite the presence of viral particles in the hippocampus. Rather, mice lacking APP exhibited a higher number of BrdU-positive cells in the DG (Coronel et al., 2019a; Li Puma et al., 2019). These results suggest that virus *per se* does not have direct effects on neurogenesis and that APP cleavage products (e.g., Aβ) may play a major role in modulating adult hippocampal neurogenesis. As extensively reviewed in Lazarov and Demars (2012), Aβ is not the only APP product affecting neurogenesis in the hippocampus of adult mice. Other APP metabolites, derived from proteolytic processing by specific secretases, such as the secreted N-terminal-soluble fragments of APP cleaved by α- (sAPPα) or β-secretase (sAPPβ), and the APP intracellular C-terminal domain (AICD), cleaved by γ-secretase, reportedly modulate various NSC functions including proliferation, neuronal vs. glial differentiation, and death (Coronel et al., 2019b). In particular, sAPPα, obtained by the physiological non-amyloidogenic cleavage of APP, has neuroprotective and neurotrophic functions by promoting proliferation of NSCs (Demars et al., 2011, 2013). In contrast, sAPPβ derived by the Aβ-producing amyloidogenic pathway of APP has a lower efficacy than α counterpart (Demars et al., 2013). However, both sAPPα and sAPPβ were found to increase proliferation of neural precursor cells derived from the SGZ of adult rats *in vitro* and to promote glial differentiation (Baratchi et al., 2012). Finally, in human embryonic teratocarcinoma cells (NT-2/D1), often used as experimental model to investigate neural differentiation, sAPPα promotes glial fate (Kwak et al., 2006) by stimulating bone morphogenic protein signaling (Kwak et al., 2014), which is involved in aged-associated cognitive decline.

Unlike sAPPα and sAPPβ, AICD seems to negatively impact on neurogenesis. In fact, as reviewed in Coronel et al. (2019b) and Lazarov and Demars (2012), AICD strongly inhibited proliferation of NSCs acting as transcriptional regulator. Indeed, in AICD transgenic mice proliferation and survival of progenitor cells were strongly reduced while neuronal differentiation was unaffected (Ghosal et al., 2010). Moreover, NSC differentiation reportedly depended on γ-secretase activity (Gadadhar et al., 2011).

Although HSV-1 infection in cultured hippocampal NSCs determined increased APP processing with the consequent intracellular accumulation of Aβ peptides and intranuclear accumulation of AICD, we found that the 4G8 antibody (recognizing the 17–24 sequence of Aβ) was able to completely revert the effects of HSV-1 on *in vitro* neurogenesis, suggesting that the contribution of other APP fragments (e.g., AICD) to HSV-1-induced impaired neurogenesis is negligible. However, we cannot exclude, *in vivo,* that other APP metabolites generated after HSV-1-induced APP amyloidogenic cleavage may participate in the alteration of neurogenesis.

Finally, although most of the functions exerted by APP and its proteolytic fragments have been described, the molecular mechanisms and the signaling pathways involved in these effects remain mostly unknown. APP belongs to a superfamily including the homologs APLP1 and APLP2, which are expressed in APP KO mice. While mouse KO for APP/APLP1 is viable, APP/APLP2, and APLP1/APLP2 KO mice do not survive, which stresses the importance of APLP2. Interestingly, the *in vivo* silencing of APLP2 in an APP/APLP1 double knockout mouse keeps cortical progenitors much longer in their undifferentiated state, which is consistent with the view that APLP2 plays a key role in the commitment of neuronal progenitors to neuronal differentiation (Shariati et al., 2013).

ALZHEIMER'S DISEASE, MEMORY LOSS, AND ALTERED NEUROGENESIS: THE ROLE OF TAU

Although this review primarily deals with the impact of APP fragments on neurogenesis, experimental evidence suggests that tau is the real bad player in AD. Specifically, tau oligomers target neurons and astrocytes involved in tripartite synapses, which affect synaptic transmission and synaptic plasticity (Guerrero-Muñoz et al., 2015; Fá et al., 2016; Piacentini et al., 2017; Puzzo et al., 2017; Li et al., 2018). Tau has also been reported to negatively affect hippocampal neurogenesis (see Fuster-Matanzo et al., 2012). In 2010, Demars et al. demonstrated that APPswe/PS1ΔE9 mice exhibited a significant increase in tau phosphorylation in several brain areas including the hippocampus, likely contributing to the development of the AD phenotype. As discussed above, exposure of these mice to an enriched environment reduced, besides ameliorating cognitive functions and neurogenesis, also accumulation of phosphorylated tau in their hippocampus (Hu et al., 2010). In agreement with these results, more recent studies reported that human tau mice and FTDP-17 mutant tau mice exhibited a decrease in proliferation of neuronal precursors (Komuro et al., 2015; Houben et al., 2019). Pallas-Bazarra et al. (2016) demonstrated a novel role played by tau in NSC survival after stressful stimuli; they demonstrated that tau is fundamental for morphological and functional maturation of newborn granule neurons using a tau KO mouse model. $Tau^{-/-}$ mice show impairment in the maturation of newborn granule neurons, and they are insensitive to the modulation of adult hippocampal neurogenesis exerted by external stimuli. Tau protein also facilitates DCX-positive cell migration from the SGZ to the granular layer of the hippocampus, a process that requires a dynamic microtubule network. Therefore, it is conceivable that the increased dynamics and destabilization of microtubules caused by hyperphosphorylation of tau protein may contribute to impaired hippocampal neurogenesis (Fuster-Matanzo et al., 2009, 2012). Very recent studies reported that pTau accumulation in DG interneurons impair adult hippocampal neurogenesis by suppressing GABAergic transmission (Zheng et al., 2020) and that tau KO mice exhibit increased neurogenesis in the DG at 14 months of age compared with WT mice matched for age (Criado-Marrero et al., 2020). In support of a role for tau in neurogenesis, Houben et al. (2019) demonstrated that deletion of tau in a transgenic mouse model of tauopathy (Tg30 mice harboring FTDP-17 mutant tau) rescued the alteration in hippocampal neurogenesis exhibited by these mice.

There is a strong interplay between Aβ and tau, and a common, although controversial, opinion in the field is that tau pathology would be triggered by Aβ (Bloom, 2014). For example, it was demonstrated that endogenously produced Aβ induces tau hyperphosphorylation in cell cultures (Wang et al., 2006) and recent *in vivo* PET-imaging studies suggested that Aβ is a prerequisite for tau pathology (Franzmeier et al., 2019; Pontecorvo et al., 2019). Two main protein kinases have been shown to be involved in aberrant tau phosphorylation: the cyclin-dependent kinase (Cdk5) and GSK-3β. A deregulation of these kinases, induced by extracellular amyloid loading, results in tau hyperphosphorylation (Maccioni et al., 2001). As discussed above, tau hyperphosphorylation was found in FAD mice in which genetic alterations account for APP and its cleaving enzymes (APPswe/PS1ΔE9; Demars et al., 2010), supporting the idea of a cross talk among Aβ and tau. Reduction of Aβ burden by *scyllo*-inositol in TgF344-AD rats reduced tau pathology and rescued adult hippocampal neurogenesis (Morrone et al., 2020). We cannot exclude that the effects of tau on adult neurogenesis are mediated by Aβ load, although another view has been recently proposed that Aβ and tau exert their detrimental action by acting in parallel, probably sharing common targets, rather than acting in series (Puzzo et al., 2020).

ALZHEIMER'S DISEASE, MEMORY LOSS, AND ALTERED NEUROGENESIS: HUMAN STUDIES

Despite the large number of studies about the relationship among altered neurogenesis and AD, some questions still remain unanswered: is this alteration disrupting the hippocampal circuitry involved in memory formation? Does it significantly contribute to memory loss in AD? Are the results obtained in *in vitro* and *in vivo* murine models translatable to humans? Is recovery/activation of neurogenesis a useful tool to prevent the onset and/or counteract the progression of AD? Some tentative answers to these questions can be found in recent reviews from Kempermann et al. (2018) and Cosacak et al. (2020), but more in-depth investigations are absolutely needed to address these issues.

What about neurogenesis in humans and its involvement in neurodegenerative diseases? Recently, some independent studies (Mathews et al., 2017; Boldrini et al., 2018; Moreno-Jiménez et al., 2019; Tobin et al., 2019) demonstrated that (i) adult hippocampal neurogenesis also occurs in human brain and it contributes to adding new granule cells to the DG throughout the lifespan even though the efficiency of this mechanism decreases with age and (ii) in AD patients, the number and maturation of newly generated neurons progressively decline as the disease proceeds. In particular, Tobin et al. found a significant inverse relationship between the number of newly formed neuroblasts and cognitive impairment, with MCI patients exhibiting fewer $DCX^+/PCNA^+$ cells than cognitive normal subjects (Tobin et al., 2019). Another study correlated adult hippocampal neurogenesis with AD and major depressive disorder, which are known to interact reciprocally elevating the risk for one another (Berger et al., 2020). Although several previous researches unsuccessfully attempted to identify adult hippocampal neurogenesis in humans, and then questioned the existence of this process in the adult brain (Paredes et al., 2018; Sorrells et al., 2018), more recent studies demonstrated the existence of this process owing to the application of new methods of tissue sample preservation from postmortem brain, thus allowing a more precise recognition of NSCs, and additionally, the application of this approach to AD patient brains.

CONCLUSIONS

Collectively, literature discussed in this review adds new layers of knowledge on the link between impairment of adult hippocampal neurogenesis and cognitive dysfunction in AD. Specifically, it is reasonable to hypothesize that altered adult hippocampal neurogenesis, due to intracellular accumulation of Aβ and pTau, may have a significant impact on the hippocampal circuitry underlying memory formation, which actively contributes to disease progression. Indeed, data obtained from murine models reminiscent of both FAD and sporadic AD clearly indicate that alterations of neurogenesis (in terms of reduced NSC proliferation, survival of neuroblasts, and functional integration of newly formed neurons) occur before the appearance of memory impairment and that stimuli, increasing hippocampal neurogenesis, ameliorate cognitive functions of AD mice. To date, a correlation between altered hippocampal neurogenesis and AD has been suggested in humans, although the cause–effect relationship between these two processes has not been ascertained yet. Therefore, strategies aimed at restoring and/or boosting adult hippocampal neurogenesis in both normal elderly people and subjects at high risk of AD (e.g., individuals with MCI) could emerge as effective strategies to prevent the onset and/or counteracting the progression of the disease. In this perspective, it is worth mentioning that in mouse models exposed to extremely low-frequency electromagnetic fields a significantly enhanced adult neurogenesis at both hippocampal DG and the subventricular zone has been reported along with memory improvement (Cuccurazzu et al., 2010; Leone et al., 2014; Podda et al., 2014; Mastrodonato et al., 2018).

AUTHOR CONTRIBUTIONS

Manuscript was written and revised by RP, DDLP, and CG. All authors approved the final version of the manuscript.

ACKNOWLEDGMENTS

Università Cattolica del Sacro Cuore contributed to funding this research project and its publication. We would like to thank Franziska M. Lohmeyer, Ph.D., Fondazione Policlinico Universitario A. Gemelli, for her support revising our manuscript.

REFERENCES

Anacker, C., and Hen, R. (2017). Adult hippocampal neurogenesis and cognitive flexibility — linking memory and mood. *Nat. Rev. Neurosci*. 18, 335–346. doi: 10.1038/nrn.2017.45

Baglietto-Vargas, D., Sánchez-Mejias, E., Navarro, V., Jimenez, S., Trujillo-Estrada, L., Gómez-Arboledas, A., et al. (2017). Dual roles of Aβ in proliferative processes in an amyloidogenic model of alzheimer's disease. *Sci. Rep*. 7:10085. doi: 10.1038/s41598-017-10353-7

Baratchi, S., Evans, J., Tate, W. P., Abraham, W. C., and Connor, B. (2012). Secreted amyloid precursor proteins promote proliferation and glial differentiation of adult hippocampal neural progenitor cells. *Hippocampus* 22, 1517–1527. doi: 10.1002/hipo.20988

Berger, T., Lee, H., Young, A. H., Aarsland, D., and Thuret, S. (2020). Adult hippocampal neurogenesis in major depressive disorder and alzheimer's disease. *Trends Mol. Med*. 26, 803–818. doi: 10.1016/j.molmed.2020.03.010

Bernabeu-Zornoza, A., Coronel, R., Palmer, C., Calero, M., Martínez-Serrano, A., Cano, E., et al. (2019). Aβ42 peptide promotes proliferation and gliogenesis in human neural stem cells. *Mol. Neurobiol*. 56, 4023–4036. doi: 10.1007/s12035-018-1355-7

Biscaro, B., Lindvall, O., Hock, C., Ekdahl, C. T., and Nitsch, R. M. (2009). Aβ immunotherapy protects morphology and survival of adult-born neurons in doubly transgenic APP/PS1 mice. *J. Neurosci*. 29, 14108–14119. doi: 10.1523/JNEUROSCI.2055-09.2009

Bloom, G. S. (2014). Amyloid-β and tau: the trigger and bullet in alzheimer disease pathogenesis. *JAMA Neurol*. 71, 505–508. doi: 10.1001/jamaneurol.2013.5847

Boldrini, M., Fulmore, C. A., Tartt, A. N., Simeon, L. R., Pavlova, I., Poposka, V., et al. (2018). Human hippocampal neurogenesis persists throughout aging. *Cell Stem Cell*. 22, 589–599.e5. doi: 10.1016/j.stem.2018.03.015

Choi, S. H., Bylykbashi, E., Chatila, Z. K., Lee, S. W., Pulli, B., Clemenson, G. D., et al. (2018). Combined adult neurogenesis and BDNF mimic exercise effects on cognition in an alzheimer's mouse model. *Science* 361:eaan8821. doi: 10.1126/science.aan8821

Chuang, T. T. (2010). Neurogenesis in mouse models of alzheimer's disease. *Biochim. Biophys. Acta* 1802, 872–880. doi: 10.1016/j.bbadis.2009.12.008

Coronel, R., Lachgar, M., Bernabeu-Zornoza, A., Palmer, C., Domínguez-Alvaro, M., Revilla, A., et al. (2019a). Neuronal and glial differentiation of human neural stem cells is regulated by amyloid precursor protein (APP) levels. *Mol. Neurobiol*. 56, 1248–1261. doi: 10.1007/s12035-018-1167-9

Coronel, R., Palmer, C., Bernabeu-Zornoza, A., Monteagudo, M., Rosca, A., Zambrano, A., et al. (2019b). Physiological effects of amyloid precursor protein and its derivatives on neural stem cell biology and signaling pathways involved. *Neural Regen Res*. 14, 1661–1671. doi: 10.4103/1673-5374.257511

Cosacak, M. I., Bhattarai, P., and Kizil, C. (2020). Alzheimer's disease, neural stem cells and neurogenesis: cellular phase at single-cell level. *Neural Regen Res.* 15, 824–827. doi: 10.4103/1673-5374.268896

Crews, L., Rockenstein, E., and Masliah, E. (2010). APP transgenic modeling of alzheimer's disease: mechanisms of neurodegeneration and aberrant neurogenesis. *Brain Struct. Func.* 214, 111–126. doi: 10.1007/s00429-009-0232-6

Criado-Marrero, M., Sabbagh, J. J., Jones, M. R., Chaput, D., Dickey, C. A., and Blair, L. J. (2020). Hippocampal neurogenesis is enhanced in adult tau deficient mice. *Cells* 9:210. doi: 10.3390/cells9010210

Cuccurazzu, B., Leone, L., Podda, M. V., Piacentini, R., Riccardi, E., Ripoli, C., et al. (2010). Exposure to extremely low-frequency (50 Hz) electromagnetic fields enhances adult hippocampal neurogenesis in C57BL/6 mice. *Exp. Neurol.* 226, 173–182. doi: 10.1016/j.expneurol.2010.08.022

De Chiara, G., Marcocci, M. E., Civitelli, L., Argnani, R., Piacentini, R., Ripoli, C., et al. (2010). APP processing induced by herpes simplex virus type 1 (HSV-1) yields several APP fragments in human and rat neuronal cells. *PLoS ONE* 5:e13989. doi: 10.1371/journal.pone.0013989

De Chiara, G., Piacentini, R., Fabiani, M., Mastrodonato, A., Marcocci, M. E., Limongi, D., et al. (2019). Recurrent herpes simplex virus-1 infection induces hallmarks of neurodegeneration and cognitive deficits in mice. *PLoS Pathog.* 15:e1007617. doi: 10.1371/journal.ppat.1007617

Demars, M., Hu, Y. S., Gadadhar, A., and Lazarov, O. (2010). Impaired neurogenesis is an early event in the etiology of familial alzheimer's disease in transgenic mice. *J. Neurosci. Res.* 88, 2103–2117. doi: 10.1002/jnr.22387

Demars, M. P., Bartholomew, A., Strakova, Z., and Lazarov, O. (2011). Soluble amyloid precursor protein: a novel proliferation factor of adult progenitor cells of ectodermal and mesodermal origin. *Stem Cell Res. Ther.* 2:36. doi: 10.1186/scrt77

Demars, M. P., Hollands, C., Zhao, K., and Lazarov, O. (2013). Soluble amyloid precursor protein-α rescues age-linked decline in neural progenitor cell proliferation. *Neurobiol. Aging* 34, 2431–2440. doi: 10.1016/j.neurobiolaging.2013.04.016

Fá, M., Puzzo, D., Piacentini, R., Staniszewski, A., Zhang, H., Baltrons, M. A., et al. (2016). Extracellular tau oligomers produce an immediate impairment of LTP and memory. *Sci. Rep.* 6:19393. doi: 10.1038/srep19393

Franzmeier, N., Rubinski, A., Neitzel, J., Ewers, M., and Alzheimer's Disease Neuroimaging Initiative (ADNI) (2019). The BIN1 rs744373 SNP is associated with increased tau-PET levels and impaired memory. *Nat. Commun.* 10:1766. doi: 10.1038/s41467-019-09564-5

Fuster-Matanzo, A., de Barreda, E. G., Dawson, H. N., Vitek, M. P., Avila, J., and Hernández, F. (2009). Function of tau protein in adult newborn neurons. *FEBS Lett.* 583, 3063–3068. doi: 10.1016/j.febslet.2009.08.017

Fuster-Matanzo, A., Llorens-Martín, M., Jurado-Arjona, J., Avila, J., and Hernández, F. (2012). Tau protein and adult hippocampal neurogenesis. *Front. Neurosci.* 6:104. doi: 10.3389/fnins.2012.00104

Gadadhar, A., Marr, R., and Lazarov, O. (2011). Presenilin-1 regulates neural progenitor cell differentiation in the adult brain. *J. Neurosci.* 31, 2615–2623. doi: 10.1523/JNEUROSCI.4767-10.2011

Gage, F. H. (2019). Adult neurogenesis in mammals. *Science* 364, 827–828. doi: 10.1126/science.aav6885

Games, D., Adams, D., Alessandrini, R., Barbour, R., Berthelette, P., Blackwell, C., et al. (1995). Alzheimer-type neuropathology in transgenic mice overexpressing V717F beta-amyloid precursor protein. *Nature* 373, 523–527. doi: 10.1038/373523a0

Ghosal, K., Stathopoulos, A., and Pimplikar, S. W. (2010). APP intracellular domain impairs adult neurogenesis in transgenic mice by inducing neuroinflammation. *PLoS ONE* 5:e11866. doi: 10.1371/journal.pone.0011866

Gonçalves, J. T., Schafer, S. T., and Gage, F. H. (2016). Adult neurogenesis in the hippocampus: from stem cells to behavior. *Cell* 167, 897–914. doi: 10.1016/j.cell.2016.10.021

Guerrero-Muñoz, M. J., Gerson, J., and Castillo-Carranza, D. L. (2015). Tau oligomers: the toxic player at synapses in alzheimer's disease. *Front. Cell. Neurosci.* 9:464. doi: 10.3389/fncel.2015.00464

Hainmueller, T., and Bartos, M. (2020). Dentate gyrus circuits for encoding, retrieval and discrimination of episodic memories. *Nat. Rev. Neurosci.* 21, 153–168. doi: 10.1038/s41583-019-0260-z

Hamilton, L. K., Aumont, A., Julien, C., Vadnais, A., Calon, F., and Fernandes, K. J. (2010). Widespread deficits in adult neurogenesis precede plaque and tangle formation in the 3xTg mouse model of alzheimer's disease. *Eur. J. Neurosci.* 32, 905–920. doi: 10.1111/j.1460-9568.2010.07379.x

Hollands, C., Bartolotti, N., and Lazarov, O. (2016). Alzheimer's disease and hippocampal adult neurogenesis; exploring shared mechanisms. *Front. Neurosci.* 10:178. doi: 10.3389/fnins.2016.00178

Hollands, C., Tobin, M. K., Hsu, M., Musaraca, K., Yu, T. S., Mishra, R., et al. (2017). Depletion of adult neurogenesis exacerbates cognitive deficits in alzheimer's disease by compromising hippocampal inhibition. *Mol. Neurodegener.* 12:64. doi: 10.1186/s13024-017-0207-7

Houben, S., Leroy, K., Ando, K., Yilmaz, Z., Widomski, C., Buée, L., et al. (2019). Genetic ablation of tau in postnatal neurons rescues decreased adult hippocampal neurogenesis in a tauopathy model. *Neurobiol. Dis.* 127, 131–141. doi: 10.1016/j.nbd.2019.02.021

Hsiao, K. (1998). Transgenic mice expressing alzheimer amyloid precursor proteins. *Exp. Gerontol.* 33, 883–889. doi: 10.1016/S0531-5565(98)00045-X

Hu, Y. S., Xu, P., Pigino, G., Brady, S. T., Larson, J., and Lazarov, O. (2010). Complex environment experience rescues impaired neurogenesis, enhances synaptic plasticity, and attenuates neuropathology in familial alzheimer's disease-linked APPswe/PS1DeltaE9 mice. *FASEB J.* 24, 1667–1681. doi: 10.1096/fj.09-136945

Jankowsky, J. L., Slunt, H. H., Ratovitski, T., Jenkins, N. A., Copeland, N. G., and Borchelt, D. R. (2001). Co-expression of multiple transgenes in mouse CNS: a comparison of strategies. *Biomol. Eng.* 17, 157–165. doi: 10.1016/S1389-0344(01)00067-3

Kempermann, G., Gage, F. H., Aigner, L., Song, H., Curtis, M. A., Thuret, S., et al. (2018). Human adult neurogenesis: evidence and remaining questions. *Cell Stem Cell* 23, 25–30. doi: 10.1016/j.stem.2018.04.004

Kim, D., Cho, J., and Kang, H. (2019). Protective effect of exercise training against the progression of alzheimer's disease in 3xTg-AD mice. *Behav. Brain Res.* 374:112105. doi: 10.1016/j.bbr.2019.112105

Kitabatake, Y., Sailor, K. A., Ming, G., and Song, H. (2007). Adult neurogenesis and hippocampal memory function: new cells, more plasticity, new memories? *Neurosurg. Clin. N. Am.* 18, 105–113. doi: 10.1016/j.nec.2006.10.008

Komuro, Y., Xu, G., Bhaskar, K., and Lamb, B. T. (2015). Human tau expression reduces adult neurogenesis in a mouse model of tauopathy. *Neurobiol. Aging* 36, 2034–2042. doi: 10.1016/j.neurobiolaging.2015.03.002

Krezymon, A., Richetin, K., Halley, H., Roybon, L., Lassalle, J. M., Francès, B., et al. (2013). Modifications of hippocampal circuits and early disruption of adult neurogenesis in the tg2576 mouse model of alzheimer's disease. *PLoS ONE* 8:e76497. doi: 10.1371/journal.pone.0076497

Kumar, D. K., Choi, S. H., Washicosky, K. J., Eimer, W. A., Tucker, S., Ghofrani, J., et al. (2016). Amyloid-β peptide protects against microbial infection in mouse and worm models of alzheimer's disease. *Sci. Trans. Med.* 8:340ra72. doi: 10.1126/scitranslmed.aaf1059

Kwak, Y. D., Brannen, C. L., Qu, T., Kim, H. M., Dong, X., Soba, P., et al. (2006). Amyloid precursor protein regulates differentiation of human neural stem cells. *Stem Cells Dev.* 15, 381–389. doi: 10.1089/scd.2006.15.381

Kwak, Y. D., Hendrix, B. J., and Sugaya, K. (2014). Secreted type of amyloid precursor protein induces glial differentiation by stimulating the BMP/Smad signaling pathway. *Biochem. Biophys. Res. Commun.* 447, 394–399. doi: 10.1016/j.bbrc.2014.03.139

Lazarov, O., and Demars, M. P. (2012). All in the family: how the APPs regulate neurogenesis. *Front. Neurosci.* 6:81. doi: 10.3389/fnins.2012.00081

Lazarov, O., and Hollands, C. (2016). Hippocampal neurogenesis: learning to remember. *Prog. Neurobiol.* 138–140, 1–18. doi: 10.1016/j.pneurobio.2015.12.006

Lazarov, O., Robinson, J., Tang, Y. P., Hairston, I. S., Korade-Mirnics, Z., Lee, V. M., et al. (2005). Environmental enrichment reduces Abeta levels and amyloid deposition in transgenic mice. *Cell* 120, 701–713. doi: 10.1016/j.cell.2005.01.015

Lee, I. S., Jung, K., Kim, I. S., and Park, K. I. (2013). Amyloid-β oligomers regulate the properties of human neural stem cells through GSK-3β signaling. *Exp. Mol. Med.* 45:e60. doi: 10.1038/emm.2013.125

Leone, L., Colussi, C., Gironi, K., Longo, V., Fusco, S., Li Puma, D. D., et al. (2019). Altered Nup153 expression impairs the function of cultured hippocampal neural stem cells isolated from a mouse model of alzheimer's disease. *Mol. Neurobiol.* 56, 5934–5949. doi: 10.1007/s12035-018-1466-1

Leone, L., Fusco, S., Mastrodonato, A., Piacentini, R., Barbati, S. A., Zaffina, S., et al. (2014). Epigenetic modulation of adult hippocampal neurogenesis by extremely low-frequency electromagnetic fields. *Mol. Neurobiol.* 49, 1472–1486. doi: 10.1007/s12035-014-8650-8

Li Puma, D. D., Piacentini, R., Leone, L., Gironi, K., Marcocci, M. E., De Chiara, G., et al. (2019). Herpes simplex virus type-1 infection impairs adult hippocampal neurogenesis via amyloid-β protein accumulation. *Stem Cells* 37, 1467–1480. doi: 10.1002/stem.3072

Li, K., Wei, Q., Liu, F. F., Hu, F., Xie, A. J., Zhu, L. Q., et al. (2018). Synaptic dysfunction in Alzheimer's disease: Aβ, tau, and epigenetic alterations. *Mol. Neurobiol.* 55, 3021–3032. doi: 10.1007/s12035-017-0533-3

Liu, P. Z., and Nusslock, R. (2018). Exercise-mediated neurogenesis in the hippocampus via BDNF. *Front. Neurosci.* 12:52. doi: 10.3389/fnins.2018.00052

López-Toledano, M. A., and Shelanski, M. L. (2004). Neurogenic effect of beta-amyloid peptide in the development of neural stem cells. *J. Neurosci.* 24, 5439–5444. doi: 10.1523/JNEUROSCI.0974-04.2004

López-Toledano, M. A., and Shelanski, M. L. (2007). Increased neurogenesis in young transgenic mice overexpressing human APP(Sw, Ind). *J. Alzheimers. Dis.* 12, 229–240. doi: 10.3233/JAD-2007-12304

Maccioni, R. B., Muñoz, J. P., and Barbeito, L. (2001). The molecular bases of alzheimer's disease and other neurodegenerative disorders. *Arch. Med. Res.* 32, 367–381. doi: 10.1016/S0188-4409(01)00316-2

Malenka, R. C., and Nicoll, R. A. (1999). Long-term potentiation–a decade of progress? *Science* 285, 1870–1874. doi: 10.1126/science.285.5435.1870

Mastrodonato, A., Barbati, S. A., Leone, L., Colussi, C., Gironi, K., Rinaudo, M., et al. (2018). Olfactory memory is enhanced in mice exposed to extremely low-frequency electromagnetic fields via Wnt/?-catenin dependent modulation of subventricular zone neurogenesis. *Sci. Rep.* 8:262. doi: 10.1038/s41598-017-18676-1

Mathews, K. J., Allen, K. M., Boerrigter, D., Ball, H., Shannon Weickert, C., and Double, K. L. (2017). Evidence for reduced neurogenesis in the aging human hippocampus despite stable stem cell markers. *Aging Cell* 16, 1195–1199. doi: 10.1111/acel.12641

McAvoy, K. M., Scobie, K. N., Berger, S., Russo, C., Guo, N., Decharatanachart, P., et al. (2016). Modulating neuronal competition dynamics in the dentate gyrus to rejuvenate aging memory circuits. *Neuron* 91, 1356–1373. doi: 10.1016/j.neuron.2016.08.009

Micci, M. A., Krishnan, B., Bishop, E., Zhang, W. R., Guptarak, J., Grant, A., et al. (2019). Hippocampal stem cells promote synaptic resistance to the dysfunctional impact of amyloid beta oligomers via secreted exosomes. *Mol. Neurodegener.* 14:25. doi: 10.1186/s13024-019-0322-8

Moon, M., Cha, M. Y., and Mook-Jung, I. (2014). Impaired hippocampal neurogenesis and its enhancement with ghrelin in 5XFAD mice. *J. Alzheimer's Dis.* 41, 233–241. doi: 10.3233/JAD-132417

Moreno-Jiménez, E. P., Flor-García, M., Terreros-Roncal, J., Rábano, A., Cafini, F., Pallas-Bazarra, N., et al. (2019). Adult hippocampal neurogenesis is abundant in neurologically healthy subjects and drops sharply in patients with alzheimer's disease. *Nat. Med.* 25, 554–560. doi: 10.1038/s41591-019-0375-9

Morrone, C. D., Bazzigaluppi, P., Beckett, T. L., Hill, M. E., Koletar, M. M., Stefanovic, B., et al. (2020). Regional differences in alzheimer's disease pathology confound behavioural rescue after amyloid-β attenuation. *Brain* 143, 359–373. doi: 10.1093/brain/awz371

Mu, Y., and Gage, F. H. (2011). Adult hippocampal neurogenesis and its role in alzheimer's disease. *Mol. Neurodegener.* 6:85. doi: 10.1186/1750-1326-6-85

Mucke, L., Masliah, E., Yu, G. Q., Mallory, M., Rockenstein, E. M., Tatsuno, G., et al. (2000). High-level neuronal expression of abeta 1-42 in wild-type human amyloid protein precursor transgenic mice: synaptotoxicity without plaque formation. *J. Neurosci.* 20, 4050–4058. doi: 10.1523/JNEUROSCI.20-11-04050.2000

Oakley, H., Cole, S. L., Logan, S., Maus, E., Shao, P., Craft, J., et al. (2006). Intraneuronal beta-amyloid aggregates, neurodegeneration, and neuron loss in transgenic mice with five familial alzheimer's disease mutations: potential factors in amyloid plaque formation. *J. Neurosci.* 26, 10129–10140. doi: 10.1523/JNEUROSCI.1202-06.2006

Oddo, S., Caccamo, A., Shepherd, J. D., Murphy, M. P., Golde, T. E., Kayed, R., et al. (2003). Triple-transgenic model of alzheimer's disease with plaques and tangles: intracellular Abeta and synaptic dysfunction. *Neuron* 39, 409–421. doi: 10.1016/S0896-6273(03)00434-3

Pallas-Bazarra, N., Jurado-Arjona, J., Navarrete, M., Esteban, J. A., Hernández, F., Ávila, J., et al. (2016). Novel function of Tau in regulating the effects of external stimuli on adult hippocampal neurogenesis. *EMBO J.* 35, 1417–1436. doi: 10.15252/embj.201593518

Pan, H., Wang, D., Zhang, X., Zhou, D., Zhang, H., Qian, Q., et al. (2016). Amyloid β is not the major factor accounting for impaired adult hippocampal neurogenesis in mice overexpressing amyloid precursor protein. *Stem Cell Rep.* 7, 707–718. doi: 10.1016/j.stemcr.2016.08.019

Paredes, M. F., Sorrells, S. F., Cebrian-Silla, A., Sandoval, K., Qi, D., Kelley, K. W., et al. (2018). Does adult neurogenesis persist in the human hippocampus? *Cell Stem Cell* 23, 780–781. doi: 10.1016/j.stem.2018.11.006

Piacentini, R., Civitelli, L., Ripoli, C., Marcocci, M. E., De Chiara, G., Garaci, E., et al. (2011). HSV-1 promotes Ca^{2+} -mediated APP phosphorylation and Aβ accumulation in rat cortical neurons. *Neurobiol. Aging* 32, 2323.e13–e26. doi: 10.1016/j.neurobiolaging.2010.06.009

Piacentini, R., Li Puma, D. D., Mainardi, M., Lazzarino, G., Tavazzi, B., Arancio, O., et al. (2017). Reduced gliotransmitter release from astrocytes mediates tau-induced synaptic dysfunction in cultured hippocampal neurons. *Glia* 65, 1302–1316. doi: 10.1002/glia.23163

Piacentini, R., Li Puma, D. D., Ripoli, C., Marcocci, M. E., De Chiara, G., Garaci, E., et al. (2015). Herpes simplex virus type-1 infection induces synaptic dysfunction in cultured cortical neurons via GSK-3 activation and intraneuronal amyloid-β protein accumulation. *Sci. Rep.* 5:15444. doi: 10.1038/srep15444

Podda, M. V., Leone, L., Barbati, S. A., Mastrodonato, A., Li Puma, D. D., Piacentini, R., et al. (2014). Extremely low-frequency electromagnetic fields enhance the survival of newborn neurons in the mouse hippocampus. *Eur. J. Neurosci.* 39, 893–903. doi: 10.1111/ejn.12465

Pontecorvo, M. J., Devous, M. D., Kennedy, I., Navitsky, M., Lu, M., Galante, N., et al. (2019). A multicentre longitudinal study of flortaucipir (18F) in normal ageing, mild cognitive impairment and alzheimer's disease dementia. *Brain* 142, 1723–1735. doi: 10.1093/brain/awz090

Puzzo, D., Argyrousi, E. K., Staniszewski, A., Zhang, H., Calcagno, E., Zuccarello, E., et al. (2020). Tau is not necessary for amyloid-beta-induced synaptic and memory impairments. *J. Clin. Invest.* 130, 4831–4844. doi: 10.1172/JCI137040

Puzzo, D., Piacentini, R., Fá, M., Gulisano, W., Li Puma, D. D., Staniszewski, A., et al. (2017). LTP and memory impairment caused by extracellular Aβ and Tau oligomers is APP-dependent. *Elife* 6:e26991. doi: 10.7554/eLife.26991

Ripoli, C., Cocco, S., Li Puma, D. D., Piacentini, R., Mastrodonato, A., Scala, F., et al. (2014). Intracellular accumulation of amyloid-β (Aβ) protein plays a major role in Aβ-induced alterations of glutamatergic synaptic transmission and plasticity. *J. Neurosci.* 34, 12893–12903. doi: 10.1523/JNEUROSCI.1201-14.2014

Ripoli, C., Piacentini, R., Riccardi, E., Leone, L., Li Puma, D. D., Bitan, G., et al. (2013). Effects of different amyloid β-protein analogues on synaptic function. *Neurobiol. Aging* 34, 1032–1044. doi: 10.1016/j.neurobiolaging.2012.06.027

Rodríguez, J. J., Jones, V. C., Tabuchi, M., Allan, S. M., Knight, E. M., LaFerla, F. M., et al. (2008). Impaired adult neurogenesis in the dentate gyrus of a triple transgenic mouse model of alzheimer's disease. *PLoS ONE* 3:e2935. doi: 10.1371/journal.pone.0002935

Saraulli, D., Costanzi, M., Mastrorilli, V., and Farioli-Vecchioli, S. (2017). The long run: neuroprotective effects of physical exercise on adult neurogenesis from youth to old age. *Curr. Neuropharmacol.* 15, 519–533. doi: 10.2174/1570159X14666160412150223

Scala, F., Fusco, S., Ripoli, C., Piacentini, R., Li Puma, D. D., Spinelli, M., et al. (2015). Intraneuronal Aβ accumulation induces hippocampal neuron hyperexcitability through A-type K^+ current inhibition mediated by activation of caspases and GSK-3. *Neurobiol. Aging* 36, 886–900. doi: 10.1016/j.neurobiolaging.2014.10.034

Selkoe, D. J. (2011). Alzheimer's disease. *Cold Spring Harb. Perspect. Biol.* 3:a004457. doi: 10.1101/cshperspect.a004457

Shariati, S. A., Lau, P., Hassan, B. A., Müller, U., Dotti, C. G., De Strooper, B., et al. (2013). APLP2 regulates neuronal stem cell differentiation during cortical development. *J. Cell Sci.* 126, 1268–1277. doi: 10.1242/jcs.122440

Sorrells, S. F., Paredes, M. F., Cebrian-Silla, A., Sandoval, K., Qi, D., Kelley, K. W., et al. (2018). Human hippocampal neurogenesis drops sharply in children to undetectable levels in adults. *Nature* 555, 377–381. doi: 10.1038/nature25975

Soscia, S. J., Kirby, J. E., Washicosky, K. J., Tucker, S. M., Ingelsson, M., Hyman, B., et al. (2010). The alzheimer's disease-associated amyloid β-protein is an antimicrobial peptide. *PLoS ONE* 5:e9505. doi: 10.1371/journal.pone.0009505

Tampellini, D., Magrané, J., Takahashi, R. H., Li, F., Lin, M. T., Almeida, C. G., et al. (2007). Internalized antibodies to the Abeta domain of APP reduce neuronal Abeta and protect against synaptic alterations. *J. Biol. Chem*. 282, 18895–18906. doi: 10.1074/jbc.M700373200

Taniuchi, N., Niidome, T., Goto, Y., Akaike, A., Kihara, T., and Sugimoto, H. (2007). Decreased proliferation of hippocampal progenitor cells in APPswe/PS1dE9 transgenic mice. *Neuroreport* 18, 1801–1805. doi: 10.1097/WNR.0b013e3282f1c9e9

Tobin, M. K., Musaraca, K., Disouky, A., Shetti, A., Bheri, A., Honer, W. G., et al. (2019). Human hippocampal neurogenesis persists in aged adults and alzheimer's disease patients. *Cell Stem Cell* 24, 974–982.e3. doi: 10.1016/j.stem.2019.05.003

Toda, T., Parylak, S. L., Linker, S. B., and Gage, F. H. (2019). The role of adult hippocampal neurogenesis in brain health and disease. *Mol. Psychiatry* 24, 67–87. doi: 10.1038/s41380-018-0036-2

Unger, M. S., Marschallinger, J., Kaindl, J., Höfling, C., Rossner, S., Heneka, M. T., et al. (2016). Early changes in hippocampal neurogenesis in transgenic mouse models for alzheimer's disease. *Mol. Neurobiol*. 53, 5796–5806. doi: 10.1007/s12035-016-0018-9

Wang, Z. F., Li, H. L., Li, X. C., Zhang, Q., Tian, Q., Wang, Q., et al. (2006). Effects of endogenous beta-amyloid overproduction on tau phosphorylation in cell culture. *J. Neurochem*. 98, 1167–1175. doi: 10.1111/j.1471-4159.2006.03956.x

Wirths, O. (2017). Altered neurogenesis in mouse models of alzheimer disease. *Neurogenesis* 4:e1327002. doi: 10.1080/23262133.2017.1327002

Yan, Y., Ma, T., Gong, K., Ao, Q., Zhang, X., and Gong, Y. (2014). Adipose-derived mesenchymal stem cell transplantation promotes adult neurogenesis in the brains of alzheimer's disease mice. *Neural Regen Res*. 9, 798–805. doi: 10.4103/1673-5374.131596

Yousef, H., Morgenthaler, A., Schlesinger, C., Bugaj, L., Conboy, I. M., and Schaffer, D. V. (2015). Age-associated increase in BMP signaling inhibits hippocampal neurogenesis. *Stem Cells* 33, 1577–1588. doi: 10.1002/stem.1943

Yu, Y., He, J., Zhang, Y., Luo, H., Zhu, S., Yang, Y., et al. (2009). Increased hippocampal neurogenesis in the progressive stage of alzheimer's disease phenotype in an APP/PS1 double transgenic mouse model. *Hippocampus* 19, 1247–1253. doi: 10.1002/hipo.20587

Zheng, J., Li, H. L., Tian, N., Liu, F., Wang, L., Yin, Y., et al. (2020). Interneuron accumulation of phosphorylated tau impairs adult hippocampal neurogenesis by suppressing GABAergic transmission. *Cell Stem Cell* 26, 331–345.e6. doi: 10.1016/j.stem.2019.12.015

Zheng, J. Y., Liang, K. S., Wang, X. J., Zhou, X. Y., Sun, J., and Zhou, S. N. (2017). Chronic estradiol administration during the early stage of alzheimer's disease pathology rescues adult hippocampal neurogenesis and ameliorates cognitive deficits in Aβ1-42 mice. *Mol. Neurobiol*. 54, 7656–7669. doi: 10.1007/s12035-016-0181-z

Conflict of Interest: The authors declare that the research was conducted in the absence of any commercial or financial relationships that could be construed as a potential conflict of interest.

frontiers in Molecular Neuroscience

MINI REVIEW
published: 24 February 2021
doi: 10.3389/fnmol.2021.635880

(Dys)regulation of Synaptic Activity and Neurotransmitter Release by β-Amyloid: A Look Beyond Alzheimer's Disease Pathogenesis

Francesca Fagiani[1,2†], *Cristina Lanni*[1*†], *Marco Racchi*[1] *and Stefano Govoni*[1]

[1] *Department of Drug Sciences, Pharmacology Section, University of Pavia, Pavia, Italy,* [2] *Istituto Universitario di Studi Superiori – IUSS, Pavia, Italy*

Beside its widely studied role in the pathogenesis of Alzheimer's disease (AD), β-amyloid (Aβ) is a normal and soluble product of neuronal metabolism that regulates several key physiological functions, exerting neuromodulatory effects on synaptic plasticity, memory, and neurotransmitter release. Such effects have been observed to occur in a hormetic fashion, with Aβ exhibiting a dual role influenced by its concentration, the different isoforms, or aggregation forms of the peptide. However, to date, our knowledge about the physiological functions of Aβ and, in particular, its modulatory role on synaptic activity and neurotransmission in the normal brain is fragmentary, thus hindering a clear comprehension of the biological mechanisms underlying the derangement from function to dysfunction. In particular, according to the amyloid cascade hypothesis, the switch from physiology to pathology is linked to the abnormal increase in Aβ levels, due to an imbalance in Aβ production and clearance. In this regard, increased Aβ levels have been hypothesized to induce early defects in synaptic function and such alterations have been suggested to account, at least in part, for the onset of neuropsychiatric symptoms (e.g., apathy, anxiety, changes in mood, depression, and agitation/aggression), frequently observed in the prodromal stage of AD. Therefore, understanding the biological mechanisms underlying early synaptic alterations in AD is a key starting point to frame the relevant time windows for AD treatment and to gain insight into AD etiopathogenesis.

Keywords: β-amyloid, Alzheimer's disease, synaptic activity, neurotransmission, neuropsychiatric symptoms, synaptic vesicle cycle

OPEN ACCESS

Edited by:
Walter Gulisano,
University of Catania, Italy

Reviewed by:
Marcello Melone,
Marche Polytechnic University, Italy
Maria Rosaria Tropea,
University of Catania, Italy
Cláudio Gouveia Roque,
Columbia University, United States
Cristian Ripoli,
Catholic University of the Sacred Heart, Italy

***Correspondence:**
Cristina Lanni
cristina.lanni@unipv.it

† *These authors have contributed equally to this work*

Received: *30 November 2020*
Accepted: *25 January 2021*
Published: *24 February 2021*

Citation:
Fagiani F, Lanni C, Racchi M and Govoni S (2021) (Dys)regulation of Synaptic Activity and Neurotransmitter Release by β-Amyloid: A Look Beyond Alzheimer's Disease Pathogenesis. Front. Mol. Neurosci. 14:635880. doi: 10.3389/fnmol.2021.635880

INTRODUCTION

β-amyloid (Aβ) is a 4-kDa peptide produced during the amyloidogenic pathway by the sequential proteolysis of the amyloid precursor protein (APP) by β- and γ-secretase (Glenner and Wong, 1984). APP is first cleaved by β-site APP cleaving enzyme one (BACE1), thereby releasing the C-terminal fragment (C99), further cleaved by γ-secretase to generate Aβ peptide. Aβ is secreted into the extracellular space and cleared by the cerebrospinal fluid (CSF) and vascular system (Iliff et al., 2012). In the CSF of healthy humans, the 40-amino-acid-long isoform ($A\beta_{1-40}$) has been reported to be the most represented isoform, which is present at ∼2–3 ng/ml, and the 42-amino-acid-long isoform ($A\beta_{1-42}$) to be the second most abundant isoform

(∼0.75 ng/ml) (Ida et al., 1996; Mo et al., 2015). Aβ is normally present in a soluble form, but it can self-assemble. In particular, $A\beta_{1-42}$ has been reported to be more prone to aggregation than $A\beta_{1-40}$, which differ from the former by two amino acid residues at the C-terminal end (Sgourakis et al., 2007). The C-terminal flexibility of the $A\beta_{1-42}$ peptide has been suggested to be responsible for its higher propensity to aggregate (Sgourakis et al., 2007). The self-assembly of Aβ produces aggregates such as oligomers that can further accrete to form protofibrils, fibrils, and, finally, insoluble plaques, one of the main histological hallmarks observed in the brain of Alzheimer's disease (AD) patients.

The pathological role of Aβ as a misfolded protein involved in the pathogenesis of AD, according to the amyloid hypothesis (Hardy and Selkoe, 2002), has been extensively investigated for decades, with different types of Aβ oligomers found to correlate with cognitive impairment and to promote neurodegeneration in AD (Walsh and Selkoe, 2007; Ono et al., 2009). Because of this evidence reporting Aβ key role in several physiological functions (for a comprehensive review on the topic see Brothers et al., 2018) has been partially overshadowed. Since Aβ is released into the extracellular space as monomer, the physiological roles of Aβ have been commonly ascribed to its monomeric form (Giuffrida et al., 2009). However, the dynamic equilibrium between monomers/oligomers in the brain under physiological conditions is still matter of scientific debate (Bemporad and Chiti, 2012). It has been suggested that a certain degree of Aβ oligomerization may also occur under physiological conditions (Gulisano et al., 2018). In this regard, although the effects of different forms and aggregation status of soluble Aβ have been widely investigated for their well-established neurotoxic potential in AD, less is known about such aspects under physiological conditions. In the following sections, we will discuss evidence from the literature reporting the effects of low (i.e., picomolar–nanomolar) concentrations of the main Aβ isoforms (i.e., $A\beta_{1-40}$ and $A\beta_{1-42}$), as well as of different aggregation status of Aβ (i.e., monomers, low-weight-soluble oligomers, and combination of both) at synaptic level, in condition not resulting in neurotoxicity.

THE NEUROMODULATORY ROLE OF Aβ

Among the physiological functions regulated by Aβ, several lines of evidence indicate that Aβ exerts a neuromodulatory role by controlling synaptic activity and neurotransmitter release from presynaptic terminals (Preda et al., 2008; Puzzo et al., 2008, 2011; Abramov et al., 2009; Grilli et al., 2010; Mura et al., 2012; Zappettini et al., 2012). Aβ has been demonstrated to act in a hormetic fashion, exhibiting a dual role on synaptic activity and neurotransmission, strictly depending upon its concentration. Accordingly, while low Aβ concentrations (picomolar and low nanomolar), resembling the endogenous levels of Aβ in the brain, have been found to positively modulate neurotransmission and memory, higher concentrations (high nanomolar–low micromolar) have been observed to negatively modulate neurotransmission, finally resulting in the well-established neurotoxic action (Puzzo et al., 2008). Moreover, these opposite Aβ effects have been demonstrated to be influenced not only by Aβ concentration but also by different isoforms or aggregation forms of the peptide (Gulisano et al., 2018).

In addition, a number of studies demonstrates that, at presynaptic terminals, Aβ regulates the release of neurotransmitters, including dopamine, γ-aminobutyric acid (GABA), glutamate, aspartate, and glycine, by mainly affecting the cholinergic control of their release, in conditions not resulting in neurotoxicity (Preda et al., 2008; Grilli et al., 2010; Mura et al., 2012; Zappettini et al., 2012). In accordance with such evidence, Aβ has been found to act as positive endogenous modulator of release probability at hippocampal synapses (Abramov et al., 2009), and a direct and indirect interplay of Aβ with different presynaptic proteins regulating the sequential steps (i.e., exocytosis, endocytosis, and trafficking) of synaptic vesicle cycle at presynaptic terminals has been reported (Russell et al., 2012; Yang et al., 2015; Lazarevic et al., 2017). However, data concerning the physiological functions of Aβ and, in particular, the modulation of synaptic activity and neurotransmission by Aβ in the normal brain are still fragmentary, thus hindering a clear comprehension of the biological mechanisms underlying the derangement from function to dysfunction. According to the amyloid cascade hypothesis, the switch from physiology to pathology is linked to the abnormal increase in Aβ levels, due to an imbalance in Aβ production and clearance (Mawuenyega et al., 2010; Murphy and Levine, 2010). In this regard, increased Aβ levels have been hypothesized to induce early defects in synaptic activity and neurotransmission, and such alterations have been suggested to account, at least in part, for the onset of early behavioral symptoms, including apathy, anxiety, changes in mood, depression, and psychosis, frequently observed in the prodromal stage of AD (reviewed by Ismail et al., 2016). Therefore, such early defects may likely be the consequences of synaptic dysfunction rather than of neurodegenerative processes. Understanding the biological mechanisms underlying early synaptic alterations in AD might represent a key starting point to better frame the relevant time windows and to gain insight into AD etiopathogenesis, as well as defining the associated early behavioral signs.

Aβ as Endogenous Regulator of Synaptic Activity

Independent *in vitro* and *in vivo* studies have demonstrated that neuronal activity directly increases Aβ production and secretion into the extracellular space at the synapses (Kamenetz et al., 2003; Cirrito et al., 2005) and that, in turn, Aβ suppresses excitatory synaptic transmission, thereby maintaining neuronal activity within a normal dynamic range (Kamenetz et al., 2003). In this regard, it has been speculated that such negative feedback loop may act as a physiological homeostatic mechanism to limit the overexcitation of brain circuits that might result in excitotoxicity (Kamenetz et al., 2003). Thus, deviation from this fine-tuning control mechanism due to Aβ derangement may suppress synaptic activity and, ultimately, lead to synaptic damage.

However, the concentrations of Aβ tested in these studies are far higher than the endogenous levels of Aβ peptides in the normal brain, estimated in the picomolar range (Seubert et al., 1992; Ida et al., 1996), and prompted investigations on the effects of low Aβ concentrations (i.e., picomolar and low nanomolar) resembling its endogenous levels. In this regard, a growing body of evidence converges to indicate that soluble Aβ acts as a crucial synaptic regulator, by modulating key physiological functions, such as synaptic plasticity and memory. Accordingly, Puzzo et al. (2008) demonstrated that the exposure of hippocampal neurons to low concentrations (i.e., picomolar–low nanomolar) of $A\beta_{1-42}$ positively modulated synaptic plasticity and memory. In contrast, the exposure to higher concentrations (i.e., high nanomolar–low micromolar) induced a neurotoxic action. In particular, $A\beta_{1-42}$ exhibited a biphasic or hormetic effect in regulating the long-term potentiation (LTP), the electrophysiological correlate of learning, and memory (Puzzo et al., 2008). Accordingly, at the synapses between Schaffer collateral fibers and CA1 neurons, picomolar concentrations of $A\beta_{1-42}$ promoted LTP enhancement, with a maximum effect around 200 pM, whereas nanomolar concentrations of $A\beta_{1-42}$ induced an impairment of LTP. Moreover, picomolar concentrations of $A\beta_{1-42}$ induced an enhancement of both hippocampal-dependent reference and contextual fear memory in mice. In line with these data, in mouse hippocampal slices, perfusion with the monoclonal antibody JRF/rAb2, recognizing a specific epitope of rodent $A\beta_{1-40}$ and $A\beta_{1-42}$, led to a decrease in contextual fear memory and reference memory, as well as significantly reduced LTP (Puzzo et al., 2011). Both these parameters were rescued by the addition of the human homolog $A\beta_{1-42}$, which is not recognized by JRF/rAb2, suggesting that endogenous Aβ might be required for synaptic plasticity in the brain. According to this hypothesis, intraneuronal delivery of a small interfering RNA (siRNA), specific for rodent APP, induced a reduction in LTP that was rescued by the addition of 200 pM $A\beta_{1-42}$.

Furthermore, the effects of soluble Aβ on synaptic plasticity and memory have been reported to rely not only on the concentration of Aβ but also on the different isoforms and aggregation status of the peptide. Accordingly, Gulisano et al. (2018) demonstrated that the exposure of rodent CA1 pyramidal neurons to 200 pM low-molecular-weight oligomeric $A\beta_{1-42}$ led to an increase of frequency in miniature excitatory postsynaptic currents, accompanied by a reduction in pair pulse facilitation. In addition, an increased number of docked vesicles at presynaptic terminals was also observed, thus suggesting that low concentrations of oligomeric $A\beta_{1-42}$ promote neurotransmitter release from the presynaptic terminals. Noteworthy, such effects were not observed when pyramidal neurons were exposed to 200 pM $A\beta_{1-40}$ oligomers. Moreover, although monomeric forms of Aβ are commonly considered as neuroprotective (Giuffrida et al., 2009), the exposure of neurons to high concentrations (200 nM) of $A\beta_{1-42}$ monomers induced an impairment in synaptic plasticity and memory (Gulisano et al., 2018). By contrast, such effect was not observed for $A\beta_{1-40}$ monomers. Indeed, the exposure to 200 nM $A\beta_{1-40}$ monomers was ineffective, whereas 200 nM $A\beta_{1-40}$ oligomers impaired synaptic plasticity and memory. However, while interpreting these results, it should be taken into account that the preparation of $A\beta_{1-42}$ monomers, which promoted the observed neurotoxic action, contained also few dimers and higher quantity of trimers and tetramers that may be responsible for neurotoxicity.

Moreover, also the time of exposure to the peptide represents a key parameter to consider. In this regard, Koppensteiner et al. (2016) observed that, in mouse hippocampal neurons, short-term exposure (minutes) to picomolar concentration (200 pM) of oligomeric $A\beta_{1-42}$ stimulated synaptic potentiation in hippocampal cultures and slices and synaptic plasticity and contextual memory in mice. Differently, longer exposures (hours) to 200 pM $A\beta_{1-42}$ induced a decrease in such parameters. In this regard, it is important to consider that dynamic Aβ changes physiologically occur in the brain, since Aβ levels undergo diurnal fluctuations. Accordingly, both in mouse hippocampal interstitial fluid as well as in human CSF, soluble Aβ levels have been reported to exhibit robust daily oscillations, with a clear 24-h period, that are in phase with circadian rhythms in activity (Kang et al., 2009; Huang et al., 2012), thus indicating the presence of physiological circadian patterns regulating fluctuations of CSF Aβ levels. Notably, Huang et al. (2012) demonstrated that aging and Aβ deposition diminish normal CSF Aβ dynamics to a flat line, possibly contributing to AD.

Aβ as Endogenous Regulator of Neurotransmitter Release

Evidence from the literature indicates that Aβ controls neurotransmitter release from presynaptic terminals in the absence of evident signs of neurotoxicity. A functional interplay between Aβ and different neurotransmitter systems, such as cholinergic, glutamatergic, GABAergic, catecholaminergic, and serotoninergic, has been reported (for a comprehensive review on the topic, see Lanni et al., 2019). It has been speculated that Aβ exhibits a neuromodulatory action fundamental for the proper balance among the different neurotransmitter systems.

Notably, Aβ has been found to regulate the cholinergic control of neurotransmitter release in several brain regions in a concentration-dependent manner in different *in vitro* and *in vivo* models, as schematized in detail in **Table 1**. Both $A\beta_{1-40}$ and $A\beta_{1-42}$ isoforms have been demonstrated to bind with high affinity to α7-containing nicotinic acetylcholine receptors (α7-nAChRs) (Wang et al., 2000; Khan et al., 2010; Tong et al., 2011). Picomolar–low nanomolar concentrations of $A\beta_{1-40}$ have been found to activate α7-nAChRs, thus triggering intracellular pathways regulating synaptic plasticity, learning, and memory. Conversely, higher concentrations (nanomolar–low micromolar), as well as prolonged exposure to $A\beta_{1-40,}$ have been found to desensitize and inactivate α7-nAChRs, thereby disrupting synaptic signaling (Mura et al., 2012; Zappettini et al., 2012). Taken together, these results converge to indicate that, while Aβ may physiologically exert a neuromodulatory action on nicotinic receptors, its accumulation, whose primary etiological factors may be an imbalance between Aβ production and its clearance (Mawuenyega et al., 2010; Murphy and Levine, 2010), may damage nicotinic transmission, by inducing the

TABLE 1 | Regulation by Aβ of cholinergic control of neurotransmitter release.

Aβ species	Concentration and timing	Effects of Aβ on neurotransmitter release	Experimental model/brain area	References
Dopamine				
Soluble $A\beta_{1-40}$ and $A\beta_{1-42}$	1–10 μM/60–80 min (for *in vivo* experiments); 100 nM/up to 10 min (for *in vitro* experiments)	Low micromolar concentrations (1 μM) of Aβ prevented the muscarinic receptor-activated dopamine release in rat nucleus accumbens. The [^{3}H]dopamine release, evoked by carbachol, was decreased by 100 nM Aβ in isolated nerve endings of the nucleus accumbens. Moreover, $A\beta_{1-42}$ (100 nM) significantly reduced the dopamine release evoked by carbachol.	*In vivo* (brain dialysis) and *in vitro* (isolated synaptosomes) models/rat nucleus accumbens	Preda et al., 2008
$A\beta_{1-40}$	100 nM	Treatment with 100 nM $A\beta_{1-40}$ prevented both nicotinic and muscarinic cholinergic modulation of dopamine release.	Synaptosomes/rat nucleus accumbens	Olivero et al., 2014
$A\beta_{1-40}$ and $A\beta_{1-42}$	10–100 nM/up to 12 min	In nerve endings, Aβ impaired the muscarinic control of dopamine release in both the nucleus accumbens and caudate putamen.	Synaptosomes/caudate-putamen-nucleus accumbens	Mura et al., 2010
GABA				
Monomers of $A\beta_{1-40}$ and $A\beta_{1-42}$	100 nM/up to 17 min	In isolated nerve endings, Aβ blocked GABA release by acting on muscarinic receptor subtypes (M3 and M5). Instead, Aβ was ineffective on muscarinic receptor subtypes negatively modulating the stimulated transmitter release (M2 and M4).	Synaptosomes/rat nucleus accumbens	Grilli et al., 2010
Monomers of $A\beta_{1-40}$	100 nM, 1 μM, and 10 μM/40–60 min (for *in vivo* experiments); 100 pM, 1 nM, and 100 nM/up to 10 min (for *in vitro* experiments)	While perfusion of 10 μM Aβ blocked the nicotine-induced release of GABA, perfusion of 100 nM Aβ potentiated the nicotine-evoked GABA overflow. In isolated nerve endings, 100 nM Aβ blocked the nicotine-induced release of GABA and 100 nM Aβ inhibited the release of GABA induced by the 4β2 selective agonist 5IA85380.	*In vivo* (microdialysis) and *in vitro* (synaptosomes in superfusion) techniques/hippocampus	Mura et al., 2012
Glycine				
$A\beta_{1-40}$	10 μM/40–60 min (for *in vivo* experiments); 10 nM and 100 nM/up to 10 min (for *in vitro* experiments)	Perfusion of 10 μM $A\beta_{1-40}$ reduced the nicotine-induced glycine overflow and also the glycine overflow induced by the α7 selective agonist PHA543613. In isolated nerve endings, both 10 and 100 nM Aβ inhibited the nicotine-induced glycine release; 100 nM Aβ inhibited the release of glycine evoked by the α7 selective agonist carbachol and by the α4β2 selective agonist 5IA85380.	*In vitro* (synaptosomes in superfusion) and *in vivo* (microdialysis) approaches/hippocampus	Zappettini et al., 2012
Aspartate				
Monomers of $A\beta_{1-40}$	100 nM, 1 μM, and 10 μM/40–60 min (for *in vivo* experiments); 100 pM, 1 nM, and 100 nM/up to 10 min (for *in vitro* experiments)	Perfusion of 10 and 1 μM Aβ inhibited the nicotine-induced release of aspartate. In isolated nerve endings, 100 nM Aβ inhibited the nicotine-induced release of aspartate; 100 nM Aβ inhibited the release of aspartate that was induced by the α7 selective agonist carbachol; 100 nM Aβ inhibited the release of aspartate induced by the α4β2 selective agonist 5IA85380; 100 pM Aβ potentiated the carbachol-induced release of aspartate.	*In vivo* (microdialysis) and *in vitro* (synaptosomes in superfusion) techniques/hippocampus	Mura et al., 2012
Glutamate				
Monomers of $A\beta_{1-40}$	100 nM, 1 μM, and 10 μM/40–60 min (for *in vivo* experiments); 100 pM, 1 nM, and 100 nM/up to 10 min (for *in vitro* experiments)	Perfusion of 10 and 1 μM Aβ inhibited the nicotine-induced release of glutamate. In isolated nerve endings, 100 nM Aβ inhibited the nicotine-induced release of glutamate and the release of glutamate induced by the α7 selective agonist carbachol. Instead, 1 nM Aβ potentiated the release of glutamate induced by carbachol; 100 nM Aβ inhibited the release of glutamate induced by the α4β2 selective agonist 5IA85380; 100 pM Aβ potentiated the carbachol-induced release of glutamate.	*In vivo* (microdialysis) and *in vitro* (synaptosomes in superfusion) techniques/hippocampus	Mura et al., 2012

inactivation of α7-nAChRs, with consequent impairment of nicotinic cholinergic neurotransmission.

Besides the interaction with cholinergic receptors, low concentrations (range pM–nM) of $A\beta_{1-40}$ also promoted the nicotine-evoked release of both excitatory (i.e., glutamate and aspartate) and inhibitory amino acids (i.e., glycine and GABA) (Mura et al., 2012; Zappettini et al., 2012), while higher concentrations of $A\beta_{1-40}$ (range nM–μM) inhibited the nicotine-elicited release of glutamate and aspartate (Mura et al., 2012; Zappettini et al., 2012). These effects are consistent with

results obtained in the nucleus accumbens and in the striatum, in the case of GABA and dopamine release upon muscarinic cholinergic stimuli (Preda et al., 2008; Grilli et al., 2010).

The Potential Interplay Between Aβ and Synaptic Vesicle Cycle

In an elegant work by Abramov et al. (2009), endogenous Aβ has been demonstrated to exert a pivotal role in the regulation of synaptic vesicle release but not to affect postsynaptic function. In particular, the increase in endogenous Aβ levels, due to the inhibition of its extracellular degradation, led to enhancement of release probability of synaptic vesicles, as well as of neuronal activity in rodent hippocampal culture (Abramov et al., 2009). Such effects increased spontaneous excitatory postsynaptic currents, but not inhibitory currents, and were specifically presynaptic and dependent on firing rates, with lower facilitation observed in hippocampal neurons showing higher firing rates. In line with such evidence reporting Aβ involvement in release probability of synaptic vesicles, evidence from literature indicates that Aβ may directly interact with key presynaptic proteins regulating the neurotransmitter release machinery, by influencing the phosphorylation of SNARE and accessory proteins and, consequently, the assembly of the soluble N-ethylmaleimide-sensitive factor attachment protein (SNAP) receptors (SNARE) complex and the consequent release of neurotransmitter from the presynaptic terminal (Russell et al., 2012; Yang et al., 2015; Marsh et al., 2017). Indeed, Aβ has been reported to interfere with different steps of the synaptic vesicle cycle, such as vesicle docking and fusion, fundamental for the exocytosis of synaptic vesicles, as well as vesicle recycling and recovery in neurons (as reviewed by Fagiani et al., 2019). Corroborating the hypothesis of Aβ implication in the exocytosis of synaptic vesicles, Russell et al. (2012) demonstrated that, at presynaptic terminals, in rat CA3–CA1 hippocampal neurons, monomeric $A\beta_{1-42}$, at nanomolar concentration (50 nM), directly competed with Synaptobrevin/vesicle-associated membrane protein (VAMP2) for the binding to Synaptophysin, thereby promoting the formation of the fusion pore complex, with consequent positive effect on neurotransmitter release. Moreover, Yang et al. (2015) reported that, in an *in vitro* assay, Aβ oligomers (1–20 nM) bind to the SNARE motif region (SynH3) of Syntaxin 1a, thereby inhibiting the fusion step between docking and lipid mixing. Finally, the exposure of rat hippocampal neurons to soluble Aβ oligomers (300 nM) induced an increase in phosphorylated Synapsin I by activating CaMKIV, thereby increasing the availability of synaptic vesicles to dock to the active zone and to promote neurotransmitter release (Marsh et al., 2017). However, these data are extremely limited and do not allow to draw definitive conclusions regarding the functional impact of Aβ on synaptic vesicle cycle. Given the key role of Aβ at presynaptic terminals as well as its effects on neurotransmitter release, discussed above, further studies investigating the interplay between Aβ and the presynaptic release machinery may provide relevant information. In particular, a comparative analysis of the effects of low and high Aβ concentrations, as well as the impact of different soluble species (i.e., monomers and low-weight oligomers) of Aβ peptides, may open new avenues in the field. In this regard, it has to be mentioned that, besides a direct interplay of Aβ with key presynaptic proteins mediating synaptic vesicle dynamics, Aβ has been reported to regulate protein kinases (e.g., calpain-cyclin-dependent kinase 5 and Ca^{2+}/calmodulin-dependent protein kinase IV) (Lazarevic et al., 2017; Park et al., 2017), thereby influencing the fine-tuning of synaptic vesicle dynamics at the presynaptic terminal (for a comprehensive review on the topic, see Fagiani et al., 2019).

Aβ-DRIVEN DYSREGULATION OF NEUROTRANSMISSION: AN EARLY EVENT TRIGGERING BEHAVIORAL SYMPTOMS IN AD?

Pathological increase in Aβ levels has been suggested to lead to the derangement of Aβ neuromodulatory action. In particular, the overall scenario depicted above suggests that increased Aβ levels might transiently affect the fine-tuning of synaptic vesicle cycling and neurotransmitter release, thereby altering synaptic homeostasis, whose accumulating transient alterations may result in long-lasting and even permanent alteration (as illustrated in **Figure 1**). Therefore, Aβ-induced early synaptic changes altering synaptic homeostasis may promote a linear progression from synaptic dysfunction to frank neurodegeneration (Fagiani et al., 2019). Noteworthy, perturbation of synaptic homeostasis and neurotransmission has been suggested to possibly contribute to the onset of neuropsychiatric symptoms (NPS) (e.g., apathy, social withdrawal, anxiety, changes in mood, depression, agitation/aggression, psychosis, and delusions), frequently observed in the prodromal stage of AD (Ismail et al., 2016). In AD, such behavioral signs have been suggested to be predictive of incipient cognitive decline and to be correlated to early synaptic dysfunction rather than to neurodegenerative processes. In this regard, when thinking of neuropsychiatric manifestations, the first observation is how Aβ-related changes in neurotransmitter release may support and translate, over the time, into the onset of behavioral symptoms (e.g., apathy, anxiety, and depression) (Ismail et al., 2016). For instance, the onset of apathy, one of the main behavioral correlates of the impairment in dopaminergic neurotransmission observed in aging, may be, at least in part, related to the inhibitory effect induced by Aβ on dopamine release (Preda et al., 2008). Furthermore, based on evidence demonstrating an inhibitory effect on GABA and glycine release induced by micromolar concentrations of Aβ (Mura et al., 2012; Zappettini et al., 2012), it can be speculated that perturbation of the inhibitory component of the excitatory/inhibitory network by Aβ may represent the neurochemical base underlying the appearance of psychotic symptoms (e.g., delusions, hallucinations, and misidentifications). In fact, the inhibitory component of the excitatory/inhibitory network plays a fundamental role in maintaining the excitatory/inhibitory functional balance in the brain, thus critically regulating cortical network function. In line with such hypothesis, mouse models recapitulating

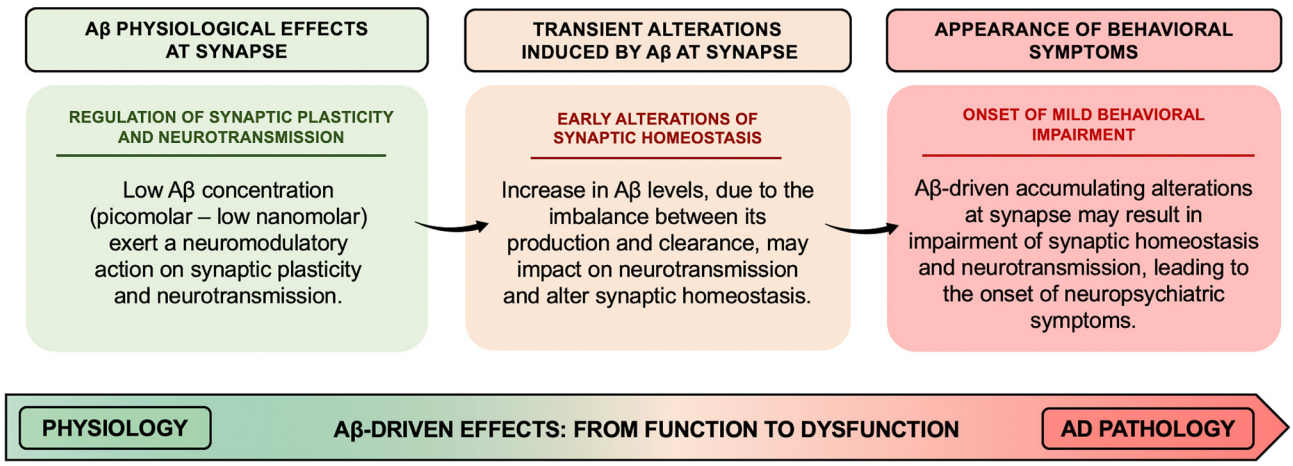

FIGURE 1 | Aβ-driven effects at synapse: the derangement from function to dysfunction. Low concentrations (picomolar–low nanomolar) of Aβ exert a neuromodulatory action on synaptic plasticity and neurotransmitter release from the presynaptic terminals. The alteration of Aβ homeostasis, due to an imbalance between Aβ production and clearance, may impact on the fine-tuning of synaptic vesicle cycling and neurotransmitter release, thus altering synaptic homeostasis. Aβ-driven accumulating alterations at synapse might result in permanent impairment of synaptic homeostasis and neurotransmission, thereby leading to the onset of neuropsychiatric symptoms frequently observed in the prodromal stage of AD.

Aβ amyloidosis, generated by knock-in (KI) of a humanized Aβ sequence, exhibited behavioral changes associated with non-cognitive, emotional domains, before the onset of definitive cognitive deficits (Sakakibara et al., 2018; Latif-Hernandez et al., 2019). In Sakakibara's et al. (2018), assessments of the emotional domains showed that *App*-KI mice, harboring three familial AD-associated mutations (i.e., Swedish–NL–, Beyreuther/Iberian–F–, and Arctic–G–) ($App^{NL-G-F/NL-G-F}$), developed progressive Aβ amyloidosis and exhibited anxiolytic-like behavior from 6 months of age, compared to wild-type mice. Instead, App-KI mice, carrying only the Swedish mutation ($App^{NL/NL}$), displayed an anxiogenic-like behavior from 15 months of age. In the contextual fear conditioning task, while both $App^{NL/NL}$ and $App^{NL-G-F/NL-G-F}$ mice showed intact learning and memory up to 15–18 months of age, $App^{NL-G-F/NL-G-F}$ mice had hyper-reactivity to painful stimuli. Such evidence indicates that anxiolytic-like behavior might be correlated with Aβ amyloidosis.

Noteworthy, although NPS are traditionally associated with frontotemporal dementia, the International Society to Advance Alzheimer's Research and Treatment (ISTAART) NPS Professional Interest Area developed diagnostic criteria to define the association between neuropsychiatric symptoms and other dementias, including AD, with the aim to define late-life appearance of sustained NPS as an at-risk condition for cognitive decline and dementia. Within this context, mild behavioral impairment (MBI) syndrome represents a diagnostic construct to identify patients with or without cognitive symptoms, prone to develop dementia, as well as a counterpart of mild cognitive impairment (MCI) and a transitional state between normal aging and dementia (Taragano et al., 2018). However, it is still unclear whether MBI represents a potentially reversible condition. Interestingly, Lussier et al. (2020) recently investigated the neuropathological correlates of MBI and found, as detailed below, an association between MBI and Aβ, but not tau or neurodegeneration, in cognitively intact elderly individuals. The authors investigated the association between the MBI Checklist (MBI-C) scores and AD imaging biomarkers (brain burden of Aβ, tau, and regional gray matter volume), in order to test whether MBI-C scores were correlated with early pathological stages of AD (Lussier et al., 2020). Higher MBI-C scores predicted higher Aβ PET labeling in the left frontal cortex, left posterior cingulate cortex, left caudate nucleus, and left thalamus, thus suggesting a correlation between MBI and amyloid pathology (Lussier et al., 2020). Notably, the areas with higher associations between MBI-C scores and Aβ PET uptake have been also reported to exhibit amyloidosis in the first phases of hierarchical amyloidosis in AD, specifically the neocortex, including frontal neocortex, followed by the striatum (Lussier et al., 2020). These results are consistent with evidence reporting that NPS are correlated with Aβ deposition in the frontal and cingulate cortices (Mori et al., 2014; Bensamoun et al., 2015) and subcortical amyloidosis (Hanseeuw et al., 2020). However, despite evidence showing that MBI represents an at-risk condition for dementia associated with Aβ deposition, it is still unknown which factors contribute to the progression from MBI to full-blown dementia and whether this progression is an extension of Aβ-driven detrimental effects.

CONCLUDING REMARKS

Data from the literature, discussed in this mini review, highlight the key role of Aβ on synaptic activity and neurotransmission, in particular as endogenous modulator of neurotransmitter release from presynaptic terminals. However, our knowledge about the regulatory role of Aβ on synaptic activity and neurotransmission in the normal brain is extremely fragmentary and the application of exogenous Aβ has produced heterogeneous data on the topic, thus complicating the interpretation of the results discussed

above. To date, it is unknown the mechanism by which endogenously released Aβ (comprising different isoforms and molecular conformations) modulates synaptic activity in normal and non-transgenic brain circuits (Abramov et al., 2009). Notably, such limitation hinders a clear comprehension of the biological mechanisms underlying the derangement from function to dysfunction and the switch of Aβ role from physiological to pathological.

Moreover, the overall scenario depicted in this paper raises a number of questions not yet fully resolved. First, a consideration comes from therapeutic endeavor targeting Aβ. Several thousands of patients have been treated with anti-Aβ drugs, ranging from strategies neutralizing Aβ with humanized monoclonal antibodies or promoting Aβ clearance, and these approaches have failed strong clinical goals. Based on the knowledge of a neuromodulatory role of Aβ, an antibody selectively binding and removing Aβ oligomers and fibrils might be more beneficial than one also directed to Aβ monomers. The failure of clinical trials testing Solanezumab, whose mechanism of action is peripheral sink and sequestration, may rely on its preference to bind to monomeric Aβ, since it recognizes a linear epitope in the center of Aβ and does not bind to larger Aβ aggregates (Willis et al., 2018). Some encouragement derives from aducanumab, a human monoclonal antibody selectively binding to Aβ fibrils and soluble oligomers, which in October 2019, after a reanalysis of the phase 3 studies, originally discounted after a futility analysis reporting no clinical advantage, showed some significant results (Schneider, 2020). However, it should be considered that the effects of aducanumab on cognitive decline were modest and severe side effects, such as cerebral edema, were observed, thus indicating that the risks may not be worth the benefits. Further considerations should be also done on the effect of a mobilization of Aβ from plaques, which appears detrimental and responsible for complications and severe side effects, such as amyloid-related imaging abnormalities (e.g., vasogenic edema and cerebral microhemorrhages) (Sperling et al., 2011; Mo et al., 2017).

Altogether, these questions suggest the importance of better analyzing the spectrum of Aβ effects to better frame the relevant time windows for intervention and to identify more appropriate targeting strategies.

AUTHOR CONTRIBUTIONS

FF, SG, and CL conceived the idea and wrote the manuscript. FF, SG, MR, and CL contributed in the critical discussion. All authors contributed to the article and approved the submitted version.

FUNDING

This research has been supported by the University of Pavia (grant from FR&G 2019, Fondo Ricerca & Giovani, to CL and PRIN 2017B9NCSX_003 to MR).

REFERENCES

Abramov, E., Dolev, I., Fogel, H., Ciccotosto, G. D., Ruff, E., and Slutsky, I. (2009). Amyloid-B as a positive endogenous regulator of release probability at hippocampal synapses. *Nat. Neurosci.* 12, 1567–1576. doi: 10.1038/nn.2433

Bemporad, F., and Chiti, F. (2012). Protein misfolded oligomers: experimental approaches, mechanism of formation, and structure-toxicity relationships. *Chem. Biol.* 19, 315–327. doi: 10.1016/j.chembiol.2012.02.003

Bensamoun, D., Guignard, R., Furst, A. J., Derreumaux, A., Manera, V., Darcourt, J., et al. (2015). Associations between neuropsychiatric symptoms and cerebral amyloid deposition in cognitively impaired elderly people. *J. Alzheimer's Dis.* 49, 387–398. doi: 10.3233/JAD-150181

Brothers, H. M., Gosztyla, M. L., and Robinson, S. R. (2018). The physiological roles of amyloid-β peptide hint at new ways to treat Alzheimer's disease. *Front. Aging Neurosci.* 10:118. doi: 10.3389/fnagi.2018.00118

Cirrito, J. R., Yamada, K. A., Finn, M. B., Sloviter, R. S., Bales, K. R., May, P. C., et al. (2005). Synaptic activity regulates interstitial fluid amyloid-β levels *in vivo*. *Neuron* 48, 913–922. doi: 10.1016/j.neuron.2005.10.028

Fagiani, F., Lanni, C., Racchi, M., Pascale, A., and Govoni, S. (2019). Amyloid-β and synaptic vesicle dynamics: a cacophonic Orchestra. *J. Alzheimer's Dis.* 72, 1–14. doi: 10.3233/JAD-190771

Giuffrida, M. L., Caraci, F., Pignataro, B., Cataldo, S., De Bona, P., Bruno, V., et al. (2009). β-amyloid monomers are neuroprotective. *J. Neurosci.* 29, 10582–10587. doi: 10.1523/JNEUROSCI.1736-09.2009

Glenner, G. G., and Wong, C. W. (1984). Alzheimer's disease: initial report of the purification and characterization of a novel cerebrovascular amyloid protein. *Biochem. Biophys. Res. Commun.* 120, 885–890. doi: 10.1016/S0006-291X(84)80190-4

Grilli, M., Lagomarsino, F., Zappettini, S., Preda, S., Mura, E., Govoni, S., et al. (2010). Specific inhibitory effect of amyloid-β on presynaptic muscarinic receptor subtypes modulating neurotransmitter release in the rat nucleus accumbens. *Neuroscience* 167, 482–489. doi: 10.1016/j.neuroscience.2010.01.058

Gulisano, W., Melone, M., Li Puma, D. D., Tropea, M. R., Palmeri, A., Arancio, O., et al. (2018). The effect of amyloid-β peptide on synaptic plasticity and memory is influenced by different isoforms, concentrations, and aggregation status. *Neurobiol. Aging* 71, 51–60. doi: 10.1016/j.neurobiolaging.2018.06.025

Hanseeuw, B. J., Jonas, V., Jackson, J., Betensky, R. A., Rentz, D. M., Johnson, K. A., et al. (2020). Association of anxiety with subcortical amyloidosis in cognitively normal older adults. *Mol. Psychiatry* 25:2644. doi: 10.1038/s41380-018-0323-y

Hardy, J., and Selkoe, D. J. (2002). The amyloid hypothesis of Alzheimer's disease: progress and problems on the road to therapeutics. *Science* 297, 353–356. doi: 10.1126/science.1072994

Huang, Y., Potter, R., Sigurdson, W., Santacruz, A., Shih, S., Ju, Y., et al. (2012). Effects of age and amyloid deposition on Aβ dynamics in the human central nervous system. *Arch. Neurol.* 69, 51–58. doi: 10.1001/archneurol.2011.235

Ida, N., Hartmann, T., Pantel, J., Schröder, J., Zerfass, R., Förstl, H., et al. (1996). Analysis of heterogeneous βA4 peptides in human cerebrospinal fluid and blood by a newly developed sensitive western blot assay. *J. Biol. Chem.* 271, 22908–22914. doi: 10.1074/jbc.271.37.22908

Iliff, J. J., Wang, M., Liao, Y., Plogg, B. A., Peng, W., Gundersen, G. A., et al. (2012). A paravascular pathway facilitates CSF flow through the brain parenchyma and the clearance of interstitial solutes, including amyloid β. *Sci. Transl. Med.* 4:147ra111. doi: 10.1126/scitranslmed.3003748

Ismail, Z., Smith, E. E., Geda, Y., Sultzer, D., Brodaty, H., Smith, G., et al. (2016). Neuropsychiatric symptoms as early manifestations of emergent dementia: provisional diagnostic criteria for mild behavioral impairment. *Alzheimer's Dement.* 12, 195–202. doi: 10.1016/j.jalz.2015.05.017

Kamenetz, F., Tomita, T., Hsieh, H., Seabrook, G., Borchelt, D., Iwatsubo, T., et al. (2003). APP processing and synaptic function. *Neuron* 37, 925–937. doi: 10.1016/S0896-6273(03)00124-7

Kang, J. E., Lim, M. M., Bateman, R. J., Lee, J. J., Smyth, L. P., Cirrito, J. R., et al. (2009). Amyloid-β dynamics are regulated by orexin and the sleep-wake cycle. *Science* 326, 1005–1007. doi: 10.1126/science.1180962

Khan, G. M., Tong, M., Jhun, M., Arora, K., and Nichols, R. A. (2010). β-Amyloid activates presynaptic α7 nicotinic acetylcholine receptors reconstituted into a model nerve cell system: involvement of lipid rafts. *Eur. J. Neurosci.* 31, 788–796. doi: 10.1111/j.1460-9568.2010.07116.x

Koppensteiner, P., Trinchese, F., Fà, M., Puzzo, D., Gulisano, W., Yan, S., et al. (2016). Time-dependent reversal of synaptic plasticity induced by physiological concentrations of oligomeric Aβ42: an early index of Alzheimer's disease. *Sci. Rep.* 6:32553. doi: 10.1038/srep32553

Lanni, C., Fagiani, F., Racchi, M., Preda, S., Pascale, A., Grilli, M., et al. (2019). Beta-amyloid short- and long-term synaptic entanglement. *Pharmacol. Res.* 139, 243–260. doi: 10.1016/j.phrs.2018.11.018

Latif-Hernandez, A., Shah, D., Craessaerts, K., Saido, T., Saito, T., De Strooper, B., et al. (2019). Subtle behavioral changes and increased prefrontal-hippocampal network synchronicity in APP NL–G–F mice before prominent plaque deposition. *Behav. Brain Res.* 364, 431–441. doi: 10.1016/j.bbr.2017.11.017

Lazarevic, V., Fieńko, S., Andres-Alonso, M., Anni, D., Ivanova, D., Montenegro-Venegas, C., et al. (2017). Physiological concentrations of amyloid beta regulate recycling of synaptic vesicles via alpha7 acetylcholine receptor and CDK5/calcineurin signaling. *Front. Mol. Neurosci.* 10:221. doi: 10.3389/fnmol.2017.00221

Lussier, F. Z., Pascoal, T. A., Chamoun, M., Therriault, J., Tissot, C., Savard, M., et al. (2020). Mild behavioral impairment is associated with β-amyloid but not tau or neurodegeneration in cognitively intact elderly individuals. *Alzheimer's Dement.* 16, 192–199. doi: 10.1002/alz.12007

Marsh, J., Bagol, S. H., Williams, R. S. B., Dickson, G., and Alifragis, P. (2017). Synapsin I phosphorylation is dysregulated by beta-amyloid oligomers and restored by valproic acid. *Neurobiol. Dis.* 106, 63–75. doi: 10.1016/j.nbd.2017.06.011

Mawuenyega, K. G., Sigurdson, W., Ovod, V., Munsell, L., Kasten, T., Morris, J. C., et al. (2010). Decreased clearance of CNS β-amyloid in Alzheimer's disease. *Science* 330:1774. doi: 10.1126/science.1197623

Mo, J. A., Lim, J. H., Sul, A. R., Lee, M., Youn, Y. C., and Kim, H. J. (2015). Cerebrospinal fluid β-amyloid1-42 levels in the differential diagnosis of Alzheimer's disease - systematic review and meta-analysis. *PLoS ONE* 10:e0116802. doi: 10.1371/journal.pone.0116802

Mo, J. J., Li, J. Y., Yang, Z., Liu, Z., and Feng, J. S. (2017). Efficacy and safety of anti-amyloid-β immunotherapy for Alzheimer's disease: a systematic review and network meta-analysis. *Ann. Clin. Transl. Neurol.* 4, 931–942. doi: 10.1002/acn3.469

Mori, T., Shimada, H., Shinotoh, H., Hirano, S., Eguchi, Y., Yamada, M., et al. (2014). Apathy correlates with prefrontal amyloid β deposition in Alzheimer's disease. *J. Neurol. Neurosurg. Psychiatry* 85, 449–455. doi: 10.1136/jnnp-2013-306110

Mura, E., Preda, S., Govoni, S., Lanni, C., Trabace, L., Grilli, M., et al. (2010). Specific neuromodulatory actions of amyloid-beta on dopamine release in rat nucleus accumbens and caudate putamen. *J. Alzheimers Dis.* 19, 1041–1053. doi: 10.3233/JAD-2010-1299

Mura, E., Zappettini, S., Preda, S., Biundo, F., Lanni, C., Grilli, M., et al. (2012). Dual effect of beta-amyloid on α7 and α4β2 nicotinic receptors controlling the release of glutamate, aspartate and GABA in rat hippocampus. *PLoS ONE* 7:e29661. doi: 10.1371/journal.pone.0029661

Murphy, M. P., and Levine, H. (2010). Alzheimer's disease and the amyloid-β peptide. *J. Alzheimer's Dis.* 19, 311–323. doi: 10.3233/JAD-2010-1221

Olivero, G., Grilli, M., Chen, J., Preda, S., Mura, E., Govoni, S., et al. (2014). Effects of soluble β-amyloid on the release of neurotransmitters from rat brain synaptosomes. *Front Aging Neurosci.* 6:166. doi: 10.3389/fnagi.2014.00166

Ono, K., Condron, M. M., and Teplow, D. B. (2009). Structure-neurotoxicity relationships of amyloid β-protein oligomers. *Proc. Natl. Acad. Sci. U. S. A.* 106, 14745–14750. doi: 10.1073/pnas.0905127106

Park, D., Na, M., Kim, J. A., Lee, U., Cho, E., Jang, M., et al. (2017). Activation of CaMKIV by soluble amyloid-β1-42 impedes trafficking of axonal vesicles and impairs activity-dependent synaptogenesis. *Sci. Signal.* 10:eaam8661. doi: 10.1126/scisignal.aam8661

Preda, S., Govoni, S., Lanni, C., Racchi, M., Mura, E., Grilli, M., et al. (2008). Acute β-amyloid administration disrupts the cholinergic control of dopamine release in the nucleus accumbens. *Neuropsychopharmacology* 33, 1062–1070. doi: 10.1038/sj.npp.1301485

Puzzo, D., Privitera, L., Fa', M., Staniszewski, A., Hashimoto, G., Aziz, F., et al. (2011). Endogenous amyloid-β is necessary for hippocampal synaptic plasticity and memory. *Ann. Neurol.* 69, 819–830. doi: 10.1002/ana.22313

Puzzo, D., Privitera, L., Leznik, E., Fà, M., Staniszewski, A., Palmeri, A., et al. (2008). Picomolar amyloid-β positively modulates synaptic plasticity and memory in hippocampus. *J. Neurosci.* 28, 14537–14545. doi: 10.1523/JNEUROSCI.2692-08.2008

Russell, C. L., Semerdjieva, S., Empson, R. M., Austen, B. M., Beesley, P. W., and Alifragis, P. (2012). Amyloid-β acts as a regulator of neurotransmitter release disrupting the interaction between synaptophysin and VAMP2. *PLoS ONE* 7:e4320. doi: 10.1371/journal.pone.0043201

Sakakibara, Y., Sekiya, M., Saito, T., Saido, T. C., and Iijima, K. M. (2018). Cognitive and emotional alterations in app knock-in mouse models of Aβ amyloidosis. *BMC Neurosci.* 19:46. doi: 10.1186/s12868-018-0446-8

Schneider, L. (2020). A resurrection of aducanumab for Alzheimer's disease. *Lancet Neurol.* 19, 111–112. doi: 10.1016/S1474-4422(19)30480-6

Seubert, P., Vigo-Pelfrey, C., Esch, F., Lee, M., Dovey, H., Davis, D., et al. (1992). Isolation and quantification of soluble Alzheimer's β-peptide from biological fluids. *Nature* 359, 325–327. doi: 10.1038/359325a0

Sgourakis, N. G., Yan, Y., McCallum, S. A., Wang, C., and Garcia, A. E. (2007). The Alzheimer's peptides Aβ40 and 42 adopt distinct conformations in water: a combined MD / NMR Study. *J. Mol. Biol.* 368, 1448–1457. doi: 10.1016/j.jmb.2007.02.093

Sperling, R. A., Jack, C. R., Black, S. E., Frosch, M. P., Greenberg, S. M., Hyman, B. T., et al. (2011). Amyloid-related imaging abnormalities in amyloid-modifying therapeutic trials: recommendations from the Alzheimer's Association Research Roundtable Workgroup. *Alzheimer's Dement.* 7, 367–385. doi: 10.1016/j.jalz.2011.05.2351

Taragano, F. E., Allegri, R. F., Heisecke, S. L., Martelli, M. I., Feldman, M. L., Sánchez, V., et al. (2018). Risk of Conversion to Dementia in a Mild Behavioral Impairment Group Compared to a Psychiatric Group and to a Mild Cognitive Impairment Group. *J. Alzheimer's Dis.* 62, 227–238. doi: 10.3233/JAD-170632

Tong, M., Arora, K., White, M. M., and Nichols, R. A. (2011). Role of key aromatic residues in the ligand-binding domain of α7 nicotinic receptors in the agonist action of β-amyloid. *J. Biol. Chem.* 286, 34373–34381. doi: 10.1074/jbc.M111.241299

Walsh, D. M., and Selkoe, D. J. (2007). Aβ oligomers - a decade of discovery. *J. Neurochem.* 101, 1172–1184. doi: 10.1111/j.1471-4159.2006.04426.x

Wang, H. Y., Lee, D. H. S., D'Andrea, M. R., Peterson, P. A., Shank, R. P., and Reitz, A. B. (2000). β-Amyloid1-42 binds to α7 nicotinic acetylcholine receptor with high affinity. Implications for Alzheimer's disease pathology. *J. Biol. Chem.* 275, 5626–5632. doi: 10.1074/jbc.275.8.5626

Willis, B. A., Sundell, K., Lachno, D. R., Ferguson-Sells, L. R., Case, M. G., Holdridge, K., et al. (2018). Central pharmacodynamic activity of solanezumab in mild Alzheimer's disease dementia. *Alzheimer's Dement* 4, 652–660. doi: 10.1016/j.trci.2018.10.001

Yang, Y., Kim, J., Kim, H. Y., Ryoo, N., Lee, S., Kim, Y. S., et al. (2015). Amyloid-β oligomers may impair SNARE-mediated exocytosis by direct binding to syntaxin 1a. *Cell Rep.* 12, 1244–1251. doi: 10.1016/j.celrep.2015.07.044

Zappettini, S., Grilli, M., Olivero, G., Mura, E., Preda, S., Govoni, S., et al. (2012). Beta amyloid differently modulate nicotinic and muscarinic receptor subtypes which stimulate *in vitro* and *in vivo* the release of glycine in the rat hippocampus. *Front. Pharmacol.* 3:146. doi: 10.3389/fphar.2012.00146

Conflict of Interest: The authors declare that the research was conducted in the absence of any commercial or financial relationships that could be construed as a potential conflict of interest.

frontiers in Molecular Neuroscience

ORIGINAL RESEARCH
published: 12 April 2021
doi: 10.3389/fnmol.2021.576038

The Neuroprotective Beta Amyloid Hexapeptide Core Reverses Deficits in Synaptic Plasticity in the 5xFAD APP/PS1 Mouse Model

*Kelly H. Forest†, Ruth Taketa, Komal Arora†, Cedomir Todorovic and Robert A. Nichols**

Department of Cell & Molecular Biology, John A. Burns School of Medicine, University of Hawai'i at Mānoa, Honolulu, HI, United States

Alzheimer's disease (AD) is the most common cause of dementia in the aging population. Evidence implicates elevated soluble oligomeric Aβ as one of the primary triggers during the prodromic phase leading to AD, effected largely via hyperphosphorylation of the microtubule-associated protein tau. At low, physiological levels (pM-nM), however, oligomeric Aβ has been found to regulate synaptic plasticity as a neuromodulator. Through mutational analysis, we found a core hexapeptide sequence within the N-terminal domain of Aβ (N-Aβcore) accounting for its physiological activity, and subsequently found that the N-Aβcore peptide is neuroprotective. Here, we characterized the neuroprotective potential of the N-Aβcore against dysfunction of synaptic plasticity assessed in *ex vivo* hippocampal slices from 5xFAD APP/PS1 mice, specifically hippocampal long-term potentiation (LTP) and long-term depression (LTD). The N-Aβcore was shown to reverse impairment in synaptic plasticity in hippocampal slices from 5xFAD APP/PS1 model mice, both for LTP and LTD. The reversal by the N-Aβcore correlated with alleviation of downregulation of hippocampal AMPA-type glutamate receptors in preparations from 5xFAD mice. The action of the N-Aβcore depended upon a critical di-histidine sequence and involved the phosphoinositide-3 (PI3) kinase pathway via mTOR (mammalian target of rapamycin). Together, the present findings indicate that the non-toxic N-Aβcore hexapeptide is not only neuroprotective at the cellular level but is able to reverse synaptic dysfunction in AD-like models, specifically alterations in synaptic plasticity.

Keywords: beta amyloid (Aβ), neuroprotection, Alzheimer's disease, hippocampal slice, long-term potentiation, long-term depression

OPEN ACCESS

Edited by:
Oliver Wirths, University Medical Center Göttingen, Germany

Reviewed by:
Igor Klyubin, Trinity College Dublin, Ireland
Takashi Saito, Nagoya City University, Japan

****Correspondence:***
Robert A. Nichols
robert.nichols@hawaii.edu
orcid.org/0000-0003-0366-0162

†Present address:
Kelly H. Forest, Department of Biology, Dartmouth College, Hanover, NH, United States
Komal Arora, Department of Biology, College of Arts and Sciences, Georgia State University, Atlanta, GA, United States

Received: *25 June 2020*
Accepted: *11 March 2021*
Published: *12 April 2021*

Citation:
Forest KH, Taketa R, Arora K, Todorovic C and Nichols RA (2021) The Neuroprotective Beta Amyloid Hexapeptide Core Reverses Deficits in Synaptic Plasticity in the 5xFAD APP/PS1 Mouse Model. Front. Mol. Neurosci. 14:576038. doi: 10.3389/fnmol.2021.576038

INTRODUCTION

Alzheimer's disease (AD) is clinically characterized by impairments in cognitive memory and function. Loss of critical pre- and post-synaptic markers have been reported for postmortem AD brain tissue (Reddy et al., 2005; Scheff et al., 2006), suggesting that AD-related cognitive impairments are based, in large part, on synaptic dysfunction and loss. Additionally, accumulating

evidence shows a strong link between excess soluble oligomeric amyloid-β (Aβ) and synaptic dysfunction in AD (Walsh et al., 2002; Glabe, 2005; Shankar and Walsh, 2009). Cognitive decline and synaptic plasticity deficits are reported to occur prior to the accumulation of Aβ plaques and tau neurofibrillary tangles in the prodromic phase leading to AD (Oddo et al., 2003), supporting the idea that synaptic dysfunction and mild cognitive impairment are early events driven by soluble oligomeric Aβ rising to abnormally high levels years prior to AD diagnosis.

Synaptic dysfunction and eventual degeneration lead to abnormal synaptic transmission and impaired long-term potentiation (LTP) and/or long-term depression (LTD), which are important in synaptic plasticity and learning and memory. Pathological levels (high nM to μM) of Aβ have been shown to inhibit LTP-induction (Cullen et al., 1997; Chapman et al., 1999; Walsh et al., 2002) and enhance LTD (Li et al., 2009; Chen et al., 2013) in the hippocampus. On the other hand, low physiological levels (pM) of Aβ was found to enhance LTP and memory, indicating a hormetic effect of Aβ on synaptic plasticity (Puzzo et al., 2008, 2012; Lawrence et al., 2014; Gulisano et al., 2019).

Dysregulation of synaptic plasticity in AD pathogenesis involves altered regulation of NMDA-type and AMPA-type glutamate receptors. In addition to mediating Aβ-induced excitotoxicity, NMDA receptors can be depressed by Aβ at high concentrations (Snyder et al., 2005), inducing LTD (Hsieh et al., 2006; D'Amelio et al., 2011) as a consequence of subsequent downstream AMPA receptor internalization (Hsieh et al., 2006; D'Amelio et al., 2011) and dendritic spine loss (D'Amelio et al., 2011).

We have shown that at low concentration (pM-nM) the N-terminal Aβ fragment comprising amino acids 1–15/16 of the Aβ sequence, an endogenous peptide cleaved from Aβ via α-secretase (Portelius et al., 2011), is more effective as a neuromodulator than full-length Aβ1–42, stimulating receptor-linked increases in neuronal Ca^{2+}, enhancing synaptic plasticity and enhancing contextual fear memory (Lawrence et al., 2014). The Aβ1–16 peptide sequence corresponds to the C-terminal 16 amino acid sequence in soluble amyloid precursor protein-α (sAPP-α), referred to as the CTα16, which has also been shown to enhance synaptic plasticity (Morrisey et al., 2019). An essential core sequence comprising amino acids 10–15 of Aβ (N-Aβcore) was identified as the active region of the N-terminal Aβ fragment and was further shown to protect against Aβ-induced neuronal toxicity (Forest et al., 2018). Here, we aimed to better understand the neuroprotective mechanism of the N-Aβcore on synaptic plasticity. We investigated whether the N-Aβcore could rescue LTP and LTD dysfunction resulting from prolonged, elevated levels of Aβ in an APP/PS1 transgenic mouse model harboring mutations found in familial Alzheimer's disease (FAD), while assessing the impact on AMPA-type glutamate receptor expression in reference to the neuroprotective action of the N-Aβcore in Aβ-synaptotoxicity (Forest et al., 2020).

MATERIALS AND METHODS

Transgenic Mice and Cannulation Surgery

All animal handling, surgery, use and euthanasia were performed under approved IACUC protocols (11-1219-6/16-2282-2), compliant with NIH and Society for Neuroscience guidelines for use of vertebrate animals in neuroscience research. The human APP/PSEN1 mouse line, 5xFAD (Tg6799), on the B6.SJL background (B6SJL-Tg (APPSwFlLOn, PSEN1*M146L*L286V) 6799 Vas/Mmjax; obtained from JAX stock #006554, MMRRC034840 hemizygous) was used as a well characterized model for human Aβ-based FAD pathology and neurodegeneration (Oakley et al., 2006), with noted limitations in regard to its application in a physiological context. As the transgenic mice are hemizygous, age-matched B6.SJL background mice (MMRRC034840 Non-carrier) were used as controls. Aged adult mice at 7- to 8-months of age of both sexes (weight range: 28–35 g), obtained from established in-house colonies and housed in ventilated enrichment cages in the John A. Burns School of Medicine AAALAC-accredited Vivarium with *ad libitum* access to food and water, were used at roughly equal numbers, this age range selected for displaying pronounced LTP deficits in the transgenic line. For comparison of B6.SJL mice for baseline treatment, adult mice at 4–5 months of age were used in one set of experiments. Inclusion/exclusion criteria were based on animal health.

For bilateral cannulation and injection, the following protocol was employed (as per Forest et al., 2018). Cannulation into the dorsal aspects of both hippocampi of the 5xFAD mice at 7- to 8-months of age of both sexes was performed under full anesthesia (general: 1.2% Avertin; local at site: lidocaine) using stereotaxis (coordinates: −1.5 mm anteroposterior; ±1 mm lateral; −2 mm depth). After the brief surgical procedure and recovery (full righting reflex), mice were subsequently housed in sound-isolated, ventilated hotels prior to peptide injection one week later. On the day of microinjection (morning), sterile saline or 500 nM N-Aβcore peptide was administered bilaterally through the cannulae in the 5xFAD mice via microinjectors over 30s (0.5μL/side) and the mice were returned to their cages in the mouse hotel. Hippocampi were collected from euthanized mice 24 h after the bilateral microinjection of the saline or peptide, and lysates extracted from the hippocampi were prepared for immunoblot analysis (30 μg each). Euthanasia was performed under approved IACUC protocols (11-1219-6/16-2282-2). This study was not preregistered and followed ARRIVE guidelines.

Aβ Peptides

Solutions of $Aβ_{1-42}$ (American Peptide; Anaspec) were prepared from aqueous stock solutions, followed by bath sonication. This preparation of full-length Aβ ($Aβ_{1-42}$) was previously shown to exist predominantly in the oligomeric state (see Lawrence et al., 2014). The N-Aβcore peptide, YEVHHQ, and the substituted peptide, SEVAAQ, previously shown to be inactive (Forest et al., 2018), and here used as a control, were prepared from aqueous stock solutions of peptides synthesized and isolated at

>98% purity (Peptide 2.0). Concentrations of the Aβ peptides used were based on previous studies of synaptic plasticity (Lawrence et al., 2014).

Extracellular Field Potential Recordings in Hippocampal Slices

Hippocampal slices were prepared from aged adult (4- or 7- to 8- month-old) B6.SJL (control) or 5xFAD (Tg6799) mice (as per Lawrence et al., 2014). Cervical dislocation and decapitation were performed under approved IACUC protocols (11-1219-6/16-2282-2), compliant with NIH and Society for Neuroscience guidelines for use of vertebrate animals in neuroscience research. Brains were removed into ice-cold artificial cerebral spinal fluid (aCSF) consisting of 130 mM NaCl, 3.5 mM KCl, 10 mM glucose, 1.25 mM NaH_2PO_4, 2.0 mM $CaCl_2$, 1.5 mM $MgSO_4$, and 24 mM $NaHCO_3$, bubbled in 95% O_2/5% CO_2. Transverse brain slices of 400μm were obtained using a Leica vibrating microtome (Leica, VT1200S) and quickly transferred to fresh ice-cold aCSF for hippocampi isolation. Extracted hippocampi slices were incubated in bubbled aCSF in a holding chamber for 30 min at room temperature (23°C) after which the holding chamber was transferred to a 32°C water bath for 1 h. The chamber was then removed from the water bath and placed at room temperature for another 1 h prior to recording. The slices were subsequently transferred to a recording chamber and perfused at 3 mL/min with aCSF (bubbled with 95% O_2/5% CO_2) at 32°C. The Schaffer collateral fibers were stimulated at a frequency 0.1 Hz using a bipolar stimulating electrode and CA1 field excitatory postsynaptic potentials (fEPSPs) were recorded with a glass electrode filled with 3M NaCl (resistance 1–1.5 MΩ). Basal synaptic transmission was assessed by comparing stimulus strength against fEPSP slope to generate input/output (I/O) curves. A minimum of 20 min baseline stimulation was then performed, recording every minute. The baseline and stimulus current were adjusted during this period so that fEPSP stabilized at 30–40% of maximum amplitude.

Long-term potentiation was induced by a 3-theta-burst stimulation (TBS) protocol, where each burst consisted of four pulses at 100 Hz with a 200-ms interburst interval. LTD was induced using a low frequency stimulation (LFS) protocol, consisting of a 1 Hz single pulse stimulus (900 pulses for 15 min). TBS and LFS were administered after a 20-min baseline recording period for aCSF alone or a 35-min baseline recording period in aCSF (15 min) followed by inclusion of N-Aβcore in the absence or presence of tested reagents (20 min). For the latter, TBS and LFS were administered in the presence of N-Aβcore in the absence or presence of tested reagents. The phosphoinositide-3 (PI3) kinase inhibitor LY294002 (Sigma, # 440202) and the mTOR inhibitor rapamycin (Sigma, #553210) were used at effective concentrations based on prior studies (Hou and Klann, 2004).

Immunoblot Analysis

Hippocampi Injected With N-Aβcore

Hippocampi removed from euthanized 8-month-old 5xFAD mice previously bilaterally injected with saline or N-Aβcore were homogenized with 250 μL of Pierce IP Lysis Buffer (Thermo Fisher Scientific, # 87788, lot# MJ162614) with 1× Halt Protease and Phosphatase Inhibitor Cocktail (Thermo Fisher Scientific, # 78441, lot# SF248390). The homogenates were centrifuged at 18,000 × *g* for 20 min at 4°C and the supernatant was collected. The total amount of protein was quantified by a Pierce™ BCA Protein Assay Kit (Thermo Fisher Scientific, # 23225).

For each condition, gel sample buffer (4×; Thermo Fisher Scientific, # B0007, lot # 1920132) and reducing agent (10×; Thermo Fisher Scientific, # B0009, lot # 1901009) were added to diluted SDS-solubilized protein samples for a final protein concentration of 2 μg/μL. The samples were boiled at 95°C for 10 min, immediately cooled on ice and then centrifuged. Equal amounts of protein were subjected to electrophoretic separation on a 4–20% Tris-Glycine polyacrylamide gel (Thermo Fisher Scientific, #XP04200), transferred to Nitrocellulose membrane (LI-COR, # 92631092) via the iBlot2 semidry system (Thermo Fisher Scientific). Recovered blots were incubated in primary antibody (see below) overnight at 4°C. The transfer blots were washed 3× (10 min each wash) in 0.1% Tween-20 in Tris-buffered saline and incubated in the appropriate IR-dye-conjugated secondary antibody (LI-COR Biosciences) for 1 h. An Odyssey IR imaging system (LI-COR Biosciences, Lincoln, NE) was used for signal detection. Analysis was performed via Image Studio v5.2.5 software (LI-COR Biosciences).

The following primary antibodies were used for detection and normalization, respectively: anti-pAMPAR1 rabbit monoclonal antibody (pS831-GluA1; Cell Signaling Technology; RRID:AB_2799873) and anti-AMPAR1 rabbit monoclonal antibody (GluA1; Cell Signaling Technology; RRID:AB_2732897), both at 1:1000 and anti-beta actin mouse monoclonal antibody (Sigma-Aldrich; RRID:AB_476697) at 1:10,000 dilution.

Cultured Hippocampal Neurons

Hippocampal neuron cultures were prepared as described (Cheng and Yakel, 2015) from neonatal mouse pups (0–2 days old; 1 litter (6–10 mice)/preparation) from female breeders housed in the John A. Burns School of Medicine AAALAC-accredited Vivarium of either gender (equivalent numbers) obtained from established colonies of wild-type B6.SJL (background) mice. All animal procedures (handling; euthanasia) followed an IACUC-approved protocol (16-2282-2), compliant with NIH and Society for Neuroscience guidelines for use of vertebrate animals in neuroscience research. Following rapid decapitation, brains were removed from the mice into ice-cold Neurobasal A medium (NB) containing B-27 supplement, 5% fetal bovine serum (FBS) and Gentamicin. Hippocampi were then dissected under a stereomicroscope (Olympus SZ61). The isolated hippocampi were treated with papain (Worthington, LS003126, Lot # 35N16202) in Hanks buffer with 10 mM cysteine at 37°C for 15 min. The partially digested tissue was washed by centrifugation in NB plus FBS. The cells were dissociated using sequential trituration (polished Pasteur pipettes of decreasing diameter) and collected by low-speed centrifugation. The dissociated cells were pre-plated in standard tissue culture dishes to remove adherent non-neuronal cells (glia;

fibroblasts) for 10–15 min. The neuron-enriched preparation was diluted to 1×10^5 cells/mL and then plated into poly-D-lysine-coated 24-well dishes in NB plus serum and Gentamicin. The cultures were washed with Neurobasal A medium containing B27 and Gentamicin to remove the serum and then cultured in this media for 7–10 days prior to treatment with Aβ, N-Aβcore or the combination for an additional 7 days.

qPCR

RNA was extracted from treated cultured hippocampal neurons using the PureLink® RNA Mini Kit (Ambion, Life Technologies, #12183025) as per the manufacturer's protocol. Genomic DNA contamination was eliminated from the RNA preparation by digesting with RNase-free DNase (Qiagen, #79254). The iScript cDNA Synthesis Kit (Bio-Rad) was used to synthesize cDNA. The expression levels of various genes were then determined using SYBR green via qPCR (Bio-Rad iCycler iQ^{TM} Multicolor Real-Time PCR Detection System) using the primers listed in **Table 1**. Cycling conditions were as follows: 95°C for 15 min, followed by 40 cycles of 94°C for 15 s and 60°C for 60 s and the fold-changes in the variously treated samples compared to untreated (vehicle control) samples were calculated after normalizing to GAPDH gene expression.

Data and Statistical Analysis

Treatment and units were randomized as to order for all assays and experiments. Biological replicates were based on independent samples (*n*). For extracellular recording, each biological replicate was one mouse hippocampal slice (only one slice from one mouse hippocampus per condition), unless otherwise noted. All experiments were repeated at least three times, unless otherwise noted. After testing for normality, multiple comparisons of the data were made using one-way ANOVA with Bonferroni or Tukey's *post hoc* tests, as indicated. Paired comparison was made using Student's *t*-tests, or as appropriate, Chi-square test. *P*-values < 0.05 were considered the minimum for significance (as rejection of the null hypothesis). Unless otherwise noted, data were analyzed and graphed with GraphPad Prism 5 (GraphPad v5.0b; RRID:SCR_002798) using the appropriate statistical tests.

TABLE 1 | Sequences of Primers for qPCR.

Gene (accession number)	Sequence (5′–3′)
GluA1 (NM_001113325)	
Forward	AAGAGAAACAAGAGAAACCT
Reverse	GATGTACGGCATATTCCTT
GluA2 (NM_001083806)	
Forward	TTTGTGGATGCTCTACTT
Reverse	ATCTGTATGCTGTTAGAAGA
Akt1 (NM_009652)	
Forward	AGAAGAGACGATGGACTT
Reverse	GCTTCAGGTACTCAAACT
Akt3 (NM_011785)	
Forward	GATGTGGACTTACCTTATC
Reverse	TTCCTCTGGTGTATCTAC
mTOR (NM_020009)	
Forward	GGCACACATTTGAAGAAG
Reverse	GTGATCTCCTCCATCTCT
PI3KCa (NM_008839)	
Forward	TGATTCTGACTCCATAAGG
Reverse	GTCACTATCATTCCATTGG
PI3KCb (NM_029094)	
Forward	GATGTTATGGAAGCAAGT
Reverse	CATATACAGCAGTTTGATTC

RESULTS

The N-Aβcore Reversed LTP Deficits Induced by Pathological Levels of Full-Length Aβ

We have previously shown that the N-terminal Aβ fragment ($A\beta_{1-15/16}$) enhances synaptic plasticity and contextual fear memory while protecting against Aβ-linked synaptic impairment (Lawrence et al., 2014). Considering the evidence that the N-Aβcore hexapeptide, YEVHHQ, accounts for the neuromodulatory activity of the N-terminal Aβ fragment, we assessed whether the N-Aβcore is capable of reversing Aβ-linked synaptic dysfunction in an *ex vivo* model. We utilized hippocampal slices from a mutant APP/PS1 transgenic AD-like endophenotype mouse model (5xFAD) and their wild-type counterparts (B6.SJL) to examine synaptic transmission. Basal synaptic transmission at the Schaffer collateral-CA1 synapses represented by input-output curves shows that the fEPSP slopes versus stimulus strength for both the 5xFAD and B6.SJL control mice were comparable (**Figure 1A**), ruling out any issues with regard to impact of the Aβ fragment peptides on baseline synaptic strength. Treatment with 500 nM N-Aβcore during baseline recordings induced increases in baseline synaptic transmissions for both 5xFAD and B6.SJL, but was only significant in the B6.SJL slices (**Figure 1B**; average increase relative to untreated controls: 110% ± 2% SD), similar to that observed for the N-terminal Aβ fragment over the same time period (Lawrence et al., 2014), where the increased fEPSPs were found to extend through the high-frequency stimulation and post-tetanic potentiation (see **Figure 1C**).

To assess sustained changes in synaptic plasticity, we used a 3×-TBS stimulation protocol at the Schaffer collaterals to measure LTP in the CA1 region (see cross-sectional diagram of the hippocampus in **Figure 1A**, inset). LTP showed a trend toward enhancement for the N-Aβcore-treated B6.SJL slices as compared to untreated slice, though it was not significant (**Figures 1C,E**). Consistent with previous findings (Crouzin et al., 2013), LTP in the 5xFAD slices was substantially reduced compared to that observed for slices from B6.SJL (**Figures 1C,E**; 24.2% of control), dropping to near baseline at 60 min post-TBS. By contrast, prestimulation treatment with 500 nM N-Aβcore restored LTP in the 5xFAD slices to the level seen for the wild-type slices (**Figures 1C,E**; 107% ± 44% SD of control). These findings demonstrate that the N-Aβcore can reverse LTP deficits

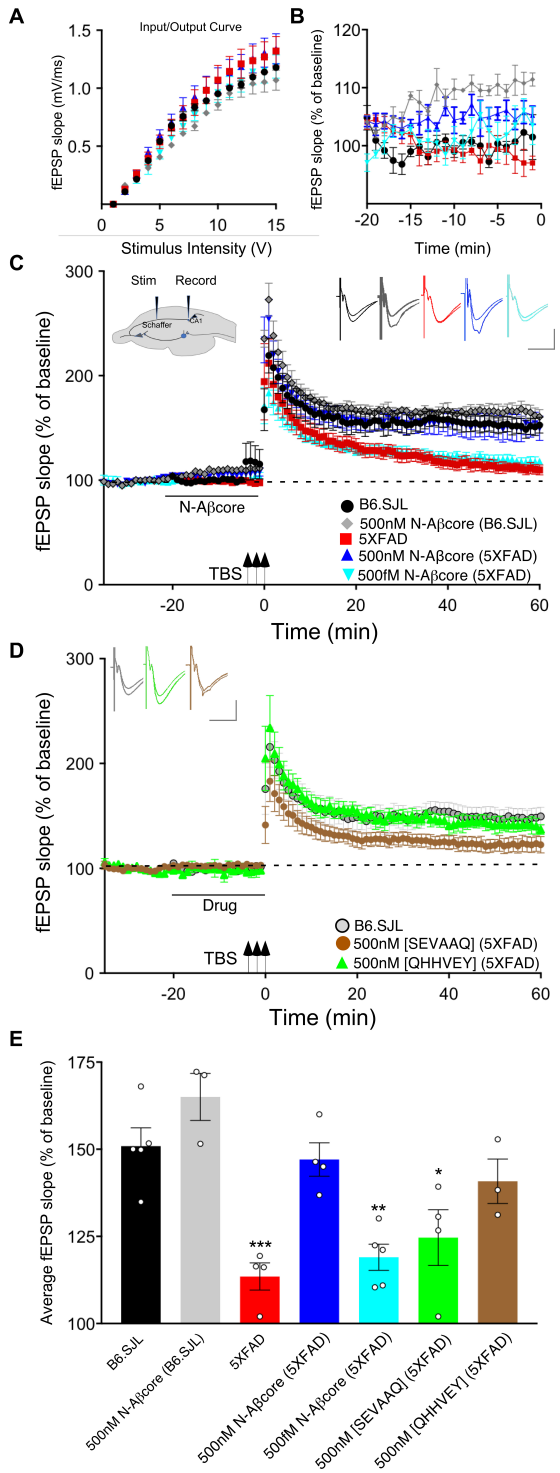

FIGURE 1 | The N-Aβcore reverses Aβ-induced synaptic impairment in APP/PSEN1 mutant mouse hippocampal slices. Input/output curves **(A)** plotting average fEPSP slopes versus stimulus strength before treatment and baseline recordings compared to panel **(B)** during the drug pretreatment period versus aCSF perfusion alone prior to stimulation for: control aCSF in B6.SJL slices (black, $n = 5$), 5xFAD slices (red, $n = 4$), 500 nM N-Aβcore in B6.SJL slices (gray, $n = 3$) and 5xFAD slices (blue, $n = 4$), plus 500 fM. *(Continued)*

FIGURE 1 | Continued
N-Aβcore in 5xFAD slices (cyan, $n = 5$). No statistically significant differences in the input/output curves **(A)** were found ($p > 0.05$, one-way repeated measures ANOVA). Averaged (last 10 min**) baseline data **(B)** were analyzed by one-way ANOVA ($F_{(4,16)} = 7.53$, $p = 0.0013$). Bonferroni *post hoc* tests revealed significant enhancement of baseline fEPSPs by 500 nM N-Aβcore on B6.SJL slices compared to aCSF-perfused B6.SJL slices ($p = 0.006$), aCSF perfused 5xFAD slices ($p = 0.002$), and by 500 fM N-Aβcore on 5xFAD slices ($p = 0.038$). **(C)** TBS-induced LTP for B6.SJL slices perfused with control aCSF (black, $N = 5$) or 500 nM N-Aβcore (gray, $N = 3$) and 5xFAD slices with aCSF (red, $N = 4$), 500 nM N-Aβcore (blue, $N = 4$) and 500 fM N-Aβcore (cyan, $N = 5$). Inset in panel **(C)**, diagram of hippocampal slice stimulation of the Schaffer collaterals (Stim) and recording fEPSPs in CA1 (Record). **(D)** TBS-induced LTP for 5xFAD slices treated with 500 nM [SEVAAQ] (green, $n = 5$) or 500 nM [QHHVEY] (brown, $n = 3$) substituted N-Aβcore peptides, and, as a reference, B6.SJL perfused with control aCSF [gray circles, $n = 5$, data from panel **(C)**]. **(E)** Quantification of average fEPSP slope values for 50–60 min post TBS. All groups shown in panels **(C,D)** were analyzed by one-way ANOVA ($F_{(6,21)} = 11.33$, $p < 0.0001$). Bonferroni *post hoc* tests: differences found for 5xFAD slices ($p = 0.0012$), 500 fM N-Aβcore in 5xFAD slices ($p = 0.0036$), and 500 nM [SEVAAQ] in 5xFAD slices ($p = 0.041$) when compared to aCSF-perfused (control) B6.SJL slices. Application of 500 nM N-Aβcore in 5xFAD slices reversed the LTP deficit in the 5xFAD slices ($p < 0.0005$). Horizontal bars in panels **(C,D)** indicate the period (20 min) of drug delivery for the color-coded conditions as indicated. Arrows indicate timing of TBS in panels **(C,D)**. Color-coded insets showing examples of fEPSPs (baseline vs. LTP). All data are means ± SEM. *N* values represent independent experiments (1 slice/mouse). Inset calibration: horizontal, 10 ms; vertical, 0.4 mV. $^*p < 0.05$; $^{**}p < 0.005$, $^{***}p < 0.0005$

induced from prolonged exposure to pathological levels of Aβ, while modestly enhancing basal synaptic transmission.

The N-Aβcore Reversed Full-Length Aβ-Linked Downregulation of Hippocampal AMPA-Type Glutamate Receptors

Regulation of synaptic expression of AMPA-type glutamate receptors (AMPARs) has been shown to underlie LTP (Makino and Malinow, 2009; Huganir and Nicoll, 2013). As downregulation of AMPARs is linked to the impairment in hippocampal LTP in APP/PS1 mice (Hsieh et al., 2006), the impact *in vitro* and *in vivo* of the N-Aβcore on the regulation of hippocampal AMPARs was assessed.

Utilizing hippocampal neuronal cultures derived from the background wild-type mice, B6.SJL, and treated with exogenous full-length Aβ ($Aβ_{42}$) for 7 days, $Aβ_{42}$ was shown to downregulate AMPAR1 (GluA1) transcript expression assessed via qPCR in this *in vitro* Aβ toxicity model as compared to untreated control cultures (**Figure 2A**), consistent with previous findings. There was no significant impact of the N-Aβcore compared to control, while there was a modest trend for the N-Aβcore on the downregulation by $Aβ_{42}$. There was no impact of any condition on AMPAR2 (GluA2) transcript expression.

Proteins solubilized from hippocampi isolated from 5xFAD mice bilaterally injected with the N-Aβcore or saline vehicle were assayed for changes in *in vivo* expression of hippocampal AMPAR1 (GluA1) via immunoblot analysis. Total GluA1 levels in the hippocampi were increased with exposure to the N-Aβcore

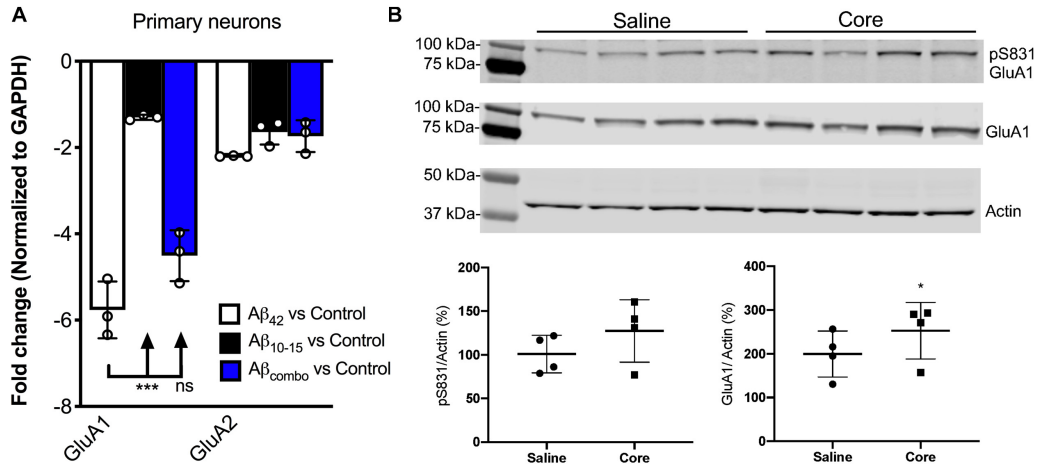

FIGURE 2 | N-AβCore normalizes AMPAR1 expression in an *in vitro* Aβ neurotoxicity model of primary hippocampal neurons and *in vivo* in hippocampi of 5xFAD APP/PS1 mice. **(A)** Normalized average expression of AMPA receptor GluA1 and GluA2 transcripts in B6.SJL mouse hippocampal neuron cultures exposed to full-length $A\beta_{1-42}$ ($A\beta_{42}$), the N-Aβcore ($A\beta_{10-15}$) or the combination (combo), as measured via qPCR. Data are means ± SD. $N = 3$ cultures for each condition. ***$p = 0.000001$ (Bonferroni *post hoc* tests for one-way ANOVA comparison between $A\beta_{42}$ and $A\beta_{10-15}$). There was no statistical difference between expression for any condition for GluA2. **(B)** Expression of pAMPAR1 (pGluA1) or total AMPAR1 (GluA1) in the hippocampi of 5xFAD mice injected with sterile saline or N-Aβcore (Core), as measured using western immunoblot. $N = 4$ mice for each condition. Total GluA1: *$p < 0.0001$ (Chi-square).

as compared to saline-injected controls (**Figure 2B**; 248% ± 67% SD; $p < 0.0001$ by Chi-square (42.3, 3df). The increase in relative pAMPAR1 (pS831) in the hippocampi exposed to N-Aβcore was accounted by the increase in total GluA1 (**Figure 2B**; 127% ± 35% SD).

Structure-Function and Concentration-Dependence of the N-Aβcore in Reversing LTP Impairment in Hippocampal Slices From 5xFAD APP/PS1 Mice

We also tested for basic concentration-dependence of the N-Aβcore in reversing LTP impairment in the 5xFAD mouse hippocampal slices. Low concentration (0.5 pM) of the N-Aβcore showed no difference on LTP compared to control 5xFAD slices (**Figures 1C,E**; 107% ± 7% SD compared to 5xFAD).

Through Aβ-interacting receptor-linked Ca^{2+} and neurotoxicity assays, we had previously shown that mutating the tyrosine residue in the N-Aβcore to a serine [Y10S] or mutating the two histidine residues to two alanines [H13A, H14A] reduces activity, indicating these amino acid residues in the N-Aβcore sequence are essential for activity (Lawrence et al., 2014; Forest et al., 2018). To confirm the specificity of the N-Aβcore in reversing LTP impairment in 5xFAD hippocampal slices, we tested the inactive triple mutant [SEVAAQ] and the reverse-sequence N-Aβcore [QHHVEY]. Treatment with the reverse-sequence N-Aβcore partially restored LTP in the 5xFAD hippocampal slices (**Figures 1D,E**). Note that the reverse-sequence peptide contains the critical di-histidine sequence. By contrast, the inactive triple mutant had no significant effect on LTP in the 5xFAD slices (**Figures 1D,E**; 110% ± 13% SD compared to 5xFAD). It is important to note that there was no change in basal synaptic transmission or a trend toward increasing LTP in the wild-type slices treated with the reverse N-Aβcore (not shown), as seen for the N-Aβcore. Taken together, these results confirm the contribution of the two essential histidine residues to the neuromodulatory activity of the N-Aβ core.

N-Aβcore Rescue of Aβ-Induced LTP Deficits Involves PI3 Kinase and mTOR

Long-term potentiation has shown to involve multiple protein kinase and phosphatase pathways (Thomas and Huganir, 2004; Kennedy, 2013). As prior evidence implicates the PI3 kinase and mTOR pathways in the regulation of Aβ neurotoxicity (Lafay-Chebassier et al., 2005; Lee et al., 2008) and in the regulation of LTP (Hoeffer and Klann, 2010), we evaluated the roles of PI3 kinase and mTOR in the action of the N-Aβcore in reversing impaired LTP via treatment of the hippocampal slice preparations with selective inhibitors. As shown in **Figure 3**, application of PI3 kinase inhibitor LY294002 had no impact on baseline responses or LTP in hippocampal slices from control (background B6.SJL) mice or 5xFAD mice. In contrast, application of LY294002 prior to treatment with the N-Aβcore prevented the rescue by the N-Aβcore of LTP in the slices from 5xFAD mice (**Figure 3**; 94.3% ± 15% SD compared to 5xFAD).

Prior inhibition of the PI3 kinase pathway effector mTOR by rapamycin also prevented the rescue by the N-Aβcore of LTP in the slices from 5xFAD mice (**Figure 4B**; 101% ± 20% SD compared to 5xFAD slices). The acute treatment with rapamycin had no significant effect on the control B6.SJL slices (**Figure 4A**). Rapamycin also had no significant effect on the reduced level of LTP in the 5xFAD slices at any point, and rapamycin prevented the rescue by N-Aβcore at all time points post-TBS. The inhibitor also did not affect baseline responses.

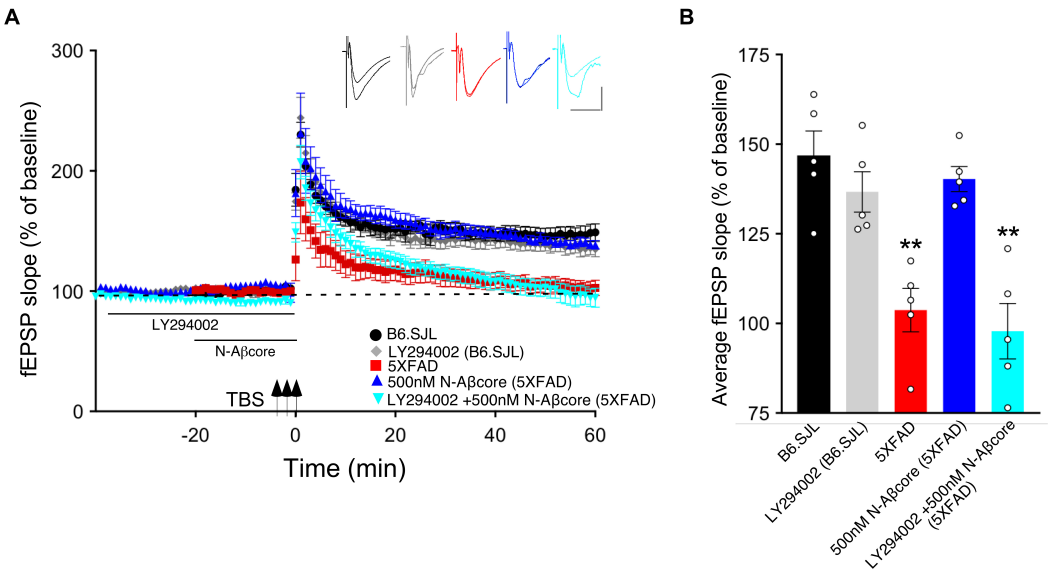

FIGURE 3 | N-Aβcore protection of Aβ-induced synaptic dysfunction involves the PI3 kinase pathway. **(A)** TBS-induced LTP for B6.SJL slices perfused with control aCSF (black) or 100 μM LY294002 (gray) and for 5xFAD slices with aCSF (red), 500 nM N-Aβcore (blue) or 500 nM N-Aβcore plus 100μM LY294002 (cyan). Color-coded inserts showing examples of fEPSPs (baseline vs. LTP). **(B)** Quantification of average fEPSP slope values for 50–60 min post-TBS (one-way ANOVA: $F_{(4,20)} = 13.63$, $p < 0.0001$). Bonferroni *post hoc* tests showed that rescue of the LTP deficit in the 500 nM N-Aβcore-treated 5xFAD slices (**$p = 0.004$, 500 nM N-Aβcore 5xFAD vs. 5xFAD; $p < 0.05$, vs. aCSF B6.SJL) was blocked by 100 μM LY294002 pretreatment (**$p = 0.0002$, 100μM LY294002 + 500 nM N-Aβcore vs. aCSF B6.SJL). Arrows indicate timing of TBS in **(A)**. All data are expressed as means ± SEM. $N = 4$ for each condition (1 slice/mouse). Inset calibration: horizontal, 10 ms; vertical, 0.4 mV. **$p < 0.005$.

To further probe the mechanism by which the N-Aβcore regulates the PI3 kinase pathway, the impact of the core peptide on Aβ-linked regulation of the PI3 kinase and its downstream effectors Akt and mTOR was investigated using mouse hippocampal neuron cultures. Treatment of neuron cultures with full-length Aβ (1–42) was shown to downregulate expression of various PI3 kinase, Akt and mTOR transcripts (**Figure 5**). While modest changes were noted on treatment with the N-Aβcore (not significant from control for mTOR), co-treatment with the N-Aβcore alleviated the Aβ-induced downregulation of Akt1 and mTOR transcripts (**Figure 5**).

Elevated Levels of Aβ Enhances LTD and the N-Aβcore Reverses Aβ-Linked LTD Enhancement in Hippocampal Slices From 5xFAD APP/PS1 Mice

Long-term depression is an essential component of synaptic plasticity underlying memory processing in the hippocampus, as synapses cycle between LTP and LTD, a process known as synaptic scaling (Nägerl et al., 2004). To date, few studies have examined the effects of pathological levels of soluble Aβ on LTD induction, and moreover, the results have been mixed. For example, while focusing on NMDA receptor-dependent LTD, administration of synthetic Aβ led to an enhancement of LTD in some cases (e.g., Kim et al., 2001; Shankar et al., 2008; Li et al., 2009), whereas other studies reported no effect (e.g., Wang et al., 2002). Here, we aimed to examine the effects of endogenous soluble Aβ on LTD in the 5xFAD hippocampal slices. Using LFS to induce LTP in the same Schaffer collateral – CA1 pathway in hippocampal slice as that used for LTP, the LTD in slices from the 5xFAD mice was more pronounced than that observed for LTD induced in slices from B6.SJL control mice (**Figures 6A,B**; −32.5% ± −5.1% SD for 5xFAD compared to −18.1% ± −4.9% SD for the control B6.SJL slices). Interestingly, treatment of 5xFAD mouse slices with the N-Aβcore prior to and during LFS resulted in a restoration of LTD to the level observed for the B6.SJL slices (**Figures 6A,B**; −21.4% ± 4.5%). The N-Aβcore had no effect on metabotropic glutamate receptor-induced LTD (**Figures 6C,D**). Taken together, these data suggest that Aβ plays a role in facilitating LTD and the N-Aβcore may protect against Aβ-induced LTD enhancement. The role of the NMDA receptor in Aβ facilitation of LTD warrants further investigation.

DISCUSSION

Previous studies have established a strong link between the progression of AD and the extent of synaptic dysfunction occurring in the early stages of the disease, prior to the formation of Aβ plaques and tau neurofibrillary tangles (Terry et al., 1991; Scheff et al., 2006; Shankar and Walsh, 2009; Koffie et al., 2011). In AD-endophenotype APP transgenic mouse models, though limited in regard to physiological context for APP expression, it has been widely demonstrated that elevated levels of soluble oligomeric Aβ drive LTP inhibition (Cullen et al., 1997; Chapman et al., 1999; Walsh et al., 2002; Kimura and Ohno, 2009), coupled to downregulation of synaptic AMPARs. By contrast,

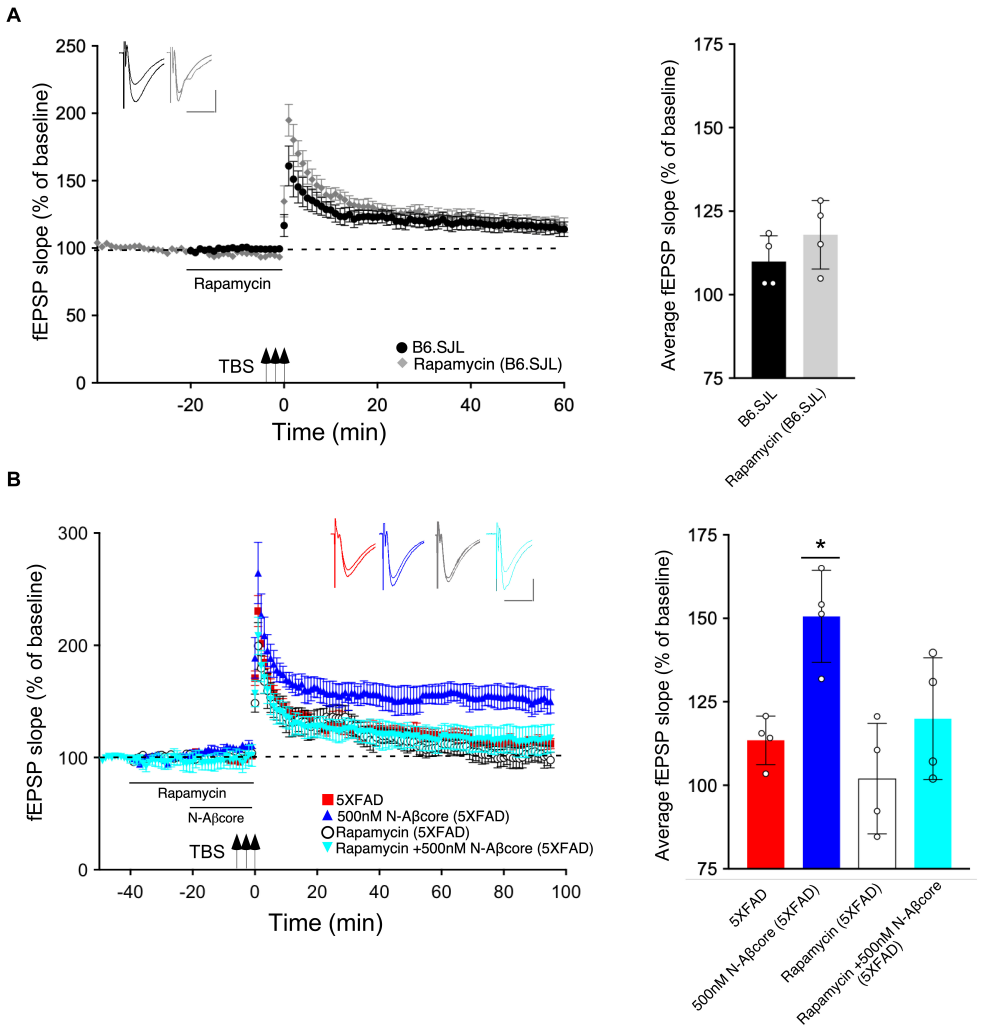

FIGURE 4 | N-Aβcore protection of Aβ-induced synaptic dysfunction involves mTOR downstream in the PI3 kinase pathway. **(A)** Left, Lack of effect of acute pretreatment of 500 nM rapamycin (gray) on TBS-induced LTP for B6.SJL slices as compared to LTP induced in aCSF-treated B6.SJL control slices (black) from 4–5 month-old mice. Right, Comparison of average fEPSP slope values for 50–60 min post-TBS for B6.SJL slices incubated in 500 nM rapamycin to aCSF-treated B6.SJL control slices ($t_{(6)}$ = 0.26, p = 0.8023; two-tailed unpaired Student's t-test). **(B)** Left, TBS-induced LTP for 5xFAD slices with aCSF (red), 500 nM rapamycin (white circle), 500 nM N-Aβcore (cyan) or 500 nM N-Aβcore plus 500 nM rapamycin (blue). Right, Rescue of LTP deficit following 20-min 500 nM N-Aβcore treatment in 5xFAD slices (*p = 0.0217, Bonferroni *post hoc* test after one-way ANOVA, $F_{(3,12)}$) was abolished with 500 nM rapamycin pretreatment (40 min) (ns, Bonferroni: rapamycin + N-Aβcore in 5xFAD vs. 5xFAD alone). There was no effect of acute pretreatment of rapamycin on LTP in 5xFAD slices (ns, Bonferroni: rapamycin in 5xFAD vs. 5xFAD alone). Arrows indicate timing of TBS in **(A)** and **(B)**. All recording data **(A,B)** are means ± SEM. Averaged data for 50–60 min post-tetanus are means ± SD. N = 4 for each condition (1 slice/mouse). Color-coded insets show examples of fEPSPs (baseline vs. LTP). Calibration bars for insets: horizontal, 10 ms; vertical, 0.4 mV.

the link between pathological levels of Aβ and LTD are less well understood, and as previously noted, investigations of the impact of Aβ on LTD have had conflicting results.

Low "physiological" levels (pM) of soluble Aβ have been shown to enhance synaptic plasticity and facilitate hippocampal-based learning and memory (Puzzo et al., 2008; Puzzo et al., 2012; Lawrence et al., 2014), suggesting a neuromodulatory role of soluble Aβ at physiological levels. Augmentation of LTP by pM Aβ correlated with enhanced expression of AMPARs. Similar results obtained using an N-terminal fragment of Aβ (1–15) implicated that sequence within Aβ as accountable for the positive neuromodulatory activity of full-length Aβ (Lawrence et al., 2014). We wondered whether the N-Aβcore (10–15; YEVHHQ), encompassing the essential sequence within the N-terminal fragment accounting for its positive neuromodulatory activity and its cellular neuroprotective activity against Aβ neurotoxicity, could itself enhance synaptic plasticity and protect against Aβ-induced synaptic dysfunction.

In accordance with previous findings (Kimura and Ohno, 2009), we found that LTP was nearly absent in the hippocampal slice model from APP/PS1 5xFAD transgenic mice, previously

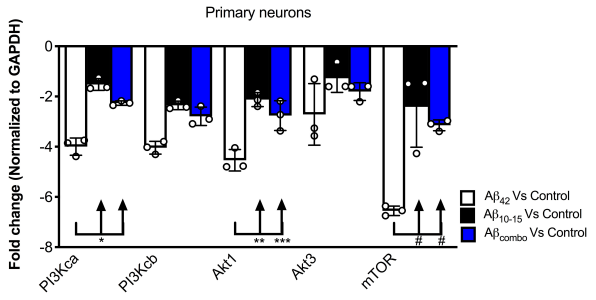

FIGURE 5 | Impact of N-Aβcore on regulation of various PI3 kinase, Akt and mTOR transcripts by Aβ. Primary mouse hippocampal neuron cultures were treated with 1 μM full-length $Aβ_{42}$, 1 μM $Aβ_{10-15}$ (N-Aβcore) or the combination (combo). Extracted RNA was subjected to qPCR, probing for Class 1 PI3 kinase catalytic subunits (CA and CB), Akt1 and Akt2 and mTOR. Data are expressed as averaged fold-change over untreated controls, after normalizing for GAPDH expression. Bars are means ± SD. $^{*}p = 0.00063$; $^{**}p = 0.000002$; $^{***}p = 0.0001$; $^{\#}p = 0.000001$ (Bonferroni *post hoc* tests for one-way ANOVA comparisons, as shown). For each condition, $N = 3$ cultures.

shown to be accounted by elevated Aβ in the brains of the transgenic model mice (Oakley et al., 2006; Crouzin et al., 2013), though the possibility of altered levels of the different sAPP variants in 5xFAD mice is to be noted and, while primarily neurotrophic (see Dar and Glazner, 2020), they may also contribute to the mutant phenotype and regulation of synaptic plasticity by the N-Aβcore. Treatment here with the N-Aβcore reversed this deficit back to the LTP observed in slices from age-matched background B6.SJL mice. Treatment of 5xFAD slices with the N-Aβcore trended toward LTP enhancement, suggesting that the reversal of the LTP deficits in the 5xFAD slices by the N-Aβcore was not solely due to competitive binding for target receptors and may possibly involve activation of a neuroprotective pathway that enhances synaptic plasticity (see Forest and Nichols, 2019). Here, we identified the PI3 kinase/Akt/mTOR in the reversal of LTP deficits in 5xFAD slices by the N-Aβcore as a primary pathway, which has been shown to be a key link to long-term memory (Bekinschtein et al., 2007). Under the conditions used for the mutant APP/PS1 5xFAD model preparation, we did not observe any evident impact of the mTOR inhibitor rapamycin, consistent with existing mTOR dysregulation of LTP in AD model mouse preparations (Ma et al., 2010), shown to be rescued by upregulation of mTOR. Our findings using selective inhibitors suggest that treatment of the 5xFAD slice preparations with the N-Aβcore upregulated PI3 kinase/Akt/mTOR, accounting, at least in part, for the rescue by the N-Aβcore of hippocampal LTP deficits in this mutant APP/PS1 5xFAD model.

Other downstream pathways engaged by the N-Aβcore are not yet definitely identified, but we suspect that key players involved in synaptic modulation may also affected, such as regulation of CREB, PKA, and/or CAMKII or downregulation of calcineurin and/or PP1, subsequently altering AMPA receptor trafficking to the synapses (Derkach et al., 2007; Makino and Malinow, 2009; Huganir and Nicoll, 2013; Herring and Nicoll, 2016). Additionally, the enhancement of the basal synaptic transmission with the treatment of the N-Aβcore suggests a receptor-linked influx of Ca^{2+}, which further supports the idea that the N-Aβcore activates an alternative neuroprotective pathway that enhances synaptic plasticity, consistent with results for neuroprotection by the N-Aβcore in Aβ-triggered neurotoxicity (Forest et al., 2018). Previously, it has been shown that BDNF enhances basal synaptic transmission (Patterson et al., 1996), and therefore, it may be that the N-Aβcore-induced Ca^{2+} influx could regulate BDNF release at the synapses, thus enhancing baseline synaptic transmission and ultimately LTP (see Lu, 2003). It would be interesting to examine the effect of the basal synaptic transmission by the N-Aβcore long-term, and whether the enhancement of LTP observed involved BDNF.

In the context of synaptic plasticity, LTD is necessary for neural homeostasis. NMDA receptor-dependent LTD involves internalization of AMPA receptors via a caspase-dependent pathway (D'Amelio et al., 2011; Li and Sheng, 2012). To date, however, there is limited understanding in regard to the effects of pathological Aβ on LTD, where some groups show that synthetic Aβ enhances LTD (Kim et al., 2001; Shankar et al., 2008; Hu et al., 2014) and others show no effect (Wang et al., 2002; Raymond et al., 2003), though the differential action of Aβ may have resulted from recording in different subregions of the hippocampus (e.g., CA1 vs. dentate gyrus). Here, we found that high concentrations of endogenous soluble Aβ shown to be present in the brains of 5xFAD mice resulted in enhanced LTD in hippocampal slices, and treatment with effective concentrations of N-Aβcore prior to and during the LFS induction of LTD reverses this enhancement. Interestingly, Hu et al. (2014) found that applying synthetic soluble Aβ prior to LFS did not affect the early phase of LFS-induced LTD (<2 h post LFS), but facilitated the late phase (3–5 h post LFS), thus, possibly accounting for different findings. It is important to note that late-phase LTP and LTD require new protein synthesis, and mTOR is linked to the regulation of protein synthesis (Wang and Proud, 2006). Indeed, as previously noted, the reversal by the N-Aβcore of LTP deficit in the 5xFAD slices was dependent upon mTOR. As LTD and LTP work in concert to allow for reversible synaptic plasticity and synaptic scaling, the LFS-induced enhancement of LTD in the 5xFAD slices could affect subsequent LTP, and this may be another reason why an LTP deficit was observed in the 5xFAD slices compared to wild-type preparations.

Although NMDA and AMPA receptors are involved in different aspects of LTP and LTD, and their expression is affected by elevated Aβ, metabotropic glutamate receptors (mGluRs) have also been implicated in Aβ-induced synaptic dysfunction (Wang et al., 2004; Chen et al., 2013; Hu et al., 2014; Haas et al., 2016). Interestingly, NMDA-independent, mGluR-induced LTD was found to be unaffected by the N-Aβcore. While mGluRs have been linked via cellular prion to Aβ-induced cellular toxicity (Haas et al., 2016), our findings support a divergence in the Aβ-linked signaling pathways affected by the N-Aβcore in synaptic plasticity. Further work is needed to elucidate the detailed molecular mechanisms involved in N-Aβcore protection or reversal of Aβ-linked synaptic dysfunction, including caspase-dependent intracellular pathways

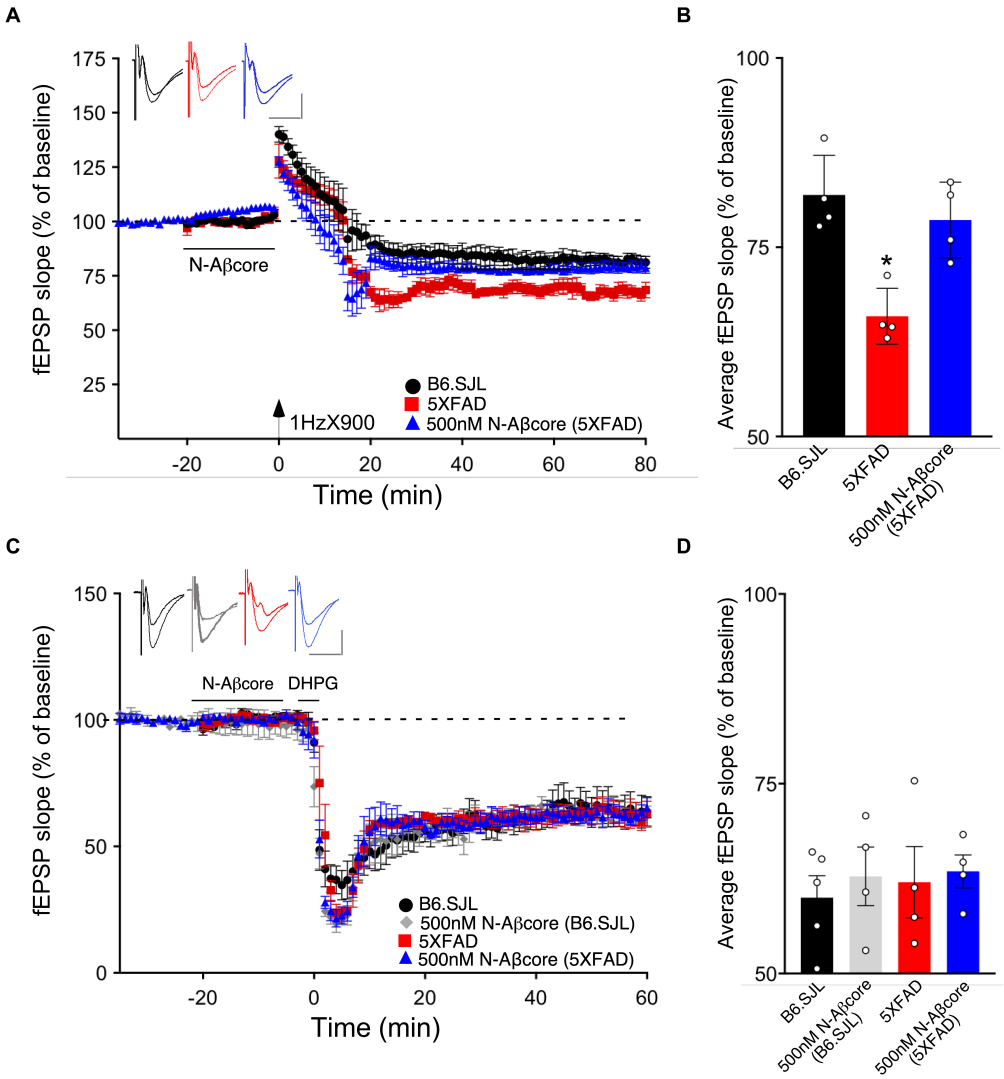

FIGURE 6 | The N-Aβcore reverses endogenous Aβ enhancement of LTD, but has no impact on NMDA-independent, metabotropic glutamate receptor-induced LTD deficits. **(A)** LFS-induced LTD in hippocampal slices from B6.SJL perfused with control aCSF (black) and 5xFAD slices perfused with aCSF (red) or 500 nM N-Aβcore (blue). Color-coded insets show examples of fEPSPs (baseline vs. LTD). **(B)** Quantification of average fEPSP slope values for 50–60 min post-LFS (one-way ANOVA $F_{(2,9)} = 13.03$, $p = 0.0022$). Bonferroni *post hoc* tests: 5xFAD slices displayed significantly more pronounced LTD as compared to control aCSF B6.SJL slices ($^*p = 0.012$). 500 nM N-Aβcore in 5xFAD slices returned LTD to the level observed in control aCSF-perfused B6.SJL slices ($p > 0.99$). Data are mean ± SEM. $N = 4$ for each condition (1 slice/mouse). Inset calibration: horizontal, 10 ms; vertical, 0.4 mV. $^*p < 0.05$. **(C)** NMDA-independent, 3,5-dihydroxyphenylglycine (DHPG, metabotropic glutamate receptor group I agonist; 100 μM)-induced LTD in hippocampal slices from B6.SJL mice perfused with control aCSF (black) or 500 nM N-Aβcore (gray) and 5xFAD slices perfused with aCSF (red) or 500 nM N-Aβcore (blue). Color-coded insets show examples of fEPSPs (baseline vs. LTD). Inset calibration: horizontal, 10 ms; vertical, 0.4 mV. **(D)** Quantification of average fEPSP slope values for 50–60 min post-LFS ($p < 0.05$, two-way ANOVA). Data are means ± SEM. $N = 4$ for each condition (1 slice/mouse).

leading to the regulation of AMPA receptors, and eventual synaptic loss in AD.

CONCLUSION

The essential core hexapeptide sequence, YEVHHQ, or N-Aβcore, within the neuroprotective N-terminal fragment of Aβ was able to effectively, selectively and potently reverse deficits in synaptic plasticity in hippocampal slices from adult APP/PS1 5xFAD transgenic mice. Attenuated LTP and enhanced LTD observed in the slices from 5xFAD mice were both rescued by the N-Aβcore, returning LTP and LTD back to the levels found for hippocampal slices from background control (B6.SJL) mice. The involvement of the PI3 kinase pathway, specifically, mTOR in the protective action of the N-Aβcore against FAD-linked deficits in synaptic plasticity indicates possible connection between N-Aβcore-linked signaling and the translation machinery at hippocampal synaptic sites (dendritic spines). It would thus be of interest to examine the specific signaling pathways engaged

by N-Aβcore at hippocampal sites, especially key downstream elements in translational control such as S6 kinase, a prominent substrate for mTORC1 in neuronal systems.

DATA AVAILABILITY STATEMENT

The datasets generated for the current study are available from the corresponding author on reasonable request.

ETHICS STATEMENT

All experiments using animals were performed under approved University of Hawai'i Institutional Animal Care and Use Committee (IACUC) protocols.

AUTHOR CONTRIBUTIONS

KF and RN contributed to the conceptualization and writing – original draft. KF, RT, KA, and CT contributed to the methodology. KF, RT, KA, CT, and RN contributed to the data analysis. KF, RT, CT, and RN contributed to writing – review and editing. All authors contributed to the article and approved the submitted version.

FUNDING

RN was supported by the University of Hawai'i Foundation, #125-8320-4.

ACKNOWLEDGMENTS

We thank Dr. Naghum Alfulaij for advice. We thank Ms. Ann Hashimoto for mouse breeding and husbandry. We thank Dr. Tessi Sherrin for help with the hippocampal microinjections. This manuscript has been released as a pre-print at bioRxiv 2020.03.17.995191 (doi: https://doi.org/10.1101/2020.03.17.995191).

REFERENCES

Bekinschtein, P., Katche, C., Slipczuk, L. N., Igaz, L. M., Cammarota, M., Izquierdo, I., et al. (2007). mTOR signaling in the hippocampus is necessary for memory formation. *Neurobiol. Learn. Mem.* 87, 303–307. doi: 10.1016/j.nlm.2006.08.007

Chapman, P. F., White, G. L., Jones, M. W., Cooper-Blacketer, D., Marshall, V. J., Irizarry, M., et al. (1999). Impaired synaptic plasticity and learning in aged amyloid precursor protein transgenic mice. *Nat. Neurosci.* 2, 271–276. doi: 10.1038/6374

Chen, X., Lin, R., Chang, L., Xu, S., Wei, X., Zhang, J., et al. (2013). Enhancement of long-term depression by soluble amyloid β protein in rat hippocampus is mediated by metabotropic glutamate receptor and involves activation of p38MAPK, STEP and caspase-3. *Neuroscience* 253, 435–443. doi: 10.1016/j.neuroscience.2013.08.054

Cheng, Q., and Yakel, J. L. (2015). Activation of α7 nicotinic acetylcholine receptors increases intracellular cAMP levels via activation of AC1 in hippocampal neurons. *Neuropharmacol* 95, 405–414. doi: 10.1016/j.neuropharm.2015.04.016

Crouzin, N., Baranger, K., Cavalier, M., Marchalant, Y., Cohen-Solal, C., Roman, F. S., et al. (2013). Area-specific alterations of synaptic plasticity in the 5XFAD mouse model of Alzheimer's disease: dissociation between somatosensory cortex and hippocampus. *PLoS One* 8:e74667. doi: 10.1371/journal.pone.0074667

Cullen, W. K., Suh, Y. H., Anwyl, R., and Rowan, M. J. (1997). Block of LTP in rat hippocampus *in vivo* by β-amyloid precursor protein fragments. *Neuroreport* 8, 3213–3217. doi: 10.1097/00001756-199710200-00006

D'Amelio, M., Cavallucci, V., Middei, S., Marchetti, C., Pacioni, S., Ferri, A., et al. (2011). Caspase-3 triggers early synaptic dysfunction in a mouse model of Alzheimer's disease. *Nat. Neurosci.* 14, 69–76. doi: 10.1038/nn.2709

Dar, N. J., and Glazner, G. W. (2020). Deciphering the neuroprotective and neurogenic potential of soluble amyloid precursor protein alpha (sAPPα). *Cell. Mol. Life Sci.* 77, 2315–2330. doi: 10.1007/s00018-019-03404-x

Derkach, V. A., Oh, M. C., Guire, E. S., and Soderling, T. R. (2007). Regulatory mechanisms of AMPA receptors in synaptic plasticity. *Nat. Rev. Neurosci.* 8, 101–113. doi: 10.1038/nrn2055

Forest, K. H., Alfulaij, N., Arora, K., Taketa, R., Sherrin, T., Todorovic, C., et al. (2018). Protection against β-amyloid neurotoxicity by a non-toxic endogenous N-terminal β-amyloid fragment and its active hexapeptide core sequence. *J. Neurochem.* 144, 201–217. doi: 10.1111/jnc.14257

Forest, K. H., and Nichols, R. A. (2019). Assessing neuroprotective agents for Aβ-induced neurotoxicity. *Trends Mol. Med.* 25, 685–695. doi: 10.1016/j.molmed.2019.05.013

Forest, K. H., Taketa, R., Arora, K., Todorovic, C., and Nichols, R. A. (2020). The neuroprotective beta amyloid hexapeptide core reverses deficits in synaptic plasticity in the 5×FAD APP/PS1 mouse model (preprint). *bioRxiv* 2020:995191. doi: 10.1101/2020.03.17.995191

Glabe, C. C. (2005). ""Amyloid accumulation and pathogenesis of Alzheimer's disease: significance of monomeric, oligomeric and fibrillar Aβ"," in *Alzheimer's disease: Cellular and molecular aspects of amyloid* β, eds J. R. Harris and F. Fahrenholz (Boston, MA: Springer), 167–177.

Gulisano, W., Melone, M., Ripoli, C., Tropea, M. R., Li Puma, D. D., Giunta, S., et al. (2019). Neuromodulatory action of picomolar extracellular Aβ42 oligomers on presynaptic and postsynaptic mechanisms underlying synaptic function and memory. *J. Neurosci.* 39, 5986–6000. doi: 10.1523/JNEUROSCI.0163-19.2019

Haas, L. T., Salazar, S. V., Kostylev, M. A., Um, J. W., Kaufman, A. C., and Strittmatter, S. M. (2016). Metabotropic glutamate receptor 5 couples cellular prion protein to intracellular signaling in Alzheimer's disease. *Brain* 139, 526–546. doi: 10.1093/brain/awv356

Herring, B. E., and Nicoll, R. A. (2016). Long-term potentiation: from CaMKII to AMPA receptor trafficking. *Annu. Rev. Physiol.* 78, 351–365. doi: 10.1146/annurev-physiol-021014-071753

Hoeffer, C. A., and Klann, E. (2010). mTOR signaling: at the crossroads of plasticity, memory and disease. *Trends Neurosci.* 33, 67–75. doi: 10.1016/j.tins.2009.11.003

Hou, L., and Klann, E. (2004). Activation of the phosphoinositide 3-kinase-Akt-mammalian target of rapamycin signaling pathway is required for metabotropic glutamate receptor-dependent long-term depression. *J. Neurosci.* 24, 6352–6361. doi: 10.1523/JNEUROSCI.0995-04.2004

Hsieh, H., Boehm, J., Sato, C., Iwatsubo, T., Tomita, T., Sisodia, S., et al. (2006). AMPAR removal underlies Aβ-induced synaptic depression and dendritic spine loss. *Neuron* 52, 831–843. doi: 10.1016/j.neuron.2006.10.035

Hu, N.-W., Nicoll, A. J., Zhang, D., Mably, A. J., O'Malley, T., Purro, S. A., et al. (2014). mGlu5 receptors and cellular prion protein mediate amyloid-β-facilitated synaptic long-term depression *in vivo*. *Nat. Commun.* 5:3374. doi: 10.1038/ncomms4374

Huganir, R. L., and Nicoll, R. A. (2013). AMPARs and synaptic plasticity: the last 25 years. *Neuron* 80, 704–717. doi: 10.1016/j.neuron.2013.10.025

Kennedy, M. B. (2013). Synaptic signaling in learning and memory. *Cold Spring Harb. Perspect. Biol.* 8:a016824. doi: 10.1101/cshperspect.a016824

Kim, J.-H., Anwyl, R., Suh, Y.-H., Djamgoz, M. B. A., and Rowan, M. J. (2001). Use-dependent effects of amyloidogenic fragments of β-amyloid precursor protein on synaptic plasticity in rat hippocampus *in vivo*. *J. Neurosci.* 21, 1327–1333. doi: 10.1523/JNEUROSCI.21-04-01327.2001

Kimura, R., and Ohno, M. (2009). Impairments in remote memory stabilization precede hippocampal synaptic and cognitive failures in 5XFAD Alzheimer mouse model. *Neurobiol. Dis.* 33, 229–235. doi: 10.1016/j.nbd.2008.10.006

Koffie, R. M., Hyman, B. T., and Spires-Jones, T. L. (2011). Alzheimer's disease: synapses gone cold. *Mol. Neurodegener.* 6:63. doi: 10.1186/1750-1326-6-63

Lafay-Chebassier, C., Paccalin, M., Page, G., Barc-Pain, S., Perault-Pochat, M. C., Gil, R., et al. (2005). mTOR/p70S6k signaling alteration by Aβ exposure as well as in APP-PS1 transgenic models and in patients with Alzheimer's disease. *J. Neurochem.* 94, 215–225. doi: 10.1111/j.1471-4159.2005.03187.x

Lawrence, J. L. M., Tong, M., Alfulaij, N., Sherrin, T., Contarino, M., White, M. M., et al. (2014). Regulation of presynaptic Ca^{2+}, synaptic plasticity and contextual fear conditioning by a N-terminal β-amyloid fragment. *J. Neurosci.* 34, 14210–14218. doi: 10.1523/JNEUROSCI.0326-14.2014

Lee, K.-Y., Koh, S.-H., Noh, M. Y., Kim, S. H., and Lee, Y. J. (2008). Phosphatidylinositol-3-kinase activation blocks amyloid beta-induced neurotoxicity. *Toxicology* 243, 43–50. doi: 10.1016/j.tox.2007.09.020

Li, S., Hong, S., Shepardson, N. E., Walsh, D. M., Shankar, G. M., and Selkoe, D. (2009). Soluble oligomers of amyloid β-protein facilitate hippocampal long-term depression by disrupting neuronal glutamate uptake. *Neuron* 62, 788–801. doi: 10.1016/j.neuron.2009.05.012

Li, Z., and Sheng, M. (2012). Caspases in synaptic plasticity. *Mol. Brain* 5:15. doi: 10.1186/1756-6606-5-15

Lu, B. (2003). BDNF and activity-dependent synaptic modulation. *Learn. Mem.* 10, 86–98. doi: 10.1101/lm.54603

Ma, T., Hoeffer, C. A., Capetillo-Zarate, E., Yu, F., Wong, H., Lin, M. T., et al. (2010). Dysregulation of the mTOR pathway mediates impairment of synaptic plasticity in a mouse model of Alzheimer's disease. *PLoS One* 5:e12845. doi: 10.1371/journal.pone.0012845

Makino, H., and Malinow, R. (2009). AMPA receptor incorporation into synapses during LTP: the role of lateral movement and exocytosis. *Neuron* 64, 381–390. doi: 10.1016/j.neuron.2009.08.035

Morrisey, J. A., Mockett, B. G., Singh, A., Kweon, D., Ohline, S. M., Tate, W. P., et al. (2019). A C-terminal peptide from secreted amyloid precursor protein-α enhances long-term potentiation in rats and a transgenic mouse model of Alzheimer's disease. *Neuropharmacology* 157:107670. doi: 10.1016/j.neuropharm.2019.107670

Nägerl, U. V., Eberhorn, N., Cambridge, S. B., and Bonhoeffer, T. (2004). Bidirectional activity-dependent morphological plasticity in hippocampal neurons. *Neuron* 44, 759–767. doi: 10.1016/j.neuron.2004.11.016

Oakley, H., Cole, S. L., Logan, S., Maus, E., Shao, P., Craft, J., et al. (2006). Intraneuronal β-amyloid aggregates, neurodegeneration, and neuron loss in transgenic mice with five familial Alzheimer's disease mutations: potential factors in amyloid plaque formation. *J. Neurosci.* 26, 10129–10140. doi: 10.1523/JNEUROSCI.1202-06.2006

Oddo, S., Caccamo, A., Shepherd, J. D., Murphy, M. P., Golde, T. E., Kayed, R., et al. (2003). Triple-transgenic model of Alzheimer's disease with plaques and tangles: intracellular Aβ and synaptic dysfunction. *Neuron* 39, 409–421. doi: 10.1016/S0896-6273(03)00434-3

Patterson, S. L., Abel, T., Deuel, T. A., Martin, K. C., Rose, J. C., and Kandel, E. R. (1996). Recombinant BDNF rescues deficits in basal synaptic transmission and hippocampal LTP in BDNF knockout mice. *Neuron* 16, 1137–1145. doi: 10.1016/s0896-6273(00)80140-3

Portelius, E., Price, E., Brinkmalm, G., Stieler, M., Olsson, M., Persson, R., et al. (2011). A novel pathway for amyloid precursor processing. *Neurobiol. Aging* 32, 1090–1098. doi: 10.1016/j.neurobiolaging.2009.06.002

Puzzo, D., Privitera, L., Leznik, E., Fà, M., Staniszewski, A., Palmeri, A., et al. (2008). Picomolar amyloid-β positively modulates synaptic plasticity and memory in hippocampus. *J. Neurosci.* 28, 14537–14545. doi: 10.1523/JNEUROSCI.2692-08.2008

Puzzo, D., Privitera, L., and Palmeri, A. (2012). Hormetic effect of amyloid-β peptide in synaptic plasticity and memory. *Neurobiol. Aging* 33, e15–e24. doi: 10.1016/j.neurobiolaging.2011.12.020

Raymond, C. R., Ireland, D. R., and Abraham, W. C. (2003). NMDA receptor regulation by amyloid-β does not account for its inhibition of LTP in rat hippocampus. *Brain Res.* 968, 263–272. doi: 10.1016/s0006-8993(03)02269-8

Reddy, P. H., Mani, G., Park, B. S., Jacques, J., Murdoch, G., Whetsell, W., et al. (2005). Differential loss of synaptic proteins in Alzheimer's disease: implications for synaptic dysfunction. *J. Alzheimers Dis.* 7, 103–117. doi: 10.3233/JAD-2005-7203

Scheff, S. W., Price, D. A., Schmitt, F. A., and Mufson, E. J. (2006). Hippocampal synaptic loss in early Alzheimer's disease and mild cognitive impairment. *Neurobiol. Aging* 27, 1372–1384. doi: 10.1016/j.neurobiolaging.2005.09.012

Shankar, G. M., Li, S., Mehta, T. H., Garcia-Munoz, A., Shepardson, N. E., Smith, I., et al. (2008). Amyloid β-protein dimers isolated directly from Alzheimer's brains impair synaptic plasticity and memory. *Nat. Med.* 14, 837–842. doi: 10.1038/nm1782

Shankar, G. M., and Walsh, D. M. (2009). Alzheimer's disease: synaptic dysfunction and Aβ. *Mol. Neurodegener.* 4:48. doi: 10.1186/1750-1326-4-48

Snyder, E. M., Nong, Y., Almeida, C. G., Paul, S., Moran, T., Choi, E. Y., et al. (2005). Regulation of NMDA receptor trafficking by amyloid-β. *Nat. Neurosci.* 8, 1051–1058. doi: 10.1038/nn1503

Terry, R. D., Masliah, E., Salmon, D. P., Butters, N., DeTeresa, R., Hill, R., et al. (1991). Physical basis of cognitive alterations in Alzheimer's disease: synapse loss is the major correlate of cognitive impairment. *Ann. Neurol.* 30, 572–580. doi: 10.1002/ana.410300410

Thomas, G. M., and Huganir, R. L. (2004). MAPK cascade signalling and synaptic plasticity. *Nat. Rev. Neurosci.* 5, 173–183. doi: 10.1038/nrn1346

Walsh, D. M., Klyubin, I., Fadeeva, J. V., Cullen, W. K., Anwyl, R., Wolfe, M. S., et al. (2002). Naturally secreted oligomers of amyloid β protein potently inhibit hippocampal long-term potentiation *in vivo*. *Nature* 416, 535–539. doi: 10.1038/416535a

Wang, H.-W., Pasternak, J. F., Kuo, H., Ristic, H., Lambert, M. P., Chromy, B., et al. (2002). Soluble oligomers of β amyloid (1-42) inhibit long-term potentiation but not long-term depression in rat dentate gyrus. *Brain Res.* 924, 133–140. doi: 10.1016/s0006-8993(01)03058-x

Wang, Q., Walsh, D. M., Rowan, M. J., Selkoe, D. J., and Anwyl, R. (2004). Block of long-term potentiation by naturally secreted and synthetic amyloid β-peptide in hippocampal slices is mediated via activation of the kinases c-Jun N-terminal kinase, cyclin-dependent kinase 5, and p38 mitogen-activated protein kinase as well as metabotropic glutamate receptor type 5. *J. Neurosci.* 24, 3370–3378. doi: 10.1523/JNEUROSCI.1633-03.2004

Wang, X., and Proud, C. G. (2006). The mTOR pathway in the control of protein synthesis. *Physiology* 21, 362–369. doi: 10.1152/physiol.00024.2006

Conflict of Interest: The authors declare that the research was conducted in the absence of any commercial or financial relationships that could be construed as a potential conflict of interest.

frontiers in Molecular Neuroscience

ORIGINAL RESEARCH
published: 03 June 2021
doi: 10.3389/fnmol.2021.661728

Amyloid-β Impairs Dendritic Trafficking of Golgi-Like Organelles in the Early Phase Preceding Neurite Atrophy: Rescue by Mirtazapine

*Elsa Fabbretti†, Giulia Antognolli† and Enrico Tongiorgi**

Department of Life Sciences, University of Trieste, Trieste, Italy

Neurite atrophy with loss of neuronal polarity is a pathological hallmark of Alzheimer's disease (AD) and other neurological disorders. While there is substantial agreement that disruption of intracellular vesicle trafficking is associated with axonal pathology in AD, comparatively less is known regarding its role in dendritic atrophy. This is a significant gap of knowledge because, unlike axons, dendrites are endowed with the complete endomembrane system comprising endoplasmic reticulum (ER), ER–Golgi intermediate compartment (ERGIC), Golgi apparatus, post-Golgi vesicles, and a recycling-degradative route. In this study, using live-imaging of pGOLT-expressing vesicles, indicative of Golgi outposts and satellites, we investigate how amyloid-β (Aβ) oligomers affect the trafficking of Golgi-like organelles in the different dendritic compartments of cultured rat hippocampal neurons. We found that short-term (4 h) treatment with Aβ led to a decrease in anterograde trafficking of Golgi vesicles in dendrites of both resting and stimulated (with 50 mM KCl) neurons. We also characterized the ability of mirtazapine, a noradrenergic and specific serotonergic tetracyclic antidepressant (NaSSA), to rescue Golgi dynamics in dendrites. Mirtazapine treatment (10 μM) increased the number and both anterograde and retrograde motility, reducing the percentage of static Golgi vesicles. Finally, mirtazapine reverted the neurite atrophy induced by 24 h treatment with Aβ oligomers, suggesting that this drug is able to counteract the effects of Aβ by improving the dendritic trafficking of Golgi-related vesicles.

Keywords: neurodegenerative disorders, amyloid-beta, neurite atrophy, neuronal polarity, Golgi-like organelles, intracellular vesicle trafficking, antidepressants, dendritic arborization

OPEN ACCESS

Edited by:
Walter Gulisano,
University of Catania, Italy

Reviewed by:
Carlos G. Dotti,
Consejo Superior de Investigaciones Científicas (CSIC), Spain
Matteo Spinelli,
University College London, United Kingdom
Domenica Donatella Li Puma,
Catholic University Medical School, Italy

***Correspondence:**
Enrico Tongiorgi
tongi@units.it

† These authors have contributed equally to this work and share first authorship

Received: *31 January 2021*
Accepted: *30 April 2021*
Published: *03 June 2021*

Citation:
Fabbretti E, Antognolli G and Tongiorgi E (2021) Amyloid-β Impairs Dendritic Trafficking of Golgi-Like Organelles in the Early Phase Preceding Neurite Atrophy: Rescue by Mirtazapine. Front. Mol. Neurosci. 14:661728. doi: 10.3389/fnmol.2021.661728

INTRODUCTION

Neurite atrophy, including abnormal morphology and retraction or loss of part of the dendritic and/or axonal arborization, is a pathological symptom underlying several neurodevelopmental and neurodegenerative brain diseases such as autism, Rett syndrome (RTT), Fragile X syndrome, schizophrenia, and Alzheimer's disease (AD) (Kaufmann and Moser, 2000; Kulkarni and Firestein, 2012). Among the possible causes of neurite atrophy is the impairment of microtubules-based motor machineries involved in vesicle and protein anterograde trafficking toward distal neurite endings, as well as in retrograde vesicle recycling mechanisms (Overk and Masliah, 2014;

Dubey et al., 2015; De Vos and Hafezparast, 2017). Trafficking mechanisms are necessary for the maintenance of the integrity and spatial organization of the secretory pathway which, in turn, is essential for stability of axons and dendrites, and synaptic function (Ramírez and Couve, 2011; Koleske, 2013; Maeder et al., 2014). Indeed, several proteins involved in the regulation of either secretory membrane trafficking or the endocytic pathway were identified by GWAS (genome wide sequencing studies) as susceptibility genes in AD (Toh and Gleeson, 2016). While there is substantial agreement that anterograde axonal transport of synaptic secretory vesicles and both anterograde and retrograde axonal traffic of endocytic vesicles are impaired in AD, comparatively less is known about how AD affects the dynamics of secretory pathway organelles in dendrites.

Unlike axons, dendrites are endowed with the complete endomembrane system comprising the forward biosynthetic route constituted by the endoplasmic reticulum (ER), the ER–Golgi intermediate compartment (ERGIC), the Golgi apparatus and post-Golgi vesicles, and a recycling-degradative route constituted by endosomes and lysosomes (Pierce et al., 2001; Ramírez and Couve, 2011). All membranous elements of the secretory pathway show dynamic rearrangements that are critical for dendrites outgrowth and neuronal polarization during development, as well as synaptic plasticity and homeostasis in adulthood (Horton and Ehlers, 2004; Tang, 2008). However, the different secretory organelles display different localization and degrees of motility. The ER forms an anatomizing network distributed throughout the entire dendritic arbor with local zones of increased complexity at dendritic branching points and upper order dendrites, in which highly dynamic domains are involved in local ER-to-Golgi protein export (Aridor et al., 2004; Cui-Wang et al., 2012). In contrast, stacks of Golgi cisternae with no connection to the somatic Golgi, also designed as Golgi outposts (GO), are stably localized in the first two segments of large dendrites (primary and secondary dendrites) and at branching points between primary/secondary and secondary/tertiary dendrites (Horton and Ehlers, 2003a; Tongiorgi, 2008). More dynamic *Trans*-Golgi network (TGN) compartments were discovered in distal dendrites where they undergo rapid anterograde and retrograde movements (Horton and Ehlers, 2003a; McNamara et al., 2004; Tongiorgi, 2008). In distal dendrites, the high dynamic features of the trafficking of these post-Golgi organelles are similar to the pre-Golgi ERGIC vesicles and to other more recently discovered Golgi-like small cisternae, known as Golgi satellites that can be identified by the expression of the pGOLT protein (Mikhaylova et al., 2016).

Aberrant folding and accumulation of the amyloid-β peptide (Aβ), an hallmark of AD, causes neurite degeneration, synapse loss, and impairment in neuronal trafficking (Serrano-Pozo et al., 2011; Plá et al., 2017). In the present study, using a live imaging approach on hippocampal neurons in culture, we investigate how $A\beta_{25-25}$ oligomers affect the dynamics of pGOLT-expressing vesicles indicative of Golgi-related organelles, such as Golgi outposts and satellites (Horton and Ehlers, 2003b; Horton et al., 2005; Mikhaylova et al., 2016). We also characterize the ability of mirtazapine, a noradrenergic and specific serotonergic tetracyclic antidepressant (NaSSA), to rescue Golgi trafficking. The neurotrophic effect of antidepressants is well known and demonstrated in several pathological models (Castrén, 2004), and we have previously shown that mirtazapine can rescue dendritic atrophy and soma size shrinkage of cortical and hippocampal neurons in a mouse model of Rett syndrome (Bittolo et al., 2016; Nerli et al., 2020).

MATERIALS AND METHODS

Primary Cultures of Rat Hippocampal Neurons

Animals were treated according to the institutional guidelines, in compliance with the European Community Council Directive 2010/63/UE for care and use of experimental animals. Authorization for animal experimentation was obtained from the local ethical committee on November 10, 2017 and was communicated to the Italian Ministry of Health, in compliance with the Italian law D. Lgs. 116/92 and the L. 96/2013, art. 13. All efforts were made to minimize animal suffering and to reduce the number of animals used. Hippocampal neurons were prepared from postnatal day 0 to 1 (P0–P1) Wistar rats as previously described (Baj et al., 2014). Cultures were maintained in Neurobasal medium (Life Technologies) supplemented with B27 (Thermo Fisher Scientific, Waltham, MA, United States), 1 mM L-glutamine and antibiotics (Euroclone, Milan, Italy) on 24-well imaging plates (Eppendorf, Hamburg, Germany) or glass coverslips pre-coated with poly-L-ornithine (100 μg/ml) and Matrigel™ (Corning, NY, United States). At days *in vitro* 3 (DIV3), cytosine 2.5 μM β-D-arabinofuranoside was added. For transfection experiments, neurons were used at a concentration of 200 cells/mm^2, used at DIV6 and analyzed 24 h later. For neurite outgrowth analysis, neurons were seeded at a concentration of 320 cell/mm^2.

Ab_{25-35} and Mirtazapine Treatment

Aggregation of $A\beta_{25-35}$ peptide (5 mg/ml, Bachem, Bubendorf, Switzerland; Copani et al., 1995) was obtained in phosphate buffer for 24 h at 37°C (Millucci et al., 2010). A-beta25–35 oligomers aggregation was previously demonstrated by atomic force microscopy, showing formation of oligomeric/protofibrillary assemblies displaying the typical beta-sheet structure (Antonini et al., 2011). Aggregated Aβ oligomers (10 μM; Gomes et al., 2014) were applied on DIV7 hippocampal cultures for 4–24 h. Mirtazapine (10 μM in DMSO; Abcam, Cambridge, United Kingdom; Fukuyama et al., 2013; Bittolo et al., 2016) was applied alone or co-applied with Aβ on DIV7 cultures. Control neurons were treated with vehicle only (DMSO). Effective concentrations of Aβ and mirtazapine (24 h) were initially chosen accordingly to data from a (3-(4,5-dimethylthiazol-2-yl)-2,5-diphenyltetrazolium bromide) tetrazolium (MTT) reduction assay performed on DIV7 hippocampal cultures. Short (4 h) incubation of hippocampal neurons with Aβ peptide (10 μM) was sufficient to significantly impair mitochondrial membrane potential with respect to control (**Supplementary Figure 1**).

Immunofluorescence and Images Acquisition

For immunofluorescence experiments, hippocampal cultures were fixed in 4% paraformaldehyde for 15 min at room temperature and incubated for 1 h with the following primary antibodies diluted in phosphate buffer with 0.1% Triton-X100 and 2% of bovine serum albumin: anti-β Tubulin III (1:1000; Sigma, Milan, Italy), anti-NeuN (1:1000; Millipore, Burlington, MA, United States), anti-GM130 (1:250; BD Transduction Laboratories, San Jose, CA, United States), anti-TGN38/46 (1:250; Abcam, Cambridge, United Kingdom), and anti-LMAN1 (1:250; Sigma, Milan, Italy). Immunolabeling was visualized with 488-/568-AlexaFluor-conjugated secondary antibodies (1:500; Thermo Fisher Scientific). Nuclei were counterstained with Hoechst 33342 (0.001%; Thermo Fisher Scientific) and visualized with a Nikon ECLIPSE T*i*-E epifluorescence microscope or an ECLIPSE C1si confocal microscope (Nikon, Tokyo, Japan). Fields were captured at a resolution of 1 pixel = 0.44 micron, using the Nikon acquisition software NIS-elements, a 40x DIC H 0.17, and an oil immersion objective with a working distance of 160 μm. NeuN- and Hoechst-positive cells were counted using the Object Analyzer option of the NIS-Elements.

Total Neurite Length (TNL) Analysis

An automated analysis approach was used to quantify the neurite retraction and recovery after 24 h of treatment. This automated analysis was performed using the open source bioinformatics toolkit NeuriteQuant, implemented in the free image analysis software ImageJ/Fiji (Dehmelt et al., 2011; Nerli et al., 2020). Following a staining of neurites using an antibody against cytoskeletal proteins such as Tubulin-β-III or MAP-2, this tool allows for the measurement of total neuritic or dendritic length on primary neuronal cultures. Moreover, by analyzing multi-channel images, it allows researchers to measure many other parameters such as total neuronal cell body area, total number of cell bodies, number of neurite-cell body attachment points, and number of neurite endpoints. To perform the analysis, 8-bit images are necessary. The NeuriteQuant analysis settings were set by a configuration file, in which the parameters for the analysis were as follows: Neurite detection width = 12; neurite detection threshold = 10; neurite cleanup threshold = 150; neurite cell body detection = 80.

Transfection of Hippocampal Neurons and Live Imaging Experiments

Plasmid transfection was done on DIV6 hippocampal neurons with Lipofectamine 2000^{TM} (Thermo Fisher Scientific) with pEGFP (Takara, Clontech) or pGOLT-mCherry (Addgene plasmid # 73297; Mikhaylova et al., 2016) and transfected cells were used 16 h later. For live imaging experiments, only low expressing pGOLT neurons with punctate fluorescence were selected while pGOLT high expressing neurons were excluded. pGOLT-positive neurons were selected from low magnification large-fields and analyzed individually with a 40x objective in a solution containing 5.3 mM KCl, 50.9 mM NaCl, HEPES 10.9 mM, $NaHPO_4$ 0.8 mM, $NaHCO_3$ 26 mM, $MgCl_2$ 0.8 mM, $CaCl_2$ 1.8 mM, and glucose 25 mM, under temperature and CO_2 atmosphere control (Nikon). Sequential time lapse images were acquired in 1 min-time intervals for a total of 10 min, with a CMOS Nikon DS-Qi2 camera at a 500–700 s exposure time and with neutral density filter 4, in order to minimize the phototoxicity. For tests at high K^+, cultures were stimulated with an isotonic solution containing 50 mM KCl and immediately analyzed for time lapse recording for 5 or 10 min. For kymographs, neurons were imaged in 5 s-time intervals for 2 min. Fluorescence peak analysis of pGOLT spots was obtained with ImageJ/Fiji, along 50 μm-long line selections (ROIs) from proximal apical, proximal basal dendrites, and higher order dendrites (**Figure 1B**). The peak values from each time were analyzed in Microsoft Office Excel. Peaks of similar intensities found in an adjacent space and persisting for more than 3 min were defined as "persistent spots." Peaks oscillating in a ±0.22 μm space were defined as "static." Only long-lasting persistent pGOLT spots were used for further analysis. A mobility index was defined as the net distance traveled by individual persistent pGOLT spots (μm) obtained by summing all anterograde and retrograde movements covered by pGOLT spots between the first and last step of a 10 min observation time.

Statistical Analysis

Statistical analysis was performed using Prism 5 software (GraphPad). Based on D'Agostino and Pearson's omnibus positive normality test, statistical significance between groups was obtained with student's *t*-test, or with the Mann–Whitney Rank Sum test. For multiple comparisons, one-way ANOVA or Kruskal–Wallis statistical analysis were performed. Data are represented as average percentage ± standard error mean (SEM).

RESULTS

Dendritic Trafficking of Golgi-Like Organelles

Golgi organelles are present in the soma and dendrites, but not in axons, and can be labeled in living neurons by overexpressing the recombinant protein pGOLT-mCherry (pGOLT) (Mikhaylova et al., 2016). To confirm the effective identification of Golgi organelles by pGOLT, we verified by confocal analysis in pGOLT-mCherry-transfected primary rat hippocampal neuronal cultures at 7 days *in vitro* (DIV7), if pGOLT-mCherry-labeled organelles were also immunostained by antibodies specific for the Golgi outposts protein GM130, or the *trans*-Golgi network marker TGN38/46, or the ERGIC-specific mannose lectin LMAN1/ERGIC-53. We used 7-day *in vitro* neurons because young neurons (DIV 6–9) are more indicated than the more mature ones (DIV 15–20) for studies on Golgi trafficking since Golgi-like organelles are more abundant at younger ages while dynamics are comparable at all ages (Mikhaylova et al., 2016).

We found that pGOLT expression was mainly located in somatic and dendritic vesicles that extensively co-localized with the Golgi-cisternae marker GM130 and the *trans*-Golgi network

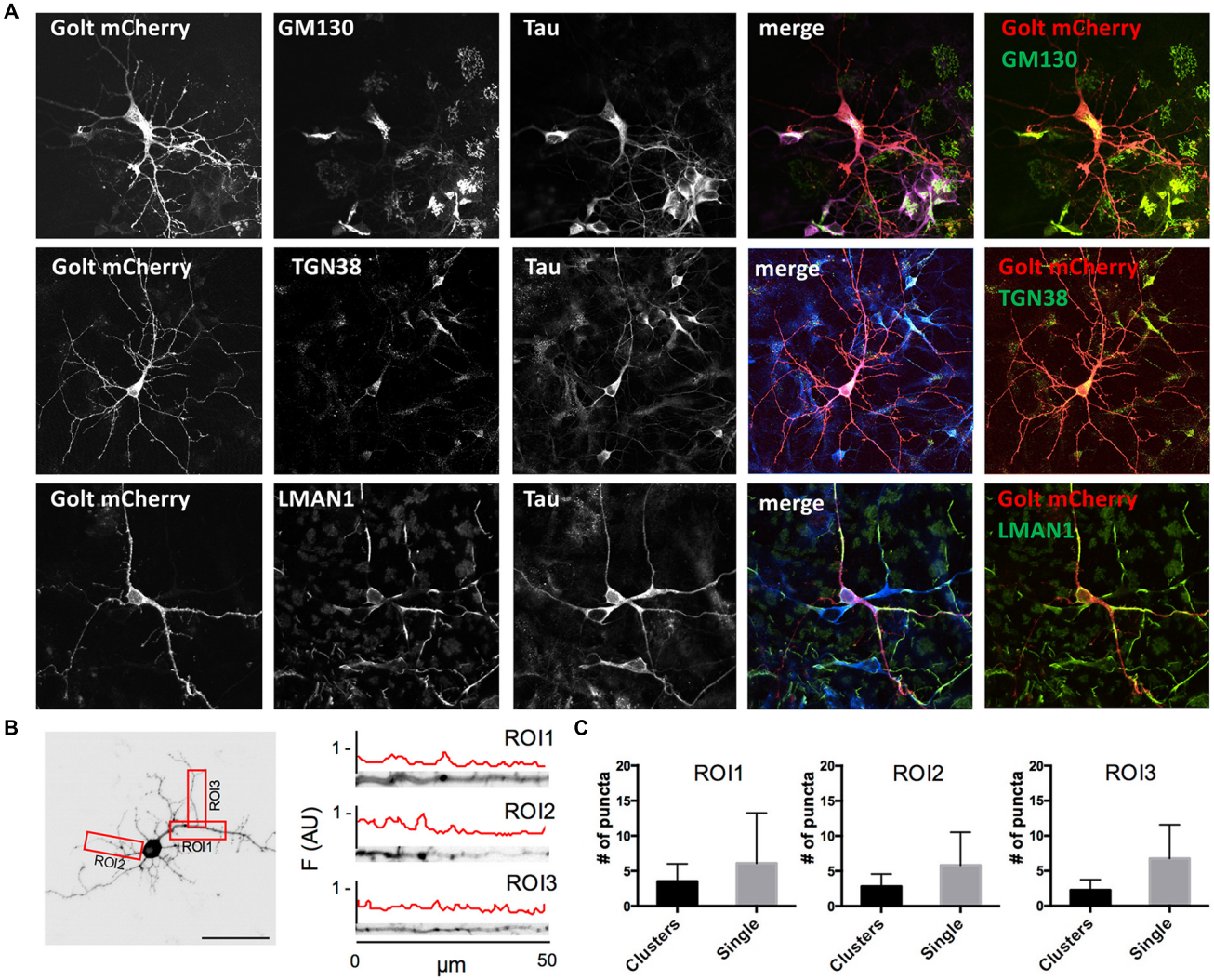

FIGURE 1 | Characterization of pGOLT signals in hippocampal neurons cultured for 7 days *in vitro*. **(A)** Representative confocal images of pGOLT-mCherry transfected neurons (red), Tau cytoskeletal marker (blue) combined with immunofluorescence (green) for either Golgi marker GM130 **(top)**, *trans*-Golgi network marker TGN38 **(mid)**, or endoplasmic reticulum marker LMAN1 **(bottom)**. Transfected neurons present a diffuse and spotted pGOLT-mCherry expression, with high intensity staining in the somatic region. Scale bars = 5 µm. **(B) Left**. Image converted in gray levels and B/W inverted of one neuron expressing low pGOLT levels. Each red rectangle represents a 50 µm-long region of interest (ROI). ROI1 corresponds to the proximal part of the apical dendrite; ROI2 to the proximal part of basal dendrite; and ROI3 to a higher order process. **(B) Right**. Straightened dendrites presenting several pGOLT spots of variable dimensions. Fluorescence is analyzed as arbitrary units in each segment by an intensity profile plot [F(AU), red line]. Peaks of the intensity plot profile coincide with pGOLT-related vesicles. **(C)** Average number of persistent pGOLT clusters or single puncta per segment in unstimulated neurons. RO1 = proximal apical, RO2 = proximal basal, RO3 = distal apical. *N* = 10 neurons per each condition.

marker TGN38/46, and to a lesser extent with the ERGIC marker LMAN1 (**Figure 1A**). To study the subcellular distribution of pGOLT-positive vesicles, living neurons expressing low pGOLT levels were analyzed in the three distinct 50 µm-long regions of interest (ROI) corresponding to proximal basal (ROI1), proximal apical (ROI2), and distal apical higher order processes (ROI3) (**Figure 1B**). We observed different types of pGOLT-labeled vesicles that we classified as follows: "Transient single puncta" with short-lived spot appearance (<3 min); "long-lasting puncta" = mobile spots covering a space >2 microns during the observation time of 10 min, and persisting for about 8–10 min; "clusters" = peaks of intensity similar to single puncta present in a contiguous space, and visible continuously for a minimum of 3 min; and "static pGOLT puncta or clusters" = stable peaks, i.e., oscillating within a space of ±0.22 microns and stable for more than 3 min. Only pGOLT-labeled long-lasting single puncta (just named single puncta) and clusters that were visualized as individual spots (pGOLT spots) and persisted for at least 3 min were further analyzed. In basal conditions, neurons exhibited large pGOLT spots (average diameter 2 ± 0.56 µm) and their average number was comparable in the three different ROIs (**Figure 1C**).

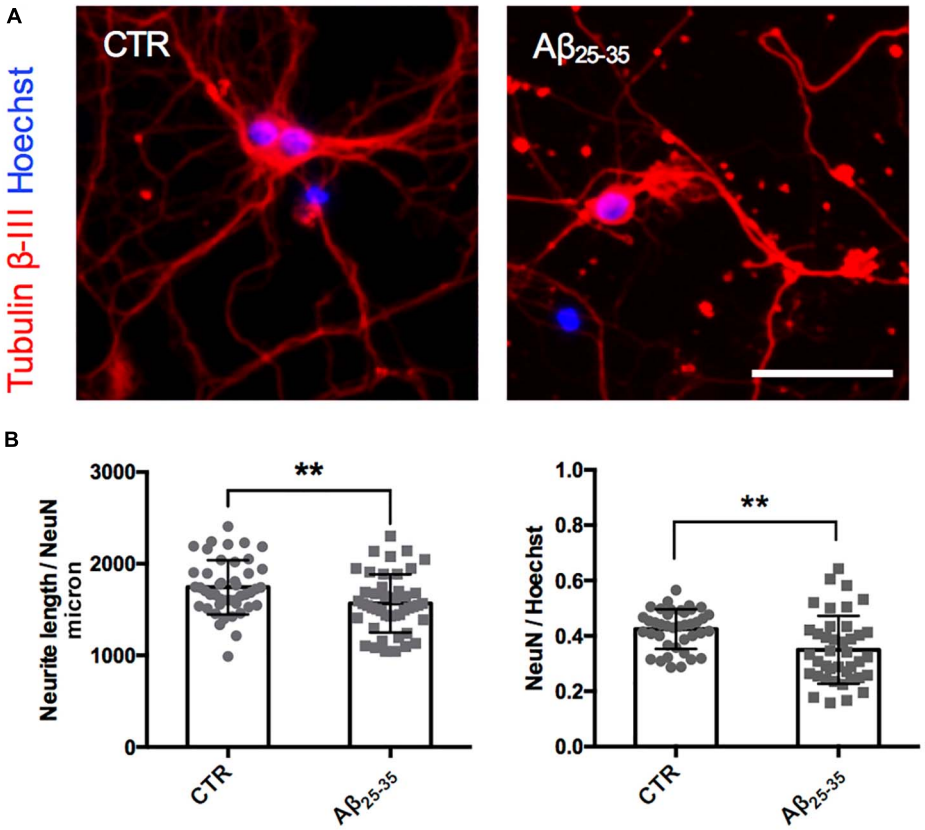

FIGURE 2 | Neurite atrophy in an *in vitro* model of Aβ injury. **(A)** Representative microscopy images (10X) of DIV7 hippocampal neurons in control condition **(left)** and after 24 h of $A\beta_{25\text{-}35}$ (10 μM) treatment **(right)** stained with anti-Tubulin β-III (red) and Hoechst (blue). Scale bar = 50 μm. **(B)** Scatter plot of total neurite length (TNL) for each neuron **(left)** expressed in μm/neuron, and neuronal density expressed as the ratio between the number of neurons on the total number of cells **(right)**. Each dot represents TNL from an image (10X) in control and after 24 h of $A\beta_{25\text{-}35}$ (10 μM) treatment, n = 40–45 fields per condition from three independent experiments. Following D'Agostino and Pearson's normality test, we performed an unpaired t-test. $^{**}p < 0.01$.

Short-Term Aβ Treatment Impairs Trafficking of pGOLT-Positive Golgi Vesicles

After having established the methodology to identify Golgi-like organelles in dendrites, we asked whether Aβ treatment could impair trafficking of pGOLT spots during the early phase of the Aβ-induced injury that precedes neurite atrophy and cell death. Toward this aim, we first verified the ability of $A\beta_{25-35}$ oligomers to induce neurite atrophy over 24 h in DIV7 neurons. The concentration of Aβ was chosen based on data from a (3-(4,5-dimethylthiazol-2-yl)-2,5-diphenyltetrazolium bromide) tetrazolium (MTT) reduction assay performed on DIV7 hippocampal cultures (**Supplementary Figure 1**). Primary rat hippocampal neuronal cultures (DIV7) were incubated with aggregated $A\beta_{25-35}$ peptide (10 μM) and 24 h later, neurons were labeled by immunofluorescence for the neuron-specific microtubule protein β-Tubulin III which labels both axonal and dendritic processes (**Figure 2A**). Aβ-induced neurite atrophy measured using the software NeuriteQuant (see section "Materials and Methods") was applied on fluorescence microscopy images for β-Tubulin III to quantify the total neurite length (TNL) in each condition (**Figure 2B** left). While control neurons presented a complex and dense neurite network, Aβ-treated neurons showed an aberrant neurite morphology with a significant TNL reduction (1743 ± 44 μm/neuron in control vs. 1566 ± 47 μm/neuron after Aβ; n = 3, p = 0.008; **Figure 2B** left), in line with previous observations (Resende et al., 2007). Aβ also significantly reduced neuronal density (**Figure 2B** right) with a significant lower number of NeuN-positive neurons, indicative of neuronal cell loss (ratio NeuN/total cells: 0.42 ± 0.01 in control vs. 0.35 ± 0.02 after Aβ; n = 3; p = 0.0013).

To explore the impact of Aβ on the trafficking of Golgi vesicles, we incubated DIV7 neurons with $A\beta_{25-35}$ peptide for 4 h and we investigated how it affected Golgi cargo trafficking during this early time-window that preceded neuronal atrophy and cell death. In these experiments, in order to perform further comparisons with pharmacological treatments, control cultures were treated for 4 h with DMSO which is the vehicle used to dilute mirtazapine in the subsequent set of rescue experiments. The effects of DMSO and $A\beta_{25-35}$ peptide were investigated in both basal conditions and after KCl stimulation (**Figure 3**). Qualitative kymograph analysis of

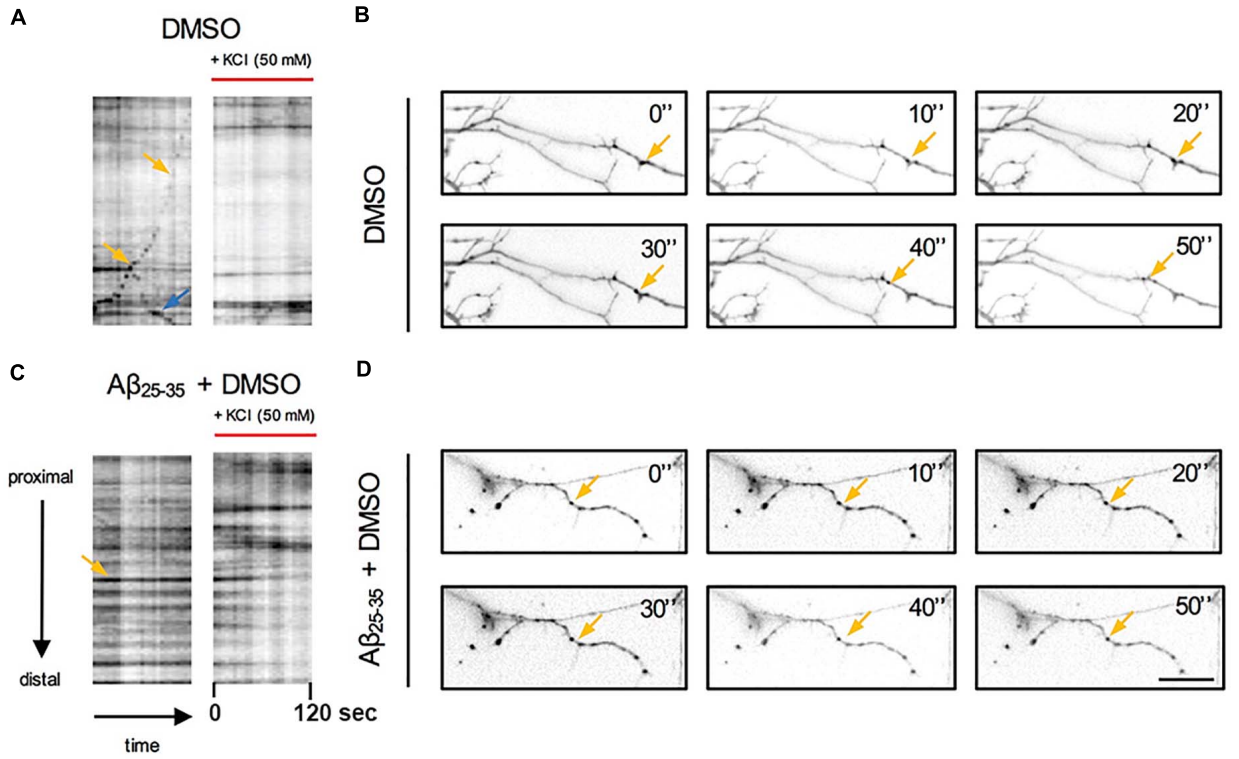

FIGURE 3 | Qualitative analysis of the effects of Aβ and KCl-induced neuronal activity on pGOLT spots trafficking. Kymograph representation of **(A)** pGOLT spots trafficking (2 min) in hippocampal neurons in control (DMSO) or **(C)** Aβ treatment (10 μM, 4 h) in basal and KCl conditions (50 mM, 2 min). **(B)** Representative images of neuronal dendrites in control and **(D)** Aβ + DMSO (bottom) in basal conditions. **(A,B)** In control conditions, retrogradely (yellow arrows) and anterogradely (blue arrows) moving pGOLT spots were detected. **(C,D)** In Aβ-treated cultures, static pGOLT spots (yellow arrows) were mostly detected. Images are acquired for 2 min with 5 s interval. Scale bar = 15 μm.

50 μm-long proximal regions of neurons treated with DMSO showed the occurrence of both anterograde and retrograde pGOLT spots trafficking (**Figures 3A–D**). However, both Aβ (10 μM, 4 h) and KCl (50 mM, 2 min) treatments apparently reduced trafficking (**Figures 3A,C**). To better define this effect, we carried out a quantitative analysis of pGOLT spots trafficking. Neurons treated with DMSO showed a similar proportion of static, retrograde, or anterograde pGOLT spots in all the ROIs analyzed (**Figure 4A** and **Table 1**). Short Aβ treatment in DMSO (4 h) of hippocampal neurons showed a small, not significant increase of static vesicles in proximal apical dendrites and proximal basal dendrites along with a larger, statistically significant increase of +15.9% (from 42.6 ± 5.0% to 58.5 ± 13.0%, $p < 0.05$) in higher order processes (**Figure 4A** and **Table 1**). Interestingly, while the percentage of pGOLT spots undergoing retrograde trafficking was substantially unmodified, the anterograde mobility after Aβ + DMSO treatment was reduced with respect to control conditions in the different regions considered, with a small, insignificant reduction in the proximal apical (21.9 ± 8.8%) and proximal basal dendrites (16.0 ± 5.9%) and a stronger, statistically significant ($p = 0.02$) reduction of −23.4% in the higher order processes (from 29.0 ± 7.0% to 5.6 ± 3.0%) (**Figure 4A** and **Table 1**).

Considering the space covered by individual pGOLT spots in 10-min observation times, similar net distances were measured in proximal apical, proximal basal, and higher order segments in all conditions for both anterograde and retrograde movements (**Figure 4B**). Of note, the net distance covered either by anterogradely or retrogradely moving pGOLT spots was not affected by the Aβ + DMSO treatment, although the population variance appeared reduced (**Figure 4B**). To further investigate the pGOLT spot velocity, the net distances were pooled together independently of the direction, creating a different representation of the data that we called "mobility index." Accordingly, the mobility index (**Figure 4C**) and the average velocity of trafficking pGOLT spots remained substantially unchanged after Aβ + DMSO treatment, being 0.05 ± 0.007 μm/min in proximal apical, 0.05 ± 0.010 μm/min in proximal basal, and 0.08 ± 0.001 μm/min in higher order dendrites under basal conditions (**Figure 4C** and **Table 2**). Interestingly, in all segments measured, 4-h treatment with Aβ + DMSO significantly reduced the number of visible pGOLT spots with respect to control conditions (**Figure 4D**). In conclusion, short-term Aβ + DMSO treatment in unstimulated neuronal cultures induced a decrease of visible pGOLT spots and a reduction in the anterograde trafficking of pGOLT spots in distal high order dendrites.

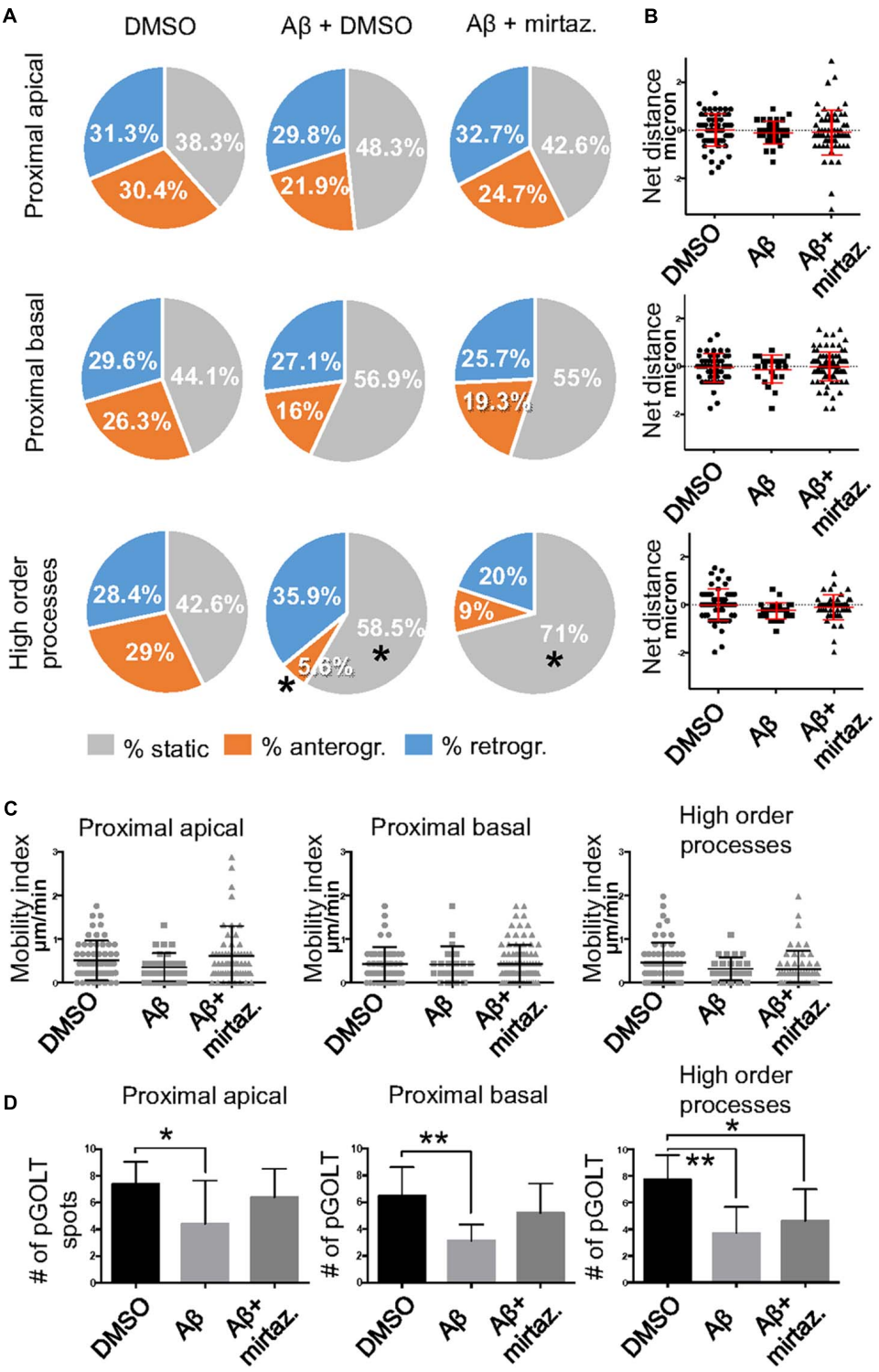

FIGURE 4 | Effects of Aβ and mirtazapine on pGOLT vesicle trafficking in unstimulated cultures. **(A)** Pie charts representation of the average percentage of anterograde, retrograde, and static pGOLT spots for each cell in cultures treated with Aβ and mirtazapine (both 10 μM, 4 h). Data were obtained from 4 to 5 ROI segments in proximal apical, proximal basal, and higher order processes. DMSO: $n = 8$; Aβ + DMSO: $n = 7$; Aβ + mirtazapine: $n = 10$. **(B)** Scatter plot representation of net distance covered by pGOLT spots in the basal condition in proximal apical, proximal basal, and higher order processes after 4-h treatments. **(C)** Mobility index represents the velocity of pGOLT spots in the different segments analyzed, expressed in μm/min, after 4 h of treatments. **(D)** Average of the number of pGOLT spots in the different segments. DMSO: $n = 8$; Aβ + DMSO: $n = 7$; Aβ + mirtazapine: $n = 10$. Following D'Agostino-Pearson's normality test, we performed an unpaired *t*-test. $^{*}p \leq 0.05$; $^{**}p \leq 0.01$.

TABLE 1 | Summary of the pGOLT dynamics in unstimulated cultures.

		DMSO	Aβ + DMSO	Aβ + mirtazapine
Proximal apical	Static	38.3 ± 5.5%	48.3 ± 9.5%	42.6 ± 8.8%
	Anterograde	30.4 ± 11.0%	21.9 ± 8.8%	24.7 ± 6.4%
	Retrograde	31.3 ± 8.4%	29.8 ± 13.0%	32.7 ± 6.0%
Proximal basal	Static	44.1 ± 9.5%	56.9 ± 13.0%	55.0 ± 5.0%
	Anterograde	26.3 ± 9.0%	16 ± 5.9.0%	19.3 ± 4.5%
	Retrograde	29.6 ± 9.7%	27.1 ± 10.0%	25.7 ± 6.0%
Higher order	Static	42.6 ± 5.0%	58.5 ± 13.0%*1	71 ± 6.0%*2
	Anterograde	29 ± 7.0%	5.6 ± 3.0%*3	9 ± 3.0%*4
	Retrograde	28.4 ± 6.0%	35.9 ± 12.0%	20 ± 5.0%

*Average percentage ± standard error of the mean (SEM) of static, anterograde, and retrograde vesicles for each neuron in control (DMSO) or after treatment with Aβ or Aβ + mirtazapine. *1: $p < 0.05$, for Aβ + DMSO vs. DMSO. *2: $p = 0.004$, for Aβ + mirtazapine vs. DMSO for static spots in high order processes. *3: $p = 0.02$, for Aβ vs. DMSO for anterograde spots in high order processes. *4: $p = 0.02$, for Aβ + mirtazapine vs. DMSO for anterograde spots in high order processes.*

TABLE 2 | Summary of the pGOLT spot velocities (μm/min).

Conditions	Proximal apical	Proximal basal	Higher order
DMSO	0.05 ± 0.005	0.05 ± 0.006	0.05 ± 0.004
Aβ	0.05 ± 0.007	0.05 ± 0.010	0.08 ± 0.010
Aβ + Mirta	0.09 ± 0.010*1,2	0.06 ± 0.007	0.08 ± 0.020

**1: $p = 0.0088$ for Aβ + Mirta vs. DMSO in proximal apical processes. *2: $p = 0.0182$ for Aβ + Mirta vs. Aβ in proximal apical processes.*

Mirtazapine Recues Aβ-Induced Impaired Traffic and Number of pGOLT Spots in Dendrites

To explore for possible protecting effects of mirtazapine on Aβ-induced insult in hippocampal neurons, we tested whether mirtazapine (10 μM, 4 h) could reverse the Aβ-induced impairment of trafficking in DIV7 hippocampal neurons cultured under basal, unstimulated conditions. First of all, we tested the effects on pGOLT vesicles speed of mirtazapine alone and we found no difference with respect to control cultures treated with the DMSO vehicle (**Supplementary Figure 2**). When mirtazapine was co-applied with Aβ, we observed in proximal apical and basal dendrites no significant change in the percentage of static vesicles with respect to cultures treated with Aβ + DMSO (**Figure 4A** and **Table 1**). However, in high order dendrites, the percentage of static spots was significantly increased in cultures treated with Aβ + mirtazapine, with respect to control cultures (static spots: 42.6 ± 5.0% in DMSO vs. 58.5 ± 13.0% in Aβ + DMSO and 71.0 ± 6.0% in Aβ + mirtazapine; $p = 0.004$). Notably, the significant reduction in the anterograde spots observed in higher order dendrites after Aβ + DMSO treatment was not recovered by mirtazapine (29.0 ± 7.0% in DMSO; 5.6 ± 3.0% in Aβ + DMSO; 9.0 ± 3.0% in Aβ + mirtazapine; $p = 0.02$; **Figure 4A** and **Table 1**). A positive effect of mirtazapine included the regaining of the fastest spots with higher net distance covered in 10 min (**Figure 4B**) and the rescue of the population variance average velocity of pGOLT spots, which was contracted after Aβ treatment (**Figure 4C**). Of note, mirtazapine promoted a significant increase in pGOLT spot velocities only in proximal apical processes (0.09 ± 0.010 μm/min for Aβ + Mirta, vs. 0.05 ± 0.005 μm/min for DMSO; $p = 0.0088$ or 0.05 ± 0.007 μm/min for Aβ; $p = 0.0182$; **Table 2**). Moreover, mirtazapine induced a recovery to basal levels of the number of pGOLT spots in the three dendritic regions, which were strongly reduced by the Aβ + DMSO treatment ($p < 0.05$; **Figure 4D**). In conclusion, in unstimulated cultures mirtazapine induced a recovery of the number of pGOLT spots and regained the fastest pGOLT movements but the percentage of anterogradely moving pGOLT spots remained as low after Aβ treatment and there was a strong increase in static vesicles in higher order dendrites.

Since in unstimulated cultures mirtazapine was unable to rescue the impairment of the anterograde trafficking induced in distal dendrites by short-term Aβ treatment, in the subsequent series of experiments we investigated how neurons were affected by Aβ in the presence of sustained neuronal activity and if mirtazapine could have a beneficial effect under these conditions (**Figure 5**). In cultures stimulated with high K^+ (50 mM, 5 min), Aβ + DMSO treatment did not significantly change the percentage of pGOLT spots with a static behavior or those moving anterogradely or retrogradely with respect to DMSO-treated cultures in proximal dendritic compartments (**Figure 5A**). However, similarly to unstimulated cultures, we observed in higher order dendrites, a trend at the limit of statistical significance toward a reduction in anterograde movements (from 46.2 ± 12.0% with DMSO + KCl to 16.3 ± 14.0% in Aβ + KCl, $p = 0.0754$; **Figure 5A** and **Table 3**) and an increase in retrograde spots following Aβ treatment (from 28.7 ± 9.0% with DMSO + KCl to 60.6 ± 16.0% in Aβ + KCl; **Figure 5A**). Interestingly, we found reduced variability of the net distance covered for both anterograde (positive values, **Figure 5B**) and retrograde pGOLT spots (negative values, **Figure 5B**). In particular, we observed that the number of fastest spots (i.e., those with longest net distance) was reduced in cultures treated with Aβ + KCl (**Figure 5B**), although the mobility index of pGOLT spots in cultures treated with Aβ + DMSO and KCl did not change with respect to controls (**Figure 5C**). Finally, we observed a significant decrease in the number of pGOLT spots following Aβ + DMSO + KCl treatment with respect to cultures incubated with DMSO + KCl (**Figure 5D**).

In cultures stimulated with high K^+ and challenged with Aβ, mirtazapine had a general stimulating effect on the mobilization of pGOLT spots. In fact, in both proximal apical and basal processes, mirtazapine induced a significant reduction in the percentage of static spots ($p < 0.04$; **Figure 5A**). In particular, in proximal apical segments the percentage of static pGOLT spots was significantly reduced from 29.3 ± 6.7% in Aβ + DMSO + KCl to 14.1 ± 7.0% in Aβ + mirtazapine + KCl ($p = 0.048$), and, in the same conditions, the percentage of retrograde vesicles was significantly increased from 22.8 ± 9.0% in Aβ to 61.4 ± 11.0% in Aβ + mirtazapine ($p = 0.03$). In basal proximal dendrites there was a significant decrease in static pGOLT spots from 40.5 ± 13.0% in Aβ + DMSO + KCl to 12.1 ± 4.0% in Aβ + mirtazapine + KCl ($p < 0.01$) along with an increase in anterograde pGOLT spots from 22.4 ± 8.4.0% in Aβ + DMSO + KCl to 45.9 ± 9.5% in Aβ + mirtazapine + KCl ($p < 0.05$). In higher order processes, mirtazapine reverted the

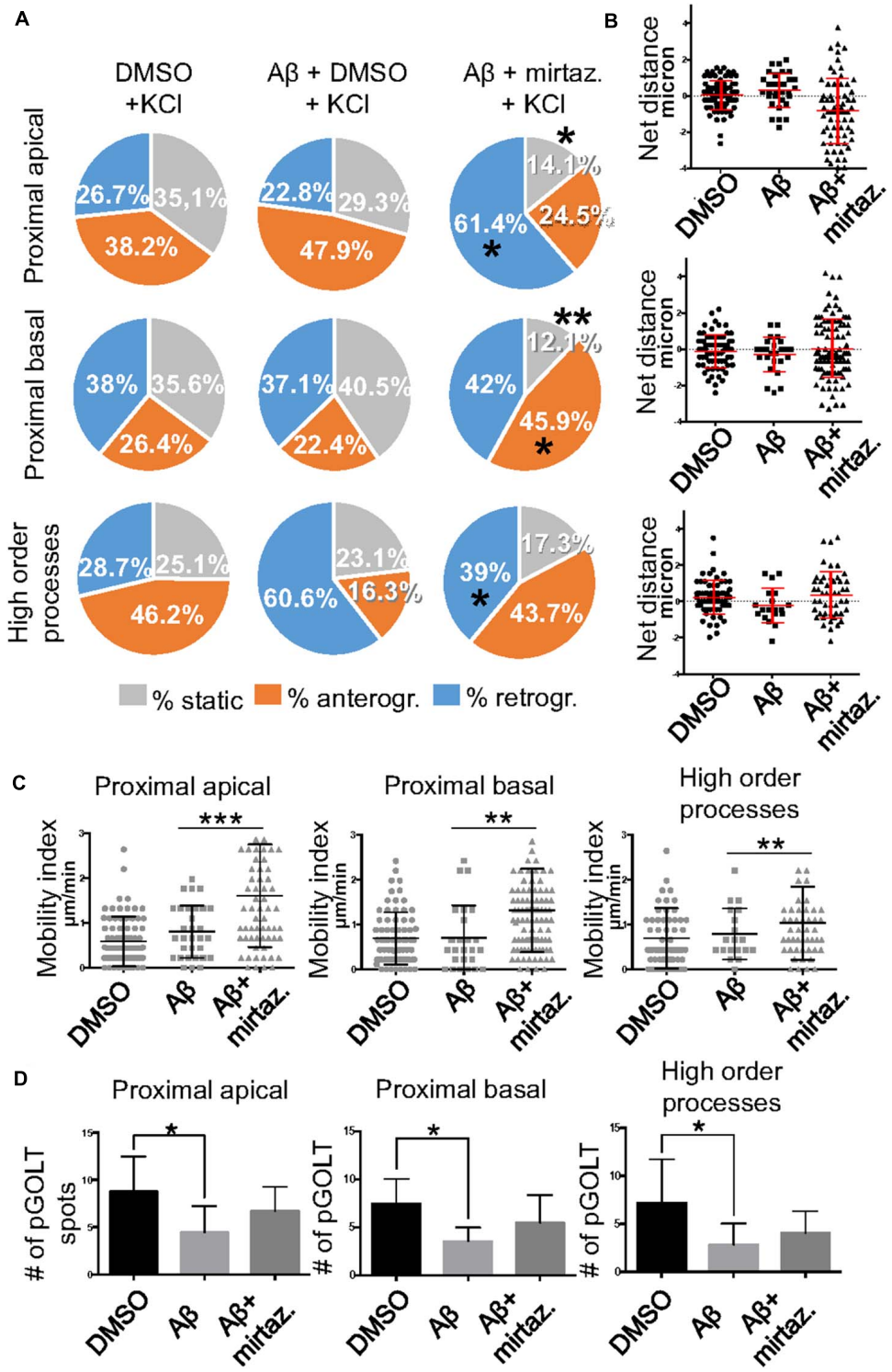

FIGURE 5 | Effects of Aβ and mirtazapine on pGOLT vesicle trafficking in 50 mM KCl-stimulated cultures. **(A)** Pie charts representation of the average percentage of anterograde, retrograde, and static pGOLT spots after KCl stimulation (50 mM, 5 min). Data were obtained from 4 to 5 segments in proximal apical, proximal basal, and higher order processes. DMSO: $n = 8$; Aβ + DMSO: $n = 7$; Aβ + mirtazapine: $n = 10$. **(B)** Scatter plot representation of net distance of pGOLT spots in KCl conditions in proximal apical, proximal basal, and higher order processes after 4 h of treatments. **(C)** Mobility index calculated as the absolute net distance traveled by pGOLT spots in apical segments, basal segments, and higher order segments. DMSO: $n = 8$, $p = 0.0004$; Aβ + DMSO: $n = 7$, $p = 0.0025$; Aβ + mirtazapine: $n = 10$, $p = 0.0173$. **(D)** Average of the number of pGOLT spots in the different segments. DMSO: $n = 8$; Aβ + DMSO: $n = 7$; Aβ + mirtazapine: $n = 10$. Following D'Agostino-Pearson's normality test, we performed a one-way ANOVA test or Kruskal Wallis test. $^{*}p \leq 0.05$; $^{**}p \leq 0.01$; $^{***}p \leq 0.001$.

TABLE 3 | Summary of the pGOLT dynamics in high KCl-stimulated cultures.

		DMSO	Aβ + DMSO	Aβ + mirtazapine
Proximal apical	Static	35.1 ± 6.6%	29.3 ± 6.7%	14.1 ± 7.0%*1
	Anterograde	38.2 ± 11.0%	47.9 ± 9.0%	24.5 ± 9.0%
	Retrograde	26.7 ± 6.0%	22.8 ± 9.0%	61.4 ± 11.0%*2
Proximal basal	Static	35.6 ± 6.0%	40.5 ± 13.0%	12.1 ± 4.0%*3
	Anterograde	26.4 ± 7.0%	22.4 ± 8.4%	45.9 ± 9.5%*4
	Retrograde	38 ± 10.0%	37.1 ± 10.0%	42 ± 8.0%
Higher order	Static	25.1 ± 6.0%	23.1 ± 13.0%	17.3 ± 8.0%
	Anterograde	46.2 ± 12.0%	16.3 ± 14.0%	43.7 ± 12.0%
	Retrograde	28.7 ± 9.0%	60.6 ± 16.0%	39 ± 12.0%*5

*Average percentage ± standard error of the mean (SEM) of static, anterograde, and retrograde vesicles for each neuron in control (DMSO) or after treatment with Aβ or Aβ + mirtazapine after treatment with high K + *1: p = 0.04, for Aβ + mirtazapine + KCl vs. Aβ + DMSO + KCl for static spots in proximal apical processes. *2: p = 0.03, for Aβ + mirtazapine + KCl vs. Aβ + DMSO + KCl for retrograde spots in proximal apical processes. *3: p = 0.01, for Aβ + mirtazapine + KCl vs. DMSO + KCl for static spots in proximal basal processes. *4: p < 0.05, for Aβ + mirtazapine + KCl vs. Aβ + DMSO + KCl for anterograde spots in proximal basal processes. *5: p < 0.05, for Aβ + mirtazapine + KCl vs. Aβ + DMSO + KCl for retrograde spots in higher order processes.*

Aβ-induced decrease in retrograde mobility of pGOLT spots from 60.6 ± 16.0% in Aβ + DMSO + KCl to 39.0 ± 12.0% in Aβ + mirtazapine + KCl ($p > 0.05$; **Table 3**). In support of the idea that mirtazapine could have a stimulating effect on Golgi vesicles trafficking, we found that mirtazapine increased the number of pGOLT spots that moved for a significantly longer net distance in each of the three dendritic compartments considered (**Figures 5B,C**). In particular, in all dendritic segments analyzed, the pGOLT mobility index was significantly higher in Aβ neurons treated with mirtazapine with respect to neurons treated with Aβ only ($p < 0.001$ for proximal apical and $p < 0.01$ for proximal basal and high order processes; **Figure 5C**). Moreover, mirtazapine treatment induced a recovery of the quantity of pGOLT spots per segment, which was reduced after incubation with Aβ (**Figure 5D**). Finally, by time-lapse recording of pGOLT spots in the same Aβ + mirtazapine-treated hippocampal neurons before and after KCl depolarization, we found that depolarization induced a significant increase in the mobility of retrograde pGOLT spots in proximal apical processes ($p = 0.0479$) and in anterograde spots in basal and distal processes ($p = 0.0165$ and $p = 0.0264$, respectively) with a corresponding significant reduction in the number of static vesicles with respect to mirtazapine (**Figure 6**).

These results indicate that neuronal depolarization induced distinct responses in proximal apical, proximal basal, or higher order processes in conditions of impaired trafficking induced by Aβ treatment, suggesting regional distinct effects of mirtazapine overcame the Aβ-induced reduction in the number and mobility of pGOLT spots.

Pharmacological Recovery of Aβ-Induced Neurite Atrophy

Considering the effects of Aβ and mirtazapine on vesicle trafficking, and the role of the Golgi apparatus in neuronal development and in the maintenance of dendritic arborization, we hypothesized that a pharmacological treatment with mirtazapine could reduce the Aβ-induced damage in cultured rat hippocampal neurons (**Figure 7**). Therefore, by applying the same methods used in **Figure 2**, we measured the total neuritic length (TNL) and the percentage of surviving neurons after 4-h treatment with $A\beta_{25-35}$ alone (with DMSO), or in the presence of mirtazapine. Mirtazapine treatment alone (10 μM, 4 h) did not affect the TNL (1058 ± 128 for DMSO, vs. 971 ± 87 μm/neuron mirtazapine) nor the ratio of the number of neurons on total cell number with respect to cultures treated with the vehicle only (0.28 ± 0.01 NeuN/DAPI positive cells for DMSO, vs. 0.26 ± 0.02 for mirtazapine; **Figures 7A,B**). In a second set of experiments, Aβ + DMSO incubation (10 μM, 4 h) caused a significant blunting of TDL and reduction of surviving neurons with respect to DMSO controls ($p = 0.0068$ for TDL; $p \leq 0.001$ for neuronal survival; **Figures 7C,D**). Co-application of Aβ and mirtazapine (both 10 μM, 4 h) to hippocampal neuronal cultures demonstrated a significant neuroprotective effect of mirtazapine with respect to Aβ-treated cultures on total neuritic length (1603 ± 47 μm/neuron in Aβ + DMSO, vs. 1754 ± 40 μm/neuron in Aβ + mirtazapine; $n = 3$ independent cultures; $p = 0.0154$; **Figures 7C,D**). The recovery effect was incomplete because cultures treated with mirtazapine showed TNL values significantly lower than control cultures treated with only DMSO (1754 ± 40 μm/neuron in Aβ + mirtazapine vs. 1906 ± 28 μm/neuron in DMSO; $n = 3$ independent cultures; $p \leq 0.05$; **Figures 7C,D**). Moreover, mirtazapine treatment was not sufficient to protect against Aβ-induced cell death with respect to control (0.24 ± 0.02 for Aβ + DMSO vs. 0.25 ± 0.02 for Aβ with mirtazapine, not significantly different; **Figure 7D** right). In **Figure 7**, TDL data shown for the DMSO condition were different between **Figures 7B,D** which were carried out at different times. We previously reported that variations in the culture density can affect the TDL (Nerli et al., 2020). However, irrespective of the actual value, the validity of each experiment is given by the comparison to its own control.

DISCUSSION

In this work we demonstrated that short-term (4 h) treatment with Aβ oligomers led to a decrease in anterograde trafficking of Golgi-like organelles in dendrites of hippocampal neurons. In neurons cultured under basal (unstimulated) conditions, the reduced percentage of Golgi vesicles undergoing anterograde trafficking is accompanied by an increase in the percentage of static Golgi spots and the effect is modest in proximal apical basal dendrites and much more marked in higher order dendrites. In contrast, in cultures stimulated with 50 mM KCl, the reduction in anterograde trafficking is visible only in higher order dendrites and is also accompanied by an increase in the percentage of static Golgi spots (summarized in **Figure 8**). We also showed the efficacy of mirtazapine in limiting the early damage induced by Aβ oligomers in hippocampal neurons, by increasing the total number and the general motility of Golgi spots in both an anterograde and retrograde direction, and reducing the percentage of static Golgi vesicles (**Figure 8**).

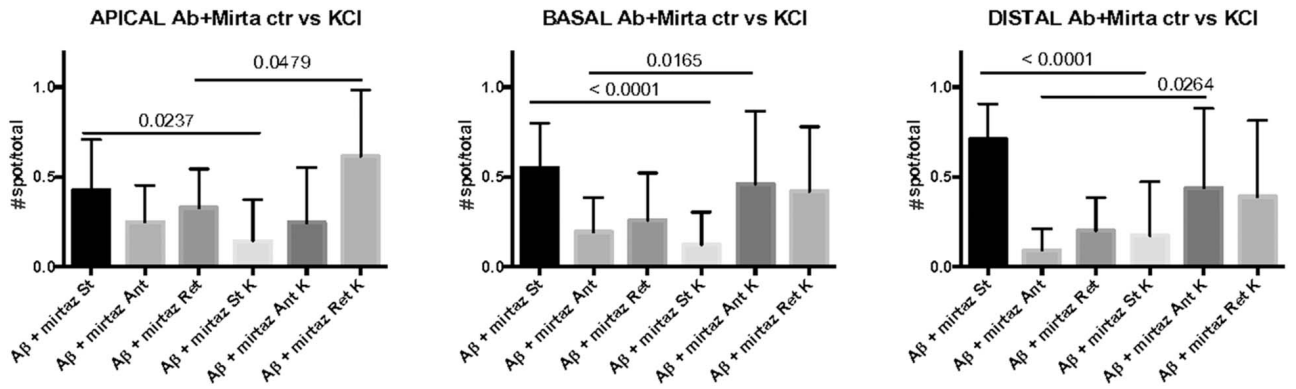

FIGURE 6 | Comparison of number of pGOLT spots in control conditions and after high K^+ treatment. The same hippocampal neurons were treated with Aβ + mirtazapine and recorded in time lapse before and after entering depolarizing conditions (K+, KCl, 50 mM, 10 min). The histograms represent the occurrence of static (St) or mobile anterograde (Ant) or retrograde (Ret) pGOLT vesicles in apical, basal, and in high order processes (distal), as indicated. Result of the statistical analysis between control and high K+ groups is indicated (*t* test). *N* = 7–18 neurons.

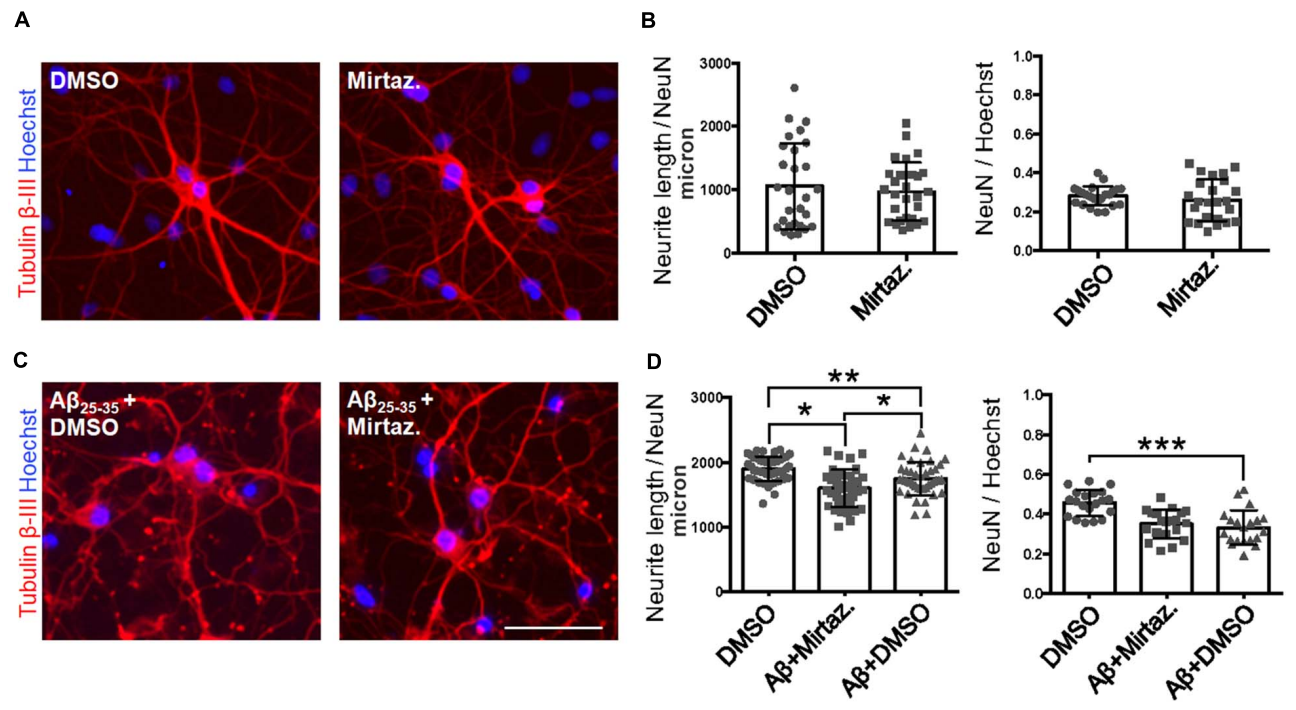

FIGURE 7 | Rescue of Aβ-induced dendritic atrophy by mirtazapine treatment. **(A)** Representative microscopy images (10X) of DIV7 hippocampal neurons after 24-h treatment in DMSO **(left)** or mirtazapine (10 μM, 4 h **right**), stained with anti-Tubulin β-III (red) and Hoechst (blue). Scale bar = 50 μm. **(B)** Scatter plot of total neurite length for each neuron (**left**) expressed in μm/neuron, and neuronal density expressed as the ratio between the number of NeuN positive neurons on the total number of cells (**right**). Each dot represents an image in the different conditions, *n* = 24–25 fields per condition. **(C)** Representative images (10X) of DIV7 hippocampal neurons after 24 h of Aβ + DMSO **(left)** or Aβ + mirtazapine treatment **(right)**, stained with anti-Tubulin β-III and Hoechst. Scale bar = 50 μm. **(D)** Scatter plot of neurite length for each neuron **(left)** expressed in μm/neuron, and neuronal density expressed as the ratio between the number of neurons on the total number of cells **(right)**. Each dot represents an image in the different conditions, *n* = 40–44 fields per condition. Following D'Agostino-Pearson's normality test, we performed an unpaired two-tailed *t*-test or one way ANOVA. *$p \leq 0.05$; **$p \leq 0.01$; ***$p \leq 0.001$.

In addition, mirtazapine largely reverted the neuronal atrophy induced by 24-h treatment with Aβ oligomers, suggesting that this drug is able to recover, at least in part, the neuronal damage by improving trafficking of the vesicles involved in the secretory route.

In this study, all experiments were carried out using the 11-amino acid sequence of Aβ25–35 which corresponds to the functional domain of the full-length Aβ1–40/42 peptides. The initial sequence of this short peptide fragment encodes a hydrophilic domain (Aβ25–28) involved in the formation of a

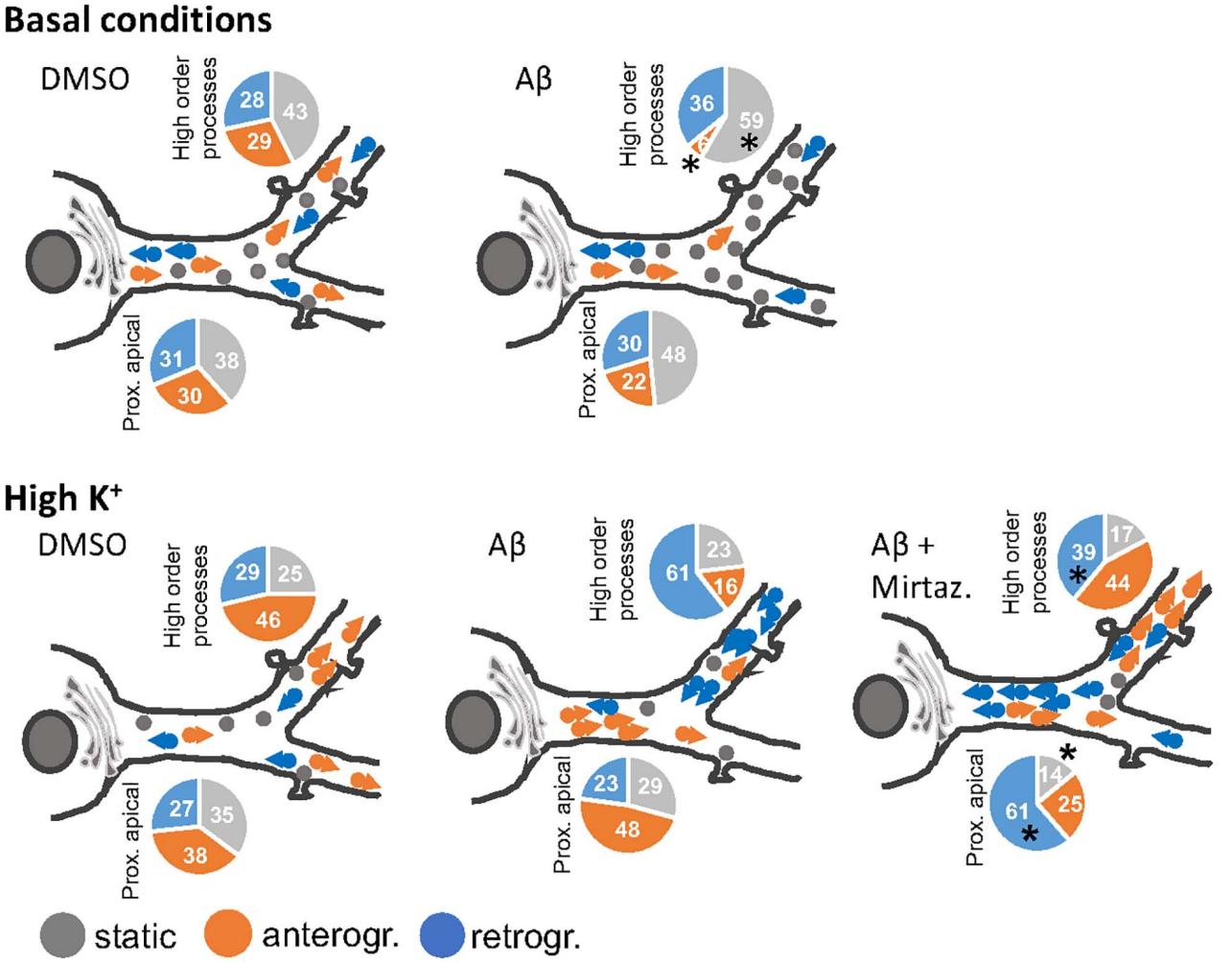

FIGURE 8 | Model of the effects of a short-term challenge with Aβ oligomers on the trafficking of Golgi-like spots in the apical dendrites of rat hippocampal neurons and its rescue with mirtazapine treatment (the effects on basal dendrites are omitted for simplicity). The pie charts indicate percentage of static, anterograde, or retrograde moving pGOLT spots observed in living neurons, asterisks indicate significant changes induced by mirtazapine with respect to Aβ.

β-sheet structure, while the terminal half is constituted by a hydrophobic domain (Aβ29–35) (Millucci et al., 2009). Similar to the Aβ1–42 or Aβ1–40 fragments, Aβ25–35 can form early intermediate aggregates such as monomeric or oligomeric soluble forms, or insoluble fibrils which are tightly associated with disease pathogenesis (Selkoe and Hardy, 2016). In particular, we chose to use Aβ25–35 because its presence was demonstrated in senile plaques of AD brains (Kubo et al., 2002), and it is the shortest fragment able to form large β-sheet fibrils, retaining the toxicity of the full length Aβ1–40/42 peptides (Kubo et al., 2002; Naldi et al., 2012).

Effect of Aβ and Mirtazapine on Golgi Vesicle Trafficking

We found that even a short-term Aβ treatment of 4 h can cause a reduction in the number of Golgi vesicles in dendrites. The reduction in neurite outgrowth caused by long-term Aβ treatment might be associated with an overall reduced number of Golgi outposts (GOPs), as observed in other neurodegenerative disease models (Chung et al., 2017). Proper organization of both GOPs and Golgi satellites is fundamental for post-Golgi trafficking and dendrite elongation (Horton and Ehlers, 2003a; Horton et al., 2005).

In our work, we have studied the acute effect of Aβ and mirtazapine on the trafficking properties of pGOLT vesicles in hippocampal neurons. pGOLT-expressing neurons exhibited discrete spots in the soma and dendrites that were partially co-localized with antibodies targeting GM130 and TGN38, in line with previous findings (Mikhaylova et al., 2016). By employing a quantitative live imaging experiment analysis, we found that pGOLT vesicles were highly mobile in the perisomatic region, while they tended to become more static or oscillate in the dendrites. In particular, under basal conditions, pGOLT-transfected neurons were characterized by an equal fraction of static, retrograde, and anterograde pGOLT vesicles, distributed along the entire dendritic tree. Short incubation with Aβ

oligomers had a strong effect on vesicle trafficking, supporting the known effects of Aβ on molecular motors (Vicario-Orri et al., 2015; Gan and Silverman, 2016; Gan et al., 2020). In fact, we observed a significant reduction in the number of pGOLT vesicles as well as significant impairment in their mobility in both directions with respect to the control in all compartments analyzed. After mirtazapine treatment, vesicles were more numerous, and had higher motility, covering significantly larger net distances with respect to control neurons.

We investigated the motility of pGOLT vesicles after depolarization with high K^+, a treatment that is known to mobilize secretory vesicles and massively reinforce signaling following synaptic activation. In control conditions, membrane depolarization with high K^+ strongly mobilized pGOLT anterograde trafficking. Similarly, in neurons treated with Aβ for only 4 h, high K^+ was indeed sufficient to promote pGOLT vesicle mobilization, suggesting that in this early phase, the Aβ injury is still reversible. In fact, mirtazapine co-applied with Aβ was sufficient to positively impact the occurrence of pGOLT vesicles and significantly change their mobility, thus suggesting a positive effect of this drug on the molecular mechanisms that were impaired in Aβ-injured neurons. In addition, mirtazapine-treated neurons were visibly more trophic, with a larger membrane surface, and displayed a larger number of smaller pGOLT vesicles with respect to control. In the presence of KCl-induced neuronal depolarization, mirtazapine significantly sped up long-distance retrograde trafficking in apical and distal endings. After KCl, in Aβ, the percentage of static vesicles was similar to the vehicle, while in higher order processes the percentage of retrograde vesicles was strongly increased. In addition, mirtazapine induced decreased static pGOLT vesicles favoring retrograde transport toward the soma, with the exception of higher order processes where we observed a decrease in the percentage of retrograde vesicles. Moreover, mirtazapine induced a significant increase in pGOLT vesicles' mobility index compared to Aβ-treated cultures.

The different dynamics observed in the dendrites of hippocampal neurons after KCl further confirmed the fact that primary dendrites exhibit a distinct trafficking mechanism compared to the higher order dendrites, as shown in basal condition (van Beuningen and Hoogenraad, 2016; **Figure 8**). Moreover, it is known that Aβ treatment may alter the ionic concentration within the neurons, interfering directly with the ion channels and pumps or intracellular organelles. In fact, several studies proved the capability of Aβ to form cationic channels permeable for Ca^{2+} in the membrane, leading to the disruption of Ca^{2+} homeostasis (Arispe et al., 1993) and further impairment of mitochondrial activity (Dong et al., 2016). The imbalance in Ca^{2+} may be further enhanced by the depolarizing effects of KCl, leading to strong activation of voltage-gated Ca^{2+} channels and synaptic activity. Ca^{2+} dyshomeostasis may interact with the activity of pGOLT, characterized by the transmembrane domain of the protein Calneuron-2, known as the Ca^{2+} sensor (Mikhaylova et al., 2016). It has been observed that sustained intracellular Ca^{2+} levels induced by high frequency stimulation by KCl prevents the inhibition activity of Calneuron-2 on the enzyme Phosphatidylinositol 4-OH kinase IIIβ (PI-4Kβ) leading to enzyme activation, increased Golgi-to-plasma membrane trafficking, and therefore retromer trafficking (Mikhaylova et al., 2009). The Calneuron-2 mechanisms may explain the fact that in Aβ-treated pGOLT-transfected neurons, high K^+ led to a strong increase in retrograde vesicles in higher order processes, which is indicative of synaptic activity and endosome-to-TGN trafficking. On the other hand, mirtazapine co-application with Aβ recovered correct trafficking in distal segments, leaving an open question regarding which intracellular mechanisms, that re-establish the vehicle rates of retromer trafficking, are induced by this antidepressant.

Differential Behavior of Vesicles in the Different Compartments of the Dendritic Arbor

It is not known whether Golgi transport mechanisms are equally regulated in the different regions of dendritic arborization and if they are functionally independent and with unique trafficking properties. Our data globally confirm the view that different segments of neuronal arborization are functionally independent and follow different trafficking rules. In particular, in resting cultures, Aβ affected the trafficking of pGOLT spots mainly in proximal apical and proximal basal processes, and both these effects were recovered by mirtazapine in the same regions (**Figure 8**). On the contrary, in higher order processes, Aβ significantly decreased the number of anterograde vesicles compared to control and mirtazapine increased the percentage of static vesicles, with little effect on their mobility (**Figure 8**). Interestingly, KCl-evoked depolarization had no effect on pGOLT spots in proximal segments, while the combination of KCl and Aβ treatments affected spots localized in apical segments and in distal endings, that are, however, differently mobilized, in anterograde and retrograde fashion, respectively. In conclusion, in proximal apical dendrites, mirtazapine partially restored vesicle mobility, presumably allowing the anterograde trafficking of vesicles necessary for the proper functionality of the neurons. Moreover, in higher order processes, mirtazapine seems to exert a dominant effect leading to an increase in Golgi outposts in distal dendrites, where elongation occurs. Regarding retrograde trafficking, mirtazapine was able to stimulate the spots mainly located in apical and distal endings, with no effect on spots on basal segments.

These data underline the differences between higher order dendrites and primary dendrites that originate from the soma and extend until the first branching point (Ye et al., 2007). Interestingly, it has already been described that organelles close to perinuclear regions may exhibit distinct functionality from those present in distal dendrites, since the concentrations of ions and proteins between these two compartments are different (Prydz et al., 2008; Britt et al., 2016).

Effect of Aβ and Mirtazapine on Neurite Outgrowth

Mirtazapine is a noradrenergic and serotoninergic tetracyclic antidepressant, which in our experiments had no effect on neurite length or neuronal density of naïve hippocampal neurons,

while it significantly counteracted the neuronal atrophy induced by Aβ, with no effect on neuronal loss. Aberrant neurite morphology caused by protein toxicity is a common feature of neurodegenerative diseases. Multiple mechanisms are involved in causing Aβ-induced neurodegeneration (Resende et al., 2007). Among others, Aβ oligomers affect the structure and function of molecular motors required for neurite elongation, trafficking, and sorting of vesicles essential for synaptic function (Brady and Morfini, 2017; Gan et al., 2020). In particular, Aβ induces Tau hyperphosphorylation and disengagement from microtubules affecting cargo transport, inducing deficits of neuronal protein transport, further leading to disruption of neuronal polarity (Ballatore et al., 2007). Furthermore, Aβ affects HDAC functioning, altering the acetylation of cytoskeleton proteins (Hubbert et al., 2002; Cohen et al., 2011) essential for microtubules dynamics.

The observed protective effects of mirtazapine on Aβ-induced neuronal atrophy can be explained by its multi-target way of action. In contrast to other antidepressants, mirtazapine does not inhibit the norepinephrine reuptake but rather antagonizes the α_2-heteroreceptors in serotoninergic terminals. Additionally, mirtazapine acts as a blocker of 5-HT_2 and 5-HT_3 receptors, while promotes 5-HT_{1A}-mediated transmission (de Boer, 1996). In particular, 5-HT_{1A} receptors were found mainly expressed in the soma and dendrites of CA1 pyramidal neurons (Ferreira et al., 2010). Serotonin production and expression of receptors, in particular 5-HT_{1A} and 5-HT_7, are involved in shaping hippocampal circuits, and the activation of 5-HT_{1A} receptors improves neurite outgrowth of secondary neurites (Fricker et al., 2005; Rojas et al., 2014), suggesting a possible mechanism of action of mirtazapine. Moreover, the protective mechanism induced by mirtazapine may be mediated by promoting BDNF expression and release (Rogóz et al., 2005) as well as by promoting HDAC-related mechanisms (Ookubo et al., 2013).

Use of Mirtazapine in Alzheimer's Patients

Depression, often associated with severe weight loss, insomnia, and anxiety, is a comorbidity frequently found in patients affected by Alzheimer's disease (Cassano et al., 2019). Unfortunately, as most antidepressant drugs were found to be ineffective, depression often presents as resistant to treatment (Elsworthy and Aldred, 2019). Among various possible explanations for the lack of efficacy of antidepressants in AD, a major hypothesis is that depression becomes resistant to treatment as a consequence of neurodegenerative events occurring at advanced stages of the pathology (Elsworthy and Aldred, 2019). To complicate this picture, meta-analysis studies have identified depression as a risk factor for AD, in that patients with a previous history of depression were more likely to develop AD later in life (Ownby et al., 2006; Tan et al., 2019). There is therefore an urgent need to understand how antidepressants may impact the cellular mechanisms underlying AD and its associated psychiatric symptoms.

Studies regarding the clinical use of mirtazapine treatment in AD are controversial. In three AD patients, mirtazapine was reported to promote a complete remission of depression, anhedonia, weight loss, sleep disturbances, and anxiety although memory deficits persisted (Raji and Brady, 2001). A 12-week open-label pilot study showed significant improvement in Cohen-Mansfield Agitation Inventory-Short form (CMAI-SF) scores and Clinical Global Impression-Severity scale (CGI-S) scores in 13 out of 16 patients (81.25%; Cakir and Kulaksizoglu, 2008). However, a large double-blind, placebo-controlled clinical study for the treatment of depression in AD conducted on 326 subjects (111 controls, 107 mirtazapine, 108 sertraline) across 9 centers in the United Kingdom found no benefit of mirtazapine or sertraline compared to placebo at 13 and 39 weeks (Banerjee et al., 2011). On the other hand, full resolution of associated symptoms such as weight loss, sleep problems, and anxiety has been consistently reported in several studies (Raji and Brady, 2001; Urrestarazu and Iriarte, 2016; Franx et al., 2017). Interestingly, recent studies have investigated non-canonical effects of antidepressants on neurobiological mechanisms, demonstrating that various antidepressants, including mirtazapine (Sun et al., 2007) are able to downregulate amyloid-β peptide levels in the serum and brain of AD patients and transgenic animal models (reviewed in Cassano et al., 2019). Our results on the effects of mirtazapine Golgi trafficking add to this emerging trend of investigations in AD.

Conclusion

In AD, transport deficits underlie neuronal dysfunction and synaptic loss. We propose that mirtazapine can exert protective effects against Aβ injury by acting on dendritic trafficking mechanisms that are required for the proper functioning of the anterograde secretory pathway as well as retrograde retromer trafficking in dendrites. Previous studies have shown that Aβ oligomers and neuroinflammation associated with AD impair axonal and dendritic retromer trafficking of BDNF, causing a downregulation in neurotrophin signaling, essential for neuronal development and maintenance of dendritic complexity (Poon et al., 2011; Gan and Silverman, 2016; Seifert et al., 2016; Carlos et al., 2017; Plá et al., 2017). In hAPP transgenic mice, the impairment in axonal retrograde trafficking induced an aberrant retention of endosomes in distal neurites and impaired endosome-TGN and lysosomal functioning (Tammineni et al., 2017). Concerning anterograde Golgi trafficking along the secretory pathway, a different outcome on BDNF or glutamate release in Aβ-treated neurons was described: while BDNF secretion is lowered by Aβ treatment, glutamate release remains unchanged, indicating a specific impairment of the protein secretory pathway (Plá et al., 2017). Thus, the efficacy of mirtazapine in restoring Golgi trafficking is promising for possible future employment in AD treatment.

DATA AVAILABILITY STATEMENT

The raw data supporting the conclusions of this article will be made available by the authors, without undue reservation.

ETHICS STATEMENT

The animal study was reviewed and approved by the Local Ethical Committee of the University of Trieste on November 10th 2017 and was communicated to the Italian Ministry of Health, in compliance with the Italian law D. Lgs.116/92 and the L. 96/2013, art. 13.

AUTHOR CONTRIBUTIONS

ET and EF designed the study, wrote the first draft of the manuscript, and edited the final manuscript. GA and EF carried out the experiments and analyzed the results. All authors contributed to the article and approved the submitted version.

FUNDING

This work was supported by funding from the intramural grant program "Fondi per la Ricerca di Ateneo (FRA-2016)" of the University of Trieste. EF was supported by a post-doctoral fellowship award of the University of Trieste (COFIN program).

ACKNOWLEDGMENTS

The authors thank the manager of the Light Microscopy Imaging Center (LMIC) Gabriele Baj, for help with setting the protocol for live imaging. The authors also thank Giampiero Leanza for the generous gift of the amyloid-beta$_{25-35}$ peptide.

SUPPLEMENTARY MATERIAL

The Supplementary Material for this article can be found online at: https://www.frontiersin.org/articles/10.3389/fnmol.2021.661728/full#supplementary-material

Supplementary Figure 1 | MTT assay dose-curve response of drug and vehicle concentrations on cell survival.

Supplementary Figure 2 | Mobility of pGOLT vesicles after DMSO or mirtazapine treatment. **(A–C)** Examples of time-lapse images of pGOLT vesicles in cultures incubated with vehicle (DMSO) or treated with mirtazapine (MIRTAZ.), under basal conditions or in high KCl medium (post K+). **(D)** Quantification of mobility index in the proximal apical, proximal basal dendrites, or high order processes.

Supplementary Table 1 | Antibodies used in this study.

REFERENCES

Antonini, V., Marrazzo, A., Kleiner, G., Coradazzi, M., Ronsisvalle, S., Prezzavento, O., et al. (2011). Anti-amnesic and neuroprotective actions of the sigma-1 receptor agonist (-)-MR22 in rats with selective cholinergic lesion and amyloid infusion. *J. Alzheimers Dis.* 24, 569–586. doi: 10.3233/jad-2011-101794

Aridor, M., Guzik, A. K., Bielli, A., and Fish, K. N. (2004). Endoplasmic reticulum export site formation and function in dendrites. *J. Neurosci. Off. J. Soc. Neurosci.* 24, 3770–3776. doi: 10.1523/jneurosci.4775-03.2004

Arispe, N., Pollard, H. B., and Rojas, E. (1993). Giant multilevel cation channels formed by Alzheimer disease amyloid beta-protein [A beta P-(1-40)] in bilayer membranes. *Proc. Natl. Acad. Sci. U S A.* 90, 10573–10577. doi: 10.1073/pnas.90.22.10573

Baj, G., Patrizio, A., Montalbano, A., Sciancalepore, M., and Tongiorgi, E. (2014). Developmental and maintenance defects in rett syndrome neurons identified by a new mouse staging system in vitro. *Front. Cell Neurosci.* 8:18. doi: 10.3389/fncel.2014.00018

Ballatore, C., Lee, V. M.-Y., and Trojanowski, J. Q. (2007). Tau-mediated neurodegeneration in Alzheimer's disease and related disorders. *Nat Rev Neurosci.* 8, 663–672. doi: 10.1038/nrn2194

Banerjee, S., Hellier, J., Dewey, M., Romeo, R., Ballard, C., Baldwin, R., et al. (2011). Sertraline or mirtazapine for depression in dementia (HTA-SADD): a randomised, multicentre, double-blind, placebo-controlled trial. *Lancet* 378, 403–411. doi: 10.1016/S0140-6736(11)60830-1

Bittolo, T., Raminelli, C. A., Deiana, C., Baj, G., Vaghi, V., Ferrazzo, S., et al. (2016). Pharmacological treatment with mirtazapine rescues cortical atrophy and respiratory deficits in MeCP2 null mice. *Sci. Rep.* 6:19796.

Brady, S. T., and Morfini, G. A. (2017). Regulation of motor proteins, axonal transport deficits and adult-onset neurodegenerative diseases. *Neurobiol Dis.* 105, 273–282. doi: 10.1016/j.nbd.2017.04.010

Britt, D. J., Farías, G. G., Guardia, C. M., and Bonifacino, J. S. (2016). Mechanisms of polarized organelle distribution in neurons. *Front. Cell Neurosci.* 10:88. doi: 10.3389/fncel.2016.00088

Cakir, S., and Kulaksizoglu, I. B. (2008). The efficacy of mirtazapine in agitated patients with Alzheimer's disease: a 12-week open-label pilot study. *Neuropsychiatr. Dis. Treat.* 4, 963–966. doi: 10.2147/ndt.s3201

Carlos, A. J., Tong, L., Prieto, G. A., and Cotman, C. W. (2017). IL-1β impairs retrograde flow of BDNF signaling by attenuating endosome trafficking. *J. Neuroinflam.* 14:29.

Cassano, T., Calcagnini, S., Carbone, A., Bukke, V. N., Orkisz, S., Villani, R., et al. (2019). pharmacological treatment of depression in Alzheimer's disease: a challenging task. *Front. Pharmacol.* 10:1067. doi: 10.3389/fphar.2019.01067

Castrén, E. (2004). Neurotrophic effects of antidepressant drugs. *Curr. Opin. Pharmacol.* 4, 58–64. doi: 10.1016/j.coph.2003.10.004

Chung, C. G., Kwon, M. J., Jeon, K. H., Hyeon, D. Y., Han, M. H., Park, J. H., et al. (2017). Golgi outpost synthesis impaired by toxic polyglutamine proteins contributes to dendritic pathology in neurons. *Cell Rep.* 20, 356–369. doi: 10.1016/j.celrep.2017.06.059

Cohen, T. J., Guo, J. L., Hurtado, D. E., Kwong, L. K., Mills, I. P., Trojanowski, J. Q., et al. (2011). The acetylation of tau inhibits its function and promotes pathological tau aggregation. *Nat. Commun.* 2:252.

Copani, A., Bruno, V., Battaglia, G., Leanza, G., Pellitteri, R., Russo, A., et al. (1995). Activation of metabotropic glutamate receptors protects cultured neurons against apoptosis induced by beta-amyloid peptide. *Mol. Pharmacol.* 47, 890–897.

Cui-Wang, T., Hanus, C., Cui, T., Helton, T., Bourne, J., Watson, D., et al. (2012). Local zones of endoplasmic reticulum complexity confine cargo in neuronal dendrites. *Cell* 148, 309–321. doi: 10.1016/j.cell.2011.11.056

de Boer, T. (1996). The pharmacologic profile of mirtazapine. *J. Clin. Psychiatry* 57 (Suppl 4), 19–25.

De Vos, K. J., and Hafezparast, M. (2017). Neurobiology of axonal transport defects in motor neuron diseases: opportunities for translational research? *Neurobiol. Dis.* 105, 283–299. doi: 10.1016/j.nbd.2017.02.004

Dehmelt, L., Poplawski, G., Hwang, E., and Halpain, S. (2011). NeuriteQuant: an open source toolkit for high content screens of neuronal morphogenesis. *BMC Neurosci.* 12:100. doi: 10.1186/1471-2202-12-100

Dong, W., Wang, F., Guo, W., Zheng, X., Chen, Y., Zhang, W., et al. (2016). Aβ25-35 suppresses mitochondrial biogenesis in primary hippocampal neurons. *Cell Mol. Neurobiol.* 36, 83–91. doi: 10.1007/s10571-015-0222-6

Dubey, J., Ratnakaran, N., and Koushika, S. P. (2015). Neurodegeneration and microtubule dynamics: death by a thousand cuts. *Front Cell Neurosci.* 9:343. doi: 10.3389/fncel.2015.00343

Elsworthy, R. J., and Aldred, S. (2019). Depression in Alzheimer's disease: an alternative role for selective serotonin reuptake inhibitors? *J. Alzheimers Dis.* 69, 651–661. doi: 10.3233/JAD-180780

Ferreira, T. A., Iacono, L. L., and Gross, C. T. (2010). Serotonin receptor 1A modulates actin dynamics and restricts dendritic growth in hippocampal neurons. *Eur. J. Neurosci.* 32, 18–26. doi: 10.1111/j.1460-9568.2010.07283.x

Franx, B. A. A., Arnoldussen, I. A. C., Kiliaan, A. J., and Gustafson, D. R. (2017). Weight loss in patients with dementia: considering the potential impact of pharmacotherapy. *Drugs Aging* 34, 425–436. doi: 10.1007/s40266-017-0462-x

Fricker, A. D., Rios, C., Devi, L. A., and Gomes, I. (2005). Serotonin receptor activation leads to neurite outgrowth and neuronal survival. *Brain Res. Mol. Brain Res.* 138, 228–235. doi: 10.1016/j.molbrainres.2005.04.016

Fukuyama, K., Tanahashi, S., Hamaguchi, T., Nakagawa, M., Shiroyama, T., Motomura, E., et al. (2013). Differential mechanisms underlie the regulation of serotonergic transmission in the dorsal and median raphe nuclei by mirtazapine: a dual probe microdialysis study. *Psychopharmacology (Berl).* 229, 617–626. doi: 10.1007/s00213-013-3122-9

Gan, K. J., Akram, A., Blasius, T. L., Ramser, E. M., Budaitis, B. G., Gabrych, D. R., et al. (2020). GSK3β impairs KIF1A transport in a cellular model of Alzheimer's disease but does not regulate motor motility at S402. *eNeuro* 7:ENEURO.0176-20.2020.

Gan, K. J., and Silverman, M. A. (2016). Imaging organelle transport in primary hippocampal neurons treated with amyloid-β oligomers. *Methods Cell Biol.* 131, 425–451. doi: 10.1016/bs.mcb.2015.06.012

Gomes, G. M., Dalmolin, G. D., Bär, J., Karpova, A., Mello, C. F., Kreutz, M. R., et al. (2014). Inhibition of the polyamine system counteracts β-amyloid peptide-induced memory impairment in mice: involvement of extrasynaptic NMDA receptors. *PLoS One* 9:e99184. doi: 10.1371/journal.pone.0099184

Horton, A. C., and Ehlers, M. D. (2003a). Dual modes of endoplasmic reticulum-to-Golgi transport in dendrites revealed by live-cell imaging. *J. Neurosci. Off J. Soc. Neurosci.* 23, 6188–6199. doi: 10.1523/jneurosci.23-15-06188.2003

Horton, A. C., and Ehlers, M. D. (2003b). Neuronal polarity and trafficking. *Neuron* 40, 277–295. doi: 10.1016/s0896-6273(03)00629-9

Horton, A. C., and Ehlers, M. D. (2004). Secretory trafficking in neuronal dendrites. *Nat. Cell Biol.* 6, 585–591. doi: 10.1038/ncb0704-585

Horton, A. C., Rácz, B., Monson, E. E., Lin, A. L., Weinberg, R. J., and Ehlers, M. D. (2005). Polarized secretory trafficking directs cargo for asymmetric dendrite growth and morphogenesis. *Neuron* 48, 757–771. doi: 10.1016/j.neuron.2005.11.005

Hubbert, C., Guardiola, A., Shao, R., Kawaguchi, Y., Ito, A., Nixon, A., et al. (2002). HDAC6 is a microtubule-associated deacetylase. *Nature* 417, 455–458. doi: 10.1038/417455a

Kaufmann, W. E., and Moser, H. W. (2000). Dendritic anomalies in disorders associated with mental retardation. *Cereb. Cortex N. Y.* 10, 981–991. doi: 10.1093/cercor/10.10.981

Koleske, A. J. (2013). Molecular mechanisms of dendrite stability. *Nat. Rev. Neurosci.* 14, 536–550. doi: 10.1038/nrn3486

Kubo, T., Nishimura, S., Kumagae, Y., and Kaneko, I. (2002). In vivo conversion of racemized beta-amyloid ([D-Ser 26]A beta 1-40) to truncated and toxic fragments ([D-Ser 26]A beta 25-35/40) and fragment presence in the brains of Alzheimer's patients. *J. Neurosci. Res.* 70, 474–483. doi: 10.1002/jnr.10391

Kulkarni, V. A., and Firestein, B. L. (2012). The dendritic tree and brain disorders. *Mol. Cell Neurosci.* 50, 10–20. doi: 10.1016/j.mcn.2012.03.005

Maeder, C. I., Shen, K., and Hoogenraad, C. C. (2014). Axon and dendritic trafficking. *Curr. Opin. Neurobiol.* 27, 165–170. doi: 10.1016/j.conb.2014.03.015

McNamara, J. O. II, Grigston, J. C., VanDongen, H. M., and VanDongen, A. M. (2004). Rapid dendritic transport of TGN38, a putative cargo receptor. *Brain Res. Mol. Brain Res.* 127, 68–78. doi: 10.1016/j.molbrainres.2004.05.013

Mikhaylova, M., Bera, S., Kobler, O., Frischknecht, R., and Kreutz, M. R. (2016). A dendritic golgi satellite between ERGIC and retromer. *Cell Rep.* 14, 189–199. doi: 10.1016/j.celrep.2015.12.024

Mikhaylova, M., Reddy, P. P., Munsch, T., Landgraf, P., Suman, S. K., Smalla, K.-H., et al. (2009). Calneurons provide a calcium threshold for trans-Golgi network to plasma membrane trafficking. *Proc. Natl. Acad. Sci. U.S.A.* 106, 9093–9098. doi: 10.1073/pnas.0903001106

Millucci, L., Ghezzi, L., Bernardini, G., and Santucci, A. (2010). Conformations and biological activities of amyloid beta peptide 25-35. *Curr. Protein Pept. Sci.* 11, 54–67. doi: 10.2174/138920310790274626

Millucci, L., Raggiaschi, R., Franceschini, D., Terstappen, G., and Santucci, A. (2009). Rapid aggregation and assembly in aqueous solution of A beta (25-35) peptide. *J. Biosci.* 34, 293–303. doi: 10.1007/s12038-009-0033-3

Naldi, M., Fiori, J., Pistolozzi, M., Drake, A. F., Bertucci, C., Wu, R., et al. (2012). Amyloid β-peptide 25-35 self-assembly and its inhibition: a model undecapeptide system to gain atomistic and secondary structure details of the Alzheimer's disease process and treatment. *ACS Chem. Neurosci.* 3, 952–962. doi: 10.1021/cn3000982

Nerli, E., Roggero, O. M., Baj, G., and Tongiorgi, E. (2020). In vitro modeling of dendritic atrophy in Rett syndrome: determinants for phenotypic drug screening in neurodevelopmental disorders. *Sci Rep.* 10:2491.

Ookubo, M., Kanai, H., Aoki, H., and Yamada, N. (2013). Antidepressants and mood stabilizers effects on histone deacetylase expression in C57BL/6 mice: brain region specific changes. *J. Psychiatr. Res.* 47, 1204–1214. doi: 10.1016/j.jpsychires.2013.05.028

Overk, C. R., and Masliah, E. (2014). Pathogenesis of synaptic degeneration in Alzheimer's disease and lewy body disease. *Biochem. Pharmacol.* 88, 508–516. doi: 10.1016/j.bcp.2014.01.015

Ownby, R. L., Crocco, E., Acevedo, A., John, V., and Loewenstein, D. (2006). Depression and risk for Alzheimer disease: systematic review, meta-analysis, and metaregression analysis. *Arch. Gen. Psychiatry* 63, 530–538. doi: 10.1001/archpsyc.63.5.530

Pierce, J. P., Mayer, T., and McCarthy, J. B. (2001). Evidence for a satellite secretory pathway in neuronal dendritic spines. *Curr. Biol.* 11, 351–355. doi: 10.1016/s0960-9822(01)00077-x

Plá, V., Barranco, N., Pozas, E., and Aguado, F. (2017). Amyloid-β impairs vesicular secretion in neuronal and astrocyte peptidergic transmission. *Front. Mol. Neurosci.* 10:202. doi: 10.3389/fnmol.2017.00202

Poon, W. W., Blurton-Jones, M., Tu, C. H., Feinberg, L. M., Chabrier, M. A., Harris, J. W., et al. (2011). β-Amyloid impairs axonal BDNF retrograde trafficking. *Neurobiol. Aging* 32, 821–833. doi: 10.1016/j.neurobiolaging.2009.05.012

Prydz, K., Dick, G., and Tveit, H. (2008). How many ways through the Golgi maze? *Traffic* 9, 299–304. doi: 10.1111/j.1600-0854.2007.00690.x

Raji, M. A., and Brady, S. R. (2001). Mirtazapine for treatment of depression and comorbidities in Alzheimer disease. *Ann. Pharmacother.* 35, 1024–1027. doi: 10.1345/aph.10371

Ramírez, O. A., and Couve, A. (2011). The endoplasmic reticulum and protein trafficking in dendrites and axons. *Trends Cell Biol.* 21, 219–227. doi: 10.1016/j.tcb.2010.12.003

Resende, R., Pereira, C., Agostinho, P., Vieira, A. P., Malva, J. O., and Oliveira, C. R. (2007). Susceptibility of hippocampal neurons to Abeta peptide toxicity is associated with perturbation of Ca2+ homeostasis. *Brain Res.* 1143, 11–21. doi: 10.1016/j.brainres.2007.01.071

Rogóz, Z., Skuza, G., and Legutko, B. (2005). Repeated treatment with mirtazepine induces brain-derived neurotrophic factor gene expression in rats. *J. Physiol. Pharmacol. Off J. Pol. Physiol. Soc.* 56, 661–671.

Rojas, P. S., Neira, D., Muñoz, M., Lavandero, S., and Fiedler, J. L. (2014). Serotonin (5-HT) regulates neurite outgrowth through 5-HT1A and 5-HT7 receptors in cultured hippocampal neurons. *J. Neurosci. Res.* 92, 1000–1009. doi: 10.1002/jnr.23390

Seifert, B., Eckenstaler, R., Rönicke, R., Leschik, J., Lutz, B., Reymann, K., et al. (2016). Amyloid-beta induced changes in vesicular transport of BDNF in hippocampal neurons. *Neural. Plast.* 2016:4145708.

Selkoe, D. J., and Hardy, J. (2016). The amyloid hypothesis of Alzheimer's disease at 25 years. *EMBO Mol. Med.* 8, 595–608.

Serrano-Pozo, A., Frosch, M. P., Masliah, E., and Hyman, B. T. (2011). Neuropathological alterations in Alzheimer disease. *Cold Spring Harb. Perspect Med.* 1:a006189. doi: 10.1101/cshperspect.a006189

Sun, X., Mwamburi, D. M., Bungay, K., Prasad, J., Yee, J., Lin, Y. M., et al. (2007). Depression, antidepressants, and plasma amyloid beta (Beta) peptides in those elderly who do not have cardiovascular disease. *Biol. Psychiatry* 62, 1413–1417. doi: 10.1016/j.biopsych.2007.01.003

Tammineni, P., Jeong, Y. Y., Feng, T., Aikal, D., and Cai, Q. (2017). Impaired axonal retrograde trafficking of the retromer complex augments lysosomal deficits in Alzheimer's disease neurons. *Hum. Mol. Genet.* 26, 4352–4366. doi: 10.1093/hmg/ddx321

Tan, E. Y. L., Köhler, S., Hamel, R. E. G., Muñoz-Sánchez, J. L., Verhey, F. R. J., and Ramakers, I. H. G. B. (2019). Depressive symptoms in mild cognitive impairment and the risk of dementia: a systematic review and comparative meta-analysis of clinical and community-based studies. *J. Alzheimers Dis.* 67, 1319–1329. doi: 10.3233/JAD-180513

Tang, B. L. (2008). Emerging aspects of membrane traffic in neuronal dendrite growth. *Biochim. Biophys. Acta* 1783, 169–176. doi: 10.1016/j.bbamcr.2007.11.011

Toh, W. H., and Gleeson, P. A. (2016). Dysregulation of intracellular trafficking and endosomal sorting in Alzheimer's disease: controversies and unanswered questions. *Biochem. J.* 473, 1977–1993. doi: 10.1042/bcj20160147

Tongiorgi, E. (2008). Activity-dependent expression of brain-derived neurotrophic factor in dendrites: facts and open questions. *Neurosci. Res.* 61, 335–346. doi: 10.1016/j.neures.2008.04.013

Urrestarazu, E., and Iriarte, J. (2016). Clinical management of sleep disturbances in Alzheimer's disease: current and emerging strategies. *Nat. Sci. Sleep* 8, 21–33. doi: 10.2147/NSS.S76706

van Beuningen, S. F., and Hoogenraad, C. C. (2016). Neuronal polarity: remodeling microtubule organization. *Curr. Opin. Neurobiol.* 39, 1–7. doi: 10.1016/j.conb.2016.02.003

Vicario-Orri, E., Opazo, C. M., and Muñoz, F. J. (2015). The pathophysiology of axonal transport in Alzheimer's disease. *J. Alzheimers Dis.* 43, 1097–1113. doi: 10.3233/jad-141080

Ye, B., Zhang, Y., Song, W., Younger, S. H., Jan, L. Y., and Jan, Y. N. (2007). Growing dendrites and axons differ in their reliance on the secretory pathway. *Cell* 130, 717–729. doi: 10.1016/j.cell.2007.06.032

Conflict of Interest: The authors declare that the research was conducted in the absence of any commercial or financial relationships that could be construed as a potential conflict of interest.

frontiers in Molecular Neuroscience

PERSPECTIVE
published: 15 June 2021
doi: 10.3389/fnmol.2021.684977

Conceptual and Methodological Pitfalls in Experimental Studies: An Overview, and the Case of Alzheimer's Disease

Daniela Puzzo[1,2]* *and Fiorenzo Conti*[3,4]

[1] Department Biomedical and Biotechnological Sciences, University of Catania, Catania, Italy, [2] Oasi Research Institute-IRCCS, Troina, Italy, [3] Department of Experimental and Clinical Medicine, Section of Neuroscience and Cell Biology, Università Politecnica delle Marche, Ancona, Italy, [4] Center for Neurobiology of Aging, INRCA IRCCS, Ancona, Italy

The main goal of scientific research is to uncover new knowledge to understand reality. In the field of life sciences, the aim of translational research—to transfer results "from bench to bedside"—has to contend with the problem that the knowledge acquired at the "bench" is often not reproducible at the "bedside," raising the question whether scientific discoveries truly mirror the real world. As a result, researchers constantly struggle to overcome the dichotomy between methodological problems and expectations, as funding agencies and industries demand expandable and quick results whereas patients, who are uninterested in the epistemological dispute, only ask for an effective cure. Despite the numerous attempts made to address reproducibility and reliability issues, some essential pitfalls of scientific investigations are often overlooked. Here, we discuss some limitations of the conventional scientific method and how researcher cognitive bias and conceptual errors have the potential to steer an experimental study away from the search for the *vera causa* of a phenomenon. As an example, we focus on Alzheimer's disease research and on some problems that may have undermined most of the clinical trials conducted to investigate it.

Keywords: scientific method, cognitive bias, *vera causa*, translational research, Alzheimer's disease

OPEN ACCESS

Edited by:
Davide Tampellini, Institut National de la Santé et de la Recherche Médicale (INSERM), France

Reviewed by:
Marco Venturin, University of Milan, Italy
Luis Quintino, Lund University, Sweden

***Correspondence:**
Daniela Puzzo
danypuzzo@yahoo.it

Specialty section:
This article was submitted to Brain Disease Mechanisms, a section of the journal Frontiers in Molecular Neuroscience

Received: *24 March 2021*
Accepted: *21 May 2021*
Published: *15 June 2021*

Citation:
Puzzo D and Conti F (2021) Conceptual and Methodological Pitfalls in Experimental Studies: An Overview, and the Case of Alzheimer's Disease. Front. Mol. Neurosci. 14:684977. doi: 10.3389/fnmol.2021.684977

INTRODUCTION

Translational or "bench to bedside" research aims to transfer knowledge from basic science to clinical practice. As theorized by Claude Bernard, the founder of Experimental Medicine (Conti, 2001, 2002), the process starts with understanding how a physiological system works and tries to uncover the pathophysiology of a disease in order to diagnose, prevent and cure it. The drug discovery process is guided by preclinical studies, where the efficacy and safety of a compound (or device) are tested in animal models before being tried in humans. However, the whole process depends on the validity of the experimental approach itself, since besides the objective risks and intrinsic difficulties of the bench to bedside transition (Seyhan, 2019), methodological and, more frequently, interpretive mistakes may lead to falls in crossing the "valley of death" (Llovera and Liesz, 2016).

Assuming researcher's *bona fide* and excluding the pressure from big pharma and funding agencies, data manipulation for personal interests, and psychiatric diseases, a number of problems

still have the potential to skew research outcomes in any field of science. However, in translational research the challenge and pressure are felt especially keenly, considering the expectations of clinical application and their public health implications. To prevent the failure of the translation process, several studies have examined the main confounding factors that might invalidate an experimental study (see **Table 1**), focusing on result reproducibility and reliability (e.g., National Academies of Sciences, Engineering, and Medicine (NASEM)., 2019). However, there are few works discussing how to avoid methodological errors due to researcher cognitive biases (Kaptchuk, 2003) and general conceptual errors. Moreover, in life sciences the issue of the scientific method is often dismissed, based on the widespread belief of the existence of only one, undoubtedly correct method (Wagensberg, 2014).

Here, we briefly discuss some of these methodological errors, hoping that this overview may be useful, especially to young researchers approaching the world of science and research.

RESEARCHER COGNITIVE BIASES MIRROR THE FALLIBILITY OF THE HUMAN BRAIN

The premise that best explains how cognitive biases may undermine the interpretation of a phenomenon is the fallibility of the human brain. Indeed, we are cognitively predisposed to interpret facts based on a number of fallible systems, whose aim is probably to facilitate the retention of information and to strengthen the force driving our actions. Accordingly we tend to draw conclusions or to find a quick solution to a given problem even though we lack all the information that is required to do so. Although this attitude is clearly advantageous in some life situations, it is a limiting factor when novel research findings confute our beliefs. *Confirmation bias* (Nickerson, 1998), i.e., our tendency to seek and accept information that confirms our prior opinions, leads us to unconsciously select data supporting our views and to ignore opposing evidence. Furthermore, when confronted with ambiguous or opposite evidence, we tend to reinterpret it, to make it consistent with our beliefs and lend more weight to it. The need for confirmation (Peters, 2020) is closely related to pleasure and satisfaction. Even though the degree of confirmation need is strongly related to self-confidence, motivation, and personality structure, the general tendency to prefer positive to negative outcomes (e.g., the Pollyanna Principle, Matlin and Stang, 1979) usually prevails.

Confirmation bias is particularly relevant in scientific research, as demonstrated throughout history by scientists' resistance to discoveries that challenge a current paradigm.

The first strategy that can help combat this tendency is awareness, which is a key prerequisite for any endeavor that needs impartial observation; impartial, maximally objective observation is a central tenet of scientific research. When conceiving an experimental design, neutrality should inform the entire process, from the generation of the hypothesis to the drawing of conclusions, which may either support or reject the hypothesis. A common pitfall is being unaware of snags

TABLE 1 | Common errors made in the different phases of an experimental study.

Phases	What to check	Common errors
Before the study	Previous literature	• Poor knowledge of previous studies • Biased interpretation of the existing literature, i.e., exclusive focus on literature supporting our hypothesis, uncritical revision, quality judgment of previous studies exclusively based on journal impact factor
	Choice of the model	• Model not adequate for the purpose of the study • Intrinsic limit of the chosen model
	Experimental design	• Experimental design unclear • Experimental design non-consequential • Experimental design not suitable to achieve the proposed objectives
	Feasibility	• Discrepancy between what you want and what you can do in terms of time, technical, financial and human resources
During the study	Sample size	• Minimum sample size to obtain statistically significant results not calculated • Unclear difference between a pilot study and a study to test a hypothesis • Wrong interpretation of "reduction" in animal research
	Inclusion and exclusion criteria	• Unclear definition of inclusion and exclusion criteria • Overlapping inclusion and exclusion criteria • Selection of inclusion criteria not related to the purpose of the study
	Randomization	• Randomization criteria not established before to start the experiments • Ambiguous randomization criteria • Randomization based on incorrect baseline information or ineligible samples
	Blinding of investigators	• No one blind in the trial • False belief that preclinical studies cannot be blind • Poor standardization when blinding is not possible
	Positive and negative controls	• Experimental plan lacks positive and negative controls, i.e., in preclinical research: to not include in the study untreated/treated healthy animals, untreated models of disease, shame-operated animals, etc.
	Method reliability	• Unreliable methods • Method not adequate to the purpose of the study • Incorrect application of the method • Modification of an existing method without sufficient evidence of its efficacy and reliability
	Environmental conditions	• Different environmental conditions used throughout the experiments • Poor attention toward environmental factors affecting the experiments, i.e., in animal studies: housing, diet, circadian rhythms, temperature, humidity, noise, etc.
	Quality of materials	• Poor quality or expired materials • Cheap but nor certified chemicals or equipment • Low quality samples
	Intrinsic limitations of techniques	• Poor knowledge of the technique, its use and limitation • Confusion between quantitative/qualitative techniques
	Errors in measurements	• Difficulties to detect random or systematic errors, depending on the measurement and the instrument precision and calibration • Undefined conditions that might affect the measurement • Artifacts

(Continued)

TABLE 1 | Continued

Phases	What to check	Common errors
	Evaluation of outliers	• To disregard how outliers might influence or even reverse the results • Inappropriate statistical test if outliers are maintained • Unfixed standard methods to remove outliers
	Replication	• Results cannot be replicated in different samples (control for errors, artifacts, environmental factors, conceptual and practical reliability of previous workplan) • Results cannot be replicated in different models (control for model intrinsic differences, adequacy of the method) • Results cannot be replicated in different labs (control for sampling errors, differences in materials, instruments, environmental conditions, procedures, fraud attempts) • Intrinsic variability of responses in living systems, the differences among populations, the low reproducibility of some aspects are not taken into account
	Operators	• Insufficient operator expertise • Inter-operator variability • Operators not blind
	Variables	• Unclear difference between dependent, independent, extraneous and controlled variables • Chosen variables not appropriate to answer the proposed question
After the study	Results interpretation	• Wrong assumptions inferred from statistical analyses • Systematic and random errors ignored • Negative or unexpected results discarded
	Conclusions	• Conclusions do not answer the study question(s) • Conclusions diverge from existing literature without sufficient explanation • Results are not justified and adequately discussed • Differences between prediction and observation not assessed • Biased evaluation of strengths and weaknesses of the study

and problems, which results in the perpetuation of familiar schemes; indeed, even cutting edge technologies cannot rescue an experiment from inadequate underlying reasoning. Assuming *a priori* the goodness of the expected results and rejecting incompatible or negative data are grave methodological mistakes, since a hypothesis is inherently a proposed explanation of reality, not reality itself. This behavior, which has been called *hypothesis myopia* (Nuzzo, 2015), focuses the attention on data supporting the hypothesis through a variety of mental stratagems.

The second strategy that can help us resist our affective loyalty to a notion is to doubt our own stance, avoiding "denial attitude," which undermines open-mindedness and prevents us from considering different viewpoints. Reasonable doubt is a pillar of scientific research, whose goal is to acquire knowledge by questioning nature through a continuous testing/proof system (Bernard, 1865). Perseverance should not be confused with *belief perseverance*, whose only consequence is to strengthen our own beliefs even in the face of evidence pointing in the opposite direction. We are prey to this phenomenon, which is sometimes called a backfire or boomerang effect (Howard, 2019), when we perceive a threat to our freedom of thought or action. The adverse consequences of such irrational attitude (e.g., the anti-vax movement, COVID-19 denialism) are there for all to see. Rather, facts that clearly contradict our assumptions should carefully be sifted, to allow us to form an unprejudiced view supported by the analysis of the events that have led to the original conclusion.

LIMITATIONS OF CONVENTIONAL METHODOLOGY IN THE SEARCH FOR THE *VERA CAUSA*

So much has been written about the scientific method that discussing here its rules, interpretation and limitations would involve inappropriate generalizations, besides being beyond the scope of this overview. However, at least for educational purposes, we feel that it may be useful to summarize some of its aspects, bearing in mind that the debate is still open and that novel variables are continuously being introduced by the philosophers of science (Novikov and Novikov, 2013; Grüne-Yanoff, 2014; Stanford Encyclopedia of Philosophy (SEP)., 2015).

In the current scientific context, "conventional methods" have replaced the authentic search for knowledge and most scientists, us included, have become accustomed to employ established methods accepted by the scientific, or in our case, the life science community. As a consequence, we use and teach this scientific method as "the sole" scientific method, advocating its uniqueness and validity and choosing to ignore that other disciplines (e.g., astrophysics, economics) might employ different approaches. In this way we probably disregard the complexity of the epistemological debate. An example of this recent attitude is the "observe-hypothesize-test" system, which most science textbooks present as "the" scientific method (Blachowicz, 2009) without specifying that such step-by-step algorithm is merely a general rule on how to conduct all investigations, as stressed by the philosopher and psychologist John Dewey in *How We Think* (Dewey, 1933). Consequently, we base our work on a rigid proposition that leaves little room for interpretation or flexibility and favors sectorial observation as long as it is verifiable, even outside its "real" context. Is this what the scientific method really prescribes?

As noted above, the observation and organization of empirical facts is at the heart of our knowledge of nature. Despite the variety of explanations provided by philosophers from medieval to modern times, the differences between inductive/deductive or synthesis/analysis reasoning are still applicable. The relevant flow of thought can be summarized as a bottom-up (observation→hypothesis→theory) or a top-down (theory→hypothesis→observation) approach. These apparently opposite methods are not necessarily exclusive, as demonstrated by Galileo Galilei (1564–1642) and subsequently clarified by the four rules of reasoning of Isaac Newton (1642–1726), who, however, overemphasized induction. Indeed, according to the fourth rule (Newton, 1726) "In experimental philosophy, propositions gathered from phenomena by induction should be considered either exactly or very nearly true not withstanding

any contrary hypotheses, until yet other phenomena make such propositions either more exact or liable to exception," paving the way for the modern debate between inductivism and hypothetico-deductivism (Krajewski, 1977). The latter has become the most common approach, especially in life sciences, as also demonstrated by the IMRAD structure of scientific publications: Introduction (the background generating the hypothesis), Methods (how the hypothesis will be demonstrated), Results (data collection), Analysis and Discussion (conclusions). Interestingly, such linear presentation, which we automatically adopt to describe our research work, rarely corresponds to the process that has actually generated our results (e.g., Grmek, 1973; Schickore, 2008), both in terms of the temporal execution of the experiments and of the conception of the experimental plan. Don't we often reorganize our data to meet the journal's or the reviewers' expectations? Thus, manuscripts are written according to the hypothetico-deductive method, even though we may have applied the inductive approach.

However, hypothesis-driven research involves at least two disadvantages. First of all, it prevents *ex novo* exploration of a phenomenon when there are no previous studies of a topic and a hypothesis cannot be clearly stated. The problem is hardly new. The physiologist Claude Bernard (1813–1878) was aware that researchers often encounter matters about which no "fact" is known beforehand. In such cases, an "exploratory experiment" (*expérience pour voir*) is conducted and becomes the starting point for a hypothesis, which is then subjected to experimental verification. Notably, an exploratory experiment led to his celebrated discovery of the effects of curare (Bernard, 1857, 1865). In more recent times, David Hubel and Torsten Wiesel wrote: "Meanwhile we had begun a completely different set of experiments, ones in which specific questions were asked, as opposed to exploration. It is not that we felt that the kind of science that explores, in the manner of Columbus sailing west, or Galileo looking at Jupiter's moons, or Darwin visiting the Galapagos (often pejoratively referred to as 'fishing trips'), is in any way inferior to the science we learn about in high school, with its laws, measurements, hypotheses, and so on. Exploration had dominated our work up to then, since we had certainly had no 'hypotheses' as we set about to explore the visual cortex. Neither were we in any way "quantitative" in our approach. The term 'anecdotal,' a favorite expression of disdain on NIH pink sheets, probably best describes the nature of most of our work, but the deprivation studies were slightly different in that we did ask somewhat more specific questions, without, to be sure, having anything that a modern study section would call a hypothesis" (Hubel and Wiesel, 1998). For the results of their exploratory studies, which today in all likelihood would neither be funded nor pass the review filter, Hubel and Wiesel were awarded the 1981 Nobel Prize for Physiology or Medicine.

Another problem with hypothesis-driven research is that it may prevent questioning the starting hypothesis even if some "facts" clearly contradict it. In his seminal work, *An Introduction to the Study of Experimental Medicine* (1865), Claude Bernard, who was the first researcher to apply the scientific method to medicine, stressed the importance of "facts," which allow questioning a pre-existing theory if they have been obtained through rigorous experiments. "When we meet a fact which contradicts a prevailing theory, we must accept the fact and abandon the theory, even when the theory is supported by great names and generally accepted." Only this continuous induction-deduction or facts-theory interaction can guide experimental science. Interestingly, Bernard was already aware that "proof that a given condition always precedes or accompanies a phenomenon does not warrant concluding with certainty that a given condition is the immediate cause of that phenomenon." This is the *vera causa* principle of Newtonian philosophy (Stanford Encyclopedia of Philosophy (SEP)., 2015; Scholl, 2020), i.e., the requirement for a cause-effect relationship to be proved by direct evidence before it can be accepted. Hypotheses are not to be rejected, but tested by the criterion of counterproof. If disproved, the hypothesis should be discarded or modified; if proved, the experimenter should still doubt. Some authors who consider this approach limiting, especially where theoretical science is concerned, have conceived consequentialist reasoning (see for example Popper's Falsificationism theory—Popper, 1963). However, the demonstration that a relationship exists and that it is causally competent and responsible for the effect is still a tenet of experimental biology.

Demonstration of the *vera causa* requires the adoption of appropriate methodological standards to obtain reliable experimental data that provide a credible representation of reality and are able to be replicated. The concept of data robustness has been introduced because the fact that a result is replicable does not entail that it is also reliable, and indicates a result that does not vary irrespective of the experimental method used. Hence, a robust conclusion requires a measure of variability through a certain number of independent repetitions conducted under consistent, controlled experimental conditions. "Scientific control" enables the researcher to isolate the effect of the independent variable: minimizing the influence of other variables reduces experimental errors and experimenter bias.

An outstanding example of this approach is found in Bernard's studies of recurrent sensitivity. Magendie had observed that, in dogs, pinching or cutting the ventral roots induced pain-like responses and that resection of the appropriate dorsal root abolished them, a mechanism he called "recurrent sensitivity." The topic became popular and was intensely debated (Conti, 2002). Bernard performed numerous experiments on recurrent sensitivity and resolved contradictions by refining the experimental conditions required for its expression, e.g., time interval between surgery and observation, time since the last meal, general conditions of the animal, species, amount of blood loss during surgery, and degree of opening of the vertebral canal (Bernard, 1858).

Nowadays, randomization, blinding and appropriate controls are the fundamentals of the scientific method, although they are not invariably applied. For example, randomization (assignment to a treatment group by a chance process, to minimize differences among groups) and blinding (the experimenter and/or the patient ignore the group to which the patient has been assigned) are mandatory in clinical research, but are not emphasized in basic or translational studies (Karanicolas et al., 2010). Although a double-blind study of cells or animals seems to make little

sense, since both are by definition "blind to treatment," operator blinding during the entire experimental process, from execution to data analysis, would still avoid several biases (see the previous paragraph), maximizing result validity while also preserving that feeling of suspense and curiosity that should drive all researchers.

More complicated is the use and selection of appropriate controls, given their multifaceted nature. As noted above, controls aim to keep variables as constant as possible, to enable isolation of the cause-effect relationship. In an experimental study, this means either using the same experimental conditions (temperature, humidity, oxygenation, chemical solutions, etc.) throughout the replications or introducing control groups that are exposed to the same generic variables with the exception of the independent variable, i.e., the proposed causal factor. A difference in the results obtained in the experimental group compared to controls is highly likely to identify the cause-effect relationship. Negative (not exposed to the experimental treatment) and positive (exposed to a treatment known to exert the effect) controls are also mandatory. Yet, in numerous studies they are either omitted or inappropriate (e.g., lack of comparison between vehicle, i.e., placebo, and drug treatment or between a healthy and a diseased model). For instance, some studies report that a certain treatment rescues a given deficit even if the animal model used to mimic the disease does not present the deficit being investigated. Although model choice is critical in any field of science, it is especially important in preclinical studies using animal models, due to a number of intrinsic variables: (i) the variability of complex systems; (ii) differences between species (e.g., mouse vs. human); (iii) the clear definition of the aspects of the diseases being modeled; (iv) manipulations that result in disease caused by "unreal" causes. Failure to consider these aspects, especially that a model is by definition a representation of reality, not reality itself, may invalidate our experiments or, worse, suggest that the scientific approach has been unsuccessful, whereas it was our interpretation that was to blame.

THE AMYLOID-BETA HYPOTHESIS: AN EXAMPLE OF FALLACIOUS INTERPRETATION

Cognitive biases and methodological errors affect several fields of biomedical research, but lately a great concern has been rising over the failure of translational research to find a cure for Alzheimer's disease (AD), the most common form of dementia arising in mid-late life. AD affects the ability to remember, understand and interact with the environment, slowly eroding the patient's identity and independence in daily life activities. Given that around 50 million people are affected by dementia worldwide and that their number is expected to climb to 74.7 million by 2030 and 131.5 million by 2050 (Giri et al., 2016), AD is a severe social and economic problem, especially in developed countries, where population aging is most advanced. However, despite significant scientific progress, intense basic and preclinical research efforts have failed to deliver applications for clinical practice. According to a growing number of researchers, we have lost our way by testing drugs based on a rationale that is far from the *vera causa*. In particular, the amyloid cascade hypothesis, which has inspired most of the research work conducted to date, is now being set aside after none of the clinical trials aimed at reducing amyloid beta (Aβ) have succeeded in preventing or slowing down the disease. Yet, thousands of preclinical studies have documented a role for it in AD pathophysiology (Sauer, 2014; de la Torre, 2017; Kepp, 2017; Gulisano et al., 2018; Makin, 2018). Where did we go wrong?

Observation is a pillar of scientific research, whether using the inductive or the hypothetico-deductive method. In the case of AD, the amyloid cascade hypothesis appeared to satisfy both the bottom-up (observation→hypothesis) and the top-down (hypothesis→observation) approach, providing a continuum that has reinforced the observation→hypothesis→observation loop. The earliest "observation," i.e., the identification of senile plaques with/without neurofibrillary tangles by Alois Alzheimer (Hippius and Neundörfer, 2003), was strengthened by post-mortem studies. At least two additional "facts"—the report that senile plaques are formed by Aβ deposits (Glenner and Wong, 1984) and the discovery of rare hereditary forms of early onset Familial Alzheimer's Disease (FAD), where genetic mutations of amyloid precursor protein and presenilins lead to increased Aβ production (Levy et al., 1990; Hardy et al., 1998)—made Aβ the key factor in AD. These reports gave rise to the amyloid cascade hypothesis (Hardy and Higgins, 1992), which has prompted a variety of studies aimed at confirming the noxious effect of Aβ on synaptic plasticity and memory as well as its increase and deposition in the AD brain. The obvious next step was to remove it from the brain to rescue memory and cure the disease. However, this "Occam's razor" strategy did not work.

TABLE 2 | Amyloid-beta hypothesis facts.

Overestimated facts	Underestimated facts
Senile plaques formed by Aβ deposits are found in AD brains	Senile plaques can be found in cognitively intact individuals
High Aβ concentrations disrupt synaptic plasticity and memory in preclinical models	Low Aβ concentrations improve synaptic plasticity and memory in preclinical models
Aβ triggers tau pathology	Aβ and tau may act independently
FAD is characterized by the same symptoms as AD	Different types of dementia present the symptoms of AD
FAD is caused by genetic mutations that lead to increased Aβ production	Sporadic AD is not due to genetic mutations directly leading to increased Aβ production
Animal models of FAD are used for AD preclinical research	Animal models of FAD do not mimic sporadic AD
Anti-Aβ drugs rescue the cognitive phenotype in FAD animal models	Anti-Aβ drugs do not work on humans with sporadic AD
The amyloid cascade hypothesis might explain AD etiology	AD is a multifactorial disorder characterized, among other factors, by mitochondrial dysfunction, glucose metabolism, ApoEe4 polymorphism, cholinergic dysfunction and vascular problems and influenced by immunity-related and environmental factors.

Given the problems hampering translational research, this failure is not really surprising. What is remarkable is that the Aβ notion thrived for decades (Cline et al., 2018) without changes in its rationale (since Aβ increases, it must be removed) and that pharmaceutical companies, funding agencies and health organizations continued to give strong support to anti-Aβ approaches. The neuroscience community is now split into two main camps. Aβ supporters argue that success is a matter of "timing" (i.e., treatment should start earlier) or "personalized therapy" (i.e., treatment should be provided to Aβ-responders). Their stance, which cannot be rejected *a priori*, may also be ascribed to researchers' "cognitive bias." The Aβ critics call for aiming at different targets, such as tau protein, whose increase, hyperphosphorylation, and deposition in neurofibrillary tangles is the other hallmark of the disease. But the underlying reasoning is the same: tau is increased in the AD brain→its levels need to be lowered; preclinical studies support the notion→anti-tau strategies must be translated into clinical practice. Altogether, the orchestra is playing the same score even if the second violin has become the first.

Notably, there is a third group of researchers, smaller and probably inadequately supported, who would like to understand where we lost our way, because if we look at the literature with a neutral attitude it is clear that some observations have been emphasized to buttress the amyloid cascade hypothesis whereas some equally important data that contrast with the hypothesis have been underestimated (**Table 2**). Please see the following reviews for a detailed description of Aβ facts and studies summarized in **Table 2**; Reitz, 2012; Herrup, 2015; Gulisano et al., 2018.

To discuss here why decades of research have supported (and continue supporting) this hypothesis is outside the scope of our work, but it would be interesting to answer this question: were previous experiments aimed at unveiling the *vera causa*? Because it appears that we have relied on the "inference to the best explanation" by selecting the simplest hypothesis; yet its simplicity does not make it true. The key question that remains unanswered is: why do Aβ and tau increase in the AD brain? The question is quite relevant, since in physiological conditions both proteins play a major role, contributing to neuronal function and structure (Puzzo et al., 2015; Wang and Mandelkow, 2015; Gulisano et al., 2018, 2019), therefore their pharmacological inhibition is potentially unsafe.

CONCLUSION

The debate on the scientific method and its inherent limitations is still animated and is expected to continue as knowledge and technology advance. In any case, we should never forget that "What we observe is not nature in itself but nature exposed to our method of questioning" (Heisenberg, 1958). Therefore, the intrinsic limitation of the method, the significance of model and control, and the differences among methodology, methods and techniques need to be pondered each time we design an experimental plan. As researchers, we should continuously strive to balance rigor and creativity, neutrality and sincere curiosity, and the desire to obtain a result and the need to learn the truth, or at least its reflection.

AUTHOR CONTRIBUTIONS

DP and FC contributed to conception of the manuscript. DP wrote the first draft of the manuscript. FC wrote sections of the manuscript. Both authors contributed to manuscript revision, read, and approved the submitted version.

REFERENCES

Bernard, C. (1857). *Leçons sur les effets des substances toxiques et medicamenteuses*. Paris: J.-B. Baillière et Fils.

Bernard, C. (1858). *Leçons sur la physiologie et la pathologie du système nerveux*. Paris: J.-B. Baillière et Fils.

Bernard, C. (1865). *Introduction à l'Etude de la Médecine Expérimentale*. Paris: J.-B. Baillière et Fils.

Blachowicz, J. (2009). How Science Textbooks Treat Scientific Method: a Philosopher's Perspective. *Br. J. Phil. Sci.* 60, 303–344. doi: 10.1093/bjps/axp011

Cline, E. N., Bicca, M. A., Viola, K. L., and Klein, W. L. (2018). The Amyloid-β Oligomer Hypothesis: beginning of the Third Decade. *J. Alzheimers Dis.* 64, S567–S610.

Conti, F. (2001). Claude Bernard: primer of the second biomedical revolution. *Nat. Rev. Mol. Cell Biol.* 2, 703–710.

Conti, F. (2002). Claude Bernard's Des Fonctions du Cerveau: an ante litteram manifesto of the neurosciences? *Nat. Rev. Neurosci.* 3, 979–985. doi: 10.1038/nrn985

de la Torre, J. (2017). *What is Wrong With Alzheimer's Disease Clinical Research?*. Amsterdam: IOS Press.

Dewey, J. (1933). *How We Think: A Restatement of the Relation of Reflective Thinking to the Educative Process*. Boston: D.C. Heath & Co Publishers.

Giri, M., Zhang, M., and Lü, Y. (2016). Genes associated with Alzheimer's disease: an overview and current status. *Clin. Interv. Aging* 11, 665–681. doi: 10.2147/cia.s105769

Glenner, G. G., and Wong, C. W. (1984). Alzheimer's disease: initial report of the purification and characterization of a novel cerebrovascular amyloid protein. *Biochem. Biophys. Res. Commun.* 120, 885–890. doi: 10.1016/s0006-291x(84)80190-4

Grmek, M. (1973). *Raisonnement expérimental et recherches toxicologiques chez Claude Bernard*. Genève: Librairie Droz.

Grüne-Yanoff, T. (2014). Teaching philosophy of science to scientists: why, what and how. *Euro. J. Phil. Sci.* 4, 115–134. doi: 10.1007/s13194-013-0078-x

Gulisano, W., Maugeri, D., Baltrons, M. A., Fà, M., Amato, A., Palmeri, A., et al. (2018). Role of Amyloid-β and Tau Proteins in Alzheimer's Disease: confuting the Amyloid Cascade. *J. Alzheimers Dis.* 64, S611–S631.

Gulisano, W., Melone, M., Ripoli, C., Tropea, M. R., Li Puma, D. D., Giunta, S., et al. (2019). Neuromodulatory Action of Picomolar Extracellular Aβ42 Oligomers on Presynaptic and Postsynaptic Mechanisms Underlying Synaptic Function and Memory. *J. Neurosci.* 39, 5986–6000. doi: 10.1523/jneurosci.0163-19.2019

Hardy, J., Duff, K., Hardy, K. G., Perez-Tur, J., and Hutton, M. (1998). Genetic dissection of Alzheimer's disease and related dementias: amyloid and its relationship to tau. *Nat. Neurosci.* 1, 355–358. doi: 10.1038/1565

Hardy, J., and Higgins, G. (1992). Alzheimer's disease: the amyloid cascade hypothesis. *Science* 256, 184–185.

Heisenberg, W. (1958). *Physics and Philosophy: The Revolution in Modern Science*. New York: HarperCollins Publishing company.

Herrup, K. (2015). The case for rejecting the amyloid cascade hypothesis. *Nat. Neurosci.* 18, 794–799. doi: 10.1038/nn.4017

Hippius, H., and Neundoörfer, G. (2003). The discovery of Alzheimer's disease. *Dialogues Clin. Neurosci.* 5, 101–108.
Howard, J. (2019). *Confirmation Bias, Motivated Cognition, the Backfire Effect. In: Cognitive Errors and Diagnostic Mistakes*. Cham: Springer.
Hubel, D. H., and Wiesel, T. N. (1998). Early exploration of the visual cortex. *Neuron* 20, 401–412. doi: 10.1016/s0896-6273(00)80984-8
Kaptchuk, T. J. (2003). Effect of interpretive bias on research evidence. *BMJ* 326, 1453–1455. doi: 10.1136/bmj.326.7404.1453
Karanicolas, P. J., Farrokhyar, F., and Bhandari, M. (2010). Blinding: who, what, when, why, how? *Can. J. Surg.* 53, 345–348.
Kepp, K. P. (2017). Ten challenges of the amyloid hypothesis of Alzheimer's disease. *J. Alzheimers Dis.* 55, 447–457. doi: 10.3233/jad-160550
Krajewski, W. (1977). *The Types of Methodological Empiricism. In: Correspondence Principle and Growth of Science*. Dordrecht: Springer.
Levy, E., Carman, M. D., Fernandez-Madrid, I. J., Power, M. D., Lieberburg, I., van Duinen, S. G., et al. (1990). Mutation of the Alzheimer's disease amyloid gene in hereditary cerebral hemorrhage, Dutch type. *Science* 248, 1124–1126. doi: 10.1126/science.2111584
Llovera, G., and Liesz, A. (2016). The next step in translational research: lessons learned from the first preclinical randomised controlled trial. *J. Neurochem.* 139, 271–279. doi: 10.1111/jnc.13516
Makin, S. (2018). The amyloid hypothesis on trial. *Nature* 559, S4–S7.
Matlin, M. W., and Stang, D. J. (1979). *The Pollyanna Principle: Selectivity in Language, Memory, and Thought*. Cambridge: Schenkman Pub. Company.
National Academies of Sciences, Engineering, and Medicine (NASEM). (2019). *Reproducibility and Replicability in Science*. Washington, DC: The National Academies Press.
Newton, I. (1726). *Philosophiae Naturalis Principia Mathematica*. Guil. & Joh. Innys, Regiae Societatis typographos. London.
Nickerson, R. S. (1998). Confirmation Bias: a Ubiquitous Phenomenon in Many Guises. *Rev. Gen. Psychol.* 2, 175–220. doi: 10.1037/1089-2680.2.2.175
Novikov, A., and Novikov, D. (2013). *Research Methodology*. London: CRC Press.
Nuzzo, R. (2015). Fooling ourselves. *Nature* 526, 182–185.
Peters, U. (2020). What Is the Function of Confirmation Bias? *Erkenntnis* 2020, 1–26.
Popper, K. (1963). *Conjectures and Refutations: The Growth of Scientific Knowledge*. London: Routledge.
Puzzo, D., Gulisano, W., Arancio, O., and Palmeri, A. (2015). The keystone of Alzheimer pathogenesis might be sought in Aβ physiology. *Neuroscience* 307, 26–36. 10.1016/j.neuroscience.2015.08.039
Reitz, C. (2012). Alzheimer's disease and the amyloid cas-cade hypothesis: a critical review. *Int. J. Alzheimers Dis.* 2012:369808.
Sauer, A. (2014). Has Alzheimer's research been wrong for 20 years? Available online at: https://www.alzheimers.net/2014-04-07-beta-amyloid-wrong-protein
Schickore, J. (2008). Doing science, writing science. *Philos. Sci.* 75, 323–343. doi: 10.1086/592951
Scholl, R. (2020). Unwarranted assumptions: claude Bernard and the growth of the vera causa standard. *Stud. Hist. Philos. Sci.* 82, 120–130. doi: 10.1016/j.shpsa.2019.12.005
Seyhan, A. A. (2019). Lost in translation: the valley of death across preclinical and clinical divide – identification of problems and overcoming obstacles. *Transl. Med. Commun.* 4:18.
Stanford Encyclopedia of Philosophy (SEP). (2015). *Scientific Method*. California: Stanford University.
Stanford Encyclopedia of Philosophy (SEP). (2017). *Experiment in Biology*. California: Stanford University.
Wagensberg, J. (2014). On the Existence and Uniqueness of the Scientific Method. *Biol. Theory* 9, 331–346. doi: 10.1007/s13752-014-0166-y
Wang, Y., and Mandelkow, E. (2015). Tau in physiology and pathology. *Nat. Rev. Neurosci.* 17, 22–35. doi: 10.1038/nrn.2015.1

Conflict of Interest: The authors declare that the research was conducted in the absence of any commercial or financial relationships that could be construed as a potential conflict of interest.

frontiers in Molecular Neuroscience

ORIGINAL RESEARCH
published: 09 July 2021
doi: 10.3389/fnmol.2021.660104

Age-Related Transcriptional Deregulation of Genes Coding Synaptic Proteins in Alzheimer's Disease Murine Model: Potential Neuroprotective Effect of Fingolimod

Henryk Jęśko[1†], Iga Wieczorek[2†], Przemysław Leonard Wencel[2], Magdalena Gąssowska-Dobrowolska[1], Walter J. Lukiw[3] and Robert Piotr Strosznajder[2]*

[1] Department of Cellular Signalling, Mossakowski Medical Research Institute, Polish Academy of Sciences, Warsaw, Poland, [2] Laboratory of Preclinical Research and Environmental Agents, Mossakowski Medical Research Institute, Polish Academy of Sciences, Warsaw, Poland, [3] LSU Neuroscience Center, Departments of Neurology and Ophthalmology, Louisiana State University School of Medicine, New Orleans, LA, United States

OPEN ACCESS

Edited by:
Daniela Puzzo, University of Catania, Italy

Reviewed by:
Carlos G. Dotti, Consejo Superior de Investigaciones Científicas (CSIC), Spain
Halina Car, Medical University of Bialystok, Poland

***Correspondence:**
Robert Piotr Strosznajder
rstrosznajder@imdik.pan.pl

[†] These authors have contributed equally to this work and share first authorship

Specialty section:
This article was submitted to Brain Disease Mechanisms, a section of the journal Frontiers in Molecular Neuroscience

Received: *28 January 2021*
Accepted: *31 May 2021*
Published: *09 July 2021*

Citation:
Jęśko H, Wieczorek I, Wencel PL, Gąssowska-Dobrowolska M, Lukiw WJ and Strosznajder RP (2021) Age-Related Transcriptional Deregulation of Genes Coding Synaptic Proteins in Alzheimer's Disease Murine Model: Potential Neuroprotective Effect of Fingolimod. Front. Mol. Neurosci. 14:660104. doi: 10.3389/fnmol.2021.660104

Alzheimer's disease (AD) induces time-dependent changes in sphingolipid metabolism, which may affect transcription regulation and neuronal phenotype. We, therefore, analyzed the influence of age, amyloid β precursor protein (AβPP), and the clinically approved, bioavailable sphingosine-1-phosphate receptor modulator fingolimod (FTY720) on the expression of synaptic proteins. RNA was isolated, reverse-transcribed, and subjected to real-time PCR. Expression of mutant (V717I) AβPP led to few changes at 3 months of age but reduced multiple mRNA coding for synaptic proteins in a 12-month-old mouse brain. Complexin 1 (*Cplx1*), SNAP25 (*Snap25*), syntaxin 1A (*Stx1a*), neurexin 1 (*Nrxn1*), neurofilament light (*Nefl*), and synaptotagmin 1 (*Syt1*) in the hippocampus, and VAMP1 (*Vamp1*) and neurexin 1 (*Nrxn1*) in the cortex were all significantly reduced in 12-month-old mice. Post mortem AD samples from the human hippocampus and cortex displayed lower expression of VAMP, synapsin, neurofilament light (NF-L) and synaptophysin. The potentially neuroprotective FTY720 reversed most AβPP-induced changes in gene expression (*Cplx1, Stx1a, Snap25*, and *Nrxn1*) in the 12-month-old hippocampus, which is thought to be most sensitive to early neurotoxic insults, but it only restored *Vamp1* in the cortex and had no influence in 3-month-old brains. Further study may reveal the potential usefulness of FTY720 in the modulation of deregulated neuronal phenotype in AD brains.

Keywords: aging, Alzheimer's disease, amyloid β, FTY720/fingolimod, neurodegeneration, sphingolipids, sphingosine-1-phosphate, synaptic proteins

INTRODUCTION

Aging creates a vulnerable background for the development of incurable neurodegenerative disorders, such as Alzheimer's disease (AD), which is characterized by the presence of extracellular senile plaques of amyloid β (Aβ) and neurofibrillary tangles of hyperphosphorylated tau protein. AD is the most common neurodegenerative disorder in the elderly. Its most frequent late-onset,

usually sporadic form, follows a long period of stealthy, relatively symptom-free development. Major neuronal populations are already lost when first easily recognizable behavioral outcomes appear, which dramatically hampers both therapy and research on its etiology. Although AD is relatively less frequently caused by inherited genetic mutations, this form of disease raises hopes for a better understanding of AD mechanisms. Aggregation of Aβ peptides is one of the hallmarks of all AD forms, and overexpression of the Aβ precursor protein (AβPP) is frequently used to generate animal models of the disease. In pathological conditions, the normally dominating AβPP cleavage by α- and γ-secretase is partially replaced by amyloidogenic proteolysis by β- and γ-secretase. AβPP mutations may be responsible for the shift in AβPP processing and for the increased Aβ tendency to aggregate. Increasing the local concentration of Aβ, along with its ongoing aggregation, seems to be an important stimulus changing its activity from the supposed physiological stimulation of synaptic plasticity into a neurotoxin (Fagiani et al., 2019).

Although the precise location of Aβ in the chain of events leading to neurodegeneration is still debated, the presence of its excessive amounts in the extracellular space leads to signaling anomalies and free radical stress. Synaptic disturbances are part of early AD, preceding neuronal death by a significant time margin (Fagiani et al., 2019). While large extracellular deposits of Aβ do not correlate precisely with cognitive decline, oligomers and intracellular soluble/aggregated Aβ associate with ultrastructural damage to synapses/distal neurites, and with disease severity (Rajmohan and Reddy, 2017; Marsh and Alifragis, 2018). Oligomers are, therefore, currently viewed as the likely Aβ species capable of driving synaptic pathology (Walsh et al., 2002), which accompanies and most likely predates extensive neurodegeneration (Zamponi and Pigino, 2019). Synaptic alterations are targeted by few treatments currently available for a transient slowing of AD symptoms (Marsh and Alifragis, 2018). The molecular interactions that mediate the detrimental influence of Aβ on synapses most likely involve members and binding partners of the SNARE (soluble N-ethylmaleimide sensitive fusion attachment protein receptor) complex, which ensure structural integrity and regulate synaptic vesicle turnover (Russell et al., 2012; Yang et al., 2015; Koppensteiner et al., 2016; Marsh and Alifragis, 2018). Low concentrations of monomeric Aβ have been suggested to stimulate neurotransmission through stimulation of vesicle fusion (during neurotransmitter secretion) and inhibition of endocytosis (which mediates neurotransmitter removal from the synaptic cleft); pathological, aggregating Aβ, in turn, would predominantly block exocytosis (Fagiani et al., 2019). Aβ has also been found to regulate receptor activities and their feedback endocytosis (Kamenetz et al., 2003; Hsieh et al., 2006). Correspondingly, accumulating evidence suggests that elusive functions of Aβ in a healthy brain could include synaptic regulation (Gulisano et al., 2019). However, while protein–protein interactions of Aβ are gaining attention, comparatively little is known on the possible influence of Aβ/AβPP on the expression of genes, such as those that code synaptic proteins. Aβ interacts with synaptic translation machinery (Ghosh et al., 2020), but there is also a possibility that it could modulate gene expression through modification of the sphingolipid-dependent modulation of transcription factors (Jeśko et al., 2019a,b).

Altered signaling pathways are a major part of the known pathomechanism of synapse and neuron loss. Disturbances in bioactive sphingolipids are observed both in aging and AD (Katsel et al., 2007; Han, 2010; Couttas et al., 2014). Interestingly, these disturbances occur very early in the disease course and seem to diminish in later stages (Han, 2010). Ceramide and its derivative sphingosine typically activate apoptosis, while their respective phosphates (C1P: ceramide-1-phosphate; S1P: sphingosine-1-phosphate) are mostly positive regulators of cellular survival. S1P has a wide array of other functions, modulating acquisition and maintenance of neuronal phenotypes, such as neurotransmission and synaptic plasticity. S1P (and probably C1P) acts either through cell surface receptors, or as second messengers within the cell. The cell membrane receptors for S1P (S1PR1−5) bind to $G_{12}/_{13}$, G_q, and G_i proteins, and are able to influence transcription factors, such as AP-1, NF-kB, p53, or the splicing regulator SRSF1 (Kaneider et al., 2004; Van Brocklyn and Williams, 2012; Patwardhan et al., 2014; Czubowicz et al., 2019; Jeśko et al., 2019a). Strikingly, Aβ is able to modify the expression of sphingolipid-related genes (Kaneider et al., 2004; Jeśko et al., 2019b, 2020). This may explain the above-mentioned shift from S1P signaling toward ceramide production, which is observed in the brain in the early stages of AD and preceding mild cognitive impairment (MCI) (Katsel et al., 2007; Han, 2010; Couttas et al., 2014). Increased ceramide production also occurs before MCI onset, leading to the idea of *pre-MCI*, a period when upstream events set the neurodegenerative processes in motion, likely with the significant engagement of sphingolipid-based pathways (Han, 2010). Besides altered survival/death signaling, changes in ceramide levels might also impact AβPP maturation and proteolytic processing, which can lead to increased generation of Aβ, closing the feedback circle of events (Puglielli et al., 2003; Sawamura et al., 2004; Tamboli et al., 2005). S1P has also been known to regulate various secretory pathways (Riganti et al., 2016). Somewhat scattered data also suggest the engagement of sphingolipids in the creation and maintenance of neuronal projections and synapses, which are among the earliest targets of Aβ neurotoxicity (Scheff et al., 2006; Ferreira et al., 2015).

The aim of the study was to characterize the influence of the expression of AβPP carrying familial AD–linked mutation (V717I) on the expression of genes coding selected synaptic proteins in the mouse brain cortex and hippocampus at the age of 3 and 12 months and to examine the impact of treatment with FTY720 (fingolimod, an S1P receptor modulator) on these

Abbreviations: Aβ, amyloid β; AβPP, Aβ precursor protein; ACTB, actin beta; AD, Alzheimer's disease; CNS, central nervous system; CPLX1, complexin 1; FTY720, fingolimod/Gilenya^{TM}; GAP43, Growth-associated protein 43/neuromodulin; GFAP, glial fibrillary acidic protein; NF-L, neurofilament light chain; NF-M, neurofilament medium chain; NRXN1, neurexin 1; S1P, sphingosine-1-phosphate; S1PR, S1P receptor; SNAP25, synaptosomal-associated protein, 25kDa; SNARE, soluble N-ethylmaleimide sensitive fusion attachment protein receptor; Sp1, specificity protein 1; STX1A, syntaxin 1A; SYN1, synapsin 1; SYT1, synaptotagmin 1; SYP, synaptophysin; t-SNARE, target membrane SNARE protein; VAMP1, vesicle-associated membrane protein 1; v-SNARE, vesicular side SNARE protein.

changes. The results were verified with alterations observed in neocortical and hippocampal samples of human AD cases.

MATERIALS AND METHODS

Three- and 12-month-old FVB-Tg (Thy1; APP LD2/B6) mice that express AβPP harboring V717I "London" mutation predominantly in the brain and spinal cord neurons were used. The "London" mutation associates with early AD and increases the amounts of Aβ, changing the isoform ratios in favor of the highly neurotoxic $A\beta_{42}$ (Ję̨śko et al., 2019b).

Animals

Female FVB-Tg (Thy1; APP LD2/B6) mice overexpressed human AβPP with V717I ("London") mutation under the control of a fragment of thy 1 promoter that ensured expression specifically in the neurons of the brain and spinal cord. The Animal House of the Mossakowski Medical Research Institute PAS, Warsaw, Poland maintained the mice under specific pathogen-free (SPF) conditions, under controlled temperature and humidity conditions, and a 12-h light/dark cycle. Animals aged 3 or 12 months were treated for 2 weeks daily (15 i.p. injections) with 1 mg/kg b.w. FTY720 (Cayman Chemical, Ann Arbor, Michigan, United States, cat. No 10006292) in 0.9% NaCl, or NaCl only (treatment controls), based on a previous study (Poti et al., 2012; Asle-Rousta et al., 2013; Ję̨śko et al., 2019b). Mice that did not inherit the transgene were used as transgene controls.

All possible measures were used to reduce the number of used animals and minimize their pain/distress. Initial experiments were performed on a minimal number of animals (typically $n = 3$–4), and only selected results were confirmed on larger cohorts. The experiments were approved by the IV Local Ethics Committee for Animal Experimentation in Warsaw and the Ministry of Environment (approval no. 67/2015 from July 2, 2016 and no. 139 from August 22, 2016, respectively) and were carried out in accordance with the EC Council Directive of November 24, 1986 (86/609/EEC) following the ARRIVE guidelines, the NIH Guide for the Care and Use of Laboratory Animals, and the "Guidelines for the Use of Animals in Neuroscience Research" by the Society for Neuroscience.

Gene Expression Measurement in Mouse Brain Parts by Real-Time Polymerase Chain Reaction

A day after the last treatment, the animals were decapitated, and cerebral cortices and hippocampi were isolated on ice and flash-frozen in liquid nitrogen. RNA was extracted using TRI-reagent according to the protocol of the manufacturer (Sigma-Aldrich/Merck) and DNA digested with DNase I (Sigma-Aldrich, St. Louis, MO, USA). RNA quantity and quality were measured spectrophotometrically (A_{260}/A_{280} method). Reverse transcription of 4 μg of total RNA was performed with avian myeloblastosis virus (AMV) enzyme and random sequence primers (High Capacity Reverse Transcription Kit, Applied Biosystems, Foster City, CA, United States). TaqMan Gene Expression Assay kits were used for real-time PCR on Applied Biosystems 7500 Real-Time PCR System (Applied Biosystems/Thermo Fisher Scientific, Foster City, California, USA, cat. No. 4331182). Mm01198853_m1 (*Cplx1*), Mm01315666_m1 (*Nefl*), Mm00456201_m1 (*Nefm*), Mm00660298_m1 (*Nrxn1*), Mm01276449_m1 (*Snap25*), Mm00444008_m1 (*Stx1a*), Mm00449772_m1 (*Syn1*), Mm00436850_m1 (*Syp*), Mm00436858_m1 (*Syt1*), Mm01185107_g1 (*Vamp1*). Gene expression in tri- to quadruplicate samples was calculated using the ddCt method and normalized against actin beta (Actb - Mm00607939_s1). All measurement plates for each brain part/age combination were calibrated with the same sample. Statistical significance was analyzed with a two-way analysis of variance (ANOVA; GraphPad Software, San Diego, CA, United States); "p" value < 0.05 was deemed statistically significant; experimental results are expressed as means ± SEM (standard error of the mean).

Gene Expression Analysis of Human Post Mortem Brain Samples by Northern Dot Blot Arrays

A guanidine isothiocyanate- and silica gel-based membrane total RNA purification system and miRNA isolation kit (PureLink™ Invitrogen, Carlsbad, CA, United States) were used to isolate total RNA; total RNA concentrations were quantified using RNA 6000 Nano LabChips and a 2100 Bioanalyzer (Caliper Technologies, Mountainview, CA, United States; Agilent Technologies, Palo Alto, CA, United States). Synaptic and cytoskeletal RNA abundances were analyzed and quantified using Northern dot blot arrays as previously described (McLachlan et al., 1988; Lukiw et al., 1990, 2008, 2020). Altered RNA levels of interest were further verified using a quantitative Northern dot blot focusing assay that utilizes a T4 PNK kinase radiolabel system employing [α-^{32}P]-dATP (6,000 Ci/m mol; Invitrogen, Carlsbad, CA, United States) that significantly interrogates the abundance of RNA and miRNA signals (Lukiw et al., 2008, 2020). Northern dot blot signal strengths were quantified using data-acquisition software provided with a GS250 molecular imager (Bio-Rad, Hercules, CA, United States), and graphic presentations (including comparative bar graphs) were performed using Excel algorithms (Microsoft, Seattle, WA, United States) and Adobe Photoshop 6.0 (Adobe Systems, San Jose, CA, United States). Alternately Northern dot blot patterns were analyzed using a cut-and count method. Statistical significance was analyzed using a two-way factorial analysis of variance (p, ANOVA; SAS Institute, Cary, NC, United States). A "p" value < 0.05 was deemed statistically significant; experimental values in the Figures are expressed as means ± standard deviation (SD) of that mean.

The acquisition, handling, experimental, and analytical procedures involving post mortem human brain tissues were carried out in an ethical manner in strict accordance with the ethics review board policies at brain and tissue donor institutions and at the Louisiana State University (LSU) Health Sciences Center. Informed consent from next of kin was obtained at brain and tissue donor institutions for all tissue samples prior to autopsy and donation; coded post mortem brain tissue samples (containing no personal identifying information of the donors)

were obtained from the brain and tissue banks listed above. The ethical use of post mortem human brain tissues and their analyses were also carried out in strict accordance with the Institutional Biosafety Committee and the Institutional Review Board Committee (IBC/IRBC) ethical guidelines IBC#18059 and IRBC#6774 at the LSU Health Sciences Center, New Orleans, LA, 70112 United States. Project identification codes: NIA AG18031 and NIA AG038834.

RESULTS

To analyze the effects of Aβ precursor protein (AβPP) expression and administration of the potentially neuroprotective drug fingolimod (FTY720, Gilenya™) on the expression of genes coding for synaptic proteins, we used a mouse model (Jeśko et al., 2019b) expressing AβPP with V717I "London" mutation. The mutation is linked to familial FAD/early onset AD and stimulates the production of Aβ, especially its most toxic 42 amino acid species. Despite obvious limitations shared with other animal models of AD, the mice display a temporal sequence of behavioral alterations characteristic for AD and relatively closely follow disturbances of sphingolipid metabolism we noted in the human brain (Moechars et al., 1999; Van Dorpe et al., 2000; Jeśko et al., 2019b, 2020).

FTY720 is an S1P receptor modulator with characterized bioavailability, currently used because of its capacity to cause internalization of the receptors in immune cells in relapsing-remitting multiple sclerosis, primarily lymphocytes but also in brain astrocytes (Choi et al., 2011). The immune component may also be important for the action of FTY720 in other neurodegeneration-linked diseases (Becker-Krail et al., 2017). FTY720 also exerts its neuroprotective potential through enhanced production of brain-derived neurotrophic factor and modulation of its downstream signaling (Doi et al., 2013; Fukumoto et al., 2014; Becker-Krail et al., 2017). However, its primary recognized biological role is to activate S1PRs, potentially leading to a strong anti-apoptotic signal. Finally, FTY720 has been shown to positively modulate synaptic signaling and to restore long-term synaptic plasticity affected by neurodegenerative insults (Nazari et al., 2016; Darios et al., 2017; Zhang et al., 2020). As Aβ is capable of altering sphingolipid (especially S1P) metabolism, it might result in FTY720-treatable disturbances in survival/death pathways (Jeśko et al., 2019b). However, it might also deregulate the known engagement of sphingolipids in gene regulation, such as those coding for synaptic proteins (Cai et al., 2008).

Results from this study show reduced *Vamp1* mRNA in the cerebral cortex of 3-month-old mice expressing V717I AβPP transgene. Administration of FTY720 had no effect (**Figure 1**). *Cplx1, Nrxn1, Syn1*, and *Snap25* remained unchanged in the 3-month-old AβPP mouse brain cortex. Similarly, *Nefl* and *Nefm* were not changed (**Supplementary Figure 1**).

The pattern of mRNA changes in the hippocampus of 3-month-old AβPP-expressing mice also included a reduction in *Vamp1*; the SNARE-interacting partner *Syt1* was also significantly reduced. FTY720 had no effect on their levels

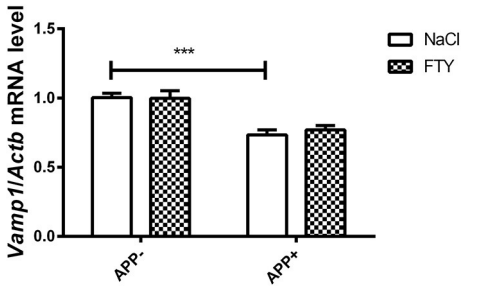

FIGURE 1 | Levels of mRNA coding for synaptic protein VAMP1 in 3-month-old mouse cortex–effect of AβPP expression and FTY720 administration. Levels of mRNAs measured with real-time PCR in the cerebral cortex of 3-month-old (adult) mice as described in Materials and methods. Results from AβPP-expressing mice were compared with those from control animals that did not inherit the transgene. Effect of FTY720 administration was assessed against vehicle-treated animals of the same group. *Vamp1*, vesicle-associated membrane protein 1; APP^{-}, animals without V717I AβPP transgene; APP^{+}, mice expressing V717I AβPP transgene. ***$p < 0.001$ vs. corresponding controls, two-way ANOVA followed by Tukey's *post-hoc* test (significances marked over the horizontal bar describe the difference between vehicle-treated control animals and vehicle-treated AβPP-expressing mice). $n = 6–7$, measured in tri- to quadruplicate ± SEM.

(**Figure 2**). Among the SNARE proteins, we did not observe any changes in the expression of *Stx1a* or *Snap25* mRNA. *Syn1* showed some tendency toward reduction but did not reach significance (**Supplementary Figure 2**). *Nefl* and *Nefm* remained unchanged (**Supplementary Figure 2**).

Twelve-month-old mice expressing V717I AβPP demonstrated reduced expression of numerous genes coding for synaptic proteins. *Vamp1* mRNA was again significantly reduced in AβPP-expressing brain cortex compared with controls that did not inherit the transgene (**Figure 3**). FTY720 treatment returned its expression to near control levels. *Nrxn1* mRNA was also reduced by AβPP expression, but FTY720 had no effect on it. No changes were observed in 12-month-old brain cortex in the mRNA levels of *Stx1a, Cplx1, Syt1, Syp, Syn1*, or *Snap25* in response to AβPP (**Figure 3**). However, FTY720 treatment increased *Cplx1, Snap25, Stx1a*, and *Syt1* in the transgenic animals. *Nefl* and *Nefm* remained unchanged (**Figure 3**).

Also, at 12 months, hippocampal mRNA levels were significantly lower in AβPP-expressing animals compared with non-transgenic controls: *Snap25, Stx1a, Nrxn1*, and *Cplx1*. FTY720 reversed these changes. *Syt1* mRNA was also reduced in AβPP-expressing hippocampus, but FTY720 did not change it significantly. *Vamp1* and *Syp* remained unaltered by AβPP expression, but both responded positively to FTY720. We also observed that *Nefl* mRNA dropped significantly in AβPP animals, while *Syn1* and *Nefm* remained unchanged (**Figure 4**).

Analysis of data from nine human AD samples (**Figure 5**) indicated a reduced expression of *VAMP*, synaptophysin, synapsin, and *NF-L* in comparison to 15 healthy controls. The changes were significant in both neocortical and hippocampal materials. Similar results were obtained using Northern dot blot array methodologies.

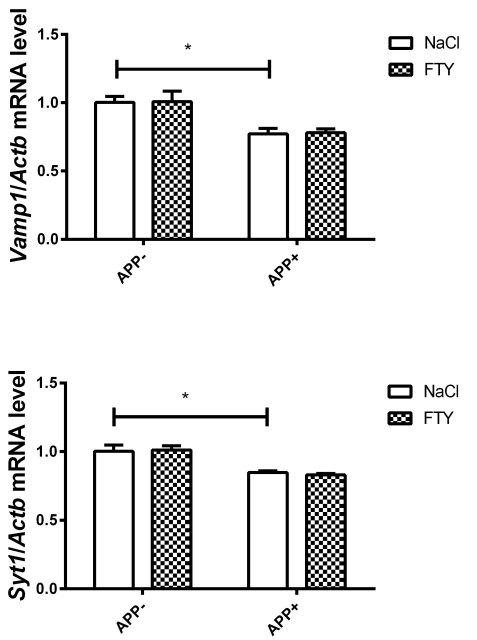

FIGURE 2 | Levels of mRNAs coding for synaptic proteins VAMP1 and SYT1 in the 3-month-old mouse hippocampus: effect of AβPP and FTY720. Levels of mRNAs measured in the hippocampus of 3-month-old (adult) mice as described in Materials and methods. mRNA levels in AβPP-expressing mice were compared with control animals that did not inherit the transgene. Effect of FTY720 administration was assessed against vehicle-treated animals in each group. *Vamp1*, vesicle-associated membrane protein 1; *Syt1*, synaptotagmin 1; APP^{-}, animals without V717I AβPP transgene; APP^{+}, mice expressing V717I AβPP transgene. *$p < 0.05$ vs. corresponding controls, two-way ANOVA followed by Tukey's *post-hoc* test (horizontal bars: effect of AβPP). $n = 3$–4, measured in triplicate ± SEM.

DISCUSSION

Our previous analysis (Jeśko et al., 2019b, 2020) has shown that the reaction of mouse brain to the expression of AβPP (V717I) transgene is highly different at various ages. The presence of AβPP in adult (3-month-old) animals was associated with elevated ceramide turnover (higher expression of both ceramide-synthesizing and -degrading enzymes of the salvage pathway of sphingolipid metabolism), but 12-month-old transgenic mice only displayed a reduction in the expression of ceramide-utilizing enzymes in the sphingomyelinase pathway. The effects of such changes may include the well-documented intensification of pro-apoptotic signaling. Literature points to an early rise in the predominantly pro-apoptotic ceramide and disturbed production of S1P, which, in most situations, supports cell survival, in human AD brains. Disturbances in ceramide/sphingolipid metabolism appear very early (leading to the proposal of *pre-MCI* phase that would precede the mild cognitive impairment), correlate with the severity of neurodegeneration, and, strikingly, diminish in later disease stages (Katsel et al., 2007; Han, 2010; Couttas et al., 2014).

Altered sphingolipid signaling may also heavily affect neuronal phenotype, as sphingolipids regulate glutamate secretion, the expression of glutamate receptor subunits, and probably the shape and structure of neurites and synapses (Riganti et al., 2016; Joshi et al., 2017). Synapse loss is one of the early features of AD and correlates with the ongoing cognitive deterioration (Scheff et al., 2006; Ferreira et al., 2015). Deregulation and eventual degeneration of synaptic connections is largely dependent on Aβ levels (Forner et al., 2019; Sharda et al., 2020). Disruption of lipid rafts, which are sphingolipid-enriched microdomains in the neuronal membrane, is a known trigger of synapse loss (Hering et al., 2003). Inhibition of ceramide synthesis, or exogenous addition of sphingosine, causes axon growth blockade and axon retraction in cultured neurons (Campenot et al., 1991; Harel and Futerman, 1993). Inhibition of ceramide synthase also disturbs dendrite formation in cultured neurons (Furuya et al., 1995). Manipulation of ceramide metabolism alters numerous neuronal signaling systems, such as NMDA, AMPA (α-amino-3-hydroxy-5-methyl-4-isoxazolepropionic acid), and acetylcholine receptors, reviewed in Olsen and Færgeman (2017). Metabolism of AβPP and production of Aβ are also highly dependent on the rafts (Czubowicz et al., 2019). The synaptic targets that bind Aβ and may mediate synapse loss could include some neurexin and neuroligin isoforms, glutamate, adrenergic, and nicotinic receptors, calcium channels, or GM1 ganglioside (Ferreira et al., 2015; Brito-Moreira et al., 2017). However, Aβ might also deregulate synaptic homeostasis through alteration of the role of sphingolipids in gene regulation (Jeśko et al., 2019b, 2020), which is mostly realized through cell surface S1P receptors (S1PR1-5), G proteins, and the PI3K (phosphoinositide 3-kinase)–Akt pathway (Jeśko et al., 2019a). PI3K/Akt–dependent transcription factors include AP-1 and NF-κB. Interestingly, promoter of the human SNAP25 synaptic protein gene contains sites binding sphingolipid-regulated transcription factors AP-1 and Sp1 (specificity protein 1) (Cai et al., 2008; Zou et al., 2011; Hsu et al., 2015). The potential of Aβ to cause synaptic disruption prompted us to analyze the levels of mRNA coding for selected synaptic proteins in the AβPP (V717I) transgenic mouse model.

The results showed decreased expression of several crucial genes coding SNARE proteins and their interacting partners in (V717I) AβPP transgenic mice. At the age of 3 months, the changes were limited to reduced *Vamp1* mRNA (both in the cerebral cortex and hippocampus) and *Syt1* (only in the hippocampus), (**Figures 1**, **2**). These changes might signify an already ongoing disruption of synaptic structure. Administration of the potentially neuroprotective S1P receptor modulator FTY720 has not changed the abnormal expression of *Syt1* or *Vamp1* in 3-month-old AβPP transgenic mice.

In contrast to the young adults, we observed numerous gene expression changes in 12-month-old AβPP-expressing animals. *Vamp1* and *Nrxn1* mRNAs were reduced in the cerebral cortex, while other measured mRNAs (such as *Cplx1, Snap25, Syp*, and *Stx1a*) remained at the same level as in non-AβPP controls (**Figure 3**). *Nrxn1* mRNA was reduced in both investigated 12-month-old brain parts. FTY720 reversed the decrease in *Vamp1* but not *Nrxn1* mRNAs; and the compound also had a positive influence on *Cplx1, Snap25, Stx1a*, and *Syt1* in the 12-month-old animals (**Figure 3**).

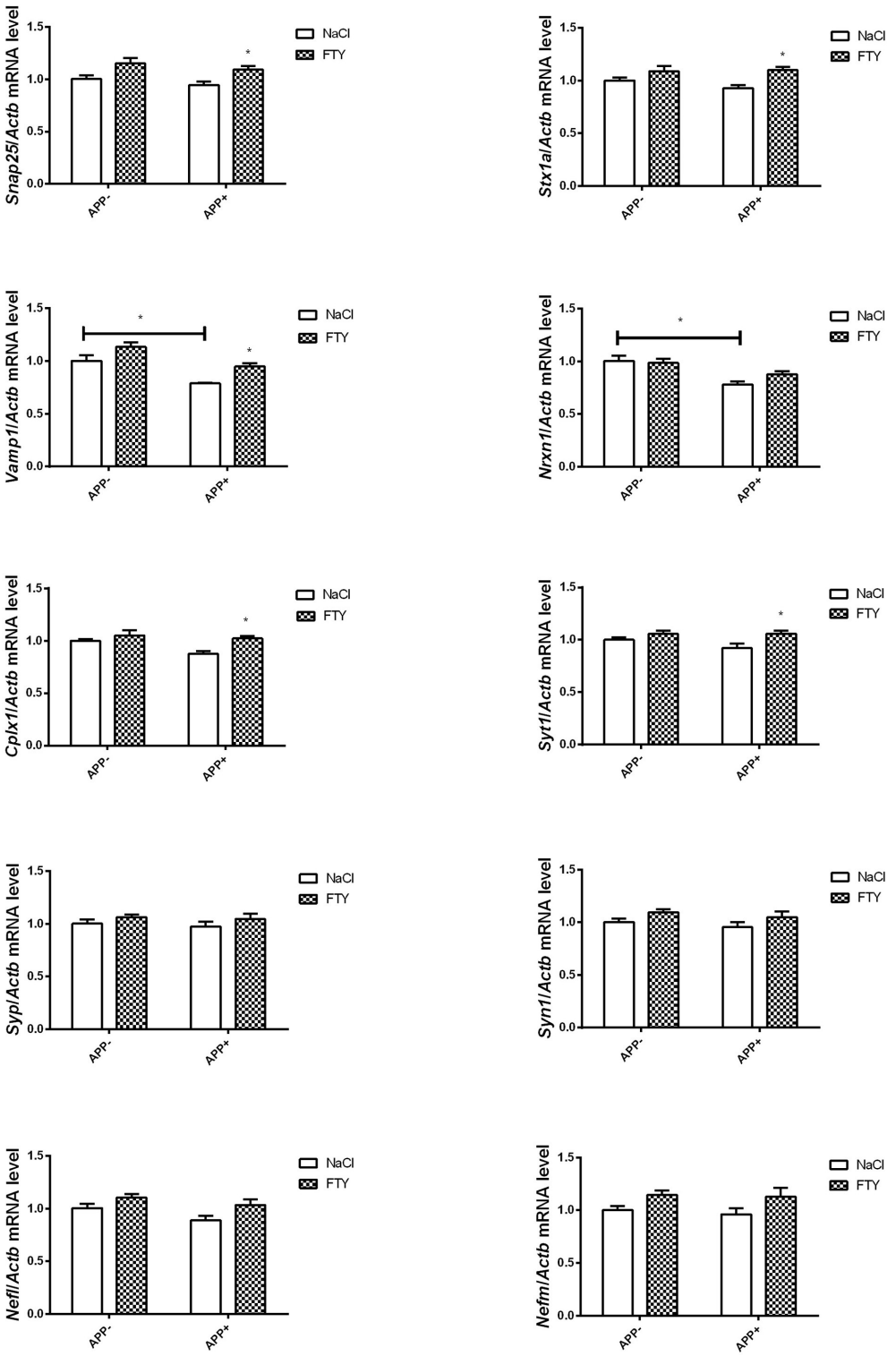

FIGURE 3 | Levels of mRNAs coding for synaptic proteins in 12-month-old cortex: effect of AβPP and FTY720. Levels of mRNAs measured with real-time PCR in the cerebral cortex of 12-month-old (old adult) mice as described in Materials and methods. mRNA levels in AβPP-expressing mice were compared with control animals that did not inherit the transgene. Effect of FTY720 administration was assessed against vehicle-treated animals in each group. *Snap25*, synaptosomal-associated protein, 25kDa; *Stx1a*, syntaxin 1A; *Vamp1*, vesicle-associated membrane protein 1; *Nrxn1*, neurexin 1; *Cplx1*, complexin 1; *Syt1*, synaptotagmin 1; *Syp*, synaptophysin; *Syn1*, synapsin 1; *Nefl*, neurofilament light; *Nefm*, neurofilament medium; APP^{-}, animals without V717I AβPP transgene; APP^{+}, mice expressing V717I AβPP transgene. *$p < 0.05$ vs. corresponding controls, two-way ANOVA followed by Tukey's *post-hoc* test (horizontal bars: effect of AβPP; significances marked over FTY720 values: effect of FTY720 treatment within each animal group). $n = 3$–6, measured in triplicate ($n = 6$–9 for *Cplx1*, *Snap25*, *Syn1*, and *Nefl*) ± SEM.

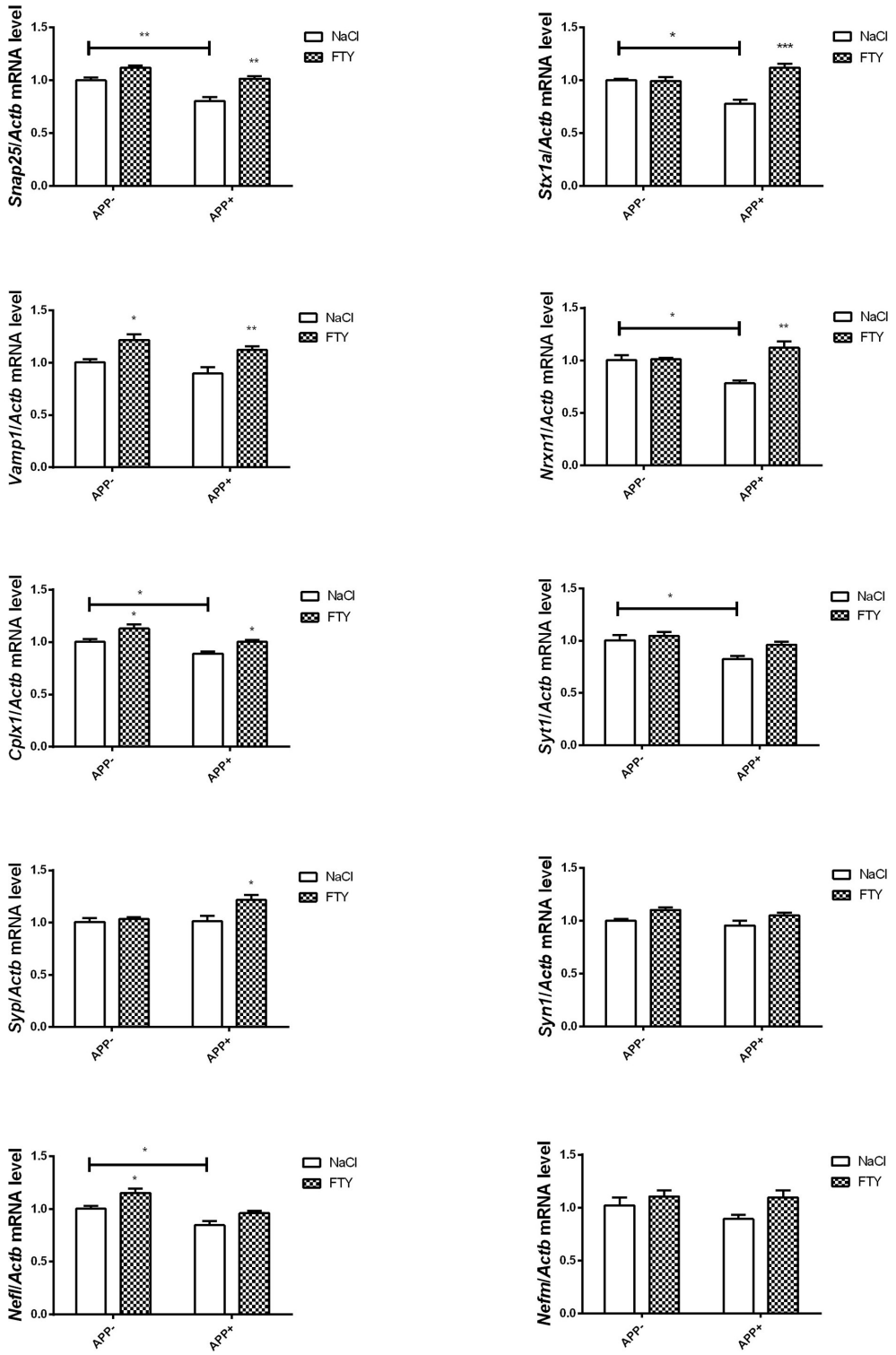

FIGURE 4 | Levels of mRNAs coding for synaptic proteins in 12-month-old hippocampus: effect of AβPP and FTY720. Levels of mRNAs measured with real-time PCR in the hippocampus of 12-month-old (old adult) mice as described in Materials and methods. mRNA levels in AβPP-expressing mice were compared with control animals that did not inherit the transgene. Effect of FTY720 administration was assessed against vehicle-treated animals in each group. *Snap25*, synaptosomal-associated protein, 25kDa; *Stx1a*, syntaxin 1A; *Vamp1*, vesicle-associated membrane protein 1; *Nrxn1*, neurexin 1; *Cplx1*, complexin 1; *Syt1*, synaptotagmin 1; *Syp*, synaptophysin; *Syn1*, synapsin 1; *Nefl*, neurofilament light; *Nefm*, neurofilament medium; APP^{-}, animals without V717I AβPP transgene; APP^{+}, mice expressing V717I AβPP transgene. $^{*}p < 0.05$; $^{**}p < 0.01$; $^{***}p < 0.001$ vs. corresponding controls, two-way ANOVA followed by Tukey's *post-hoc* test (horizontal bars: effect of AβPP; significances marked over FTY720 values: effect of FTY720 treatment within each animal group). $n = 3$–6, measured in triplicate ($n = 7$–14 for *Cplx1*, *Syp*, *Syn1*, *Vamp1*, and *Nefl*) ± SEM.

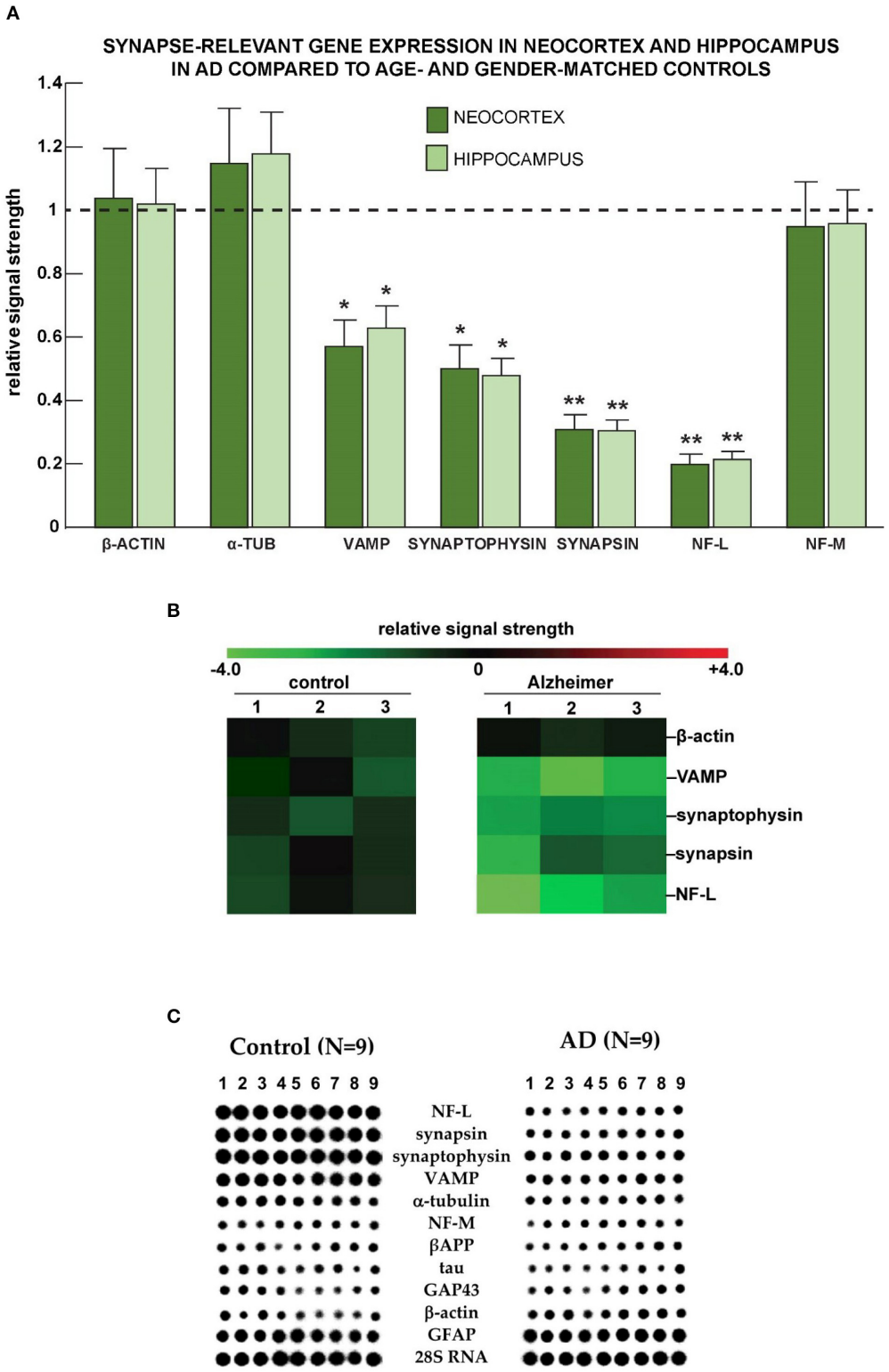

FIGURE 5 | Selective down-regulation of the expression of genes coding for synaptic proteins in AD. **(A)** Neocortical and hippocampal down-regulation of VAMP, synaptophysin, synapsin, and the neuron-specific neurofilament light (NF-L) chain messenger RNA in Alzheimer's disease vs. age-, gender-, and post mortem interval-matched controls using the β-actin cytoskeletal as an internal "housekeeping gene" and expression control. Importantly, the low abundance of the

(Continued)

FIGURE 5 | neuron-specific NF-L mRNA cannot be adequately accounted for by a non-specific effect of brain damage, neuron cell loss, or loss of neurons with neurofibrillary degeneration (McLachlan et al., 1988; Lukiw et al., 2018). The AD group ($N = 3$) had a mean age of 76.1 ± 11.4 years and a mean post mortem (PMI; death to brain-freezing period) of ∼3.4 h and the control group ($N = 3$) had a mean age of 75.5 ± 12.7 years and a mean PMI of ∼3.5 h; all brain samples were from female donors; there was no significant difference in the mean age, gender, PMI, or yield of total RNA between the AD and control groups. Total RNA was extracted and probed for α-tubulin, VAMP, synaptophysin, synapsin, the neurofilament light and medium neurofilaments, and quantified based on unchanging β-actin control levels in the same sample using methods explained in detail in previously published study from our laboratories (McLachlan et al., 1988; Lukiw et al., 2008, 2018); deficits in synapse-relevant gene expression were consistently found to be NF-L < synapsin < synaptophysin < VAMP; these observations are also consistent with synaptic signaling deficits in AD brain compared to three unchanging biomarkers: β-actin, α-tubulin, and the NF-M chain protein; $^{*}p < 0.05$; $^{**}p < 0.01$ (ANOVA). **(B)** Down-regulation of mRNAs coding for vesicle-associated membrane protein (VAMP), synaptophysin (SYP), synapsin, and NF-L in Alzheimer's disease vs. age- gender- and post-mortem interval-matched controls using the β-actin cytoskeletal as a "housekeeping gene" and expression control using DNA array analysis (McLachlan et al., 1988; Lukiw et al., 2008, 2018); the numbers 1–3 along the top represent results from $N = 3$ control and $N = 3$ Alzheimer cases; again, all were age-matched from female donors; there was no significant difference in the mean age, PMI, or yield of total RNA between the AD and control groups. **(C)** Selective deficits for synapse-relevant gene expression were also observed in AD temporal lobe neocortex compared with age- and gender-matched controls using Northern dot blot analysis. Deficits in gene expression for synaptic components in control ($N = 9$) vs. AD ($N = 9$) female superior temporal lobe (Brodmann A22) neocortices using quantitative Northern dot blots for signal quantitation; the PMI for all tissues was ∼4 h or less; a 288-gene matrix was generated using a Biomek 2000 robot (Beckman-Coulter Life Sciences, Indianapolis, IN, United States) at a Northern dot blot density of about 30 genes/cm^2; in **(C)**, each vertical column represents the Northern dot blot signature of one control or one AD brain, and each horizontal row represents the hybridization signals from one particular synaptic-relevant probe; signal intensity of each dot in the dot blot is proportional to the abundance of that specific mRNA in the sample; note significant deficits in signal strength (signal intensity of the dot blot) for NF-L, synapsin, synaptophysin, and vesicle-associated membrane protein (VAMP) and negligible changes between control and AD for α-tubulin, NF-M, the amyloid precursor protein (APP), tau, the 43 kDa growth associated protein GAP43 (neuromodulin), the cytoskeletal protein β-actin, glial fibrillary acidic protein (GFAP), and the large ribosomal subunit 28S RNA. In these DNA array studies, the control group ($N = 9$) had a mean age of 77.5 ± 13.5 years, and the AD group ($N = 9$) had a mean age of 78.5 ± 11.8 years; all brain samples were from female donors; again, there was no significant difference in the mean age, gender, PMI, or yield of total RNA between the AD and control groups. Experimental values in all of the Figures are expressed as mean ± standard deviation of that mean. This figure represents updated and additional new information for NF-L gene expression data adapted from earlier studies on specific cytoskeletal gene abundance in control and AD neocortex (McLachlan et al., 1988; Lukiw et al., 1990).

Opposite to the cerebral cortex, the 12-month-old hippocampus displayed a nearly uniform reduction in *Cplx1, Snap25, Stx1a, Nrxn1, Syt1*, and *Nefl* but not *Vamp1* mRNA, which seems to reflect unique sensitivity of the brain part to the gradually accumulating effects of Aβ/AβPP. The reduction in *Snap25, Syt1* as well as *Vamp1* hippocampal gene expression is consistent with previously observed changes in the human AD hippocampus (Berchtold et al., 2013). Importantly, reduction in *Cplx1, Snap25, Stx1a*, and *Nrxn1* could be reversed by FTY720, which also increased the levels of *Vamp1* and *Syp*.

We next evaluated the expression of selected synaptic protein-coding genes in samples from high quality human brain tissues with post mortem intervals (PMIs) of 2.4 h or less (**Figure 5**). Interestingly, the patterns of AD-linked changes in the human hippocampus and neocortex were very similar to each other, but the set of genes affected showed a noticeable similarity to the mouse model. We observed reduced expression of *VAMP, SYP, SYN*, and *NF-L* (*NEFL*) mRNAs, in both brain regions.

VAMP1, STX1A, and SNAP25 belong to the SNARE complex critically implicated in vesicular secretion of neurotransmitters, in the membrane insertion of receptor proteins, and also in synaptic plasticity, axon guidance, or nerve regeneration (Ulloa et al., 2018; Madrigal et al., 2019). Several lines of evidence suggest the possible engagement of SNARE proteins in AD, although data are rather limited: polymorphisms in *VAMP1* and *STX* genes associate with AD; VAMP1 can modulate Aβ secretion; while VAMP2 levels are disturbed in AD (Sevlever et al., 2015; Vallortigara et al., 2016; Costa et al., 2019). The SNARE trimer binds a multitude of other proteins, such as regulators (synaptotagmin–SYT, complexin–CPLX), and also α-synuclein (Almandoz-Gil et al., 2018; Alford et al., 2019; Hawk et al., 2019; Karmakar et al., 2019). SYT1 is engaged in Ca^{2+} sensing and coupling of calcium signal to neurotransmitter release; genetic *SYT* ablation can lead to disturbed synaptic vesicle exocytosis, such as uncontrolled (spontaneous) release (Volynski and Krishnakumar, 2018). SYT1, -2, -7, and -9 bind AβPP; SYT1 probably supports AβPP processing by β-secretase (Gautam et al., 2015; Barthet et al., 2018). SYT1 also interacts with presenilin 1, and experimental disruption of their interaction increases the proportion of the highly neurotoxic $Aβ_{42}$ (Zoltowska et al., 2017). Moreover, SYT1 levels and SYT1–presenilin 1 binding are disturbed in the brain of humans with AD (Zoltowska et al., 2017).

Neurexins (NRXN) are single-pass transmembrane proteins located predominantly in the presynaptic part; they bind post-synaptic neuroligins (NLGN), neurexophilins, and dystroglycan systems ensuring structural properties of neuronal connections. Neurexins also influence differentiation and synaptic vesicle production. Their sensitivity to calcium allows for direct regulation of NLGN–NRXN binding by neuron activity (Sindi et al., 2014). Neurexin mutations may predispose to AD (Sindi et al., 2014). Aβ impairs the expression of *NRXN1β* and can bind NRXN2A (Brito-Moreira et al., 2017; Naito et al., 2017). Interactions of NRXN with Aβ/secretases can lead to, e.g., accumulation of NRXN fragments in the extracellular space, membranes, and pre-synaptic cytoplasm, and finally to altered efficiency of synaptic transmission [discussed in Sindi et al. (2014)] but also to structural disruption and loss of synapses (Brito-Moreira et al., 2017; Naito et al., 2017). The reduction of *Nrxn1* and *Vamp1* expression we observed might be a part of advancing synaptic deterioration. However, the known association of AD risk with *VAMP1* polymorphisms that cause increased transcription, and the positive influence of VAMP1 on Aβ secretion (Sevlever et al., 2015) suggest an ambiguous role for the protein. We cannot rule out a neuroprotective outcome of *Vamp1* reduction, and some potentially homeostatic reactions might occur even relatively late in the disease progression.

Synaptophysin (SYP) is a cholesterol-binding membrane protein that transiently interacts with VAMP in an activity-dependent manner (Hübner et al., 2002; Khvotchev and Südhof, 2004). The significance of SYP for synaptic function/maintenance is unclear because of the lack of gross gene ablation-induced phenotypes. However, reduced synaptophysin has long been noted in aging and in a disease-specific, spatially-restricted manner in early stages of AD and some other neurodegeneration types (Masliah et al., 1989; Lippa, 2004; Martin et al., 2014). Reduced SYP also correlates with AD severity (Sze et al., 1997; Heffernan et al., 1998). Loss of SYP staining is observed in neurons in the vicinity of Aβ oligomer deposits (Ishibashi et al., 2006); interaction of SYP with internalized Aβ and Aβ-induced preferential SYP nitration have been suggested to mediate synaptic disturbances observed in AD (Tran et al., 2003; Russell et al., 2012). Reduction of *Syp* expression was also observed in neurons containing neurofibrillary tangles (Callahan et al., 1999).

Synapsins (SYN) are highly abundant, neuron-specific pre-synaptic vesicle proteins engaged in synaptogenesis, regulation of vesicle storage, fusion, and resulting neurotransmitter release (Song and Augustine, 2015). SYN disturbances are noted in multiple neurodegenerative/psychiatric disorders, including AD (Qin et al., 2004; Song and Augustine, 2015). Specifically, loss of SYN1 has been previously observed in some layers of CA1 and dentate gyrus of patients with AD hippocampus (Qin et al., 2004). Moreover, a reduction in *Syn1* mRNA levels was observed in the CA3 layer of the hippocampus of rats with sporadic AD (Bolognin et al., 2012). Similar results were also reported by Berchtold et al. who observed structure-specific downregulation of *SYN1* mRNA levels in the hippocampus of patients with AD. Interestingly, cortical *SYN1* mRNA reduction was observed in the aged control group (69–99 vs. 20–50 years) (Berchtold et al., 2013).

The results also confirm reduced expression of *NEFL* (NF-L), which encodes the 68 kDa neurofilament protein. NF-L is a neuron-specific intermediate filament being a critical scaffolding component of neurite extensions, the primary regulator of axon diameter, overall neuronal cytoarchitecture, neuron shape and morphology, and an integral component of synaptic complexes (Palermo et al., 2020). Down-regulated NF-L within degenerating neocortical neurons, such as those seen in AD, correlates well with the neuronal atrophy and deterioration widely observed in progressive neurological degeneration (Berchtold et al., 2013). Diminished brain levels of NF-L have been reported by several independent laboratories in AD and in transgenic murine models for AD (TgAD) irrespective of reduced neuron count (Lukiw et al., 1990, 2018; Loeffler et al., 2020). NF-L may be a diagnostic biomarker of brain atrophy and disease progression in multiple nervous system disorders (Gaetani et al., 2019; Antonell et al., 2020).

The difference between human and rodent samples could stem from several sources. First, although the (V717I) AβPP-expressing mice relatively successfully recreate a spectrum of AD pathology aspects, they still share the obvious limitations of all rodent AD models. Second, human post mortem samples are collected at much more advanced stages of widespread, massive neurodegeneration, in contrast to the mild degenerative changes observed in 12-month-old (V717I) AβPP mouse brains. Moreover, some differences in the spatial distribution of sensitivity to Aβ neurotoxicity between the human and mouse brains might also modify the outcome.

The results, therefore, show that the impact of Aβ/AβPP on critical synaptic components is highly dependent on age/disease stage and is brain part specific, with the highest number of changes occurring in the 12-month-old hippocampi (all changes that were observed in 12-month-old transgenic mice were presented in **Figure 6**). FTY720 is capable of reversing many of Aβ/AβPP-induced changes in the expression of synaptic proteins, suggesting its value as a research tool and possibly a repurposed drug. Although the mouse model obviously examines the disease at a much earlier stage (and at a much younger age) than observed in human tissues, we noted several striking similarities in the obtained results. Therefore, we can suggest that the sensitivity of several key synaptic components to FTY720 administration may also be present in the human nervous system. Synaptic deterioration is a relatively early stage of degeneration in AD, but its biochemical manifestations appear to persist to the end stage.

The pleiotropic activities of FTY720 require further attention to the potential mechanism of its restorative action. One plausible explanation is the ability of S1P receptors to modulate transcription factors, such as AP-1 or NF-kappa B, therefore relatively directly and specifically affecting the transcription of multiple genes (including feedback regulation of sphingolipid metabolic enzymes) (Jeśko et al., 2019a,b; Jeśko et al., 2020). S1P and its receptors also have a complex influence on PI3 kinase/Akt and their signaling target mTOR, potentially influencing gene transcription and translation through ribosomal protein S6 kinases, eukaryotic translation initiation factor 4E-binding proteins, and FOXO transcription factors (Jeśko et al., 2019a). Both sphingosine kinase 2 and its product S1P can modulate histone deacetylases (Jeśko et al., 2019a). More general influences of FTY720 on AβPP metabolism and inflammation may add further layers of complexity. FTY720, acting as a ligand, can cause regulatory internalization of S1PR protein, effectively inhibiting S1PR signaling in lymphocytes and blocking their egress from secondary lymphoid organs. This effect is exploited in the therapy of relapsing remitting multiple sclerosis (Sica et al., 2019). FTY720 also reduces the numbers of activated microglia and astrocytes in the brain of rodent AD models, normalizing cytokines, synaptic morphology, plasticity, and learning performance (Hemmati et al., 2013; Aytan et al., 2016). Anti-inflammatory effects of FTY720 have also been shown in other diseases, such as amyotrophic lateral sclerosis (ALS), Parkinson's disease (PD), Huntington's disease (HD), neuronal ceroid lipofuscinoses, and neonatal hyperoxia (Bascuñana et al., 2020). Although feedback S1PR internalization upon ligation has been considered the main mechanism of the anti-inflammatory action of FTY720, the atypical dose-response characteristics suggest that agonistic action on S1PRs may also be important in this case, possibly involving two different mechanisms depending on compound concentration (Aytan et al., 2016). Moreover, FTY720 might be most effective in concentrations that reduce microglia and astrocyte activation but do not affect peripheral lymphocytes (Carreras et al., 2019).

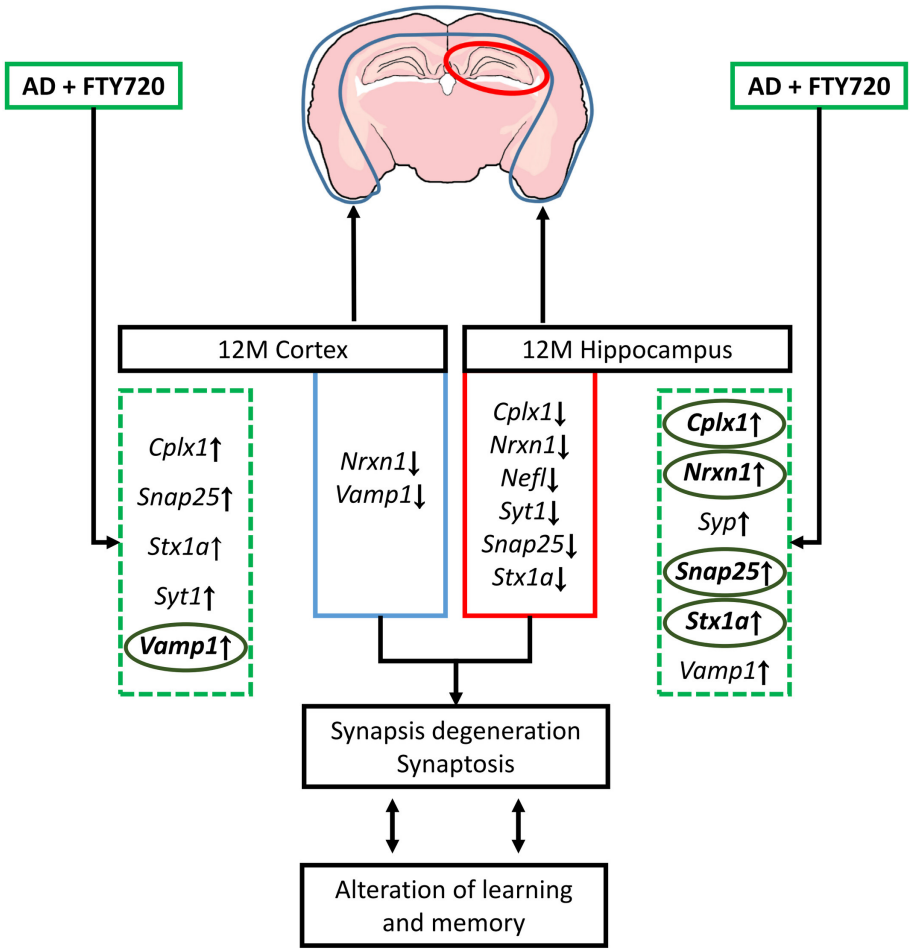

FIGURE 6 | Schematic representation of changes in genes coding synaptic proteins and their possible consequences observed in 12-month (12 M) FVB/AβPP (V717I) mice cortex and hippocampus. The effect of fingolimod (FTY720, marked by green dashed square) on genes that expression was altered in AD mice brain was bolded and marked with circles (ellipses). *Snap25*, synaptosomal-associated protein, 25kDa; *Stx1a*, syntaxin 1A; *Vamp1*, vesicle-associated membrane protein 1; *Nrxn1*, neurexin 1; *Cplx1*, complexin 1; *Syt1*, synaptotagmin 1; *Syp*, synaptophysin; *Nefl*, neurofilament light.

Much study has also been conducted on the effects of FTY720 on amyloid beta accumulation. FTY720 can decrease the accumulation of soluble and plaque Aβ, probably through an increased phagocytic capacity of astrocytes and reduced microgliosis (McManus et al., 2017; Kartalou et al., 2020). Takasugi observed that reduction of Aβ load by FTY720 and change in the proportions between Aβ40 and Aβ42 may occur in the presence of Gi inhibitor suramin, therefore likely independently of the currently known S1PR-dependent signaling pathways, possibly through direct binding of FTY720 to γ-secretase or AβPP (FTY720 decreased the γ-secretase mediated cleavage of AβPP) (Takasugi et al., 2013).

The gradual evolution of the Aβ/AβPP-associated changes in synaptic composition we observed in aging AβPP transgenic mice occurs along with the known Aβ-induced disruption of synaptic protein-protein interactions (Marsh and Alifragis, 2018). This phenomenon suggests the necessity of wide, in-depth characterization of the feasibility of Aβ-induced synaptic changes as a potential druggable target in AD. Irrespective of the mentioned cautions, the observed effects of FTY720 administration on synaptic protein expression suggest restorative potential, in accordance with the currently prevailing view on the action of FTY720 in AD and other neurodegenerative disorders.

DATA AVAILABILITY STATEMENT

The original contributions presented in the study are included in the article/**Supplementary Material**, further inquiries can be directed to the corresponding author/s.

ETHICS STATEMENT

The studies involving human participants were reviewed and approved by the ethical use of postmortem human brain tissues and their analyses were also carried out in strict accordance with the Institutional Biosafety Committee

and the Institutional Review Board Committee (IBC/IRBC) ethical guidelines IBC#18059 and IRBC#6774 at the LSU Health Sciences Center, New Orleans LA 70112 USA. Project identification codes: NIA AG18031 and NIA AG038834. Written informed consent for participation was not required for this study in accordance with the national legislation and the institutional requirements. The animal study was reviewed and approved by the IV Local Ethics Committee for Animal Experimentation in Warsaw and the Ministry of Environment (approval no. 67/2015 from 2nd July 2016 and no. 139 from 22nd August 2016, respectively) and were carried out in accordance with the EC Council Directive of November 24, 1986 (86/609/EEC) following the ARRIVE guidelines, the NIH Guide for the Care and Use of Laboratory Animals, and the Guidelines for the Use of Animals in Neuroscience Research by the Society for Neuroscience.

AUTHOR CONTRIBUTIONS

RS and WL: conceptualization and formal analysis. HJ, IW, PW, RS, and WL: methodology and investigation. RS: validation, resources, supervision, project administration, and funding acquisition. RS and PW: data curation. HJ: writing – original draft preparation. HJ and RS: writing – review and editing. IW and PW: visualization. All authors contributed to the article and approved the submitted version.

FUNDING

The study was supported by the National Science Centre (PL) (Grant no. NCN 2014/15/B/NZ3/01049) and the statutory budget of MMRI PAS theme no. 7 (**Figures 1**–**4**). Research on synaptic and neurofilament gene expression involving synaptogenesis and neuro-inflammation in AD and in other human neurological- and plant-viroid-based diseases (**Figure 5**) was supported through an unrestricted grant to the LSU Eye Center from Research to Prevent Blindness (RPB); the Louisiana Biotechnology Research Network (LBRN) and NIH grants NEI EY006311, NIA AG18031, and NIA AG038834 (WL). AD and age-matched control human hippocampus and temporal lobe and/or neocortical tissues were obtained from brain and tissue repositories including the LSU Health Sciences Center archives, the University of Oregon Health Sciences Center (OHSC), NIH collaborators and researchers, and by the Institute for Memory Impairments and Neurological Disorders and the University of California at Irvine Alzheimer's Disease Research Center (UCI-ADRC). Funding for the UCI-ADRC was provided by NIH/NIA Grant P50 AG16573. Funding bodies had no role in the design, execution, interpretation, or writing of the study.

ACKNOWLEDGMENTS

We would like to sincerely thank the many neuropathologists, physicians, and researchers of Canada, Europe, the Russian Federation, and the USA for their cooperation and provision of high-quality, short postmortem interval (PMI) human CNS or brain tissues for scientific analysis and study.

SUPPLEMENTARY MATERIAL

The Supplementary Material for this article can be found online at: https://www.frontiersin.org/articles/10.3389/fnmol.2021.660104/full#supplementary-material

Supplementary Figure 1 | Levels of mRNA coding for synaptic proteins in 3-month-old mouse cortex: effect of AβPP expression and FTY720 administration. Levels of mRNAs measured with real-time PCR in the cerebral cortex of 3-month-old (adult) mice as described in Materials and methods. Results from AβPP-expressing mice were compared with those from control animals that did not inherit the transgene. Effect of FTY720 administration was assessed against vehicle-treated animals of the same group. *Snap25*, synaptosomal-associated protein, 25kDa; *Stx1a*, syntaxin 1A; *Nrxn1*, neurexin 1; *Cplx1*, complexin 1; Syt, synaptotagmin 1; *Syp*, synaptophysin; *Syn1*, synapsin 1; *Nefl*, neurofilament light; *Nefm*, neurofilament medium; APP^{-}, animals without V717I AβPP transgene; APP^{+}, mice expressing V717I AβPP transgene. $n = 3$–4 (for *Nrxn1*, *Cplx1*, *Syt1*, and *Syp*), $n = 6$–8 (for *Snap25*, *Stx1a, Syn1, Nefl,* and *Nefm*) measured in triplicate.

Supplementary Figure 2 | Levels of mRNA coding for synaptic proteins in 3-month-old mouse hippocampus: effect of AβPP expression and FTY720 administration. Levels of mRNAs measured with real-time PCR in the hippocampus of 3-month-old (adult) mice as described in Materials and methods. Results from AβPP-expressing mice were compared with those from control animals that did not inherit the transgene. Effect of FTY720 administration was assessed against vehicle-treated animals of the same group. *Snap25*, synaptosomal-associated protein, 25kDa; *Stx1a*, syntaxin 1A; *Nrxn1*, neurexin 1; *Cplx1*, complexin 1; *Syp*, synaptophysin; *Syn1*, synapsin 1; *Nefl*, neurofilament light; *Nefm*, neurofilament medium; APP^{-}, animals without V717I AβPP transgene; APP^{+}, mice expressing V717I AβPP transgene. $n = 3$–4 measured in triplicate (for *Snap25, Nrxn1, Syp, Syn1, Nefl,* and *Nefm*) ($n = 6$–8 for *Stx1a* and *Cplx1*).

REFERENCES

Alford, S., Hamm, H., Rodriguez, S., and Zurawski, Z. (2019). Gβγ SNARE interactions and their behavioral effects. *Neurochem. Res.* 44, 636–649. doi: 10.1007/s11064-018-2531-x

Almandoz-Gil, L., Persson, E., Lindström, V., Ingelsson, M., Erlandsson, A., and Bergström, J. (2018). *In situ* proximity ligation assay reveals co-localization of alpha-synuclein and SNARE proteins in murine primary neurons. *Front. Neurol.* 9:180. doi: 10.3389/fneur.2018.00180

Antonell, A., Tort-Merino, A., Ríos, J., Balasa, M., Borrego-Écija, S., Auge, J. M., et al. (2020). Synaptic, axonal damage and inflammatory cerebrospinal fluid biomarkers in neurodegenerative dementias. *Alzheimers Dement.* 16, 262–272. doi: 10.1016/j.jalz.2019.09.001

Asle-Rousta, M., Kolahdooz, Z., Oryan, S., Ahmadiani, A., and Dargahi, L. (2013). FTY720 (fingolimod) attenuates beta-amyloid peptide (Aβ42)-induced impairment of spatial learning and memory in rats. *J. Mol. Neurosci.* 50, 524–532. doi: 10.1007/s12031-013-9979-6

Aytan, N., Choi, J. K., Carreras, I., Brinkmann, V., Kowall, N. W., Jenkins, B. G., et al. (2016). Fingolimod modulates multiple neuroinflammatory markers in a mouse model of Alzheimer's disease. *Sci. Rep.* 6:24939. doi: 10.1038/srep24939

Barthet, G., Jordà-Siquier, T., Rumi-Masante, J., Bernadou, F., Müller, U., and Mulle, C. (2018). Presenilin-mediated cleavage of APP regulates synaptotagmin-7 and presynaptic plasticity. *Nat. Commun.* 9:4780. doi: 10.1038/s41467-018-06813-x

Bascuñana, P., Möhle, L., Brackhan, M., and Pahnke, J. (2020). Fingolimod as a treatment in neurologic disorders beyond multiple sclerosis. *Drugs R D* 20, 197–207. doi: 10.1007/s40268-020-00316-1

Becker-Krail, D., Farrand, A. Q., Boger, H. A., and Lavin, A. (2017). Effects of fingolimod administration in a genetic model of cognitive deficits. *J. Neurosci. Res.* 95, 1174–1181. doi: 10.1002/jnr.23799

Berchtold, N. C., Coleman, P. D., Cribbs, D. H., Rogers, J., Gillen, D. L., and Cotman, C. W. (2013). Synaptic genes are extensively downregulated across multiple brain regions in normal human aging and Alzheimer's disease. *Neurobiol. Aging* 34, 1653–1661. doi: 10.1016/j.neurobiolaging.2012.11.024

Bolognin, S., Blanchard, J., Wang, X., Basurto-Islas, G., Tung, Y. C., Kohlbrenner, E., et al. (2012). An experimental rat model of sporadic Alzheimer's disease and rescue of cognitive impairment with a neurotrophic peptide. *Acta Neuropathol.* 123, 133–151. doi: 10.1007/s00401-011-0908-x

Brito-Moreira, J., Lourenco, M. V., Oliveira, M. M., Ribeiro, F. C., Ledo, J. H., Diniz, L. P., et al. (2017). Interaction of amyloid-β (Aβ) oligomers with neurexin 2α and neuroligin 1 mediates synapse damage and memory loss in mice. *J. Biol. Chem.* 292, 7327–7337. doi: 10.1074/jbc.M116.761189

Cai, F., Chen, B., Zhou, W., Zis, O., Liu, S., Holt, R. A., et al. (2008). SP1 regulates a human SNAP-25 gene expression. *J. Neurochem.* 105, 512–523. doi: 10.1111/j.1471-4159.2007.05167.x

Callahan, L. M., Vaules, W. A., and Coleman, P. D. (1999). Quantitative decrease in synaptophysin message expression and increase in cathepsin D message expression in Alzheimer disease neurons containing neurofibrillary tangles. *J. Neuropathol. Exp. Neurol.* 58, 275–287. doi: 10.1097/00005072-199903000-00007

Campenot, R. B., Walji, A. H., and Draker, D. D. (1991). Effects of sphingosine, staurosporine, and phorbol ester on neurites of rat sympathetic neurons growing in compartmented cultures. *J. Neurosci.* 11, 1126–1139. doi: 10.1523/JNEUROSCI.11-04-01126.1991

Carreras, I., Aytan, N., Choi, J.-K., Tognoni, C. M., Kowall, N. W., Jenkins, B. G., et al. (2019). Dual dose-dependent effects of fingolimod in a mouse model of Alzheimer's disease. *Sci. Rep.* 9, 10972–10972. doi: 10.1038/s41598-019-47287-1

Choi, J. W., Gardell, S. E., Herr, D. R., Rivera, R., Lee, C. W., Noguchi, K., et al. (2011). FTY720 (fingolimod) efficacy in an animal model of multiple sclerosis requires astrocyte sphingosine 1-phosphate receptor 1 (S1P1) modulation. *Proc. Natl. Acad. Sci. U. S. A.* 108, 751–756. doi: 10.1073/pnas.1014154108

Costa, A. S., Guerini, F. R., Arosio, B., Galimberti, D., Zanzottera, M., Bianchi, A., et al. (2019). SNARE complex polymorphisms associate with alterations of visual selective attention in Alzheimer's disease. *J. Alzheimers Dis.* 69, 179–188. doi: 10.3233/JAD-190147

Couttas, T. A., Kain, N., Daniels, B., Lim, X. Y., Shepherd, C., Kril, J., et al. (2014). Loss of the neuroprotective factor Sphingosine 1-phosphate early in Alzheimer's disease pathogenesis. *Acta Neuropathol. Commun.* 2:9. doi: 10.1186/2051-5960-2-9

Czubowicz, K., Jeśko, H., Wencel, P., Lukiw, W. J., and Strosznajder, R. P. (2019). The Role of ceramide and sphingosine-1-phosphate in Alzheimer's disease and other neurodegenerative disorders. *Mol. Neurobiol.* 56, 5436–5455. doi: 10.1007/s12035-018-1448-3

Darios, F. D., Jorgacevski, J., Flašker, A., Zorec, R., García-Martinez, V., Villanueva, J., et al. (2017). Sphingomimetic multiple sclerosis drug FTY720 activates vesicular synaptobrevin and augments neuroendocrine secretion. *Sci. Rep.* 7:5958. doi: 10.1038/s41598-017-05948-z

Doi, Y., Takeuchi, H., Horiuchi, H., Hanyu, T., Kawanokuchi, J., Jin, S., et al. (2013). Fingolimod phosphate attenuates oligomeric amyloid β-induced neurotoxicity via increased brain-derived neurotrophic factor expression in neurons. *PLoS ONE* 8:e61988. doi: 10.1371/journal.pone.0061988

Fagiani, F., Lanni, C., Racchi, M., Pascale, A., and Govoni, S. (2019). Amyloid-β and synaptic vesicle dynamics: a cacophonic orchestra. *J. Alzheimers Dis.* 72, 1–14. doi: 10.3233/JAD-190771

Ferreira, S. T., Lourenco, M. V., Oliveira, M. M., and De Felice, F. G. (2015). Soluble amyloid-β oligomers as synaptotoxins leading to cognitive impairment in Alzheimer's disease. *Front. Cell Neurosci.* 9:191. doi: 10.3389/fncel.2015.00191

Forner, S., Martini, A. C., Prieto, G. A., Dang, C. T., Rodriguez-Ortiz, C. J., Reyes-Ruiz, J. M., et al. (2019). Intra- and extracellular β-amyloid overexpression via adeno-associated virus-mediated gene transfer impairs memory and synaptic plasticity in the hippocampus. *Sci. Rep.* 9:15936. doi: 10.1038/s41598-019-52324-0

Fukumoto, K., Mizoguchi, H., Takeuchi, H., Horiuchi, H., Kawanokuchi, J., Jin, S., et al. (2014). Fingolimod increases brain-derived neurotrophic factor levels and ameliorates amyloid β-induced memory impairment. *Behav. Brain Res.* 268, 88–93. doi: 10.1016/j.bbr.2014.03.046

Furuya, S., Ono, K., and Hirabayashi, Y. (1995). Sphingolipid biosynthesis is necessary for dendrite growth and survival of cerebellar Purkinje cells in culture. *J. Neurochem.* 65, 1551–1561. doi: 10.1046/j.1471-4159.1995.65041551.x

Gaetani, L., Blennow, K., Calabresi, P., Di Filippo, M., Parnetti, L., and Zetterberg, H. (2019). Neurofilament light chain as a biomarker in neurological disorders. *J. Neurol. Neurosurg. Psychiatry* 90, 870–881. doi: 10.1136/jnnp-2018-320106

Gautam, V., D'Avanzo, C., Berezovska, O., Tanzi, R. E., and Kovacs, D. M. (2015). Synaptotagmins interact with APP and promote Aβ generation. *Mol. Neurodegener.* 10:31. doi: 10.1186/s13024-015-0028-5

Ghosh, A., Mizuno, K., Tiwari, S. S., Proitsi, P., Gomez Perez-Nievas, B., Glennon, E., et al. (2020). Alzheimer's disease-related dysregulation of mRNA translation causes key pathological features with ageing. *Transl. Psychiatry* 10:192. doi: 10.1038/s41398-020-00882-7

Gulisano, W., Melone, M., Ripoli, C., Tropea, M. R., Li Puma, D. D., Giunta, S., et al. (2019). Neuromodulatory action of picomolar extracellular Aβ42 oligomers on presynaptic and postsynaptic mechanisms underlying synaptic function and memory. *J. Neurosci.* 39, 5986–6000. doi: 10.1523/JNEUROSCI.0163-19.2019

Han, X. (2010). Multi-dimensional mass spectrometry-based shotgun lipidomics and the altered lipids at the mild cognitive impairment stage of Alzheimer's disease. *Biochim. Biophys. Acta* 1801, 774–783. doi: 10.1016/j.bbalip.2010.01.010

Harel, R., and Futerman, A. H. (1993). Inhibition of sphingolipid synthesis affects axonal outgrowth in cultured hippocampal neurons. *J. Biol. Chem.* 268, 14476–14481. doi: 10.1016/S0021-9258(19)85263-8

Hawk, B. J. D., Khounlo, R., and Shin, Y. K. (2019). Alpha-synuclein continues to enhance SNARE-dependent vesicle docking at exorbitant concentrations. *Front. Neurosci.* 13:216. doi: 10.3389/fnins.2019.00216

Heffernan, J. M., Eastwood, S. L., Nagy, Z., Sanders, M. W., McDonald, B., and Harrison, P. J. (1998). Temporal cortex synaptophysin mRNA is reduced in Alzheimer's disease and is negatively correlated with the severity of dementia. *Exp. Neurol.* 150, 235–239. doi: 10.1006/exnr.1997.6772

Hemmati, F., Dargahi, L., Nasoohi, S., Omidbakhsh, R., Mohamed, Z., Chik, Z., et al. (2013). Neurorestorative effect of FTY720 in a rat model of Alzheimer's disease: comparison with memantine. *Behav. Brain Res.* 252, 415–421. doi: 10.1016/j.bbr.2013.06.016

Hering, H., Lin, C. C., and Sheng, M. (2003). Lipid rafts in the maintenance of synapses, dendritic spines, and surface AMPA receptor stability. *J. Neurosci.* 23, 3262–3271. doi: 10.1523/JNEUROSCI.23-08-03262.2003

Hsieh, H., Boehm, J., Sato, C., Iwatsubo, T., Tomita, T., Sisodia, S., et al. (2006). AMPAR removal underlies Abeta-induced synaptic depression and dendritic spine loss. *Neuron* 52, 831–843. doi: 10.1016/j.neuron.2006.10.035

Hsu, C. K., Lee, I. T., Lin, C. C., Hsiao, L. D., and Yang, C. M. (2015). Sphingosine-1-phosphate mediates COX-2 expression and PGE2 /IL-6 secretion via c-Src-dependent AP-1 activation. *J. Cell Physiol.* 230, 702–715. doi: 10.1002/jcp.24795

Hübner, K., Windoffer, R., Hutter, H., and Leube, R. E. (2002). Tetraspan vesicle membrane proteins: synthesis, subcellular localization, and functional properties. *Int. Rev. Cytol.* 214, 103–159. doi: 10.1016/S0074-7696(02)14004-6

Ishibashi, K., Tomiyama, T., Nishitsuji, K., Hara, M., and Mori, H. (2006). Absence of synaptophysin near cortical neurons containing oligomer Abeta in Alzheimer's disease brain. *J. Neurosci. Res.* 84, 632–636. doi: 10.1002/jnr.20952

Jeśko, H., Stepień, A., Lukiw, W. J., and Strosznajder, R. P. (2019a). The cross-talk between sphingolipids and insulin-like growth factor signaling: significance for aging and neurodegeneration. *Mol. Neurobiol.* 56, 3501–3521. doi: 10.1007/s12035-018-1286-3

Jeśko, H., Wencel, P. L., Lukiw, W. J., and Strosznajder, R. P. (2019b). Modulatory effects of fingolimod (FTY720) on the expression of sphingolipid metabolism-related genes in an animal model of Alzheimer's disease. *Mol. Neurobiol.* 56, 174–185. doi: 10.1007/s12035-018-1040-x

Jeśko, H., Wencel, P. L., Wójtowicz, S., Strosznajder, J., Lukiw, W. J., and Strosznajder, R. P. (2020). Fingolimod affects transcription of genes encoding enzymes of ceramide metabolism in animal model of Alzheimer's disease. *Mol. Neurobiol.* 57, 2799–2811. doi: 10.1007/s12035-020-01908-3

Joshi, P., Gabrielli, M., Ponzoni, L., Pelucchi, S., Stravalaci, M., Beeg, M., et al. (2017). Fingolimod limits acute Aβ neurotoxicity and promotes synaptic versus extrasynaptic NMDA receptor functionality in hippocampal neurons. *Sci. Rep.* 7:41734. doi: 10.1038/srep41734

Kamenetz, F., Tomita, T., Hsieh, H., Seabrook, G., Borchelt, D., Iwatsubo, T., et al. (2003). APP processing and synaptic function. *Neuron* 37, 925–937. doi: 10.1016/S0896-6273(03)00124-7

Kaneider, N. C., Lindner, J., Feistritzer, C., Sturn, D. H., Mosheimer, B. A., Djanani, A. M., et al. (2004). The immune modulator FTY720 targets sphingosine-kinase-dependent migration of human monocytes in response to amyloid beta-protein and its precursor. *FASEB J.* 18, 1309–1311. doi: 10.1096/fj.03-1050fje

Karmakar, S., Sharma, L. G., Roy, A., Patel, A., and Pandey, L. M. (2019). Neuronal SNARE complex: a protein folding system with intricate protein-protein interactions, and its common neuropathological hallmark, SNAP25. *Neurochem. Int.* 122, 196–207. doi: 10.1016/j.neuint.2018.12.001

Kartalou, G.-I., Salgueiro-Pereira, A. R., Endres, T., Lesnikova, A., Casarotto, P., Pousinha, P., et al. (2020). Anti-inflammatory treatment with FTY720 starting after onset of symptoms reverses synaptic deficits in an AD mouse model. *Int. J. Mol. Sci.* 21:8957. doi: 10.3390/ijms21238957

Katsel, P., Li, C., and Haroutunian, V. (2007). Gene expression alterations in the sphingolipid metabolism pathways during progression of dementia and Alzheimer's disease: a shift toward ceramide accumulation at the earliest recognizable stages of Alzheimer's disease? *Neurochem. Res.* 32, 845–856. doi: 10.1007/s11064-007-9297-x

Khvotchev, M. V., and Südhof, T. C. (2004). Stimulus-dependent dynamic homo- and heteromultimerization of synaptobrevin/VAMP and synaptophysin. *Biochemistry* 43, 15037–15043. doi: 10.1021/bi048290+

Koppensteiner, P., Trinchese, F., Fà, M., Puzzo, D., Gulisano, W., Yan, S., et al. (2016). Time-dependent reversal of synaptic plasticity induced by physiological concentrations of oligomeric Aβ42: an early index of Alzheimer's disease. *Sci. Rep.* 6:32553. doi: 10.1038/srep32553

Lippa, C. F. (2004). Synaptophysin immunoreactivity in Pick's disease: comparison with Alzheimer's disease and dementia with Lewy bodies. *Am. J. Alzheimers Dis. Other Demen.* 19, 341–344. doi: 10.1177/153331750401900606

Loeffler, T., Schilcher, I., Flunkert, S., and Hutter-Paier, B. (2020). Neurofilament-light chain as biomarker of neurodegenerative and rare diseases with high translational value. *Front. Neurosci.* 14:579. doi: 10.3389/fnins.2020.00579

Lukiw, W. J., Cong, L., Jaber, V., and Zhao, Y. (2018). Microbiome-derived lipopolysaccharide (LPS) selectively inhibits neurofilament light chain (NF-L) gene expression in human neuronal-glial (HNG) cells in primary culture. *Front. Neurosci.* 12:896. doi: 10.3389/fnins.2018.00896

Lukiw, W. J., Pogue, A., and Hill, J. M. (2020). SARS-CoV-2 infectivity and neurological targets in the brain. *Cell Mol. Neurobiol.* 1–8. doi: 10.1007/s10571-020-00947-7

Lukiw, W. J., Wong, L., and McLachlan, D. R. (1990). Cytoskeletal messenger RNA stability in human neocortex: studies in normal aging and in Alzheimer's disease. *Int. J. Neurosci.* 55, 81–88. doi: 10.3109/00207459008985953

Lukiw, W. J., Zhao, Y., and Cui, J. G. (2008). An NF-kappaB-sensitive micro RNA-146a-mediated inflammatory circuit in Alzheimer disease and in stressed human brain cells. *J. Biol. Chem.* 283, 31315–31322. doi: 10.1074/jbc.M805371200

Madrigal, M. P., Portalés, A., SanJuan, M. P., and Jurado, S. (2019). Postsynaptic SNARE proteins: role in synaptic transmission and plasticity. *Neuroscience* 420, 12–21. doi: 10.1016/j.neuroscience.2018.11.012

Marsh, J., and Alifragis, P. (2018). Synaptic dysfunction in Alzheimer's disease: the effects of amyloid beta on synaptic vesicle dynamics as a novel target for therapeutic intervention. *Neural Regen. Res.* 13, 616–623. doi: 10.4103/1673-5374.230276

Martin, S. B., Dowling, A. L., Lianekhammy, J., Lott, I. T., Doran, E., Murphy, M. P., et al. (2014). Synaptophysin and synaptojanin-1 in Down syndrome are differentially affected by Alzheimer's disease. *J. Alzheimers Dis.* 42, 767–775. doi: 10.3233/JAD-140795

Masliah, E., Terry, R. D., DeTeresa, R. M., and Hansen, L. A. (1989). Immunohistochemical quantification of the synapse-related protein synaptophysin in Alzheimer disease. *Neurosci. Lett.* 103, 234–239. doi: 10.1016/0304-3940(89)90582-X

McLachlan, D. R., Lukiw, W. J., Wong, L., Bergeron, C., and Bech-Hansen, N. T. (1988). Selective messenger RNA reduction in Alzheimer's disease. *Brain Res.* 427, 255–261. doi: 10.1016/0169-328X(88)90048-4

McManus, R. M., Finucane, O. M., Wilk, M. M., Mills, K. H. G., and Lynch, M. A. (2017). FTY720 Attenuates infection-induced enhancement of Aβ accumulation in APP/PS1 mice by modulating astrocytic activation. *J. Neuroimmune Pharmacol.* 12, 670–681. doi: 10.1007/s11481-017-9753-6

Moechars, D., Dewachter, I., Lorent, K., Revers,é, D., Baekelandt, V., Naidu, A., et al. (1999). Early phenotypic changes in transgenic mice that overexpress different mutants of amyloid precursor protein in brain. *J. Biol. Chem.* 274, 6483–6492. doi: 10.1074/jbc.274.10.6483

Naito, Y., Tanabe, Y., Lee, A. K., Hamel, E., and Takahashi, H. (2017). Amyloid-β oligomers interact with neurexin and diminish neurexin-mediated excitatory presynaptic organization. *Sci. Rep.* 7:42548. doi: 10.1038/srep42548

Nazari, M., Keshavarz, S., Rafati, A., Namavar, M. R., and Haghani, M. (2016). Fingolimod (FTY720) improves hippocampal synaptic plasticity and memory deficit in rats following focal cerebral ischemia. *Brain Res. Bull.* 124, 95–102. doi: 10.1016/j.brainresbull.2016.04.004

Olsen, A. S. B., and Færgeman, N. J. (2017). Sphingolipids: membrane microdomains in brain development, function and neurological diseases. *Open Biol.* 7:170069. doi: 10.1098/rsob.170069

Palermo, G., Mazzucchi, S., Della Vecchia, A., Siciliano, G., Bonuccelli, U., Azuar, C., et al. (2020). Different clinical contexts of use of blood neurofilament light chain protein in the spectrum of neurodegenerative diseases. *Mol. Neurobiol.* 57, 4667–4691. doi: 10.1007/s12035-020-02035-9

Patwardhan, G. A., Hosain, S. B., Liu, D. X., Khiste, S. K., Zhao, Y., Bielawski, J., et al. (2014). Ceramide modulates pre-mRNA splicing to restore the expression of wild-type tumor suppressor p53 in deletion-mutant cancer cells. *Biochim. Biophys. Acta* 1841, 1571–1580. doi: 10.1016/j.bbalip.2014.08.017

Poti, F., Costa, S., Bergonzini, V., Galletti, M., Pignatti, E., Weber, C., et al. (2012). Effect of sphingosine 1-phosphate (S1P) receptor agonists FTY720 and CYM5442 on atherosclerosis development in LDL receptor deficient (LDL-R?/?) mice. *Vascul Pharmacol.* 57, 56–64. doi: 10.1016/j.vph.2012.03.003

Puglielli, L., Ellis, B. C., Saunders, A. J., and Kovacs, D. M. (2003). Ceramide stabilizes beta-site amyloid precursor protein-cleaving enzyme 1 and promotes amyloid beta-peptide biogenesis. *J. Biol. Chem.* 278, 19777–19783. doi: 10.1074/jbc.M300466200

Qin, S., Hu, X. Y., Xu, H., and Zhou, J. N. (2004). Regional alteration of synapsin I in the hippocampal formation of Alzheimer's disease patients. *Acta Neuropathol.* 107, 209–215. doi: 10.1007/s00401-003-0800-4

Rajmohan, R., and Reddy, P. H. (2017). Amyloid-beta and phosphorylated tau accumulations cause abnormalities at synapses of Alzheimer's disease neurons. *J. Alzheimers Dis.* 57, 975–999. doi: 10.3233/JAD-160612

Riganti, L., Antonucci, F., Gabrielli, M., Prada, I., Giussani, P., Viani, P., et al. (2016). Sphingosine-1-phosphate (S1P) impacts presynaptic functions by regulating synapsin I localization in the presynaptic compartment. *J. Neurosci.* 36, 4624–4634. doi: 10.1523/JNEUROSCI.3588-15.2016

Russell, C. L., Semerdjieva, S., Empson, R. M., Austen, B. M., Beesley, P. W., and Alifragis, P. (2012). Amyloid-β acts as a regulator of neurotransmitter release disrupting the interaction between synaptophysin and VAMP2. *PLoS ONE* 7:e43201. doi: 10.1371/journal.pone.0043201

Sawamura, N., Ko, M., Yu, W., Zou, K., Hanada, K., Suzuki, T., et al. (2004). Modulation of amyloid precursor protein cleavage by cellular sphingolipids. *J. Biol. Chem.* 279, 11984–11991. doi: 10.1074/jbc.M309832200

Scheff, S. W., Price, D. A., Schmitt, F. A., and Mufson, E. J. (2006). Hippocampal synaptic loss in early Alzheimer's disease and mild cognitive impairment. *Neurobiol. Aging* 27, 1372–1384. doi: 10.1016/j.neurobiolaging.2005.09.012

Sevlever, D., Zou, F., Ma, L., Carrasquillo, S., Crump, M. G., Culley, O. J., et al. (2015). Genetically-controlled vesicle-associated membrane protein 1 expression may contribute to Alzheimer's pathophysiology and susceptibility. *Mol. Neurodegener.* 10:18. doi: 10.1186/s13024-015-0047-2

Sharda, N., Pengo, T., Wang, Z., and Kandimalla, K. K. (2020). Amyloid-β peptides disrupt interactions between VAMP-2 and SNAP-25 in neuronal cells as determined by FRET/FLIM. *J. Alzheimers Dis.* 77, 423–435. doi: 10.3233/JAD-200065

Sica, F., Centonze, D., and Buttari, F. (2019). Fingolimod immune effects beyond its sequestration ability. *Neurol. Ther.* 8, 231–240. doi: 10.1007/s40120-019-00162-7

Sindi, I. A., Tannenberg, R. K., and Dodd, P. R. (2014). Role for the neurexin-neuroligin complex in Alzheimer's disease. *Neurobiol. Aging* 35, 746–756. doi: 10.1016/j.neurobiolaging.2013.09.032

Song, S. H., and Augustine, G. J. (2015). Synapsin isoforms and synaptic vesicle trafficking. *Mol. Cells* 38, 936–940. doi: 10.14348/molcells.2015.0233

Sze, C. I., Troncoso, J. C., Kawas, C., Mouton, P., Price, D. L., and Martin, L. J. (1997). Loss of the presynaptic vesicle protein synaptophysin in hippocampus correlates with cognitive decline in Alzheimer disease. *J. Neuropathol. Exp. Neurol.* 56, 933–944. doi: 10.1097/00005072-199708000-00011

Takasugi, N., Sasaki, T., Ebinuma, I., Osawa, S., Isshiki, H., Takeo, K., et al. (2013). FTY720/fingolimod, a sphingosine analogue, reduces amyloid-β production in neurons. *PLoS ONE* 8:e64050. doi: 10.1371/journal.pone.0064050

Tamboli, I. Y., Prager, K., Barth, E., Heneka, M., Sandhoff, K., and Walter, J. (2005). Inhibition of glycosphingolipid biosynthesis reduces secretion of the beta-amyloid precursor protein and amyloid beta-peptide. *J. Biol. Chem.* 280, 28110–28117. doi: 10.1074/jbc.M414525200

Tran, M. H., Yamada, K., Nakajima, A., Mizuno, M., He, J., Kamei, H., et al. (2003). Tyrosine nitration of a synaptic protein synaptophysin contributes to amyloid beta-peptide-induced cholinergic dysfunction. *Mol. Psychiatry* 8, 407–412. doi: 10.1038/sj.mp.4001240

Ulloa, F., Cotrufo, T., Ricolo, D., Soriano, E., and Araújo, S. J. (2018). SNARE complex in axonal guidance and neuroregeneration. *Neural Regen. Res.* 13, 386–392. doi: 10.4103/1673-5374.228710

Vallortigara, J., Whitfield, D., Quelch, W., Alghamdi, A., Howlett, D., Hortobágyi, T., et al. (2016). Decreased levels of VAMP2 and monomeric alpha-synuclein correlate with duration of dementia. *J. Alzheimers Dis.* 50, 101–110. doi: 10.3233/JAD-150707

Van Brocklyn, J. R., and Williams, J. B. (2012). The control of the balance between ceramide and sphingosine-1-phosphate by sphingosine kinase: oxidative stress and the seesaw of cell survival and death. *Comp. Biochem. Physiol. B Biochem. Mol. Biol.* 163, 26–36. doi: 10.1016/j.cbpb.2012.05.006

Van Dorpe, J., Smeijers, L., Dewachter, I., Nuyens, D., Spittaels, K., Van Den Haute, C., et al. (2000). Prominent cerebral amyloid angiopathy in transgenic mice overexpressing the london mutant of human APP in neurons. *Am. J. Pathol.* 157, 1283–1298. doi: 10.1016/S0002-9440(10)64644-5

Volynski, K. E., and Krishnakumar, S. S. (2018). Synergistic control of neurotransmitter release by different members of the synaptotagmin family. *Curr. Opin. Neurobiol.* 51, 154–162. doi: 10.1016/j.conb.2018.05.006

Walsh, D. M., Klyubin, I., Fadeeva, J. V., Cullen, W. K., Anwyl, R., Wolfe, M. S., et al. (2002). Naturally secreted oligomers of amyloid beta protein potently inhibit hippocampal long-term potentiation *in vivo*. *Nature* 416, 535–539. doi: 10.1038/416535a

Yang, Y., Kim, J., Kim, H. Y., Ryoo, N., Lee, S., Kim, Y., et al. (2015). Amyloid-β oligomers may impair SNARE-mediated exocytosis by direct binding to syntaxin 1a. *Cell Rep.* 12, 1244–1251. doi: 10.1016/j.celrep.2015.07.044

Zamponi, E., and Pigino, G. F. (2019). Protein misfolding, signaling abnormalities and altered fast axonal transport: implications for Alzheimer and prion diseases. *Front. Cell Neurosci.* 13:350. doi: 10.3389/fncel.2019.00350

Zhang, J., Xiao, B., Li, C. X., and Wang, Y. (2020). Fingolimod (FTY720) improves postoperative cognitive dysfunction in mice subjected to D-galactose-induced aging. *Neural Regen. Res.* 15, 1308–1315. doi: 10.4103/1673-5374.272617

Zoltowska, K. M., Maesako, M., Lushnikova, I., Takeda, S., Keller, L. J., Skibo, G., et al. (2017). Dynamic presenilin 1 and synaptotagmin 1 interaction modulates exocytosis and amyloid β production. *Mol. Neurodegener.* 12:15. doi: 10.1186/s13024-017-0159-y

Zou, X., Gao, Y., Ruvolo, V. R., Gardner, T. L., Ruvolo, P. P., and Brown, R. E. (2011). Human glycolipid transfer protein gene (GLTP) expression is regulated by Sp1 and Sp3: involvement of the bioactive sphingolipid ceramide. *J. Biol. Chem.* 286, 1301–1311. doi: 10.1074/jbc.M110.127837

Disclaimer: The content of this manuscript is solely the responsibility of the authors and does not necessarily represent the official views of the National Institute on Aging, the National Center for Research Resources, or the National Institutes of Health.

Conflict of Interest: The authors declare that the research was conducted in the absence of any commercial or financial relationships that could be construed as a potential conflict of interest.

frontiers in Molecular Neuroscience

REVIEW
published: 02 December 2021
doi: 10.3389/fnmol.2021.757515

Calcium Ions Aggravate Alzheimer's Disease Through the Aberrant Activation of Neuronal Networks, Leading to Synaptic and Cognitive Deficits

*Pei-Pei Guan†, Long-Long Cao†, Yi Yang and Pu Wang**

College of Life and Health Sciences, Northeastern University, Shenyang, China

OPEN ACCESS

Edited by:
Daniela Puzzo, University of Catania, Italy

Reviewed by:
Balaji Krishnan, University of Texas Medical Branch at Galveston, United States
Maud Gratuze, Washington University in St. Louis, United States
Roberto Piacentini, Catholic University of the Sacred Heart, Italy

***Correspondence:**
Pu Wang
wangpu@mail.neu.edu.cn

†These authors have contributed equally to this work

Specialty section:
This article was submitted to Brain Disease Mechanisms, a section of the journal Frontiers in Molecular Neuroscience

Received: *12 August 2021*
Accepted: *04 November 2021*
Published: *02 December 2021*

Citation:
Guan P-P, Cao L-L, Yang Y and Wang P (2021) Calcium Ions Aggravate Alzheimer's Disease Through the Aberrant Activation of Neuronal Networks, Leading to Synaptic and Cognitive Deficits. Front. Mol. Neurosci. 14:757515. doi: 10.3389/fnmol.2021.757515

Alzheimer's disease (AD) is a neurodegenerative disease that is characterized by the production and deposition of β-amyloid protein (Aβ) and hyperphosphorylated tau, leading to the formation of β-amyloid plaques (APs) and neurofibrillary tangles (NFTs). Although calcium ions (Ca^{2+}) promote the formation of APs and NFTs, no systematic review of the mechanisms by which Ca^{2+} affects the development and progression of AD has been published. Therefore, the current review aimed to fill the gaps between elevated Ca^{2+} levels and the pathogenesis of AD. Specifically, we mainly focus on the molecular mechanisms by which Ca^{2+} affects the neuronal networks of neuroinflammation, neuronal injury, neurogenesis, neurotoxicity, neuroprotection, and autophagy. Furthermore, the roles of Ca^{2+} transporters located in the cell membrane, endoplasmic reticulum (ER), mitochondria and lysosome in mediating the effects of Ca^{2+} on activating neuronal networks that ultimately contribute to the development and progression of AD are discussed. Finally, the drug candidates derived from herbs used as food or seasoning in Chinese daily life are summarized to provide a theoretical basis for improving the clinical treatment of AD.

Keywords: calcium ions, transporters, mechanisms, Alzheimer's disease, review

INTRODUCTION

Alzheimer's disease (AD) is a neurodegenerative disease with cognitive deficit as the main characteristic (Elgh et al., 2006). During the course of AD development and progression, calcium ion (Ca^{2+}) concentrations are obviously increased in the brains of patients with AD and APP/PS1 Tg mice (Cao et al., 2019). One report has shown that β-amyloid protein $(Aβ)_{1–40}$ has the ability to increase Ca^{2+} influx in rat cortical synaptosomes and cultured cortical neurons (MacManus et al., 2000). Similar to $Aβ_{1–40}$, $Aβ_{1–42}$ induce the Ca^{2+} influx *via* RyRs in primary cultured hippocampal neurons (Marcantoni et al., 2020). Furthermore, the $Aβ_{25–35}$ peptide promotes Ca^{2+} influx by activating L- and T-type Ca^{2+} channels in rat hippocampal slices (Li et al., 2010). The APP intracellular domain (AICD), a APP cleavage fragment, may act as a transcription

factor to activate the Ca^{2+} signaling system (Cao and Südhof, 2001; Leissring et al., 2002). Because of the self-aggregating characteristics of Aβ, Aβ oligomers can promote Ca^{2+} influx through N-methyl-D-aspartic acid receptor (NMDAR) channels in a short period of time (Kelly and Ferreira, 2006). More directly, Arispe et al. (2010) found that the aggregates of $Aβ_{1–40}$ and $Aβ_{1–42}$ form a cation channel on the surface of an artificial lipid membrane that allows the passage of Ca^{2+}. The pore formation ability of Aβ was confirmed and corroborated by atomic force microscopy (Lin et al., 2001), electron microscopy (Lashuel et al., 2002, 2003), and a theoretical model (Durell et al., 1994; Jang et al., 2008).

Reciprocally, Ca^{2+} is not a passive contributor to the development and progression of AD. In PS-mutant AD brain tissue, a Ca^{2+} metabolic disorder was evident before the formation of APs or NFTs (Etcheberrigaray et al., 1998), which indicated that the metabolic disorder caused by Ca^{2+} located in the cytoplasm might be the cause of AD. Based on this hypothesis, previous studies have shown that Ca^{2+} influx increases the production and aggregation of Aβ and the phosphorylated tau protein, which affects the learning and memory of patients with AD (Etcheberrigaray et al., 1998; Zempel et al., 2010; Tong et al., 2018). Moreover, Ca^{2+} imbalance leads to dysregulated metabolism that affects many neurophysiological functions related to AD, including the regulation of neuroinflammation, response to neuronal injury, neuronal regeneration, neurotoxicity and autophagy (Wahlestedt et al., 1993; Liu and Zukin, 2007; Decuypere et al., 2011a; Sama and Norris, 2013; Song et al., 2019). These actions of Ca^{2+} may finally contribute to neuronal death, which results in cognitive decline during the course of AD development and progression.

Given the multiple functions of Ca^{2+} in AD, its transporters in the cell membrane, endoplasmic reticulum (ER), mitochondria and lysosomes must be involved in regulating the development and progression of AD. As an antagonist of NMDAR, a Ca^{2+} transporter on the surface of the nerve cell membrane, memantine significantly inhibits Ca^{2+} influx and was the first Food and Drug Administration (FDA)-approved drug for the treatment of moderate to severe AD in patients (Bullock, 2006). Regarding the important reservoir of Ca^{2+} in neurons, the ER has been reported to release Ca^{2+} to the cytosol, which contributes to the development and progression of AD (Guan et al., 2021). Although direct evidence showing the relationship between Ca^{2+} transport from mitochondria and lysosomes and the learning ability of patients with AD is unavailable, voltage-dependent anion channel protein 1 (VDAC1) is a hub protein that interacts with phosphorylated tau, Aβ, and γ-secretase, and it contributes to their toxic effects on triggering cell death and potentially leading to the dementia that is a characteristic of AD (Shoshan-Barmatz et al., 2018). All this evidence prompted us to summarize the roles of Ca^{2+} transporters located in different organelles in regulating the development and progression of AD.

Therefore, this review mainly summarizes the molecular mechanisms by which a Ca^{2+} imbalance in individuals with AD affects the regulation of neuroinflammation, neuronal injury, neuronal regeneration, neurotoxicity, neuroprotection, and autophagy, specifically from the perspective of Ca^{2+} transporters in the cell, mitochondria, endoplasmic reticulum and lysosomal membranes. By addressing these mechanisms, we will fill the gaps between increased Ca^{2+} concentrations and the fate of neurons, which results in dementia.

CROSSTALK BETWEEN FACTORS RESPONSIBLE FOR Ca^{2+} DYSHOMEOSTASIS AND NEUROINFLAMMATION

Ca^{2+} Increases the Production of Proinflammatory Cytokines

Neuroinflammation is widely accepted to be mediated by Ca^{2+} dyshomeostasis and induces the cognitive decline associated with AD. This process is studied to understand the inherent mechanisms by which Ca^{2+} exerts an effect. For example, Ca^{2+} increases the production of interleukin (IL)-1β and tumor necrosis factor α (TNF-α) *via* calcineurin (CaN) in glial cells (Sama and Norris, 2013). Consistently, an indirect blockade of Ca^{2+} entry into lipopolysaccharide (LPS)-activated microglia stimulates the production of proinflammatory cytokines, such as TNF-α and IL-6 (Dolga et al., 2012). These observations revealed critical roles for Ca^{2+} in inducing neuroinflammation by concurrently increasing the production of proinflammatory cytokines and decreasing the levels of anti-inflammatory cytokines.

Transporters on the Cell Membrane Mediate the Effects of Ca^{2+} on the Secretion of Proinflammatory Cytokines

Based on these observations, Ca^{2+} transporters were found to be involved in regulating neuroinflammation. More specifically, NMDAR is critical for mediating the effects of Ca^{2+} on stimulating the production of proinflammatory cytokines, such as IL-1β and TNF-α, in primary mouse hippocampal neurons and lamina II neurons of isolated spinal cord slices (Kawasaki et al., 2008; Huang et al., 2011). By deactivating NMDAR, sevoflurane, an NMDAR antagonist, inhibits the production of IL-1β, TNF-α, IL-6, and IL-8, whereas the addition of the NMDAR agonist D-cycloserine restores the suppression of ageing phenotype acquisition in rats (Yang Z. Y. et al., 2020). NMDAR overexpression in primary cultured microglial cells was induced to synthesize nitric oxide (NO) by activating the NF-κB signaling pathway and to exclude the nonspecific action of these pharmacological interventions (Murugan et al., 2011). In the context of inflammation, NMDAR blockade attenuates the clinical symptoms of glutamate excitotoxicity, suggesting that NMDAR exerts potential neuroprotective effects (Wallström et al., 1996). Similar to this observation, blocking the AMPA/kainate receptor also results in the neuroprotection of encephalomyelitis-sensitized mice (Pitt et al., 2000; Smith et al., 2000). Based on this observation, researchers have readily deduced that α-amino-3-hydroxy-5-methyl-4-isoxazole propionate receptor (AMPAR) might also be involved in regulating neuroinflammation. In SG neurons and lamina II neurons isolated from spinal cord slices, AMPAR was reported

to mediate Ca^{2+}-stimulated secretion of proinflammatory cytokines, such as IL-1β and TNF-α (Liu et al., 2013). Perampanel, an AMPAR antagonist, concurrently suppressed the expression of proinflammatory cytokines, including IL-1β and TNF-α, and upregulates the expression of anti-inflammatory cytokines, including IL-10 and Transforming Growth Factor Beta 1 (TGF β1), in a rat model of traumatic brain injury (TBI; Chen T. et al., 2017).

In addition to glutamate receptors serving as transporters of Ca^{2+}, some Ca^{2+} transporters in the cell membrane are reported to be involved in regulating neuroinflammation. For example, the blockade of L-type voltage-gated calcium channels (L-VGCC) by bepridil, nitrendipine or nimodipine attenuates neuroinflammation by deactivating astrocytes and microglial cells in LPS-stimulated or artificial cerebrospinal fluid (aCSF)-injected (i.c.v.) rats and astrocytes from the CA1 region of the hippocampus (Brand-Schieber and Werner, 2004; Daschil et al., 2013; Espinosa-Parrilla et al., 2015; Hopp et al., 2015). These observations were corroborated by the ability of Ca^{2+} to induce TNF-α production in cultured rat hippocampal neurons through an L-VGCC-dependent mechanism (Furukawa and Mattson, 1998). In addition, transient receptor potential channels (TRPs) have been identified in mammals and are grouped into six families associated with the onset of neurodegenerative diseases of the central nervous system (CNS): vanilloid TRP (TRPV), melastatin TRP (TRPM), ankyrin TRP (TRPA), polycystin TRP (TRPP), and canonical or classical TRP (TRPC) channels (Morelli et al., 2013). Among these channels, TRPM2 deletion suppresses cytokine production by deactivating microglial cells in TRPM2-knockout mice (Miyanohara et al., 2018; Kakae et al., 2019). Activation of the TRPV1 channel increases the production of proinflammatory cytokines, such as IL-6, in microglial cells (Sappington and Calkins, 2008). The roles of TRPV4 in inflammation are still being debated. By blocking TRPV4 channels, the release of IL-1β and TNF-α is inhibited because of the reduced Ca^{2+} influx, leading to the attenuation of glial cell-mediated inflammation (Shi et al., 2013). In contrast, the opening of TRPV4 channels by a selective TRPV4 agonist, 4α-phorbol 12, 13-didecanoate (4α-PDD), prevents microglial activation and TNF-α release after LPS treatment, and TRPV4 knockdown eliminates the inhibitory effect of agonists on the release of TNF-α from cultured microglial cells (Konno et al., 2012). According to these findings, TRPV4 activation may be induced by microglial cell swelling after activation with LPS. Channel activation may thus serve as an autoregulator to avoid excess microglial activation. In addition, TRPC1-mediated negative regulation may exert an immunosuppressive effect by blocking the initiation of inflammatory pathways in primary microglial cells (Sun Y. et al., 2014; **Figure 1**). Although Apolipoprotein E4 (APOE4) is not regarded as a canonical Ca^{2+} transporter, human APOE4 increases the activity of microglial cells by inducing the expression of IL-1β in E4F AD mice (Rodriguez et al., 2014). In contrast to APOE4, other isoforms of APOEs inhibit the synthesis of inflammatory mediators, including COX-2, PGE_2, and IL-1β, in primary cultured microglia obtained from the adult rat brain cortex (Chen et al., 2005).

The Endoplasmic Reticulum Is Involved in Regulating the Production of Proinflammatory Cytokines and Represents Intracellular Ca^{2+} Stores

Regarding intracellular stores, genetic ablation of type 2 inositol 1,4,5-triphosphate receptor (InsP3R2) increases the production of cytokines in $SOD1^{G93A}$ mice (Staats et al., 2016). By blocking the activity of Ryanodine Receptor (RyR) with dantrolene, the secretion of inflammatory markers is attenuated because of the deactivation of microglia in LPS-infused rats (Hopp et al., 2015). Treatment with PK11195, a mitochondrial ligand, inhibits store-operated calcium entry (SOCE)-mediated Ca^{2+} influx, resulting in the downregulation of COX-2 expression in human microglial cells (Hong et al., 2006). Thus, the endoplasmic reticulum (ER), as an intracellular Ca^{2+} store, is critical for regulating neuroinflammation *via* InsP3R-, RyR- and SOCE-dependent mechanisms. Interferon α/β (IFNα/β) induce cell apoptosis through Ca^{2+} release-activated Ca^{2+} (CRAC; Yue et al., 2012). As an important component of the mitochondrial permeability transition pore (mPTP), cyclophilin (CypD) knockdown decreases the secretion of proinflammatory cytokines, including Vascular Cell Adhesion Molecule 1 (VCAM-1), IL-6 and TNF-α, in the arteries of mice (Liu et al., 2019; **Figure 3**).

With opposite effects, proinflammatory cytokines have the ability to modulate the Ca^{2+} balance *via* their transporters. For example, TNF-α, IL-1β, and IFNγ increase the influx of Ca^{2+} into microglial cells, which indicates crosstalk between Ca^{2+} and neuroinflammatory factors in cultured hippocampal neurons (Goghari et al., 2000; McLarnon et al., 2001; Franciosi et al., 2002). IL-1β increases the expression of AMPAR on the cell surface, which potentially contributes to the entry of Ca^{2+} into hippocampal neurons (Viviani et al., 2003; Simões et al., 2012). In contrast to AMPAR, IL-1β inhibits L-VGCC activity by suppressing the protein expression of Ca^{2+} channels in primary cultured neurons (Zhou et al., 2006; Zhou, 2010). In addition, IL-1β is responsible for increasing the expression of TRPM2, leading to the influx of Ca^{2+} to microglial cells (Fonfria et al., 2006). Similar to IL-1β, IL-6 potentiates Ca^{2+} entry through NMDARs in hippocampal neurons (Orellana et al., 2005). Although IL-6 is not expressed in neuronal cells, it downregulates the expression of SERCA2, which blocks Ca^{2+} entry into the ER, thus maintaining high levels of cytosolic Ca^{2+} in cardiac myocytes (Villegas et al., 2000). Similar to other cytokines, TNF-α increases Ca^{2+} currents through NMDARs in cultured rat hippocampal neurons (Furukawa and Mattson, 1998). In addition, TNF-α induces the rapid insertion of AMPAR into the membranes of hippocampal pyramidal neurons (Ogoshi et al., 2005). In addition, the colocalization of GluA1, GluA2 and GluA4 and synaptophysin on the neural crest also indicates the transportation of AMPAR to synapses (Wigerblad et al., 2017). In contrast, TNF-α decreases Ca^{2+} influx by inhibiting the activity of L-VGCCs in cultured rat hippocampal neurons and hippocampal CA1 neurons (Furukawa and Mattson, 1998; Sama et al., 2012). Regarding the regulation of intracellular stores, impaired TNF-α signaling disrupts the

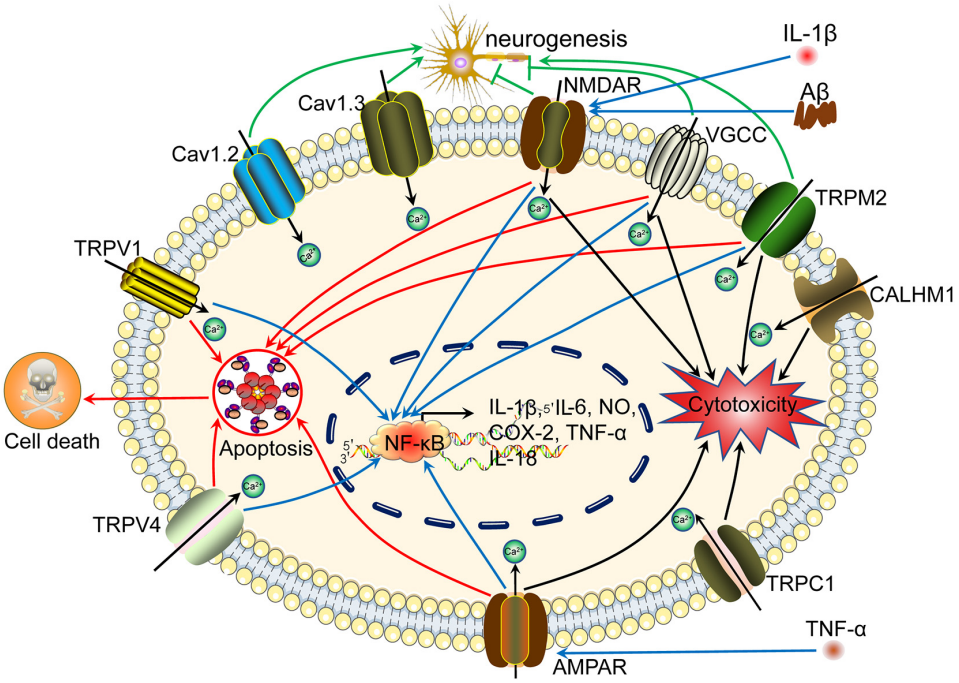

FIGURE 1 | Ca^{2+} participates in regulating neuroinflammation, neuronal injury, neurogenesis, neurotoxicity, neuroprotection, autophagy and apoptosis *via* its transporters located on the cell membrane. Aβ activates Ca^{2+} transporters, including NMDAR, AMPAR, LTCC, Na^+/K^+ -ATPase, CALHM1, TRPV1, and Cav1.2, which promote Ca^{2+} entry into the cytoplasm and increase the concentration of Ca^{2+} in neuronal cells. More importantly, these Ca^{2+} transporters mediate the effects of Ca^{2+} on neuroinflammation, neuronal injury, neurogenesis, neurotoxicity, neuroprotection, autophagy, and apoptosis through different mechanisms. Aβ activates NMDAR, LTCC, CALHM1, and TRPV1, which result in apoptosis induction, leading to cell death. Regarding neuroinflammation, NMDARs mediate the effects of Aβ on activating NF-κB through a Ca^{2+}-dependent mechanism, which results in transcriptional regulation of the secretion of IL-1β, IL-6, NO, and TNF-α. Moreover, NMDARs induce LC3 II production, leading to autophagy.

effects of InsP3R on mediating Ca^{2+} release from the ER to the cytosol in 3xTg mice (Park et al., 2010). Moreover, calcineurin (CaN) is activated by the proinflammatory cytokine TNF-α in astrocytes (Fernandez et al., 2007; Sama et al., 2008; Furman et al., 2012). TNF-α activates a more complicated mechanism to regulate Ca^{2+} currents. In addition to TNF-α itself, the TNF-α receptor mobilizes Ca^{2+} through an RyR-dependent mechanism in cultured neonatal rat dorsal root ganglion (DRG) neurons (Pollock et al., 2002). In addition to proinflammatory cytokines, most investigations have focused on the roles of anti-inflammatory cytokines on Ca^{2+} transporters. Based on this information, researchers also found that anti-inflammatory cytokines, such as IL-10, reduced the intracellular Ca^{2+} levels in microglial cells by decreasing Ca^{2+} release from the ER through the deactivation of the InsP3R-dependent mechanism in cultured hippocampal neurons (Turovskaya et al., 2012). Therefore, the existence of crosstalk between Ca^{2+} and neuroinflammation will result in the aggravation of AD (**Figure 2**).

Proinflammatory Cytokines Reciprocally Regulate the Activities of Transporters Expressed on Lysosomes to Regulate the Basal Ca^{2+} Levels in Glial Cells

In SH-SY5Y cells, IFNγ also induces Ca^{2+} influx by activating TRPM2, leading to the apoptosis of cultured neurons (Sama et al., 2012). Furthermore, IFNγ reduces the activity of ATPase Sarcoplasmic/Endoplasmic Reticulum Ca^{2+} Transporting 2b (SERCA2b) in IL-1β-stimulated OSCC cells (Cardozo et al., 2005; Gkouveris et al., 2018). In addition to these cytokines, inflammatory factors, such as H_2O_2, increase TRPM2 activity, which might lead to increased basal Ca^{2+} levels in cultured rat microglial cells (Kraft et al., 2004). Poly ADP-ribose polymerase-1 (PARP-1) induces Ca^{2+} influx by activating TRPM2 in PARP-2 knockout mice (Kraft et al., 2004). All this evidence revealed crosstalk between Ca^{2+} and neuroinflammatory factors, which aggravates AD *via* the actions of different transporters (**Table 1**).

Ca^{2+} SIGNALING IMPAIRS NEURONAL FUNCTION

The Effects of Ca^{2+} on Impairing Neuronal Functions

Given the crosstalk between Ca^{2+} and neuroinflammatory factors, we continued to elucidate the roles of Ca^{2+} in impairing neuronal functions and its effects on the relationship between neuroinflammation and neuronal apoptosis and death (**Table 2**). For example, accumulating evidence has revealed that appropriate activation of microglial cells may exert beneficial effects by attenuating neuronal apoptosis, increasing

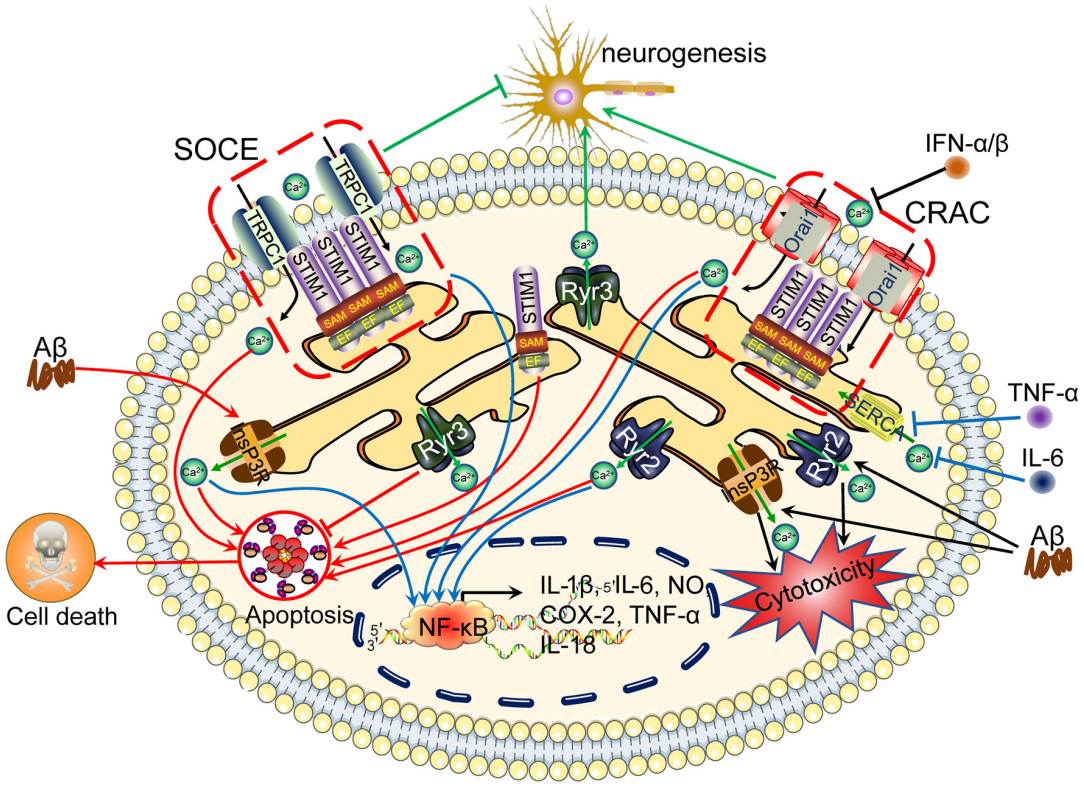

FIGURE 2 | Ca^{2+} channels in the ER are involved in regulating neuroinflammation, apoptosis, tau phosphorylation and Aβ deposition, leading to cognitive impairment. The accumulation of Aβ in neuronal cells induces Ca^{2+} influx from the intracellular Ca^{2+} store, namely, the ER. In addition, Ca^{2+} depletion from the ER triggers sustained extracellular Ca^{2+} influx to the cytosol *via* a SOCE pathway, including TRPC1 and Orai1, by activating the Stim. During these processes, InsP3R and RyR2 play important roles in inducing Ca^{2+} influx from the ER to the cytosol, regulating apoptosis, neurogenesis, tau phosphorylation and Aβ deposition and subsequently leading to cognitive impairment. ER, endoplasmic reticulum; SOCE, store-operated calcium entry.

neurogenesis, and promoting functional recovery after cerebral ischaemia (Neumann et al., 2008). In contrast, overactivation of microglial cells may result in the apoptosis or death of neurons (Brown and Neher, 2014). Based on these findings, excessive release of Ca^{2+} initially protects neuronal cells from death by inducing the expression of Bcl-2 through the activated transcription factor NF-κB (Pahl and Baeuerle, 1996; Mattson and Furukawa, 1997), whereas sustained increases in cytosolic Ca^{2+} concentrations induced by neuronal depolarization result in $A\beta_{1-42}$ production and subsequent neuronal death (Pierrot et al., 2004). Moreover, a series of studies reviewed in our previous work described the effects of Ca^{2+} on cell apoptosis *via* multiple signaling pathways, and this information is not repeated in the present review (Wang and Wang, 2017).

Proinflammatory Cytokines Induce Neuronal Apoptosis or Death *via* Ca^{2+} Transporters Located on the Cell Membranes

However, transporters have not been considered critical for mediating the effects of Ca^{2+} on the apoptosis or death of neurons. Therefore, we further addressed the roles of different types of Ca^{2+} transporters in regulating the apoptosis or death of neuronal cells, especially during the course of AD development and progression. Due to its close association with neuroinflammation, neuronal apoptosis in the rat hippocampus is induced by IL-1β through an NMDAR-mediated Ca^{2+} influx mechanism (Dong et al., 2017). By coculturing glial cells with primary hippocampal neurons, IL-1β secreted from glial cells triggers neuronal death *via* tyrosine phosphorylation and NMDAR trafficking mechanisms (Viviani et al., 2006; Dong et al., 2017). In contrast to the action of IL-1β, IL-6 reduces Ca^{2+} overload by deactivating NMDARs, which resulted in the death of cultured cerebellar granule neurons (CGNs) *via* the JAK/CaN pathways (Ma et al., 2015). As another type of glutamate receptor involved in Ca^{2+} transport, AMPAR, which is trafficked to the plasma membrane, mediates the effects of TNF-α on exacerbating the effects of spinal cord injury on cell death (Ferguson et al., 2008; Beattie et al., 2010). By inhibiting the activities of L-VGCC, Gas6 or nimodipine suppresses Aβ-induced neuronal apoptosis by attenuating Ca^{2+} influx into primary cultured cortical and hippocampal neurons (Ueda et al., 1997; Yagami et al., 2002). In addition, NMDARs and L-VGCCs mediate the effects of perfluorohexanesulfonate (PFHxS) on activating the AMPK and ERK pathways, leading to the apoptosis

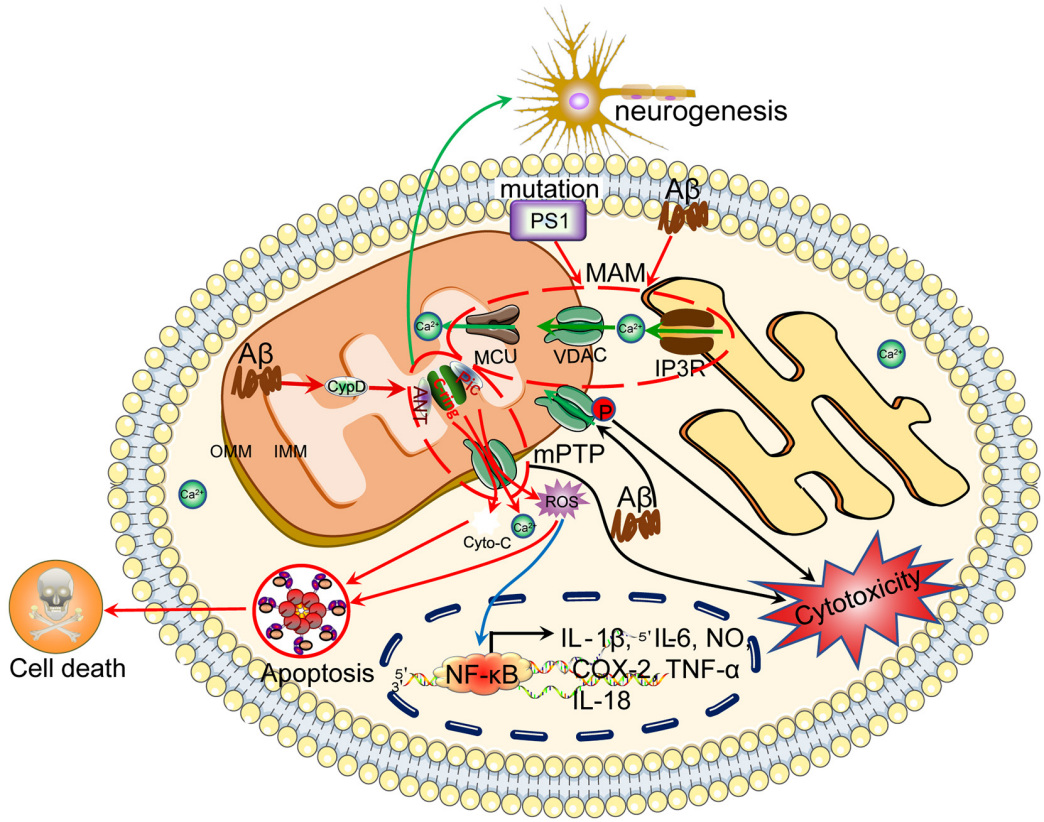

FIGURE 3 | Ca^{2+} efflux from mitochondria regulates the apoptosis of neuronal cells, which results in cognitive dysfunction. Ca^{2+} is transported to the mitochondria *via* MCU. Under physiological or pathological conditions, Ca^{2+} is continuously shuffled between the ER and mitochondria *via* VDAC. Moreover, Ca^{2+} in mitochondria induces the formation of the mPTP, which transports Ca^{2+} and small molecules, such as ROS and cytochrome C, from the mitochondria to the cytosol, leading to neuronal apoptosis. The loss of neurons will cause cognitive dysfunction.

of P12 cells (Lee et al., 2016). Among the Ca^{2+} transporters located in the cell membrane, TRPV1 overexpression disrupts mitochondrial function and induces cytochrome c release, which results in the death of a human microglial cell line (HMO6; Kim et al., 2006; Zhang and Liao, 2015). Similarly, ectopically expressed TRPV4 in glial cells induces neuronal damage *via* an apoptotic mechanism (Shi et al., 2013). Consistent with these findings, pharmacological or genetic interventions targeting TRPV4 suppress neuronal cell death by decreasing the expression of proinflammatory cytokines, such as IL-1β and TNF-α (Konno et al., 2012; Shi et al., 2013). As another type of TRP family protein, TRPM2 is activated to induce Ca^{2+} influx, resulting in the death of RIN-5F rat insulinoma cells and rat cortical neurons (Kaneko et al., 2006). TRPM2 knockdown reduces the toxicity of Aβ and subsequent death of primary rat neuron cultures (Fonfria et al., 2005; Li and Jiang, 2018; **Figure 1**).

Ca^{2+} Transporters Located on the ER Membrane Are Responsible for Regulating Neuronal Apoptosis

Although APOE4 is not a canonical Ca^{2+} transporter, APOE4 overexpression induces Ca^{2+} influx, resulting in neuronal apoptosis (Veinbergs et al., 2002; Jiang et al., 2015). Through a more complicated mechanism, APOE4 induces neuronal apoptosis in APOE4 knockout mice by activating NMDAR-mediated Calcium/Calmodulin dependent protein kinase II (CaMKII) pathways (Qiao et al., 2017). Moreover, TBI induces apoptosis in the cortex and hippocampus of Tg mice overexpressing human APOE4 by activating APOE4 (Giarratana et al., 2020). In addition, ER stress also mediates the effects of the unfolded protein response (UPR) and misfolded proteins on inducing apoptosis through mechanisms related to Ca^{2+} influx (Nishitoh et al., 2009; Moreno et al., 2013). Specifically, Ca^{2+} transporters located on the ER membrane, including InsP3R and RyR, are reported to be involved in regulating neuronal apoptosis. For example, type 3 InsP3R regulates cell death by modulating Ca^{2+} release from the ER to the cytosol in postnatal cerebellar granule cells (Blackshaw et al., 2000; Wang and Zheng, 2019). Isoflurane treatment induces Ca^{2+} influx, leading to caspase-3 activation by cleavage in DT40 cells (Joseph et al., 2014). Upon the stimulation of P2X7R by isoflurane and sulforaphane, InsP3R mediates the effects of Ca^{2+} on inducing apoptosis or cell death of NG108-15 and PC12 neuronal cells and cells in nude mice (Wei et al., 2008; Chao et al., 2012; Hudecova et al., 2016). Specifically, $A\beta_{25-35}$ induces the apoptosis of murine astrocytes *via* InsP3R- and Ca^{2+}-activating pathways

TABLE 1 | Crosstalk between Ca^{2+} dysregulation and neuroinflammation.

Cat.	Stimulator/Mediator	Mechanism	Experimental model	References
Ca^{2+}	CaN	Ca^{2+}→IL-1β and TNF-α	Glial cells	Sama and Norris (2013)
	CyPPA	LPS→Ca^{2+}→TNF-α and IL-6	Primary mouse microglial cells	Dolga et al. (2012)
CM	NMDAR	NMDAR→Ca^{2+}→IL-1β and TNF-α	Primary mouse hippocampal neurons and lamina II neurons of isolated spinal cord slices	Kawasaki et al. (2008) and Huang et al. (2011)
		Sevoflurane ⊣ NMDAR→IL-1β/-6/-8 and TNF-α D-cycloserine→NMDAR→IL-1β/-6/-8 and TNF-α	Ageing rats	Yang Z. Y. et al. (2020)
		NMDAR→NF-κB→NO	Primary microglial cells	Murugan et al. (2011)
	AMPAR	AMPAR→Ca^{2+}→IL-1β and TNF-α	SG neurons and lamina II neurons of isolated spinal cord slices	Kawasaki et al. (2008), Park et al. (2008) and Liu et al. (2013)
		Perampanel ⊣ AMPAR→IL-1β and TNF-α ∪ ⊣ IL-10 and TGF-β1.	TBI model in rats	Chen T. et al. (2017)
	L-VGCC	Bepridil, nitrendipine and nimodipine ⊣ L-VGCC→astrocytes and microglia cells→neuroinflammation	Encephalomyelitis (EAE)-induced multiple sclerosis (MS) animal model; LPS or aCSF-injected (i.c.v) rats; astrocytes in the CA1 region of the hippocampus	Brand-Schieber and Werner (2004), Daschil et al. (2013), Espinosa-Parrilla et al. (2015), and Hopp et al. (2015)
		L-VGCC→Ca^{2+}→TNF-α	Rat hippocampal neurons	Furukawa and Mattson (1998)
	TRPM2	$TRPM2^{-/-}$ ⊣ microglial cells→cytokines	$TRPM2^{-/-}$ mice	Miyanohara et al. (2018) and Kakae et al. (2019)
	TRPV1	TRPV1→IL-6	Microglial cells	Sappington and Calkins (2008)
	TRPV4	Blocking TRPV4 channels ⊣ Ca^{2+} influx→IL-1β and TNF-α→inflammation	Glial cells	Shi et al. (2013)
		4α-phorbol 12, 13-didecanoate (4α-PDD)→TRPV4 ⊣ microglial activation→TNF-α	Rat microglial cells	Konno et al. (2012)
	TRPC1	TRPC1→microglia-mediated inflammation	Primary microglial cells	Sun Y. et al. (2014)
	APOE4	hAPOE4→IL-1β→microglia cells	E4F AD mice	Rodriguez et al. (2014)
	APOEs	APOE1–3 ⊣ COX-2, PGE_2 and IL-1β	Primary microglial cells from the rat brain cortex	Chen et al. (2005)
ER	InsP3R2	$InsP3R2^{-/-}$→cytokines	$SOD1^{G93A}$ mice	Staats et al. (2016)
	RyR	Dantrolene ⊣ RyR→deactivation of microglia→inflammatory markers	LPS-infused rats	Hopp et al. (2015)
	SOCE	PK11195, a mitochondrial ligand ⊣ SOCE→Ca^{2+} influx→COX-2	Human microglial cells	Hong et al. (2006)
MD		CypD→mPTP→IL-6 ∪ TNFα	CypD KO mouse	Liu et al. (2019)
LM		$PS1/2^{-/-}$→Ca^{2+} efflux from lysosomes	$PS1/2^{-/-}$ MEFs	Coen et al. (2012) and McBrayer and Nixon (2013)
IL-1β/TNF-α/IFNγ	Ca^{2+}	TNF-α, IL-1β, and IFNγ→Ca^{2+} influx	Microglial cells	Goghari et al. (2000), McLarnon et al. (2001), and Franciosi et al. (2002)
IL-10	InsP3R	IL-10 ⊣ InsP3R→Ca^{2+} efflux from the ER	Hippocampal neurons	Turovskaya et al. (2012)
IL-1β	NMPAR	IL-1β→NMPAR→Ca^{2+} influx	Hippocampal neurons	Viviani et al. (2003) and Simões et al. (2012)
	L-VGCC	IL-1β ⊣ Ca^{2+} channels→L-VGCC	Primary neurons	Zhou et al. (2006) and Zhou (2010)
	TRPM2	IL-1β→TRPM2→Ca^{2+} influx	Human C13 microglia cells	Fonfria et al. (2006)
IL-6	NMDAR	IL-6→NMDAR→Ca^{2+} influx	Hippocampal neurons	Orellana et al. (2005)

(Continued)

TABLE 1 | Continued

Cat.	Stimulator/Mediator	Mechanism	Experimental model	References
	SERCA	IL-6 ⊣ SERCA	Cardiac myocytes	Villegas et al. (2000)
TNF-α	NMDAR	TNF-α→NMDAR→Ca^{2+} currents	Rat hippocampal neurons	Furukawa and Mattson (1998)
	TRPM2			
	CP-AMPAR	TNF-α→CP-AMPAR	Hippocampal neurons	Ogoshi et al. (2005)
		TNF-α→GluA1	Male Holtzman rats	Wigerblad et al. (2017)
	TRPM2	IFNγ→TRPM2→Ca^{2+} influx	SH-SY5Y cells	Güzel et al. (2021)
	L-VGCC	TNF-α ⊣ L-VGCC→Ca^{2+} influx	Rat hippocampal neurons and hippocampal CA1 neurons	Furukawa and Mattson (1998) and Sama et al. (2012)
	InsP3R	TNF-$\alpha^{-/-}$ ⊣ InsP3R→Ca^{2+} efflux from the ER	3xTg mice	Park et al. (2010)
	Calcineurin	TNF-α→CaN	Astrocytes	Fernandez et al. (2007), Sama et al. (2008), and Furman et al. (2012)
TNFα	RyR	TNFα→RyR→Ca^{2+} mobilization	Neonatal rat DRG neurons	Pollock et al. (2002)
IFNγ/LPS	TRPM2	IFNγ and LPS→TRPM2→Ca^{2+} influx	Microglial cells in TRPM2$^{-/-}$ mice	Miyake et al. (2014)
IL-1β/IFNγ	SERCA2b	IL-1β and IFNγ ⊣ SERCA2b	Pancreatic cells	Cardozo et al. (2005)
		IFNγ ⊣ SERCA2b	Human OSCC cell line	Gkouveris et al. (2018)
H_2O_2	TRPM2	H_2O_2→TRPM2→Ca^{2+} influx	Rat microglial cells	Kraft et al. (2004)
		PARP1→TRPM2→Ca2 + influx	PARP1 KO mice	Raghunatha et al. (2020)

(Oseki et al., 2014). In addition to InsP3R, the posttranslational modification of RyR2 by S-glutathionylation increases channel activity, resulting in the death of rat cortical neurons (Bull et al., 2008). In contrast, the suppression of RyR3 expression in TgCRND8 neurons increases the neuronal death rate, which suggests a protective role for RyR in the late stages of AD pathogenesis (Supnet et al., 2010).

Based on these observations, ethanol dose-dependently increases the intracellular Ca^{2+} concentration, which damages HepG2 hepatocytes by upregulating the expression of the Orai1 and Stromal interaction molecule 1 (Stim1) mRNAs and proteins (Liu et al., 2012). Although the pathophysiological effects of decreased Store-operated calcium entry (SOCE) levels in AD remain unclear, several lines of evidence have shown that SOCE deficits lead to neuronal cell death and decreased synaptic plasticity (Soboloff and Berger, 2002; Calvo-Rodriguez et al., 2020). As expected, Stim1 silencing alleviates the apoptosis of H_2O_2-treated endothelial progenitor cells (Wang et al., 2016). Moreover, the downregulation of Stim1 by an siRNA concurrently increases neuronal viability and inhibits apoptotic cell death by decreasing the intracellular Ca^{2+} levels (Selvaraj et al., 2016). In PC3 and DU145 cells, both Stim1 and Orai1 separately mediate the effects of resveratrol (RSV), a natural polyphenol, on activating autophagic cell death (Selvaraj et al., 2016). In addition, resveratrol can mediate the release of Ca^{2+} from intracellular stores (Santoro et al., 2020). As a method to exclude nonspecific effects of pharmacological interventions, silencing the expression of Stim1 and Orai1 reduces the apoptosis rate of LPS-treated pulmonary microvascular endothelial cells by blocking SOCE in pulmonary microvascular endothelial cells (Wang et al., 2016). Researchers excluded the effects of Stim1 on cell apoptosis by transfecting Orai1 mutants and observed decreases in both SOCE and the rate of thapsigargin-induced apoptosis in human prostate cancer (PCa) cells (Flourakis et al., 2010; **Figure 2**).

Mitochondrial Dysfunction Is Also Involved in Mediating the Effects of Ca^{2+} on Neuronal Apoptosis

However, ER stress is not the only mechanism by which the effects of Ca^{2+} on neuronal apoptosis are mediated: mitochondrial dysfunction is also reported to be involved in this process (Yoon et al., 2011). Consistently, Stim1 or Orai1 knockdown attenuates the intracellular Ca^{2+} overload, restores the mitochondrial membrane potential, decreases the release of cytochrome c and inhibits ethanol-induced apoptosis (Cui et al., 2015). Without affecting ER stress, curcumin protects mitochondria from oxidative damage by attenuating the apoptosis of cortical neurons (Zhu et al., 2004). In primary cultured spinal neurons, salidroside (Sal) treatment decreases apoptosis by activating PINK-Parkin pathways, leading to mitophagy of mitochondria (Gu et al., 2020). Similar to its effects on AD, $A\beta_{1-42}$ induces neuronal apoptosis by concurrently upregulating mitochondrial fission protein dynamin-related protein 1 (Drp1) and downregulating mitofusin 1/2 (Mfn1/2) and dynamin-like GTPase (OPA-1) in primary cultures of mouse cerebral cortical neurons (Han et al., 2017). In addition, $A\beta_{25-35}$ induces cytochrome c-mediated apoptosis of NT2 cells through a functional mitochondria-dependent mechanism (Morais Cardoso et al., 2002). In this mechanism, Ca^{2+} transport by InsP3R to mitochondria induced by opening

TABLE 2 | The effect of Ca^{2+} on impairing neuronal functions.

Cat.	Stimulator or Mediator	Mechanism	Experimental model	References
Ca^{2+}		Ca^{2+}→NF-κB→Bcl-2 ⊣ neuronal death	Primary rat hippocampal neurons	Pahl and Baeuerle (1996) and Mattson and Furukawa (1997)
		Ca^{2+}→$A\beta_{1-42}$→neuronal death	Rat cortical neurons	Pierrot et al. (2004)
		XeC ⊣ $A\beta_{1-42}$→IP3→Ca^{2+}→apoptosis	Primary hippocampal neurons	Wang et al. (2019)
CM	NMDAR	IL-1β→NMDAR→Ca^{2+} influx→neuronal apoptosis	Rat hippocampus	Dong et al. (2017)
		IL-1β→NMDAR ∪ tyrosine phosphorylation→neuronal death	Co-culture of primary hippocampal neurons and glial cells	Viviani et al. (2006)
		IL-6 ⊣ NMDAR→Ca^{2+}→JAK/CaN →neuronal death	Cerebellar granule neurons (CGNs)	Ma et al. (2015)
	AMPAR	TNF-α→trafficking GluR2-lacking AMPARs to the plasma membrane→cell death	Spinal cord neurons	Ferguson et al. (2008) and Beattie et al. (2010)
	L-VGCC	Gas6 ⊣ L-VGCC→Aβ-induced apoptosis	Cortical neurons	Yagami et al. (2002)
		Nimodipine ⊣ L-VGCC→Ca^{2+} influx→Aβ-induced neuronal apoptosis	Primary cortical and hippocampal neurons	Ueda et al. (1997) and Yagami et al. (2002)
		PFHxS→NMDAR ∪ L-VGCC→AMPK ∪ ERK→apoptosis	PC12 cells	Lee et al. (2016)
	TRPV1	$TRPV1^{+/+}$→mitochondria→cytochrome c→cell death	Human microglia cell line (HMO6)	Kim et al. (2006) and Zhang and Liao (2015)
	TRPV4	$TRPV4^{+/+}$→neuronal apoptosis	Rats with neuronal injury	Shi et al. (2013)
		$TRPV4^{-/-}$ ⊣ IL-1β and TNF-α→neuronal cell death	Glial cells	Shi et al. (2013)
		$TRPV4^{-/-}$ ⊣ infrasound-induced neuronal death	Rat microglial cells	Konno et al. (2012)
	TRPM2	TRPM2→Ca^{2+}→neuronal death	Rat insulinoma RIN-5F cells and rat cortical neurons	Kaneko et al. (2006)
		TRPM2 siRNA ⊣ Aβ-induced neuronal death	Primary rat neurons	Fonfria et al. (2005)
	APOE4	APOE4→Ca^{2+} influx→neuronal death APOE4→NMDAR ∪ CaMKII→apoptosis	SH-SY5Y cells $APOE^{-/-}$ mice and primary cultures of cerebral cortical neurons from $APOE^{-/-}$ mice	Veinbergs et al. (2002) Xu and Peng (2017)
		APOE4 overexpression→Ca^{2+} influx→neuronal apoptosis	APOE4-expressing neurons	Jiang et al. (2015)
ER		TBI→APOE4→apoptosis	Tg mice overexpressing human APOE4/APOE3	Giarratana et al. (2020)
	UPR	ER stress→UPR→cell apoptosis	Prion protein-infected mice	Moreno et al. (2013)
	Misfolded proteins	Misfolded proteins accumulate→ER stress→Ca^{2+} influx→apoptosis	Patients with AD, PD and ALS	Nishitoh et al. (2009)
	InsP3R	InsP3R3→Ca^{2+} efflux from the ER→cell death	Postnatal cerebellar granule cells	Blackshaw et al. (2000)
		Isoflurane→InsP3R→caspase-3→apoptosis	DT40 cells	Joseph et al. (2014)
		P2X7R, isoflurane and sulforaphane→InsP3R-mediated Ca^{2+} efflux from the ER→apoptosis or cell death	NG108–15 and PC12 neurons and nude mice	Wei et al. (2008), Chao et al. (2012), and Hudecova et al. (2016)
		$A\beta_{25-35}$→InsP3R→Ca^{2+} efflux from the ER→apoptosis of astrocytes	Murine astrocytes	Oseki et al. (2014)
	RyR	S-gluthathionylation→$RyR2^{PMT}$→cortical neuronal death	Rats with cerebral ischaemia	Bull et al. (2008)
		RyR3 suppression→neuronal death	TgCRND8 neurons	Supnet et al. (2010)
	Stim1	$Stim1^{-}$ ⊣ H_2O_2-induced apoptosis	Endothelial progenitor cells	Wang et al. (2016)
		Stim1 siRNA ⊣ Ca^{2+} influx ⊣ neuronal viability ∪ →apoptotic cell death	*In vitro* traumatic neuronal injury	Hou et al. (2015)

(Continued)

TABLE 2 | Continued

Cat.	Stimulator or Mediator	Mechanism	Experimental model	References
	Stim1/Orai	Resveratrol (RSV) ⊣ Stim1 and Orai1 ⊣ autophagic cell death	PC3 and DU145 cells	Selvaraj et al. (2016)
		$Stim1^{-}$ and $Orai^{-}$ ⊣ SOCE→LPS-induced apoptosis	Pulmonary microvascular endothelial cells	Wang et al. (2016)
	Orai	$Orai1^{mut}$ ⊣ SOCE and thapsigargin-induced apoptosis	Human prostate cancer (PCa) cells	Flourakis et al. (2010)
MT		Curcumin ⊣ mitochondrial damage from oxidative stress→neuronal apoptosis	Rat cortical neurons	Zhu et al. (2004)
		Sal→mitophagy ⊣ apoptosis	Primary cultures of spinal neurons	Gu et al. (2020)
	Aβ	$Aβ_{1-42}$→Drp1 ∪ ⊣ Mfn1/2 and OPA-1→neuronal apoptosis	Primary mouse cortical neurons	Han et al. (2017)
		$Aβ_{25-35}$→mitochondria→cytochrome c→apoptosis	NT2 cells	Morais Cardoso et al. (2002)
	mPTP	InsP3R→Ca^{2+}→mPTP→cytochrome c→cell apoptosis	HepG2 cells	Szalai et al. (1999)
		CBD→mPTP→ROS→cytochrome c→apoptosis	Human monocytes	Wu et al. (2018)
		$Mortalin^{+}$ ⊣ mPTP→Aβ-induced neuronal apoptosis	SH-SY5Y cells	Qu et al. (2012)
		$CyPD^{-/-}$ ⊣ mPTP→cell death	mAPP mice	Du et al. (2008)
	VDAC	$VDAC1^{+}$→Ca^{2+}→cell death and apoptosis	A549 cells	Weisthal et al. (2014)
		Antibody ⊣ VDAC1→Aβ induced neuronal apoptosis	Hippocampal neurons	Thinnes (2011)
		VDAC→cell apoptosis	Lymphoblastoid cells carrying the mitochondrial DNA mutation	Yuqi et al. (2009)
		VDAC→cytochrome c ∪ Bax→permeating membranes	VDAC1-deficient mitochondria from a mutant yeast	Shimizu et al. (1999)
		Caspase-8→cleaves Bid→VDAC closure→protein release from mitochondria→apoptosis	Planar phospholipid membranes	Rostovtseva et al. (2004)
		Bcl-xL→VDAC open ⊣ apotosis.	FL5.12 cells	Vander Heiden et al. (2001)
		FABP5→VDAC1 ∪ BAX→apoptosis	Human KG-1C oligodendroglial cells	Cheng et al. (2020)
		BAPTA-AM ⊣ Ca^{2+}→VDAC1 oligomerization→ mitochondria-mediated apoptosis	HeLa or T-REx-293 cells	Keinan et al. (2013)
		DIDS, SITS, H2DIDS, DNDS, and DPC ⊣ VDAC1 oligomerization→apoptosis	$VDAC1^{+}$ HeLa cells	Ben-Hail and Shoshan-Barmatz (2016)
		DIDS ⊣ VDAC1→Ca^{2+}→apoptosis	THP-1 macrophages	Chen et al. (2014)

the mPTP induces the release of cytochrome c, which results in the apoptosis of cells (Szalai et al., 1999). In fact, mPTP opening induces matrix swelling, the subsequent rupture of the outer membrane, and nonspecific release of proteins in the intermembrane space into the cytosol upon cannabidiol (CBD) induction of human monocyte apoptosis (Wu et al., 2018). By inhibiting the opening of the mPTP in mitochondria, mortalin overexpression blocks Aβ-induced SH-SY5Y cell apoptosis (Qu et al., 2012). In AD mice, CyPD knockout decreases the cell death rate by attenuating the opening of the mPTP in mitochondria (Du et al., 2008; Pahrudin Arrozi et al., 2020).

VDAC1 expression induces cell death and apoptosis by activating the Ca^{2+} signaling cascade in A549 cells (Weisthal et al., 2014). VDAC is involved in the apoptosis of lymphoblastoid cells carrying a mitochondrial DNA mutation (Yuqi et al., 2009). Through a direct interaction with Bax, VDAC induces the transport of cytochrome c through membranes (Shimizu et al., 1999). Moreover, the cleavage of the pro-apoptotic protein Bid by caspase-8 induces the closure of VDAC, which leads to protein release from mitochondria and apoptosis (Rostovtseva et al., 2004). In contrast, Bcl-xL promotes the opening of the VDAC, which results in a reduced apoptosis rate of cultured FL5.12 cells (Vander Heiden et al., 2001; Bessou et al., 2020). Fatty acid binding protein 5 (FABP5), which is expressed in oligodendrocytes, induces mitochondrial macropore formation through VDAC-1 and Bax, thus accelerating mitochondria-induced glial cell death. These two proteins mediate mitochondrial outer membrane

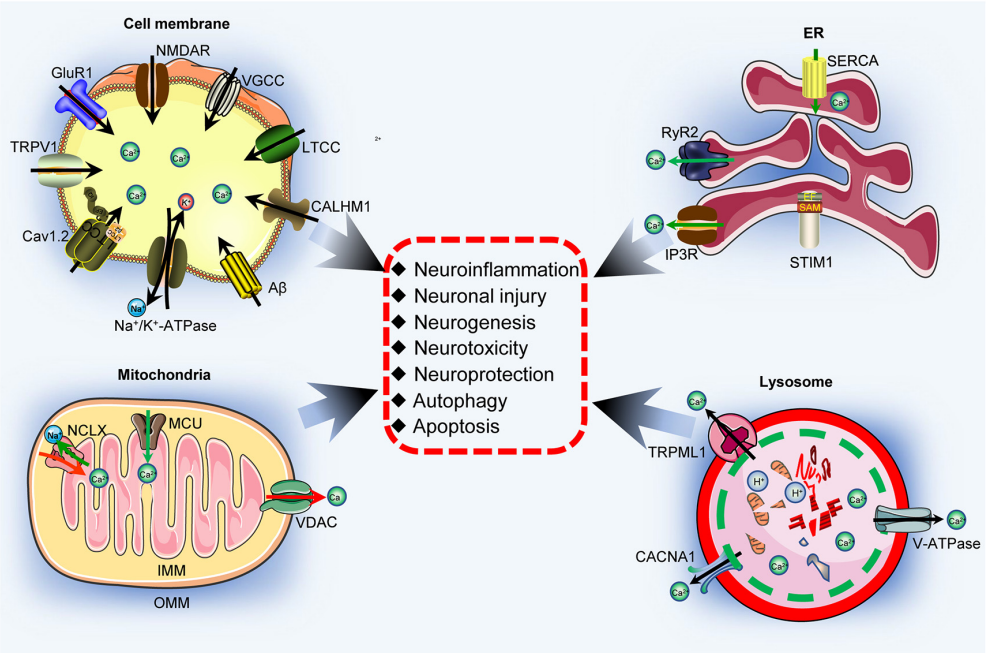

FIGURE 4 | Ca^{2+} transporters are responsible for activating neuronal networks. Ca^{2+} transporters located in the cell membrane, ER, mitochondria, and lysosome are responsible for regulating neuroinflammation, neuronal injury, neurogenesis, neurotoxicity, neuroprotection, autophagy, and apoptosis.

permeability, resulting in the release of mitochondrial DNA and cytochrome c into the cytoplasm and activation of apoptotic caspases (Cheng et al., 2020). More interestingly, BAPTA-AM, a Ca^{2+}-chelating reagent, inhibits mitochondria-mediated apoptosis by decreasing the oligomerization of VDAC1 in HeLa and T-REx-293 cells (Keinan et al., 2013). Consistent with this observation, anion transport inhibitors, including 4'-diisothiocyano-2,2'-stilbenedisulfonic acid (DIDS), SITS, H_2DIDS, DNDS, and DPC, inhibit apoptosis-associated VDAC1 oligomerization (Ben-Hail and Shoshan-Barmatz, 2016). In addition, blockade of plasmalemmal VDAC1 with a specific antibody suppresses Aβ-induced neuronal apoptosis (Thinnes, 2011; Lim et al., 2021a). In THP-1 macrophages, DIDS disodium salt, an inhibitor of VDAC1, attenuates the apoptosis of THP-1 macrophages by decreasing intracellular Ca^{2+} levels (Chen et al., 2014). Similarly, Ca^{2+} transporters generally mediate the regulatory effects of Ca^{2+} on neuronal apoptosis, especially in the context of AD (**Figure 3**).

Ca^{2+} INHIBITS THE REGULATION OF NEURONAL STEM CELLS

Ca^{2+} Modulates Neuronal Differentiation, Migration and Self-renewal During the Course of Neurogenesis

During the course of AD development and progression, neurogenesis is markedly inhibited in the brains of patients with AD and mouse models (Rash et al., 2016). Given the potential roles of Ca^{2+} in AD, we summarize the effects of Ca^{2+} on neurogenesis during the course of AD development and progression. Indeed, higher frequencies of Ca^{2+} oscillations increase the differentiation of hippocampus-derived neural stem cells (NSCs) into neurons in adult rats (Wang Q. et al., 2015). Moreover, Epac2 mediates PACAP-induced differentiation of neural progenitor cells (NPCs) into astrocytes along with an increase in intracellular Ca^{2+} levels, which also activated the signaling pathway for astrocytogenesis in Epac2-knockout (KO) mice (Seo and Lee, 2016). NSC differentiation is closely related to the expression of VGCC, especially Caveolin 1 (Cav1) through regulating Ca^{2+} influx (D'Ascenzo et al., 2006). Moreover, exposure in extremely low-frequency electromagnetic fields (ELFEF) promotes the differentiation of NSCs by upregulating the expression and function of Cav1 (Piacentini et al., 2008c). Furthermore, bidirectional radial Ca^{2+} activity elongates the fiber of radial glial cells (RGCs) and simultaneously induces neurogenesis during early cortical column development (Rash et al., 2016). By upregulating the Notch signaling pathway after brain injury, Ca^{2+} waves generated in neighboring astrocytes propagate to NPCs, inducing neurogenic behavior, including the self-renewal and migration of progenitor cells (Kraft et al., 2017). Based on these observations, Ca^{2+} induces neuronal differentiation, migration and self-renewal during the course of neurogenesis.

Ca^{2+} Transporters Located on the Cell Membranes Are Required for Neurogenesis

Given the key roles of Ca^{2+} in neurogenesis, its transporters are also required for neurogenesis. In the developing cerebellum,

granule cell precursors differentiate upon activation of a homodimeric G protein-coupled receptor that is sensitive to Ca^{2+} levels called calcium-sensing receptor (CaSR). CaSR activation *in vivo* induces the homing of granule cell precursors during differentiation, mainly through CaSR interactions with integrin complexes (Tharmalingam et al., 2016). Among these CaSRs, the lower activity of NMDARs in $NR1^{+/-}$ mice contributes to increased cell proliferation and neurogenesis compared to the activity in the brains of adult $NR1^{+/+}$ mice (Bursztajn et al., 2007). In contrast, intraperitoneal injection of the NMDAR agonist NMDA (2 mg/kg/day) promotes cell proliferation in the subventricular zone (SVZ) of rats (Fan et al., 2012). Unfortunately, the researchers did not extend their investigations to Ca^{2+}, although NMDAR affects neurogenesis. Compared to NMDARs, the roles of AMPARs in neurogenesis are relatively simple. In rats administered chronic corticosterone (CORT), S47445, a novel AMPAR-positive allosteric modulator (AMPA-PAM), exerted significant neurogenic effects on the proliferation, survival and maturation of new hippocampal neurons (Mendez-David et al., 2017). Moreover, AMPAR mediates kainate-induced radial glia-like stem cell proliferation (Shtaya et al., 2018). Human NPCs contain Ca^{2+}-permeable AMPARs; however, AMPARs were engineered to become Ca^{2+}-impermeable receptors during the course of differentiation from NPCs to neurons or astrocytes through RNA editing of the AMPA receptor subunit GluR2 at the Q/R site (Whitney et al., 2008). Then, the NMDAR subunits NR1 and NR2B and the AMPAR subunit GluR2 in Ca^{2+}-impermeable AMPARs were upregulated at the mRNA level in differentiated neuroepithelial precursors, indicating their likely contribution to neurotransmission after first establishing neuronal networks (Muth-Köhne et al., 2010; Wang et al., 2018).

In addition to NMDARs and AMPARs, different types of VGCCs and TRPs in cell membranes are also involved in regulating neurogenesis. For example, the differentiation of dental pulp stem cells (DPSCs) into neural cells is markedly inhibited by regulating the levels of the distal C-terminus (DCT) upon treatment with nimodipine and knock down of Cav1.2 expression (Ju et al., 2015). In the dentate gyrus (DG) region, deletion of Cav1.2 decreases the numbers of doublecortin-positive adult-born neurons, suggesting important roles for Cav1.2 in adult neurogenesis (Temme et al., 2016). Consistent with these findings, Cav1.3 knockout impairs hippocampal neurogenesis and inhibits neuronal differentiation (Marschallinger et al., 2015). More importantly, Ca^{2+} mediates the effects of L-VGCC on the neurogenesis of interneurons in nifedipine-treated NPCs (Brustein et al., 2013). Similar to L-VGCCs, blockade of other types of VGCCs, such as N- and T-VGCCs, decreases the migration and neurite extension of developing neurons (Komuro and Rakic, 1992; Louhivuori et al., 2013). On the other hand, TRPs are also reported to be involved in regulating neurogenesis. For instance, TRPM2 deficiency results in impaired embryonic neurogenesis because it regulates neural progenitor self-renewal through an SP5-dependent mechanism (Li and Jiao, 2020). In addition, the antisense oligonucleotide-mediated knockdown of TRPC1 expression reduces the effects of bFGF on the proliferation of embryonic rat NSCs (Fiorio Pla et al., 2005; Toth et al., 2016). Blocking SOCE activity with YM-58483 (BPT2) decreases the proliferation of SVZ and neural stem cells (Domenichini et al., 2018). By stereotactically injecting a recombinant adeno-associated virus expressing TRPC1 into the DG of the bilateral hippocampus, we observed that neurogenesis, LTP induction, and cognitive enhancement related to environmental enrichment (EE) were effectively rescued in TRPC1 knockout mice (Du et al., 2017). Consistent with this observation, TRPC3 knockout reduces the effect of Ca^{2+} on mGluR5-mediated radial glial processes, reducing the neuronal migration rate (Louhivuori et al., 2015; Toth et al., 2016). In addition to these classical Ca^{2+} transporters in the cell membrane, both APOE1–3 knockout and APOE4 overexpression suppress neurogenic responses *in vivo* (Hong et al., 2013; Rijpma et al., 2013; Geffin et al., 2017). Based on this evidence, transporters are involved in mediating the effects of Ca^{2+} on the neurogenesis of NPCs and NSCs (**Figure 1**).

Intracellular Ca^{2+} Stores Mediate the Effects of Ca^{2+} on Neurogenesis

The ER and mitochondria are major intracellular Ca^{2+} stores and thus mediate the regulatory effects of Ca^{2+} on neurogenesis. In PC12 cells, ER stress and BDNF-TrkB signaling pathways are involved in the induction of neurogenesis by 3β, 23, 28-trihydroxy-12-oleanene 3β-caffeate from *Desmodium sambuense* (Cheng et al., 2019). In addition, ER stress mediates the effects of tunicamycin and HRD1 deletion on the aberrant induction of neuronal differentiation and inhibition of dendrite outgrowth in retinoic acid-treated P19 mouse embryonic carcinoma cells (Kawada et al., 2014). More interestingly, transcripts encoding the three main isoforms of the two families of intracellular calcium release channels, namely, InsP3R and RyR, were detected during early neurogenesis in the mouse cerebral cortex (Faure et al., 2001). In particular, an antagonist of the InsP3 pathway, wortmannin, prevents neurogenesis in neural crest cells (Evrard et al., 2004). In addition, Ca^{2+} waves propagate through radial glial cells in the proliferative cortical ventricular zone (VZ) and require connexin hemichannels, P2Y1 ATP receptors, and intracellular InsP3-mediated Ca^{2+} release, suggesting critical roles for radial glial signaling mechanisms in cortical neuronal production (Weissman et al., 2004; Lim et al., 2021b). In this process, the G protein-coupled receptor GPR157, an orphan G protein-coupled receptor, is involved in regulating the neuronal differentiation of radial glial progenitors through Gq-InsP3-mediated Ca^{2+} cascades (Takeo et al., 2016). In mesenchymal stem cells, caffeine, an RyR agonist, induces an intracellular Ca^{2+} response that increases throughout neuronal differentiation (Resende et al., 2010). Specifically, RyR2 knockout decreases the neurogenesis of embryonic stem cells (Yu et al., 2008). Associated with the aforementioned mechanisms, the proliferation of embryonic and adult NPCs cultured as neurospheres and progenitors in the subventricular zone (SVZ) of adult mice *in vivo*

was attenuated by depleting the expression of Stim1 and Orai1, suggesting pivotal roles for SOCE channel-mediated Ca^{2+} entry in mammalian neurogenesis (Somasundaram et al., 2014). In addition to Orai1, single knock down of Stim1, a Ca^{2+} sensor that mediates SOCE, impairs early and late embryonic stem cell differentiation into neural progenitors, neurons or astrocytes, increasing the cell death rate and suppressing the proliferation of neural progenitors (Hao et al., 2014; Deb et al., 2020). Similarly, pharmacological blockade of SOCE decreases the proliferation and self-renewal of NSCs, driving asymmetric division to the detriment of symmetric proliferative division, reducing the population of stem cells in the adult brain, and impairing the ability of SVZ cells to form neurospheres in culture (Domenichini et al., 2018). CRAC channels serve as a major route of Ca^{2+} entry in NSCs/NPCs and regulate key effector functions, including gene expression and proliferation, indicating that CRAC channels are important regulators of mammalian neurogenesis (Somasundaram et al., 2014). Similar to the ER, mitochondria are intracellular Ca^{2+} stores involved in regulating the neurogenesis of NPCs. For example, the inhibition of mPTPs and a selective reduction in mitochondrial superoxide spikes significantly ameliorates the negative effects of $A\beta_{1-42}$ on NPC proliferation and survival (Hou et al., 2014). Moreover, cyclosporin A inhibits neuronal differentiation by suppressing mPTP opening (Hou et al., 2013; Namba et al., 2020). All these observations confirm the involvement of Ca^{2+} and its transporters in regulating neurogenesis (**Table 3**).

THE EFFECTS OF Ca^{2+} ON NEUROTOXICITY

Ca^{2+} Induces Excitotoxicity *via* Its Transporters Located on Cell Membranes

Neurotoxicity might be the inherent cause of the Ca^{2+}-mediated impairment of neuronal functions. In primary cultured cerebral cortical neurons, increased levels of Ca^{2+} induce excitotoxicity, whereas reduced Ca^{2+} release exerts neuroprotective effects (Frandsen and Schousboe, 1991). As the natural ligand of NMDAR, NMDA induces neurotoxicity by activating NMDAR in cerebellar granule cells (Xia et al., 1995). In addition to its natural ligand, the exposure of neurons to ethanol and glutamate also induces neurotoxicity by activating NMDARs (Thomas and Morrisett, 2000; Miao et al., 2012). Similar to its effect on the AD pathway, $A\beta_{25-35}$ induces neurotoxicity by deactivating the pCRMP2 and NMDAR2B signaling pathways in SH-SY5Y cells (Ji et al., 2019). However, the researchers did not extend their observations to the involvement of Ca^{2+} in neurotoxicity. In cultured cerebellar granule neurons, domoic acid induces neurotoxicity through NMDAR-mediated Ca^{2+} influx (Berman et al., 2002). By blocking NMDAR-mediated Ca^{2+} influx, dantrolene and ionomycin prevent neurotoxicity in cultured rat cortical and retinal ganglion cell neurons (Lei et al., 1992). Drug-induced inhibition of Glutamate ionotropic receptor NMDA type subunit 2A (GluN2A) NMDAR or deletion of the GluN2A subunit gene attenuates the effects of homocysteine on increasing intracellular Ca^{2+} concentrations, leading to neurotoxicity (Deep et al., 2019). In hippocampal neurons, Aβ-induced Ca^{2+} influx mediated by NMDARs leads to calpain-dependent neurotoxicity (Kelly and Ferreira, 2006; Deep et al., 2019). Based on these observations, NMDARs have the ability to mediate Aβ-induced neurotoxicity *via* Ca^{2+}-dependent mechanisms. In addition, AMPAR was also reported to be involved in regulating neurotoxicity as another glutamate receptor type functioning as a Ca^{2+} transporter. For example, cannabinoid receptor activation attenuates the effects of TNF-α on the surface localization of AMPAR, which resulted in excitotoxicity in cultured hippocampal neurons (Zhao et al., 2010; Ganguly et al., 2019). AMPAR trafficking to the cell membrane of CNS neurons regulates excitotoxicity induced by TNF-α (Ferguson et al., 2008). TNF-α induces a rapid reduction in AMPAR-mediated Ca^{2+} entry by increasing the expression of the GluR2 subunit on the cell surface, which results in excitotoxicity during the progression of neurodegeneration (Rainey-Smith et al., 2010). Moreover, AMPAR mediated AMPA- and kainite-induced neurotoxicity *via* Ca^{2+} influx mechanisms in cultured rat hippocampal neurons (Ambrósio et al., 2000). In addition, ethanol induces neurotoxicity in hippocampal slices by activating AMPAR (Gerace et al., 2021). Of note, either Aβ or trimethyltin has the ability to induce neuronal death *via* activating L-VGCC, leading to the Ca^{2+} overload (Piacentini et al., 2008a,b). Therefore, NMDARs and AMPARs are critical for inducing neurotoxicity by triggering Ca^{2+} influx.

In the cell membrane, L-VGCC is also involved in mediating AMPA/Zn^{2+}-induced neurotoxicity in primary cultured rat cortical neurons (Ambrósio et al., 2000; Lee et al., 2016). In these cells, L-VGCCs were further reported to be critical for iron-induced neurotoxicity (Xu Y. Y. et al., 2020). In cerebral cortical cells, CXCL12 induces neurotoxicity *via* NMDAR and L-VGCC-dependent p38 MAPK activation (Sanchez et al., 2016). By blocking the L/N-type Ca^{2+} channel, cilnidipine protects the retina from neurotoxicity in ischaemia-reperfusion-treated rats (Sakamoto et al., 2009).

Another family of Ca^{2+} transporters, TRPs, was also reported to be involved in regulating neurotoxicity. In primary cultures of mouse DRG neurons, the inhibition of TRPV1 with specific blockers, such as capsaicin or resiniferatoxin, reduces the prooxidant capacity of microglial neurotoxicity (Ma et al., 2009). In addition, TRPV1 mediates vanilloid- and low pH-induced neurotoxicity in cultured rat cortical neurons (Shirakawa et al., 2007; Ertilav et al., 2021). In contrast, the inhibition of TRPV1 by the antagonist capsazepine attenuates its neuroprotective effects, indicating that TRPV1 activation contributes to the survival of rat nigral neurons (Park et al., 2012). To the best of our knowledge, no report has reconciled these conflicting results. With respect to TRPC1, neurotoxicity in SH-SY5Y cells is markedly induced by treatment with 1-methyl-4-phenylpyridinium ion (MPP^+) through TRPC1-deactivating Ca^{2+}-dependent mechanisms (Bollimuntha et al., 2005). TRPC1 overexpression inhibits neurotoxicity by inhibiting the release of cytochrome c and the

TABLE 3 | Ca^{2+} regulates the neurogenesis of neuronal stem cells.

Cat.	Stimulator or Mediator	Mechanism	Experimental model	References
Ca^{2+}		Ca^{2+} oscillations→differentiation	Adult rat NSCs	Wang Q. et al. (2015)
		PACAP→Epac2→Ca^{2+}→differentiation	NPCs from Epac2$^{-/-}$ mice	Seo and Lee (2016)
		Ca^{2+}→elongate the fibers of radial glial cells (RGCs)→neurogenesis	Mouse embryonic forebrain/radial glial cells	Rash et al. (2016)
		Brain injury→Notch→Ca^{2+}→neurogenic behavior, including the self-renewal and migration of neurons	NPCs obtained after permanently occluding the middle cerebral artery of mice	Kraft et al. (2017)
CM	NMDAR	NR1$^{+/-}$ ⊣ NMDAR ⊣ cell proliferation and neurogenesis	NR1$^{+/-}$ vs. NR1$^{+/+}$ mice	Bursztajn et al. (2007)
		NMDA→NMDAR→cell proliferation	Rat subventricular zone (SVZ)	Fan et al. (2012)
	AMPAR	S47445→AMPAR→neurogenic effects on the proliferation, survival and maturation of hippocampal newborn neurons	Chronic CORT-treated rats	Mendez-David et al. (2017)
		Kainate→AMPAR→proliferation	Radial glia (RG)-like stem cells	Shtaya et al. (2018)
	L-VGCC/Cav1.2	Nimodipine ∪ Cav1.2^{-} ⊣ differentiation	Rat DPSCs	Ju et al. (2015)
		Cav1.2$^{-/-}$ ⊣ neurogenesis	Cav1.2$^{-/-}$ mice	Temme et al. (2016)
	L-VGCC/Cav1.3	Cav1.2$^{-/-}$ ⊣ hippocampal neurogenesis and neuronal differentiation	Cav1.3$^{-/-}$ mice	Marschallinger et al. (2015)
	L-VGCC	Nifedipine ⊣ L-VGCC→Ca^{2+}→neurogenesis	NPCs	Brustein et al. (2013)
	N-VGCC	Antagonist ⊣ N-VGCC→migration of granule cells	Granule cells	Komuro and Rakic (1992)
	T-VGCC	T-VGCC^{-} ⊣ migration and neurite extensions	Neurosphere cultures of neural progenitor cells	Louhivuori et al. (2013)
	TRPM2	TRPM2^{-} ⊣ embryonic neurogenesis	NSCs	Li and Jiao (2020)
	TRPC1	TRPC1^{-} ⊣ bFGF→proliferation	Rat embryonic NSCs	Fiorio Pla et al. (2005) and Toth et al. (2016)
		BTP2 ⊣ TRPC1→SOCE→proliferation	C57BL/6 mice	Domenichini et al. (2018)
		TRPC1→neurogenesis ∪ ERK/CREB	TRPC1$^{-/-}$ mice	Du et al. (2017)
	TRPC3	TRPC3$^{-/-}$ ⊣ Ca^{2+}→mGluR5→neuronal migration	NPCs	Louhivuori et al. (2015) and Toth et al. (2016)
	APOE	$APOE_{1-3}^{-}$ ∪ $APOE_4^{+}$ ⊣ neurogenic responses	C57BL/6 mice	Hong et al. (2013)
		$APOE_4^{+}$ ∪ $APOE_{1-3}^{-}$ ⊣ neurogenesis	Aged $APOE_4$-overexpressing and $APOE_{1-3}$ knockout mice	Rijpma et al. (2013)
ER		3β, 23, 28-Trihydroxy-12-oleanene 3β-caffeate from *Desmodium sambuense*→ER stress and BDNF-TrkB signaling pathways→neurogenesis	PC12 cells	Cheng et al. (2019)
		Tunicamycin ∪ HRD1-→ER stress→neuronal differentiation ∪ ⊣ dendrite outgrowth	Mouse embryonic carcinoma P19 cells exposed to retinoic acid	Kawada et al. (2014)
	InsP3	Wortmannin ⊣ InsP3→neurogenesis	Neural crest cells	Evrard et al. (2004)
		P2Y1 ATP receptors ∪ InsP3→Ca^{2+}→cortical neuronal production	Embryonic cortical ventricular zone (VZ)	Weissman et al. (2004)
		GPR157→Gq-IP3→Ca^{2+}→neuronal differentiation of radial glial progenitors	Mouse neocortices at E13 and P0	Takeo et al. (2016)
	RyR	Caffeine→RyR→Ca^{2+}→neuronal differentiation	Mesenchymal stem cells	Resende et al. (2010)
		RyR2$^{-/-}$ ⊣ neurogenesis	Embryonic stem cells	Yu et al. (2008)
	Stim1/Orai1	Stim1^{-} ∪ Orai1^{-} ⊣ SOCE→Ca^{2+}→proliferation	NPC neurospheres or NPCs in the SVZ of adult mice	Somasundaram et al. (2014)

(Continued)

TABLE 3 | Continued

Cat.	Stimulator or Mediator	Mechanism	Experimental model	References
	Stim1	$STIM1^{-}$ ⊣ SOCE→embryonic stem cell differentiation into neural progenitors, neurons or astrocytes ∪ ⊣ cell death and suppressing the proliferation of neural progenitors	Embryonic stem cells and neural progenitors	Hao et al. (2014)
		$SOCE^{-}$ ⊣ proliferation and self-renewal of NSCs	Cultured NSCs and NSCs in the SVZ	Domenichini et al. (2018)
MT	mPTP	$mPTP^{-}$ ∪ mitochondrial superoxide $flash^{-}$ ⊣ $A\beta_{1-42}$ ⊣ proliferation and survival of NPC	NPCs	Hou et al. (2014)
		Cyclosporine A ⊣ mPTP→neuronal differentiation	NPCs	Hou et al. (2013)

expression of the Bax and Apaf-1 proteins in SH-SY5Y cells (Morelli et al., 2013). In contrast to TRPC1, TRPC6 deletion attenuates the effects of NMDAR-mediated Ca^{2+} entry, resulting in a disruption of the effect of Ca^{2+} on neurotoxicity in primary cultured neurons (Chen J. et al., 2017). Blocking TRPV4-mediated Ca^{2+} influx reduces the neurotoxicity of paclitaxel to small and medium dorsal root ganglion neurons (Boehmerle et al., 2018). Regarding TRPM2, cisplatin-induced neurotoxicity in primary DRG cells is attenuated by treatment with its antagonist, 2-aminoethoxydiphenyl borate (Chen J. et al., 2017). TRPM2 knockout blocks Aβ oligomer-induced neurotoxicity, which results in impaired memory in APP/PS1 mice (Ostapchenko et al., 2015). In hippocampal neurons, $A\beta_{1-42}$ induces neurotoxicity by activating TRPM2 (Li and Jiang, 2018).

In addition to these canonical Ca^{2+} transporters, decreasing the expression of CALHM1 exerts neuroprotective effects on oxygen and glucose deprivation in hippocampal slices (Garrosa et al., 2020). On the other hand, APOE has been reported to be involved in regulating neurotoxicity. For example, APOE4 promotes the neurotoxicity induced by Aβ aggregation in AD (Ma et al., 1996). Extracellular APOE4 is cytotoxic to human neuroblastoma SK-N-SH cells, and $A\beta_{1-42}$ enhances the cytotoxicity of APOE4. The carboxyl terminal mutation of L279Q, K282A or Q284A decreases the ability of APOE4 to form SDS-stable oligomers and decreases its cytotoxicity. Structural and thermodynamic analyses showed that all three APOE4 mutants contain significantly increased α-helical and β-sheet structures, which resulted in reduced exposure of the hydrophobic surface to the solvent and reduced conformational stability during chemical denaturation (Dafnis et al., 2018). In $N2a\text{-}APP_{695}$ cells, APOE4 exacerbates the effects of ethanol on inducing neurotoxicity by increasing oxidative stress and apoptosis (Ji et al., 2019). In contrast, APOE1–3 has been shown to protect primary cultures of rat cortical neurons from the neurotoxic effects of the nonfibrillar C-terminal domain of Aβ (Drouet et al., 2001; Brookhouser et al., 2021). APOE isoforms play different roles in neurotoxicity by modulating Aβ deposition in the mouse brain (Drouet et al., 2001). Ca^{2+} mediates the effects of truncated APOE on neurotoxicity in cultured embryonic rat hippocampal neurons (Tolar et al., 1999). Through these mechanisms, APOE-related neurotoxicity might be a therapeutic target for AD (Marques and Crutcher, 2003; **Figure 1**).

The ER Mediates the Effects of Ca^{2+} on Inducing Neurotoxicity as an Intracellular Store

Since Ca^{2+} regulates neurotoxicity *via* transporters located in the cell membrane, the roles of Ca^{2+} derived from intracellular stores in neurotoxicity are further addressed in **Table 4**. For example, Aβ induces neurotoxicity in cortical neurons *via* an ER-mediated apoptotic pathway (Ferreiro et al., 2006; Goswami et al., 2020). In the spinal cord, Ca^{2+} mediates the effects of ER stress on neurotoxicity (Li et al., 2014). By alleviating ER stress, nicotine suppresses the activity of MPP^{+}/MPTP associated with neurotoxicity in PC12 cells (Cai et al., 2017). Similar to its role in AD, Aβ induces neurotoxicity in cortical neurons by promoting ER stress (Song et al., 2008).

As Ca^{2+} mediates the effects of ER stress on neurotoxicity, Ca^{2+} transporters in ER membranes must be associated with neurotoxicity. For example, The generation of InsP3 by activated M3 muscarinic receptors contributes to increased Ca^{2+} influx and subsequent cytotoxicity in rat cerebellar granule cells (Limke et al., 2004). Furthermore, cyanide induces the formation of InsP3, which triggers intracellular neurotoxic signaling events in PC12 cells (Yang et al., 1996). In hippocampal neurons, Ca^{2+} was also found to be the critical cause of microcystin-LR-induced neurotoxicity through PLC- and InsP3-dependent pathways (Cai et al., 2015). Regarding the receptors of InsP3, InsP3R triggers Ca^{2+} influx to mediate isoflurane-induced neurotoxicity, which is facilitated by an APP mutant in SH-SY5Y cells (Liu et al., 2016). In primary cultures of cortical cells, Aβ induces neurotoxic effects by inducing Ca^{2+} release from the ER *via* InsP3R- and RyR-dependent mechanisms (Ferreiro et al., 2004). After inhibiting the activity of InsP3R and RyR, the cytotoxicity and increased Ca^{2+} levels are attenuated. More interestingly, the combined inhibition of both receptors paradoxically increases the amount of cytosolic Ca^{2+} entering PC12 cells from the extracellular space, increasing cytotoxicity

TABLE 4 | The effects of Ca^{2+} on neurotoxicity (including neuroprotection).

Cat.	Stimulator or mediator	Mechanism	Experimental model	References
Ca^{2+}		Ca^{2+}→excitotoxicity ⊣ neuroprotective effects	Primary cerebral cortical neurons	Frandsen and Schousboe (1991)
CM	NMDAR	NMDA→NMDAR→neurotoxicity	Cerebellar granule cells	Xia et al. (1995)
		Ethanol→NMDAR→neurotoxicity	Hippocampal slices	Thomas and Morrisett (2000)
		glutamate→NMDAR→neurotoxicity	Primary rat retinal neurons	Miao et al. (2012)
		$A\beta_{25-35}$ ⊣ pCRMP2 and NMDAR2B ⊣ neurotoxicity	SH-SY5Y cells	Ji et al. (2019)
		Domoic acid→NMDAR→Ca^{2+} influx→neurotoxicity	Cerebellar granule neurons	Berman et al. (2002)
		Dantrolene and ionomycin ⊣ NMDAR→Ca^{2+} influx→neurotoxicity	Rat cortical and retinal ganglion neurons	Lei et al. (1992)
		Homocysteine→GluN2A-NMDAR Ca^{2+} influx→neurotoxicity	Primary cultured cortical neurons	Deep et al. (2019)
		Aβ→NMDAR→Ca^{2+} influx→calpain→neurotoxicity	Hippocampal neurons	Kelly and Ferreira (2006)
	AMPAR	Cannabinoid receptor ⊣ TNF-α→CM-AMPAR→excitotoxicity	Hippocampal neurons	Zhao et al. (2010)
		TNF-α→AMPAR trafficking→excitotoxicity	Spinal neurons	Ferguson et al. (2008)
		TNF-α→GluR2 ⊣ AMPAR→Ca^{2+}→excitotoxicity→neurodegeneration	Primary mouse motor and cortical neurons	Rainey-Smith et al. (2010)
		AMPA ∪ kainate→AMPAR→Ca^{2+} →neurotoxicity	Rat hippocampal neurons	Ambrósio et al. (2000)
		Ethanol→AMPAR→neurotoxicity	Hippocampal slices	Gerace et al. (2021)
	L-VGCC	AMPA/Zn^{2+}→L-VGCC→neurotoxicity	Primary rat cortical neurons	Ambrósio et al. (2000)
		Iron→L-VGCC→neurotoxicity	Primary rat ventral mesencephalic neurons	Xu Y. Y. et al. (2020)
		CXCL12→NMDAR ∪ L-VGCC→p38→neurotoxicity	Cerebrocortical cells	Sanchez et al. (2016)
		Cilnidipine ⊣ L/N-type Ca^{2+} channel →neurotoxicity	Retina from ischaemia-reperfusion-treated rats	Sakamoto et al. (2009)
	TRP	Capsaicin or resiniferatoxin ⊣ TRPV1→microglial neurotoxicity	Primary mouse DRG neurons	Ma et al. (2009)
		Vanilloids and low pH→TRPV1→neurotoxicity	Rat cortical neurons	Shirakawa et al. (2007)
		Capsazepine ⊣ TRPV1→neuronal survival	Rat nigral neurons	Park et al. (2012)
	TRPC1	MPP^+ ⊣ TRPC1→Ca^{2+} influx ⊣ neurotoxicity	SH-SY5Y cells	Bollimuntha et al. (2005)
		$TRPC1^+$ ⊣ neurotoxicity→cytochrome c, Bax and Apaf-1	SH-SY5Y cells	Morelli et al. (2013)
	TRPV4	Paclitaxel→TRPV4→Ca^{2+}→neurotoxicity	DRG neurons	Boehmerle et al. (2018)
	TRPC6	$TRPC6^-$ ⊣ NMDAR→Ca^{2+} influx→ neurotoxicity	Primary neurons	Chen J. et al. (2017)
	TRPM2	2-Aminoethoxydiphenyl borate ⊣ TRPM2→cisplatin→neurotoxicity	Primary DRG neurons	Chen J. et al. (2017)
		$TRPM2^{-/-}$ ⊣ Aβ oligomers→neurotoxicity ⊣ memory	$TRPM2^{-/-}$ APP/PS1 mice	Ostapchenko et al. (2015)
		$A\beta_{1-42}$→TRPM2→neurotoxicity	Hippocampal neurons	Li and Jiang (2018)
	CALHM1	CALHM1−/− ⊣ oxygen and glucose deprivation ⊣ neuroprotective effects	Hippocampal slices from WT $Calhm1^{+/+}$, $Calhm1^{+/-}$, and $Calhm1^{-/-}$ mice	Garrosa et al. (2020)

(Continued)

TABLE 4 | Continued

Cat.	Stimulator or mediator	Mechanism	Experimental model	References
	APOE	APOE4→Aβ aggregates→neurotoxicity→AD	Human cortical neurons	Ma et al. (1996)
		APOE4→Aβ42→neurotoxicity	SK-N-SH cells	Dafnis et al. (2018)
		APOE4 ∪ ethanol→oxidative stress and apoptosis→neurotoxicity	$N2a\text{-}APP_{695}$ cells	Ji et al. (2019)
		$APOE_{2-3}$ ⊣ non-fibrillar C-terminal domain of Aβ→neurotoxicity	Primary rat cortical neurons	Drouet et al. (2001)
		APOE isoforms→Aβ→neurotoxicity	Mouse brain	Hudry et al. (2013)
		Truncated APOE→Ca^{2+} influx→neurotoxicity	Embryonic rat hippocampal neurons	Tolar et al. (1999)
		APOE→neurotoxicity→AD	Embryonic rat hippocampal neurons	Marques and Crutcher (2003)
ER		Aβ→ER→apoptotic pathway→neurotoxicity	Cortical neurons	Ferreiro et al. (2006)
		Ozone (O_3) →ER→Ca^{2+} influx→neurotoxicity	Spinal cord neurons	Li et al. (2014)
		Nicotine ⊣ MPP^+ /MPTP→ER stress→neurotoxicity	PC12 cells	Cai et al. (2017)
		Sevoflurane→ER stress→neurotoxicity	Neuronal cells	Komita et al. (2013)
		Aβ→ER stress→neurotoxicity	Cortical neurons	Song et al. (2008)
	IP3	Cyanide→IP3→neurotoxicity	PC12 cells	Yang et al. (1996)
		M3 muscarinic receptors→IP3→Ca^{2+}→cytotoxicity	Rat cerebellar granule cells	Limke et al. (2004)
		Microcystin-LR→PLC ∪ IP3→Ca^{2+}→neurotoxicty	Hippocampal neurons	Cai et al. (2015)
	InsP3R	Isoflurane ∪ APP^{mut}→InsP3R→Ca^{2+} influx→neurotoxicity	SH-SY5Y cells	Liu et al. (2016)
	InsP3R/RyR	Aβ→InsP3R ∪ RyR→Ca^{2+} efflux from the ER→neurtoxicity	Primary cortical cells	Ferreiro et al. (2004)
		InsP3R ∪ RyR→cytotoxicity	$PS1^{L286V}$ mutant PC12 cells	Yang et al. (2019)
	RyR	RyR→neurotoxicity	Human microglial and THP-1 cells	Klegeris et al. (2007)
		Xbpls ⊣ Aβ→RyR→neurotoxicity	Mammalian neurons	Fernandez-Funez et al. (2010)
MT	VDAC	Aβ→VDAC1→neurotoxicity→AD	PC12 and SH-SY5Y cells	Smilansky et al. (2015)
		Hesperidin ⊣ Aβ ⊣ p-VDAC1 ⊣ neurotoxicity	PC12 cells	Wang et al. (2013)
		Aβ ⊣ p-VDAC1 ⊣ neurotoxicity	Murine septal SN56, SH-SY5Y and hippocampal HT22 cells	Fernandez-Echevarria et al. (2014) and Shoshan-Barmatz et al. (2018)
		VDAC ∪ mERα→Aβ-induced neurotoxicity	SN56 and hippocampal HT22 cells	Marin et al. (2007)
		Antibody ⊣ VDAC2→intracellular Ca^{2+}→neurotoxicity	SH-SY5Y cells	Marin et al. (2007)
	mPTP	Cyclosporin A ⊣ mPTP→neurotoxicity	SH-SY5Y and PC12 cells	Ye et al. (2016)
		4-Hydroxy-2(E)-nonenal ∪ NMDA→mPTP→Ca^{2+} influx→neurotoxicity	Primary rat cortical neurons	Choi et al. (2013)
		NMDA→mPTP→neurotoxicity	Mouse cortical neurons	Kinjo et al. (2018)

(Yang et al., 2019). In addition to InsP3R, RyR alone might be critical for modulating neurotoxicity in human microglia and THP-1 cells (Klegeris et al., 2007; Holland and Pessah, 2021). In cultured mammalian neurons, Xbpls ameliorates Aβ-induced neurotoxicity through an RyR-dependent mechanism (Fernandez-Funez et al., 2010). Thus, the ER is an important intracellular Ca^{2+} store for regulating neurotoxicity in neurons (**Figure 2**).

Mitochondria Are Critical for Regulating Neurotoxicity Through a Ca^{2+}-Dependent Mechanism

In addition to the ER, mitochondria are reported to be critical for regulating neurotoxicity through a Ca^{2+}-dependent mechanism. In particular, VDAC1, a transporter located in mitochondria, mediates Aβ-induced neurotoxicity in PC12 and SH-SY5Y cells and thus represents a potential target for AD treatment (Smilansky et al., 2015). In addition, the dephosphorylation of VDAC1 by hesperidin blocks Aβ-induced neurotoxicity in PC12 cells through a mitochondria-dependent mechanism (Wang et al., 2013). Aβ directly induces neurotoxicity *via* the dephosphorylation of VDAC1 in murine septal SN56, SH-SY5Y and hippocampal HT22 cells (Fernandez-Echevarria et al., 2014; Shoshan-Barmatz et al., 2018). In these cells, the interaction between VDAC and mERα at the plasma membrane may lead to the modulation of Aβ-induced neurotoxicity (Marin et al., 2007). In addition to VDAC1, an anti-VDAC2 antibody reduces neurotoxicity by decreasing intracellular Ca^{2+} levels in SH-SY5Y cells (Marin et al., 2007; Nagakannan et al., 2019). By inhibiting the opening of the mPTP, cyclosporin A protects SH-SY5Y and PC12 cells from neurotoxicity (Ye et al., 2016). In primary cultures of rat cortical neurons, 4-hydroxy-2(E)-nonenal facilitates NMDA-induced neurotoxicity by opening the mPTP, which results in Ca^{2+} influx (Choi et al., 2013). This observation is further supported by a report showing that NMDA induced neurotoxicity *via* the mPTP in cultured murine cortical neurons (Kinjo et al., 2018). Based on this evidence, intracellular Ca^{2+} stores are involved in mediating the effects of Ca^{2+} on neurotoxicity, which potentially contributes to neuronal apoptosis or death (**Table 4**, **Figure 3**).

Ca^{2+} DISRUPTS THE AUTOPHAGIC CLEARANCE OF AGGREGATED PROTEINS

Ca^{2+} Transporters on the Cell Membranes Are Presumably Involved in Regulating Autophagy and Are Responsible for Clearing Aβ or Phosphorylated Tau

As a protein clearing function, autophagy deficiency might be the cause of the aggregation and deposition of Aβ or hyperphosphorylation of tau in APs and NFTs (Pickford et al., 2008; Heckmann et al., 2019). Ca^{2+} signaling plays a crucial role in autophagy in various experimental models (Shaikh et al., 2016; Zhang et al., 2016). Logically, Ca^{2+} transporters are proposed to be involved in regulating autophagy. According to preliminary evidence, NMDARs on the cell membrane contribute to autophagy and the membrane potential in leukaemic megakaryoblasts (Nursalim, 2016). Specifically, exposure to low-dosage NMDA increases LC3 II production, which results in the degradation of GluR1, a subunit of AMPAR, in cultured rat hippocampal neurons (Shehata et al., 2012). Treatment with an antagonist of NMDAR, memantine, induces the NMDAR1-mediated autophagic cell death of T-98G cells (Yoon et al., 2017). In cultured hippocampal neurons, the NR2B antagonist Ro25-6981 markedly attenuates NMDA- and global ischaemia-induced activation of the autophagy pathway by disrupting the association of NR2B and Beclin1, resulting in cell death (Borsello et al., 2003; Liu and Zhao, 2013). In contrast, autophagy upregulates the expression of AMPAR subunits, including GluR1, GluR2, and GluR3, in oxygen- and glucose-deprived and reoxygenated injured neurons (Bao et al., 2017). These observations indicate the involvement of Ca^{2+} transporters located in the cell membranes in regulating autophagy. Similarly, VGCC induces Ca^{2+} influx to inhibit autophagy by activating calpains that cleave ATG5, an important factor for elongating autophagosomes, in H4 cells (Williams et al., 2008). As an atypical Ca^{2+} transporter in the cell membrane, APOE4 potentiates the effects of Aβ on the destabilization and permeabilization of lysosomal membranes, which results in impaired autophagy and the degradation of lysosomes in N2a cells (Ji et al., 2006; Nasiri-Ansari et al., 2021). In addition, rapamycin, an autophagy inducer, enhances mitochondrial autophagy and restores mitochondrial function in APOE4-expressing astrocytes (Schmukler et al., 2020). In astrocytes, APOE4 also impairs autophagy, resulting in attenuated clearance of Aβ (Simonovitch et al., 2016; **Figure 1**).

ER Stress Induces Autophagy by Modulating the Dyshomeostasis of Ca^{2+}

In terms of intracellular Ca^{2+} stores, ER stress induces autophagy in propofol-stimulated C2C12 myoblast cells (Chen et al., 2018). In SK-N-SH cells, ER stress activates autophagy in UPR-stimulated SK-N-SH cells, which indicates its roles in AD (Nijholt et al., 2011). Specifically, polyglutamine induces LC3 conversion *via* ER stress, which initiates the onset of autophagy in C2C5 myoblast cells (Kouroku et al., 2007). Similarly, inducers of ER stress, including tunicamycin, DTT and MG132, concurrently decrease the activity of mTOR and increase the conversion of LC3 I to LC3 II in MEFs (Qin et al., 2010). Lithium induces autophagy by suppressing inositol monophosphatase, leading to the depletion of free inositol and InsP3 in SK-N-SH and COS-7 cells (Sarkar et al., 2005). This observation was also confirmed in lithium-treated IMPA1 knockout mice (Sade et al., 2016). In another study, Ca^{2+} was reported to be located downstream of InsP3R and mediated 2-aminoethoxydiphenyl borate (2-APB)-induced autophagy flux in neonatal rat ventricular myocytes (NRVMs) and HeLa cells (Wong et al., 2013). In addition, by inhibiting InsP3-mediated Ca^{2+} signaling, glucocorticoids induce autophagy in T lymphocytes (Harr et al., 2010). Blockade of InsP3R, the receptor of InsP3, restores autophagy and mitochondrial function in muscle fibers from WT and MDX mice (Valladares et al., 2018). InsP3R knockout upregulates the expression of autophagy markers compared to the WT controls (Cárdenas et al., 2010; Khan and Joseph, 2010). Researchers further emphasized the involvement of Ca^{2+} in autophagy by inducing autophagy through starvation and the activation of the InsP3R-mediated Ca^{2+} signaling pathway, as evidenced by the abolishment of LC3 lipidation and the formation of GFP-LC3 puncta in

HeLa cells; these changes were blocked by the Ca^{2+} chelator BAPTA-AM and the InsP3R inhibitor xestospongin B (Cárdenas et al., 2010). In PC12 cells, isoflurane induced autophagy-dependent cell death *via* InsP3R-Ca^{2+}-dependent mechanisms (Peng et al., 2011). Moreover, InsP3R-mediated transfer of Ca^{2+} from the ER to mitochondria is required to maintain the proper production of ATP, and Ca^{2+} blockade inhibits AMPK activity, leading to the suppression of autophagy in DT40 cells (Cárdenas et al., 2010; Lim et al., 2021a). Regarding the other Ca^{2+} transporters in ER membranes, RyR mediates the effects of propofol on inducing autophagy in cortical neuronal progenitor cells (Qiao et al., 2017). In primary cultured cortical neurons, RyR1 and RyR3 upregulation induced by insulin deprivation increase Ca^{2+} release from the ER, which increases the production of LC3II, an important autophagy marker (Edinger and Thompson, 2004; Chung et al., 2016). As an antagonist of RyRs, ryanodine stimulates autophagy by decreasing the cytosolic levels of Ca^{2+}, leading to neuroprotection in CBE-N2a cells (Liou et al., 2016). By blocking RyR activity, dantrolene and an inhibitory dose of ryanodine reduce the conversion of LC3I to LC3II in HEK293 and C2C12 cells (Vervliet et al., 2017). Similarly, the downregulation of RyR2-mediated Ca^{2+} release decreases ATP production by suppressing mitochondrial metabolism, resulting in an increase in the autophagy-dependent death of rat neonatal cardiomyocytes (Pedrozo et al., 2013; McDaid et al., 2020). By depleting Ca^{2+} from the ER, SOCE exerts a biological effect on Ca^{2+} influx. In PC3 and DU145 cells, autophagic cell death was induced by resveratrol, which downregulated the expression of Stim1 and disrupted its association with TRPC1 and Orai1 (Selvaraj et al., 2016). The overexpression of Stim1 and Orai1 inhibits the effects of starvation- and rapamycin-induced autophagy on A7R5 rat arterial smooth muscle cells (Michiels et al., 2015). Moreover, caerulein promotes the interaction between Stim1 and Orai1, which activates CaN by inducing Ca^{2+} overload, leading to the expression of autophagy-related genes in mice with acute pancreatitis (Zhu et al., 2018). These observations revealed the involvement of ER Ca^{2+} stores in regulating autophagy (**Figure 2**).

Based on the aforementioned observations, InsP3R was found to connect mitochondria, potentially contributing to apoptosis and autophagy (Decuypere et al., 2011b). In Aβ-treated PC12 cells, moderate activation of autophagy regulates intracellular Ca^{2+} levels and the mitochondrial membrane potential (Xue et al., 2016). Reciprocally, mitochondrial fission-mediated Ca^{2+} signaling induces the expression of Stim1 and subsequent SOCE, which promoted autophagy through Ca^{2+}/CAMKK/AMPK signaling cascades (Huang et al., 2017). Regarding Ca^{2+} transporters in mitochondria, VDAC recruits Parkin to defective mitochondria, resulting in the induction of mitochondrial autophagy in HEK293 cells (Sun et al., 2012). In addition, p53 is actively recruited to the outer membrane of mitochondria during nutrient deprivation, resulting in opening of the mPTP, an increase in the conversion of LC3BII to LC3BI, and the formation of LC3-GFP puncta in ventricular myocytes (Eydelnant et al., 2009; Xu H. X. et al., 2020).

Ca^{2+} Transporters on the Lysosomal Membranes Are Responsible for Regulating the Degradation of Aggregated Proteins

As the lysosome is the organelle responsible for degrading proteins, studies aiming to elucidate the roles of Ca^{2+} transporters located in lysosomes in regulating autophagy would be interesting. For example, Ca^{2+} stimulates lysosomal v-ATPase and mTORC1 pathways, which potentially contribute to the effects of orexin and hypocretin on autophagy in HEK293T cells (Wang et al., 2014). Rapamycin treatment inhibits mTOR activity by decreasing phosphorylation at two serine residues, leading to the induction of autophagy *via* a Ca^{2+}-dependent mechanism (Onyenwoke et al., 2015). Furthermore, v-ATPase deficiency in Presenilin 1 (PS1) loss-of-function states causes deficits in lysosomes and autophagy, which contributes to abnormal cellular Ca^{2+} homeostasis (Lee et al., 2015). In addition, accumulating evidence is showing that the functional regulation of TRP channels contributes to Ca^{2+} signaling and subsequent autophagy initiation (Sukumaran et al., 2016). Transient receptor potential cation channel mucolipin subfamily member 1 (TRPML1) is a lysosomal Ca^{2+} channel, which can mediate the release of Ca^{2+} from lysosomes to cytoplasm. TRPML1 mutation increases the formation of autophagosomes, disrupts the fusion of autophagosomes and lysosomes, and induces the accumulation of p62 and insufficient removal of ubiquitinated proteins and/or defective mitochondria in fibroblasts from patients with mucolipidosis type IV (MLIV; Vergarajauregui et al., 2008; Nakamura et al., 2020). Under nutrient starvation conditions, TRPML1 upregulation is critical for increasing lysosomal proteolytic activity in COS-1 cells (Wang W. et al., 2015). Moreover, the overexpression of TRPML3/MCOLN3 induces autophagy in HeLa cells *via* a Ca^{2+}-dependent mechanism (Kim et al., 2009). Similarly, both exogenous and endogenous Ca^{2+} modulate autophagy *via* different transporters (**Table 5**).

THE HERBS USED AS FOOD AND SEASONINGS IN CHINESE DAILY LIFE POTENTIALLY CONTRIBUTE TO AD TREATMENT BY RESTORING THE Ca^{2+} CONCENTRATION THROUGH EFFECTS ON ITS TRANSPORTERS

As discussed above, Ca^{2+} overload plays important roles in aggravating AD *via* its transporters. In particular, Ca^{2+} overload perturbs the activities of the brain network, which increases the risk of AD and contributes causally to synaptic and cognitive deficits in hAPP mice. Since Ca^{2+} homeostasis is regulated by different transporters, transporters might be potential therapeutic targets for treating AD by modulating Ca^{2+} homeostasis. However, the outcome is not always consistent with our expectation. For instance, memantine, a noncompetitive NMDA antagonist, is an effective drug approved by the FDA

TABLE 5 | Ca^{2+} disrupts the effects of autophagy on clearing aggregated proteins.

Cat.	Stimulator or mediator	Mechanism	Experimental model	References
Ca^{2+}		Mitochondria damage→ROS→TRPML1→Ca^{2+} →autophagy	MCOLN1$^{-/-}$ cells	Zhang et al. (2016)
		Ca^{2+}→autophagy	Cardiomyocytes	Shaikh et al. (2016)
CM	NMDAR	Memantine ⊣ NMDAR1 ⊣ autophagic cell death	T-98G cells	Yoon et al. (2017)
		Ro25–6981 ⊣ NMDA ∪ global ischaemia→NR2B ∪ Beclin1→autophagy	Hippocampal neurons	Borsello et al. (2003)
		MiR-93–5p ⊣ PTEN→AKT/mTOR→ NMDA→autophagy	Retinal ganglion cells	Li et al. (2018)
	NMDAR/AMPAR	Low dosage NMDA→LC3 II ⊣ GluR1, a subunit of AMPAR	Rat hippocampal neurons	Shehata et al. (2012)
	AMPAR	Oxygen/glucose-deprived and reoxygenated injured neurons→autophagy→AMPAR, including the subunits of GluR1, GluR2, and GluR3	Primary rat hippocampal neurons	Bao et al. (2017)
	VGCC	VGCC→Ca^{2+} influx→calpains →ATG5 cleavage ⊣ autophagosomes →autophagy	H4 cells	Williams et al. (2008)
	APOE4	APOE4→Aβ→destabilization and permeabilization of lysosomal membranes→degradation of lysosomes ⊣ autophagy	N2a cells	Ji et al. (2006)
		APOE4 ⊣ mitophagy and mitochondrial function	APOE4-expressing astrocytes	Schmukler et al. (2020)
		APOE4 ⊣ autophagy→Aβ clearance	Astrocytes	Simonovitch et al. (2016)
ER		propofol→ER stress→autophagy	C2C12 myoblast cells	Chen et al. (2018)
		UPR→ER stress→autophagy	SK-N-SH cells	Nijholt et al. (2011)
		Polyglutamine→ER stress→LC3 conversion→autophagy	C2C5 myoblast cells	Kouroku et al. (2007)
		Tunicamycin, DTT and MG132→ER stress ⊣ mTOR ∪ →conversion of LC3 I to LC3 II	MEF cells	Qin et al. (2010)
	Ca^{2+}	Rapamycin→Ca^{2+} efflux from the ER→autophagy	MCF-7 cells	Høyer-Hansen et al. (2007)
		BAPTA-AM ⊣ Ca^{2+}-mobilizing agents→autophagy	MEFs	Grotemeier et al. (2010)
	IP3	Lithium ⊣ inositol monophosphatase→inositol and IP3 ⊣ autophagy	SK-N-SH and COS-7 cells	Sarkar et al. (2005)
		IP3→Beclin1→autophagy	Li-treated IMPA1 KO mice	Sade et al. (2016)
		Glucocorticoids ⊣ IP3→Ca^{2+} efflux from ER ⊣ autophagy	T-lymphocytes	Harr et al. (2010)
	InsP3R	InsP3R ⊣ autophagy	Muscle fibers from WT and MDX mice	Valladares et al. (2018)
		2-aminoethoxydiphenyl borate (2-APB) ⊣ InsP3R→Ca^{2+} release from the ER ⊣ autophagy flux	Neonatal rat ventricular myocytes (NRVMs) and HeLa cells	Wong et al. (2013)
		InsP3R$^{-/-}$→autophagy markers	Chicken DT40B lymphocytes (TKO cells)	Cárdenas et al. (2010) and Khan and Joseph (2010)
		Starvation ⊣ (xestospongin B ⊣)InsP3R→(BAPTA-AM ⊣)Ca^{2+} ⊣ LC3 lipidation ∪ GFP-LC3 puncta→autophagy	HeLa cells	Cárdenas et al. (2010)

(Continued)

TABLE 5 | Continued

Cat.	Stimulator or mediator	Mechanism	Experimental model	References
		Isoflurane ⊣ InsP3R→Ca^{2+} ⊣ autophagic cell death	PC12 cells	Peng et al. (2011)
		InsP3R→Ca^{2+} efflux from the ER→ATP→Ca^{2+} uptake by mitochondria ⊣ AMPK→autophagy	DT40 cells	Cárdenas et al. (2010)
	RyR	ryanodine ⊣ RyRs→autophagy	CBE-N2a cells	Liou et al. (2016)
		Insulin deprivation→RyR1/3→Ca^{2+} efflux from the ER→LC3 II→autophagy	Primary cortical neurons	Edinger and Thompson (2004) and Chung et al. (2016)
		Dantrolene ⊣ RyR→conversion of LC3 I to LC3 II	HEK293 and C2C12 cells	Vervliet et al. (2017)
		RyR^- ⊣ Ca^{2+}→mitochondrial metabolism→ATP ⊣ autophagic cell death	Rat neonatal cardiomyocytes	Pedrozo et al. (2013)
	SOCE	Resveratrol ⊣ Stim1 ⊣ TRPC1 ∪ Orai1 →autophagic cell death	PC3 and DU145 cells	Selvaraj et al. (2016)
		$Stim1^+$ ∪ $Orai1^+$ ⊣ starvation ∪ rapamycin →autophagy	A7R5, rat arterial smooth muscle cells	Michiels et al. (2015)
		Caerulein→Stim1 ∪ Orai1→CaN Ca^{2+}→autophagy-related genes	Mice with acute pancreatitis	Zhu et al. (2018)
MT	VDAC	VDAC ∪ Parkin→mitochondrial autophagy.	HEK293 cells	Sun et al. (2012)
	mPTP	Nutrient deprivation→p53 ∪ outer membrane of mitochondria→mPTP→conversion from LC3B II to LC3B I ∪ LC3-GFP puncta	Ventricular myocytes	Eydelnant et al. (2009)
LM	v-ATPase	Orexin ∪ hypocretin→v-ATPase→Ca^{2+} influx into lysosomes ∪ mTORC1→autophagy	HEK293T cells	Wang et al. (2014)
		$PS1^{mut}$ ⊣ vATPase→Ca^{2+} influx into lysosomes→autophagy	$PS1^{mut}$ cells	Lee et al. (2015)
	TRPML1	$TRPML1^{mut}$→autophagosomes ∪ ⊣ fusion of autophagosomes and lysosomes→removing p62 and ubiquitinated proteins	Fibroblasts from patients with MLIV	Vergarajauregui et al. (2008)
		Nutrient starvation→TRPML1→lysosomal proteolytic activity	COS-1 cells	Wang W. et al. (2015)
		Rapamycin ⊣ mTOR ⊣ autophagy	HEK293 cells	Onyenwoke et al. (2015)
	TRPML3	$TRPML3/MCOLN3^+$→Ca^{2+} →autophagy	HeLa cells	Kim et al. (2009)

for the treatment of AD. The VGCC inhibitor levetiracetam, an antiepileptic drug, exerts positive effects on patients with AD (Cumbo and Ligori, 2010; Vogl et al., 2012), whereas no beneficial therapeutic effect on AD was observed for the VGCC antagonist nilvadipine (Lawlor et al., 2018).

Although several FDA-approved chemical drugs are currently available for treating AD, the identification of new compounds targeting Ca^{2+} transporters to prevent, halt and reverse the dyshomeostasis of Ca^{2+} is urgently needed. We thereby summarized the drug candidates derived from herbs used as food or seasonings in Chinese daily life used to restore Ca^{2+} homeostasis in animals (**Table 6**). For example, asiatic acid from *Centella asiatica* reduces intracellular Ca^{2+} levels by inhibiting N- and P/Q-type calcium channels in the rat hippocampus (Lu et al., 2019). In rat cerebrocortical synaptosomes, silymarin derived from *Silybum marianum* similarly reduces intracellular Ca^{2+} concentrations by inhibiting N- and P/Q-type Ca^{2+} channels (Lu et al., 2020a). In addition, the I3C derivative [1(4-chloro-3-nitrobenzenesulfonyl)-1H-indol-3-yl]-methanol (CIM) from broccoli, cauliflower, and brussels sprouts inhibits Ca^{2+} influx by suppressing the activities of P/Q-type Ca^{2+} channels in rats (Lu et al., 2020b). In addition, numerous active compounds, such as uncarialin A, emodin, flavones, aconitine, patchouli alcohol (PA), coutareagenin, neferine, salvianolic acid B (Sal B), danshensu, tetrandrine, osthole, and hydroxy-safflor yellow A, derived from herbs, including *Uncaria rhynchophylla*,

TABLE 6 | The effects of herbal medicines on regulating Ca^{2+} dyshomeostasis.

Cat.	Herbs	Active compounds	Mechanism	Experimental model	Reference
CM	*Centella asiatica*	Asiatic acid	Asiatic acid ⊣ N- and P/Q-type calcium channels→Ca^{2+} influx	Rat hippocampus	Lu et al. (2019)
	Silybum marianum	Silymarin	Silymarin ⊣ N- and P/Q-type Ca^{2+} channels→Ca^{2+} influx	Rat cerebrocortical synaptosomes	Lu et al. (2020a)
	Broccoli, cauliflower and brussels sprouts	I3C derivative [1(4-chloro-3-nitrobenzenesulfonyl)-1H-indol-3-yl]-methanol (CIM)	CIM ⊣ P/Q-type Ca^{2+} channels→Ca^{2+} influx	Rat	Lu et al. (2020b)
	Uncaria rhynchophylla	Uncarialin A	Uncarialin A ⊣ L-type calcium channel subunit alpha-1C (Cav1.2)→Ca^{2+} influx	SD rats	Yun et al. (2020)
	Rhubarb	Emodin	Emodin ⊣ L-type Ca^{2+} channels	Isolated beating rabbit atria	Zhou et al. (2014)
	Acanthopanax senticosus (AS)	Flavones	Total flavones from AS (TFAS) ⊣ L-type Ca^{2+} channel	SD rats	Guan et al. (2015)
	Aconitum	Aconitine	Aconitine→L-type Ca^{2+} channels→intracellular Ca^{2+} levels	Wistar rats	Sun G. B. et al. (2014)
	Cablin	Patchouli alcohol (PA)	PA ⊣ VDCC and ROCC→Ca^{2+} influx	Vascular smooth muscle cells (VSMCs)	Li et al. (2018)
	Dandelion and *Astragalus*	Coutareagenin	Coutareagenin ⊣ G protein→Ca^{2+} influx	Rat aortic (A10) cells	Vierling et al. (2014)
	Plantule of *Nelumbo nucifera*	Neferine	Neferine→Gi/o protein ⊣ Ca^{2+} influx	SD rats	Yeh et al. (2020)
	Salvia miltiorrhiza	Salvianolic acid B (Sal B)	Sal B ⊣ TRPC3 and TRPC6→intracellular Ca^{2+} levels	Male SD rats	Chen R. C. et al. (2017)
	Radix *Salvia miltiorrhiza*	Danshensu	Danshensu ⊣ p-JNK and NF-κB→TRPC6→Ca^{2+} influx	H9C2 cells	Meng et al. (2016)
	Stephania tetrandra	Tetrandrine	Tetrandrine ⊣ RhoA/ROCK pathway→TRPC6→intracellular Ca^{2+} levels	Murine podocytes	Yu et al. (2020)
	Cnidium monnieri	Osthole	Osthole ⊣ TRPV1→Ca^{2+} influx	Cultured DRG neurons	Yang et al. (2016)
	Carthamus tinctorius L.	Hydroxy-safflor yellow A	HSYA→Endothelial TRPV4→Ca^{2+} influx	Wistar rats	Yang J. et al. (2020)
ER	*Cephalotaxus fortunei*	Homoharringtonine	Homoharringtonine→Histamine H receptor →Ca^{2+} released from the ER→ cytosolic free Ca^{2+} levels	HEK293 cells	Guo et al. (2014)
	Magnolia tree	Magnolol	Magnolol→PKC-sensitive store-operated Ca^{2+}→Ca^{2+} influx Magnolol ⊣ endoplasmic reticulum Ca^{2+}-ATP pump ⊣ Ca^{2+} release	OC2 cells	Matsubara et al. (2005) and Hsieh et al. (2018)
	Polygonum cuspidatum	Polydatin (PD)	PD ⊣ SOCE→intracellular Ca^{2+} levels	Mast cells	Yang et al. (2013)
MT	*Ginkgo biloba*	*Ginkgo biloba* extracts (EGb)	EGb ⊣ mitochondrial Ca^{2+} overload	C57BL/6 mice	Li et al. (2019)

CM, cell membrane; MT, mitochondria; LM, lysosome; PTM, posttranslational modification; →, stimulate, activate, induce, result in, lead to; ⊣, inhibit, block, suppress, deactivate, degrade; +, overexpress, activate, upregulate, induce; -, knockdown, deplete, ablate, siRNA, deactivate, downregulate, deficiency; –/–, knock out; ∪, interact, facilitate, associate, potentiate, recruit.

rhubarb, *Acanthopanax senticosus* (AS), Aconitum, Cablin, dandelion and *Astragalus*, plantule of *Nelumbo nucifera*, *Salvia miltiorrhiza*, Radix *Salvia miltiorrhiza*, *Stephania tetrandra*, *Cnidium monnieri*, and *Carthamus tinctorius* L., respectively, inhibit Ca^{2+} influx by deactivating Ca^{2+} transporters on the cell membrane, such as L-type Ca^{2+} channels, VDCC, G protein-coupled receptors, TRPCs, and TRPVs in different animal and cell models (Sun G. B. et al., 2014; Vierling et al., 2014; Zhou et al., 2014; Guan et al., 2015; Meng et al., 2016; Yang et al., 2016; Chen R. C. et al., 2017; Li et al., 2018; Yang J. et al., 2020; Yeh et al., 2020; Yu et al., 2020; Yun et al., 2020). Moreover, active compounds, including homoharringtonine, magnolol, polydatin (PD), and *Ginkgo biloba* extracts (EGb), derived from herbs, such as *Cephalotaxus fortunei*, magnolia tree, *Polygonum cuspidatum*, and *Ginkgo biloba*, respectively, modulate Ca^{2+} homeostasis by regulating the activities of transporters located in the ER through mechanism partially dependent on SOCE or mitochondria (Matsubara et al., 2005; Yang et al., 2013; Guo et al., 2014; Hsieh et al., 2018; Li et al., 2019). Although these herbs have not been used in clinical trials, all this evidence suggests that the herbs used as food and seasonings in Chinese daily life potentially contribute to treating

AD by targeting Ca^{2+} transporters to restore Ca^{2+} concentrations (**Table 6**).

CONCLUSIONS

During the development and progression of AD, Ca^{2+} concentrations are increased in the cytosol of neuronal cells *via* transportation from the extracellular space and intracellular stores through transporter-dependent mechanisms. Ca^{2+} accumulation in neuronal cells induces the production and deposition of Aβ and hyperphosphorylated tau in APs and NFTs, leading to impaired learning ability in patients with AD. Moreover, transporters in the cell membrane, endoplasmic reticulum, mitochondria, and lysosomal membranes are critical for mediating the effects of Ca^{2+} on neuroinflammation, neuronal injury, neurogenesis, neurotoxicity, neuroprotection, autophagy, and synaptic plasticity, which contribute to the cognitive decline associated with AD (**Figure 4**). Based on these theoretical investigations, some bioactive components from Chinese herbal medicines have the potential to treat AD by targeting Ca^{2+} transporters. Moreover, Ca^{2+} transporters are progressively becoming new therapeutic targets for treating AD.

AUTHOR CONTRIBUTIONS

P-PG and L-LC contributed to conceptualizing and drafting the manuscript. YY contributed to summarizing the data presented in **Table 6**. PW contributed to conceptualizing, writing, reviewing, and editing the manuscript. All authors have agreed to publish the manuscript. All authors contributed to the article and approved the submitted version.

FUNDING

This work was supported in part or in whole by the National Natural Science Foundation of China (CN; 81771167 and 81870840).

REFERENCES

Ambrósio, A. F., Silva, A. P., Malva, J. O., Mesquita, J. F., Carvalho, A. P., and Carvalho, C. M. (2000). Role of desensitization of AMPA receptors on the neuronal viability and on the $[Ca^{2+}]$i changes in cultured rat hippocampal neurons. *Eur. J. Neurosci.* 12, 2021–2031. doi: 10.1046/j.1460-9568.2000.00091.x

Arispe, N., Diaz, J., Durell, S. R., Shafrir, Y., and Guy, H. R. (2010). Polyhistidine peptide inhibitor of the Abeta calcium channel potently blocks the Abeta-induced calcium response in cells. Theoretical modeling suggests a cooperative binding process. *Biochemistry* 49, 7847–7853. doi: 10.1021/bi1006833

Bao, L., Li, R. H., Li, M., Jin, M. F., Li, G., Han, X., et al. (2017). Autophagy-regulated AMPAR subunit upregulation in *in vitro* oxygen glucose deprivation/reoxygenation-induced hippocampal injury. *Brain Res.* 1668, 65–71. doi: 10.1016/j.brainres.2017.05.019

Beattie, M. S., Ferguson, A. R., and Bresnahan, J. C. (2010). AMPA-receptor trafficking and injury-induced cell death. *Eur. J. Neurosci.* 32, 290–297. doi: 10.1111/j.1460-9568.2010.07343.x

Ben-Hail, D., and Shoshan-Barmatz, V. (2016). VDAC1-interacting anion transport inhibitors inhibit VDAC1 oligomerization and apoptosis. *Biochim. Biophys. Acta* 1863, 1612–1623. doi: 10.1016/j.bbamcr.2016.04.002

Berman, F. W., LePage, K. T., and Murray, T. F. (2002). Domoic acid neurotoxicity in cultured cerebellar granule neurons is controlled preferentially by the NMDA receptor Ca^{2+} influx pathway. *Brain Res.* 924, 20–29. doi: 10.1016/s0006-8993(01)03221-8

Bessou, M., Lopez, J., Gadet, R., Deygas, M., Popgeorgiev, N., Poncet, D., et al. (2020). The apoptosis inhibitor Bcl-xL controls breast cancer cell migration through mitochondria-dependent reactive oxygen species production. *Oncogene* 39, 3056–3074. doi: 10.1038/s41388-020-1212-9

Blackshaw, S., Sawa, A., Sharp, A. H., Ross, C. A., Snyder, S. H., and Khan, A. A. (2000). Type 3 inositol 1,4,5-trisphosphate receptor modulates cell death. *FASEB J.* 14, 1375–1379. doi: 10.1096/fj.14.10.1375

Boehmerle, W., Huehnchen, P., Lee, S. L. L., Harms, C., and Endres, M. (2018). TRPV4 inhibition prevents paclitaxel-induced neurotoxicity in preclinical models. *Exp. Neurol.* 306, 64–75. doi: 10.1016/j.expneurol.2018.04.014

Bollimuntha, S., Singh, B. B., Shavali, S., Sharma, S. K., and Ebadi, M. (2005). TRPC1-mediated inhibition of 1-methyl-4-phenylpyridinium ion neurotoxicity in human SH-SY5Y neuroblastoma cells. *J. Biol. Chem.* 280, 2132–2140. doi: 10.1074/jbc.M407384200

Borsello, T., Croquelois, K., Hornung, J. P., and Clarke, P. G. (2003). N-methyl-d-aspartate-triggered neuronal death in organotypic hippocampal cultures is endocytic, autophagic and mediated by the c-Jun N-terminal kinase pathway. *Eur. J. Neurosci.* 18, 473–485. doi: 10.1046/j.1460-9568.2003.02757.x

Brand-Schieber, E., and Werner, P. (2004). Calcium channel blockers ameliorate disease in a mouse model of multiple sclerosis. *Exp. Neurol.* 189, 5–9. doi: 10.1016/j.expneurol.2004.05.023

Brookhouser, N., Raman, S., Frisch, C., Srinivasan, G., and Brafman, D. A. (2021). APOE2 mitigates disease-related phenotypes in an isogenic hiPSC-based model of Alzheimer's disease. *Mol. Psychiatry* [Online ahead of print]. doi: 10.1038/s41380-021-01076-3

Brown, G. C., and Neher, J. J. (2014). Microglial phagocytosis of live neurons. *Nat. Rev. Neurosci.* 15, 209–216. doi: 10.1038/nrn3710

Brustein, E., Côté, S., Ghislain, J., and Drapeau, P. (2013). Spontaneous glycine-induced calcium transients in spinal cord progenitors promote neurogenesis. *Dev. Neurobiol.* 73, 168–175. doi: 10.1002/dneu.22050

Bull, R., Finkelstein, J. P., Gálvez, J., Sánchez, G., Donoso, P., Behrens, M. I., et al. (2008). Ischemia enhances activation by Ca^{2+} and redox modification of ryanodine receptor channels from rat brain cortex. *J. Neurosci.* 28, 9463–9472. doi: 10.1523/JNEUROSCI.2286-08.2008

Bullock, R. (2006). Efficacy and safety of memantine in moderate-to-severe Alzheimer disease: the evidence to date. *Alzheimer Dis. Assoc. Disord.* 20, 23–29. doi: 10.1097/01.wad.0000201847.29836.a5

Bursztajn, S., Falls, W. A., Berman, S. A., and Friedman, M. J. (2007). Cell proliferation in the brains of NMDAR NR1 transgenic mice. *Brain Res.* 1172, 10–20. doi: 10.1016/j.brainres.2007.07.045

Cai, F., Liu, J., Li, C., and Wang, J. (2015). Intracellular calcium plays a critical role in the microcystin-LR-elicited neurotoxicity through PLC/IP3 pathway. *Int. J. Toxicol.* 34, 551–558. doi: 10.1177/1091581815606352

Cai, Y., Zhang, X., Zhou, X., Wu, X., Li, Y., Yao, J., et al. (2017). Nicotine suppresses the neurotoxicity by MPP(+)/MPTP through activating α7nAChR/PI3K/Trx-1 and suppressing ER stress. *Neurotoxicology* 59, 49–55. doi: 10.1016/j.neuro.2017.01.002

Calvo-Rodriguez, M., Hernando-Pérez, E., López-Vázquez, S., Núñez, J., Villalobos, C., and Núñez, L. (2020). Remodeling of intracellular Ca(2+) homeostasis in rat hippocampal neurons aged *in vitro*. *Int. J. Mol. Sci.* 21:1549. doi: 10.3390/ijms21041549

Cao, L. L., Guan, P. P., Liang, Y. Y., Huang, X. S., and Wang, P. (2019). Calcium ions stimulate the hyperphosphorylation of tau by activating microsomal prostaglandin E synthase 1. *Front. Aging Neurosci.* 11:108. doi: 10.3389/fnagi.2019.00108

Cao, X., and Südhof, T. C. (2001). A transcriptionally [correction of transcriptively] active complex of APP with Fe65 and histone acetyltransferase Tip60. *Science* 293, 115–120. doi: 10.1126/science.1058783

Cárdenas, C., Miller, R. A., Smith, I., Bui, T., Molgó, J., Müller, M., et al. (2010). Essential regulation of cell bioenergetics by constitutive InsP3 receptor Ca2+ transfer to mitochondria. *Cell* 142, 270–283. doi: 10.1016/j.cell.2010.06.007

Cardozo, A. K., Ortis, F., Storling, J., Feng, Y. M., Rasschaert, J., Tonnesen, M., et al. (2005). Cytokines downregulate the sarcoendoplasmic reticulum pump Ca2+ ATPase 2b and deplete endoplasmic reticulum Ca2+, leading to induction of endoplasmic reticulum stress in pancreatic beta-cells. *Diabetes* 54, 452–461. doi: 10.2337/diabetes.54.2.452

Chao, C. C., Huang, C. C., Lu, D. Y., Wong, K. L., Chen, Y. R., Cheng, T. H., et al. (2012). Ca2+ store depletion and endoplasmic reticulum stress are involved in P2X7 receptor-mediated neurotoxicity in differentiated NG108–15 cells. *J. Cell. Biochem.* 113, 1377–1385. doi: 10.1002/jcb.24010

Chen, S., Averett, N. T., Manelli, A., Ladu, M. J., May, W., and Ard, M. D. (2005). Isoform-specific effects of apolipoprotein E on secretion of inflammatory mediators in adult rat microglia. *J. Alzheimers Dis.* 7, 25–35. doi: 10.3233/jad-2005-7104

Chen, T., Dai, S. H., Jiang, Z. Q., Luo, P., Jiang, X. F., Fei, Z., et al. (2017). The AMPAR antagonist perampanel attenuates traumatic brain injury through anti-oxidative and anti-inflammatory activity. *Cell. Mol. Neurobiol.* 37, 43–52. doi: 10.1007/s10571-016-0341-8

Chen, H., Gao, W., Yang, Y., Guo, S., Wang, H., Wang, W., et al. (2014). Inhibition of VDAC1 prevents Ca^2-mediated oxidative stress and apoptosis induced by 5-aminolevulinic acid mediated sonodynamic therapy in THP-1 macrophages. *Apoptosis* 19, 1712–1726. doi: 10.1007/s10495-014-1045-5

Chen, J., Li, Z., Hatcher, J. T., Chen, Q. H., Chen, L., Wurster, R. D., et al. (2017). Deletion of TRPC6 attenuates NMDA receptor-mediated Ca(2+) entry and Ca(2+)-induced neurotoxicity following cerebral ischemia and oxygen-glucose deprivation. *Front. Neurosci.* 11:138. doi: 10.3389/fnins.2017.00138

Chen, X., Li, L. Y., Jiang, J. L., Li, K., Su, Z. B., Zhang, F. Q., et al. (2018). Propofol elicits autophagy *via* endoplasmic reticulum stress and calcium exchange in C2C12 myoblast cell line. *PLoS One* 13:e0197934. doi: 10.1371/journal.pone.0197934

Chen, R. C., Sun, G. B., Ye, J. X., Wang, J., Zhang, M. D., and Sun, X. B. (2017). Salvianolic acid B attenuates doxorubicin-induced ER stress by inhibiting TRPC3 and TRPC6 mediated Ca(2+) overload in rat cardiomyocytes. *Toxicol. Lett.* 276, 21–30. doi: 10.1016/j.toxlet.2017.04.010

Cheng, A., Kawahata, I., and Fukunaga, K. (2020). Fatty acid binding protein 5 mediates cell death by psychosine exposure through mitochondrial macropores formation in oligodendrocytes. *Biomedicines* 8:635. doi: 10.3390/biomedicines8120635

Cheng, L., Muroi, M., Cao, S., Bian, L., Osada, H., Xiang, L., et al. (2019). 3β,23,28-Trihydroxy-12-oleanene 3β-caffeate from desmodium sambuense-induced neurogenesis in PC12 cells mediated by ER stress and BDNF-TrkB signaling pathways. *Mol. Pharm.* 16, 1423–1432. doi: 10.1021/acs.molpharmaceut.8b00939

Choi, I. Y., Lim, J. H., Kim, C., Song, H. Y., Ju, C., and Kim, W. K. (2013). 4-hydroxy-2(E)-nonenal facilitates nmda-induced neurotoxicity *via* triggering mitochondrial permeability transition pore opening and mitochondrial calcium overload. *Exp. Neurobiol.* 22, 200–207. doi: 10.5607/en.2013.22.3.200

Chung, K. M., Jeong, E. J., Park, H., An, H. K., and Yu, S. W. (2016). Mediation of autophagic cell death by type 3 ryanodine receptor (RyR3) in adult hippocampal neural stem cells. *Front. Cell. Neurosci.* 10:116. doi: 10.3389/fncel.2016.00116

Coen, K., Flannagan, R. S., Baron, S., Carraro-Lacroix, L. R., Wang, D., Vermeire, W., et al. (2012). Lysosomal calcium homeostasis defects, not proton pump defects, cause endo-lysosomal dysfunction in PSEN-deficient cells. *J. Cell. Biol.* 198, 23–35. doi: 10.1083/jcb.201201076

Cui, R., Yan, L., Luo, Z., Guo, X., and Yan, M. (2015). Blockade of store-operated calcium entry alleviates ethanol-induced hepatotoxicity *via* inhibiting apoptosis. *Toxicol. Appl. Pharmacol.* 287, 52–66. doi: 10.1016/j.taap.2015.05.014

Cumbo, E., and Ligori, L. D. (2010). Levetiracetam, lamotrigine and phenobarbital in patients with epileptic seizures and Alzheimer's disease. *Epilepsy Behav.* 17, 461–466. doi: 10.1016/j.yebeh.2010.01.015

Dafnis, I., Argyri, L., and Chroni, A. (2018). Amyloid-peptide β 42 enhances the oligomerization and neurotoxicity of apoE4: The C-terminal residues Leu279, Lys282 and Gln284 modulate the structural and functional properties of apoE4. *Neuroscience* 394, 144–155. doi: 10.1016/j.neuroscience.2018.10.026

D'Ascenzo, M., Piacentini, R., Casalbore, P., Budoni, M., Pallini, R., Azzena, G. B., et al. (2006). Role of L-type Ca2+ channels in neural stem/progenitor cell differentiation. *Eur. J. Neurosci.* 23, 935–944. doi: 10.1111/j.1460-9568.2006.04628.x

Daschil, N., Obermair, G. J., Flucher, B. E., Stefanova, N., Hutter-Paier, B., Windisch, M., et al. (2013). CaV1.2 calcium channel expression in reactive astrocytes is associated with the formation of amyloid-β plaques in an Alzheimer's disease mouse model. *J. Alzheimers Dis.* 37, 439–451. doi: 10.3233/JAD-130560

Deb, B. K., Chakraborty, P., Gopurappilly, R., and Hasan, G. (2020). SEPT7 regulates Ca(2+) entry through Orai channels in human neural progenitor cells and neurons. *Cell Calcium* 90:102252. doi: 10.1016/j.ceca.2020.102252

Decuypere, J. P., Bultynck, G., and Parys, J. B. (2011a). A dual role for Ca(2+) in autophagy regulation. *Cell Calcium* 50, 242–250. doi: 10.1016/j.ceca.2011.04.001

Decuypere, J. P., Monaco, G., Bultynck, G., Missiaen, L., De Smedt, H., and Parys, J. B. (2011b). The IP(3) receptor-mitochondria connection in apoptosis and autophagy. *Biochim. Biophys. Acta* 1813, 1003–1013. doi: 10.1016/j.bbamcr.2010.11.023

Deep, S. N., Mitra, S., Rajagopal, S., Paul, S., and Poddar, R. (2019). GluN2A-NMDA receptor-mediated sustained Ca(2+) influx leads to homocysteine-induced neuronal cell death. *J. Biol. Chem.* 294, 11154–11165. doi: 10.1074/jbc.RA119.008820

Dolga, A. M., Letsche, T., Gold, M., Doti, N., Bacher, M., Chiamvimonvat, N., et al. (2012). Activation of KCNN3/SK3/K(Ca)2.3 channels attenuates enhanced calcium influx and inflammatory cytokine production in activated microglia. *Glia* 60, 2050–2064. doi: 10.1002/glia.22419

Domenichini, F., Terrié, E., Arnault, P., Harnois, T., Magaud, C., Bois, P., et al. (2018). Store-operated calcium entries control neural stem cell self-renewal in the adult brain subventricular zone. *Stem Cells* 36, 761–774. doi: 10.1002/stem.2786

Dong, Y., Kalueff, A. V., and Song, C. (2017). N-methyl-d-aspartate receptor-mediated calcium overload and endoplasmic reticulum stress are involved in interleukin-1beta-induced neuronal apoptosis in rat hippocampus. *J. Neuroimmunol.* 307, 7–13. doi: 10.1016/j.jneuroim.2017.03.005

Drouet, B., Fifre, A., Pinçon-Raymond, M., Vandekerckhove, J., Rosseneu, M., Guéant, J. L., et al. (2001). ApoE protects cortical neurones against neurotoxicity induced by the non-fibrillar C-terminal domain of the amyloid-beta peptide. *J. Neurochem.* 76, 117–127. doi: 10.1046/j.1471-4159.2001.00047.x

Du, H., Guo, L., Fang, F., Chen, D., Sosunov, A. A., McKhann, G. M., et al. (2008). Cyclophilin D deficiency attenuates mitochondrial and neuronal perturbation and ameliorates learning and memory in Alzheimer's disease. *Nat. Med.* 14, 1097–1105. doi: 10.1038/nm.1868

Du, L. L., Wang, L., Yang, X. F., Wang, P., Li, X. H., Chai, D. M., et al. (2017). Transient receptor potential-canonical 1 is essential for environmental enrichment-induced cognitive enhancement and neurogenesis. *Mol. Neurobiol.* 54, 1992–2002. doi: 10.1007/s12035-016-9758-9

Durell, S. R., Guy, H. R., Arispe, N., Rojas, E., and Pollard, H. B. (1994). Theoretical models of the ion channel structure of amyloid beta-protein. *Biophys. J.* 67, 2137–2145. doi: 10.1016/S0006-3495(94)80717-9

Edinger, A. L., and Thompson, C. B. (2004). Death by design: apoptosis, necrosis and autophagy. *Curr Opin Cell Biol* 16, 663–669. doi: 10.1016/j.ceb.2004.09.011

Elgh, E., Lindqvist Astot, A., Fagerlund, M., Eriksson, S., Olsson, T., and Näsman, B. (2006). Cognitive dysfunction, hippocampal atrophy and glucocorticoid feedback in Alzheimer's disease. *Biol. Psychiatry* 59, 155–161. doi: 10.1016/j.biopsych.2005.06.017

Ertilav, K., Nazıroğlu, M., Ataizi, Z. S., and Yıldızhan, K. (2021). Melatonin and selenium suppress docetaxel-induced TRPV1 activation, neuropathic pain and oxidative neurotoxicity in mice. *Biol. Trace Elem. Res.* 199, 1469–1487. doi: 10.1007/s12011-020-02250-4

Espinosa-Parrilla, J. F., Martínez-Moreno, M., Gasull, X., Mahy, N., and Rodríguez, M. J. (2015). The L-type voltage-gated calcium channel modulates microglial pro-inflammatory activity. *Mol. Cell. Neurosci.* 64, 104–115. doi: 10.1016/j.mcn.2014.12.004

Etcheberrigaray, R., Hirashima, N., Nee, L., Prince, J., Govoni, S., Racchi, M., et al. (1998). Calcium responses in fibroblasts from asymptomatic members of

Alzheimer's disease families. *Neurobiol. Dis.* 5, 37–45. doi: 10.1006/nbdi.1998.0176

Evrard, Y. A., Mohammad-Zadeh, L., and Holton, B. (2004). Alterations in Ca2+-dependent and cAMP-dependent signaling pathways affect neurogenesis and melanogenesis of quail neural crest cells *in vitro*. *Dev. Genes Evol.* 214, 193–199. doi: 10.1007/s00427-004-0395-3

Eydelnant, I. A., Zhang, T., Bednarczyk, J., and Gang, H. Y. (2009). Abstract 3994: recruitment of p53 to mitochondrial VDAC1 triggers autophagy of ventricular myocytes during metabolic stress. *Circulation* 120:S902.

Fan, H., Gao, J., Wang, W., Li, X., Xu, T., and Yin, X. (2012). Expression of NMDA receptor and its effect on cell proliferation in the subventricular zone of neonatal rat brain. *Cell Biochem. Biophys.* 62, 305–316. doi: 10.1007/s12013-011-9302-5

Faure, A. V., Grunwald, D., Moutin, M. J., Hilly, M., Mauger, J. P., Marty, I., et al. (2001). Developmental expression of the calcium release channels during early neurogenesis of the mouse cerebral cortex. *Eur. J. Neurosci.* 14, 1613–1622. doi: 10.1046/j.0953-816x.2001.01786.x

Ferguson, A. R., Christensen, R. N., Gensel, J. C., Miller, B. A., Sun, F., Beattie, E. C., et al. (2008). Cell death after spinal cord injury is exacerbated by rapid TNF alpha-induced trafficking of GluR2-lacking AMPARs to the plasma membrane. *J. Neurosci.* 28, 11391–11400. doi: 10.1523/JNEUROSCI.3708-08.2008

Fernandez, A. M., Fernandez, S., Carrero, P., Garcia-Garcia, M., and Torres-Aleman, I. (2007). Calcineurin in reactive astrocytes plays a key role in the interplay between proinflammatory and anti-inflammatory signals. *J. Neurosci.* 27, 8745–8756. doi: 10.1523/JNEUROSCI.1002-07.2007

Fernandez-Echevarria, C., Díaz, M., Ferrer, I., Canerina-Amaro, A., and Marin, R. (2014). Aβ promotes VDAC1 channel dephosphorylation in neuronal lipid rafts. Relevance to the mechanisms of neurotoxicity in Alzheimer's disease. *Neuroscience* 278, 354–366. doi: 10.1016/j.neuroscience.2014.07.079

Fernandez-Funez, P., Casas-Tinto, S., Zhang, Y., and Rincon-Limas, D. (2010). P4-078: Xbp1s prevents amyloid-β neurotoxicity by regulating ryanodine Ca2+ channels. *Alzheimer's Dement.* 6, e45–e45. doi: 10.1016/j.jalz.2010.08.139

Ferreiro, E., Oliveira, C. R., and Pereira, C. (2004). Involvement of endoplasmic reticulum Ca2+ release through ryanodine and inositol 1,4,5-triphosphate receptors in the neurotoxic effects induced by the amyloid-beta peptide. *J. Neurosci. Res.* 76, 872–880. doi: 10.1002/jnr.20135

Ferreiro, E., Resende, R., Costa, R., Oliveira, C. R., and Pereira, C. M. (2006). An endoplasmic-reticulum-specific apoptotic pathway is involved in prion and amyloid-beta peptides neurotoxicity. *Neurobiol. Dis.* 23, 669–678. doi: 10.1016/j.nbd.2006.05.011

Fiorio Pla, A., Maric, D., Brazer, S. C., Giacobini, P., Liu, X., Chang, Y. H., et al. (2005). Canonical transient receptor potential 1 plays a role in basic fibroblast growth factor (bFGF)/FGF receptor-1-induced Ca2+ entry and embryonic rat neural stem cell proliferation. *J. Neurosci.* 25, 2687–2701. doi: 10.1523/JNEUROSCI.0951-04.2005

Flourakis, M., Lehen'kyi, V., Beck, B., Raphaël, M., Vandenberghe, M., Abeele, F. V., et al. (2010). Orai1 contributes to the establishment of an apoptosis-resistant phenotype in prostate cancer cells. *Cell Death Dis.* 1:e75. doi: 10.1038/cddis.2010.52

Fonfria, E., Marshall, I. C., Boyfield, I., Skaper, S. D., Hughes, J. P., Owen, D. E., et al. (2005). Amyloid beta-peptide(1–42) and hydrogen peroxide-induced toxicity are mediated by TRPM2 in rat primary striatal cultures. *J. Neurochem.* 95, 715–723. doi: 10.1111/j.1471-4159.2005.03396.x

Fonfria, E., Mattei, C., Hill, K., Brown, J. T., Randall, A., Benham, C. D., et al. (2006). TRPM2 is elevated in the tMCAO stroke model, transcriptionally regulated and functionally expressed in C13 microglia. *J. Recept. Signal Transduct. Res.* 26, 179–198. doi: 10.1080/10799890600637522

Franciosi, S., Choi, H. B., Kim, S. U., and McLarnon, J. G. (2002). Interferon-gamma acutely induces calcium influx in human microglia. *J. Neurosci. Res.* 69, 607–613. doi: 10.1002/jnr.10331

Frandsen, A., and Schousboe, A. (1991). Dantrolene prevents glutamate cytotoxicity and Ca2+ release from intracellular stores in cultured cerebral cortical neurons. *J. Neurochem.* 56, 1075–1078. doi: 10.1111/j.1471-4159.1991.tb02031.x

Furman, J. L., Sama, D. M., Gant, J. C., Beckett, T. L., Murphy, M. P., Bachstetter, A. D., et al. (2012). Targeting astrocytes ameliorates neurologic changes in a mouse model of Alzheimer's disease. *J. Neurosci.* 32, 16129–16140. doi: 10.1523/JNEUROSCI.2323-12.2012

Furukawa, K., and Mattson, M. P. (1998). The transcription factor NF-kappaB mediates increases in calcium currents and decreases in NMDA- and AMPA/kainate-induced currents induced by tumor necrosis factor-alpha in hippocampal neurons. *J. Neurochem.* 70, 1876–1886. doi: 10.1046/j.1471-4159.1998.70051876.x

Ganguly, P., Honeycutt, J. A., Rowe, J. R., Demaestri, C., and Brenhouse, H. C. (2019). Effects of early life stress on cocaine conditioning and AMPA receptor composition are sex-specific and driven by TNF. *Brain Behav. Immun.* 78, 41–51. doi: 10.1016/j.bbi.2019.01.006

Garrosa, J., Paredes, I., Marambaud, P., López, M. G., and Cano-Abad, M. F. (2020). Molecular and pharmacological modulation of CALHM1 promote neuroprotection against oxygen and glucose deprivation in a model of hippocampal slices. *Cells* 9:664. doi: 10.3390/cells9030664

Geffin, R., Martinez, R., de Las Pozas, A., Issac, B., and McCarthy, M. (2017). Apolipoprotein E4 suppresses neuronal-specific gene expression in maturing neuronal progenitor cells exposed to HIV. *J. Neuroimmune. Pharmacol.* 12, 462–483. doi: 10.1007/s11481-017-9734-9

Gerace, E., Ilari, A., Caffino, L., Buonvicino, D., Lana, D., Ugolini, F., et al. (2021). Ethanol neurotoxicity is mediated by changes in expression, surface localization and functional properties of glutamate AMPA receptors. *J. Neurochem.* 157, 2106–2118. doi: 10.1111/jnc.15223

Giarratana, A. O., Zheng, C., Reddi, S., Teng, S. L., Berger, D., Adler, D., et al. (2020). APOE4 genetic polymorphism results in impaired recovery in a repeated mild traumatic brain injury model and treatment with Bryostatin-1 improves outcomes. *Sci. Rep.* 10:19919. doi: 10.1038/s41598-020-76849-x

Gkouveris, I., Nikitakis, N. G., Aseervatham, J., and Ogbureke, K. U. E. (2018). Interferon γ suppresses dentin sialophosphoprotein in oral squamous cell carcinoma cells resulting in antitumor effects, *via* modulation of the endoplasmic reticulum response. *Int. J. Oncol.* 53, 2423–2432. doi: 10.3892/ijo.2018.4590

Goghari, V., Franciosi, S., Kim, S. U., Lee, Y. B., and McLarnon, J. G. (2000). Acute application of interleukin-1beta induces Ca(2+) responses in human microglia. *Neurosci. Lett.* 281, 83–86. doi: 10.1016/s0304-3940(00)00824-7

Goswami, P., Afjal, M. A., Akhter, J., Mangla, A., Khan, J., Parvez, S., et al. (2020). Involvement of endoplasmic reticulum stress in amyloid β ((1–42))-induced Alzheimer's like neuropathological process in rat brain. *Brain Res. Bull.* 165, 108–117. doi: 10.1016/j.brainresbull.2020.09.022

Grotemeier, A., Alers, S., Pfisterer, S. G., Paasch, F., Daubrawa, M., Dieterle, A., et al. (2010). AMPK-independent induction of autophagy by cytosolic Ca2+ increase. *Cell. Signal.* 22, 914–925. doi: 10.1016/j.cellsig.2010.01.015

Gu, C., Li, L., Huang, Y., Q25an, D., Liu, W., Zhang, C., et al. (2020). Salidroside ameliorates mitochondria-dependent neuronal apoptosis after spinal cord ischemia-reperfusion injury partially through inhibiting oxidative stress and promoting mitophagy. *Oxid. Med. Cell. Longev.* 2020:3549704. doi: 10.1155/2020/3549704

Guan, P. P., Cao, L. L., and Wang, P. (2021). Elevating the levels of calcium ions exacerbate Alzheimer's disease *via* inducing the production and aggregation of β-amyloid protein and phosphorylated Tau. *Int. J. Mol. Sci.* 22:5900. doi: 10.3390/ijms22115900

Guan, S., Ma, J., Chu, X., Gao, Y., Zhang, Y., Zhang, X., et al. (2015). Effects of total flavones from Acanthopanax senticosus on L-type calcium channels, calcium transient and contractility in rat ventricular myocytes. *Phytother. Res.* 29, 533–539. doi: 10.1002/ptr.5278

Guo, Y., Han, S., Cao, J., Liu, Q., and Zhang, T. (2014). Screening of allergic components mediated by H(1)R in homoharringtonine injection through H(1)R/CMC-HPLC/MS. *Biomed. Chromatogr.* 28, 1607–1614. doi: 10.1002/bmc.3188

Güzel, M., Nazıroğlu, M., Akpınar, O., and Çınar, R. (2021). Interferon gamma-mediated oxidative stress induces apoptosis, neuroinflammation, zinc ion influx, and TRPM2 channel activation in neuronal cell line: modulator role of curcumin. *Inflammation* 44, 1878–1894. doi: 10.1007/s10753-021-01465-4

Han, X. J., Hu, Y. Y., Yang, Z. J., Jiang, L. P., Shi, S. L., Li, Y. R., et al. (2017). Amyloid β-42 induces neuronal apoptosis by targeting mitochondria. *Mol. Med. Rep.* 16, 4521–4528. doi: 10.3892/mmr.2017.7203

Hao, B., Lu, Y., Wang, Q., Guo, W., Cheung, K. H., and Yue, J. (2014). Role of STIM1 in survival and neural differentiation of mouse embryonic stem cells independent of Orai1-mediated Ca2+ entry. *Stem Cell Res.* 12, 452–466. doi: 10.1016/j.scr.2013.12.005

Harr, M. W., McColl, K. S., Zhong, F., Molitoris, J. K., and Distelhorst, C. W. (2010). Glucocorticoids downregulate Fyn and inhibit IP(3)-mediated calcium signaling to promote autophagy in T lymphocytes. *Autophagy* 6, 912–921. doi: 10.4161/auto.6.7.13290

Heckmann, B. L., Teubner, B. J. W., Tummers, B., Boada-Romero, E., Harris, L., Yang, M., et al. (2019). LC3-associated endocytosis facilitates β-amyloid clearance and mitigates neurodegeneration in murine Alzheimer's disease. *Cell* 178, 536–551.e514. doi: 10.1016/j.cell.2019.05.056

Holland, E. B., and Pessah, I. N. (2021). Non-dioxin-like polychlorinated biphenyl neurotoxic equivalents found in environmental and human samples. *Regul. Toxicol. Pharmacol.* 120:104842. doi: 10.1016/j.yrtph.2020.104842

Hong, S. H., Choi, H. B., Kim, S. U., and McLarnon, J. G. (2006). Mitochondrial ligand inhibits store-operated calcium influx and COX-2 production in human microglia. *J. Neurosci. Res.* 83, 1293–1298. doi: 10.1002/jnr.20829

Hong, S., Kim, A., and Kernie, S. (2013). Apoe4 impairs injury-induced neurogenesis. *Critical Care Med.* 41, A39–A40. doi: 10.1097/01.ccm.0000439329.97813.61

Hopp, S. C., Royer, S. E., D'Angelo, H. M., Kaercher, R. M., Fisher, D. A., and Wenk, G. L. (2015). Differential neuroprotective and anti-inflammatory effects of L-type voltage dependent calcium channel and ryanodine receptor antagonists in the substantia nigra and locus coeruleus. *J. Neuroimmune Pharmacol.* 10, 35–44. doi: 10.1007/s11481-014-9568-7

Hou, Y., Ghosh, P., Wan, R., Ouyang, X., Cheng, H., Mattson, M. P., et al. (2014). Permeability transition pore-mediated mitochondrial superoxide flashes mediate an early inhibitory effect of amyloid beta1–42 on neural progenitor cell proliferation. *Neurobiol. Aging* 35, 975–989. doi: 10.1016/j.neurobiolaging.2013.11.002

Hou, P. F., Liu, Z. H., Li, N., Cheng, W. J., and Guo, S. W. (2015). Knockdown of STIM1 improves neuronal survival after traumatic neuronal injury through regulating mGluR1-dependent Ca(2+) signaling in mouse cortical neurons. *Cell. Mol. Neurobiol.* 35, 283–292. doi: 10.1007/s10571-014-0123-0

Hou, Y., Mattson, M. P., and Cheng, A. (2013). Permeability transition pore-mediated mitochondrial superoxide flashes regulate cortical neural progenitor differentiation. *PLoS One* 8:e76721. doi: 10.1371/journal.pone.0076721

Høyer-Hansen, M., Bastholm, L., Szyniarowski, P., Campanella, M., Szabadkai, G., Farkas, T., et al. (2007). Control of macroautophagy by calcium, calmodulin-dependent kinase kinase-beta and Bcl-2. *Mol. Cell* 25, 193–205. doi: 10.1016/j.molcel.2006.12.009

Hsieh, S. F., Chou, C. T., Liang, W. Z., Kuo, C. C., Wang, J. L., Hao, L. J., et al. (2018). The effect of magnolol on Ca(2+) homeostasis and its related physiology in human oral cancer cells. *Arch. Oral Biol.* 89, 49–54. doi: 10.1016/j.archoralbio.2018.02.006

Huang, Q., Cao, H., Zhan, L., Sun, X., Wang, G., Li, J., et al. (2017). Mitochondrial fission forms a positive feedback loop with cytosolic calcium signaling pathway to promote autophagy in hepatocellular carcinoma cells. *Cancer Lett* 403, 108–118. doi: 10.1016/j.canlet.2017.05.034

Huang, Y., Smith, D. E., Ibáñez-Sandoval, O., Sims, J. E., and Friedman, W. J. (2011). Neuron-specific effects of interleukin-1β are mediated by a novel isoform of the IL-1 receptor accessory protein. *J. Neurosci.* 31, 18048–18059. doi: 10.1523/JNEUROSCI.4067-11.2011

Hudecova, S., Markova, J., Simko, V., Csaderova, L., Stracina, T., Sirova, M., et al. (2016). Sulforaphane-induced apoptosis involves the type 1 IP3 receptor. *Oncotarget* 7, 61403–61418. doi: 10.18632/oncotarget.8968

Hudry, E., Dashkoff, J., Roe, A. D., Takeda, S., Koffie, R. M., Hashimoto, T., et al. (2013). Gene transfer of human Apoe isoforms results in differential modulation of amyloid deposition and neurotoxicity in mouse brain. *Sci. Transl. Med.* 5:212ra161. doi: 10.1126/scitranslmed.3007000

Jang, H., Ma, B., Lal, R., and Nussinov, R. (2008). Models of toxic beta-sheet channels of protegrin-1 suggest a common subunit organization motif shared with toxic alzheimer beta-amyloid ion channels. *Biophys. J.* 95, 4631–4642. doi: 10.1529/biophysj.108.134551

Ji, Y., Hu, Y., Ren, J., Khanna, R., Yao, Y., Chen, Y., et al. (2019). CRMP2-derived peptide ST2–104 (R9-CBD3) protects SH-SY5Y neuroblastoma cells against Aβ(25–35)-induced neurotoxicity by inhibiting the pCRMP2/NMDAR2B signaling pathway. *Chem. Biol. Interact* 305, 28–39. doi: 10.1016/j.cbi.2019.03.005

Ji, Z. S., Müllendorff, K., Cheng, I. H., Miranda, R. D., Huang, Y., and Mahley, R. W. (2006). Reactivity of apolipoprotein E4 and amyloid beta peptide: lysosomal stability and neurodegeneration. *J. Biol. Chem.* 281, 2683–2692. doi: 10.1074/jbc.M506646200

Jiang, L., Zhong, J., Dou, X., Cheng, C., Huang, Z., and Sun, X. (2015). Effects of ApoE on intracellular calcium levels and apoptosis of neurons after mechanical injury. *Neuroscience* 301, 375–383. doi: 10.1016/j.neuroscience.2015.06.005

Joseph, J. D., Peng, Y., Mak, D. O., Cheung, K. H., Vais, H., Foskett, J. K., et al. (2014). General anesthetic isoflurane modulates inositol 1,4,5-trisphosphate receptor calcium channel opening. *Anesthesiology* 121, 528–537. doi: 10.1097/ALN.0000000000000316

Ju, Y., Ge, J., Ren, X., Zhu, X., Xue, Z., Feng, Y., et al. (2015). Cav1.2 of L-type calcium channel is a key factor for the differentiation of dental pulp stem cells. *J. Endod.* 41, 1048–1055. doi: 10.1016/j.joen.2015.01.009

Kakae, M., Miyanohara, J., Morishima, M., Nagayasu, K., Mori, Y., Shirakawa, H., et al. (2019). Pathophysiological role of TRPM2 in age-related cognitive impairment in mice. *Neuroscience* 408, 204–213. doi: 10.1016/j.neuroscience.2019.04.012

Kaneko, S., Kawakami, S., Hara, Y., Wakamori, M., Itoh, E., Minami, T., et al. (2006). A critical role of TRPM2 in neuronal cell death by hydrogen peroxide. *J. Pharmacol. Sci.* 101, 66–76. doi: 10.1254/jphs.fp0060128

Kawada, K., Iekumo, T., Saito, R., Kaneko, M., Mimori, S., Nomura, Y., et al. (2014). Aberrant neuronal differentiation and inhibition of dendrite outgrowth resulting from endoplasmic reticulum stress. *J. Neurosci. Res.* 92, 1122–1133. doi: 10.1002/jnr.23389

Kawasaki, Y., Zhang, L., Cheng, J. K., and Ji, R. R. (2008). Cytokine mechanisms of central sensitization: distinct and overlapping role of interleukin-1beta, interleukin-6 and tumor necrosis factor-alpha in regulating synaptic and neuronal activity in the superficial spinal cord. *J. Neurosci.* 28, 5189–5194. doi: 10.1523/JNEUROSCI.3338-07.2008

Keinan, N., Pahima, H., Ben-Hail, D., and Shoshan-Barmatz, V. (2013). The role of calcium in VDAC1 oligomerization and mitochondria-mediated apoptosis. *Biochim. Biophys. Acta* 1833, 1745–1754. doi: 10.1016/j.bbamcr.2013.03.017

Kelly, B. L., and Ferreira, A. (2006). beta-Amyloid-induced dynamin 1 degradation is mediated by N-methyl-D-aspartate receptors in hippocampal neurons. *J. Biol. Chem.* 281, 28079–28089. doi: 10.1074/jbc.M605081200

Khan, M. T., and Joseph, S. K. (2010). Role of inositol trisphosphate receptors in autophagy in DT40 cells. *J. Biol. Chem.* 285, 16912–16920. doi: 10.1074/jbc.M110.114207

Kim, S. R., Kim, S. U., Oh, U., and Jin, B. K. (2006). Transient receptor potential vanilloid subtype 1 mediates microglial cell death *in vivo* and *in vitro via* Ca2+-mediated mitochondrial damage and cytochrome c release. *J. Immunol.* 177, 4322–4329. doi: 10.4049/jimmunol.177.7.4322

Kim, H. J., Soyombo, A. A., Tjon-Kon-Sang, S., So, I., and Muallem, S. (2009). The Ca(2+) channel TRPML3 regulates membrane trafficking and autophagy. *Traffic* 10, 1157–1167. doi: 10.1111/j.1600-0854.2009.00924.x

Kinjo, T., Ashida, Y., Higashi, H., Sugimura, S., Washida, M., Niihara, H., et al. (2018). Alleviation by GABA(B) receptors of neurotoxicity mediated by mitochondrial permeability transition pore in cultured murine cortical neurons exposed to N-Methyl-D-aspartate. *Neurochem. Res.* 43, 79–88. doi: 10.1007/s11064-017-2311-z

Klegeris, A., Choi, H. B., McLarnon, J. G., and McGeer, P. L. (2007). Functional ryanodine receptors are expressed by human microglia and THP-1 cells: their possible involvement in modulation of neurotoxicity. *J. Neurosci. Res.* 85, 2207–2215. doi: 10.1002/jnr.21361

Komita, M., Jin, H., and Aoe, T. (2013). The effect of endoplasmic reticulum stress on neurotoxicity caused by inhaled anesthetics. *Anesth. Analg.* 117, 1197–1204. doi: 10.1213/ANE.0b013e3182a74773

Komuro, H., and Rakic, P. (1992). Selective role of N-type calcium channels in neuronal migration. *Science* 257, 806–809. doi: 10.1126/science.1323145

Konno, M., Shirakawa, H., Iida, S., Sakimoto, S., Matsutani, I., Miyake, T., et al. (2012). Stimulation of transient receptor potential vanilloid 4 channel suppresses abnormal activation of microglia induced by lipopolysaccharide. *Glia* 60, 761–770. doi: 10.1002/glia.22306

Kouroku, Y., Fujita, E., Tanida, I., Ueno, T., Isoai, A., Kumagai, H., et al. (2007). ER stress (PERK/eIF2alpha phosphorylation) mediates the polyglutamine-induced LC3 conversion, an essential step for autophagy formation. *Cell Death Differ.* 14, 230–239. doi: 10.1038/sj.cdd.4401984

Kraft, R., Grimm, C., Grosse, K., Hoffmann, A., Sauerbruch, S., Kettenmann, H., et al. (2004). Hydrogen peroxide and ADP-ribose induce TRPM2-mediated calcium influx and cation currents in microglia. *Am. J. Physiol. Cell Physiol.* 286, C129–137. doi: 10.1152/ajpcell.00331.2003

Kraft, A., Jubal, E. R., von Laer, R., Döring, C., Rocha, A., Grebbin, M., et al. (2017). Astrocytic calcium waves signal brain injury to neural stem and progenitor cells. *Stem Cell Rep.* 8, 701–714. doi: 10.1016/j.stemcr.2017.01.009

Lashuel, H. A., Hartley, D. M., Petre, B. M., Wall, J. S., Simon, M. N., Walz, T., et al. (2003). Mixtures of wild-type and a pathogenic (E22G) form of Abeta40 *in vitro* accumulate protofibrils, including amyloid pores. *J. Mol. Biol.* 332, 795–808. doi: 10.1016/s0022-2836(03)00927-6

Lashuel, H. A., Hartley, D., Petre, B. M., Walz, T., and Lansbury, P. T.,Jr. (2002). Neurodegenerative disease: amyloid pores from pathogenic mutations. *Nature* 418:291. doi: 10.1038/418291a

Lawlor, B., Segurado, R., Kennelly, S., Olde Rikkert, M. G. M., Howard, R., Pasquier, F., et al. (2018). Nilvadipine in mild to moderate Alzheimer disease: a randomised controlled trial. *PLoS Med.* 15:e1002660. doi: 10.1371/journal.pmed.1002660

Lee, Y. J., Choi, S. Y., and Yang, J. H. (2016). AMP-activated protein kinase is involved in perfluorohexanesulfonate-induced apoptosis of neuronal cells. *Chemosphere* 149, 1–7. doi: 10.1016/j.chemosphere.2016.01.073

Lee, J. H., McBrayer, M. K., Wolfe, D. M., Haslett, L. J., Kumar, A., Sato, Y., et al. (2015). Presenilin 1 maintains lysosomal Ca(2+) homeostasis *via* TRPML1 by regulating vATPase-mediated lysosome acidification. *Cell Rep.* 12, 1430–1444. doi: 10.1016/j.celrep.2015.07.050

Lei, S. Z., Zhang, D., Abele, A. E., and Lipton, S. A. (1992). Blockade of NMDA receptor-mediated mobilization of intracellular Ca2+ prevents neurotoxicity. *Brain Res.* 598, 196–202. doi: 10.1016/0006-8993(92)90183-a

Leissring, M. A., Murphy, M. P., Mead, T. R., Akbari, Y., Sugarman, M. C., Jannatipour, M., et al. (2002). A physiologic signaling role for the gamma -secretase-derived intracellular fragment of APP. *Proc. Natl. Acad. Sci. U S A* 99, 4697–4702. doi: 10.1073/pnas.072033799

Li, X., and Jiang, L. H. (2018). Multiple molecular mechanisms form a positive feedback loop driving amyloid β42 peptide-induced neurotoxicity *via* activation of the TRPM2 channel in hippocampal neurons. *Cell Death Dis.* 9:195. doi: 10.1038/s41419-018-0270-1

Li, Y., and Jiao, J. (2020). Deficiency of TRPM2 leads to embryonic neurogenesis defects in hyperthermia. *Sci. Adv.* 6:eaay6350. doi: 10.1126/sciadv.aay6350

Li, R., Jin, Y., Li, Q., Sun, X., Zhu, H., and Cui, H. (2018). MiR-93–5p targeting PTEN regulates the NMDA-induced autophagy of retinal ganglion cells *via* AKT/mTOR pathway in glaucoma. *Biomed. Pharmacother.* 100, 1–7. doi: 10.1016/j.biopha.2018.01.044

Li, Y., Lin, X., Zhao, X., Xie, J., JunNan, W., Sun, T., et al. (2014). Ozone (O3) elicits neurotoxicity in spinal cord neurons (SCNs) by inducing ER Ca(2+) release and activating the CaMKII/MAPK signaling pathway. *Toxicol. Appl. Pharmacol.* 280, 493–501. doi: 10.1016/j.taap.2014.08.024

Li, L., Tsai, H. J., Li, L., and Wang, X. M. (2010). Icariin inhibits the increased inward calcium currents induced by amyloid-beta(25–35) peptide in CA1 pyramidal neurons of neonatal rat hippocampal slice. *Am. J. Chin. Med.* 38, 113–125. doi: 10.1142/S0192415X10007701

Li, T., Zhang, Y., Tian, J., Yang, L., and Wang, J. (2019). Ginkgo biloba pretreatment attenuates myocardial ischemia-reperfusion injury *via* mitoBK(Ca). *Am. J. Chin. Med.* 47, 1057–1073. doi: 10.1142/S0192415X1950054X

Lim, D., Dematteis, G., Tapella, L., Genazzani, A. A., Calì, T., Brini, M., et al. (2021a). Ca(2+) handling at the mitochondria-ER contact sites in neurodegeneration. *Cell Calcium* 98:102453. doi: 10.1016/j.ceca.2021.102453

Lim, D., Semyanov, A., Genazzani, A., and Verkhratsky, A. (2021b). Calcium signaling in neuroglia. *Int. Rev. Cell Mol. Biol.* 362, 1–53. doi: 10.1016/bs.ircmb.2021.01.003

Limke, T. L., Bearss, J. J., and Atchison, W. D. (2004). Acute exposure to methylmercury causes Ca2+ dysregulation and neuronal death in rat cerebellar granule cells through an M3 muscarinic receptor-linked pathway. *Toxicol. Sci.* 80, 60–68. doi: 10.1093/toxsci/kfh131

Lin, H., Bhatia, R., and Lal, R. (2001). Amyloid beta protein forms ion channels: implications for Alzheimer's disease pathophysiology. *FASEB J* 15, 2433–2444. doi: 10.1096/fj.01-0377com

Liou, B., Peng, Y., Li, R., Inskeep, V., Zhang, W., Quinn, B., et al. (2016). Modulating ryanodine receptors with dantrolene attenuates neuronopathic phenotype in Gaucher disease mice. *Hum. Mol. Genet.* 25, 5126–5141. doi: 10.1093/hmg/ddw322

Liu, X., Du, H., Chen, D., Yuan, H., Chen, W., Jia, W., et al. (2019). Cyclophilin D deficiency protects against the development of mitochondrial ROS and cellular inflammation in aorta. *Biochem. Biophys. Res. Commun.* 508, 1202–1208. doi: 10.1016/j.bbrc.2018.12.064

Liu, H., Jia, X., Luo, Z., Guan, H., Jiang, H., Li, X., et al. (2012). Inhibition of store-operated Ca(2+) channels prevent ethanol-induced intracellular Ca(2+) increase and cell injury in a human hepatoma cell line. *Toxicol. Lett* 208, 254–261. doi: 10.1016/j.toxlet.2011.11.007

Liu, T., Jiang, C. Y., Fujita, T., Luo, S. W., and Kumamoto, E. (2013). Enhancement by interleukin-1β of AMPA and NMDA receptor-mediated currents in adult rat spinal superficial dorsal horn neurons. *Mol. Pain* 9:16. doi: 10.1186/1744-8069-9-16

Liu, X., Song, S., Wang, Q., Yuan, T., and He, J. (2016). A mutation in β-amyloid precursor protein renders SH-SY5Y cells vulnerable to isoflurane toxicity: the role of inositol 1,4,5-trisphosphate receptors. *Mol. Med. Rep.* 14, 5435–5442. doi: 10.3892/mmr.2016.5930

Liu, S. B., and Zhao, M. G. (2013). Neuroprotective effect of estrogen: role of nonsynaptic NR2B-containing NMDA receptors. *Brain Res. Bull.* 93, 27–31. doi: 10.1016/j.brainresbull.2012.10.004

Liu, S. J., and Zukin, R. S. (2007). Ca2+-permeable AMPA receptors in synaptic plasticity and neuronal death. *Trends Neurosci.* 30, 126–134. doi: 10.1016/j.tins.2007.01.006

Louhivuori, L. M., Jansson, L., Turunen, P. M., Jäntti, M. H., Nordström, T., Louhivuori, V., et al. (2015). Transient receptor potential channels and their role in modulating radial glial-neuronal interaction: a signaling pathway involving mGluR5. *Stem Cells Dev.* 24, 701–713. doi: 10.1089/scd.2014.0209

Louhivuori, L. M., Louhivuori, V., Wigren, H. K., Hakala, E., Jansson, L. C., Nordström, T., et al. (2013). Role of low voltage activated calcium channels in neuritogenesis and active migration of embryonic neural progenitor cells. *Stem Cells Dev.* 22, 1206–1219. doi: 10.1089/scd.2012.0234

Lu, C. W., Lin, T. Y., Chiu, K. M., Lee, M. Y., Huang, J. H., and Wang, S. J. (2020a). Silymarin inhibits glutamate release and prevents against kainic acid-induced excitotoxic injury in rats. *Biomedicines* 8:486. doi: 10.3390/biomedicines8110486

Lu, C. W., Lin, T. Y., Yang, H. C., Hung, C. F., Weng, J. R., Chang, C., et al. (2020b). [1–(4-chloro-3-nitrobenzenesulfonyl)-1H-indol-3-yl]-methanol, an indole-3-carbinol derivative, inhibits glutamate release in rat cerebrocortical nerve terminals by suppressing the P/Q-type Ca(2+) channels and Ca(2+)/calmodulin/protein kinase a pathway. *Neurochem. Int.* 140:104845. doi: 10.1016/j.neuint.2020.104845

Lu, C. W., Lin, T. Y., Wang, S. J., and Huang, S. K. (2019). Asiatic acid, an active substance of Centella asiatica, presynaptically depresses glutamate release in the rat hippocampus. *Eur. J. Pharmacol.* 865:172781. doi: 10.1016/j.ejphar.2019.172781

Ma, J., Brewer, H. B.Jr., and Potter, H. (1996). Alzheimer A beta neurotoxicity: promotion by antichymotrypsin, ApoE4; inhibition by A beta-related peptides. *Neurobiol. Aging* 17, 773–780. doi: 10.1016/0197-4580(96)00112-1

Ma, F., Zhang, L., and Westlund, K. N. (2009). Reactive oxygen species mediate TNFR1 increase after TRPV1 activation in mouse DRG neurons. *Mol. Pain* 5:31. doi: 10.1186/1744-8069-5-31

Ma, S. H., Zhuang, Q. X., Shen, W. X., Peng, Y. P., and Q25u, Y. H. (2015). Interleukin-6 reduces NMDAR-mediated cytosolic Ca^2 overload and neuronal death *via* JAK/CaN signaling. *Cell Calcium* 58, 286–295. doi: 10.1016/j.ceca.2015.06.006

MacManus, A., Ramsden, M., Murray, M., Henderson, Z., Pearson, H. A., and Campbell, V. A. (2000). Enhancement of (45)Ca(2+) influx and voltage-dependent Ca(2+) channel activity by beta-amyloid-(1–40) in rat cortical synaptosomes and cultured cortical neurons. Modulation by the proinflammatory cytokine interleukin-1beta. *J. Biol. Chem.* 275, 4713–4718. doi: 10.1074/jbc.275.7.4713

Marcantoni, A., Cerullo, M. S., Buxeda, P., Tomagra, G., Giustetto, M., Chiantia, G., et al. (2020). Amyloid Beta42 oligomers up-regulate the excitatory synapses by potentiating presynaptic release while impairing postsynaptic NMDA receptors. *J. Physiol.* 598, 2183–2197. doi: 10.1113/JP279345

Marin, R., Ramírez, C. M., González, M., González-Muñoz, E., Zorzano, A., Camps, M., et al. (2007). Voltage-dependent anion channel (VDAC) participates in amyloid beta-induced toxicity and interacts with plasma membrane estrogen receptor alpha in septal and hippocampal neurons. *Mol. Membr. Biol.* 24, 148–160. doi: 10.1080/09687860601055559

Marques, M. A., and Crutcher, K. A. (2003). Apolipoprotein E-related neurotoxicity as a therapeutic target for Alzheimer's disease. *J. Mol. Neurosci.* 20, 327–337. doi: 10.1385/JMN:20:3:327

Marschallinger, J., Sah, A., Schmuckermair, C., Unger, M., Rotheneichner, P., Kharitonova, M., et al. (2015). The L-type calcium channel Cav1.3 is required for proper hippocampal neurogenesis and cognitive functions. *Cell Calcium* 58, 606–616. doi: 10.1016/j.ceca.2015.09.007

Matsubara, M., Tamura, T., Ohmori, K., and Hasegawa, K. (2005). Histamine H1 receptor antagonist blocks histamine-induced proinflammatory cytokine production through inhibition of Ca2+-dependent protein kinase C, Raf/MEK/ERK and IKK/I kappa B/NF-kappa B signal cascades. *Biochem. Pharmacol.* 69, 433–449. doi: 10.1016/j.bcp.2004.10.006

Mattson, M. P., and Furukawa, K. (1997). Anti-apoptotic actions of cycloheximide: blockade of programmed cell death or induction of programmed cell life? *Apoptosis* 2, 257–264. doi: 10.1023/a:1026433019210

McBrayer, M., and Nixon, R. A. (2013). Lysosome and calcium dysregulation in Alzheimer's disease: partners in crime. *Biochem. Soc. Trans.* 41, 1495–1502. doi: 10.1042/BST20130201

McDaid, J., Mustaly-Kalimi, S., and Stutzmann, G. E. (2020). Ca(2+) dyshomeostasis disrupts neuronal and synaptic function in Alzheimer's disease. *Cells* 9:2655. doi: 10.3390/cells9122655

McLarnon, J. G., Franciosi, S., Wang, X., Bae, J. H., Choi, H. B., and Kim, S. U. (2001). Acute actions of tumor necrosis factor-alpha on intracellular Ca(2+) and K(+) currents in human microglia. *Neuroscience* 104, 1175–1184. doi: 10.1016/s0306-4522(01)00119-1

Mendez-David, I., Guilloux, J. P., Papp, M., Tritschler, L., Mocaer, E., Gardier, A.M., et al. (2017). S 47445 produces antidepressant- and anxiolytic-like effects through neurogenesis dependent and independent mechanisms. *Front. Pharmacol.* 8:462. doi: 10.3389/fphar.2017.00462

Meng, Y., Li, W. Z., Shi, Y. W., Zhou, B. F., Ma, R., and Li, W. P. (2016). Danshensu protects against ischemia/reperfusion injury and inhibits the apoptosis of H9c2 cells by reducing the calcium overload through the p-JNK-NF-κB-TRPC6 pathway. *Int. J. Mol. Med.* 37, 258–266. doi: 10.3892/ijmm.2015.2419

Miao, Y., Dong, L. D., Chen, J., Hu, X. C., Yang, X. L., and Wang, Z. (2012). Involvement of calpain/p35–p25/Cdk5/NMDAR signaling pathway in glutamate-induced neurotoxicity in cultured rat retinal neurons. *PLoS One* 7:e42318. doi: 10.1371/journal.pone.0042318

Michiels, C. F., Fransen, P., De Munck, D. G., De Meyer, G. R., and Martinet, W. (2015). Defective autophagy in vascular smooth muscle cells alters contractility and Ca^2 homeostasis in mice. *Am. J. Physiol. Heart Circ. Physiol.* 308, H557–567. doi: 10.1152/ajpheart.00659.2014

Miyake, T., Shirakawa, H., Kusano, A., Sakimoto, S., Konno, M., Nakagawa, T., et al. (2014). TRPM2 contributes to LPS/IFNγ-induced production of nitric oxide *via* the p38/JNK pathway in microglia. *Biochem. Biophys. Res. Commun.* 444, 212–217. doi: 10.1016/j.bbrc.2014.01.022

Miyanohara, J., Kakae, M., Nagayasu, K., Nakagawa, T., Mori, Y., Arai, K., et al. (2018). TRPM2 channel aggravates CNS inflammation and cognitive impairment *via* activation of microglia in chronic cerebral hypoperfusion. *J. Neurosci.* 38, 3520–3533. doi: 10.1523/JNEUROSCI.2451-17.2018

Morais Cardoso, S., Swerdlow, R. H., and Oliveira, C. R. (2002). Induction of cytochrome c-mediated apoptosis by amyloid beta 25–35 requires functional mitochondria. *Brain Res.* 931, 117–125. doi: 10.1016/s0006-8993(02)02256-4

Morelli, M. B., Amantini, C., Liberati, S., Santoni, M., and Nabissi, M. (2013). TRP channels: new potential therapeutic approaches in CNS neuropathies. *CNS Neurol. Disord. Drug Targets* 12, 274–293. doi: 10.2174/18715273113129990056

Moreno, J.A., Halliday, M., Molloy, C., Radford, H., Verity, N., Axten, J. M., et al. (2013). Oral treatment targeting the unfolded protein response prevents neurodegeneration and clinical disease in prion-infected mice. *Sci. Transl. Med.* 5:206ra138. doi: 10.1126/scitranslmed.3006767

Murugan, M., Sivakumar, V., Lu, J., Ling, E. A., and Kaur, C. (2011). Expression of N-methyl D-aspartate receptor subunits in amoeboid microglia mediates production of nitric oxide *via* NF-κB signaling pathway and oligodendrocyte cell death in hypoxic postnatal rats. *Glia* 59, 521–539. doi: 10.1002/glia.21121

Muth-Köhne, E., Pachernegg, S., Karus, M., Faissner, A., and Hollmann, M. (2010). Expression of NMDA receptors and Ca2+-impermeable AMPA receptors requires neuronal differentiation and allows discrimination between two different types of neural stem cells. *Cell Physiol. Biochem.* 26, 935–946. doi: 10.1159/000324002

Nagakannan, P., Islam, M. I., Karimi-Abdolrezaee, S., and Eftekharpour, E. (2019). Inhibition of VDAC1 protects against glutamate-induced oxytosis and mitochondrial fragmentation in hippocampal HT22 cells. *Cell Mol. Neurobiol.* 39, 73–85. doi: 10.1007/s10571-018-0634-1

Nakamura, S., Shigeyama, S., Minami, S., Shima, T., Akayama, S., Matsuda, T., et al. (2020). LC3 lipidation is essential for TFEB activation during the lysosomal damage response to kidney injury. *Nat. Cell Biol.* 22, 1252–1263. doi: 10.1038/s41556-020-00583-9

Namba, T., Dóczi, J., Pinson, A., Xing, L., Kalebic, N., Wilsch-Bräuninger, M., et al. (2020). Human-specific ARHGAP11B acts in mitochondria to expand neocortical progenitors by glutaminolysis. *Neuron* 105, 867–881.e9. doi: 10.1016/j.neuron.2019.11.027

Nasiri-Ansari, N., Nikolopoulou, C., Papoutsi, K., Kyrou, I., Mantzoros, C. S., Kyriakopoulos, G., et al. (2021). Empagliflozin attenuates non-alcoholic fatty liver disease (NAFLD) in high fat diet fed ApoE((-/-)) mice by activating autophagy and reducing ER stress and apoptosis. *Int. J. Mol. Sci.* 22:818. doi: 10.3390/ijms22020818

Neumann, J., Sauerzweig, S., Rönicke, R., Gunzer, F., Dinkel, K., Ullrich, O., et al. (2008). Microglia cells protect neurons by direct engulfment of invading neutrophil granulocytes: a new mechanism of CNS immune privilege. *J. Neurosci.* 28, 5965–5975. doi: 10.1523/JNEUROSCI.0060-08.2008

Nijholt, D. A., de Graaf, T. R., van Haastert, E. S., Oliveira, A. O., Berkers, C. R., Zwart, R., et al. (2011). Endoplasmic reticulum stress activates autophagy but not the proteasome in neuronal cells: implications for Alzheimer's disease. *Cell Death Differ.* 18, 1071–1081. doi: 10.1038/cdd.2010.176

Nishitoh, H., Kadowaki, H., Takeda, K., and Ichijo, H. (2009). ER quality control, ER stress-induced apoptosis and neurodegenerative diseases. *Protein Misfolding Disord. Trip ER* 94–102. doi: 10.2174/978160805013010901010094

Nursalim, Y. (2016). *Preliminary Evidence for NMDAR Contribution Towards Autophagy and Membrane Potential in Leukaemic Megakaryoblasts.* Masters Thesis. University of Auckland.

Ogoshi, F., Yin, H. Z., Kuppumbatti, Y., Song, B., Amindari, S., and Weiss, J. H. (2005). Tumor necrosis-factor-alpha (TNF-alpha) induces rapid insertion of Ca2+-permeable alpha-amino-3-hydroxyl-5-methyl-4-isoxazole-propionate (AMPA)/kainate (Ca-A/K) channels in a subset of hippocampal pyramidal neurons. *Exp. Neurol.* 193, 384–393. doi: 10.1016/j.expneurol.2004.12.026

Onyenwoke, R. U., Sexton, J. Z., Yan, F., Díaz, M. C., Forsberg, L. J., Major, M. B., et al. (2015). The mucolipidosis IV Ca2+ channel TRPML1 (MCOLN1) is regulated by the TOR kinase. *Biochem. J.* 470, 331–342. doi: 10.1042/BJ20150219

Orellana, D. I., Quintanilla, R. A., Gonzalez-Billault, C., and Maccioni, R. B. (2005). Role of the JAKs/STATs pathway in the intracellular calcium changes induced by interleukin-6 in hippocampal neurons. *Neurotox. Res.* 8, 295–304. doi: 10.1007/BF03033983

Oseki, K. T., Monteforte, P. T., Pereira, G. J., Hirata, H., Ureshino, R. P., Bincoletto, C., et al. (2014). Apoptosis induced by Aβ25–35 peptide is Ca(2+) -IP3 signaling-dependent in murine astrocytes. *Eur. J. Neurosci.* 40, 2471–2478. doi: 10.1111/ejn.12599

Ostapchenko, V. G., Chen, M., Guzman, M. S., Xie, Y. F., Lavine, N., Fan, J., et al. (2015). The transient receptor potential melastatin 2 (TRPM2) channel contributes to β-Amyloid oligomer-related neurotoxicity and memory impairment. *J. Neurosci.* 35, 15157–15169. doi: 10.1523/JNEUROSCI.4081-14.2015

Pahl, H. L., and Baeuerle, P. A. (1996). Activation of NF-kappa B by ER stress requires both Ca2+ and reactive oxygen intermediates as messengers. *FEBS Lett* 392, 129–136. doi: 10.1016/0014-5793(96)00800-9

Pahrudin Arrozi, A., Shukri, S. N. S., Wan Ngah, W. Z., Mohd Yusof, Y. A., Ahmad Damanhuri, M. H., Jaafar, F., et al. (2020). Comparative effects of alpha- and gamma-tocopherol on mitochondrial functions in Alzheimer's disease *in vitro* model. *Sci. Rep.* 10:8962. doi: 10.1038/s41598-020-65570-4

Park, E. S., Kim, S. R., and Jin, B. K. (2012). Transient receptor potential vanilloid subtype 1 contributes to mesencephalic dopaminergic neuronal survival by inhibiting microglia-originated oxidative stress. *Brain Res. Bull.* 89, 92–96. doi: 10.1016/j.brainresbull.2012.07.001

Park, K. M., Yule, D. I., and Bowers, W. J. (2008). Tumor necrosis factor-alpha potentiates intraneuronal Ca^{2+} signaling *via* regulation of the inositol 1,4,5-trisphosphate receptor. *J. Biol. Chem.* 283, 33069–33079. doi: 10.1074/jbc.M802209200

Park, K. M., Yule, D. I., and Bowers, W. J. (2010). Impaired TNF-alpha control of IP3R-mediated Ca^{2+} release in Alzheimer's disease mouse neurons. *Cell Signal* 22, 519–526. doi: 10.1016/j.cellsig.2009.11.006

Pedrozo, Z., Torrealba, N., Fernández, C., Gatica, D., Toro, B., Quiroga, C., et al. (2013). Cardiomyocyte ryanodine receptor degradation by chaperone-mediated autophagy. *Cardiovasc. Res.* 98, 277–285. doi: 10.1093/cvr/cvt029

Peng, Y., Cheung, K. H., Liang, G., Inan, S., Vais, H., Joseph, D., et al. (2011). General anesthetics influence autophagy and neurodegeneration through actions on the inositol 1,4,5-trisphosphate receptor calcium channel. *Alzheimer's Demen.* 7:S573. doi: 10.1016/j.jalz.2011.05.1618

Piacentini, R., Gangitano, C., Ceccariglia, S., Del Fà, A., Azzena, G. B., Michetti, F., et al. (2008a). Dysregulation of intracellular calcium homeostasis is responsible for neuronal death in an experimental model of selective hippocampal degeneration induced by trimethyltin. *J. Neurochem.* 105, 2109–2121. doi: 10.1111/j.1471-4159.2008.05297.x

Piacentini, R., Ripoli, C., Leone, L., Misiti, F., Clementi, M. E., D'Ascenzo, M., et al. (2008b). Role of methionine 35 in the intracellular Ca2+ homeostasis dysregulation and Ca2+-dependent apoptosis induced by amyloid beta-peptide in human neuroblastoma IMR32 cells. *J. Neurochem.* 107, 1070–1082. doi: 10.1111/j.1471-4159.2008.05680.x

Piacentini, R., Ripoli, C., Mezzogori, D., Azzena, G. B., and Grassi, C. (2008c). Extremely low-frequency electromagnetic fields promote in vitro neurogenesis *via* upregulation of Ca(v)1-channel activity. *J. Cell Physiol.* 215, 129–139. doi: 10.1002/jcp.21293

Pickford, F., Masliah, E., Britschgi, M., Lucin, K., Narasimhan, R., Jaeger, P. A., et al. (2008). The autophagy-related protein beclin 1 shows reduced expression in early Alzheimer disease and regulates amyloid beta accumulation in mice. *J. Clin. Invest.* 118, 2190–2199. doi: 10.1172/JCI33585

Pierrot, N., Ghisdal, P., Caumont, A. S., and Octave, J. N. (2004). Intraneuronal amyloid-beta1–42 production triggered by sustained increase of cytosolic calcium concentration induces neuronal death. *J. Neurochem.* 88, 1140–1150. doi: 10.1046/j.1471-4159.2003.02227.x

Pitt, D., Werner, P., and Raine, C. S. (2000). Glutamate excitotoxicity in a model of multiple sclerosis. *Nat. Med.* 6, 67–70. doi: 10.1038/71555

Pollock, J., McFarlane, S. M., Connell, M. C., Zehavi, U., Vandenabeele, P., MacEwan, D. J., et al. (2002). TNF-alpha receptors simultaneously activate Ca2+ mobilisation and stress kinases in cultured sensory neurones. *Neuropharmacology* 42, 93–106. doi: 10.1016/s0028-3908(01)00163-0

Qiao, H., Li, Y., Xu, Z., Li, W., Fu, Z., Wang, Y., et al. (2017). Propofol affects neurodegeneration and neurogenesis by regulation of autophagy *via* effects on intracellular calcium homeostasis. *Anesthesiology* 127, 490–501. doi: 10.1097/ALN.0000000000001730

Qin, L., Wang, Z., Tao, L., and Wang, Y. (2010). ER stress negatively regulates AKT/TSC/mTOR pathway to enhance autophagy. *Autophagy* 6, 239–247. doi: 10.4161/auto.6.2.11062

Qu, M., Zhou, Z., Chen, C., Li, M., Pei, L., Yang, J., et al. (2012). Inhibition of mitochondrial permeability transition pore opening is involved in the protective effects of mortalin overexpression against beta-amyloid-induced apoptosis in SH-SY5Y cells. *Neurosci. Res.* 72, 94–102. doi: 10.1016/j.neures.2011.09.009

Raghunatha, P., Vosoughi, A., Kauppinen, T. M., and Jackson, M. F. (2020). Microglial NMDA receptors drive pro-inflammatory responses *via* PARP-1/TRMP2 signaling. *Glia* 68, 1421–1434. doi: 10.1002/glia.23790

Rainey-Smith, S. R., Andersson, D. A., Williams, R. J., and Rattray, M. (2010). Tumour necrosis factor alpha induces rapid reduction in AMPA receptor-mediated calcium entry in motor neurones by increasing cell surface expression of the GluR2 subunit: relevance to neurodegeneration. *J. Neurochem.* 113, 692–703. doi: 10.1111/j.1471-4159.2010.06634.x

Rash, B. G., Ackman, J. B., and Rakic, P. (2016). Bidirectional radial Ca(2+) activity regulates neurogenesis and migration during early cortical column formation. *Sci. Adv.* 2:e1501733. doi: 10.1126/sciadv.1501733

Resende, R. R., da Costa, J. L., Kihara, A. H., Adhikari, A., and Lorençon, E. (2010). Intracellular Ca2+ regulation during neuronal differentiation of murine embryonal carcinoma and mesenchymal stem cells. *Stem Cells Dev.* 19, 379–394. doi: 10.1089/scd.2008.0289

Rijpma, A., Jansen, D., Arnoldussen, I. A., Fang, X. T., Wiesmann, M., Mutsaers, M. P., et al. (2013). Sex differences in presynaptic density and neurogenesis in middle-aged ApoE4 and ApoE knockout mice. *J. Neurodegener. Dis.* 2013:531326. doi: 10.1155/2013/531326

Rodriguez, G. A., Tai, L. M., LaDu, M. J., and Rebeck, G. W. (2014). Human APOE4 increases microglia reactivity at Aβ plaques in a mouse model of Aβ deposition. *J. Neuroinflammation* 11:111. doi: 10.1186/1742-2094-11-111

Rostovtseva, T. K., Antonsson, B., Suzuki, M., Youle, R. J., Colombini, M., and Bezrukov, S. M. (2004). Bid, but not bax, regulates VDAC channels. *J. Biol. Chem.* 279, 13575–13583. doi: 10.1074/jbc.M310593200

Sade, Y., Toker, L., Kara, N.Z., Einat, H., Rapoport, S., Moechars, D., et al. (2016). IP3 accumulation and/or inositol depletion: two downstream lithium's effects that may mediate its behavioral and cellular changes. *Transl. Psychiatry* 6:e968. doi: 10.1038/tp.2016.217

Sakamoto, K., Kawakami, T., Shimada, M., Yamaguchi, A., Kuwagata, M., Saito, M., et al. (2009). Histological protection by cilnidipine, a dual L/N-type Ca(2+) channel blocker, against neurotoxicity induced by ischemia-reperfusion in rat retina. *Exp. Eye Res.* 88, 974–982. doi: 10.1016/j.exer.2008.12.011

Sama, M. A., Mathis, D. M., Furman, J. L., Abdul, H. M., Artiushin, I. A., Kraner, S. D., et al. (2008). Interleukin-1beta-dependent signaling between astrocytes and neurons depends critically on astrocytic calcineurin/NFAT activity. *J. Biol. Chem.* 283, 21953–21964. doi: 10.1074/jbc.M800148200

Sama, D. M., Mohmmad Abdul, H., Furman, J. L., Artiushin, I. A., Szymkowski, D. E., Scheff, S. W., et al. (2012). Inhibition of soluble tumor necrosis factor ameliorates synaptic alterations and Ca2+ dysregulation in aged rats. *PLoS One* 7:e38170. doi: 10.1371/journal.pone.0038170

Sama, D. M., and Norris, C. M. (2013). Calcium dysregulation and neuroinflammation: discrete and integrated mechanisms for age-related synaptic dysfunction. *Ageing Res. Rev.* 12, 982–995. doi: 10.1016/j.arr.2013.05.008

Sanchez, A. B., Medders, K. E., Maung, R., Sánchez-Pavón, P., Ojeda-Juárez, D., and Kaul, M. (2016). CXCL12-induced neurotoxicity critically depends on NMDA receptor-gated and L-type Ca(2+) channels upstream of p38 MAPK. *J. Neuroinflammation* 13:252. doi: 10.1186/s12974-016-0724-2

Santoro, M., Piacentini, R., Perna, A., Pisano, E., and Silvestri, G. (2020). Resveratrol corrects aberrant splicing of RYR1 pre-mRNA and Ca 2+ signal in myotonic dystrophy type 1 myotubes. *Neural Regen. Res.* 15, 1757–1766. doi: 10.4103/1673-5374.276336

Sappington, R. M., and Calkins, D. J. (2008). Contribution of TRPV1 to microglia-derived IL-6 and NFkappaB translocation with elevated hydrostatic pressure. *Invest. Ophthalmol. Vis. Sci.* 49, 3004–3017. doi: 10.1167/iovs.07-1355

Sarkar, S., Floto, R. A., Berger, Z., Imarisio, S., Cordenier, A., Pasco, M., et al. (2005). Lithium induces autophagy by inhibiting inositol monophosphatase. *J. Cell Biol.* 170, 1101–1111. doi: 10.1083/jcb.200504035

Schmukler, E., Solomon, S., Simonovitch, S., Goldshmit, Y., Wolfson, E., Michaelson, D. M., et al. (2020). Altered mitochondrial dynamics and function in APOE4-expressing astrocytes. *Cell Death Dis.* 11:578. doi: 10.1038/s41419-020-02776-4

Selvaraj, S., Sun, Y., Sukumaran, P., and Singh, B. B. (2016). Resveratrol activates autophagic cell death in prostate cancer cells *via* downregulation of STIM1 and the mTOR pathway. *Mol. Carcinog.* 55, 818–831. doi: 10.1002/mc.22324

Seo, H., and Lee, K. (2016). Epac2 contributes to PACAP-induced astrocytic differentiation through calcium ion influx in neural precursor cells. *BMB Rep.* 49, 128–133. doi: 10.5483/bmbrep.2016.49.2.202

Shaikh, S., Troncoso, R., Criollo, A., Bravo-Sagua, R., García, L., Morselli, E., et al. (2016). Regulation of cardiomyocyte autophagy by calcium. *Am. J. Physiol. Endocrinol. Metab.* 310, E587–E596. doi: 10.1152/ajpendo.00374.2015

Shehata, M., Matsumura, H., Okubo-Suzuki, R., Ohkawa, N., and Inokuchi, K. (2012). Neuronal stimulation induces autophagy in hippocampal neurons that is involved in AMPA receptor degradation after chemical long-term depression. *J. Neurosci.* 32, 10413–10422. doi: 10.1523/JNEUROSCI.4533-11.2012

Shi, M., Du, F., Liu, Y., Li, L., Cai, J., Zhang, G. F., et al. (2013). Glial cell-expressed mechanosensitive channel TRPV4 mediates infrasound-induced neuronal impairment. *Acta Neuropathol.* 126, 725–739. doi: 10.1007/s00401-013-1166-x

Shimizu, S., Narita, M., and Tsujimoto, Y. (1999). Bcl-2 family proteins regulate the release of apoptogenic cytochrome c by the mitochondrial channel VDAC. *Nature* 399, 483–487. doi: 10.1038/20959

Shirakawa, H., Yamaoka, T., Sanpei, K., Nakagawa, T., and Kaneko, S. (2007). TRPV1 mediates vanilloids and low pH-induced neurotoxicity in rat cortical cultures. *Neurosci. Res.* 58, S207–S207. doi: 10.1016/j.neures.2007.06.946

Shoshan-Barmatz, V., Nahon-Crystal, E., Shteinfer-Kuzmine, A., and Gupta, R. (2018). VDAC1, mitochondrial dysfunction and Alzheimer's disease. *Pharmacol. Res.* 131, 87–101. doi: 10.1016/j.phrs.2018.03.010

Shtaya, A., Sadek, A. R., Zaben, M., Seifert, G., Pringle, A., Steinhäuser, C., et al. (2018). AMPA receptors and seizures mediate hippocampal radial glia-like stem cell proliferation. *Glia* 66, 2397–2413. doi: 10.1002/glia.23479

Simões, A.P., Duarte, J.A., Agasse, F., Canas, P.M., Tomé, A.R., Agostinho, P., et al. (2012). Blockade of adenosine A2A receptors prevents interleukin-1β-induced exacerbation of neuronal toxicity through a p38 mitogen-activated protein kinase pathway. *J. Neuroinflammation* 9:204. doi: 10.1177/0003134821048845

Simonovitch, S., Schmukler, E., Bespalko, A., Iram, T., Frenkel, D., Holtzman, D. M., et al. (2016). Impaired autophagy in APOE4 astrocytes. *J. Alzheimers Dis.* 51, 915–927. doi: 10.3233/JAD-151101

Smilansky, A., Dangoor, L., Nakdimon, I., Ben-Hail, D., Mizrachi, D., and Shoshan-Barmatz, V. (2015). The voltage-dependent anion channel 1 mediates amyloid β toxicity and represents a potential target for alzheimer disease therapy. *J. Biol. Chem.* 290, 30670–30683. doi: 10.1074/jbc.M115.691493

Smith, T., Groom, A., Zhu, B., and Turski, L. (2000). Autoimmune encephalomyelitis ameliorated by AMPA antagonists. *Nat. Med.* 6, 62–66. doi: 10.1038/71548

Soboloff, J., and Berger, S. A. (2002). Sustained ER Ca2+ depletion suppresses protein synthesis and induces activation-enhanced cell death in mast cells. *J. Biol. Chem.* 277, 13812–13820. doi: 10.1074/jbc.M112129200

Somasundaram, A., Shum, A. K., McBride, H. J., Kessler, J. A., Feske, S., Miller, R. J., et al. (2014). Store-operated CRAC channels regulate gene expression and proliferation in neural progenitor cells. *J. Neurosci.* 34, 9107–9123. doi: 10.1523/JNEUROSCI.0263-14.2014

Song, S., Lee, H., Kam, T. I., Tai, M. L., Lee, J. Y., Noh, J. Y., et al. (2008). E2–25K/Hip-2 regulates caspase-12 in ER stress-mediated Abeta neurotoxicity. *J. Cell Biol.* 182, 675–684. doi: 10.1083/jcb.200711066

Song, Y., Li, D., Farrelly, O., Miles, L., Li, F., Kim, S. E., et al. (2019). The mechanosensitive ion channel piezo inhibits axon regeneration. *Neuron* 102, 373–389.e376. doi: 10.1016/j.neuron.2019.01.050

Staats, K. A., Humblet-Baron, S., Bento-Abreu, A., Scheveneels, W., Nikolaou, A., Deckers, K., et al. (2016). Genetic ablation of IP3 receptor 2 increases cytokines and decreases survival of SOD1G93A mice. *Hum. Mol. Genet.* 25, 3491–3499. doi: 10.1093/hmg/ddw190

Sukumaran, P., Schaar, A., Sun, Y., and Singh, B. B. (2016). Functional role of TRP channels in modulating ER stress and Autophagy. *Cell Calcium* 60, 123–132. doi: 10.1016/j.ceca.2016.02.012

Sun, G. B., Sun, H., Meng, X. B., Hu, J., Zhang, Q., Liu, B., et al. (2014). Aconitine-induced Ca2+ overload causes arrhythmia and triggers apoptosis through p38 MAPK signaling pathway in rats. *Toxicol. Appl. Pharmacol.* 279, 8–22. doi: 10.1016/j.taap.2014.05.005

Sun, Y., Chauhan, A., Sukumaran, P., Sharma, J., Singh, B. B., and Mishra, B. B. (2014). Inhibition of store-operated calcium entry in microglia by helminth factors: implications for immune suppression in neurocysticercosis. *J. Neuroinflammation* 11:210. doi: 10.1186/s12974-014-0210-7

Sun, Y., Vashisht, A. A., Tchieu, J., Wohlschlegel, J. A., and Dreier, L. (2012). Voltage-dependent anion channels (VDACs) recruit Parkin to defective mitochondria to promote mitochondrial autophagy. *J. Biol. Chem.* 287, 40652–40660. doi: 10.1074/jbc.M112.419721

Supnet, C., Noonan, C., Richard, K., Bradley, J., and Mayne, M. (2010). Up-regulation of the type 3 ryanodine receptor is neuroprotective in the TgCRND8 mouse model of Alzheimer's disease. *J. Neurochem.* 112, 356–365. doi: 10.1111/j.1471-4159.2009.06487.x

Szalai, G., Krishnamurthy, R., and Hajnóczky, G. (1999). Apoptosis driven by IP(3)-linked mitochondrial calcium signals. *EMBO J.* 18, 6349–6361. doi: 10.1093/emboj/18.22.6349

Takeo, Y., Kurabayashi, N., Nguyen, M. D., and Sanada, K. (2016). The G protein-coupled receptor GPR157 regulates neuronal differentiation of radial glial progenitors through the Gq-IP3 pathway. *Sci. Rep.* 6:25180. doi: 10.1038/srep25180

Temme, S. J., Bell, R. Z., Fisher, G. L., and Murphy, G. G. (2016). Deletion of the mouse homolog of CACNA1C disrupts discrete forms of hippocampal-dependent memory and neurogenesis within the dentate gyrus. *eNeuro* 3:ENEURO.0118-16.2016. doi: 10.1523/ENEURO.0118-16.2016

Tharmalingam, S., Wu, C., and Hampson, D. R. (2016). The calcium-sensing receptor and integrins modulate cerebellar granule cell precursor differentiation and migration. *Dev. Neurobiol.* 76, 375–389. doi: 10.1002/dneu.22321

Thinnes, F. P. (2011). Apoptogenic interactions of plasmalemmal type-1 VDAC and Aβ peptides *via* GxxxG motifs induce Alzheimer's disease - a basic model of apoptosis. *Wien Med. Wochenschr.* 161, 274–276. doi: 10.1007/s10354-011-0887-5

Thomas, M. P., and Morrisett, R. A. (2000). Dynamics of NMDAR-mediated neurotoxicity during chronic ethanol exposure and withdrawal. *Neuropharmacology* 39, 218–226. doi: 10.1016/s0028-3908(99)00107-0

Tolar, M., Keller, J. N., Chan, S., Mattson, M. P., Marques, M. A., and Crutcher, K. A. (1999). Truncated apolipoprotein E (ApoE) causes increased intracellular calcium and may mediate ApoE neurotoxicity. *J. Neurosci.* 19, 7100–7110. doi: 10.1523/JNEUROSCI.19-16-07100.1999

Tong, B. C., Wu, A. J., Li, M., and Cheung, K. H. (2018). Calcium signaling in Alzheimer's disease and therapies. *Biochim. Biophys. Acta Mol. Cell Res.* 1865, 1745–1760. doi: 10.1016/j.bbamcr.2018.07.018

Toth, A. B., Shum, A. K., and Prakriya, M. (2016). Regulation of neurogenesis by calcium signaling. *Cell Calcium* 59, 124–134. doi: 10.1016/j.ceca.2016.02.011

Turovskaya, M. V., Turovsky, E. A., Zinchenko, V. P., Levin, S. G., and Godukhin, O. V. (2012). Interleukin-10 modulates [Ca2+]i response induced by repeated NMDA receptor activation with brief hypoxia through inhibition of InsP(3)-sensitive internal stores in hippocampal neurons. *Neurosci. Lett.* 516, 151–155. doi: 10.1016/j.neulet.2012.03.084

Ueda, K., Shinohara, S., Yagami, T., Asakura, K., and Kawasaki, K. (1997). Amyloid beta protein potentiates Ca2+ influx through L-type voltage-sensitive Ca2+ channels: a possible involvement of free radicals. *J. Neurochem.* 68, 265–271. doi: 10.1046/j.1471-4159.1997.68010265.x

Valladares, D., Utreras-Mendoza, Y., Campos, C., Morales, C., Diaz-Vegas, A., Contreras-Ferrat, A., et al. (2018). IP(3) receptor blockade restores autophagy and mitochondrial function in skeletal muscle fibers of dystrophic mice. *Biochim. Biophys. Acta Mol. Basis. Dis.* 1864, 3685–3695. doi: 10.1016/j.bbadis.2018.08.042

Vander Heiden, M. G., Li, X. X., Gottleib, E., Hill, R. B., Thompson, C. B., and Colombini, M. (2001). Bcl-xL promotes the open configuration of the voltage-dependent anion channel and metabolite passage through the outer mitochondrial membrane. *J. Biol. Chem.* 276, 19414–19419. doi: 10.1074/jbc.M101590200

Veinbergs, I., Everson, A., Sagara, Y., and Masliah, E. (2002). Neurotoxic effects of apolipoprotein E4 are mediated *via* dysregulation of calcium homeostasis. *J. Neurosci. Res.* 67, 379–387. doi: 10.1002/jnr.10138

Vergarajauregui, S., Connelly, P. S., Daniels, M. P., and Puertollano, R. (2008). Autophagic dysfunction in mucolipidosis type IV patients. *Hum. Mol. Genet.* 17, 2723–2737. doi: 10.1093/hmg/ddn174

Vervliet, T., Pintelon, I., Welkenhuyzen, K., Bootman, M. D., Bannai, H., Mikoshiba, K., et al. (2017). Basal ryanodine receptor activity suppresses autophagic flux. *Biochem. Pharmacol.* 132, 133–142. doi: 10.1016/j.bcp.2017.03.011

Vierling, C., Baumgartner, C. M., Bollerhey, M., Erhardt, W. D., Stampfl, A., and Vierling, W. (2014). The vasodilating effect of a Hintonia latiflora extract with antidiabetic action. *Phytomedicine* 21, 1582–1586. doi: 10.1016/j.phymed.2014.07.009

Villegas, S., Villarreal, F. J., and Dillmann, W. H. (2000). Leukemia inhibitory factor and Interleukin-6 downregulate sarcoplasmic reticulum Ca2+ ATPase (SERCA2) in cardiac myocytes. *Basic Res. Cardiol.* 95, 47–54. doi: 10.1007/s003950050007

Viviani, B., Bartesaghi, S., Gardoni, F., Vezzani, A., Behrens, M. M., Bartfai, T., et al. (2003). Interleukin-1beta enhances NMDA receptor-mediated intracellular calcium increase through activation of the Src family of kinases. *J. Neurosci.* 23, 8692–8700. doi: 10.1523/JNEUROSCI.23-25-08692.2003

Viviani, B., Gardoni, F., Bartesaghi, S., Corsini, E., Facchi, A., Galli, C. L., et al. (2006). Interleukin-1 beta released by gp120 drives neural death through tyrosine phosphorylation and trafficking of NMDA receptors. *J. Biol. Chem.* 281, 30212–30222. doi: 10.1074/jbc.M602156200

Vogl, C., Mochida, S., Wolff, C., Whalley, B. J., and Stephens, G. J. (2012). The synaptic vesicle glycoprotein 2A ligand levetiracetam inhibits presynaptic Ca2+ channels through an intracellular pathway. *Mol. Pharmacol.* 82, 199–208. doi: 10.1124/mol.111.076687

Wahlestedt, C., Golanov, E., Yamamoto, S., Yee, F., Ericson, H., Yoo, H., et al. (1993). Antisense oligodeoxynucleotides to NMDA-R1 receptor channel protect cortical neurons from excitotoxicity and reduce focal ischaemic infarctions. *Nature* 363, 260–263. doi: 10.1038/363260a0

Wallström, E., Diener, P., Ljungdahl, A., Khademi, M., Nilsson, C. G., and Olsson, T. (1996). Memantine abrogates neurological deficits, but not CNS inflammation, in Lewis rat experimental autoimmune encephalomyelitis. *J. Neurol. Sci.* 137, 89–96. doi: 10.3390/ijms22105335

Wang, W., Gao, Q., Yang, M., Zhang, X., Yu, L., Lawas, M., et al. (2015). Up-regulation of lysosomal TRPML1 channels is essential for lysosomal adaptation to nutrient starvation. *Proc. Natl. Acad. Sci. U S A* 112, E1373–1381. doi: 10.1073/pnas.1419669112

Wang, S. E., Ko, S. Y., Kim, Y. S., Jo, S., Lee, S. H., Jung, S. J., et al. (2018). Capsaicin upregulates HDAC2 *via* TRPV1 and impairs neuronal maturation in mice. *Exp. Mol. Med.* 50:e455. doi: 10.1038/emm.2017.289

Wang, D. M., Li, S. Q., Zhu, X. Y., Wang, Y., Wu, W. L., and Zhang, X. J. (2013). Protective effects of hesperidin against amyloid-β (Aβ) induced neurotoxicity through the voltage dependent anion channel 1 (VDAC1)-mediated mitochondrial apoptotic pathway in PC12 cells. *Neurochem. Res.* 38, 1034–1044. doi: 10.1007/s11064-013-1013-4

Wang, Z., Liu, S., Kakizaki, M., Hirose, Y., Ishikawa, Y., Funato, H., et al. (2014). Orexin/hypocretin activates mTOR complex 1 (mTORC1) *via* an Erk/Akt-independent and calcium-stimulated lysosome v-ATPase pathway. *J. Biol. Chem.* 289, 31950–31959. doi: 10.1074/jbc.M114.600015

Wang, P., and Wang, Z. Y. (2017). Metal ions influx is a double edged sword for the pathogenesis of Alzheimer's disease. *Ageing Res. Rev.* 35, 265–290. doi: 10.1016/j.arr.2016.10.003

Wang, Q., Yang, L., and Wang, Y. (2015). Enhanced differentiation of neural stem cells to neurons and promotion of neurite outgrowth by oxygen-glucose deprivation. *Int. J. Dev. Neurosci.* 43, 50–57. doi: 10.1016/j.ijdevneu.2015.04.009

Wang, G., Zhang, J., Xu, C., Han, X., Gao, Y., and Chen, H. (2016). Inhibition of SOCs attenuates acute lung injury induced by severe acute pancreatitis in rats and PMVECs injury induced by lipopolysaccharide. *Inflammation* 39, 1049–1058. doi: 10.1007/s10753-016-0335-1

Wang, Z. J., Zhao, F., Wang, C. F., Zhang, X. M., Xiao, Y., Zhou, F., et al. (2019). Xestospongin C, a reversible IP3 receptor antagonist, alleviates the cognitive and pathological impairments in APP/PS1 mice of Alzheimer's disease. *J. Alzheimers Dis.* 72, 1217–1231. doi: 10.3233/JAD-190796

Wang, X., and Zheng, W. (2019). Ca(2+) homeostasis dysregulation in Alzheimer's disease: a focus on plasma membrane and cell organelles. *FASEB J* 33, 6697–6712. doi: 10.1096/fj.201801751R

Wei, H., Liang, G., Yang, H., Wang, Q., Hawkins, B., Madesh, M., et al. (2008). The common inhalational anesthetic isoflurane induces apoptosis *via* activation of inositol 1,4,5-trisphosphate receptors. *Anesthesiology* 108, 251–260. doi: 10.1097/01.anes.0000299435.59242.0e

Weissman, T. A., Riquelme, P. A., Ivic, L., Flint, A. C., and Kriegstein, A. R. (2004). Calcium waves propagate through radial glial cells and modulate proliferation in the developing neocortex. *Neuron* 43, 647–661. doi: 10.1016/j.neuron.2004.08.015

Weisthal, S., Keinan, N., Ben-Hail, D., Arif, T., and Shoshan-Barmatz, V. (2014). Ca(2+)-mediated regulation of VDAC1 expression levels is associated with cell death induction. *Biochim. Biophys. Acta* 1843, 2270–2281. doi: 10.1016/j.bbamcr.2014.03.021

Whitney, N. P., Peng, H., Erdmann, N. B., Tian, C., Monaghan, D. T., and Zheng, J. C. (2008). Calcium-permeable AMPA receptors containing Q/R-unedited GluR2 direct human neural progenitor cell differentiation to neurons. *FASEB J.* 22, 2888–2900. doi: 10.1096/fj.07-104661

Wigerblad, G., Huie, J. R., Yin, H. Z., Leinders, M., Pritchard, R. A., Koehrn, F. J., et al. (2017). Inflammation-induced GluA1 trafficking and membrane insertion of Ca(2+) permeable AMPA receptors in dorsal horn neurons is dependent on spinal tumor necrosis factor, PI3 kinase and protein kinase A. *Exp. Neurol.* 293, 144–158. doi: 10.1016/j.expneurol.2017.04.004

Williams, A., Sarkar, S., Cuddon, P., Ttofi, E. K., Saiki, S., Siddiqi, F. H., et al. (2008). Novel targets for Huntington's disease in an mTOR-independent autophagy pathway. *Nat. Chem. Biol.* 4, 295–305. doi: 10.1038/nchembio.79

Wong, A., Grubb, D. R., Cooley, N., Luo, J., and Woodcock, E. A. (2013). Regulation of autophagy in cardiomyocytes by Ins(1,4,5)P(3) and IP(3)-receptors. *J. Mol. Cell Cardiol.* 54, 19–24. doi: 10.1016/j.yjmcc.2012.10.014

Wu, H. Y., Huang, C. H., Lin, Y. H., Wang, C. C., and Jan, T. R. (2018). Cannabidiol induced apoptosis in human monocytes through mitochondrial permeability transition pore-mediated ROS production. *Free Radic. Biol. Med.* 124, 311–318. doi: 10.1016/j.freeradbiomed.2018.06.023

Xia, Y., Ragan, R. E., Seah, E. E., Michaelis, M. L., and Michaelis, E. K. (1995). Developmental expression of N-methyl-D-aspartate (NMDA)-induced neurotoxicity, NMDA receptor function and the NMDAR1 and glutamate-binding protein subunits in cerebellar granule cells in primary cultures. *Neurochem. Res.* 20, 617–629. doi: 10.1007/BF01694545

Xu, H. X., Cui, S. M., Zhang, Y. M., and Ren, J. (2020). Mitochondrial Ca(2+) regulation in the etiology of heart failure: physiological and pathophysiological implications. *Acta Pharmacol. Sin.* 41, 1301–1309. doi: 10.1038/s41401-020-0476-5

Xu, D., and Peng, Y. (2017). Apolipoprotein E 4 triggers multiple pathway-mediated Ca2+ overload, causes CaMK II phosphorylation abnormity and aggravates oxidative stress caused cerebral cortical neuron damage. *Eur. Rev. Med. Pharmacol. Sci.* 21, 5717–5728. doi: 10.26355/eurrev_201712_14018

Xu, Y. Y., Wan, W. P., Zhao, S., and Ma, Z. G. (2020). L-type calcium channels are involved in iron-induced neurotoxicity in primary cultured ventral mesencephalon neurons of rats. *Neurosci. Bull.* 36, 165–173. doi: 10.1007/s12264-019-00424-2

Xue, Z., Guo, Y., and Fang, Y. (2016). Moderate activation of autophagy regulates the intracellular calcium ion concentration and mitochondrial membrane potential in beta-amyloid-treated PC12 cells. *Neurosci. Lett.* 618, 50–57. doi: 10.1016/j.neulet.2016.02.044

Yagami, T., Ueda, K., Asakura, K., Kuroda, T., Hata, S., Sakaeda, T., et al. (2002). Effects of endothelin B receptor agonists on amyloid beta protein (25–35)-induced neuronal cell death. *Brain Res.* 948, 72–81. doi: 10.1016/s0006-8993(02)02951-7

Yang, C. W., Borowitz, J. L., Gunasekar, P. G., and Isom, G. E. (1996). Cyanide-stimulated inositol 1,4,5-trisphosphate formation: an intracellular neurotoxic signaling cascade. *J. Biochem. Toxicol.* 11, 251–256. doi: 10.1002/(SICI)1522-7146(1996)11:5<251::AID-JBT6>3.0.CO;2-J

Yang, B., Li, J. J., Cao, J. J., Yang, C. B., Liu, J., Ji, Q. M., et al. (2013). Polydatin attenuated food allergy *via* store-operated calcium channels in mast cell. *World J. Gastroenterol.* 19, 3980–3989. doi: 10.3748/wjg.v19.i25.3980

Yang, Z. Y., Liu, J., and Chu, H. C. (2020). Effect of NMDAR-NMNAT1/2 pathway on neuronal cell damage and cognitive impairment of sevoflurane-induced aged rats. *Neurol. Res.* 42, 108–117. doi: 10.1080/01616412.2019.1710393

Yang, N. N., Shi, H., Yu, G., Wang, C. M., Zhu, C., Yang, Y., et al. (2016). Osthole inhibits histamine-dependent itch *via* modulating TRPV1 activity. *Sci. Rep.* 6:25657. doi: 10.1038/srep25657

Yang, J., Wang, R., Cheng, X., Qu, H., Qi, J., Li, D., et al. (2020). The vascular dilatation induced by Hydroxysafflor yellow A (HSYA) on rat mesenteric artery through TRPV4-dependent calcium influx in endothelial cells. *J. Ethnopharmacol.* 256:112790. doi: 10.1016/j.jep.2020.112790

Yang, M., Wang, Y., Liang, G., Xu, Z., Chu, C. T., and Wei, H. (2019). Alzheimer's disease presenilin-1 mutation sensitizes neurons to impaired autophagy flux and propofol neurotoxicity: role of calcium dysregulation. *J. Alzheimers Dis.* 67, 137–147. doi: 10.3233/JAD-180858

Ye, F., Li, X., Li, F., Li, J., Chang, W., Yuan, J., et al. (2016). Cyclosporin s protects against Lead neurotoxicity through inhibiting mitochondrial permeability transition pore opening in nerve cells. *Neurotoxicology* 57, 203–213. doi: 10.1016/j.neuro.2016.10.004

Yeh, K. C., Hung, C. F., Lin, Y. F., Chang, C., Pai, M. S., and Wang, S. J. (2020). Neferine, a bisbenzylisoquinoline alkaloid of nelumbo nucifera, inhibits glutamate release in rat cerebrocortical nerve terminals through 5-HT(1A) receptors. *Eur. J. Pharmacol.* 889:173589. doi: 10.1016/j.ejphar.2020.173589

Yoon, H., Kim, D. S., Lee, G. H., Kim, K. W., Kim, H. R., and Chae, H. J. (2011). Apoptosis induced by manganese on neuronal SK-N-MC cell line: endoplasmic reticulum (ER) stress and mitochondria dysfunction. *Environ. Health Toxicol.* 26:e2011017. doi: 10.5620/eht.2011.26.e2011017

Yoon, W. S., Yeom, M. Y., Kang, E. S., Chung, Y. A., Chung, D. S., and Jeun, S. S. (2017). Memantine induces NMDAR1-mediated autophagic cell death in malignant glioma cells. *J. Korean Neurosurg. Soc.* 60, 130–137. doi: 10.3340/jkns.2016.0101.006

Yu, H. M., Wen, J., Wang, R., Shen, W. H., Duan, S., and Yang, H. T. (2008). Critical role of type 2 ryanodine receptor in mediating activity-dependent neurogenesis from embryonic stem cells. *Cell Calcium* 43, 417–431. doi: 10.1016/j.ceca.2007.07.006

Yu, J., Zhu, C., Yin, J., Yu, D., Wan, F., Tang, X., et al. (2020). Tetrandrine suppresses transient receptor potential cation channel protein 6 overexpression- induced podocyte damage *via* blockage of RhoA/ROCK1 signaling. *Drug. Des. Devel. Ther.* 14, 361–370. doi: 10.2147/DDDT.S234262

Yue, C., Soboloff, J., and Gamero, A. M. (2012). Control of type I interferon-induced cell death by Orai1-mediated calcium entry in T cells. *J. Biol. Chem.* 287, 3207–3216. doi: 10.1074/jbc.M111.269068

Yun, W. J., Zhang, X. Y., Liu, T. T., Liang, J. H., Sun, C. P., Yan, J. K., et al. (2020). The inhibition effect of uncarialin A on voltage-dependent L-type calcium channel subunit alpha-1C: inhibition potential and molecular stimulation. *Int. J. Biol. Macromol.* 159, 1022–1030. doi: 10.1016/j.ijbiomac.2020.05.100

Yuqi, L., Lei, G., Yang, L., Zongbin, L., Hua, X., Lin, W., et al. (2009). Voltage-dependent anion channel (VDAC) is involved in apoptosis of cell lines carrying the mitochondrial DNA mutation. *BMC Med. Genet.* 10:114. doi: 10.1186/1471-2350-10-114

Zempel, H., Thies, E., Mandelkow, E., and Mandelkow, E. M. (2010). Abeta oligomers cause localized Ca(2+) elevation, missorting of endogenous tau into dendrites, tau phosphorylation and destruction of microtubules and spines. *J. Neurosci.* 30, 11938–11950. doi: 10.1523/JNEUROSCI.2357-10.2010

Zhang, E., and Liao, P. (2015). Brain transient receptor potential channels and stroke. *J. Neurosci. Res.* 93, 1165–1183. doi: 10.1002/jnr.23529

Zhang, X., Yu, L., and Xu, H. (2016). Lysosome calcium in ROS regulation of autophagy. *Autophagy* 12, 1954–1955. doi: 10.1080/15548627.2016.1212787

Zhao, P., Leonoudakis, D., Abood, M. E., and Beattie, E. C. (2010). Cannabinoid receptor activation reduces TNFalpha-induced surface localization of AMPAR-type glutamate receptors and excitotoxicity. *Neuropharmacology* 58, 551–558. doi: 10.1016/j.neuropharm.2009.07.035

Zhou, C. (2010). [Inhibition effect of IL-1beta on calcium channels currents in cultured cortical neurons of rat]. *Dongwuxue Yanjiu* 31, 89–93. doi: 10.3724/sp.j.1141.2010.01089

Zhou, C., Tai, C., Ye, H. H., Ren, X., Chen, J. G., Wang, S. Q., et al. (2006). Interleukin-1beta downregulates the L-type Ca2+ channel activity by depressing the expression of channel protein in cortical neurons. *J. Cell Physiol.* 206, 799–806. doi: 10.1002/jcp.20518

Zhou, G. H., Zhang, F., Wang, X. N., Kwon, O. J., Kang, D. G., Lee, H. S., et al. (2014). Emodin accentuates atrial natriuretic peptide secretion in cardiac atria. *Eur. J. Pharmacol.* 735, 44–51. doi: 10.1016/j.ejphar.2014.04.014

Zhu, Y. G., Chen, X. C., Chen, Z. Z., Zeng, Y. Q., Shi, G. B., Su, Y. H., et al. (2004). Curcumin protects mitochondria from oxidative damage and attenuates apoptosis in cortical neurons. *Acta Pharmacol. Sin.* 25, 1606–1612.

Zhu, Z. D., Yu, T., Liu, H. J., Jin, J., and He, J. (2018). SOCE induced calcium overload regulates autophagy in acute pancreatitis *via* calcineurin activation. *Cell Death Dis.* 9:50. doi: 10.1038/s41419-017-0073-9

Conflict of Interest: The authors declare that the research was conducted in the absence of any commercial or financial relationships that could be construed as a potential conflict of interest.

Publisher's Note: All claims expressed in this article are solely those of the authors and do not necessarily represent those of their affiliated organizations, or those of the publisher, the editors and the reviewers. Any product that may be evaluated in this article, or claim that may be made by its manufacturer, is not guaranteed or endorsed by the publisher.

Advantages of publishing in Frontiers

OPEN ACCESS
Articles are free to read for greatest visibility and readership

FAST PUBLICATION
Around 90 days from submission to decision

HIGH QUALITY PEER-REVIEW
Rigorous, collaborative, and constructive peer-review

TRANSPARENT PEER-REVIEW
Editors and reviewers acknowledged by name on published articles

Frontiers
Avenue du Tribunal-Fédéral 34
1005 Lausanne | Switzerland

Visit us: www.frontiersin.org
Contact us: frontiersin.org/about/contact

REPRODUCIBILITY OF RESEARCH
Support open data and methods to enhance research reproducibility

DIGITAL PUBLISHING
Articles designed for optimal readership across devices

FOLLOW US
@frontiersin

IMPACT METRICS
Advanced article metrics track visibility across digital media

EXTENSIVE PROMOTION
Marketing and promotion of impactful research

LOOP RESEARCH NETWORK
Our network increases your article's readership